ЖУРНАЛ
ЭКСПЕРИМЕНТАЛЬНОЙ И ТЕОРЕТИЧЕСКОЙ
ФИЗИКИ
АКАДЕМИЯ НАУК СССР

SOVIET PHYSICS

JETP

VOLUME 5 NUMBER 5

A Translation

of the

Journal of Experimental and Theoretical Physics

of the

Academy of Sciences of the USSR

Volume 32

DECEMBER 1, 1957

Published by the

AMERICAN INSTITUTE OF PHYSICS
INCORPORATED

SOVIET PHYSICS
JETP

A translation of the Journal of Experimental and Theoretical Physics of the USSR.

A publication of the

AMERICAN INSTITUTE OF PHYSICS

Editor of SOVIET PHYSICS—JETP

J. GEORGE ADASHKO, DEPARTMENT OF ELECTRICAL ENGINEERING
THE CITY COLLEGE OF NEW YORK, CONVENT AVENUE AND
139TH STREET, NEW YORK, NEW YORK.

SOVIET PHYSICS is a monthly journal published by the American Institute of Physics for the purpose of making available in English reports of current Soviet research in physics as contained in the Journal of Experimental and Theoretical Physics of the Academy of Sciences of the USSR. The page size of SOVIET PHYSICS will be 7⅛" x 10½", the same as other Institute journals.

Transliteration of the names of Russian authors follows the system employed by the Library of Congress.

This translating and publishing project was undertaken by the Institute in the conviction that dissemination of the results of researches everywhere in the world is invaluable to the advancement of science. The National Science Foundation of the United States encouraged the project initially and is supporting it in large part by a grant.

The American Institute of Physics and its translators propose to translate faithfully all the material in the Journal of EXPERIMENTAL AND THEORETICAL PHYSICS OF THE USSR appearing after January 1, 1955. The views expressed in the translated material, therefore, are intended to be those expressed by the original authors, and not those of the translators nor of the American Institute of Physics.

Two volumes are published annually, each of six issues. Each volume contains the translation of one volume of the Journal of EXPERIMENTAL AND THEORETICAL PHYSICS OF THE USSR. New volumes begin in February and August.

Subscription Prices:

Per year (12 issues)
United States and Canada $60.00
Elsewhere 64.00

Back Numbers
Single copies ..... $ 6.00

Subscriptions should be addressed to the American Institute of Physics, 335 East 45th Street, New York 17, New York.

SOVIET PHYSICS

JETP

A translation of the Journal of Experimental and Theoretical Physics of the USSR.

SOVIET PHYSICS JETP Vol. 5, No. 5, pp 779-1032 DECEMBER, 1957

Energy Spectrum of γ-Quanta from the Decay of π^0-Mesons Produced by 660 Mev Protons on Hydrogen Nuclei

IU. D. BAIUKOV AND A. A. TIAPKIN

Joint Institute for Nuclear Studies

(Submitted to JETP editor October 26, 1956)

J. Exptl. Theor. Phys. (U.S.S.R.) 32, 953-956 (May, 1957)

The energy spectrum of γ-quanta from the decay of π^0-mesons produced by 660 Mev protons on hydrogen nuclei has been measured. The angular and energy distribution of π^0-mesons produced in $p - p$ collisions has been obtained by analyzing the γ-quantum spectrum.

1. IN THE AVAILABLE INFORMATION on meson generation, there has been absent up to now information on the energy spectrum of π^0-mesons produced in $p - p$ collisions. This can be explained by the difficulty of investigating the γ-spectrum produced in the decay of π^0-mesons, formed in this reaction with relatively small cross section.

The investigation of this γ-spectrum becomes possible at a proton energy of 660 Mev, because of an increase in the cross section for the formation of π^0-mesons on hydrogen nuclei. In the present work, a differential method was used to measure the gammas from targets of polythene and carbon, continuously bombarded by protons in the integral beam of the synchroton. Relative γ-intensities from the targets were measured by a magnetic pair spectrometer described in Ref. 1.

The basic difficulties in investigating the spectra by the differential method were due to the small cross section for π^0-formation on hydrogen compared to the formation on carbon. The necessary precision of measurement was achieved in the present work by applying the method of cyclic interchange of targets. The change of targets located inside the vacuum chamber of the accelerator was performed automatically every minute. The method of automatically changing targets was developed and applied previously in work described in Ref. 2. Synchronously with the change of targets, the registering system of the spectrometer was also switched, permitting separate counting of γ-quanta formed on separate targets. In this way measurements were made in different parts of the spectra, of the γ-intensity ratios from the polythene and carbon targets. Simultaneously with this, the total γ-intensities from the two targets were measured by means of a telescope containing a scintillation counter and a Cerenkov counter. The telescope registering equipment was also switched in synchronism with the targets.

This method of measuring relative γ-intensities greatly reduced the errors associated with changes in efficiency with time of the registering apparatus, as well as errors due to normalization of the results of separate measurements in different parts of the spectra.

2. The γ-spectrum formed on hydrogen $F_H(\varepsilon_\gamma, \theta)$, is expressed as follows in terms of the γ-spectrum formed on carbon, $F_C(\varepsilon_\gamma, \theta)$, and the ratio of

γ-intensities from the polythene and carbon targets:

$$F_{\mathrm{H}}(\varepsilon_\gamma, \theta) = \frac{1}{2}[F_{\mathrm{CH_2}}(\varepsilon_\gamma, \theta) - F_{\mathrm{C}}(\varepsilon_\gamma, \theta)] = \\ = \frac{1}{2} F_{\mathrm{C}}(\varepsilon_\gamma, \theta)\left\{[1 + 2(d\sigma^\gamma_{\mathrm{H}}/d\omega)/(d\sigma^\gamma_{\mathrm{C}}/d\omega)]\ \frac{k(\varepsilon_\gamma)}{k_0} - 1\right\}. \quad (1)$$

Here $(d\sigma^\gamma_{\mathrm{H}}/d\omega)/(d\sigma^\gamma_{\mathrm{C}}/d\omega)$ is the ratio of the differential cross sections for γ-production on hydrogen and carbon as measured at an angle θ; $k(\varepsilon_\gamma)$ is the ratio of the γ-intensities from polythene and carbon at energy ε_γ and angle θ; k_0 is the ratio of the total γ-intensities from these targets at angle θ.

In the present work the measurements of γ-intensities were carried out at an angle of 0° with the direction of the incident protons. The spectrum of gammas formed at 0° by 660 Mev protons on carbon has been measured previously[3]. The magnitude of the relative cross section $(d\sigma^\gamma_{\mathrm{H}}/d\omega)/(d\sigma^\gamma_{\mathrm{C}}/d\omega)$ for the angle 0° was taken from Ref. 4. The magnitudes of the ratios $k(\varepsilon_\gamma)$ and k_0 were measured simultaneously by means of the pair spectrometer and the γ-telescope.

The γ-spectrum of the π^0-decay, due to 660 Mev protons on hydrogen, is shown in Fig. 1. The error bars include the errors in all quantities entering Eq. (1). The gamma energy from the decay of π^0-mesons formed on hydrogen should not exceed the maximum possible energy, which for a bombarding energy of 660 Mev is 470 ± 7 Mev at 0°. The spectrum actually obtained spreads to a somewhat larger energy because of errors in the measurements.

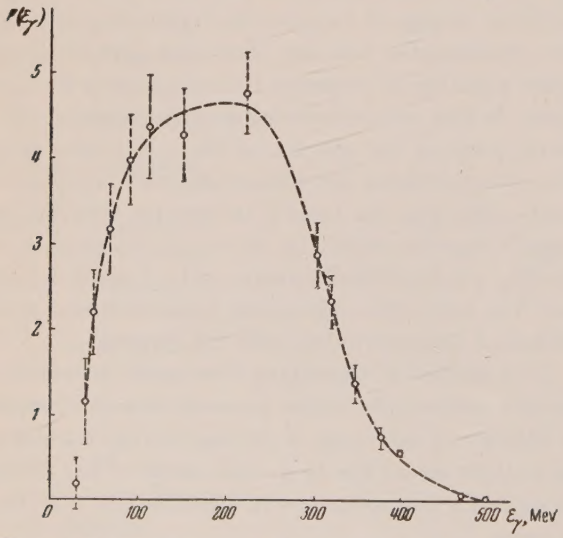

FIG. 1. Energy spectrum of γ-quanta from the decay of π^0-mesons produced in $p - p$ collisions at a proton energy of 660 Mev.

3. The measured spectrum of γ-quanta permits one to determine the energy spectrum and angular distribution of π^0-mesons formed in $p - p$ collisions. The analysis of the γ-spectrum formed on hydrogen is similar to the analysis of the spectrum formed on carbon, and described in Ref. 3. It differs from the latter in that approximations concerning the motion of nucleons in a complex nucleus need not be made.

The gamma spectrum, transformed to the center of mass system of the colliding nucleons, and represented on a semi-logarithmic plot, is almost symmetrical about an energy one half the rest energy of the π^0-mesons. This means that the angular distribution of the π^0-mesons is close to isotropic. In order to determine the energy distribution of π^0-mesons corresponding to the hard gammas ($\varepsilon_\gamma > m_0c^2/2$) represented in Fig. 1 by the smooth curve, the angular π^0-distribution was assumed isotropic. The π^0-energy distribution in the center of mass system found by this means is shown in Fig. 2.

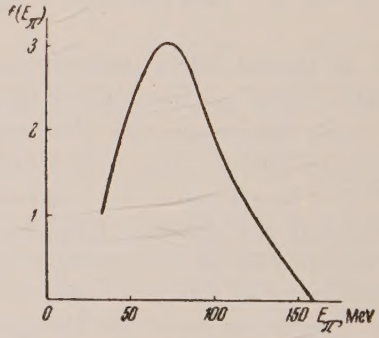

FIG. 2. Energy spectrum of π^0-mesons in the center of mass system of the colliding protons.

The π^0-energy distribution corresponding to the hard γ-spectrum was then further used for a more accurate determination of the π^0-angular distribution corresponding to gammas in the energy region $\varepsilon_\gamma \leqslant m_0c^2/2$. We took a π^0-angular distribution of the form $1 + b\cos^2\theta$, with different values of the constant b, and computed the resulting γ-energy spectrum (Fig. 3). Comparison of the computed with the measured curves shows that the π^0-angular distribution is $1 + (0.3 \pm 0.1)\cos^2\theta$, and consequently only (9 ± 3)% of the total number of π^0-mesons are distributed according to $\cos^2\theta$.

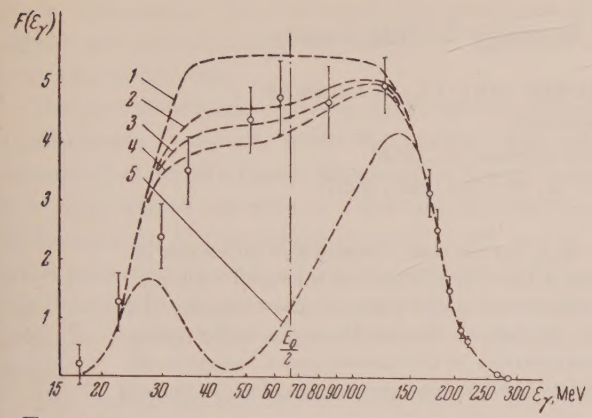

FIG. 3. Energy spectrum of γ-quanta in the center of mass system of the colliding nucleons. o – Experimental points. Dotted curves – spectra computed with different values of the constant b in the meson angular distribution: $1 - b = 0$; $2 - b = 0.2$; $3 - b = 0.3$; $4 - b = 0.4$; $5 - \varphi(\theta) \sim \cos^2\theta$.

This π^0-angular distribution could in turn be used for an improved estimate of the π^0-energy distribution. However, the calculation of the π^0-spectrum with the above determined deviation from isotropicity of the angular distribution leads only to an insignificant change in the energy distribution, substantially smaller than the uncertainties in the spectrum due to measurement errors in the γ-spectrum.

4. It is known that at small collision energies π-mesons are effectively formed in p-states, while the nucleons are emitted in S-states. In the meson angular distribution the term proportional to $\cos^2\theta$ plays the main role, and because of the strong nucleon interaction in the final state, the meson energy is close to the maximum possible. However, for the production of π^0-mesons in $p - p$ collisions, conservation of angular momentum and parity forbids the transition, basic at low energies, wherein the mesons are created in p-states, the nucleons in S-states. The fast increase with energy of the cross section for this reaction means that the transition in which mesons and nucleons are both emitted in s- and S-states cannot be of basic importance. Thus one has to assume that in the reaction $p + p \to \pi^0 + p + p$, the mesons or nucleons are emitted with higher angular momenta. It is clear therefore that the angular and energy distribution of the π^0-mesons may differ from distributions corresponding to emission of π's in p-states and nucleons in S-states. The small transition probabilities for high angular momentum transitions at low collision energies constitute one of the reasons that the π^0-formation cross section in $n - p$ collisions is considerably larger than in $p - p$ collisions.

On the basis of the γ-spectrum analysis in this work, we conclude that the angular distribution of π^0-mesons formed in $p - p$ collisions is nearly isotropic. This result is in agreement with the data of π^0-angular distributions in Ref. 2 and 5, obtained by investigating the angular distribution of gamma quanta.

From the π^0-spectrum formed in $p - p$ collisions, as obtained in the present work, it follows that the π^0-mesons are emitted with energies considerably smaller than the maximum possible: the mean kinetic energy of the mesons is about 45% of the maximum possible. One can try to explain this fact by the absence of strong nucleon interactions in the final state. If all the particles (two nucleons and π^0-meson) would not interact strongly in the final state, then the free energy of the reaction would be distributed among them according to the statistical factor. In this case the π^0-spectrum would be a semicircle on the abscissa with its maximum at an energy equal to one half of $E_{\pi\,\max}$ [6]. The angular distribution would be isotropic.

The π^0-spectrum due to 660 Mev protons incident on hydrogen has a maximum at an energy $E_\pi \approx 75$ Mev (Fig. 2), but it looks different from the one described above. The meson angular distribution also deviates somewhat from isotropic. Consequently, at this proton energy, the final state particle interactions should not be neglected. Of special interest in this case would be the analysis of π^0-energy distributions on the basis of a strong bond between the meson and one of the nucleons.

We are grateful to M. S. Kozodaev and Iu. D. Prokoshkin for their help in this work and for discussion of the results.

[1] Baiukov, Kozodaev, Markov, Sinaev, and Tiapkin, Report, Inst. Nucl. Prob., Acad. Sci. U.S.S.R. (1955).

[2] Iu. D. Prokoshkin, and A. A. Tiapkin, J. Exptl. Theoret. Phys. (U.S.S.R.) 32, 750 (1957), Soviet Physics, JETP 5, 618, (1957).

[3] Baiukov, Kozodaev, and Tiapkin, J. Exptl. Theoret. Phys. (U.S.S.R.) 32, 667 (1957), Soviet Physics, JETP 5, 552, (1957).

[4] Tiapkin, Kozodaev, and Prokoshkin, Dokl. Akad. Nauk SSSR 100, 689 (1955).

[5] Balashov, Zhukov, Pontecorvo, and Selivanov, Report, Inst. Nucl. Prob. Acad. Sci. U.S.S.R. p. 60, 1955.

[6] E. Fermi, *Elementary Particles.* (Russian Translation, 1953) Yale University Press, 1951.

Translated by C. R. Lubitz
209

Structural Characteristics of Antimony Sulfide Layers

V. N. VERTSNER, B. V. GORBUNOV AND IA. A. OKSMAN
State Optics Institute

(Submitted to JETP editor November 27, 1956)
J. Exptl. Theoret. Phys. (U.S.S.R.) 32, 957-961 (May, 1957)

The nature of the sensitization processes in Sb_2S_3 layers was investigated by means of electron diffraction. It was established that when a layer condenses on a heated backing it consists of an amorphous mass of antimony sulfide and a thin surface film of Sb_2O_3. The dependence of the orientation of the small oxide crystals on the condensation temperature was determined. It is suggested that the photosensitivity of the investigated layers is determined by the crystalline oxide which provides additional trapping centers for the current carriers.

THE PHOTOELECTRIC PROPERTIES of antimony sulfide layers produced by vacuum evaporation are determined principally by the condensation conditions. In distinction from the majority of sulfides and selenides, the properties of the layer are well reproducible; this suggests that the sensitization processes in this instance are less complex than in PbS, for example.

Since photosensitivity is principally dependent on temperature two thermal activation mechanisms can be conceived. The first process is associated with crystallization of the basic material; the second is associated with the formation of oxides. The experiments which will be described here were intended, first, to determine the character of the activation processes and, secondly, to indicate the relation between the structural characteristics of the layers and their photoelectric properties. The second purpose required a study of the photoelectric properties of the layers. The principal results of our investigation will be presented here.

The resistivity of the layers lies between 10^{10} and 10^{13} ohm-cm and shows little dependence on the temperature of the backing or the subsequent heat treatment. The material of the contacts has almost no effect on the resistance of the specimens. The sign of the thermal emf indicates the predominance of *p*-type conductivity. Photoconduction is observed only in layers evaporated on a backing which had been heated to 100–120° C, or on a backing at room temperature but subsequently heating for 1 to 2 minutes to 250–300° C in air. The latter method of activation yields less stable and less reproducible results.

The curves in Fig. 1 give an idea of the spectral characteristics of the photosensitivity at room temperature. These curves were not converted to

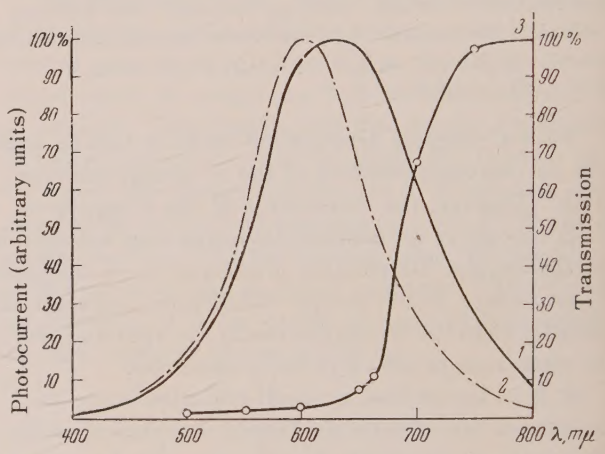

FIG. 1. Spectral distribution of photosensitivity in a layer of Sb_2S_3 at room temperature. 1—field along the specimen; 2—field at right angles to specimen; 3—optical transmission of specimen.

units of incident energy (an incandescent lamp being used as the source). The most important property of the curves is that in the strong absorption region they are independent of the direction of the electric field. If it is assumed that the carrier drift distance is considerably smaller than the layer thickness, then when the photoconductivity is measured perpendicular to the surface layer, under strongly absorbed radiation, the resistance will vary only on the surface of the specimen. Measurements along the layer should not be influenced by the same circumstance and in this case the photoconductivity curve in the strong absorption region should reveal a smaller decline.

Since the short-wave ends of the curves are of identical character we can assume that carrier drift in this case exceeds the layer thickness (1–2μ).

A temperature rise from 20 to 100° C results in an exponential rise of both the dark current and

the photocurrent. The corresponding activation energies are approximately 0.3 and 0.1 ev and vary with the specimens.

The photoconductivity relaxation time measured transversely is usually somewhat greater than when measured along the layer; its absolute value under low illumination amounts to a fraction of a second. Relaxation is characterized by both a fast and a slow process; as with all high-resistance semiconductors the latter process is apparently associated with the thermal liberation of carriers from deep traps.

The introduction of donors (Cu, Sb, Cd) does not essentially alter the properties of the layers. A small quantity of antimony oxide in the evaporated material increases the dark resistance.

It should be noted that antimony sulfide layers are of considerable practical interest because they are used extensively in "vidicon" photoconductive television camera tubes [1,2].

We have investigated two kinds of antimony sulfide layers: thin free films and ordinary layers on glass. The thin films were prepared by vacuum evaporation of Sb_2S_3 which condensed on organic backings at room temperature, 100° C and in some instances a little above or below 100° C. Backings at room temperature are designated as "cold".

All electron diffraction patterns from such layers are characterized by a common strong background. As the temperature of the backing was raised there was an increase in the definition, intensity, and number of observed reflections. Fig. 2 is the electron diffraction pattern of a layer of Sb_2S_3 evaporated on a hot backing (100° C). Table 1 gives the interplanar spacings that were calculated according to diffraction patterns from thin Sb_2S_3 layers evaporated on cold and 100° C backings. The interplanar spacings of Sb_2O_3 found in structural tables are also given. A comparison shows that in both cases the reflections were produced by small Sb_2O_3 crystals.

Thus thin films produced by vacuum evaporation of Sb_2S_3 contain amorphous Sb_2S_3 and crystalline Sb_2O_3. The presence of amorphous Sb_2S_3 in the

FIG. 2. Electron diffraction pattern of a Sb_2S_3 film evaporated on a cold backing.

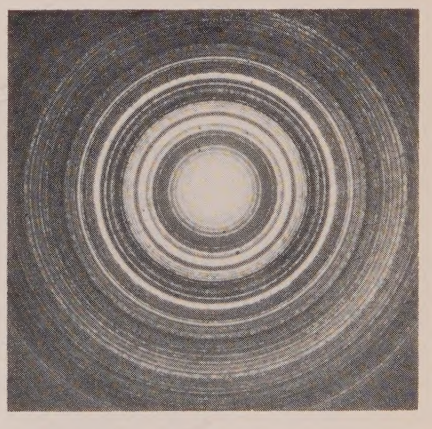

FIG. 3. Electron diffraction pattern of a Sb_2S_3 film heated at 300° C for 2 minutes.

FIG. 4. Electron diffraction pattern of a Sb_2S_3 layer evaporated on cold glass and heated at 300° C for 2 minutes.

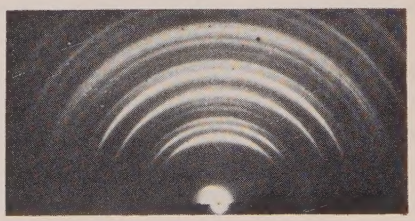

FIG. 5. Electron diffraction pattern of a Sb_2S_3 layer evaporated on hot glass and heated at 300° C for 2 minutes.

TABLE I. Interplanar spacings calculated from electron diffraction patterns of thin Sb_2S_3 layers evaporated on cold backings and backings heated to 100° C.

Sb_2S_3 layer on cold backing		Sb_2S_3 layer on hot backing		Tabulated values (Sb_2O_3)	
d, A	Intensity	*d*, A	Intensity	*d*, A	Intensity in %
		6.4	strong	6.4	10
3.26	strong	3.22	v. strong	3.22	100
2.78	weak	2.82	medium	2.78	30
		2.58	medium	2.56	8
		2.31	v. weak		
		2.16	v. weak		
1.96	weak	1.98	strong	1.96	50
1.68	weak	1.70	strong	1.68	50
		1.64	weak	1.61	10
		1.58	medium	1.56	10
				1.45	2
		1.39	v. weak	1.39	6
				1.36	4
		1.29	v. weak	1.28	15
		1.26	v. weak	1.25	10

TABLE II. Interplanar spacing calculated from electron diffraction patterns of Sb_2S_3 films heated at 300° C for two minutes.

Calculated values		Tabulated values					
		Sb_2O_3		Sb_2S_3		Sb	
d, A	Intensity	*d*, A	Intensity in %	*d*, A	Intensity in %	*d*, A	Intensity in %
				8.2	6		
7.95	medium						
6.35	strong	6.4	10				
5.61	medium			5.6	23		
5.02	medium			5.0	46		
3.93	medium			3.97	2.3		
3.64	medium					3.71	15
3.55	medium			3.57	100		
3.46	medium						
3.22	v. strong	3.22	100				
3.12	medium					3.10	100
3.04	v. strong			3.02	86		
2.82	weak						
2.76	strong	2.78	30	2.75	86		
2.67	medium			2.66	34		
2.60	medium			2.60	6		
2.52	medium	2.56	8	2.50	34		
2.42	medium			2.42	23		
2.28	weak					2.24	63
2.22				2.23	29	2.14	63
2.18	weak						
2.10	strong			2.09	40		

original films is confirmed by electron diffraction patterns of antimony sulfide films heated at 300° C for 2 minutes (the original films were produced by condensation on 100° backings). Fig. 3 and Table 2 show that the amorphous antimony sulfide of the original layer is well crystallized under these con-

ditions. In addition to the Sb_2S_3 the layers contain Sb_2O_3, possibly some metallic antimony and still unidentified compounds, whose interplanar spacings are also given in Table 2.

Thick antimony sulfide layers on glass are crystallized somewhat differently than the condensate on organic films. The reflection patterns show a

TABLE III. Interplanar spacings calculated from electron diffraction patterns of Sb_2S_3 layers on glass heated for 2 minutes at 300° C.

Calculated values		Tabulated values for Sb_2O_3	
d, Å	Intensity	d, Å	Intensity in %
4.08	extr. weak		
3.20	v. strong	3.22	100
2.84	strong	2.78	30
2.57	medium	2.56	8
2.3	weak		
2.16	weak		
1.96	v. strong	1.96	50
1.91*	extr. weak		
1.70	v. strong	1.68	50
1.62	extr. weak	1.61	10
1.57	medium	1.56	10
1.46	weak	1.45	2
1.39	extr. weak	1.394	6
1.37	medium	1.36	4
1.32	extr. weak		
1.28	medium	1.28	15
1.25	weak-med.	1.25	10
1.18	extr. weak	1.18	1
1.14	medium	1.138	4
1.08	strong	1.073	8

*For Sb_2S_3 the $d = 1.92$ reflection has 100% intensity.

very strong background which is evidently caused by scattering from amorphous Sb_2S_3. The reflections are very broad. The broadening and the background are much less apparent for layers evaporated on hot backings. When both types of layers are heated for 2 minutes at 300° C the diffraction patterns show reflection arcs, which are evidence of the formation of oriented crystals on the surface of the sublimate. Table 3 and Figs. 4 and 5 show that the Sb_2O_3 crystals have different orientations in these layers.

In the case of samples produced by heating sensitive layers previously evaporated on a hot backing the crystals of cubic Sb_2O_3 are oriented predominantly with the (111) atomic planes parallel to the backing. Heating of insensitive layers orients the oxide crystals with cube faces (100 planes) parallel to the backing. The orientation of Sb_2O_3 crystals which we observed in heated sensitive layers of Sb_2S_3 coincides with the orientation of BiO crystals in oxidized thin layers of similar compounds—Bi_2Se_3 and Bi_3Te_3[3].

We also obtained Debye X-ray patterns of the original material and of the material of layers in the form of powders scraped from glass and containing the original and oxidized Sb_2S_3 sublimates. The X-ray patterns of the original sublimates revealed only individual and very diffuse reflections. This is confirmation that the material of such layers is amorphous. After heating, the powder taken from the glass produced X-ray patterns with clear strong reflections. The system of reflections was identical with that obtained in X-ray patterns of the original material and corresponded to Sb_2S_3.

The absence of Sb_2O_3 lines in the X-ray patterns and the absence of reflections from Sb_2O_3 in the electron reflection patterns is confirmation that the oxide phase is a small fraction of the layer material and is mainly concentrated on its surface.

CONCLUSIONS

Structural studies show that thin layers of photosensitive antimony sulfide consist mainly of amorphous Sb_2S_3, an oxide surface film composed of cubic Sb_2O_3 crystals, and possibly metallic antimony. Heating of the sublimates is accompanied by growth of the crystals. Crystals of the oxide phase which form on the surface have very different orientations depending on the temperature of the backing during the condensation process. It can thus be assumed that photosensitivity is associated not with crystallization of the bulk of the layer but rather with the processes that accompany the formation of the oxide. The literature contains detailed studies of the sensitization of layers by impurities which increase carrier lifetime[4]. It is also known that in many sulfides and selenides oxygen acts as such an impurity. It is thus reasonable to interpret our findings as follows:

The formation of a thin film of definitely oriented oxide crystals on the surface results in the appearance of new recombination centers in antimony sulfide layers. The influence of the oxide surface film on the volume photoconductivity of the photolayers can be attributed to the thinness of the layers and to the large carrier drift length.

Any free antimony contained in the layers is unlikely to act as a sensitizer, as experiments with

the introduction of donor impurities have produced negative results.

In conclusion the authors must thank Academician A. A. Lebedev for his interest and valuable suggestions. The authors are also grateful to G. V. Anan'eva and A. I. Kuznetsov for their assistance.

[1] Artem'ev, Sokolov and Temiriazeva, Radiotekhn. i Elektronika (Radio Engg. and Electronics) 1, 245 (1956).

[2] Forgue, Goodrich and Cope, RCA Rev. 12, 335 (1951).

[3] S. A. Semiletov and Z. G. Pinsker, J. Tech. Phys. (U.S.S.R.) 25, 2336 (1955).

[4] A. Rose, Phys. Rev. 97, (1955).

Translated by I. Emin
210

SOVIET PHYSICS JETP VOLUME 5, NUMBER 5 DECEMBER, 1957

Energy Distribution of Neutrons Emitted from Beryllium Bombarded by 680 Mev Protons

V. KISELEV AND V. B. FLIAGIN

Joint Institute for Nuclear Research

(Submitted to JETP editor November 29, 1956)
J. Exptl. Theoret. Phys. (U.S.S.R.) 32, 962-964 (May, 1957)

The neutron energy spectra were measured at angles of 0 and 18° in the laboratory system. A peak not observed at lower primary-proton energies was detected in the 100–400 Mev region. The existence of this peak is explained by π-meson production processes.

THE PRESENT NOTE is to describe one of the experiments carried out to investigate the main characteristics of the fast neutron beams formed when beryllium targets are bombarded by 680-Mev protons.

In the present experiment the target was placed inside the synchro-cyclotron chamber and was 2.5 cm thick. The experiment was performed at angles $\theta = 0°$ and $\theta = 18°$ between the neutron beam and the direction of the velocity of the protons impinging on the target. The neutron energy distribution was investigated by determining the energy spectra of the recoil protons, emitted at a 30° laboratory angle, as a result of elastic n–p scattering. For this purpose, paraffin or graphite scatterers were placed in the path of the neutron beam; the effect due to hydrogen was determined from the difference between the effects of these two scatterers.

The measurements were performed principally by the differential method. In this case the detector, a telescope with four scintillation counters (three were connected for coincidence, the fourth for anticoincidence), was used to measure the intensity of the recoil proton current in some relatively narrow energy interval. The width of this interval and its position on the energy scale were fixed by means of copper and tungsten filters, placed between the third and fourth and between the second and third counters, respectively. A system of controlling experiments made it possible to make all the necessary corrections, in particular to take into account the loss of protons in filters, their scattering in the scintillators, etc.

The main source of error in our experiment could have been the admixture of charged particles emitted from the following reactions in the scatterer:

$$n + p \rightarrow \pi^0 + (n + p); \quad n + p \rightarrow \pi^- + p + p;$$

$$n + p \rightarrow \pi^+ + n + n.$$

The corrections related to meson production processes included only in the high energy part of the neutron spectrum ($E_n > 450$ Mev), for which Kazarinov and Simonov,, in a special experiment[1], have measured the integral $\pi^{\pm}$-meson yield from these reactions. Unfortunately, there are no experimental data on the energy spectrum of $\pi^{\pm}$-mesons formed in n–p collisions. These corrections have therefore been calculated on the assumption that the energy distribution of the $\pi^{\pm}$-mesons corresponding to different incident neutron energies has a form similar to the spectra of $\pi^{\pm}$-mesons from the

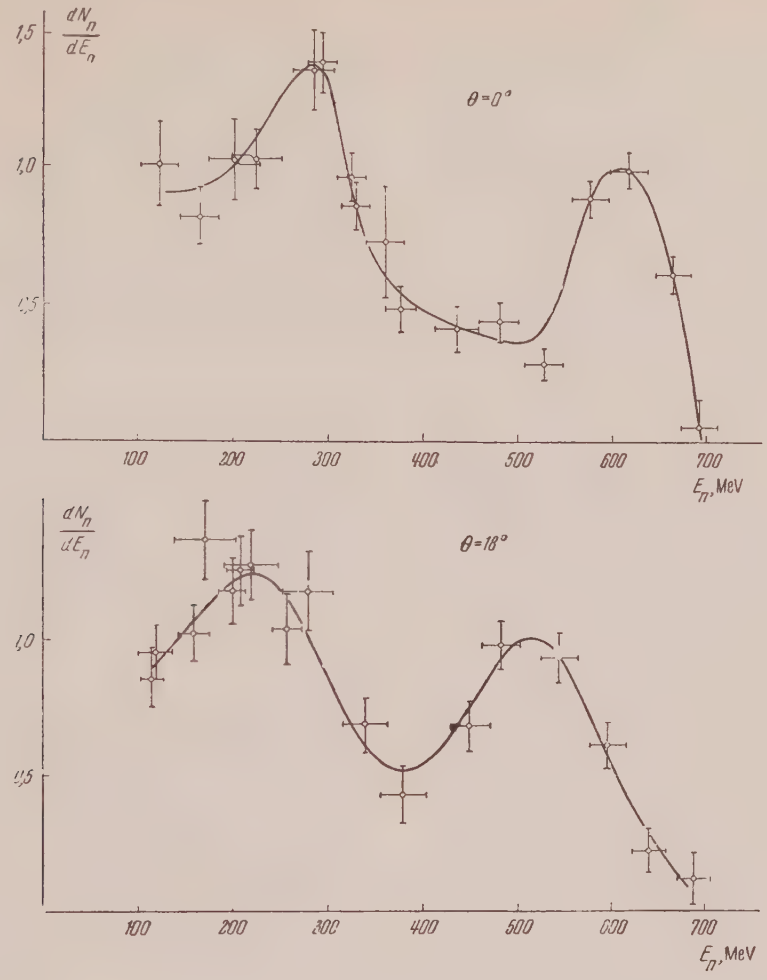

Neutron energy spectra.

reaction $p + p \rightarrow p + n + \pi^+$, spectra which have been studied for 657 and 556 Mev protons. The same calculations indicate that the admixture of charged particles from the above-mentioned reactions constitutes, in the part of the spectrum with $E_n < 450$ Mev, an average of $\sim 5\%$ of the number of the protons emitted in elastic n–p scattering.

The neutron energy distributions determined from the experiments are shown in the figure. The errors are statistical errors due only to the present measurements. One can see from the figure that for $\theta = 0°$ the maximum in the high energy region (600 Mev) is ~ 80 Mev lower than the upper limit of the spectrum. This decrease of the neutron energy with respect to the maximum energy of the protons impinging on the target is mainly related to the proton energy spread. The latter is due mostly to the radical oscillation of the synchro-cyclotron beam[3] and to the loss of energy by ionization during multiple passage of the protons through the target. The mean value of the energy lost by such processes constitutes 20 to 25 Mev. The angular spread of the beam due to multiple scattering and the angular spread of the proton incidence on the target are too small to affect this value. The additional energy losses should therefore be attributed to the proton-beryllium interaction process itself.

It is interesting to note that, in the impulse approximating, owing to the energy and momentum conservation laws, the pair collision of protons with nuclear neutrons should give for the neutrons emitted at an angle $\theta = 0°$ a spectrum identical to the spectrum of the primary protons. In this case, however, because of the exchange character of the p–n interaction, the nucleus is left out with a low energy proton instead of a neutron. The probability of

such a process should decrease considerably because of the Pauli principle. It is possible that a considerable role is played by multiple collisions and also by collisions in which part of the energy is carried away by a third particle. In this case, the restriction made by the Pauli principle can be removed and the energy of the neutrons coming out of the nucleus must then be considerably different from the primary proton energy; the neutron spectrum will then be strongly smeared out. Quantitative calculations of all these processes are difficult at the present time, and our remarks have only a qualitative character.

A new fact observed when changing the primary proton energy from 480 Mev[5] to 680 Mev is the presence of a second maximum in the neutron energy spectrum, located in the 100–400 Mev region. The presence of this peak is mainly due to neutrons emitted in the reactions with π-meson production on beryllium nuclei:

$$p + p \to \pi^+ + n + p; \quad p + n \to \pi^0 + n + p;$$

$$p + n \to \pi^+ + n + n.$$

The proposed explanation is confirmed by the following facts:

1. The total cross section for neutron yield (calculated per nucleon) from the mentioned reactions is close to the total elastic p–n scattering cross-section.

2. The position and the shape of the second maximum of the neutron energy spectrum for $\theta = 0°$ coincides within experimental accuracy with the position and shape of the maximum of the spectrum of the protons emitted in the elementary process $p + p \to \pi^+ + n + p$ at an angle close to 0°. This follows from the comparison of our data with the proton spectrum from the above-mentioned reaction, which was carefully measured[4] for an emission angle of 7°.

3. As the angle is changed to $\theta = 18°$, the second maximum shifts towards lower energies; the part of the neutrons in the low-energy region of the spectrum (from 100 to 400 Mev) decreases considerably with respect to the part of the neutrons in the high-energy region (from 400 to 680 Mev); this is in qualitative agreement with the proposed explanation for the nature of these neutrons.

4. For a proton energy of 480 Mev, when the cross section for π-meson production in nucleon-nucleon collision is not large, an analogous (second) maximum is not observed (within experimental accuracy)[5].

These data also permit to say that the mechanism of nuclear emission in π-meson production on nucleons bound in the nucleus retain in a definite way the character of free nucleon-nucleon collisions.

In conclusion, the authors express their gratitude to V. P. Dzhelepov for discussions and constant interest in this work.

---

[1] Iu. M. Kazarinov, Thesis; see also Iu. M. Kazarinov and Iu. N. Simonov, J. Exptl. Theoret. Phys. (U.S.S.R.) 31, 169 (1956), Soviet Physics JETP 4, 161 (1957).

[2] Meshcheriakov, Zrelov, Neganov, Vzorov and Shabudin, J. Exptl. Theoret. Phys. (U.S.S.R.) 31, 45 (1956), Soviet Physics, JETP 4, 60 (1957).

[3] Iu. D. Prokoshkin and G. N. Tentiukova, Prib. i Tekh. Eksperim. (Instruments and Measurement Engg.) 2, 18 (1957).

[4] Meshcheriakov, Neganov, Vzorov, Zrelov and Shabudin, Dokl. Akad. Nauk SSSR, 109, 499 (1956).

[5] Dzhelepov, Kazarinov, Golovin, Fliagin and Satarov, Izv. Akad. Nauk SSSR Ser. Fiz., 19, 573 (1955).

Translated by E. S. Troubetzkoy
211

Equilibrium Distribution of Nitrogen Ion Charges

V. S. NIKOLAEV, L. N. FATEEVA, I. S. DMITRIEV,
IA. A. TEPLOVA

(Submitted to JETP editor December 11, 1956)
J. Exptl. Theoret. Phys. (U.S.S.R.) 32, 965-968 (May, 1957)

The equilibrium distribution of charges in a beam of nitrogen ions after traversal of films of beryllium, celluloid, nickel and gold was determined in the energy range from 0.95 to 9.4 Mev. The dependence of the mean charge on the velocity was obtained. A small difference was detected in the charge distribution after traversal of various substances by the ions.

RECENTLY PUBLISHED PAPERS on the equilibrium distribution of nitrogen ion charges after passage through matter[1-4], contain no data for energies from 1 to 6 Mev. The present experiment deals with the measurement of the charge distribution in a nitrogen ion beam after its passage through plates of beryllium, celluloid, nickel and gold, in the energy range from 0.95 to 9.4 Mev.

$^{14}N^{+2}$, $^{14}N^{+3}$ and $^{14}N^{+4}$ ions were accelerated in the 72-cm cyclotron. The beam was focused at a distance of 8 meters from the cyclotron, traversed the target, and was then analyzed by a magnet which deflected the ions in a horizontal direction. The beam was limited, in front of the target, by a 1 mm slit. The metallic target was prepared by evaporating the metal in vacuum on celluloid films. The thickness of the celluloid film was ~ 10 $\mu g/cm^2$, The thickness of the beryllium or nickel layer was ~ 10 $\mu g/cm^2$, and that of gold was 15 and 30 $\mu g/cm^2$. The particles were registered by two consecutive proportional counters with an entrance window in the form of a horizontal 110×0.1 mm slit covered by a 70 $\mu g/cm^2$ celluloid film. Particles of all charges passed through the first counter which acted as a monitor; only particles with a given charge were allowed to pass through the second counter, through a movable partition between the counters. The position and the degree of separation of the charge groups were determined by the measurement of the dependence of the number of pulses in the second counter on the position of the 2 mm slit between the counters (Fig. 1). When measuring the intensity of the charge groups, the slit between the counters was widened to 14 – 20 mm in order that the second counter register the entire given charge group.

The error in the relative intensity Φ_i of the charge groups with $\Phi_i \geqslant 0.02$ was caused, for large velocities, by the small differences in the thicknesses of the entrance slit – in front of the first counter – and by the inaccuracy in placing this slit in the direction of the beam's deflection; this error amounted to 2%. For small velocities, the error was principally due to the incomplete separation of the charge groups because of scattering in the target and amounted to 6 – 8%. This is related to the fact that there were no diaphragms between the target and the entrance slit of the counter to limit the beam in the horizontal plane. In order to reduce the errors in the comparison of the equilibrium charge distribution after traversal of different elements, targets were prepared with different elements on the opposite side of the film. By turning the target, it was possible to compare independently the distribution after traversal of Be and celluloid, celluloid and Au, or Au and Ni. With this method, the inaccuracy was due entirely to the statistical error which, in almost all the cases, was considerably smaller than the errors mentioned above.

The velocity of the particles was calculated from the intensity of the magnetic field of the focusing magnet, which was calibrated using protons and deuterons of known energy. The error in the determination of the ion velocity, taking into account the energy loss in the target, did not exceed 1.5 – 2%.

The results of the measurements of equilibrium charge distribution in a beam after the ions traversed a celluloid film are shown on Fig. 2 for different velocities v. Fig. 3 shows the dependence of the intensity ratio Φ_{i+1}/Φ_i of two neighboring ion groups with charges $i + 1$ and i on the particle velocities. As can be seen from the graph, our results for large velocities agree very well with the results of the measurement of charge distribution of a beam of ions passing through formvar (polyvinyl of formal), for energies above 6.2 Mev[1]

On the basis of the obtained data, one can conclude that Φ_{i+1}/Φ_i is proportional to v^{k_i}, where k_i

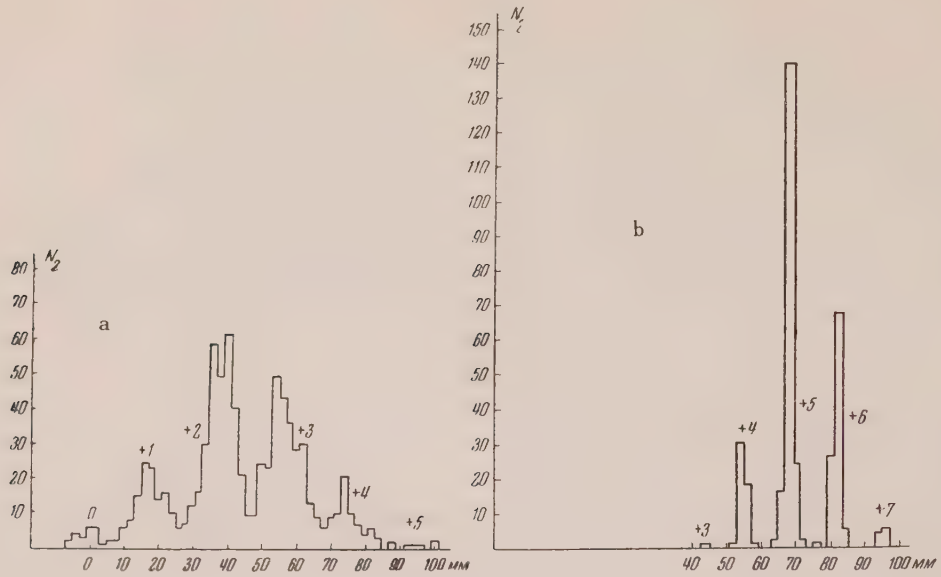

FIG. 1. Dependence of the number of pulses N_2 in the second counter on the position of the 2-mm slit between the counters: a – $v = 3.6 \times 10^8$; b – $v = 11.4 \times 10^8$ cm/sec.

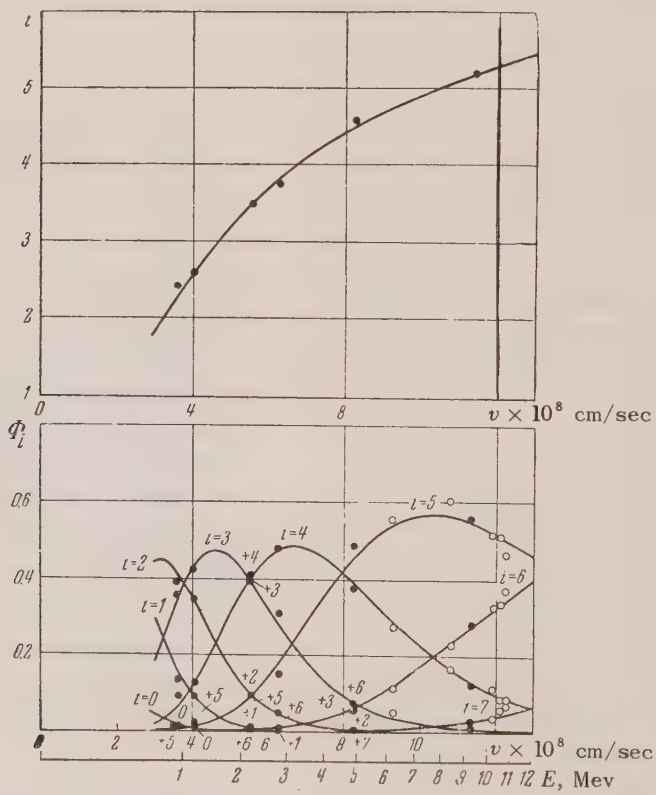

FIG. 2. Equilibrium distribution and mean charge of nitrogen ions after passing through: ●—celluloid (our data) and ○—formvar (Ref. 1).

increases in general with i (see Fig. 3). The equilibrium distribution and the mean charge were computed in the energy range from 3×10^8 to 13×10^8 cm/sec from the most probable values of k_i (see solid lines of Fig. 2).

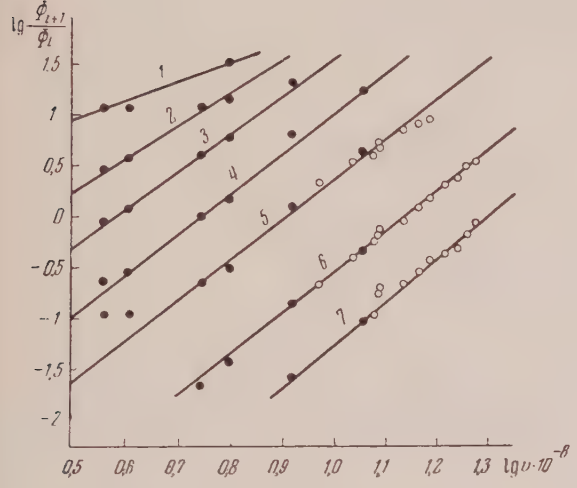

FIG. 3. Dependence of the ratio Φ_{i+1}/Φ_i on the velocity after the passage of nitrogen ions through: ● — celluloid (our data) and ○ — formvar (Ref. 1).
1 — Φ_1/Φ_0, $k_0 = 2 \pm 1$; *2* — Φ_2/Φ_1, $k_1 = 3{,}3 \pm 0{,}3$; *3* — Φ_3/Φ_2, $k_2 = 3{,}8 \pm 0{,}2$; *4* — Φ_4/Φ_3, $k_3 = 4{,}0 \pm 0{,}2$; *5* — Φ_5/Φ_4, $k_4 = 4{,}0 \pm 0{,}2$; *6* — Φ_6/Φ_5, $k_5 = 4{,}0 \pm 0{,}2$; *7* — Φ_7/Φ_6, $k_6 = 4{,}3 \pm 0{,}2$

When investigating the mean ion charge, one sometimes uses the coefficients γ_1 and γ_2 introduced by Brunings, Knipp and Teller, which equal respectively the ratio of the velocity of the least bound and of the most remote electrons of the ion to the velocity of the ion. If the above mentioned velocities are computed from the Thomas-Fermi model, it follows from the obtained mean value for the nitrogen ion charge that, as the parameter $v/v_0 Z^{2/3}$ (where $v_0 = e^2/\hbar$, Z — nuclear charge) is varied from 0.5 to 1.5, γ_1 changes approximately from 1.3 to 0.9; if the velocity is increased further γ_1 increases again[1]. As far as γ_2 is concerned, it is of the order of 0.6 in the mentioned velocity region and increases by about 10% as the velocity is increased. As the velocity is further increased, γ_2 approaches the value of γ_1, *i.e.*, it rises sharply.

The equilibrium charge distribution after the nitrogen ions pass through different elements turns out to be somewhat different. A decrease of the mean charge $\bar{i}$ with increasing atomic number is observed in all the cases; in comparison with the celluloid film, the mean charge after traversal of Be is bigger by about 0.1 – 0.3%, whereas after passing through Ni and Au, it is smaller by 0.5% and 1 – 2% respectively, with the statistical error of $\bar{i}$ being approximately 0.1%.

In the experiments using targets maintained in vacuum for a longer time, the observed difference is smaller; this is probably due to the thin film of oil from the diffusion pump forming on the surface of the target. One also observes a certain difference in the charge distribution with the same mean charge. In those cases where these differences exceed the statistical errors, the charge distribution of the beam after the ions pass through lighter elements turns out to be smoother, *i.e.*, the relative intensity Φ_i of the most probable states decreases, while for the low-intensity group Φ_i increases. This law shows up most clearly in the comparison of the charge distributions of a nitrogen ion beam passing through beryllium and celluloid at large velocities (Fig. 4). For low velocities, the differences in the distribution are considerably smaller and do not exceed the statistical errors. The smoother charge distribution in a nitrogen ion beam passing through beryllium corresponds to a smaller value of the exponent k_i for beryllium compared to the value of k_i for a celluloid plate. The difference between the exponents for beryllium and celluloid amounts to 0.1 – 0.2.

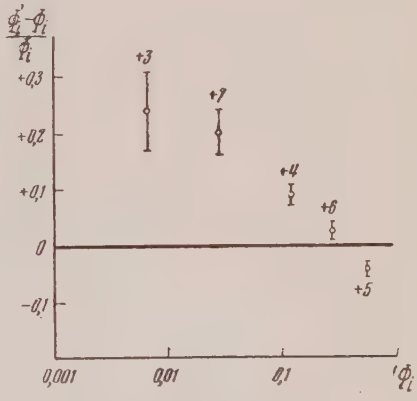

FIG. 4. Difference between the charge distribution Φ_i' after passage of nitrogen ions through beryllium and the distribution Φ_i after passage through celluloid at $v = 11.4 \times 10^8$ cm/sec. The value i of the charge is indicated close to each point.

In conclusion, we express our deep gratitude to C. C. Vasil'ev who initiated the work on multiple charge ions as well as to the cyclotron group, es-

pecially to G. V. Kosheliaev, A. A. Danilov and V. P. Khlapov.

[1] Reynolds, Wyly and Zucker, Phys. Rev. 98, 474 (1954).

[2] K. G. Stephens and D. Walker, Proc. Roy. Soc. (London), 229, 376 (1955).

[3] Stier, Barnett and Evans, Phys. Rev. 96, 973 (1954).

[4] Korsunskii, Pivovar, Markus and Levitan, Dokl. Akad. Nauk SSSR 103, 399 (1955).

[5] Brunings, Knipp and Teller, Phys. Rev. 60, 657 (1941).

Translated by E. S. Troubetzkoy
212

SOVIET PHYSICS JETP VOLUME 5, NUMBER 5 DECEMBER, 1957

Multiple Electron Production in a High Energy Electron-Photon Shower

A. A. VARFOLOMEEV, R. I. GERASIMOVA, V. A. TUMANIAN

(Submitted to the JETP editor December 24, 1956)
J. Exptl. Theoret. Phys. (U.S.S.R.) 32, 969-973 (May, 1957)

An unusual electron-photon shower produced by an electron of $> 10^{11}$ ev initial energy has been detected in a stack of emulsion layers without backing, exposed in the stratosphere. Experimental data obtained on the basis of a study of this shower are presented which indicate the occurrence of three cases of simultaneous formation of four electrons (two electron-positron pairs).

THE INVESTIGATION of electron-photon showers by means of nuclear emulsions exposed in the stratosphere has considerable interest in view of the possibility of elucidating the details of high energy electromagnetic processes. Despite some contradictions in the existing experimental data on certain aspects of electron-photon showers, one can definitely say that anomalies exist with respect to accepted theoretical views. Among these one can mention problems such as the occurrence of multiphoton showers[1] and in connection with this, the question of the source of closely correlated gamma rays; the bremsstrahlung spectrum and its possible deviations from theoretical[2]. Indications[3] also exist that the cross section for electron-positron pair formation directly by the electron without intermediaries exceeds considerably the theoretical value at energies greater than 10^{10} ev. These conclusions cannot be considered final, however, because in certain other experiments similar effects have not been found[4]. The solutions to these problems have great significance, not only for quantum electrodynamics, but as noted by Heisenberg[5], for quantum field theory in general.

Examples of multiple formation of electrons detected in an electron-photon shower are described below. Information on similar cases, together with data on pair formation by electrons, will permit the evaluation of the role (at higher energies) of higher-order processes than pair formation by photons.

GENERAL CHARACTERISTICS OF SHOWERS. EXPERIMENTAL DATA ON CORRELATED PAIRS

During a systematic investigation of electron-photon showers, using stacked emulsions without backing exposed in the stratosphere, an unusual electron-photon shower was discovered.

The emulsion stack consisted of 150 layers of type R, having a thickness of 400 μ and a diameter of 10 cm. Irradiation took place at an altitude of 20–24 km for about 10 hours. Grain density in the minimum ionizing paths was 37 grains (or 31 conglomerates) per 100 μ.

The shower was initiated by a single electron entering the stack from outside. In each emulsion layer the electron travelled ~ 0.5 cm, its total path in the emulsion was 8 cm. On the first two radiation lengths from its point of entry into the stack are registered 21 secondary electron-positron pairs, of which 12 had energies $E_i > 10^8$ ev. The most probable value of the primary electron's energy, deter-

mined from the cascade curve, turned out to be $E_0 = (0.6 - 2) \cdot 10^{12}$ ev.

The shower under consideration had the following peculiarity: six of the electron pairs formed were pairwise correlated. The appearance of two pairs in each case resembled, if one may so express oneself, a "quadrident": one heavy track beginning not far from the axis of the shower, gradually thickening and spreading out, and splitting into four separate tracks. The latter were in every case ascribed to electrons (positrons) because of the characteristic electromagnetic processes occurring along them. The following table gives the coordinates of the vertices of the quadridents (R–distance from the primary electron track in microns, t–distance from primary electron entrance point into stack, in millimeters) and the energies of the individual electrons, determined by the relative multiple scattering with an accuracy of 30–50%.

t, mm	R, μ	E_1, ev	E_2, ev	E_3, ev	E_4, ev
3.94	0.5	$2.1 \cdot 10^3$	$0.8 \cdot 10^9$	$1.7 \cdot 10^9$	$2.5 \cdot 10^9$
31.02	0.4	$2.0 \cdot 10^8$	$2.7 \cdot 10^8$	$3.2 \cdot 10^9$	$\sim 10^{10}$
40.51	2.0	$1.7 \cdot 10^8$	$1 \cdot 10^9$	$2.0 \cdot 10^9$	$3 \cdot 10^9$

Careful measurements of ionization were made along the quadrident tracks. Basically, a grain counting method was used. In the first two cases the total density of the primary and quadrident electron tracks was measured, since the distances between them were very small. In Fig. 1 – 3 the black dots indicate the results of measurements of ionization along the quadrident tracks, while the triangles denote the results of grain counting along the tracks of several relativistic electrons (evidently from the same shower). Because a diminution in grain density is observed near the emulsion surface, (sections $a'b'$ in Fig. 1 and $a''b''$ in Fig. 2) corrections have been introduced in the measurements (circles). The errors indicated are statistical.

As an additional check on the measurements, the graphic-photometric method [6] was used to measure track density (contours of the track grains, magnified 5500 times were traced on a fixed X-ray film and filled in with india ink, after which they were read with a photometer). The results obtained for the first quadrident are shown in Fig. 4. As can be seen from Figs. 1 and 4, the results of both methods are in complete agreement. In all three cases one observes the following pattern of change in ionization by the quadrident electrons: a jump to double (or somewhat greater) the value, a gradual increase, and a transition to a fourfold ionization $4I_0$. Figure 5 is a microphotograph of the third quadrident (composite).

INTERPRETATION

Two different interpretations of the appearance of the quadridents are possible: 1) the pairs were formed sequentially at small distances from each other; 2) four electrons were formed simultaneously. From a detailed examination of the structure of the tracks and of the ionization curves, it follows that the distance between the points of sequential formation of the pairs could not exceed 300–500 μ. From this one can estimate the probability w_1 of sequential pair formation (first possibility). From the number of pairs with energy $> 10^8$ ev discovered in the shower within a radius $R \leqslant 2$ μ, and assuming in first approximation that they are formed with equal probability volume-wise, one can obtain a value $w_1 \sim 10^{-7}$. (It was considered that in the plane perpendicular to the shower axis the coordinates of the pair formation points could not differ by more than 0.2–0.5 μ.) If one assumes the second pair to be formed by the bremsstrahlung from the first pair, then taking into account the conversion and radiation lengths in emulsion, the probability becomes $w_1 \sim 10^{-9}$. One must observe that consideration of all the electron-photon showers registered in the emulsion (in agreement with published data) cannot lead to a value $w_1 > 10^{-4}$. Furthermore, with sequential pair formation one ought to observe stepwise changes in ionization along the quadrident tracks.

The quadridents are therefore difficult to explain as sequentially formed pairs. This leaves the second possibility – the multiple process or simultaneous formation of four electrons. In this case the gradual increase in ionization can be primarily attributed to mutual shielding of the electrons and positrons at close distances[2,7], an effect discovered earlier in electron-positron pairs of energy

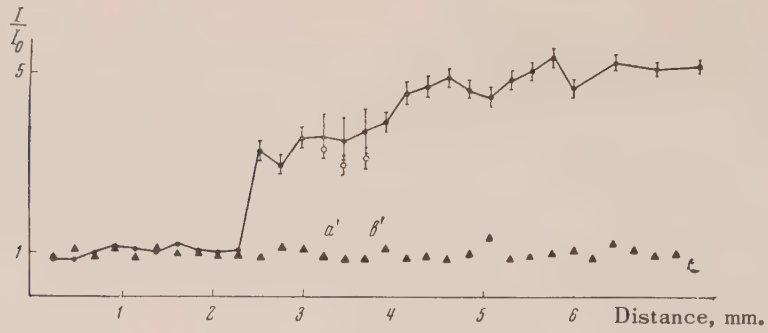

FIG. 1.

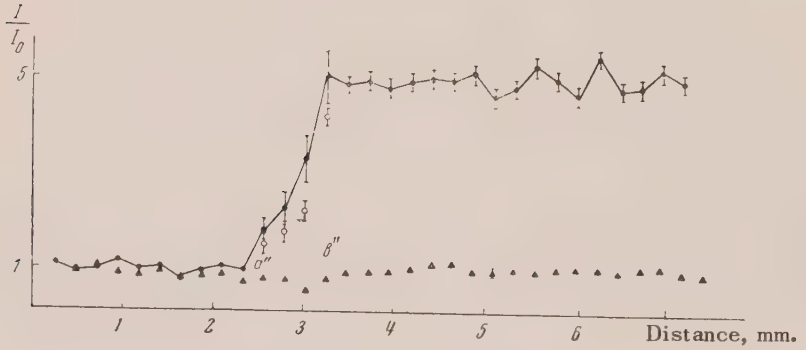

FIG. 2

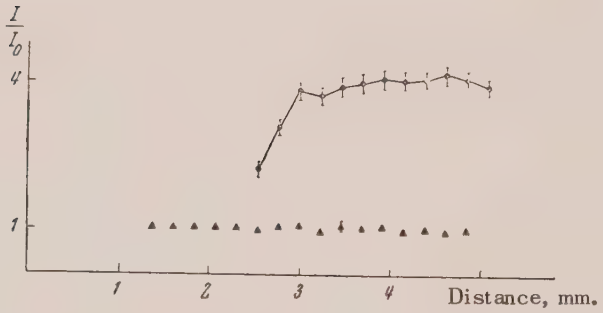

FIG. 3.

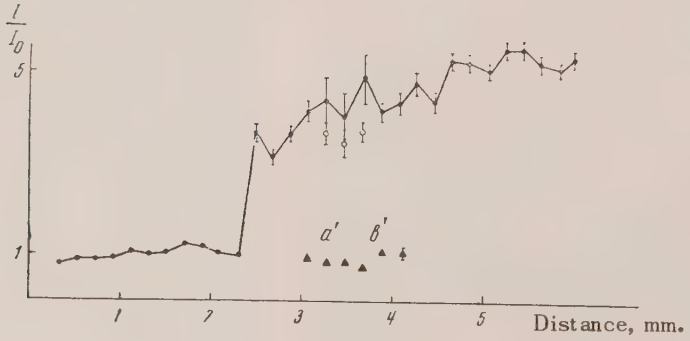

FIG. 4.

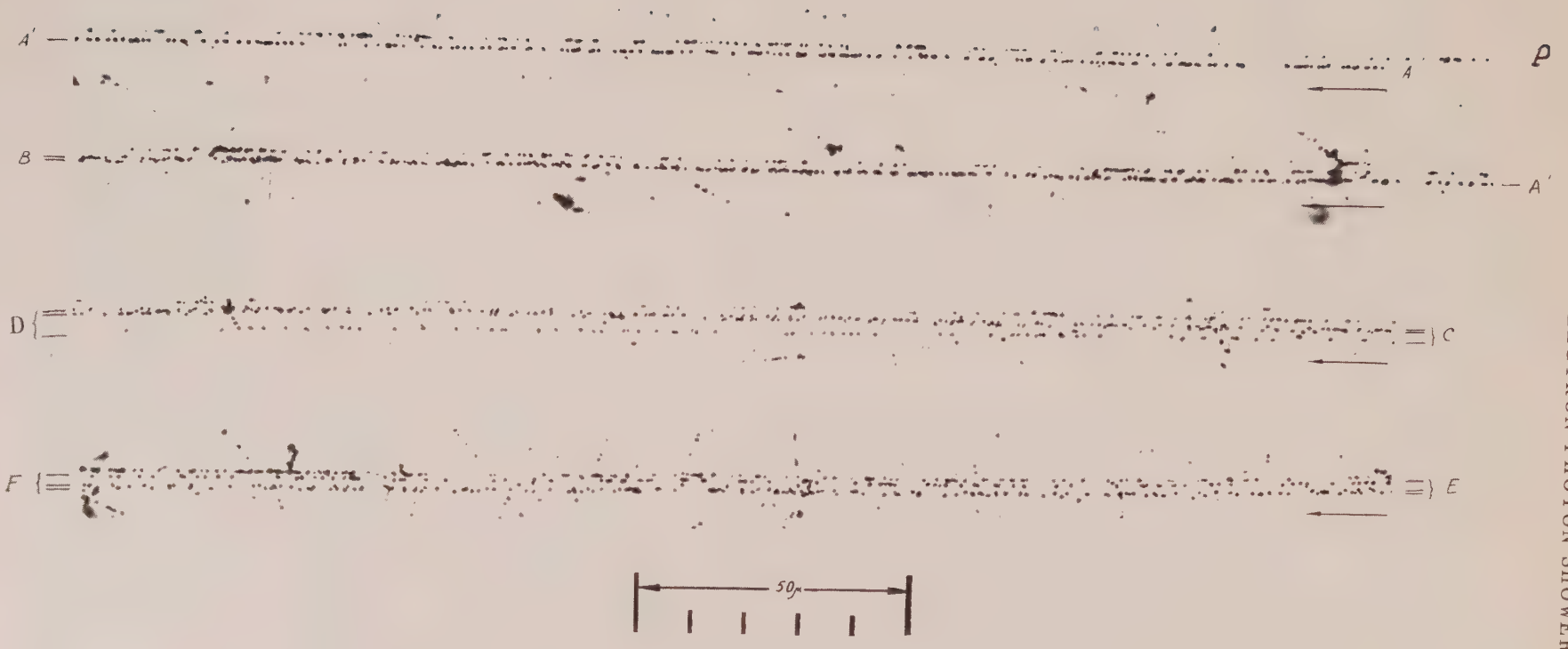

FIG. 5. Microphotograph of the tracks of two electron-positron pairs formed at a distance $t = 40.51$ mm and $R = 2\mu$ (third quadrident). AB – initial segment of the quadrident; the splitting into two separate tracks may be seen. CD – segment at a distance 3.2 – 4.1 mm from the point of formation of the pairs; the quadrident track consists of three separate tracks, of which the lower one deviates from the track axis. EF – segment at a distance 6.7 – 7.6 mm; the body of the quadrident track consists of three separate electron tracks; on this segment the fourth electron had deviated and is not seen on the photograph. The track of the primary electron P is seen alongside the quadrident tracks.

$10^{10} - 10^{11}$ ev.[8] In the second and third quadrident the track sections along which the ionization increases are approximately the same as those of the pairs, and in the first quadrident considerably longer.

DISCUSSION

If one notes that up to the present time about 150 electron-photon showers have been examined, and that on the average some 15 – 20 pairs have been noted in each, then the appearance of the three quadridents corresponds to the evaluation of the relative probability of simultaneous two-pair production performed by Hooper and King[9] on the basis of two quadridents found by them among $\sim$ 1400 pairs. Yet the fact that all three quadridents were formed in a single shower, with energy $E_0 > 10^{11}$ ev, and that in each case the total energy of the quadrident electrons exceeded $5 \cdot 10^9$ ev, is remarkable. Moreover, the energy estimates are only lower limits to the actual values. The question presents itself whether quadridents are not formed by gammas with relatively greater cross section at higher energies?

According to Heitler's calculation[10], simultaneous formation of two pairs is $\sim$ 137 or even 137π times less frequent than ordinary pair formation.* If this relationship is correct, one would expect three quadridents approximately for every $(137/10)^3 \approx 2500$ showers with energy $E_0 \gtrsim 10^{11}$ ev. But up till now, according to published data, the detailed structure of the first two radiation lengths has been examined in not more than $\sim$ 50 showers with energy $E_0 \gtrsim 10^{11}$ ev. In addition, in a number of showers (notably at higher energy) the tracks of pairs were situated close to the shower axis, forming a continuous dense track and obscuring the possible occurrence of multiple electron production.

Hence the appearance of three quadridents in a single shower is something of an indication that multiple electromagnetic processes play an increasing role at higher energies. Of course the data from this shower are insufficient for any kind of quantitative deduction. But roughly speaking, the simplest explanation of this event is that the multiple process is 2 – 3 times more probable than theory predicts.

In conclusion the authors thank I. I. Gurevich for his interest in the work and for his valuable advice, M. L. Ter-Mikaelian, I. I. Gol'dman, and L. A. Maksimov for evaluation of the results, and L. A. Makar'in, A. S. Romantsev, and S. A. Chuev for help with the measurements.

*More accurate calculations lead to a value of the relative probability $(1/137)^2 \log (K/mc^2)$, where K is the gamma energy, mc^2 the electron rest energy.

[1] Schein, Haskin, and Glasser, Phys. Rev. **95**, 855 (1954); M. Koshiba and M. F. Kaplon, Phys. Rev. **100**, 327 (1955); Debenedetti, Garelli, Tallone, Vigone, and Wataghin, Nuovo cimento **3**, 226 (1956).

[2] Miesowicz, Stanisz, and Wolter, Bull. Acad. Polon. Sci. Cl. 3, 4, 811 (1956); W. Wolter and M. Miesowicz, Nuovo cimento **4**, 648 (1956).

[3] M. Koshiba and M. F. Kaplon, Phys. Rev. **97**, 193 (1955).

[4] Debenedetti, Garelli, Tallone, and Vigone, Nuovo cimento **4**, 1151 (1956); Brisbout, Dahanayke, Engler, and Perkins, Nuovo cimento **4**, 1496 (1956).

[5] W. Heisenberg, Usp. Fiz. Nauk **60**, 413 (1956).

[6] Varfolomeev, Gerasimova, and Karpova, Dokl. Akad. Nauk SSSR **110**, 758 (1956).

[7] A. E. Chudakov, Izv. Akad. Nauk SSSR, Phys. Ser. **19**, 651 (1955).

[8] D. H. Perkins, Phil. Mag. **46**, 1146 (1955).

[9] J. E. Hooper and D. T. King, Phil. Mag. **41**, 1194 (1950).

[10] W. Heitler, *The Quantum Theory of Radiation* (Oxford, 1954) 3rd ed., p. 228.

Translated by C. R. Lubitz
213

On the Interaction Between Lithium Ions and Matter

IA. A. TEPLOVA, I. S. DMITRIEV, V. S. NIKOLAEV, AND L. N. FATEEVA

(Submitted to JETP editor December 25, 1956)
J. Exptl. Theoret. Phys. (U.S.S.R.) 32, 974-978 (May, 1957).

The following quantities have been measured for Li^7 ions possessing energies between 0.5 and 5 Mev: specific ionization in hydrogen and air, ranges in hydrogen, air and NIKFI Ia-2 photographic emulsions, and the equilibrium charge distribution after passage through a celluloid film.

AT THE PRESENT TIME there exists only unsystematic evidence about the drag of Li ions in various environments[1-11]. Absence of full data about the average effective charge of Li ions makes it difficult to calculate the magnitude of their characteristic electronic interactions with matter.

In this work, specific ionization in hydrogen and air were measured for Li^7 ions. The equilibrium charge distribution after passage through a celluloid film, and ranges in hydrogen, air and photographic emulsion NIKFI-Ia-2 were also measured. The energy of Li^7 ions, accelerated in 72-cm cyclotron, was variable from .5 to 5 Mev. The velocity of the ions in the beam was determined from the intensity of the focusing magnetic field, calibrated by α-particles and deuterons of known energies. The error in velocity determination did not exceed 2%.

The focused beam of ions was passed through a retarding chamber 240 mm long after a passage through a system of collimating diaphragms and celluloid film 120 $\mu g/cm^2$ thick was used to measure the specific ionization. The pressure in the chamber was chosen so that the range of ions was fully within the chamber. The ions were registered by a proportional counter 6 mm thick, whose pulses were measured visually on the screen of a cathode-ray oscilloscope and the film of a loop oscillograph. The dependence of the number of pulses on the range of particles can be measured by moving the counter along the beam. The specific ionization is obtained in relative units. The curves thus obtained for the specific ionization are normalized according to the initial energy of the particles, assuming that the energy loss is proportional to the ionization. Figure 1 shows the results of the measurements (the solid curves are obtained by averaging several series of measurements). The extreme error in the specific ionization for ion velocities $v \geq 3 \times 10^8$ cm/sec did not exceed 9% in air and 13% in hydrogen.

The ranges of Li^7 ions of various velocities were measured simultaneously with the specific ionization. The points on Fig. 2 represent the values obtained for the ranges. These results agree within the limits of experimental accuracy with the solid line obtained by integration of the corresponding specific ionization curves shown in Fig. 1-A.

The apparatus described by Nikolaev[12] was used to measure the equilibrium charge distribution. Celluloid films approximately 10 and 20 $\mu g/cm^2$ thick were used, and it became evident during the experiment that the equilibrium was reached with film thickness of only 10 $\mu g/cm^2$. The results of the measurements of the equilibrium distribution (Fig. 3) show that for $v \leq 8 \times 10^8$ cm/sec the ratio of the intensities of the neighboring groups Φ_{i+1}/Φ_i with charges $i + 1$ and i is proportional to v^{k_i}, where $k_i = 2.7$, 3.9, and 5.1 for $i = 1$, 2, and 3 repectively. If at the same time we substitute Φ_{i+1}/Φ_i in the region $v > 8 \times 10^8$ cm/sec, then k_i can be decreased at most to 2.9 for $i = 2$ and to 3.4 for $i = 3$. The equilibrium distribution and the average charge $\bar{i}$ calculated by using such a dependence of Φ_{i+1}/Φ_i on v, are shown solid in Fig. 3. The experimental values Φ_i and $\bar{i}$, shown in the same figure, are determined with an accuracy of $\pm 2\%$ for Φ_i and 0.5% for $\bar{i}$. With the resulting velocity dependence of the average charge one can hardly expect the breaks in the specific ionization curve, on the order of 20%, discovered by Kuznetzev *et al.*[8] and interpreted as discrete charge redistributions of the Li ions at definite velocities. (Such breaks were not found in our measurements of the specific ionization in air and hydrogen.)

The ranges of Li^7 ions obtained in the photographic NIKFI-Ia-2 emulsion and shown in Fig. 4 agreed with the results of range measurements in the Ilford C-2 emulsion reported previously[3-7,11] (the data for Li^6 and Li^8 ions were recalculated for Li^7 ions).

The Locher and Stoll[9] range data for the Kodak NTA emulsion were apparently somewhat lower since in the process of developing the authors chemically lifted from the emulsion surface the tracks of singly charged ions, thus possibly affecting the length of the measured tracks. The range data obtained in Refs. 8 and 9 do not agree with the results of other experiments[3-7,11] and with our data. We sought to explain the velocity dependence of the range by using our experimental data on the charge of Li^7 ions after passage through a celluloid film, since practically i does not depend on the material[12-14] in hard materials. The range was calculated from

$$R = \int mvdv/\langle i\rangle^2 f(v),$$

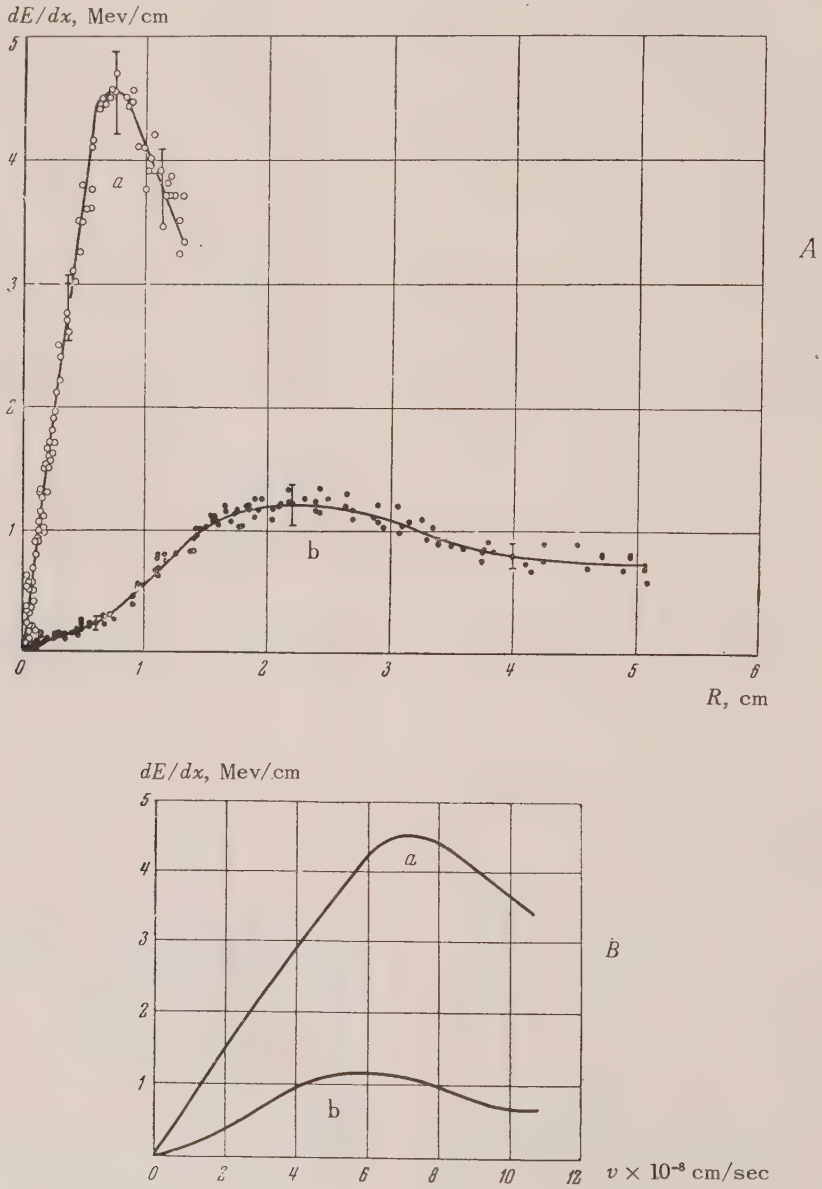

FIG. 1. Dependence of the energy loss of Li^7 ions in Mev per cm: A—on the residual range; B—on the velocity; a—in air, b—in hydrogen (760 mm Hg).

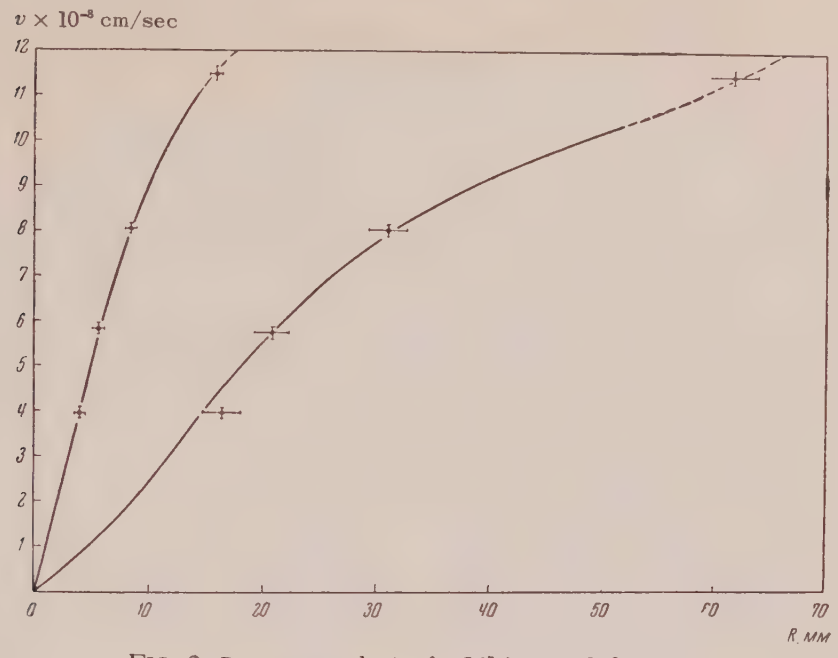

FIG. 2. Range *vs.* velocity for Li^7 ions at 760 mm Hg: *a*–in air, *b*–in hydrogen.

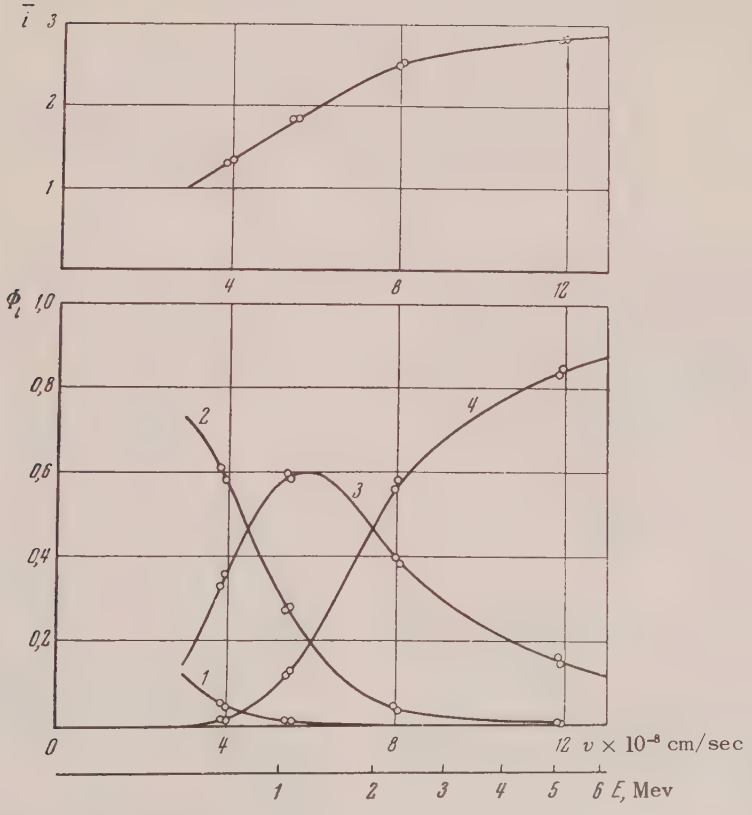

FIG. 3. Equilibrium charge distribution Φ_i and average charge $\bar{i}$ of Li^7 ions after passage through a celluloid film. 1 – $i=0$, 2 – $i=1$, 3 – $i=2$, 4 – $i=3$.

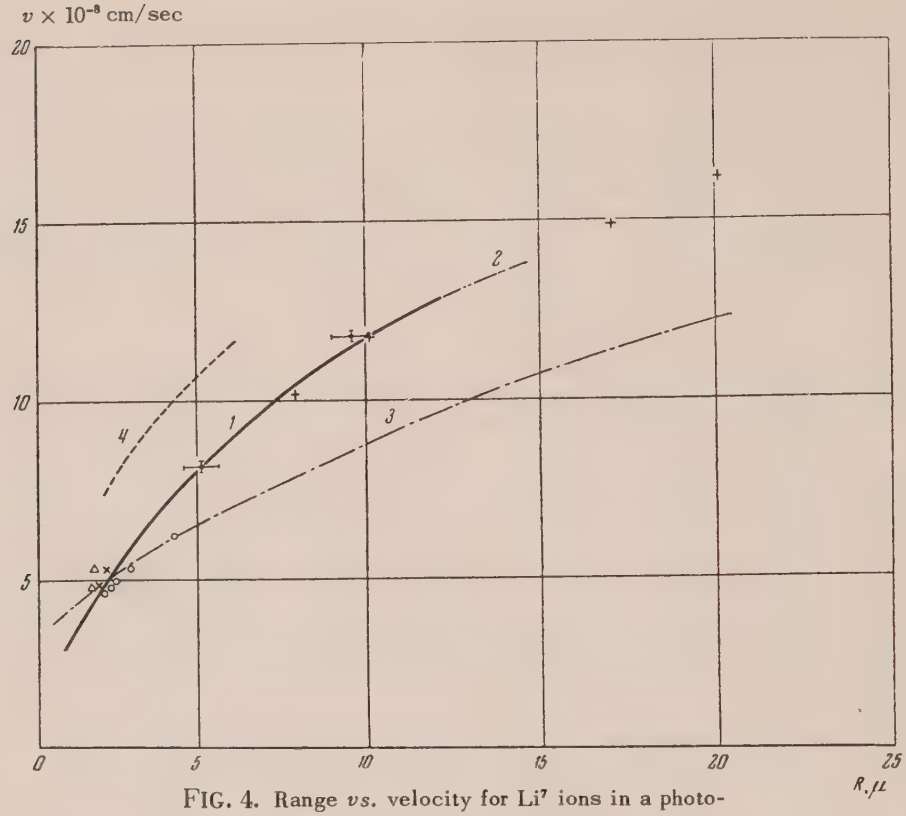

FIG. 4. Range *vs.* velocity for Li^7 ions in a photographic emulsion. Curve 1—calculated curve. The remaining curves and points correspond to the data from the following: 2—Ref. 3, 3—Ref. 8, 4—Ref. 9, +—Ref. 4, o—Ref. 5, △—Ref. 6, ×—Ref. 7, ●—our data.

where m is the mass of the ion, $f(v) = 1.04\, v^{-1.15}$ Mev/μ (*cf.* Ref. 3), $\langle \overline{i} \rangle$ is the mean-square charge. Since $\overline{i}$ is not known for low velocities, the calculated curve was compared with the experimental data on ranges for $v = 8.1 \times 10^8$ cm/sec. It is evident from Fig. 4 that the calculated curve (solid curve) agrees both with our results and with the data obtained by Livesey[3], Barkas[4], and others.

In conclusion the authors express their gratitude to the cyclotron group headed by G. V. Kosheliaev.

[1] H. A. Wilcox, Phys. Rev. 74, 1743 (1948).
[2] L. Rosario, Phys. Rev. 74, 304, (1948).
[3] D. L. Livesey, Can. Journ. Res. 34, 261 (1956).
[4] W. H. Barkas, Phys. Rev. 89, 1019 (1953).
[5] Neuendorfer, Inglis, and Hanna, Phys. Rev. 81, 75 (1951).
[6] P. Cuer, J. P. Lonchamp, Compt. Rend. 232, 1824 (1951).
[7] H. Faraggi, Ann. Physik 6, 325 (1951).
[8] Kuznetzov, Lukirskii, and Perfilov, Dokl. Akad, Nauk SSSR 100, 655 (1955).
[9] K. Locher and P. Stoll, Phys. Rev. 90, 164 (1953).
[10] S. Devons and J. H. Towle, Proc. Phys. Soc. 69, 345 (1956).
[11] A. H. Armstrong and G. M. Frye, Phys. Rev. 103, 335 (1956).
[12] V. S. Nikolaev *et al.*, J. Exptl. Theoret. Phys. (U.S.S.R.) this issue, p. 965, Soviet Physics JETP 5, 789 (1957).
[13] T. Hall, Phys. Rev. 79, 504 (1950).
[14] G. A. Dissanaike, Phil. Mag. 44, 1051 (1953).

Translated by M. J. Stevenson

214

Soft Gamma Rays Emitted by Nuclei in the Capture of Thermal Neutrons

I. V. ESTULIN, L. F. KALINKIN, A. S. MELIORANSKII
Moscow State University

(Submitted to JETP editor December 26, 1956)
J. Exptl. Theoret. Phys. (U.S.S.R.) 32, 979-992 (May, 1957)

A luminescent spectrometer was used to measure the energy and absolute intensities of gamma rays emitted by Co^{59}, Rh^{103}, I^{127}, Sm^{149}, Au^{197} and Hg^{199} nuclei capturing thermal neutrons. It is shown that the detected gamma lines which lie in the 50 – 500 kev energy range can be ascribed to transitions from the lowest excited states of the investigated nuclei.

DURING THE LAST FEW YEARS many investigations were made of gamma rays emitted by nuclei in the capture of thermal neutrons. Particularly valuable measurements were made with magnetic spectrometers by two independent groups of scientists in the U.S.S.R.[1] and Canada[2]. Both groups obtained similar results. However, the softest gamma rays emitted in the (n, γ) reaction have not been studied extensively. The energy data for soft-gamma lines given by previous experimenters[3-5] require remeasurement; the intensity of the soft gamma quanta have not been determined.

In the present work a single crystal luminescent spectrometer was used to measure the energy and the absolute yields of gamma quanta in the energy interval of 50–500 kev, emitted by nuclei in the capture of thermal neutrons. Several preliminary results have been reported previously[6].

1. EXPERIMENTAL GEOMETRY AND LUMINESCENT SPECTROMETER

An experimental physical heavy water reactor[7] was used as a neutron source. A neutron collimator consisting of thick layers of B_4C and Pb was placed in a horizontal channel within the reactor shield. A 12 cm thick Bi shield to prevent the gamma rays from the reactor from entering the collimation channel was affixed close to the reactor vessel. The intensity of the collimated beam of thermal neutrons brought out of the reactor was $\sim 10^7$ neutrons/cm^2 sec.

The geometry of the experiment is shown in Fig. 1. In most of the experiments target *1* had the shape of an ellipse with semiaxes $a = 18$ mm and $b = 10$ mm. It was placed on an aluminum stand at an angle α relative to the neutron beam. The target was placed above a duct *3* in the lead which was used as a collimator of gamma rays (the length of the duct was 75 mm and its diameter 10 and 15 mm). To protect the NaI(Tl) crystal *4* from thermal neutrons scattered from the target, the opening aperture of the gamma ray collimator was covered by B_4C *2* 0.3 g/cm^2 thick. In the experiments with Co, Rh and Au metallic targets were used. In the studies of powdered materials, such material was contained within aluminum foil .07 mm thick. The aluminum foil did not emit an observable intensity of gamma rays when placed in the neutron beam.

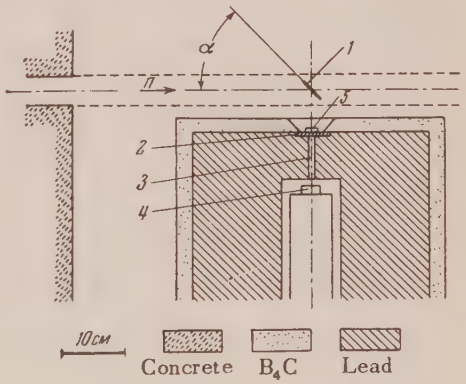

FIG. 1. Diagram of the apparatus: *1* – target, *2* – B_4C shield, *3* – γ-ray collimation channel, *4* – NaI(Tl) crystal, *5* – lead filter.

The luminescent spectrometer employed a type S photoelectric multiplier and a NaI(Tl) crystal of cylindrical shape 9 mm thick and 28 mm in diameter. The crystal was packed in a reflector made of MgO. The pulses from the photo multiplier tube had an amplitude 0.5 V and were amplified to 100 V and analyzed by a single channel amplitude analyzer with dead time of 3 μsec.

The spectrometer characteristics (resolution, the line shape and the absolute efficiency) were studied as a function of γ-quanta energy by measurements on Mo^{99}, Hg^{203}, $B^{10}(n, \alpha)Li^{7*}$, Cu^{64}, Cs^{137}, and Zn^{65}. The geometry of these measurements was similar to that in measurements of the energy and intensity of γ-rays in the (n, γ) reaction. The dependence of the resolution of the spectrometer η on the energy of the γ-rays E_γ is shown in Fig. 2. Fig. 3 shows the spectrum of pulses from γ-rays emitted in the $B^{10}(n, \alpha)Li^{7*}$ reaction (the target in the neutron beam was made of B_4C). A photopeak for γ-rays at 482 kev (peak *1*) is particularly clearly evident. This peak corresponds to the maximum energy distribution of Compton electrons, while peaks *2* originates in the apparatus and are due to γ-rays passing through the NaI(Tl) crystal and scattered back in the apparatus. Peak *3* is due to the characteristic emission of lead and thus also due to the apparatus. Analogous spectra were obtained with other sources of γ-rays, but the position

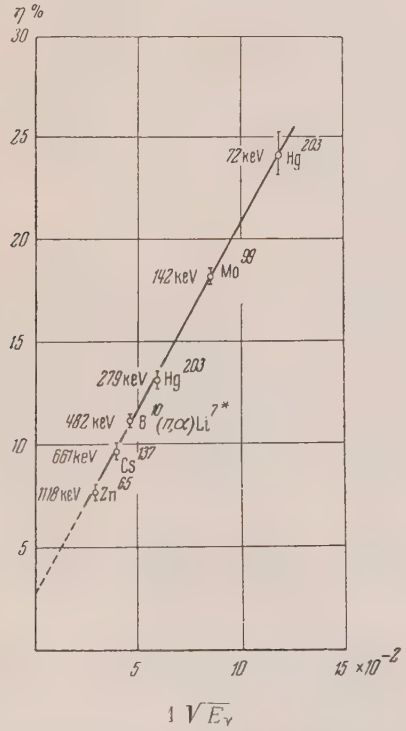

FIG. 2. Dependence of spectrometer resolving power η (in %) on the energy of the γ-rays (E_γ is in kev).

and the relative height of the peaks *1*, *2*, *3* and also of the photopeak were substantially dependent on the γ-ray energy. Graphs prepared from the experimental data allowed determination of the remaining part of the spectra from the position of the photopeak. As a result it turned out to be possible to interpret the complex spectrum of pulses generated by the γ-rays, by separating parts of the spectra related to individual gamma lines. The area of the photopeak S_p was determined most accurately. By a photopeak in a spectrum of monochromatic γ-rays we understand a peak whose position corresponds to pulses of maximum amplitude (*cf.* Fig. 3).

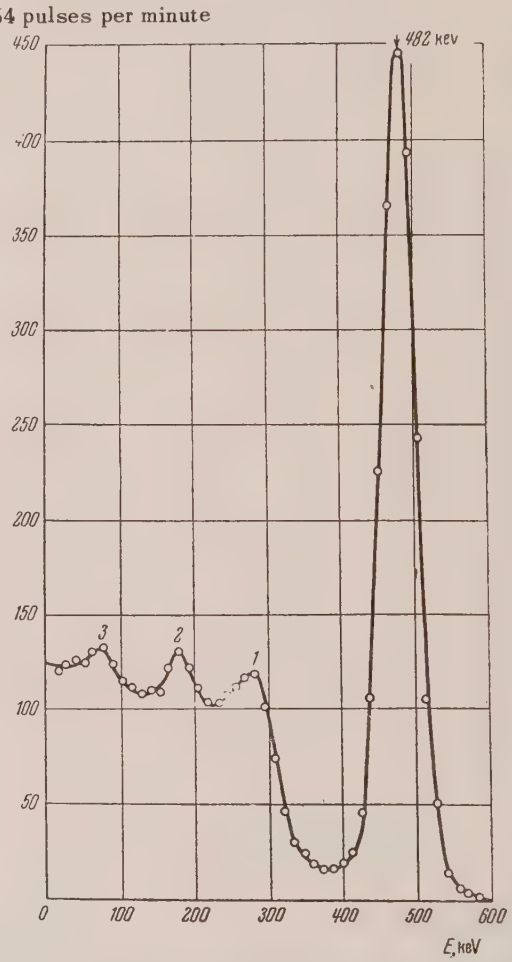

FIG. 3. Gamma ray spectrum for reaction $B^{10}(n, \alpha)Li^{7*}$

We introduce the absolute efficiency ε_p of the spectrometer for photopeaks:

$$\varepsilon_p = \frac{S_p}{S_t}(1 - e^{-\mu x}) \qquad (1)$$

where μ is the absorption coefficient of γ-rays in the crystal NaI(Tl), x is the thickness of the crystal, S_t is the total area of the spectrum of pulses, $S_t = S_p + S_C + S_{em}$ (S_p is the area of the photopeak,

S_C is the area of the Compton distribution, and S_{em} is the area of the peak due to the emission of iodine X-rays from NaI(Tl) crystal). The experimental values of the ratio S_p/S_t were found as functions of the energy of the γ-rays (Curve *2*, Fig. 4). For the sake of comparison, Curve *1* shows the energy dependence of the ratio $\sigma_p/(\sigma_p + \sigma_c)$ for the NaI crystal (σ_p and σ_c are the cross-sections of photoelectric absorption and Compton scattering of the γ-rays). The discrepancy between Curves *1* and *2* is explained by absorption of the secondary γ emission in the NaI crystal, which is due to the Compton scattering in the crystal. For γ-rays of energy $E_\gamma < 100$ kev one notices the effect of the emission of X-rays from the crystal. The efficiency of the spectrometer ε_p (Curve *3*, Fig. 4) is determined from Eq. (1) taking into account the experimental Curve 2. The spectrometer is only slightly sensitive to hard γ-rays and it can be used for measurements of soft γ-rays of $E_\gamma < 500$ kev even in the presence of the harder γ-lines.

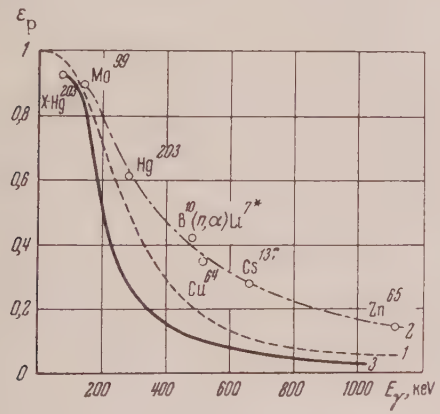

FIG. 4. Spectrometer efficiency as a function of the γ-quanta energy. *1* – dependence of the ratio $\sigma_p/\sigma_p + \sigma_c$ on E_γ; *2* – the experimental values of the ratio S_p/S_{tot}; *3* – ε_p.

2. METHOD OF MEASUREMENT OF γ-SPECTRA

The spectrum of pulses observed in the presence of a target in the neutron beam was measured with an open beam of neutrons (N_0) and with beam covered at the exit of neutron collimator (Fig. 1) by a layer of B_4C 0.3 g/cm² thick (N_1). The foil of B_4C absorbed thermal neutrons but did not change the flux of fast neutrons and γ-quanta. N_1 did not depend on the presence of the target. The effect of thermal neutrons corresponds to the difference in the readings $N = N_0 - N_1$. In the absence of a target, N was very small. In the great majority of experiments with a target, the integral count did not exceed 2,500 pulse/sec with $N_1 \sim 700$ pulse/sec. When the beam of neutrons was obstructed by a thick layer of B_4C which absorbed both thermal and fast neutrons, the counting rate dropped to 300 pulse/sec.

Thin targets were used during the experiments since in measurements carried out with thick targets, the photopeaks were considerably wider due to the Compton scattering of the γ-quanta in the target. In several cases the photopeaks were somewhat wider because of slight instability of the spectrometer. As an example of the distribution of pulses in the counts of N_0 and N_1, the results of measurements with Co_2O_3 target are shown in Fig. 5. Curve *1* shows the spectrum of pulses with an open beam of neutrons (N_0), Curve *2* shows the results with the same neutron beam but shielded with a B_4C foil (N_1), Curve *3* shows the net effect of the thermal neutrons (N). The spectrum of pulses measured in the open beam of neutrons shows peaks at 40–60 and 140 kev and a slight rise at 480 kev due to the emission from the boron shield of the spectrometer. The presence of peaks in Curve *2* makes it somewhat difficult to detect the low-intensity γ-lines in the regions of these peaks. The maximum at 140 kev is interpreted as absorption of neutrons in the NaI(Tl) crystal [γ-rays of the $I(n, \gamma)$ reaction[6]]. The smeared out maximum at 450 to 550 kev, seen in Fig. 5 in the spectrum of γ-rays from neutron capture by the target nuclei is primarily due to γ-emission from the boron shield and annihilation emission.

The target both absorbed thermal neutrons and scattered them. In a control experiment, it was shown that in measurements carried out with B_4C in the γ-ray collimator (*2* in Fig. 1) the correction for neutrons scattered by thin targets used in this work was negligible in comparison with the effect of thermal neutrons captured in the target.

Photopeaks of soft γ-lines appeared on a "base" of pulses caused by hard γ-quanta. This fact limited the accuracy in the determination of the area of the photopeak in an effort to measure the absolute number of the γ-quanta. To decrease the above-mentioned "base" and to separate more clearly the apparatus peaks and photopeak from γ-quanta emitted from the target, measurements with lead filters 0.532 – 2.55 g/cm² thick were carried out. The filters were placed in the γ-ray collimator. Fig. 6 shows the results of such measurements with Sm. Curve *1* represents the pulse distribution in the measurement without a lead filter, while Curve *2* shows the measurements with a 2.02 g/cm²

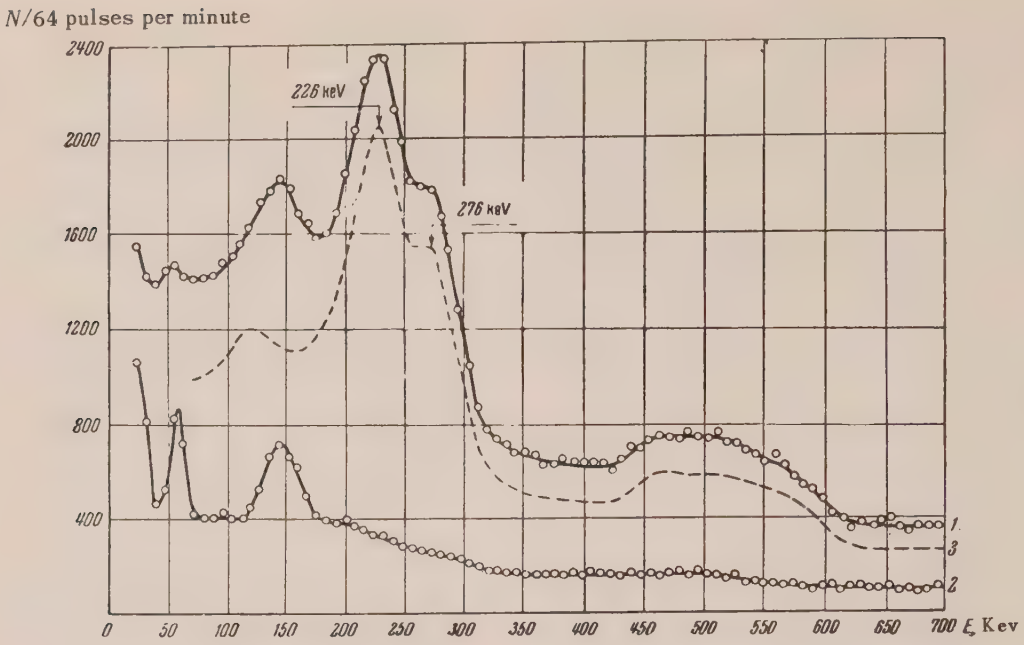

FIG. 5. Spectrum of pulses from Co_2O_3: *1* – neutron beam open (N_0), *2* – neutron beam covered by B_4C (N_1), *3* – effect of thermal neutrons $N = N_0 - N_1$.

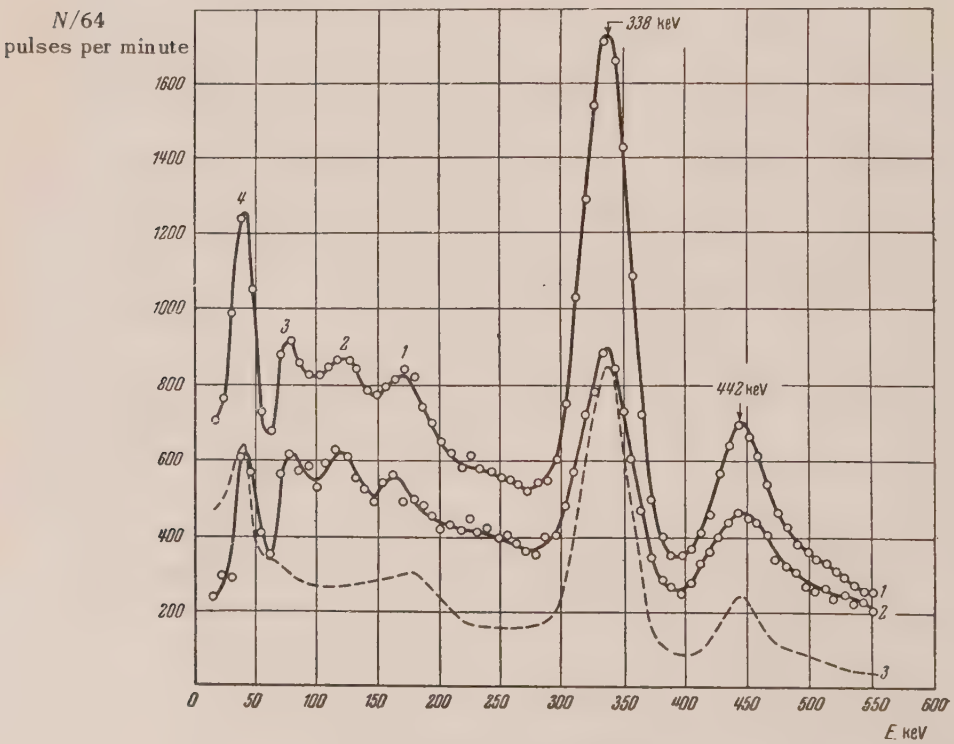

FIG. 6. Spectrum of pulses of Sm^{149} (n, γ) Sm^{150} γ-rays: *1* – without lead filter; *2* – with 2.02 g/cm² lead filter; *3* – spectrum of pulses due to radiation absorbed in the lead filter.

lead filter. The areas of the photopeaks due to the 442 and 338 kev γ-quanta decrease in the measurements with lead filters, corresponding to absorption of the γ-rays emitted by the target. Peaks *2* and *3* do not disappear in the measurements carried out with a filter and therefore cannot be interpreted as photopeaks due to soft γ-quanta from the target, but appear to be due to the apparatus. Thus, peak *3* is caused by the X-rays from the spectrometer lead shield (*cf.* also Fig. 3) and peak *2* is caused by the γ-rays from the I(n, γ) reaction within the NaI(Tl) crystal. The origin of the peaks *1* and *4* will be discussed below (Sec. 3, *Samarium*). In reducing the results of the measurements, the pulse spectra of γ-rays absorbed in the lead filters were utilized (Curve *3*).

Measurement of the area of the photopeak S_p alone is not sufficient to determine the number of γ-quanta emitted in the capture of neutrons by the target. To determine this quantity it is necessary to know the solid angle subtended by the target at the NaI(Tl) crystal and the neutron flux. Independent determinations of these quantities would serve as a source of additional errors. In an effort to obviate such errors in the present work, the area of the sought photopeaks S_p^i was compared with the area of the photopeak due to the 482 kev γ-quanta S_p^B which was determined in measurements with a B_4C target in an identical manner as with the target made of the studied material. The B_4C target was placed in the beam of thermal neutrons in place of the target prepared from the investigated isotope and its thickness was such that the absorption of thermal neutrons was almost complete. Then

$$\frac{S_p^i}{S_p^B} = \frac{n_{\gamma i}}{n_{482}} \frac{\varepsilon_p^i}{\varepsilon_p^{482}} \frac{k_i}{k_{482}} \sigma_{capt} \frac{pL}{A} \varkappa. \qquad (2)$$

In Eq. (2) $n_{\gamma i}$ is the unknown number of γ-quanta emitted per single captured neutron, n_{482} is the same number for B^{10} (n, α) Li^{7*} $(n_{482} = .93)$, k_i and k_{482} are correction factors for the absorption of γ-quanta in the path from the target to the NaI(Tl) crystal. The quantity $\sigma_{capt}\, pN_0/A$ is the probability of the neutron capture by the target nuclei (σ_{capt} is the neutron capture cross-section, p is the mass of the target, L is the Avogadro's number, and A is the molecular weight). The factor $\varkappa$ takes into account the absorption of neutrons and γ-quanta in a target of thickness l:

$$\varkappa = \frac{1 - \exp\{-(\mu_n + \mu_\gamma \tan\alpha)\, l/\sin\alpha\}}{(\mu_n + \mu_\gamma \tan\alpha)\, l/\sin\alpha}, \qquad (3)$$

where μ_n and μ_γ are the absorption coefficients of neutrons and γ-quanta, and α is the angle at which the target is oriented relative to the direction of neutron beam (Fig. 1). In the calculations of $\varkappa$, the values of μ_γ were taken from the work of Davisson and Evans[8].

3. RESULTS OF MEASUREMENTS

Cobalt

In the measurements on cobalt the target was prepared of powdered cobalt oxide (6.94 g) and metal (2.21 g). The powdered cobalt oxide was packed in a cylindrical case made of aluminum foil. The metallic target had an elliptical shape. From the known contents of impurities in the targets it was concluded that the γ-rays due to neutron capture in the target are practically entirely due to capture by Co^{59}. In the pulse spectrum from the Co_2O_3 target (Fig. 5) there are two not fully resolved peaks of energies 226 ±4 and 276 ±4 kev, which are interpreted as photopeaks due to γ-quanta of the same energies. The possibility of the presence of peaks due to γ-rays from cobalt with the intensity of the order of several percent in the 450–550 kev energy range cannot be excluded. The small peak at 120 kev was shown by additional experiments on absorption of γ-rays in lead filters to originate in the apparatus. Four independent series of measurements were carried out on the γ-ray spectra of cobalt absorbed by lead filter 2.02 g/cm² thick: two with a cobalt oxide target and two with a metallic target. These measurements were combined with the measurements of the area of the photopeak from a B_4C target. The resultant intensities of the γ-lines were found to be $n_{226} = (23 \pm 4)\%$ and $n_{276} = (23 \pm 4)\%$. The effective cross-section for capture of thermal neutrons in cobalt was taken to be 35.4 barns.

The values of the γ-transition energies obtained in the present work are close to the results of Hamermesh and Hummel[3] (220 kev) and agree with the results of Reier and Shamos[4] (237 and 289 kev). In these experiments the γ-rays from the Co(n, γ) reaction were measured by luminescent spectrometers. From measurements of hard γ-rays of the Co(n, γ) reaction[9] and the energies of proton groups in the Co(d, p) reaction[10] the energies of the excited levels of Co^{60} nucleus were determined and found to be in good agreement with each other. The lowest of these energies are shown in Fig. 7 together with the γ-transitions whose energies are

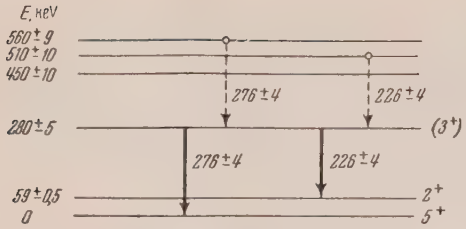

FIG. 7. Lowest energy levels of Co^{60}.

close to the energies of the γ lines measured in our experiment. It is possible to have either a combination of the shown transitions with transitions between several high-energy levels of the excited nucleus with various relative intensities, or their individual combinations. The case of a cascade transition containing only one of the pair of γ-rays of energies 280 and 220–230 kev is highly unlikely. Indeed, for $n_{226} = n_{276}$ the transitions of cascades from higher levels to the intermediate levels would have to be considered in this case as forbidden without any reasons for such an assumption. Because of the comparatively high intensity of the γ-lines observed by us, it is most probable that the transitions corresponding to these lines take place between the lowest levels of Co^{60}, *i.e.*, from the 200 kev level to the ground and isomeric levels, and that the remaining possible transitions of similar energies introduce only a small contribution to the intensities n_{226} and n_{276} (such an assumption is not in a contradiction with the values of the activation cross sections for the ground and isomeric states of Co^{60}). In this case it is possible to make several assumptions about the characteristics of the 280 kev energy level. In consequence of the equality of transition probabilities from the 280 kev energy level to the isomeric and ground levels, it is possible to assume that the angular momentum of the 280 kev level is equal to either 3 or 4, since the characteristics of the ground and isomeric levels are 5^+ and 2^+, respectively[11]. A comparison of the data reported previously[9,10] results in the conclusion that there are no transitions from the initial state of Co^{60} (which is formed after the capture of thermal neutrons by Co^{59}) to the isomeric level. This fact shows that the initial state of Co^{60} has a characteristic 4^- and not 3^- (the ground state of Co^{59} has a characteristic $7/2^-$).[12] The transitions from the initial state of Co^{60} to the ground state and to the 280 kev energy level have approximately the same intensity, namely 3 and 4% respectively[9]. Since the transition to the ground state is $E1$, then the transition to the 280 kev energy level should also be $E1$, *i.e.*, the parity of this level is positive. From the two possible values of the angular momentum for the 280 kev energy level the most preferred value is $I = 3$. In this case the transition to the isomeric level with lower energy should be $M1$ and the higher energy transition to the ground state should be $E2$.

Rhodium

A metallic plate of elliptical shape 0.1 mm thick and weighing 0.669 grams was used as a target for experiments on rhodium. Rhodium has one stable isotope Rh^{103}, so that the γ-rays of the radiative neutron capture belong to Rh^{104}. In this experiment the energy range up to 300 kev was studied in detail. Fig. 8 shows the pulse spectrum of γ-rays absorbed by a 1.01 g/cm² lead filter. The separation of this spectrum into the individual components, shown in the figure by dotted lines made possible a determination of the areas of those photopeaks for which the experiments on absorption of γ-rays reliably show their origin to be in the target. An analogous technique was used for the pulse spectrum of γ-rays absorbed by a 0.532 g/cm² filter. The energies and absolute intensities of γ-lines were found to be: $E_1 = 96 \pm 3$, $E_2 = 133 \pm 3$, $E_3 = 176 \pm 3$, $E_4 = 217 \pm 4$ kev and similarly $n_1 = 17\%$, $n_2 \leq 8\%$, $n_3 = 19\%$, $n_4 = 9\%$. The effective cross-section for capture of thermal neutrons

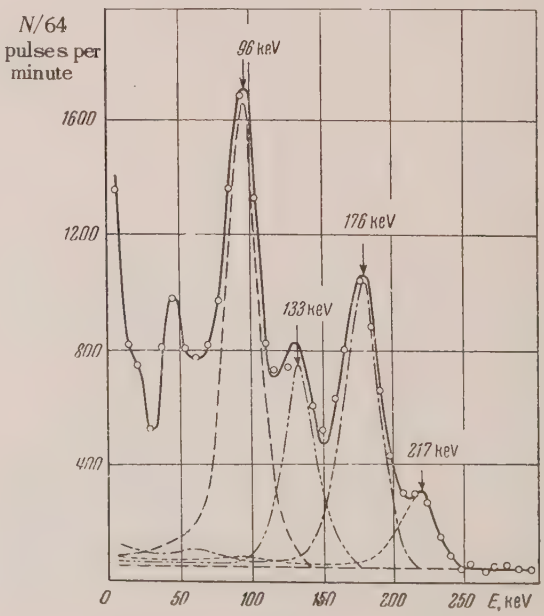

FIG. 8. Spectrum of pulses due to γ-rays from Rh (n, γ) reaction, absorbed by lead filter 1.01 g/cm² thick.

in rhodium was taken to be 150 barns. The errors in the determination of $n_1 - n_4$ are 15 to 20%. For the 133 kev line only the upper limit of intensity is shown since in that energy range there is a background peak (Fig. 5), which is not entirely eliminated in the difference of readings with open and closed neutron beams. The energy peak at 45 kev did not disappear in measurements with lead filters and consequently was due to the equipment.

It was observed previously[6] that the 80 and 160 kev γ-quanta discovered by Hamermesh and Hummel[3] in the γ-ray spectrum of radiative capture of neutrons in rhodium apparently correspond to the most intense γ-lines measured in the present work. The measurements of the hard γ-rays in the Rh(n, γ) reaction carried out previously[13] permit determinations of the energies of the lower levels of the Rh^{104} nucleus. The characteristics of the ground and the first two excited levels are determined from the β-decay of Rh^{104} [14]. It should be noted that only for 0^-, the characteristics of the initial state of Rh^{104}, produced by absorption of thermal neutrons by Rh^{103}, and 2^+ of the first excited level, is it possible to explain the absence of transitions from the initial level to the first excited level[13]. The principles which were used in Ref. 13 to assume $I = 1$ for the ground state should be reevaluated.

The energies of γ-lines found in this work do not fit directly into the energy level scheme constructed from the data of previous experiments[13,14] (Fig. 9, solid lines). If the presence of an additional 230 kev level is assumed, then these γ-lines are distributed in the scheme as shown by the dotted line in Fig. 9. In this case, however, there is a discrepancy between the intensity of the 96 kev γ-transition to the isomeric level (17 ±3)% and the probability of activation of the 4.3 minute isomer Rh^{104} (8 ± 3)%. This discrepancy exceeds the experimental error. Furthermore, it is difficult to reconcile the approximately equal intensities of the 96 and 176 kev γ-lines with the values of the radiative transition probabilities for the values of the angular momenta and parities of the first and the second excited levels of Rh^{104} shown in Fig. 9. At the most suitable characteristics of the introduced level (3^-), transitions with these energies will be $E2$ and $M2$, respectively. The ratio of the transition probabilities calculated by the Weisskopf formula[15] is approximately 5. A satisfactory arrangement of the energies of the observed γ-lines in the energy level scheme of Rh^{104} can be accomplished by introducing two additional levels. However, the possible energies of these levels cannot be determined uniquely.

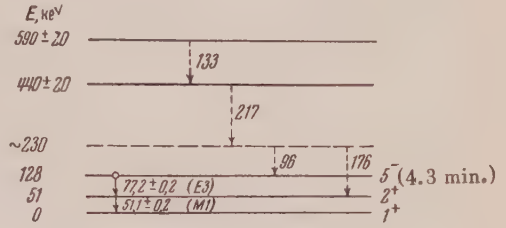

FIG. 9. Energy levels of Rh^{104}.

Iodine

A target of powdered iodine (3.96 g) was used. The γ-ray pulse spectrum of the I^{127} (n, γ) I^{128} reaction showed an intense 135 ±3 kev γ-line[6]. Existence of low-intensity γ-lines in the 255 kev energy range is possible[4]. The discrepancy with the data of Reier and Shamos[4] can apparently be explained by the fact that no shielding of the NaI(Tl) crystal from neutrons scattered by the target was used in the luminescent spectrometer. It is important to note that the scattering cross section of neutrons by iodine is approximately equal to the capture cross-section. In the measurements with any target carried out without B_4C in the γ-ray collimator (2 in Fig. 1) peaks at energies 85, 135 and 255 kev were observed. It is probable that for this reason the γ-quanta of 135 kev energy were attributed by the authors of the above work to background noise while the 80 kev peak they attributed erroneously to γ-rays from the I(n, γ) reaction.

From twelve distinct series of measurements, which included six measurements of γ-ray spectra using a lead filter, the intensity of 135-kev γ-lines was determined with an accuracy of 15%. This intensity is $n = 32\%$ per single captured neutron. The capture cross section in iodine was taken to be 6.7 barns. The absence of other intense γ-lines in the energy range up to 600 kev and the great intensity of γ-quanta of energy 135 kev shows that these γ-quanta are indeed connected with a transition from the first excited level of I^{128} to the ground state.

Samarium

The target in the experiments on samarium was powdered Sm_2O_3 (76.5 mg), packed in an aluminum foil case in the shape of a disk 10 mm in diameter.

The spectrum of pulses from the samarium target is shown in Fig. 6. Two well resolved peaks of γ-quanta at energies 442 ± 5 and 338 ± 4 kev are clearly visible in the pulse spectrum of γ-rays absorbed by a lead filter (Curve *3*). A smaller maximum appearing as a decrease in peak *1* in measurements with a lead filter was interpreted as the maximum of the Compton distribution of electrons from γ-quanta of 338 kev energy. The origin of peaks *2* and *3* was discussed in Sec. 2. The energy of peak *4* corresponds to the X-ray emission from Sm within the experimental accuracy. However, an intense peak due to the experimental equipment is observed in the spectrum at the same energy and its presence makes it impossible to measure the X-ray emission of Sm when its intensity is less than 10%. Thus, γ-lines of observable intensities are absent at energies below 300 kev. From the experiments the intensities of the observed γ-lines were determined to be (34 ± 5)% (E_γ = 442 kev) and (70 ± 10)% (E_γ = 338 kev) per single captured neutron. The capture cross section of neutron by the Sm^{149} isotope was taken to be 66,200 barns[17]. This result depends only very slightly on the error in the determination of the cross section since the target absorbed almost all the thermal neutrons incident on it. The energies of the γ-lines are in excellent agreement with the data of other authors[5,16] who studied the spectra of γ-rays in the Sm (n, γ) reaction, while the intensity of the γ-line at 338 kev is approximately twice the intensity found by Adiasevich *et al*[16]. The γ-lines investigated should be attributed to transitions to two lowest excited levels of Sm^{150}, since the major contribution to the cross section for capture of thermal neutrons in the existing composition of Samarium isotopes is due to Sm^{149}. The fact that the discussed levels appear in the decay of Pm^{150} [18] adds to the likelihood of such an assumption. From the relationship of the γ-line intensities it follows that the first excited level of Sm^{150} is the energy level at 338 ± 4 kev. This conclusion is in agreement with the data of Ref. 18. The second excited level has an energy 777 kev[5,19]. The low intensity of hard γ-lines in the spectrum of Sm (n, γ)[16,19] shows that the radiative transition of the Sm^{150} nucleus from the state originating by capture of a thermal neutron takes place through cascade γ-transitions which result with equal probability in a ground state or in one of the two above levels of Sm^{150}. The decay scheme of Sm^{150} proposed previously[16] thus appears to be incomplete.

Gold

The measurements for gold were carried out with two metallic targets of pure gold: *I* – 0.277 g/cm² thick, (1.56 g) and *II* – 0.554 g/cm² thick. Figure 10 shows the pulse spectrum of γ-quanta absorbed in a 2.02 g/cm² lead filter. In this diagram one can identify three not fully resolved photopeaks whose energies are 252, 210 and 174 kev (target *II*). The accuracy of the energy determination was ± 4 kev. In separating the spectrum into the individual components (the dotted lines of Fig. 10) a small remaining contribution in the energy region of about 140 kev is probably due to the background noise (*cf.* Fig. 5). Table I gives the intensities n_γ of the observed γ-lines measured with an accuracy of ± 20%. The capture cross section of thermal neutrons was taken to be 98 barns[20].

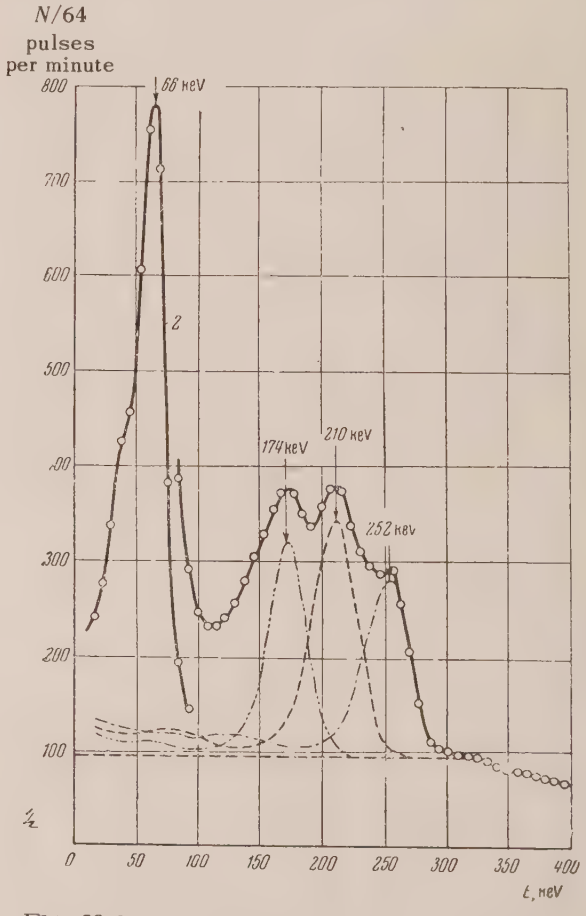

FIG. 10 Spectrum of pulses due to Au (n, γ) γ-rays absorbed in 2.02 g/cm² lead filter.

Besides the photopeaks mentioned above, an additional maximum at 66 ± 3 kev is clearly evident in Fig. 10. This maximum is also due to the capture

of neutrons in gold. The thin target (I) was used in the measurements of the intensity of this emission. The absorption of γ-quanta in the target was determined experimentally. Gold plates were used instead of lead filters 5 of Fig. 1 and the absorption was determined from the decrease in the area of the peak. In this way the coefficient of γ absorption 66 ± 3 kev γ-quanta in Au was determined to be $\mu = 2.9 \pm .2$ cm^2/g. The intensity of the considered radiation is shown in Table I.

TABLE I. Soft γ-quanta of Au (n, γ) reaction

E in kev	No. of γ-quanta per single captured neutron %	Theoretical values of internal conversion coefficient α_K in K shell		
		$E2$	$M1$	$M2$
252	22	0.0955	0.447	1.66
210	19	0.152	0.775	3.47
174	11	0.278	1.47	7.42
66	40	—	—	—

Reier and Shamos[4] discovered 248-kev γ-lines in the spectrum of Au(n, γ), which correspond apparently to a summary peak composed of the three γ-lines disclosed in the present work. From an experimental point of view the conclusions of Bartholomew and Kinsey[13] that the neutron binding energy in Au^{198} exceeds 6.5 Mev are hardly conclusive. A similar doubt has also been expressed previously[4]. It is more likely, in agreement with London and Sailar[21], that the 6.494 ± .008 Mev γ-quanta are due to direct transition of the nucleus into the ground state. Then the lowest excited states of Au^{198} (from the data of Ref. 13) have excitation energies 32 ± 20, 184 ± 16, 245 ± 17, 348 ± 20, 518 ± 20, and 792 ± 20 kev. The γ-lines discovered in the present work can be interpreted as due to transitions between the lowest levels of Au^{198} (Fig. 11). At the same time the 210-kev

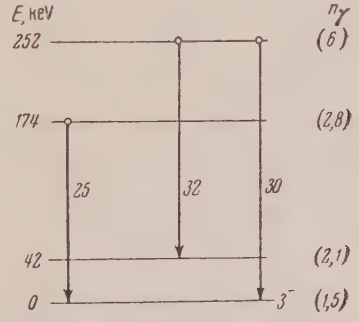

FIG. 11. Transition scheme for Au^{198}.

γ-quanta of energy cannot be considered as due to a transition between any one of the above levels, while the other two γ-quanta can correspond to transitions between somewhat higher levels. In our opinion, the transition scheme shown in Fig. 11 is the more probable. In our measurements, the 42-kev γ-rays were not observed because of strong absorption in the target and the presence of a neighboring background peak (*cf.* Fig. 5).

The 66 ± 3 kev gamma quanta cannot be reconciled with any transition between the lowest excited states. This emission was interpreted as X-ray emission from Au and due to internal conversion of γ-quanta in the K shell of the atom. Taking into account the K fluorescence from Au$(f = 0.94)$[22] we find the number of conversions in the K shell to be $K = 42 \pm 6\%$ per captured neutron. It is not possible in our work to attribute the X-rays to conversion of a soft line that cannot be detected because of its low intensity. Such an explanation is impossible since one would have to allow a complete conversion of such hypothetical line and the Au^{198} nucleus does not have a metastable state. It is most likely that the conversion is connected with the γ-quanta detected in this work: $K = K_{252} + K_{210} + K_{174}$. Table I gives the theoretical values of the coefficients α_K of the internal conversion of γ-rays by the K shell electrons of Au for dipole and quadrupole transitions[23]. The higher multipoles do not enter because of the long lifetime. The gamma-quanta intensity n_γ found in this work permits the use of α_K to determine the number K of conversion events in the K shell of the atom, which depends on the multipole order of all three γ-lines. The multipole orders of the γ-transitions were so chosen as to satisfy the experimental values of K.

The experimental results exclude the possibility that all three transitions are of the $E2$ type $(K = 7.6 \pm 1.5)$ or $M2$ $(K = 161 \pm 30)$. If the γ-transition of 252 kev energy is attributed to $M2$, and the other two transitions to $M1$ or $E2$, then one

obtains a satisfactory agreement with the experimental data. However, this variant is rather improbable, since the $M2$ transitions could not compete with $M1$ and $E2$ transitions in the above transition scheme (Fig. 11). A better agreement with the experiment is achieved if all three transitions are assumed to be $M1$ ($K = 38 \pm 8$). The case of two $M1$ transitions (one of which should be the transition at 174 kev) and one $E2$ transition is also possible. Fig. 11 shows (in percent per single captured neutron) the total number of transition events from excited states, equal to the sum of probabilities of transitions by γ-quantum emission (Table I), and of the transitions by conversion of γ-quanta conversion of atomic K electrons assuming that the transitions are of the $M1$ type.

The Au^{198} nucleus has negative parity and spin $I = 3$ in the ground state[3]. The excited levels shown in Fig. 11 should also have negative parity, since only $M1$ or $E2$ transitions are possible between them. According to Ref. 25, the initial state of Au^{198}, produced when Au^{197} captures a thermal neutron, has a spin 1^+. Bartholomew and Kinsey[13] showed that the probabilities of transitions from the initial state to the particular levels of Au^{198} considered here are of the same order of magnitude. The number of γ-transitions from the initial state to the state corresponding to a given energy level is shown in parentheses of Fig. 11 in percent per single captured neutron. The above facts can be brought into agreement by an assumption that the lowest excited levels have the same spin 3, even though such degeneracy seems unlikely to us. Furthermore, the transitions from the initial state to the considered levels, including the ground level, will be $M2$ transitions, which should be suppressed by the $E1$ and $M1$ transitions. Here it is expedient to reconsider the conclusion of Titman and Sheer[25] about the spin of the initial state. The results of a later work[20] disagree with the data used in their work to obtain 1^+ for the spin and parity of the initial state. If the initial state of Au^{198} is 2^+, the transitions into the considered levels will be $E1$ and the spins and parities of the corresponding states of Au^{198} will be 1^-, 2^-, and 3^- for small excitation energies.

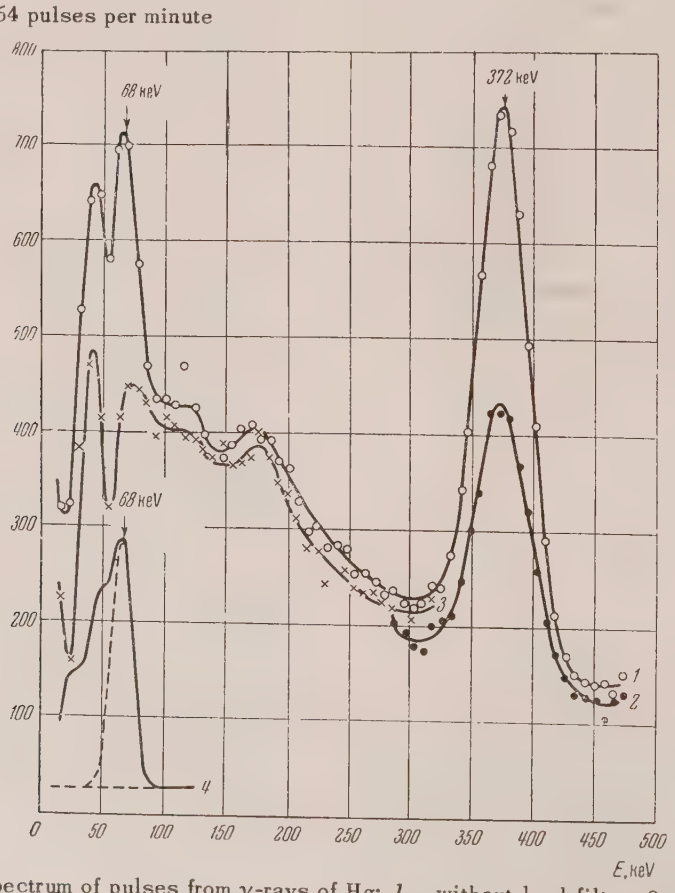

FIG. 12. Spectrum of pulses from γ-rays of Hg: *1* – without lead filter; *2* – with 2.02 g/cm^2 lead filter; *3* – with 0.5 mm lead filter; *4* – emission spectrum absorbed by 0.5 mm of lead.

Mercury

The measurements on Hg were carried out using a powdered target of HgO (1.2 g) packed in disc-shaped aluminum case 20 mm in diameter. The spectrum obtained with this target (Curve *1* Fig. 12) shows a particularly noticeable photopeak due to 372 ± 5 kev γ-quanta. Peaks corresponding to somewhat softer radiation are also apparent. Curve *2* of Fig. 12 refers to measurements with a 2.02 g/cm² lead filter. From the spectrum of the radiation absorbed by the lead filter (difference of Curves *1* and *2*) the area of the photopeak was determined, and $n_\gamma = 45 \pm 7\%$ per single captured neutron was obtained for the intensity of the radiation at 372 kev. The capture cross section of thermal neutrons was taken to be 380 barns. From a comparison of Curves *1* and *3* (the pulse spectrum of γ-rays which passed through a lead filter 0.5 mm thick) it is evident that the 68 ± 3 kev radiation originates in the target, while the 45-kev peak appears to be due to the experimental apparatus. In the lower left-hand corner of Fig 12 is shown a spectrum of radiation absorbed by 0.55 mm Pb (Curve *4*). From this curve, the intensity of the 68 ± 3 kev radiation was determined to be $1.4\% < n_\gamma < 4\%$ per single captured neutron. The apparatus peak makes it difficult to establish this intensity more accurately.

The γ-quanta observed in these experiments should be ascribed to Hg^{200} since the isotope Hg^{199} has the largest thermal neutron capture cross section of the mercury isotopes. The 372-kev γ-quanta correspond here to the transition of Hg^{200} from the first excited state to the ground state, well known[25] from the radioactive decay of Au^{200} and Tl^{200}. Gamma quanta of similar energy were detected[16] in the study of γ-rays emitted after capture of neutrons in Hg, except that our measured intensity is greater by approximately a factor of two. A similar discrepancy from the above work[16] has appeared in our data on the intensity of the soft line of the Sm(n, γ) reaction.

The 68 ± 3 kev radiation can naturally be interpreted as mercury X-rays and can be ascribed to 372 kev γ-ray conversion in the K shell of the atom. The experimental values of the internal conversion coefficient α_K in the K shell is between the limits $0.03 < \alpha_K < 0.09$. A theoretical value can be found within these limits only for $E2$ transitions ($\alpha_K \sim 0.04$)[22]. Consequently, the first excited state of Hg^{200} should have spin 2 and positive parity in agreement with a previous work[26].

SUMMARY OF RESULTS

Table II gives the values of energies E_γ and intensities n_γ of the γ-lines (number of γ-quanta per single captured neutron). The absolute intensities were determined with an accuracy of 15 ± 20%.

TABLE II.

Emitting nucleus	Energy E of the γ-quanta in kev	No. of γ-quanta per single captured neutron, n_γ, %	Emitting nucleus	Energy E of the γ-quanta in kev	No. of γ-quanta per single captured neutron, n_γ, %
Co^{60}	226±4	23	Sm^{150}	338±4	70
	276±4	23		442±5	34
Rh^{104}	96±3	17	Au^{198}	66±3	40
	133±3	⩽8		174±4	11
	176±3	19		210±4	19
	217±4	9		252±4	22
I^{128}	135±3	32	Hg^{200}	68±3	1.4—4
				372±5	45

In conclusion the authors express their gratitude to I. M. Frank for his interest in this work, I. S. Shapiro for evaluation of the results, A. M. Safronov, V. F. Tsarakev, Ia. A. Kleinman and associates, who operated the reactor, for their help in this work.

[1] Groshev, Adiasevich, and Demidov, *Papers by the Russian Delegation to the International Conference of Peaceful Uses of Atomic Energy*, Published by U.S.S.R. Acad. Sci., p. 252 (1955).

[2] B. B. Kinsey and G. A. Bartholomew, Can. Journ. Phys. **31**, 537 (1953).

[3] B. Hamermesh and V. Hummel, Phys. Rev. **88**, 916 (1952).

[4] M. Reier and M. H. Shamos, Phys. Rev. **100**, 1302 (1955).

[5] C. T. Hibdon and C. D. Muehlhause, Phys. Rev. **88**, 945 (1952).

[6] Estulin, Kalinkin, and Melioranskii, J. Exptl. Theoret. Phys. (U.S.S.R.) **31**, 886 (11956), Soviet Physics JETP **4**, 752 (1957).

[7] Alikhanov, Vladimirskii, Nikitin, Galanin, Gavrilov, and Burgov, *Papers by the Russian Delegation to the International Conference of Peaceful Uses of Atomic Energy*, p. 105 (1955).

[8] C. M. Davisson and R. D. Evans, Rev. Mod. Phys. **24**, 79 (1952).

[9] G. A. Bartholomew and B. B. Kinsey, Phys. Rev. **89**, 368 (1953).

[10] G. M. Foglesong and D. G. Foxwell, Phys. Rev. **96**, 1001 (1954).

[11] M. Deutch and G. Scharff – Goldhaber, Phys. Rev. **83**, 1059 (1951).

[12] L. K. Peker and L. A. Sliv, Izv. Akad. Nauk SSSR, Ser. Fiz. **27**, 411 (1953).

[13] G. A. Bartholomew and B. B. Kinsey, Can. Journ. Phys. **31**, 1025 (1953).

[14] Jordan, Cork, and Burson, Phys. Rev. **90**, 362 (1953).

[15] J. M. Blatt and V. F. Weisskopf, *Theoretical Nuclear Physics* (John Wiley & Sons, New York, 1952).

[16] Adiasevich, Groshev, and Demilov, U.S.S.R. Acad. Sci., *Conference on Peaceful Uses of Atomic Energy*, p. 270 (1955).

[17] Melaike, Parker, Petruske, and Tomlinson, Can. Journ. Chem. **33**, 830 (1955).

[18] V. Kistiakov – Fischer, Phys. Rev. **96**, 1549 (1956).

[19] B. B. Kinsey and G. A. Bartholomew, Can. Journ. Phys. **31**, 1051 (1953).

[20] H. H. London and V. L. Sailar, Phys. Rev **93**, 1030 (1954).

[21] A. Harvey, Phys. Rev. **81**, 353 (1951).

[22] Brogles, Thomas, and Haynes, Phys. Rev. **89**, 715 (1953).

[23] L. A. Sliv and H. N. Brand, *Tables of Internal Conversion Coefficients*, 1956.

[24] Elliot, Preston, and Wolfson, Can. Journ. Phys. **32**, 153 (1954).

[25] J. Titman and C. Sheer, Phys. Rev. **83**, 747 (1953).

[26] Berostrom, Hill, and de Pasquali, Phys. Rev. **92**, 918 (1953).

Translated by M. J. Stevenson
215

SOVIET PHYSICS JETP VOLUME 5, NUMBER 5 DECEMBER, 1957

Ignition of the High Voltage Discharge in Hydrogen at Low Pressures

A. S. POKROVSKAIA-SOBOLEVA AND B. N. KLIARFEL'D

(Submitted to JETP editor January 14, 1957)
J. Exptl. Theoret. Phys. (U.S.S.R.) **32**, 993-1000 (May, 1957)

It has been found that the striking voltages for discharges in hydrogen, corresponding to the left-hand branch of the Paschen curve, do not obey the similarity rules.

After an ignition on the left-hand branch of the Paschen curve, the resultant high-voltage discharge is characterized by electrode voltage drops which are independent of the current. In hydrogen discharges, this constancy of voltage drop is maintained over a very wide range of currents. For discharges produced by 4-μsec voltage pulses, the transition from the high-voltage form to the arc takes place only at currents exceeding 1000 amp.

IN UNIFORM ELECTRIC FIELDS, the striking voltage for a discharge satisfies the similarity rule; *i.e.*, it is a function of the product pd, where p is the pressure and d the distance between electrodes. A number of investigations[1,2] have shown noticeable deviations from the similarity rule when the electric field at the cathode begins to exceed 10^6 v/cm, and spontaneous emission of electrons begins. This situation may arise either at very high gas pressures, on the order of tens of atmospheres, where the electrode voltage reaches hundreds of kilovolts, or at very small gap widths where even at a few hundred volts the field strength at the cathode reaches the above-mentioned figure. In the work re-

ported herein, we first investigated the hydrogen-discharge striking voltage to study those deviations from similarity in the left-hand of the Paschen curve which were not of the nature of spontaneous electron emission. In the second place, we studied those particular forms of discharge which had a high voltage drop at the electrodes.

1. MEASUREMENT PROCEDURE

The tube intended for the study of discharges under the conditions of the left-hand branch of the Paschen curve was constructed to prevent any discharge by way of the "long" path. To test the applicability of Paschen's law, a construction was used in which the electrodes could be kept fixed, or one electrode could be moved so as to vary the separation d between 4 and 32 mm. The electrode diameter was 80 mm to make the interelectric field sufficiently uniform. Before use, the polished nickel electrodes were baked out with a high-frequency current in vacuum, and conditioned by a glow discharge in hydrogen. Control of the hydrogen pressure was obtained by heating titanium hydride placed in a side-arm of the discharge tube. The voltage applied to the electrodes was supplied by a high-voltage rectifier circuit, provided with a filter to smooth out the voltage pulsations. This voltage could be regulated continuously from zero to 40 kv, and its value was measured with an electrostatic voltmeter. The ignition point was indicated by the needle kick of a microammeter connected in series with the low-voltage electrode. The striking of a discharge could also be detected visually through the fine mesh screen surrounding the discharge space. In a darkened room it is possible to establish the occurrence of ignition at currents as low as about 10^{-7} ampere.

2. TEST OF THE APPLICABILITY OF PASCHEN'S LAW TO THE IGNITION OF HYDROGEN DISCHARGES

Repeated measurements of striking potentials U_s have shown the existence of very serious deviations from the similarity rule. Curves of $U_s = f(pd)$ for for different values of d are given in Fig. 1; these curves are quite widely separated. Such effects can be repeated reproducibly in tubes of different constructions, and also in tubes where both the distance d and the hydrogen pressure p can be varied. In these tubes the cathode is kept the same during all changes; this avoids any errors which might

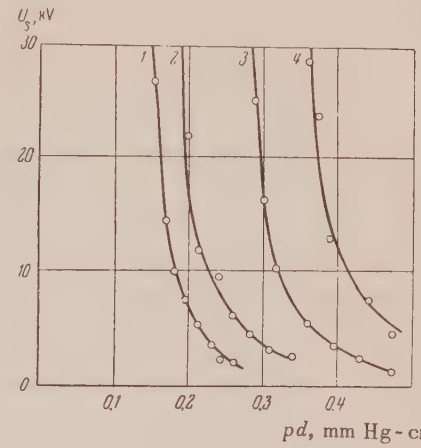

FIG. 1. Deviations from the Paschen law in hydrogen. Curves of $U_s = f(pd)$ at $T = 20°$ C. 1—$d = 4$ mm; 2—$d = 8$ mm; 3—$d = 16$ mm; 4—$d = 28$ mm.

creep in during the exchange of one cathode for another, due to changes in the coefficient γ, which is very sensitive to the condition of the surface. Repeated experiments have also shown the absence of local effects at the electrodes, and that the results are the same when the electrode polarities are interchanged. All this proves that the deviations from the similarity law are not experimental errors or peculiarities of the apparatus, but are inherent in the nature of the hydrogen discharge. In fact, if hydrogen is replaced by air in the same tubes, the curves of $U_s = f(pd)$ taken at different distances d and pressures p coincide very well (*cf.* Fig. 2) whereas the same curves in hydrogen (Fig. 1) are widely separated. If, following Slepian and Mason[3] we plot $\log p$ *vs.* $\log d$ for constant U_s, we obtain for hydrogen a family of straight lines intersecting the coordinate axes at a very nearly constant angle, differing from 45°. This implies that the striking potential is a function of the derived quantity pd^k. This function is assumed to be of the form

$$U_s = A/(pd^k)^B. \tag{1}$$

If U_s is in kilovolts, the experimental data for hydrogen are well represented by the expression

$$U_s = 46 \cdot 10^{-3}/(pd^{0,58})^6\,(\text{kV}). \tag{2}$$

Formula (2), whose validity has been verified up to a potential of 30 kv, shows that U_s is more sensitive to variations in pressure than to variations in the distance between electrodes.

The data obtained at different values of d agree

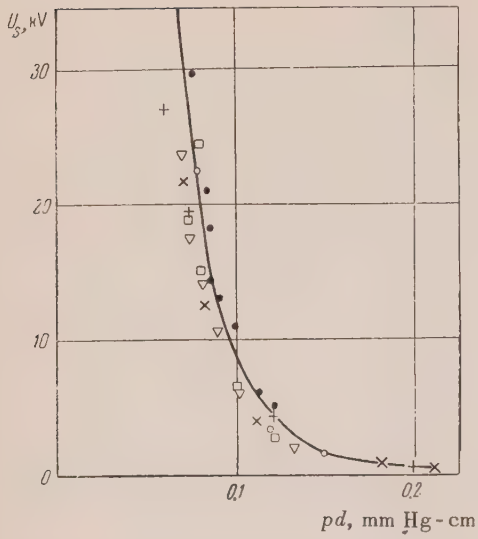

FIG. 2. Curves of $U_s = f(pd)$ for air at $T = 20°$ C. +—d = 20 mm; □—d = 8 mm; pressure varied. ×—p = 0.04 mm Hg; ▽—p = 0.06; ○—p = 0.1; ●—p = 0.14; interelectrode distance varied.

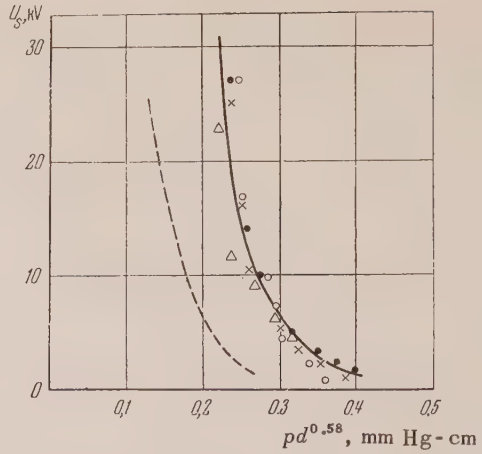

FIG. 3. Striking voltage of hydrogen discharge as function of $pd^{0.58}$. ●—d = 2.8 mm; ×—d = 16 mm; ▽—d = 8 mm; ○—d = 4 mm. Dashed curve is from data by Quinn.

well with the relation $U_s = f(pd^{0.58})$ as shown in Fig. 3. Quinn's results for hydrogen[4], shown dotted in Fig 3, give a value of U_s which is lower by almost a full order of magnitude. Apparently the electrodes in Quinn's experiments were not sufficiently outgassed, so that the coefficient γ of his cathode was much larger than in the present work. This is also confirmed by the much lower values of U_s which Quinn obtained in comparison with the results of Dikidzhi and Kliarfel'd[5]. In the high sensitivity of its striking voltage to contamination of the cathode surface, hydrogen is similar to the inert gases or mercury vapor[5,6] and differs from the other molecular gases.

The reasons why hydrogen discharges deviate from the similarity rule can be stated only in relatively general terms as yet. Field emulsion cannot be playing any part here, since the deviations are observed even when the field strength at the cathode is below 10^4 v/cm. Some reasons for the deviations might be: a) ionization processes in the gas space, which may arise in various ways in molecular gases; b) cathode surface effects, explainable by the fact that the coefficient γ depends not only on the energy of the ions, but also on the field strength at the cathode.

Experiments which have been carried out by the probe method in the positive column of hydrogen discharges[7] have shown that the mean mass of the hydrogen ions definitely exceeds the mass of a proton. A number of studies of hydrogen ions[8-10] have indicated the presence of at least three different types of ions in the hydrogen discharge: H^+, H_2^+, and H_3^+. When hydrogen is ionized by an electric spark discharge the yield of H_2^+ ions, at the maximum in the curve of ionization efficiency, is 250 times larger than the yield of protons[11]. The H_3^+ ion is formed from the H_2^+ ion by the reaction[12,13] $H_2^+ + H_2 \rightarrow H_3^+ + H$. The probability of this process falls off as the energy of the H_2^+ ion increases. The H_3^+ ion thus formed can break up again during various types of collisions with hydrogen molecules; hence the disintegration probability of H_3^+ increases with its velocity. Conditions are most favorable for the production and stability of H_3^+ ions when the surrounding medium is made up of other hydrogen ions. The value of γ for different types of hydrogen ions increases with the number of atoms in the given type of ion[14]. Thus a change in the composition of the hydrogen ion mixture striking the cathode will case corresponding changes in U_s. It is entirely possible that some of the processes by which hydrogen ions of different types are formed or destroyed[15] on their way to the cathode may not satisfy the similarity rule. In this case the striking voltage of the discharge will also deviate from the rule.

A second reason for the failure of the similarity rule could be a dependence of the coefficient γ for H^+, H_2^+ and H_3^+ ions on the potential gradient at the cathode. Unfortunately only one study of this dependence has been reported—for H^+ and H_2^+ ions with an energy of 250 kv[16]. It was found that the coefficient γ increased somewhat faster for H_2^+ ions than for protons as the field at the cathode increased. It is very probable that for the slower H_3^+ ion, the coef-

ficient γ increases still more rapidly, and that the increase is effective at still lower cathode field strengths. In this case, the curves $U_s = f(pd)$ for small values of d would be displaced to the left of those for large d, because of the increase of γ. This is what is observed experimentally (Fig. 1).

3. HIGH-VOLTAGE FORM OF THE DISCHARGE AT VERY LOW PRESSURES

On the left-hand branch of the Paschen curve the discharge occurring after ignition is characterized by a running voltage almost exactly equal to the striking voltage[6], whereas on the right-hand branch the transition to a glow discharge is always accompanied by a considerable reduction in the potential drop across the discharge. Hence formula (2) gives the running voltage as well as the striking voltage, provided that the current density in the discharge does not exceed about 0.1 a/cm², as will be shown below. On the left-hand branch of the Paschen curve the normal glow discharge cannot in general occur, since the thickness of the normal region of cathode potential drop is greater than the distance between electrodes. The high-voltage form of discharge occurring in the left-hand branch of the curve therefore has the characteristics of a silent discharge, in that there is only a weak space charge between the electrodes; it also has the characteristics of a hindered discharge, since increasing the distance between the electrodes results in a decreased potential drop across the discharge. The low space charge of this type is a result of the high speed of the charged particles due to the high field and particularly to the fact that when pd is reduced the discharge changes from a slow diffusion of ions and electrons in a gas, characterized by a mobility coefficient in the electric field, to a free fall to the cathode. Particular attention should be paid to the current-voltage characteristics of the high-voltage discharge in hydrogen, where the ionic space charge is least effective. Such characteristic curves, taken at different pressures, are shown in Fig. 4. In these curves the potential drop across the discharge is inpendent of the current over a very wide range of current densities. From the outside, the discharge appears as a diffuse glow, whose intensity falls off continuously from the cathode to the anode, corresponding to the drop in the excitation efficiency of electrons in the energy range 10^3 to 10^5 ev.

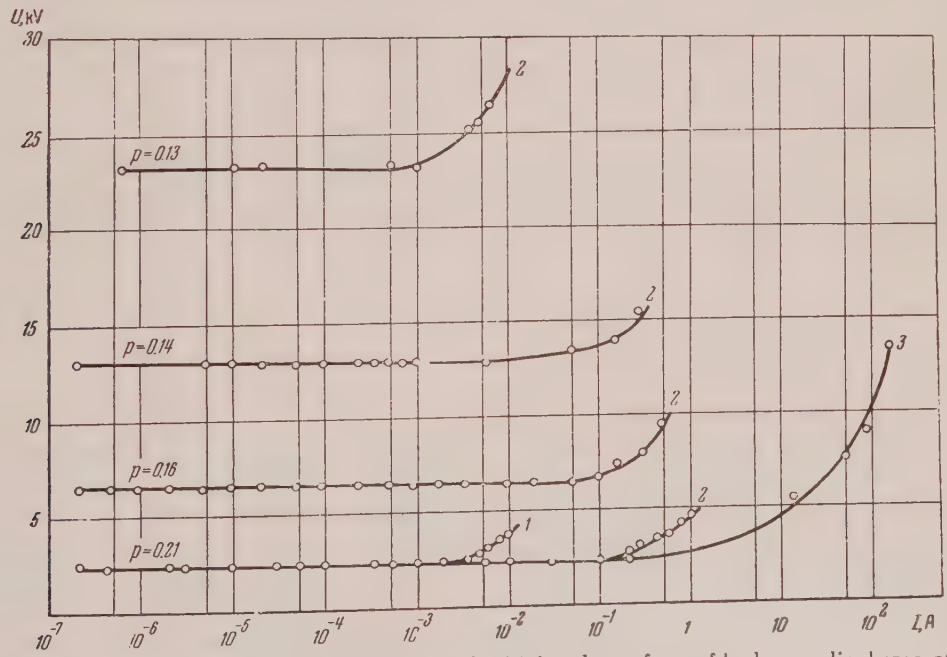

FIG. 4. Current-voltage characteristics for high-voltage form of hydrogen discharge at constant field strength. d = 16 mm; cathode surface = 50 cm²; pressure p in mm Hg. 1—thin nickel foil electrodes, 2—massive copper electrodes, 3—massive copper electrodes with pulsed operation.

The heating of the electrodes, which increases with the current, causes a lowering of the hydrogen density in the interelectrode space. Because of the very steep rise which occurs in the striking voltage (and in the concomitant running voltage) of the high-voltage hydrogen discharge when the value of

$pd^{0.58}$ is reduced, even a slight reduction in gas density is sufficient to raise the voltage necessary to maintain the discharge. Curve 1 of Fig. 4, taken at a pressure of 0.21 mm Hg in a tube with thin nickel-foil electrodes, shows a rise even at current densities of the order of 0.1 ma/cm². Curve 2 was measured in a tube with massive electrodes of electrolytic copper; the discharge was switched on for short periods only. Because of the lower electrode heating, the upward rise in the curve begins only at a current density of a few ma/cm². In order to eliminate the effect of electrode heating, curve 3 was taken by applying voltage pulses of 4 microseconds duration at a repetition rate of 200 per second. By this means the average heat dissipation at the electrodes was reduced by three orders of magnitude. The heating during each pulse could not have caused any rarefaction of the gas, since in 4 microseconds the hydrogen molecules would travel only about one centimeter, and would not be able to leave the discharge space. The rise in curve 3 begins at a current density on the order of 100 ma/cm². The remaining current-voltage characteristics were all measured at lower hydrogen pressures in the tube with massive copper electrodes already referred to, using discharges of short duration. The lower the hydrogen pressure, the smaller is the current density at which the voltage rise begins, since the left-hand branch of the Paschen curve becomes steeper for lower pressures and even a very small amount of heating is sufficient to produce a noticeable voltage rise. If the heating effect is reduced (as in Curve 3) it is possible to obtain a constant voltage drop over a range of at least seven orders of magnitude of current, from 10^{-7} to 1 ampere. It appears likely that this constancy would be maintained for several more orders of magnitude below 10^{-7} ampere.

The rise in voltage across the discharge when the current density increases above 100 ma/cm² cannot be due entirely to heating of the gas. The appearance of a positive-ion space charge at high current densities (the electron space can be neglected, since electrons are removed from the interelectrode space with almost two orders of magnitude faster than the ions) leads to a redistribution of the electric field between the electrodes. This causes an increase in the potential drop at the cathode and a decreased drop at the anode. The results of this will be: 1) a reduction in the number of ionizations caused by electrons on their way from cathode to anode, because it diminishes the region in which the electrons attain energies of 20 to 1000 ev, where they have the greatest effective cross-section for ionization ($Q_i > 1$ cm²/cm³); and 2) an increase in the average value of γ for ions which reach the cathode owing to the increased anode region in which U has a higher value, and a corresponding increase in the proportion of higher-energy ions that strike the cathode. Whether this redistribution of the field will lead to an increase or a decrease of the discharge voltage depends upon the nature of the dependence of γ and Q_i on the energies of the corresponding ions and electrons. An increased potential difference across the discharge will result when the drop in the number of ionizations by electron impact is not compensated by the increase in γ. In the opposite case, there will be a decrease in the running voltage of the discharge due to the more rapid growth of γ with increased ion energy U. In hydrogen, γ rises slowly in the energy interval 0 to 30 kv[14,17]. Therefore for a high-voltage discharge, one would predict that the positive space charge would cause the current-voltage characteristic to rise rather than drop.

It is possible to estimate the order of magnitude of the current density j at which the positive space charge is known to cause a change in the current-voltage characteristic of a high-voltage discharge (regardless of the sign of this change). All the approximations necessary for this estimate are made in such a way that the value obtained for j is an upper limit.

For simplicity let us assume that there is a constant positive space-charge density between the electrodes. If $\rho = 0$, the potential increases linearly from cathode to anode, while the field E is con-

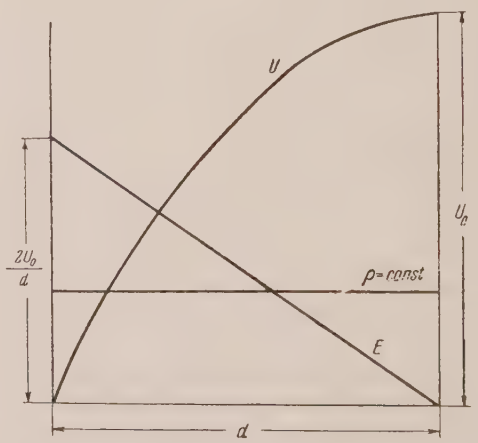

FIG. 5. Assumed conditions of U, E and ρ corresponding to the onset of a change in the running voltage of a high-voltage discharge, as the discharge current is increased.

stant and equal to $E = U_0/d$, where U_0 is the potential difference between the electrodes. Let us find the value of ρ for the case where the mean value of E is still equal to U_0/d, but where E varies from the value $2U/d$ at the cathode to zero at the anode. Since ρ is constant, E must decrease linearly from cathode to anode. The potential U varies in this case as shown in Fig. 5. When the potential deviates from linearity as much as this, it is quite reasonable to expect variations in the running voltage of the discharge.

If x is the distance from the cathode, we obtain

$$E = \frac{2U_0}{d}\left(1 - \frac{x}{d}\right), \tag{3}$$

$$dE/dx = -4\pi\rho = -2U_0/d^2, \quad \rho = U_0/2\pi d^2. \tag{4}$$

On the other hand, the positive-ion space charge produced by a current of j/e electrons passing through one square centimeter each second is equal to

$$\rho = (j/e)\, sp\tau e, \tag{5}$$

where sp is the product of the effective cross-section for ionization by electron impact and the gas pressure, and τ is the mean lifetime of the ions in the discharge. Here we are assuming that spd is considerably smaller than unity, *i.e.*, that most of the discharge current is carried by electrons.

We now determine an approximate lifetime τ as the time for the free fall of an ion from a distance of $d/2$ to the cathode in a field E_1, which is the mean value of E between $x = 0$ and $x = d/2$. (In this derivation we ignore collisions of the ion with gas molecules, which will in fact lead to an increase of τ.) Then

$$E_1 = 3U_0/2d, \quad \tau = \sqrt{2d^2M/3U_0e}, \tag{6}$$

where M is the mass of the ion and e is its charge.

The value of current density j in the discharge, for which the interelectrode field becomes distorted in the manner shown in Fig. 5, is found from Eqs. (4) to (6):

$$j = \sqrt{3/8}\, eU_0^{3/2}/\pi d^3 sp M^{1/2}. \tag{7}$$

For the case corresponding to curve 3 of Fig. 4 we have $U_0 = 2500$ v, $sp = 0.2$ cm^{-1} at electron energies of the order of 1000 ev, $d = 1.6$ cm, and $M = 2.33 \times 10^{-24}$ g (we assume that the ions are H_2^+). This gives a value for j of about 2 a/cm^2. At this current density, Curve 3 of Fig. 4 already shows a noticeable rise in the running voltage. Thus, the rise in running voltage with increasing current density in a hydrogen discharge can be due either to a rarefaction of the gas caused by heating of the electrodes, or to distortion of the field under the influence of the ionic space charge.

A dc high-voltage discharge does not turn into an arc until the discharge current reaches 1 ampere. In pulsed discharges, transition to the arc occurs for currents of 1000 ampere only at pressures above 0.2 mm Hg. At lower hydrogen pressures, transition to the arc does not occur until the total discharge current is above 1000 amperes ($j \geq 20$ a/cm^2). This result indicates that the high voltage form of discharge can be supported for short periods of time without going over into an arc, at extremely high current densities, probably considerably in excess of 100 a/cm^2.

For a comparison of the nature of discharge effects on the left- and right-hand branches of the

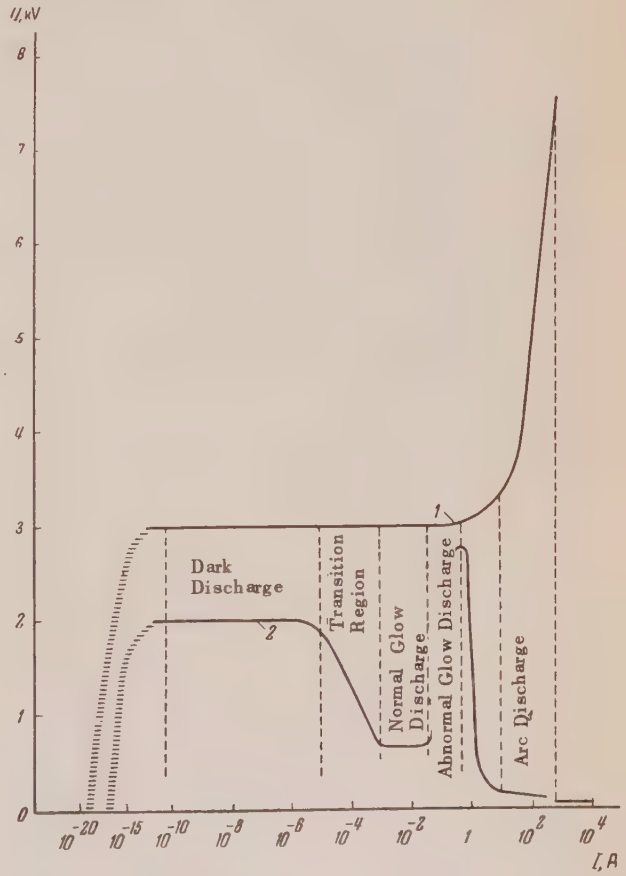

FIG. 6. Schematic form of the current-voltage characteristics of a discharge: 1—for $pd < pd_{min}$; 2— for $pd > pd_{min}$ (after Druyvesteyn and Penning[18]).

Paschen curve, Fig. 6 shows schematically the current-voltage characteristics of a high-voltage discharge (Curve 1) and a discharge on the right-hand branch (Curve 2); the latter curve is borrowed from a well-known survey article[18]. For convenience of comparison, the ordinates of Curve 2 have been increased by ten times. The curves of Fig. 6 demonstrate the relative simplicity of the effects on the left-hand branch of the Paschen curve. The constant potential difference across the discharge agrees very well with Townsend's assumption that the ignition of the discharge is a process in which the current goes to infinity when the voltage on the electrodes exceeds a certain value—the striking voltage.

The high-voltage form of discharge, characterized by voltages in kilovolts or even tens of kilovolts, and a current density up to tens of amperes per cm^2, undoubtedly deserves detailed study, not only in the steady but also in the dynamic state. This form of discharge, at low current densities, was used a great deal in former years, when such discharges were the only source of electron and positive-ion beams with energies of several tens of kilovolts. Methods have recently been sought for obtaining high temperatures with the aid of super-powerful discharges[19,20]. The high-voltage form of discharge appears to be the first stage in the development of a super-powerful discharge of this type, in which the cross-section area of the discharge is still uniformly filled with current.

In conclusion, the authors wish to express their thanks to N. G. Kashnikov and T. B. Fogel'son for valuable critical comment.

[1] W. Boyle and P. Kisliuk, Phys. Rev. **97**, 255 (1955).

[2] E. Finkelmann, Arch. Elektrotech. **31**, 282 (1937).

[3] J. Slepian and R. Mason, J. Appl. Phys. **8**, 618 (1937).

[4] R. Quinn, Phys. Rev. **55**, 482 (1939).

[5] A. Dikidzhi and B. Kliarfel'd, J. Tech. Phys. (U.S.S.R.) **25**, 1038 (1955).

[6] L. Guseva and B. Kliarfel'd, J. Tech. Phys. (U.S.S.R.) **24**, 1170 (1954).

[7] A. Pokrovskaia, J. Tech. Phys. (U.S.S.R.) **21**, 617 (1951).

[8] Simons, Fontana, Muschlitz, and Jackson, J. Chem. Phys. **11**, 307 (1943).

[10] R. Holzer, Phys. Rev. **36**, 1204 (1940).

[11] H. Newhall, Phys. Rev. **62**, 11 (1942).

[12] R. Murray, J. Appl. Phys. **23**, 6 (1952).

[13] H. Massey and E. Burhop, *Electronic and Ionic Impact Phenomena*, Oxford, (1952).

[14] V. Tel'kovskii, Dokl. Akad. Nauk SSSR, **108**, 444 (1956).

[15] N. Fedorenko, J. Tech. Phys. (U.S.S.R.) **24**, 769 (1954).

[16] Webster, Van de Graaff, Trump, J. Appl. Phys. **23**, 264 (1952).

[17] H. Bourne, Doctoral thesis, Electrical Engineering, Mass. Inst. of Technology, (1952).

[18] M. Druyvesteyn and F. Penning, Rev. Mod. Phys. **12**, 89 (1940).

[19] Artsimovich, Andrianov, Bazilevskaia, Prokhorov, and Filippov, Atomnaia Energiia (U.S.S.R.) No. 3, 76 (1956).

[29] M. Leontovich and S. Osovets, Atomnaia Energiia (U.S.S.R.) No 3, 81 (1956).

Translated by D. C. West
216

Separation of Helium Isotopes by Rectification and Thermo-Osmosis

V. M. KUZNETSOV
Institute of Physical Problems, Academy of Sciences U.S.S.R.
(Submitted to JETP editor January 15, 1956)
J. Exptl. Theoret. Phys. (U.S.S.R.) 32, 1001-1011 (May, 1957)

The main characteristics of a packed rectification column for separation of a He^3 – He^4 mixture and of a filter for enriching the solution with the light helium isotope by means of the thermomechanical effect have been determined experimentally. The results are compared with theory. A brief description of a continuous-action double ray mass spectrographic gas analyzer is presented.

IN RECENT YEARS much work has been devoted to the experimental study of the properties of He^3 and its solutions in He^4. However the light helium isotope is interesting not only as a subject for investigation. Evaporation of liquid He^3 under evacuation makes it possible to obtain temperatures of the order of 0.3 – 0.4° K and thus to increase significantly the scale of low-temperature experiments.

At the present time the basic source of He^3 is tritium ($T_1^3 \rightarrow He_2^3 + \beta + \nu$, with a half-life of 12 years), a very expensive hydrogen isotope which is obtained in atomic reactors. It is known that He^3 is contained also in natural helium, which, however, practically worthless for obtaining anywhere near reasonable amounts[1,2] of He^3, since the concentration of the light isotope in the natural gas is extremely low, about 10^{-5} – 10^{-6} %. In working with He^3 – He^4 mixtures it is often necessary to extract the He^3 from mixtures containing no less than 0.01 – 0.1 % of the light isotope.

The extreme value of He^3 necessitates the fullest possible separation of the mixture even when small quantities of the original product limit the yield of He^3. Furthermore, the separation process should be sufficiently rapid, and this is particularly important when dealing with low concentrations. He^3 and He^4 have different boiling points, and in the liquid state the two isotopes are miscible in all respects.* Solutions of He^3 – He^4 have no azeotropic points[4]. Under these conditions rectification is the simplest and most convenient method for separation of the mixture, especially since the separation coefficient

$$\alpha = y(1-x)/x(1-y)$$

(y, x are the relative molar concentrations $He^3/(He^3 + He^4)$ in the vapor and the liquid, respectively), which characterizes the ideal degree of rectification, is very large: $\alpha = 3 - 7$ (Fig. 1).

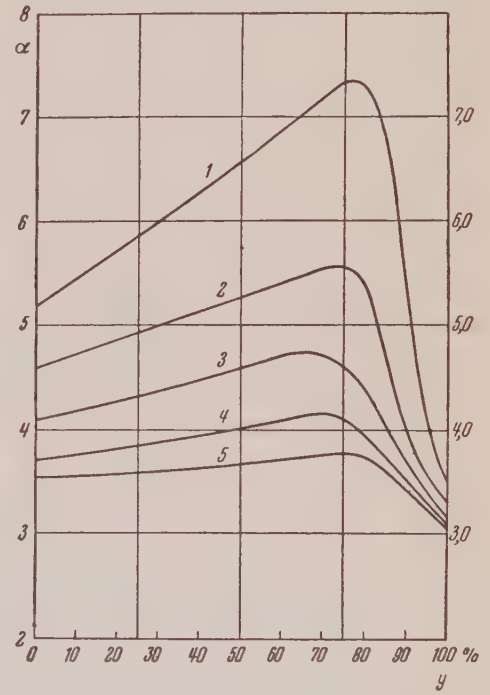

FIG. 1. The dependence of the separation coefficient α on the vapor concentration y for various pressures, calculated from experimental data[4,30].

There exist in addition many special methods for the separation of helium isotopes, which make use of the superfluidity of the He II in the solution. These involve enrichment with the aid of a thermal flux[2,5,6], conducting away the He^4 in a film[7,8], or through a thin filter[1,2] (thermo-osmosis). As is shown by experiment, the best results are obtained by thermo-osmosis, which makes possible reliable extraction of He^3 with sufficient output[1,2].

In the present work we investigate the fundamen-

*Below a temperature of 0.8° K, He^3 and He^4 are no longer mutually soluble[3].

tal results of an experimental study of the rectification and thermo-osmosis processes which are necessary for the calculation and effective use of rectification columns and filters.

RECTIFICATION

Experiments on rectification were conducted with an adiabatic column whose design is shown in Fig. 2. The column *1* itself (a 7.5 × 8 tube of stainless steel) consists of two sections, 3 and 4 cm long, filled with 2.5 mm rings of constantan wire 0.25 mm in diameter. Vapor intake *2* in the central part of the column, valve *3*, and tube *4* serve to draw off the mixture for analysis. Column chamber *5* is a copper cylinder externally heated by heater *6*. A resistance thermometer *7* made of phosphor bronze is wound on the side surface of the chamber. The chamber is filled with the mixture through coil 8. Column condenser *9* serves also as the bottom of upper bath *10* which can be filled through valve *12* by liquid helium from Dewar flask *11* (lower bath). The temperature of the condenser is regulated by the evacuation rate of the upper bath. The column itself is surrounded by a vacuum jacket *13* which, after the apparatus is assembled, is evacuated to a pressure of 10^{-3} mm Hg. The vapor is removed from the condenser by tube *14* and from the chamber through coil *8*. The glass parts of the apparatus (the upper bath and the upper part of the vacuum jacket) are joined to the metal by the copper-glass bonds *15*. Wire-mesh cone 16 supports the packing and improves the conditions for the entry of vapor into the column.

In the experiments on rectification, we determined the dependence of the vapor concentration y_l in the intake *2* as well as the vapor concentration y_u in the condenser on the pressure in the column at a constant heating rate of the chamber, and the dependence of y_l and y_u on the mass velocity of the vapor at a constant pressure in the column. All the experiments were performed on a mixture with an initial concentration y_0 of 2.6% under full reflux return (circulating system). Fig. 3 shows typical curves for y_l and y_u as functions of the pressure in the column at a constant vapor mass-velocity. For the calculations which follow we used smoothed out values for y_l and y_u (Tables 1 and 2). Since the liquid concentration in the chamber was no greater than $x = 0.2 - 0.3\%$ during the measurements, the vapor pressure in the column was assumed to be due to pure He^4, and on this basis the chamber temperature

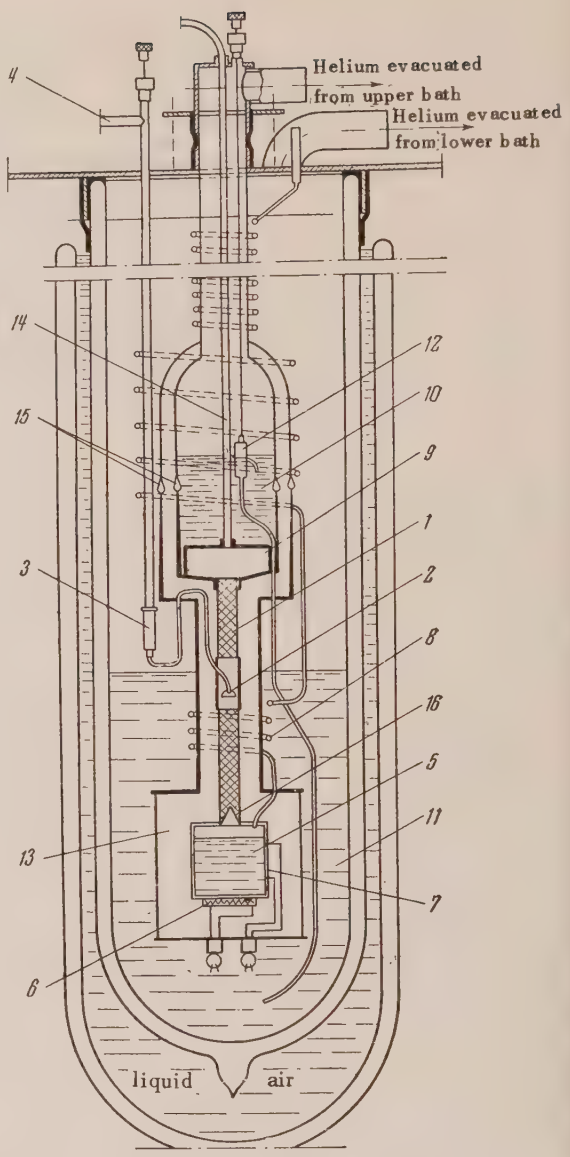

FIG. 2. Packed rectification column.

was determined.* The mass velocity U_M (measured in gm/cm²-sec) of the vapor for the total input (lower) cross section of the column was determined from the power output of the electric heater and the heat of vaporization[11] of He^4, and the Reynolds number Re corresponding to it was calculated from the usual relations

$$\mathrm{Re} = U_M d_e/\psi\eta \qquad (1)$$

$$d_e = 4\psi/f', \qquad (2)$$

*For the determination of temperature from the He^4 vapor pressure, 1949 tables were used in all cases[10].

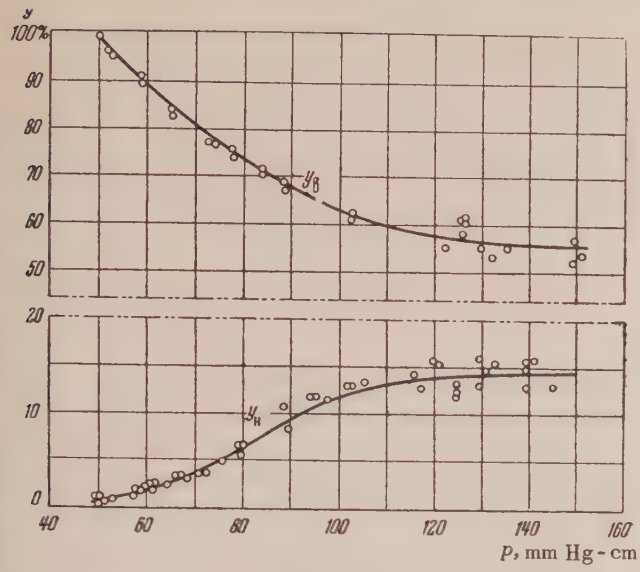

FIG. 3. The vapor concentration y_l in the intake and y_u in the condenser as functions of the pressure in the column at constant vapor mass-velocity.

where $d_e = 0.107$ cm is the equivalent diameter, $\psi = 0.811$ is the free volume of the packing (that fraction of the volume of the column which is not occupied by packing material), and f' is the area of the packing per cm³ of column. The magnitudes of ψ and f' are found from the weight of one cubic meter of dry, granular material and the geometry of the packing, and η is the viscosity. The measurements were performed with Re ranging from 35 to 175, which is essentially turbulent motion of the vapor [12].

The separation capacity of a column is usually characterized by the height of a transfer unit [13,14] Φ_0, given by

$$\Phi_0 = \frac{H}{\zeta} = H \Big/ \int_{y_l}^{y_u} \frac{dy}{y^* - y}, \qquad \int_{y_l}^{y_u} \frac{dy}{y^* - y} = \zeta, \tag{3}$$

where ζ is the number of transfer units, H is the length of the section of the filled column at whose ends the He³ concentration in the vapor is y_l and y_u, respectively, y is the vapor concentration at the core of the flow, and y^* is the vapor concentration which is equilibrium for the core of the liquid flow. The quantity $y^* - y$ is a measure of the diffusion pressure, so that Φ_0 is the height of a section of the column which gives an enrichment equal to the mean diffusion pressure in this section.

If the resistance to mass transfer in the liquid may be neglected, $y^* - y = y_i - y$ (where y_i is the vapor concentration in equilibrium with the liquid at the phase boundary), and

$$\Phi_0 = \Phi = H \Big/ \int_{y_l}^{y_u} \frac{dy}{y_i - y} = \frac{V}{k_g f},$$

where V is the volumetric rate of vapor production (in cm³/sec), k_g is the mass-transfer coefficient in the vapor (in cm/sec), and f is the packing surface per centimeter of column height. Using the mass-transfer equation in the form [15]

$$\mathrm{Nu}' = A\,\mathrm{Re}^m \mathrm{Pr}'^k \tag{4}$$

(where A is a constant, $\mathrm{Pr}' = \eta/\rho D$ is the Prandtl diffusion number for the vapor, D is the molecular diffusion coefficient, ρ is the vapor density, and

$$\mathrm{Nu}' = k_g d_e / D \tag{5}$$

is the Nusselt diffusion number), we arrive at [16]

$$\Phi = (\psi / f' A)\,\mathrm{Re}^{1-m}\,\mathrm{Pr}'^{1-k}. \tag{6}$$

An evaluation of the resistance to mass transfer in the vapor and liquid by Peshkov's method [17] shows that in the first approximation one may neglect the resistance in the liquid. This makes it possible to use Eq. (6). Bearing in mind, however, that Re depends only weakly on the pressure, Pr′ is practically constant, and*

$$\zeta = \frac{1}{\alpha - 1} \ln \frac{y_u (1 - y_l)}{y_l (1 - y_u)} + \ln \frac{1 - y_l}{1 - y_u}, \tag{7}$$

(which means that a very small change of α with pressure may cause a large change in $\alpha - 1$ and therefore in ζ), Eq. (6) should be written in the form

$$\Phi = (\psi / f' A)\,\mathrm{Re}^{1-m}\mathrm{Pr}'^{1-k} \varphi(p), \tag{8}$$

where $\varphi(p)$ is a function which accounts for the pressure-dependence of α.

The quantity $\Phi = \Phi_0$ was calculated by graphical integration of Eq. (3), with the aid of a graph of y *vs.* x (Fig. 4). The calculated height of the column

*Equation (7) is valid only for a circulating system with constant α.[14]

H was determined with the rectifying action of the condenser taken into account. As was shown by measurements of the vapor concentration in the chamber, in the center of the column, and in the condenser, all at the same state of operation, about 25% of the total number of transfer units (ζ) may be assigned to the condenser. The values of Φ obtained in this way for the packed part of the column satisfy the empirical equation

$$\Phi = 353\ \mathrm{Re}^{-1.03}\ \varphi(p). \qquad (9)$$

The values of $\varphi(p)$ are shown in Table 1. The accuracy of this equation, taking account of the spread in y_l and y_u, is ±20%. From Eq. (4) and (9) we obtain $\mathrm{Nu}' \sim \mathrm{Re}^{2.03}$. The exponent on Re usually[16] lies between 0.75 and 1.18. The stronger dependence is probably explained by the poorer distribution of the liquid through the packing at low thermal loads on the column[18].

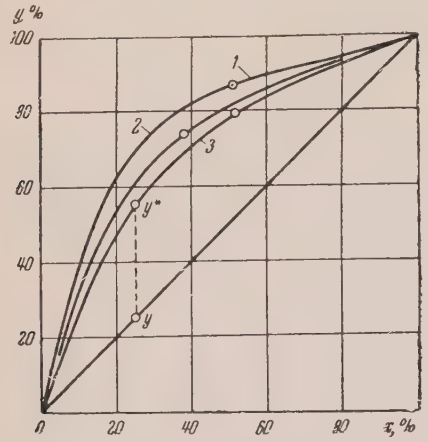

FIG. 4. Graph of y vs. x. Smoothed-out data is used[4,30]. *1)* $p = 50$, *2)* $p = 100$, *3)* $p = 150$ mm Hg.

TABLE I

Chamber temperature °K	Chamber pressure, mm Hg	y_l, %	y_u, %	ζ	Φ	Re	φ (p)
2.3	50	0.75	98.5	6.52	0.865	75.2	0.246
2.49	75	5.1	76.5	2.45	2.30	71.5	0.618
2.64	100	11.8	63.1	1.63	3.47	69.0	0.903
2.77	125	14.0	57.2	1.39	4.07	66.8	1.01
2.88	150	14.5	55.2	1.38	4.10	65.0	0.995

Note. The mass velocity was 0.00492 gm/cm²-sec.

In addition to the experimental determination of the separating capacity of the column, there exist several works[17,19,20] in which an analytic expression for the column efficiency is obtained by integration of the differential equations of mass transfer. Of particular interest are the results obtained by Peshkov[17], since they include many practically important cases.

For non-extracting operation, constant-velocity vapor motion throughout the column,* and no resistance in the liquid, y_l and y_u are related by[17]:

$$(1 - y_l)\, y_l^{-1/\alpha} = (1 - y_u) y_u^{-1/\alpha} e^{\beta H}, \qquad (10)$$

$$1/\beta = (|w|\, d_e^2/4 D_{\mathrm{eff}} 4\varkappa_y)\, \alpha/(\alpha - 1). \qquad (11)$$

Equation (10) is derived for an empty column. On going over to a packed column, the radius of the tube in Eq. (11) is replaced by $d_e/2$. In addition, Eq. (10) is strictly speaking valid for concentrations which have been averaged in a particular way over the cross section and velocities[17], although when the vapor motion is turbulent this averaging gives the values which are actually measured in experiment; here w is the velocity of the vapor averaged over the cross section (in cm/sec), $D_{\mathrm{eff}} = D + D_t$, where D_t is the coefficient of turbulent diffusion (in cm²/sec), the coefficient $\varkappa_y$ is defined by the equation[17]

$$\left|\left(\frac{\partial y}{\partial n}\right)_i\right| = 2\varkappa_y \frac{y_i - y}{d_e} \cdot 2, \qquad (12)$$

and n is the normal to the surface of phase separation. Since

$$k_g(y_i - y) = D_{\mathrm{eff}} \left|\left(\frac{\partial y}{\partial n}\right)_i\right|,$$

*At a condenser temperature of about 1.5 °K (almost pure He^3) and a chamber temperature of about 2.3 °K (almost pure He^4) the vapor velocity at the condenser is about 25% greater than at the bottom of the column, so that in the first approximation the constant-velocity condition is fulfilled.

Eq. (5) and (12) lead to

$$D_{\text{eff}} = \text{Nu}' D/4\varkappa_y. \tag{13}$$

Inserting (13) into (11) and making use of (4), (2), and (6), we obtain

$$1/\beta = \Phi\alpha/(\alpha - 1). \tag{14}$$

The values of $1/\beta$ as calculated according to Eq. (10) and (14) are sufficiently close (Fig. 5). The coefficients α necessary for the calculation were averaged according to Eq. (7).

In the case of extraction and when the molar vapor production rate remains constant along the column, we use the same initial equations and assumptions as in deriving Eq. (10) and (14), and obtain the following expression for the number of unit transfers:

$$\zeta = \frac{H}{\Phi} = \frac{\alpha}{\alpha - 1}\beta H = \frac{1}{2}\ln\frac{-(1-y_l)^2 + F(1-y_l) + M}{-(1-y_u)^2 + F(1-y_u) + M} + \frac{2G - F}{2\sqrt{4M + F^2}}\ln\left[\frac{-2(1-y_l) + F - \sqrt{4M+F^2}}{-2(1-y_l) + F + \sqrt{4M+F^2}} \cdot \frac{-2(1-y_u) + F + \sqrt{4M+F^2}}{-2(1-y_u) + F - \sqrt{4M+F^2}}\right], \tag{15}$$

where

$$F = \frac{(\alpha - 1)(1 - y_u\gamma) - \gamma}{\alpha - 1}; \quad G = \frac{\alpha(1-\gamma)}{\alpha - 1} + \gamma(1 - y_u);$$
$$M = (1 - y_u)\frac{\gamma}{\alpha - 1};$$

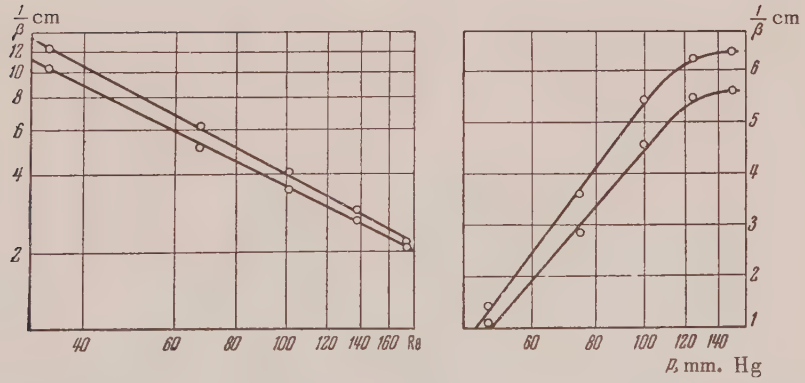

FIG. 5. Values of $1/\beta$ as calculated according to Eq. (10) (lower curve) and Eq. (14) (upper curve) for various pressures p in the column (Re = const) and various Re (p = const).

TABLE II

Chamber heating rate, watts	$10^2 U_M$ gm/cm^2-sec	y_l, %	y_u, %	ζ	Φ	Re
0.0259	0.25	23	46	0.7	8.05	34
0.0517	0.50	11.7	57	1.45	3.98	68
0.0777	0.75	4.0	65.2	2.29	2.46	102
0.104	1.0	1.1	70.5	2.92	1.93	136
0.130	1.25	0.2	73	3.73	1.51	171

Note. The column pressure is 125 mm Hg.

and γ is the fraction of the vapor stream in the column which is extracted. If $\gamma \leqslant 0.1$ and $1 - y_u \ll 1$, then $(\alpha - 1)/\alpha \geqslant 0.6$, and expanding $1/F$ in a power series in γ and neglecting terms of order γ^2 and higher, Eq. (15) leads to

$$\zeta = \frac{1}{2} \ln\left[\frac{(1-y_u)^2}{1-y_u}\left(\frac{y_l}{1-y_l} - \frac{\alpha}{\alpha-1}\gamma\right)\right] \quad (16)$$
$$+ \frac{\alpha^2 - 1 + 2\alpha\gamma}{2(\alpha-1)^2} \ln\left[\frac{y_u}{1-y_u}\left(\frac{y_l}{1-y_l} - \frac{\alpha}{\alpha-1}\gamma\right)^{-1}\right]$$

When $\gamma = 0$, Eqs. (15) and (16) reduce to (10).

In rectification of a $He^3 - He^4$ mixture the vapor production rate at the top of the column is greater than that at the bottom by a factor of about 2, assuming that the chamber contains pure He^4 and the condenser pure He^3. Therefore Eq. (15) and (16) can in this case be used only for a rough estimate.

If we increase the initial concentration y_0 of the mixture, we increase the allowable (*i.e.*, for given y_l, y_u, and U_M) extraction rate of the product (an increase of y_0 by 1.5 to 4% makes it possible to increase the extraction rate by a factor of 1.5 – 2), so that the column should be supplemented with an apparatus for the preliminary enrichment of the mixture to a y_0 value of several per cent. This is most easily done by thermo-osmosis.

To determine the maximum output of the column, one should find the critical vapor velocity, *i.e.*, the velocity at which the vapor begins to drag liquid along into the condenser (percolate).

It is known that for equal vapor velocity the pressure drop across a wet column is much greater than that across a dry one.

As has been shown by Kapitza[21], under certain definite conditions the wave motion of a thin film of viscous liquid is more stable than laminary motion. By taking account of the disruptions in the gas current flowing across the waving surface of the liquid, one is able not only to obtain a quantitative determination of the pressure drop in a wet tube, but also to calculate the critical vapor velocity in it with good accuracy. In general, the vapor mass-velocity at the moment of percolation (U_M^{cr}) depends[21] on the geometry of the column, the densities ρ and ρ_l of the vapor and liquid, the discharge of the liquid, its density η, and its surface tension. For the circulating state, a small temperature interval, and a given column diameter, the dependence is essentially $U_M^{cr} \sim (\rho/\rho_l)^n$, since the change of σ due to temperature is of little import ($U_M^{cr} \sim \sigma^{0.3}$), and the viscosity variation is even less ($U_M^{cr} \sim \eta^{0.2}$).

An investigation of percolation was carried out on a single-section column 200 mm long, similar design to the rectification column (Fig. 2). The moment of percolation was found from the different increases in the pressure difference between the chamber and condenser which accompanies small changes in the heating rate of the chamber. Measurements were performed both on pure He^4 and on a mixture ($y_0 = 2.6\%$). All calculations on percolation were performed for the total column cross section. From the chamber pressure p_c immediatedly before percolation, the chamber temperature T_c was found, and the ratio of the vapor to liquid densities (ρ/ρ_l) was calculated. In performing the calculation the modulus of compressibility of the vapor $Z = 1 + Bp_c/RT_c$ was accounted for, where B is the second virial coefficient of He^4 (in n. cm³/mole)[22]. For temperatures on the order of 2.8 – 2.9° K, the ideal gas equation gives too low a value for ρ (by 10 – 12%). Further, U_M^{cr} was calculated from the heater power and the heat of vaporization of He^4. With a statistical error no greater than ± (4 – 5%), both for the mixture and for pure He^4,

$$U_M^{cr} = 0{,}153\,(\rho/\rho_l)^{0{,}46},$$
$$0{,}013 \leqslant \rho/\rho_l \leqslant 0{,}033;\ T_c = 2{,}4 \div 3{,}0^\circ\,\mathrm{K}. \quad (17)$$

The slope of the U_M^{cr} curve as a function of ρ/ρ_l when calculated according to Kapitza's equation is close to the experimental value, so that this dependence for a packed column is the same as for a film column. A similar dependence is given by empirical equations presented in other works[23-25]. The amount of liquid trapped by the packing in the operation of the column is an important characteristic of the separation process. In periodic rectification, an increase of the ratio between the entrapment and the chamber content limits the output of the product and in many cases decreases the degree of separation[26]. The magnitude of the entrapment makes it possible to determine the incomplete product Π, that is the minimum amount of He^3 which must be in the column during its operation. In the circulating state[17] $\Pi = (S/H)\int_0^H y dH$, where S is the entrapment in the whole column; using Eq. (10) and (15) we obtain

$$\Pi = \frac{S}{\zeta}\left[\frac{\alpha}{\alpha-1}\ln\frac{1-y_l}{1-y_u} + \frac{1}{\alpha-1}(y_u - y_l)\right]. \quad (18)$$

In order to determine the entrapment (Fig. 2), a known amount of mixture (2.6%) was condensed in the chamber, and then the chamber heat supply was gradually increased until all the liquid was trapped by the packing. In this case the chamber content is equal to the entrapment and the heat supply and chamber temperature determine the vapor mass velocity at the bottom end of the column. The time at which the liquid left the chamber was fixed from the readings of resistance thermometer 7 (Fig 2) which was connected into a self-balancing bridge circuit based on the EPD-17 potentiometer.

An evaluation of the entrapment for various values of U_M in calculating the thickness of the liquid film uniformly covering the packing gives a quantity on the order of $(0.7 - 1) \cdot 10^{-2}$ cm for $U_M^{cr} = 0.005 - 0.02$ gm/cm²-sec.

THERMO-OSMOSIS

The apparatus for thermo-osmosis is shown in Fig. 6. Condenser 1 is soldered to filter 2 consisting of a copper tube of diameter 2×4 mm and length 4.5 cm tightly packed with crocus. The filter and upper bath are surrounded by a vacuum jacket which is evacuated through tube 3 during assembly of the apparatus. In experiments on the efficiency of thermo-osmosis the condenser was filled through tube 6 with a known quantity of a mixture of given concentration. Evacuation of the upper and lower baths was used to establish temperatures at the end of the filter such that the He^4 in the solution was superfluid[2]. Calibrated collector 5 was then filled through tube 7 with gaseous He^4 to the equilibrium pressure, thus improving[2] the He^3 extraction from the solution. When valve 4 was opened, the superfluid helium flows into collector 5, and the He^3 concentration in the condenser gradually increases. The calculated enrichment coefficient of the filter $\delta = x/x_0$ (where x and x_0 are the liquid concentrations in the condenser and collector, respectively) is on the order of[2] $10^4 - 10^6$ (complete separation is not obtained, since He^3 penetrates through the filter due to diffusion in the liquid). Measurements show that δ is in any case greater than 500. After closing valve 4 the enriched remainder was pumped into a graduated gas holder, and as a control its concentration was measured in a mass-spectrographic gas analyzer. From the known initial and final mixture concentrations and volumes, as well as from the amount of liquid in the container at a time τ, the concentration of the mixture in the condenser was

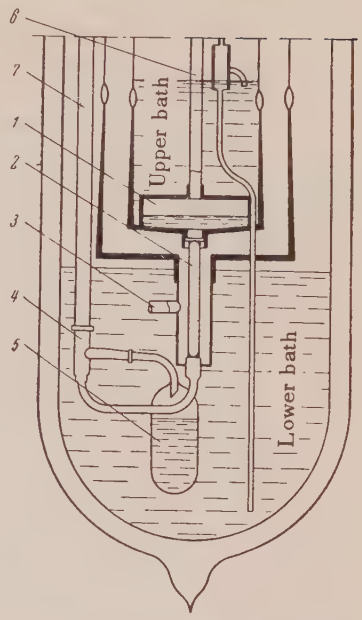

FIG. 6. Thermo-osmosis apparatus

calculated for given τ. The concentration of the liquid was calculated on the basis of the distrubution coefficients y/x as given by Esel'son and Berezniak[4], and the vapor volume of the condenser. The output Q (in l/he) of the filter is calculated from the rate at which the collector is filled. The results obtained are shown in Fig. 7. For a given filter output and condenser temperature, the enrichment is greater for greater temperature between the ends of the filter. Qualitatively speaking, the temperature dependence of the enrichment is of the same form also for equilibrium, that is when the total discharge of liquid through the filter vanishes. The equilibrium values of x have been calculated previously[2]. Since the output decreases rapidly as x increases, the use of thermo-osmosis at concentrations greater than 4 – 5% is not worthwhile.

MASS SPECTROGRAPHIC GAS ANALYZER (MG)

The gas analyzer is based on the PTI-4 helium leak-detector, and is a double-ray mass spectrograph with 180° deflection and separate amplification circuits for the He^3 and He^4 ion currents. The MG can be used for continuous analysis of a gas mixture in the concentration range between 0.2% for $He^3/(He^3 + He^4)$ and 0.2% for $He^4/(He^3 + He^4)$ with an accuracy of ± 5% of the measured quantity. Unlike Nier's[27,28] double-ray instrument and the domestic[29] MS-2M, the gas analyzer has a pulsating ion

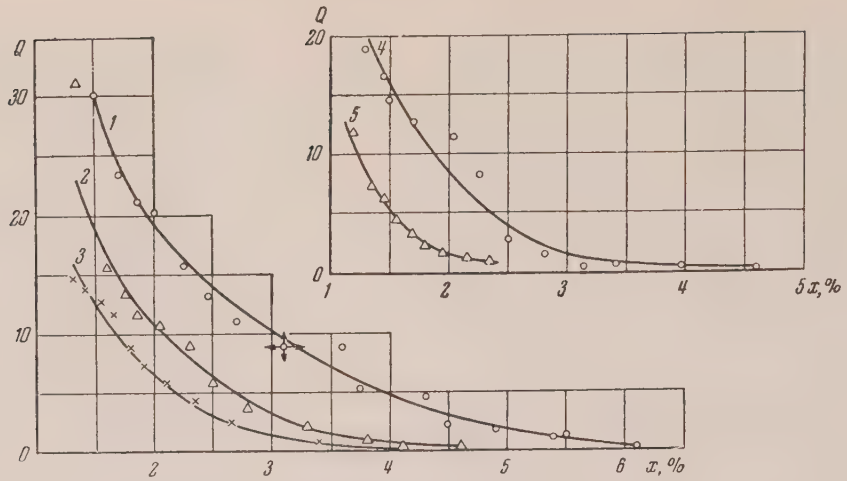

FIG. 7. The dependence of the filter output Q on the concentration of the liquid being enriched at various temperatures. Curve *1)* 1.43° (solution) – 2.15° (He^4 collector); Curve *2)* 1.43 – 2.02° K; Curve *3)* 1.43 – 1.86° K; Curve *4)* 1.86 – 2.15° K; Curve *5)* 1.86 – 2.02° K.

current and ac amplification. The method for obtaining an ac voltage on the collector is the same as in the leak detector. The construction of the ion source (cathode *1* and ionizer *2*, Fig. 8) is not changed. Between the ionizer and the exit slit *4* is an accelerating diaphragm *3* (with a slit of about 0.2 mm). The radii of the ion trajectories are 3.5 cm for He^{3+} and 4 cm for He^{4+}. The distance between the slit centers of the collector diaphragm *5* is about 10 mm. In the vacuum chamber of the MG are placed two acorn-tube electrometer stages 6Zh1Zh connected as triodes. The grid-leak resistors (5×10^8 ohm) are the same for both tubes. The signals from the electrometer stages are fed into ac amplifiers (the He^4 circuit uses the amplifier of the leak detector) and are then rectified. The maximum current gain, found from the ratio between the output dc current and the effective current in the input resistance of the acorn tubes, is about 5×10^8. An electronic potentiometer EPD-17 is used to measure the ratio of the ion currents: voltages proportional to the output currents of the amplifiers are applied, with opposite polarity, to the input of the potentiometer amplifier (the output current of the He^4 circuit flows along the EPD-17 slide wire). When so connected, the apparatus gives the ion current ratio, or the molar concentration of the mixture in terms of He^3/He^4.

Different ranges of measurement are obtained by switches which change the ratio of the gains of the amplifiers from 1 to 100. In order to test the amplifiers, an ac voltage from a PTI-4 generator can be applied to the input of the electrometer stages.

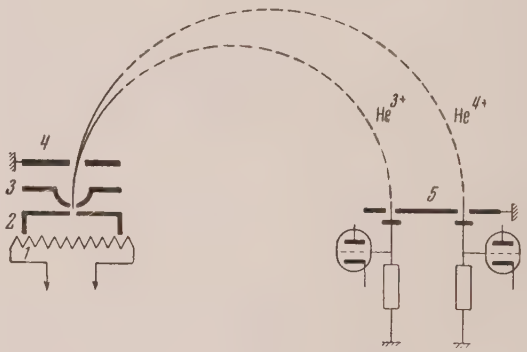

FIG. 8. Gas-analyzer vacuum chamber. The potential of cathode *1* and diaphragm *3* is +220 v, that of ionizer *2* is $U_{dc} + U_{ac} = 316 + 21$ v.

Under continuous analysis the gas consumption is 0.1 – 0.2 cm^3/hr. During measurement, the gas pressure ahead of the input valve (PTI-4 throttle valve) is no greater than 20 – 30 mm Hg, and the gas input is easily regulated; the readings of the apparatus do not depend on the gas pressure ahead of the valve within the limits of accuracy of the analysis. The background of HHH^+ ions is between 0.03 and 0.04% of the He^3 after a half hour of cathode heating. In order to obtain readings relative to zero concentration, regulation of the output current in the He^3 circuit is provided for while the ratio between the amplification factors is held constant. The resolving power of the mass spectrograph (with a maximum half-width of about 12) and the shape of the ion beams make it possible, in principle, to increase the sensitivity of the apparatus by a factor of at least 3 – 4.

CONCLUSIONS

A combination of thermo-osmosis and rectification is a simple and effective method for extracting He^3 from a mixture. The filter used in thermo-osmosis is easily connected to the column so that the whole apparatus can be placed into a single cryostat[2].

The results of the present work show that a packed column 8 – 10 cm long makes it possible to obtain practically pure He^3 when dealing with a mixture containing only 1 – 2% of the light isotope. Using a column from 7 – 8 mm in diameter, the He^3 extraction rate under these conditions may be as great as 8 – 10 l/hr. The amount of the incomplete product is then of the order of 200 – 300 cm^3 of He^3. However, successive rectification of the remainder at lower heating rates of the column makes it possible to decrease the amount of the incomplete product substantially.

For the column and filter together, the total coefficient of enrichment is of the order of $10^5 - 10^6$.

Several expressions have been obtained for the calculation of the rectification process with turbulent motion of the vapor in the column, and the dependence of the filter output on the concentration of the mixture to be enriched has been determined.

In order to study the separation processes, a double-ray mass spectrographic gas analyzer has been constructed, and in spite of its relatively simple design it can be used to obtain sufficiently accurate measurements of the concentrations in various mixtures.

The author expresses his deep gratitude to M. P. Malkov, V. P. Peshkov, A. G. Zel'dovich and N. E. Alekseev for very valuable advice and comments.

[1] B. N. Esel'son and B. G. Lazarev, J. Exptl. Theoret. Phys. (U.S.S.R.) **20**, 743 (1950).

[2] V. P. Peshkov, J. Exptl. Theoret. Phys. (U.S.S.R.) **30**, 850 (1956), Soviet Physics JETP **3**, 706 (1956).

[3] W. M. Fairbank, Phys. Rev. **103**, 262 (1956).

[4] B. N. Esel'son and N. T. Berezniak, J. Exptl. Theoret. Phys. (U.S.S.R.) **30**, 628 (1956), Soviet Physics JETP **3**, 568 (1956).

[5] Lane, Fairbank, Aldrich, and Nier, Phys. Rev. **73**, 256 (1948).

[6] Reynolds, Fairbank, Lane, McInteer, and Nier, Phys. Rev. **76**, 64 (1949).

[7] Daunt, Probst, Jonston, Adrich, and Nier, Phys. Rev. **72**, 502 (1947).

[8] Esel'son, Lazarev, and Lifshitz, J. Exptl. Theoret. Phys. (U.S.S.R.) **20**, 749 (1950).

[9] K. Atkins and J. R. Lovejoy, Canad. Journ. of Phys. **32**, 702 (1954).

[10] H. van Dijk and D. Shoenberg, Nature **164**, 151 (1949).

[11] W. Keesom, *Helium*, IIL, 149 (a translation of a book published by Elsevier Publishing Co., N. Y., 1942).

[12] *Processes and Apparatus in Chemical Engineering*, ed, A. G. Kasatkin, Goskhimizdat, 1953, p. 48.

[13] T. H. Chilton and A. P. Coburn, Ind. Eng. Chem. **26**, 1183 (1934).

[14] T. H. Chilton and A. P. Colburn, Ind. Eng. Chem **27**, 255 (1935).

[15] D. A. Frank-Kamenetskii, *Diffusion and Heat Transfer in Chemical Kinetics*, Publ. Acad. Sci. U.S.S.R., 1947, p. 41.

[16] I. P. Usiukin and L. S. Aksel'rod, Kislorod (Oxygen) **3**, 1 (1952).

[17] K. P. Peshkov, J. Tech. Phys. (U.S.S.R.) **26**, 664 (1956).

[18] D. W. Dunkan, J. H. Koffolt, J. R. Withrow, Trans. Am. Inst. Chem. Engrs. **38**, 259 (1942).

[19] W. Kuhn, Helv. Chim. Acta **25**, 252 (1942); **37**, 1407 (1954).

[20] J. M. Westhaver, Ind. Eng. Chem. **34**, 126 (1942).

[21] P. L. Kapitza, J. Exptl. Theoret. Phys. (U.S.S.R.) **18**, (1948).

[22] Kilpatrick, Keller, and Hammel, Phys. Rev. **94**, 1103 (1954).

[23] M. P. Malkov and K. F. Pavlov, *Very Low Temperature Handbook*, Gostekhizdat, 1947, p. 227.

[24] N. M. Zhavoronkov, Chemical Industry **2-3**, 12 (1947).

[25] C. S. Robinson and E. R. Gilliland, *Elements of Fractional Distillation*, 4th ed. McGraw-Hill Book Co. (1950), p. 440.

[26] *Distillation*, (Ed. American edition, A. Weisberg) IIL, 1954, pp. 126, 130.

[27] Nier, Ney, and Inghram, Rev. Sci. Instr. **18**, 749 (1947).

[28] A. O. Nier, Rev. Sci. Instr. **18**, 398 (1947).

[29] Trans. (Trudy) of Sci. Res. Inst. of the Radio Industry, Gosenergoizdat 4, (24), 1955, p. 26.

[30] V. P. Peshkov and V. N. Kachinskii, J. Exptl. Theoret. Phys. (U.S.S.R.) **31**, 720 (1956), Soviet Physics JETP **4**, 607 (1957).

Translated by E. J. Saletan
217

The Photoconductivity of Cuprite

A. N. KRONGAUZ, V. K. LIAPIDEVSKII, AND IU. S. DEEV
National Institute of Roentgenology and Radiology

(Submitted to JETP editor June 15, 1956; re-submitted after revision February 9, 1957)
J. Exptl. Theoret. Phys. (U.S.S.R.) 32, 1012-1017 (May, 1957)

A further investigation has been carried out on the photoconductivity of cuprite under various conditions of illumination. The kinetics of photoconductivity have been studied at various field strengths and light intensities by a "light probe" method. Investigations of the temperature dependence of photoconductivity indicate the presence of a peak of negative as well as positive photoconductivity. The combined action of various types of radiation on the photoconductivity has been studied, and it has been found that the nature of the observed effects depends on the sequence of the illumination processes.

IN A PREVIOUS PUBLICATION[1] the authors studied the effects of field strength and illumination intensity upon the negative photoconductivity of the mineral cuprite. Further work has now been done to study more fully this negative photoconductivity and the conditions under which it arises.

The studies were carried out on single crystals of cuprite whose structure was verified by Debye patterns taken in an X-ray camera using an X-ray tube with a copper anode. Comparison of these measurements with the data in the literature gave very good agreement (measured $a = 4.258$ A; literature value, $a = 4.252$ A).* The measuring circuit is shown in Fig. 1. Light from an incandescent or mercury lamp S is passed through a monochromator with quartz optics, and focussed on the Cu_2O crystal in the form of a narrow ribbon parallel to the electrodes. By reversing the sign of the voltage applied to the crystal, without changing the position of the light beam, it was possible to apply the illumination to either the positive or the negative electrode region.

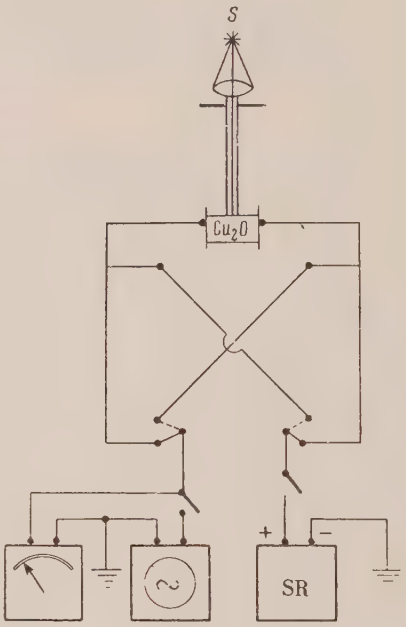

FIG. 1. Diagram of the measuring apparatus.

Since cuprite crystals show both positive and negative photoconductivity in different parts of the spectrum, experiments were carried out to study the spectral distribution of the photoconductivity of cuprite. Typical curves showing the dependence of photoconductivity on the wavelength of the incident light are shown in Fig. 2. The curves have been reduced to constant incident energy. The maximum negative photoconductivity is generally found in the long-wave region of the spectrum ($\lambda = 6400$ A) and the maximum positive photoconductivity in the short-wave region ($\lambda = 4200$ A). From the curves it is evident that the relative magnitudes of the negative and positive photoconductivity depend upon the location of the light probe with respect to the electrodes.

It has been shown previously that as the light intensity is increased, the negative photoconductivity increases, attains a maximum, and then begins to decrease, changing over to positive photoconductivity at a point which depends on the voltage applied to the crystal. With increasing applied

*The X-ray structure analysis was carried out at the Giredmet (State Inst. of Rare Metals) in the laboratory of Prof. G. F. Komovskii.

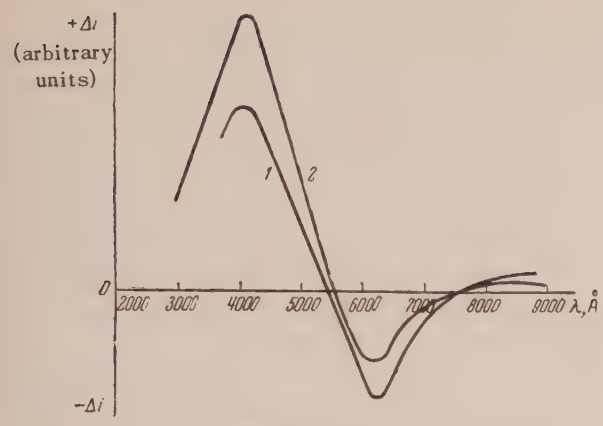

FIG. 2. Spectral distribution of photoconductivity in cuprite for low light intensity. *1*—region of positive electrode (+700 v) illuminated. *2*—region of negative electrode (—700 v) illuminated.

voltage, the transition point shifts to a more intense illumination. The dependence of negative photoconductivity on the intensity of illumination is shown in Fig. 3.

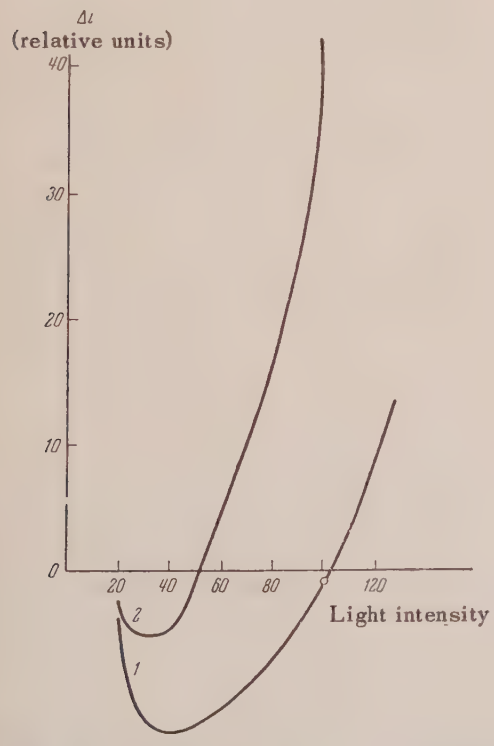

FIG. 3. Dependence of negative photoconductivity on light intensity (λ = 6400 A). *1*—region of positive electrode (+700 v) illuminated. *2*—region of negative electrode (—700 v) illuminated.

When studying the spectral distribution of photoconductivity in cuprite, one must take into account the fact that the relative magnitude of the effects, and even their sign, depend upon the experimental conditions; in particular, they depend to a marked degree upon the conditions of illumination. The spectral distribution curves shown in Fig. 4 were taken at high light intensity. Comparison of these

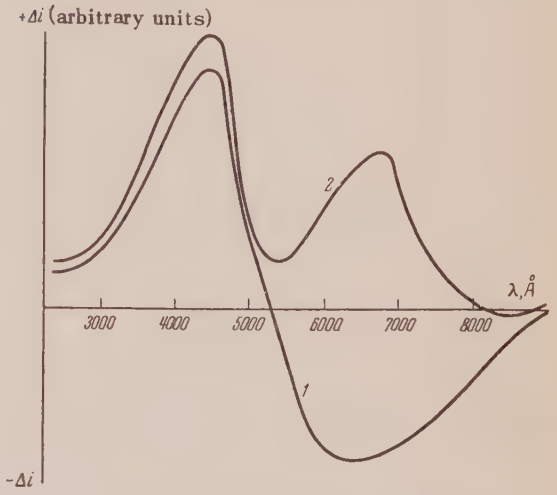

FIG. 4. Spectral distribution of photoconductivity in cuprite at high light intensity. *1*—region of positive electrode (+700 v) illuminated. *2*—region of negative electrode (—700 v) illuminated.

curves with those of Fig. 2 shows that a mere change in light intensity is all it takes to alter the whole character of the spectral distribution. A change in the voltage applied to the crystal can also produce a change in the nature of the spectral curves, since the negative photoconductivity changes more rapidly with field intensity than does the positive (Fig. 5).

When the strip of light producing the negative photoconductivity was moved from the cathode toward the anode, it was observed that the magnitude of the negative photoconductivity increased. If the crystal was illuminated with light which gave positive photoconductivity, the same direction of movement of the light probe gave a decreased positive photoconductivity. This effect was independent of the orientation of the crystal with respect to the electrodes.

Because of the effect of wavelengths and the polarity of the illuminated region of the crystal upon the magnitude, sign and character of the photoconductivity, all further observations were made under conditions which ensured a peak value of photoconductivity, namely: for negative photoconductivity,

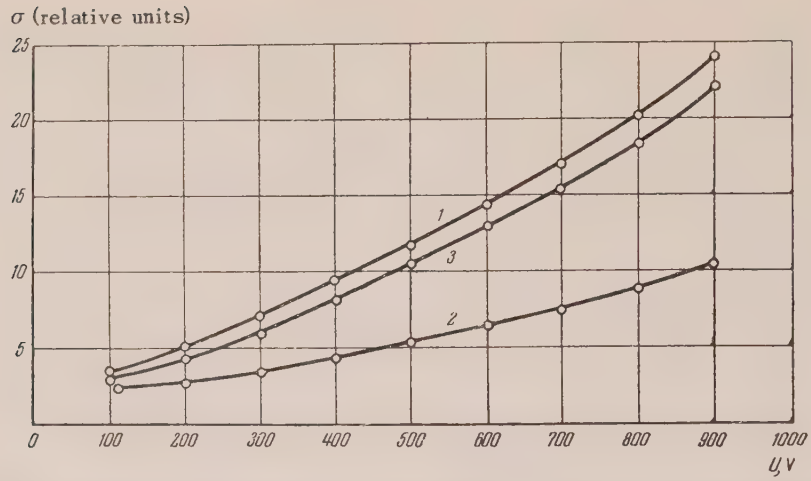

FIG. 5. Dependence of negative and positive photoconductivity of cuprite on the voltage applied to the crystal. *1*–λ = 4200 A; *2*–λ = 6400 A; *3*–dark.

light of wavelength λ = 6400 A applied to a region of the crystal adjacent to the positive electrode; and for positive photoconductivity, λ = 4200 A applied to the negative electrode region.

The time dependence of the negative photoconductivity produced when a region of the crystal in the neighborhood of the positive electrode is illuminated with low-intensity light of 6400 A wavelength is shown in the oscillogram of Fig. 6. When the direction of the electric field is reversed, so that the illuminated region of the crystal is near the negative electrode, it is evident from this figure that the negative photoconductivity is noticeably less than when the positive electrode region is illuminated.

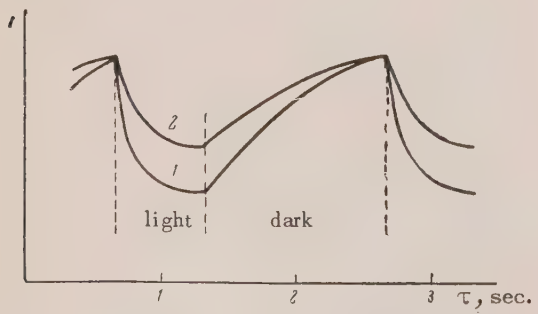

FIG. 6. Oscillogram of current flowing through the crystal. Light of wavelength 6400 A at low intensity applied to positive electrode region (*1*), and negative electrode region (2).

The oscilloscope traces obtained with high illumination (Fig. 7) seem to be the result of a superposition of both positive and negative photoconductivity. A further increase of light intensity leads to a growth of the positive photoconductivity and the complete disappearance of the negative effect.

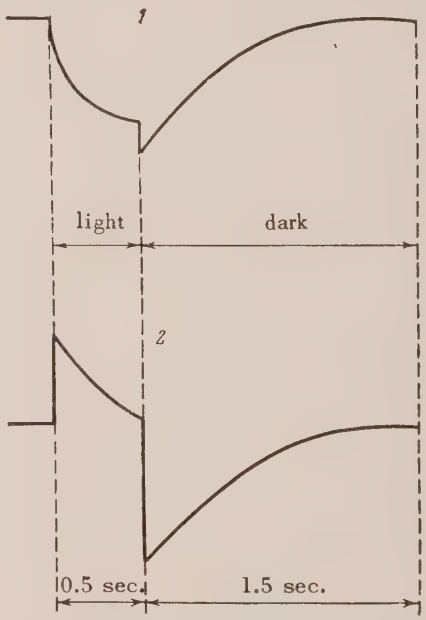

FIG. 7. Oscillogram of current flowing through the crystal for high intensity light of wavelength 6400 A, applied to the positive electrode region (*1*), and to the negative electrode region (*2*).

The observed difference between the magnitudes of the positive and negative photoconductivities produced by illuminating the positive and negative electrode regions indicates that the current carriers are of both signs. Negative photoconductivity is caused by the recombination of the dark-current carriers (holes) with the photo-current carriers,

leading to a decrease in the number of positive carriers (holes). The positive photoconductivity is basically due to the increased number of electrons.

Studies of the temperature dependence of photoconductivity have shown that at higher temperatures both the positive (Fig. 8) and negative (Fig. 9) photoconductivities increase, passing through a maximum. Upon raising the temperature higher than this, the photoconductivity drops off, although the dark current continues to increase. When a crystal which has been heated to 100° C is cooled, its original properties are recovered. However, if the cooled crystal is immediately re-heated to 100°, the temperature dependence of photoconductivity has quite a different character (Curve 2 of Fig. 8).

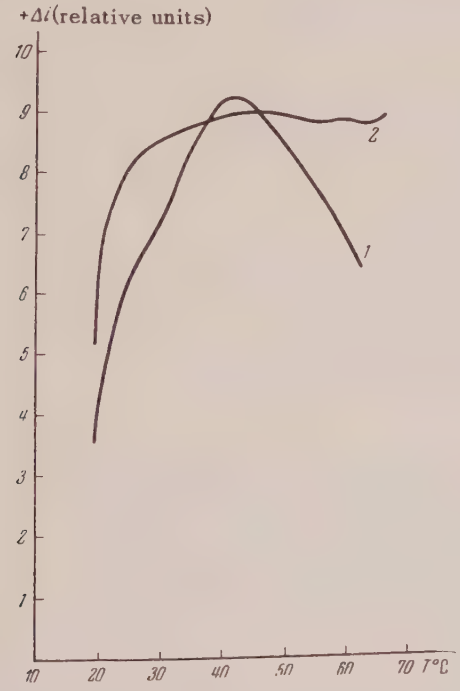

FIG. 8. Dependence of positive photoconductivity on temperature. Curve 2 was measured immediately after a preliminary heating of the crystal.

Heating the crystal to 200°C leads to a complete disappearance of the negative photoconductivity, which is not re-established upon cooling to room temperature. The positive photoconductivity does recover after cooling, but there is a considerable drop in the dark conductivity.

We have studied the effect of overall illumination on the photoconductivity of cuprite. If we apply a beam of red light, of intensity required to give the maximum negative photoconductivity n_1 and then a general illumination of blue light which by itself would give a positive photoconductivity n_2, the resulting effect is $n_1 + n_2$. On the other hand, if a general red illumination is applied to a crystal together with a blue beam, its photoconductivity does not change from the value n_1 due to the beam alone.

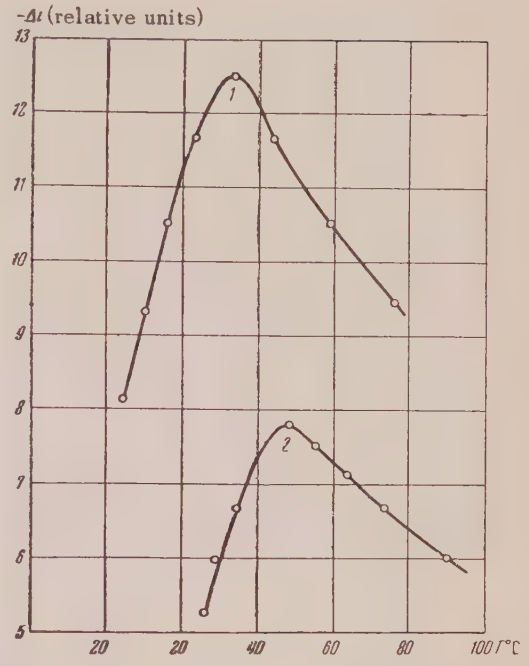

FIG. 9. Dependence of negative photoconductivity on temperature. *1*– $U = 1000$ v. *2*– $U = 700$ v.

When the cuprite crystal is irradiated with X-rays[2], the same basic phenomena of negative photoconductivity are observed as in the case of visible light. The irradiation of the crystal with an X-ray beam was carried out using an X-ray tube with a beryllium window, giving a high intensity of soft radiation. For a potential of 50 kv and a plate current of 20 ma, the intensity at the exit window was 30,000 roentgens/min. Upon irradiating the crystal it was observed that as the X-ray tube voltage was raised, the negative photoconductivity also increased. Increasing the anode current above a certain value, while at the same time keeping the voltage constant, had no effect on the negative photoconductivity. These effects are possibly caused by saturation of the negative photoconductivity in the relatively thin layer of cuprite where practically all of the soft X-rays are absorbed. In this case the increased intensity of irradiation due to the increased anode current would not increase the negative photoconductivity, and further increases in intensity might even lead to a decrease. When the voltage applied

to the X-ray tube is raised, the rays can penetrate deeper into the crystal and consequently affect a larger volume of the semiconductor, so that we observe a larger value of the negative photoconductivity.

When X-rays and visible light are both applied, the observed effects depend on the order of application. When X-rays are applied to a crystal which is already illuminated with visible light so as to give a maximum of negative photoconductivity, we observe a decrease in the negative photoconductivity, or even the appearance of a positive effect. When visible light is applied to a crystal already irradiated with X-rays, we observe an increase in the negative photoconductivity. A satisfactory simple explanation of these observations is obtained if we assume that visible light is absorbed throughout the whole volume of the crystal, while the soft X-rays are absorbed only in a very thin layer. If the X-ray and visible radiation are both sufficiently intense to produce saturation of their individual negative photoconductivities—the visible light in the whole crystal, and the X-rays in their own thin layer—then the addition of X-rays to light and light to X-rays must lead to different effects, as is actually observed.

[1] A. N. Krongauz and V. K. Liapidevskii, J. Exptl. Theoret. Phys. (U.S.S.R.) **26**, 115 (1954).

[2] A. N. Krongauz, *Studies in X-ray Technique*, Medgiz (1955).

Translated by D. C. West
218

SOVIET PHYSICS JETP VOLUME 5, NUMBER 5 DECEMBER, 1957

The Alpha Decay of Pu^{239}

G. I. NOVIKOVA, L. N. KONDRAT'EV, IU. P. SOBOLEV, AND D. L. GOL'DIN

(Submitted to JETP editor February 13, 1957)
J. Exptl. Theoret. Phys. (U.S.S.R.) **32**, 1018-1021 (May, 1957)

The α-spectrum of Pu^{239} has been investigated. Three new lines with energies 5064 ± 2, 4999 ± 5 and 4917 ± 5 kev and intensities (0.037 ± 0.005), (0.013 ± 0.005), and (0.005 ± 0.002) percent have been detected. It is shown that the principal α-line of Pu^{239} is related to the decay to an excited level of U^{235} having a spin of ½. Three previously detected lines and two of the newly detected lines belong to the rotational band of this level. The existence of a metastable state of U^{235} with an excitation energy of ~ 3 kev is predicted. A doublet splitting parameter equal to $a = -0.276$ has been found.

THE PRINCIPAL LINES in the α-spectrum of Pu^{239} are well-known[1,2]. These lines have energies 5.147, 5.134 and 5.096 Mev. The intensities of the corresponding transitions are 72, 16.8 and 10.7 percent. From the data presented it is seen that the transition to the lowest of the known levels takes place with great probability. The decay coefficient for this transition is equal to 0.3 (*cf.* Ref. 3), *i.e.*, this transition is allowed. As is known, the spin of the nucleus must not change in an allowed transition. Direct measurements of the spins lead however to $I = ½$ for Pu^{239} [4] and to $I = 7/2$ for the daughter nucleus U^{235} [5]. Such difference in spins of the ground states of the parent and daughter nuclei made it necessary to assume[6] that the most intense transition is not to the ground state of U^{235}.

This hypothesis received supporting evidence in experiments on Coulomb excitation[7,8]. The Coulomb excitation of the U^{235} nucleus has led to the observation of a system of levels starting naturally from the ground state of U^{235} and having nothing in common with the levels observed in the α-decay of Pu^{239} (see the level scheme below).

Bohr, Froman and Mottelson[3] have stated the hypothesis that the lowest most intense level known from α-decay has $I = ½$ and is the first level starting the rotational spectrum.

As is known, the excitation energy for the rotational levels with $K = ½$ are determined from the two-parameter formula suggested by Bohr[9]

$$E_{rot} = (\hbar^2/2J)\,[I\,(I+1) + a\,(-1)^{I+1/2}\,(I+1/2) - 3/4 - a]. \quad (1)$$

Assuming that the levels with excitation energies of 13.2 and 52 kev have spins ½ and ⅝, Bohr, Froman and Mottelson have computed, according to formula (1), the excitation energy of the next level with spin ⅞. It turned out to be equal to 83 kev.

The investigation of $\gamma - \gamma$ coincidences in the decay of Pu^{239} carried out by Asaro's group (see reference given in Ref. 10) did not confirm the existence of a level with such an excitation energy in the α-spectrum of plutonium. From the data obtained by this group it was concluded that the levels present have energies 172, 379, and 430 kev and α-decay intensities 0.02, 0.006 and 0.006 percent (see the level diagram). It is not difficult to convince oneself that these levels do not fit into the rotational system predicted by Bohr.

We carried out an investigation of the alpha spectrum of Pu^{239} with the help of a magnetic alpha-spectrometer[11] in the energy region 4.850–5.120 Mev. The measurements were carried out with a source, prepared by vacuum evaporation of the element, and containing Pu^{239} and Pu^{240} in ratio 100 : 0.7*.

The alpha spectrum in the energy region from 5.025 to 5.120 Mev is shown in Fig. 1, and displays clearly a line corresponding to an 84-kev level. The intensity of this line is only equal to (0.037 ±0.005) percent.† In order to resolve a line with such an intensity at a distance of ~ 30 kev from a line with an intensity 300 times larger, it was necessary to consider very carefully the choice of the optimal thickness of the source. The half width of our peak was ~ 13 kev.

Figure 2 shows a plot of the spectrum in the 4.850–5.080 Mev region taken with another source of greater intensity. The peak related to the 84-kev level is hardly noticeable here. However, an α-line corresponding to a level with excitation energy of 151 kev appears clearly. The intensity of the transition is (0.013 ±0.005) percent. A small part of the intensity of this line comes from the 4^+ level of Pu^{240} (the energy of this level and the intensity

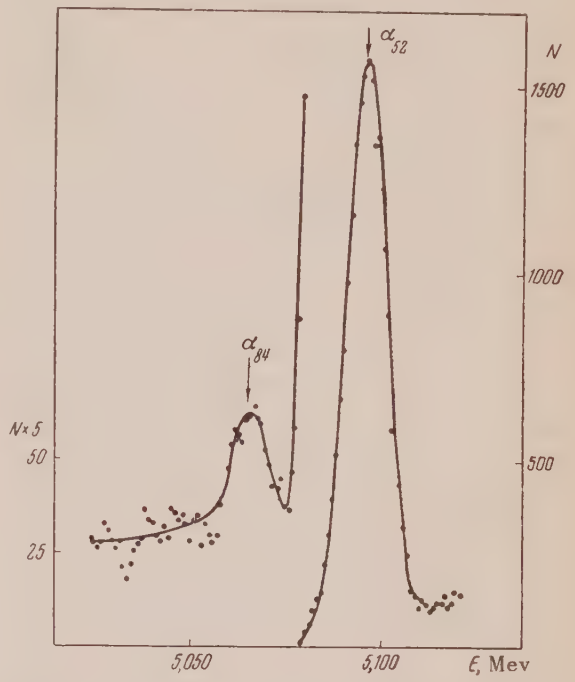

FIG. 1. The alpha spectrum of Pu^{239} in the 5.025–5.120 Mev region.

of the corresponding transition are well known[12]). The corrected curve is shown dashed.

It is not difficult to calculate, from Eq. (1), that the excitation energy of the level belonging to the rotational band with $K = ½$ and having $I = ⅝$ is 153 kev, that is, that it coincides with the energy of the level observed by us. The level with 171 kev energy and 0.02 percent intensity, indicated in Ref. 9, was not observed by us. If this level does exist, its intensity is in any case less than 0.005 percent.

The energies of five consecutive levels are thus well described by Eq. (1). Therefore the lowest level has indeed a spin ½ and is the first of the evolved system of rotational levels with $K = ½$ (see Fig. 3).

From the separation of the levels it is possible to calculate the ground state characteristics of the nucleus: $\hbar^2/2J = 6.1$ kev and $a = -0.276$ [see Eq. (1)].

A line with 0.005 percent intensity, 230 kev away from the most intense line, is also seen on Fig. 2. This line does not fit into the rotational scheme. One should mention that this line cannot be attributed to any admixture of a known α-active isotope in the material used to prepare the source. It re-

*The Pu^{240} content was determined by a mass spectroscopic method using a double isotope source.

†Bohr predicted an intensity ten times larger for this level.

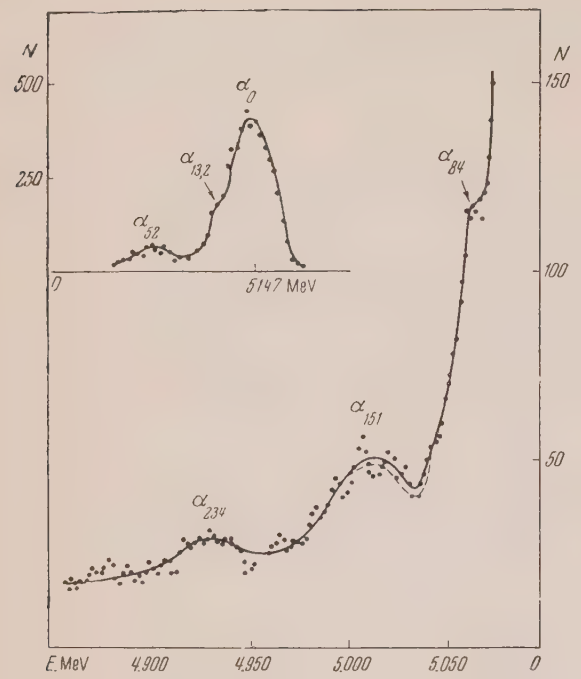

FIG. 2. The alpha-spectrum of Pu^{239} in the 4.850–5.080 Mev region.

mains to assume that this line corresponds to a single transition to a U^{235} level with 234 kev excitation energy.

Data on the investigation of γ-rays observed in the α-decay of Pu^{239} are shown in the work of Refs. 13–17. Several of the known γ-rays (E_γ = 39, 53 and 100 kev) fit in well with the U^{235} level scheme; however, it is not yet possible to find corresponding transitions in this scheme for several of these γ-rays (for instance, with E_γ = 124 kev).

Shliagin[17], studying the decay of Pu^{239}, observed a very intense group of conversion electrons with an energy of approximately 2 kev. However the interpretation of these electrons proposed by him seems rather unconvincing to us. We think that this group of electrons is related to the γ-rays corresponding to the transition of the lowest level of the rotational band with $I = 1/2$ to the ground state of U^{235} with $I = 7/2$.

Returning to the system of rotational levels in the α-spectrum of Pu^{239} (see Fig. 3) it is necessary to note the regularity which appears in the intensities of these levels.

The intensities of the transitions to states with $I = 3/2$ and $I = 5/2$ differ little from each other but are 5–7 times smaller than the intensity of the transition to the $I = 1/2$ level. The intensities of the transitions to the $I = 7/2$ and $I = 9/2$ levels again differ little from each other but they are several hundred times less intense than the transitions to to the two levels mentioned earlier.

From the doublet structure one can deduce that the α-particles corresponding to the transition between the ground state of Pu^{239} and the $I = 1/2$ level of U^{235} carry off $l = 0$, which means that the ground state of Pu^{239} and the lowest level of the rotational band have the same parity (which confirms also the large value of the decay coefficient for this transition). The transitions to the levels with energies 13.2 and 52 kev take place with $l = 2$, while the transitions to levels with energies 84 and 151 kev involve $l = 4$. It is interesting to note that the wide separation of the doublets (the 13.2-kev level, for instance, is closer to the ground state than to its pair member level with 52-kev energy) does not disturb the pronounced doublet character of the intensity of the lines.

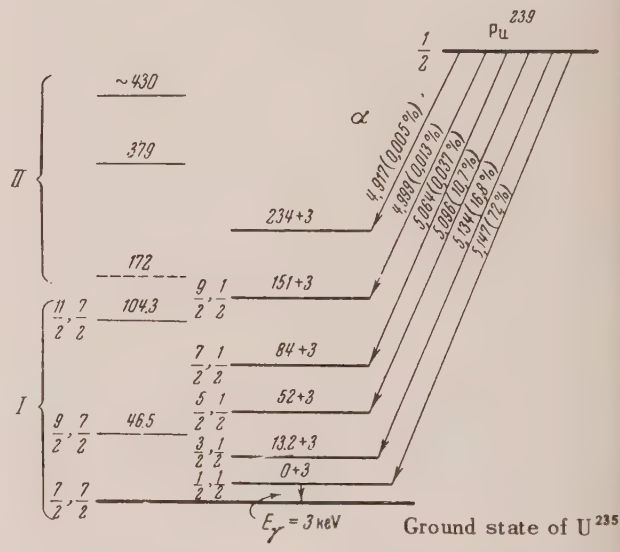

FIG. 3. α-decay scheme of Pu^{239} and the levels of U^{235}. *I* denotes the levels determined from the Coulomb excitation[8], and *II* the levels determined from the $\gamma-\gamma$ coincidences[10].

Let us discuss in greater detail the γ-transition between the $I = 1/2$ and $7/2$ levels. As L. Peker has shown (private communication), one should expect the ground states of Pu^{239} and U^{235} to have even parity. Thus the parities of the $I = 1/2$ and $I = 7/2$ levels of U^{235} are the same. The corresponding γ-transition must be of the *M*3 type with an energy of approximately 3 kev. The $I = 1/2$ level must therefore be isomeric and must have a long lifetime.

The authors are grateful to R. N. Ivanov and G. M. Kukavadze for their mass spectrometric measurements of the plutonium samples, and I. I.

Agapkin and G. I. Griskuk for their assistance in the work.

Note added in proof (April 19, 1957). Later measurements with a thinner source force one to believe that the level with 172 kev energy apparently exists. The intensity of the α-decay to this level lies within the stated limits.

In the 4.675–4.850 Mev region, levels with excitation energies 373 kev ($\sim$ 0.002%), 426 kev ($\sim$ 0.005%), 497 kev ($\sim$ 0.0015%) and, apparently, 336 kev (0.0035%) have been discovered. The first two of these levels correspond to states observed in $\gamma - \gamma$ coincidences.

[1] F. Asaro and I. Perlman, Phys. Rev. **88**, 828 (1952).

[2] Gol'din, Tret'iakov and Novikova, Collected *Papers of the Session of the U.S.S.R. Academy of Sciences Meeting of the Div. of Phys. and Math. Sciences*, p. 226 (1955).

[3] Bohr, Froman and Mottelson, Kong. Danske Vid. Selsk. Mat.-fys. Medd. **29**, 10 (1955).

[4] Bleaney, Llewellyn, Pryce, and Hall, Phil. Mag. **45**, 991 (1945).

[5] K. L. Van der Sluis and J. R. McNally, J. Opt. Soc. Amer. **45**, 65 (1955).

[6] Hollander, Perlman and Seaborg, Rev. Mod. Phys. **25**, 469 (1953).

[7] W. D. Allen and P. A. Egelsaff, Nature **175**, 1027 (1955).

[8] B. S. Dzhelepov and L. K. Peker, *"Decay Schemes of Radioactive Isotopes"*, U.S.S.R. Acad. Sci. Press (1957).

[9] A. Bohr, *Rotational States of Atomic Nuclei*, Copenhagen (1954).

[10] I. Perlman and J. O. Rasmussen, *Alpha Radioactivity*, U.C.R.L. 3424 (1956).

[11] L. L. Gol'din and E. F. Tret'iakov, Izv. Akad. Nauk SSSR, Ser. Fiz **20**, 859 (1956).

[12] Kondrat'ev, Novikova, Sobolev and Gol'din, J. Exptl. Theoret. Phys. (U.S.S.R.) **31**, 771 (1956), Soviet Phys. JETP **4**, 645 (1957).

[13] G. Albony and I. Teillac, Compt. rend. **232**, 326 (1951).

[14] D. Dunlaveya and G. T. Seaborg, Phys. Rev. **87**, 165 (1952).

[15] D. West and Y. K. Dawson, Proc. Phys. Soc. **A64**, 586 (1951).

[16] Freedman, Wagner and Engelkemeir, Phys. Rev. **88**, 1155 (1952).

[17] K. N. Shliagin, J. Exptl. Theoret. Phys. (U.S.S.R.) **30**, 817 (1956), Soviet Phys. JETP **3**, 663 (1956).

Translated by Fay Ajzenberg-Selove
219

SOVIET PHYSICS JETP VOLUME 5, NUMBER 5 DECEMBER, 1957

Reactions Involving Polarized Particles

M. I. SHIROKOV
Academy of Sciences of the U.S.S.R.

(Submitted to JETP editor June 9, 1956)
J. Exptl. Theoret. Phys. (U.S.S.R.) **32**, 1022-1035 (May, 1957)

The statistical tensors of particles produced in reactions of the types $a + b \to c + d$ and $a \to c + d$ have been obtained in the most general case, when the incident beam and the target particles are in definite spin states. New selection rules are deduced which supplement the general selection rules of Simon and Welton[1,2]. The first of these rules can be regarded as a generalization of the rule according to which the polarization vector of the particles produced in the reaction is perpendicular to the plane of the reaction if the incident and target particles are unpolarized. The second rule states that the statistical tensor of a particle produced in the reaction, defined relative to the direction of its momentum, is either purely real or purely imaginary if the incident and target particles are unpolarized. As a particular case, the decay of an unstable particle into particles of spins $\frac{1}{2}$ and 0 is considered, and it is shown that the polarization and angular distribution of these particles depend only on the spin and spin state of the decaying particle.

THE GENERAL THEORY of nuclear reactions has already been broadly developed in the papers of Simon and Welton[1, 2]. In the present paper a new method is proposed for obtaining the statistical tensors (for definition see Appendix I) of particles produced in a reaction. It has been given brief-

ly and in a somewhat different form in Ref. 3 (for a method of very similar conception, see Ref. 4). This approach permits a relativistic generalization and also immediate generalization to the case of nuclear reactions with more than two particles in the final state. In a similar fashion one can use the diagonal character of the S matrix with respect to other conserved physical quantities to obtain a number of general properties of processes in quantum-mechanical systems.

In this paper the formalism of Dirac[5] is widely used (*cf.* Ch. I-IV, especially Sec. 17).

1. We consider reactions of the types $a + b \to c + d$ and $a \to c + d$. a, b, c, d denote either "elementary" particles or nuclei, with spins i_a, i_b, i_c, i_d. The spin is treated in the Pauli approximation, and in this sense the treatment will be nonrelativistic (in particular, particles with rest mass zero are not considered). Knowing the initial state of the system (before the reaction), and assuming as known the elements of the S matrix in the corresponding representation, we can obtain the wave function of the final state*.

$$ {}_{\eta'}\Psi_{\xi_0}' = (\eta' \mid S \mid \xi)_\xi \Psi_{\xi_0}. \tag{1.1} $$

Summation or integration with respect to ξ is understood. The indices ξ and η denote a complete set of quantities characterizing the states of the system (type of particle, etc., see below the complete set for a system of two particles). ${}_{\eta'}\Psi'_{\xi_0}$ is the probability amplitude for the quantities η to have the values η' in the final state, if the system was initially in the state ξ_0.[5]

But the initial and final states must be described not by wave functions, but by density matrices, since the states of the system before and after the reaction are, generally speaking, mixed ensembles[7, 13].

*The relation (1.1) is ordinarily written as applied to reactions of the type $a + b \to c + d$. In this case $\hat{S} = \hat{U}(\infty, -\infty)$, where the operator $\hat{U}(t, t_0)$, for example, satisfies the Schroedinger equation (in the interaction representation)[6]

$$ ih\partial \hat{U}(t, t_0)/\partial t = \hat{H}_{\text{int}} \hat{U}(t, t_0). $$

But if the particle a has sufficiently long lifetime so that one can speak approximately about a definite (quasistationary) initial state (with definite energy, etc.), then (1.1) can be written also for the reaction $a \to c + d$, where now $\hat{S} = \hat{U}(\infty, 0)$ (the time is counted from the instant of production of the unstable particle).

For example, an unpolarized beam of particles incident on the target is described by an ensemble in which the probabilities of all possible orientations of the spin are equal. We define the density matrix as

$$ (\xi_1 \mid \rho \mid \xi_2) = \sum_\alpha P_\alpha \Psi_{\alpha\xi_1} \Psi^*_{\alpha\xi_2}, \tag{1.2} $$

where the P_α are the weights of the pure states $\left(\sum_\alpha P_\alpha = 1\right)$.

By means of Eq. (1.1) we find that the density matrix of the final state is given by:

$$ (\eta_{i1}' \mid \rho' \mid \eta_{i2}') = (\eta_{i1}' \mid S \mid \xi_1)(\eta_{i2}' \mid S \mid \xi_2)^* (\xi_1 \mid \rho \mid \xi_2) $$
$$ = (\eta_{i1}' \mid S\rho S^+ \mid \eta_{i2}'), \tag{1.3} $$

the diagonal elements $(\eta' \mid \rho' \mid \eta')$ give the probability that after the reaction the system will be in the state η' if the initial state was characterized by the density matrix (1.2).

We shall use henceforth instead of the S matrix the scattering matrix $\hat{R} = \hat{S} - 1$, all elements of which are the same as those of the S matrix with the exception of those for transitions without change of state[6].

It is well known that in an isolated system the total angular momentum J, its projection M, the total momentum $\mathbf{P}$, and the total energy E are conserved. An expression of this fact is the diagonal character of the S (or R) matrix with respect to these quantities. Generally speaking, however, J, M, $\mathbf{P}$, and E cannot belong to the same complete set. Therefore in the general case one has to write down the condition of the diagonal character of the elements of the R matrix with respect to J, M, and E in the representation of a set including J, M, and E, then express in terms of these elements the matrix elements of the R matrix in the representation of another complete set including $\mathbf{P}$, and write the condition that the matrix be diagonal with respect to $\mathbf{P}$. The performance of these operations in practice would require rather cumbersome unitary transformations.

There does exist, however, a system of coordinates in which we can make use of the diagonal character of the R matrix with respect to J, M, E and $\mathbf{P}$ all at once. Namely, if for the description of a system of two particles we have chosen the system of coordinates in which $P^2 = 0$, then in a set including J, M, and E there can also be included: the spins i_c and i_d of the two particles, the to-

tal spin s, the total orbital angular momentum l of the particles relative to the center of mass*, the orbital angular momentum L of the entire system relative to the origin of coordinates (see below), the total orbital angular momentum $\mathfrak{L}(\hat{\mathfrak{L}} = \hat{L} + \hat{l})$, and the absolute value P of the total momentum of the system (equal to zero)† . Since the operator $\hat{L}$ can be written $[\hat{\mathbf{R}}_c \times \mathbf{P}]$, where $\hat{\mathbf{R}}_c$ is the operator of the center of mass, then in those states in which $\mathbf{P} = 0$ we have also $L = 0$ (and we are indeed considering only states of the system for which $P = 0$ and consequently $\mathbf{P} = 0$). Since P^2 is conserved, then $L = 0$ always, and the total orbital angular momentum of the system is equal to l. For a reaction of the type $a + b \to c + d$, for example, we have in the the representation of this complete set

$$(i_c i_d s' l' L' \mathfrak{L}' P' J' M' E' \alpha' \mid R \mid i_a i_b s l L \mathfrak{L} 0 J M E \alpha) = (i_c i_d s' l' 0 l' \alpha' \mid R_0^{0JE} \mid i_a i_b s l 0 l \alpha) \times \delta(\mathbf{P}' - 0)\, \delta_{J'J} \delta_{M'M} \delta(E' - E). \quad (1.4)$$

The upper indices indicate the dependence of the diagonal elements on P, J, and E; it can be shown that they are independent of M. In what follows the indices i_c, i_d, etc., for the spins of the particles will not be written out, and also the indices for the total momentum and the quantities L and $\mathfrak{L}$ are dropped, both in the elements of the R matrix and in those of the density matrix (in other words, no indication is shown of the motion of the system as a whole, *i.e.*, of the fact that it is at rest in the chosen system of coordinates).

In the representation of the complete set s, l, J, M, E, a, and with the use of Eq. (1.4), Eq. (1.3) takes the form:

$$(s_1' l_1' J_1 M_1 E_1 \alpha_1' \mid \rho' \mid s_2' l_2' J_2 M_2 E_2 \alpha_2') = (s_1' l_1' \alpha_1' \mid R^{J_1 E_1} \mid s_1 l_1 \alpha_1)\, (s_2' l_2' \alpha_2' \mid R^{J_2 E_2} \mid s_2 l_2 a_2)^* \times (s_1 l_1 J_1 M_1 E_1 \alpha_1 \mid \rho \mid s_2 l_2 J_2 M_2 E_2 \alpha_2). \quad (1.5)$$

*In the center-of-mass system

$$\hat{l} = [(\hat{\mathbf{r}}_c - \hat{\mathbf{R}}_c)\hat{\mathbf{p}}_c] + [(\hat{\mathbf{r}}_d - \hat{\mathbf{R}}_c)\hat{\mathbf{p}}_d] = [(\hat{\mathbf{r}}_c - \hat{\mathbf{R}}_c)\hat{\mathbf{p}}_c] + [(\hat{\mathbf{r}}_c - \hat{\mathbf{R}}_c)(-\hat{\mathbf{p}}_c)] = [(\hat{\mathbf{r}}_c - \hat{\mathbf{r}}_d)\hat{\mathbf{p}}_c].$$

Here $\hat{\mathbf{p}}_c = -\hat{\mathbf{p}}_a$ are the momentum operators of the particles in the center-of-mass system.

† We remark that, generally speaking, a complete set must also include the masses of the particles. For brevity they are not written out explicitly. The complete set may also include a number of other variables, for example the intrinsic parities of the two particles. All of these are denoted by the letter α.

2. The meaning of Eq. (1.1) or (1.3) consists in the expression of the unknown parameters that determine ψ' or ρ' in the form of elements of the S matrix. The conservation laws reduce the number of these parameters. We must now find out how this manifests itself in the description of the angular distribution and spin state of the products c and d of the reaction in question. The essence of what follows is comprised in transformations (for the most part unitary) from the representation of the final and initial states of the reaction in the quantities s, l, J, M, E, which are not directly measured, into a representation of quantities that are experimentally measured.

To characterize the final state we require the elements of the density matrix that are diagonal with respect to $\mathbf{p}_c$ (the momentum in the center-of-mass system), and also the statistical tensors (briefly: the c-tensors) describing the spin state of the products of the reaction (*cf.* Appendix I). We denote the set of these quantities by the symbol $\rho'(\mathbf{p}_c;\ q_c \nu_c q_d \nu_d)$. We note that according to Eqs. (1.1)–(1.3) the indices $\mathbf{p}_c$ can be regarded also as parameters of the c-tensors of particles c and d (these being quantities proportional to the mean values of the corresponding spin operators in the ensemble of particles with momentum $\mathbf{p}_c$).

In a problem of the type $a + b \to c + d$ the initial state is characterized by a definite value of the quantity $\mathbf{p}_a$ and by c-tensors. The symbolic notation is

$$\rho(\mathbf{p}_a;\ q_a \nu_a q_b \nu_b)\, (\mathbf{p}_a' \mid \mathbf{p}_a)\, (\mathbf{p}_a'' \mid \mathbf{p}_a)$$

(*cf.* Appendix II).

Hereafter we shall specify momenta $\mathbf{p}$ in terms of their absolute values p and the corresponding unit vectors n with spherical angles ϑ, φ.

Thus we have to express

$$\rho'(\mathbf{n}_c,\ p_c,\ \alpha';\ q_c \nu_c q_d \nu_d) \text{ in terms of}$$

$$(s_1' l_1' J_1' M_1' E_1' \alpha' \mid \rho' \mid s_2' l_2' J_2' M_2' E_2' \alpha'),\ [cf.\ (1.4)] \text{ and}$$

$$(s_1 l_1 J_1 M_1 E_1 \alpha_1 \mid \rho \mid s_2 l_2 J_2 M_2 E_2 \alpha_2)$$

in terms of $(\mathbf{n}_a,\ p_a;\ q_a \nu_a q_b \nu_b)\, (\mathbf{p}_a' \mid \mathbf{p}_a)\, (\mathbf{p}_a'' \mid \mathbf{p}_a)$.

This is accomplished by means of successive transformations from one representation to another, using the Clebsch-Gordan coefficients $(j_1 j_2 m_1 m_2 \mid j_1 j_2 j m)$ or $C^{jm}_{j_1 m_1 j_2 m_2}$[8,9] and the correctly normalized (*cf.* Appendix II) transformation functions $(\vartheta \varphi p \mid l \mu E)$:

$$\varrho'(\mathbf{n}_c, p_c, \alpha'; q_c\nu_c q_d\nu_d) = [(2i_c+1)(2i_d+1)]^{1/2}$$

$$\times \sum_{m_c, m_c', m_d, m_d'} (-1)^{i_c - m_c' + i_d - m_d'} (i_c i_c m_c - m_c' | i_c i_c q_c\nu_c)(i_d i_d m_d - m_d' | i_d i_d q_d\nu_d)$$

$$\times \sum (i_c i_d m_c m_d | i_c i_d s_1' m_1')(\mathbf{n}_c p_c | l_1' \mu_1' E_1')(s_1' l_1' m_1' \mu_1' | s_1' l_1' J_1' M_1') \tag{2.1}$$

$$\times (s_1' l_1' J_1' M_1' E_1' \alpha' | \varrho' | s_2' l_2' J_2' M_2' E_2' \alpha')$$

$$\times (s_2' l_2' J_2' M_2' | s_2' l_2' m_2' \mu_2')(l_2' \mu_2' E_2' | \mathbf{n}_c p_c)(i_c i_d s_2' m_2' | i_c i_d m_c' m_d').$$

Σ denotes summation or integration (with respect to E_1' and E_2') over all indices occurring twice. We insert into Eq. (2.1) the expression (II.2) for $(\vartheta\varphi p\ l\mu E)$ and use the formula

$$Y_{l_1\mu_1}(\mathbf{n})\, Y_{l_2\mu_2}(\mathbf{n}) = \sum_{L, m_L} \left[\frac{(2l_1+1)(2l_2+1)}{4\pi(2L+1)}\right]^{1/2} C^{L0}_{l_1 0 l_2 0} C^{L m_L}_{l_1\mu_1 l_2\mu_2} Y_{L m_L}(\mathbf{n}). \tag{2.2}$$

The majority of the sums over magnetic quantum numbers in Eq. (2.1) actually do not contribute, by virtue of the properties of the Clebsch-Gordan coefficients, but it is convenient to keep them for the carrying-out of the summation over these indices. For this we use the following typical formula:

$$\sum_{m_1 m_2 \mu_1 \mu_2} C^{s_1\sigma_1}_{j_1 m_1 l_1 \mu_1} C^{s_2\sigma_2}_{j_2 m_2 l_2 \mu_2} C^{j m_j}_{j_1 m_1 j_2 - m_2} C^{l m_l}_{l_1 \mu_1 l_2 - \mu_2}$$

$$= (-1)^{s_2 - j_2 - l_2} [(2s_1+1)(2s_2+1)(2j+1)(2l+1)]^{1/2} \tag{2.3}$$

$$\times \sum_{g, m_g} C^{g m_g}_{s_1\sigma_1 s_2 - \sigma_2} C^{g m_g}_{j m_j l m_l} X(j_1 j j_2;\ s_1 g s_2;\ l_1 l l_2).$$

The relation (2.3) can be obtained by means of Eq. (1), (18), and (19) of Ref. 9, and also from Eq. (3) in Ref. 10, and the coefficients X are defined in Ref. 10 and 1. By means of Eq. (2.3) one at once carries out in Eq. (2.1) the sum over m_c, m_c', m_d, m_d' of the product of the first, second, third, and last Clebsch-Gordan coefficients (we note that $-m_c' - m_d' = -m_2'$). After this one can take the sum over m_1', m_2', μ_1', μ_2' [again a sum of the type (2.3)], and one finally gets from Eq. (2.1):

$$\varrho'(\mathbf{n}_c, p_c, \alpha'; q_c\nu_c q_d\nu_d) = N_1' N_2' (4\pi)^{-1/2} [(2i_c+1)(2i_d+1)]^{1/2}$$

$$\times \sum (\mathbf{n}_c | L' m_L') C^{J'M'}_{q'\nu' L' m_L'} C^{q'\nu'}_{q_c\nu_c q_d\nu_d} C^{L'0}_{l_1' 0 l_2' 0} (-1)^{J_2' - M_2'} C^{J'M'}_{J_1' M_1' J_2' - M_2'}$$

$$\times [(2s_1'+1)(2s_2'+1)(2q_c+1)(2q_d+1)]^{1/2} X(i_c q_c i_c;\ s_1' q' s_2';\ i_d q_d i_d) \tag{2.4}$$

$$\times [(2l_1'+1)(2l_2'+1)(2J_1'+1)(2J_2'+1)(2q'+1)]^{1/2}$$

$$\times X(s_1' q' s_2';\ J_1' J' J_2';\ l_1' L' l_2') i^{-l_1' - l_2'} (s_1' l_1' J_1' M_1' E_1' \alpha' | \varrho' | s_2' l_2' J_2' M_2' E_2' \alpha').$$

The sum Σ is taken over s_1', s_2', l_1', l_2'; J_1', J_2', q', L', J' and over ν', M_L', M_1', M_2', M'; and

$$N_{1,2}' = 2\sqrt{2}\,\pi h\,[R/V]^{1/2} p_c^{-1}\,(p_c \mid E_{1,2}')$$

(*cf.* Appendix II).

Equations (2.1) and (2.4) are written in the center-of-mass coordinate system, the z, y, and x directions being so far arbitrary. For the flux of particles the most obvious distinguished direction in space is the direction $\mathbf{n}$ of this flux. We introduce the c-tensors $\rho'(\mathbf{n}_c, p_c, \alpha'; q_c\tau_c q_d\tau_d)$ with indices τ referred to $\mathbf{n}_c$ as axis of quantization. The expression of these tensors in terms of the old c-tensors has the form:

$$\rho'(\mathbf{n}_c, p_c, \alpha'; q_c\tau_c q_d\tau_d) = \sum_{\nu_c\nu_d} D^{q_c}_{\tau_c\nu_c}(-\pi, \vartheta_c, \pi - \varphi_c) \times D^{q_d}_{\tau_d\nu_d}(-\pi, \vartheta_c, \pi - \varphi_c)\,\rho'(\mathbf{n}_c, p_c, \alpha'; q_c\nu_c q_d\nu_d), \tag{2.5}$$

$\pi - \varphi_c$, ϑ_c, and $-\pi$ are the Eulerian angles* of the rotation g_c of the axes zyx that makes the z axis coincide with the direction of $\mathbf{n}_c$ and the y axis perpendicular to the old direction of the z axis and to $\mathbf{n}_c$; the rotation inverse to $g_c = \{-\pi, \vartheta_c, \pi - \varphi_c\}$, is written $g_c^{-1} = \{\varphi_c, \vartheta_c, 0\}$. We note that the spherical angles are reckoned as before from the old axes zyx; one has only introduced a new axis of quantization for the spin indices.

Substituting Eq. (2.4) into Eq. (2.5), we can first carry out the summation over ν_c and ν_d:

$$\sum_{\nu_c,\nu_d} D^{q_c}_{\tau_c\nu_c}(g)\, D^{q_d}_{\tau_d\nu_d}(g)\, C^{q'\nu'}_{q_c\nu_c q_d\nu_d} = D^{q'}_{\tau_c+\tau_d,\nu'}(g)\, C^{q'\tau_c+\tau_d}_{q_c\tau_c q_d\tau_d}. \tag{2.6}$$

We introduce the notation $\tau' = \tau_c + \tau_d$. Using this same formula $(2.6)^1$, we can carry out the sum over ν' and m_L', if we use the relation

$$Y_{ln}(\vartheta, \pi - \varphi_1) = [(2l+1)/4\pi]^{1/2} D^l_{0,n}(\varphi_2, \vartheta, \varphi_1).$$

The final result is:

$$\rho'(\mathbf{n}_c, p_c; \alpha';\ q_c\tau_c q_d\tau_d) = N_1' N_2' (4\pi)^{-1} [(2i_c+1)(2i_d+1)]^{1/2} \times \sum D^{J'}_{\tau',M'}(-\pi, \vartheta_c, \pi - \varphi_c)\, C^{q'\tau'}_{q_c\tau_c q_d\tau_d} (-1)^{q'+\tau'} (-1)^{J_2' - M_2'} C^{J'M'}_{J_1'M_1'J_2'-M_2'} \times [(2q_c+1)(2q_d+1)]^{1/2} X(i_c q_c i_c;\ s_1' q' s_2';\ i_d q_d i_d) \times G^*_{\tau'}(J_1'l_1's_1';\ J'q';\ J_2'l_2's_2')\,(s_1'l_1'J_1'M_1'E_1'\alpha' \mid \rho' \mid s_2'l_2'J_2'M_2'E_2'\alpha'), \tag{2.7}$$

where the coefficient $G_{\tau'}$ is defined in Ref. 2, Eq. (3.3); the sum is taken over s_1', s_2', l_1', l_2', q', J_1', J_2', J' and over M_1', M_2', M'.

Similarly one gets the expressions of $(s_1l_1J_1M_1E_1\alpha_1 \mid \rho \mid s_2l_2M_2E_2\alpha_2)$ in terms of $\rho_{\alpha_1\alpha_2}(\mathbf{n}_a, p_a; q_a\nu_a q_b\nu_b)$ or of $\rho_{\alpha_1\alpha_2}(\mathbf{n}_a, p_a; q_a\tau_a q_b\tau_b)$; [we refer to the corresponding formulas as Eqs. (2.8) and (2.9)].

Refraining from a change in notation, we remark that the corresponding transformation functions are obtained by simply taking complex conjugates of the transformation functions in Eqs. (2.4) and (2.7) (*i.e.*, taking complex conjugates of all the coefficients of $(s_1'l_1'J_1'M_1'E_1'\alpha' \mid \rho' \mid s_2'l_2'J_2'M_2'E_2'\alpha')$ in Eqs. (2.4) and (2.7) and replacing $[(2i_c+1)(2i_d+1)]^{1/2}$ by $[(2i_a+1)(2i_b+1)]^{-1/2}$ [*cf.* Eqs. (1.3) and (1.4)].

Combination of Eqs. (2.4), (1.5), and (2.8) gives the first final formula [we shall call it Eq. (2.10)];

---

*The indices ν (or τ) of the c-tensors are "contravariant" (indices of the representation). Therefore $\rho(q\nu)$ transforms on three-dimensional rotation like $Y^*_{q\nu}(\theta, \Phi) = (q\nu \mid \theta\Phi)$. Equation (2.5) is obtained by simply taking the complex conjugate of the formula for transforming the spherical functions, which we write in the form

$$Y_{qn}(\mathbf{n}') = \sum_m Y_{qm}(\mathbf{n})\, D^q_{m,n}(g^{-1}),$$

if the transformation of a unit vector by the rotation g is written $\mathbf{n}' = \hat{g}\mathbf{n}$. If the rotation g is treated as a rotation of the coordinate system (right-handed), it can be specified by the Eulerian angles φ_1 (rotation around the z axis), ϑ (rotation around the y' axis), and φ_2 (rotation around the z' axis). All rotations are clockwise. We emphasize that the Eulerian angle ϑ is ordinarily defined as a rotation around the x' axis, but only with our definition will the formula written above be correct.

$$D^l_{m,n}(\varphi_2\vartheta_1\varphi_1) = \exp(-im\varphi_2)\, i^{n-m} P^l_{mn}(\cos\vartheta) \exp(-in\varphi_1),$$

with the functions P^l_{mn} as in Ref. 11. See this reference also for the definition of the spherical functions.

all spin indices and spherical angles are referred to an arbitrarily chosen system of axes zyx. Since $J_1' = J_1$, $J_2' = J_2$, $M_1' = M_1$, and $M_2' = M_2$, the sum over M_1 and M_2 is easily carried out.

$$\sum_{M_1 M_2} (J_1 J_2 M_1 - M_2 \mid J_1 J_2 J' M') \times (J_1 J_2 M_1 - M_2 \mid J_1 J_2 J M) = \delta_{J'J} \delta_{M'M}$$

and thus we also have $J' = J$, $M' = M$. Moreover,

$$(p_c \mid E_1)(E_1 \mid p_a) = (p_c \mid E_2)(E_2 \mid p_a) = (p_c; p_a),$$

where the symbol $(p_c; p_a)$ expresses the law of conservation of energy in the momentum representation. All the transformations are exhausted by this, and Eq. (2.10) can easily be written out in final form, but it is very cumbersome.

Combination of Eqs. (2.7), (1.5) and (2.8) gives the second final formula, Eq. (2.11). If in Eq. (8)* of Ref. 3 we replace $\lambda_a^2/4$ by the normalizing factor $N/(4\pi)^2$ (*cf.* Appendix II) and $D^j_{\varkappa,\varkappa'}(\varphi_A, \vartheta_A, 0)$ by

$$\sum_M D^J_{\tau' M}(-\pi, \vartheta_c, \pi - \varphi_c) D^{J^*}_{\tau M}(-\pi, \vartheta_a, \pi - \varphi_a) = D^J_{\tau'\tau}(g_c g_a^{-1}) \tag{2.12}$$

[this is required by the change of definition of the c-tensors, *cf.* Eq. (5) in Ref. 3 and Eq. (II.3)], then the combination of Eqs. (7), (8), and (9) in Ref. 3 will also be Eq. (2.11).

It can be shown that it follows from Eq. (2.12) that the c-tensors of the final state depend essentially on the parameters of the rotation $g_c g_a^{-1}$ of the system of axes $z_a y_a x_a$ distinguished by the initial state (the axis $z_a \parallel \mathbf{n}_a$, and the direction of the axis y_a can be given by the spin state; for example, it can be directed along the component of the polarization vector perpendicular to $\mathbf{n}_a$) into the system of axes $z_c y_c x_c$ (the axis $z_c \parallel \mathbf{n}_c$, and axis $y_c \parallel [\mathbf{n}_a \times \mathbf{n}_c]$). Thus all the quantities in Eq. (2.11) can be defined relatively to a number of physical directions of the reaction $a + b \to c + d$, so that for Eq. (2.11) one can dispense with the introduction of any auxiliary coordinate system. In the coordinate system ordinarily used, coinciding with the system of axes $z_a y_a x_a$, we have $g_c g_a^{-1} = \{-\pi, \vartheta, \pi - \varphi\}$, where ϑ, φ are the spherical angles of the direction $\mathbf{n}_c$ in such a system of coordinates.

If the spin state of the incident beam a and the target particles b is completely unpolarized or has axial symmetry

$$\rho(q_a \tau_a q_b \tau_b) = \rho(q_a 0 q_b 0)\, \delta_{\tau_a 0} \delta_{\tau_b 0},$$

then the sum over τ in Eq. (2.11) there remains only (*cf.* note * on page 839)

$$D^J_{\tau' 0}(-\pi, \vartheta, \pi - \varphi) = P^J_{\tau' 0}(\cos\vartheta)$$

and the c-tensors of the final state [including the angular distribution $\rho(\mathbf{n}_c, p_c, a'; 0000)$] do not depend on φ. This is natural, since in this case the choice of the axis y_a is completely arbitrary and nothing can depend physically on such a choice.

By a procedure analogous to that explained for Eq. (2.11), the general formula for a reaction of the type $a \to c + d$ can be obtained:

$$\begin{aligned}
&\rho'(\mathbf{n}_c, p_c, \alpha'; q_c \tau_c q_d \tau_d) \\
&= N_0^2 (4\pi)^{-1} [(2i_c + 1)(2i_d + 1)]^{1/2} (2s + 1)^{-1/2} \\
&\times \sum (-1)^{q' + \tau'} C^{q'\tau'}_{q_c \tau_c q_d \tau_d} [(2q_c + 1) \\
&\times (2q_d + 1)]^{1/2} X(i_c q_c i_c;\ s_1' q' s_2';\ i_d q_d i_d) \\
&\times G^{z}_{\tau'\nu}(s l_1' s_1'; q\ q';\ s l_2' s_2') \\
&\times (s_1' l_1' \alpha' \mid R^{sE} \mid \alpha_1)(s_2' l_2' \alpha' \mid R^{sE} \mid \alpha_2)^* \\
&\times D^{q}_{\tau'\nu}(-\pi, \vartheta_c, \pi - \varphi_c)\, \rho_{\alpha_1 \alpha_2}(q\nu).
\end{aligned} \tag{2.13}$$

The sum is taken over q', τ', s_1', s_2', l_1', l_2', q, ν; and

$$N_0 = 2\pi h [R/V]^{1/2} p_c^{-1} (p_c E);$$

$\rho(q\nu)$ are the c-tensors of particle a, s is its spin, and E is its total energy. The symbol $(p_c \mid E)$ is equal to unity if p_c is a root of the equation

$$\sqrt{p_c^2 c^2 + \varkappa_c^2 c^4} + \sqrt{p_c^2 c^2 + \varkappa_d^2 c^4} = E = \varkappa_a c^2,$$

and zero if p_c does not satisfy this equation (*cf.* Appendix II).

Let us analyze the case in which particles a and b are identical (and/or particles c and d). Let the variables of the complete set ξ_1 (and ξ_2) in the definition of the density matrix (1.2) be the momenta $\mathbf{p}_1$ and $\mathbf{p}_2$ of the particles and their spin components m_1 and m_2. Then it is necessary that

* There is a mistake in Eq. (8) of Ref. 3: the exponent on the square brackets $[(2s_1 + 1)(2s_2 + 1)(2s_1' + 1)(2s_2' + 1)]$ must be $-\frac{1}{2}$, not $+\frac{1}{2}$.

$$(\xi_1 \mid \rho \mid \mathbf{p}_1, \mathbf{p}_2, m_1, m_2) = (-1)^{2i} (\xi_1 \mid \rho \mid \mathbf{p}_2, \mathbf{p}_1, m_2, m_1), \tag{2.14}$$

i.e., the elements of the density matrix with fixed ξ_1 must either change sign, if the identical particles have half-integral spin, or remain unchanged, for Bose particles, depending on whether we ascribe to the "first" particle a the momentum $\mathbf{p}_1$ and the spin component m_1 and to the "second" the momentum $\mathbf{p}_2$ and the component m_2, or ascribe $\mathbf{p}_2$ and m_2 to the "first" and $\mathbf{p}_1$ and m_1 to the "second". The same must hold independently for the indices ξ_1 with fixed ξ_2. Introducing instead of $\mathbf{p}_1$ and $\mathbf{p}_2$ the total momentum $\mathbf{P}$ and the momentum in the center-of-mass system $\mathbf{p}$, we can write Eq. (2.14) in the form:

$$(\xi_1 \mid \rho \mid \mathbf{P}, \mathbf{p}, m_1, m_2) = (-1)^{2i} (\xi_1 \mid \rho \mid \mathbf{P}, -\mathbf{p}, m_2, m_1).$$

Taking into account the fact that

$$\begin{aligned}
&(\xi_1 \mid \rho \mid -\mathbf{p}, i, i, m_2, m_1) \\
&= (\xi_1 \mid \rho \mid l\mu piism)\,(l\mu p \mid \pi - \vartheta, \varphi + \pi, p)\,(iism \mid iim_2m_1) \\
&= (\xi_1 \mid \rho \mid l\mu piism)\,(-1)^l\,(l\mu p \mid \vartheta, \varphi, p)\,(-1)^{s-2i}\,(iism \mid iim_1m_2)
\end{aligned}$$

(index P omitted), we find that the element of the density matrix symmetrized with respect to the right-hand indices [satisfying Eq. (2.14)] has the form

$$\begin{aligned}
(\xi_1 \mid \rho \mid \mathbf{p}, m_1, m_2)\mathrm{sym} &= 2^{-1/2}[(\xi_1 \mid \rho \mid \mathbf{p}\, m_1m_2) + (-1)^{2i}\,(\xi_1 \mid \rho \mid -\mathbf{p}, m_2m_1)] \\
&= 2^{-1/2}\,(\xi_1 \mid \rho \mid l\mu psm)\,[1 + (-1)^{l+s}]\,(l\mu p \mid \vartheta\varphi p)\,(iism \mid iim_1m_2).
\end{aligned} \tag{2.15}$$

Therefore, if particles a and b are identical, then in addition to making the corresponding indices equal ($i_a = i_b = i$, etc.) in Eqs. (2.10) and (2.11) we must insert under the sign of summation a factor

$$1/2\,[1 + (-1)^{l_1+s_1}]\,[1 + (-1)^{l_2+s_2}]$$

A similar factor (with primes on l and s) is inserted in Eqs. (2.4), (2.7), (2.11), etc., if c and d are identical.

3. The final state of a reaction of the type $a + b \to c + d$ is described, generally speaking, by $(2i_c + 1)^2 + (2i_d + 1)^2$ c-tensors (*cf.* Appendix I). But it turns out that in the case of a completely unpolarized initial state a happy choice of the axis of quantization reduces the number of the c-tensors of the final state, for the calculation of which a knowledge of the matrix elements (1.4) is necessary.

Ordinarily the z axis of the coordinate system in which a formula of the type of Eq. (2.10) is written is directed along $\mathbf{n}_a$. Let us direct it perpendicular to the plane of the reaction, *i.e.*, along the vector $[\mathbf{n}_a \times \mathbf{n}_c]$. Thus for each case of the reaction its own z axis is chosen. We then direct the x axis along $\mathbf{n}_a$, so that the direction of the incident beam is always described in the same way: $\vartheta_a = \pi/2$, $\varphi_a = 0$*. The angle φ_c now is the angle between the directions of the momentum $\mathbf{p}_c$ and of the incident beam. For the following considerations we need the following factor in the general term of the sum Σ of Eq. (2.10), in the chosen coordinate system:

$$\begin{aligned}
&C^{J,M}_{q'\nu'L'm_L'}\,C^{JM}_{q\nu Lm_L}\,C^{L'0}_{l_1'0l_2'0}\,C^{L0}_{l_10l_20}\cdot Y_{L',m_L'} \\
&\times(\pi/2, \varphi_c)\,Y^*_{L,m_L}(\pi/2, 0).
\end{aligned} \tag{3.1}$$

From the properties of the coefficients $(l_1'l_2'00 \mid l_1'l_2'L'0)$ and $(l_1l_200 \mid l_1l_2L0)$ and from the

*But the c-tensors of the spin states of the beam and the target will, generally speaking, be different for different z axes. They can be expressed in terms of c-tensors referred, for example, to $\mathbf{n}_a$ as axis of quantization, by the formulas of Sec. 2 [of the type of Eq. (2.5)].

law of conservation of spatial parity of the system it follows that $l_1' + l_2' + L'$, $l_1 + l_2 + L$, and $l_1' + l_2' + l_1 + l_2$ must be even numbers. Therefore $L' + L$ is also even. This fact is a sort of selection rule that does not depend on the choice of the coordinate system.

In virtue of the properties of associated Legendre polynomials of the first kind, the functions $Y_{l\mu}(\pi/2, \varphi)$ are nonvanishing only for $l + \mu$ even. Therefore the only terms in Eq. (2.10) not equal to zero are those with even $L' + m_L'$, $L + m_L$ and consequently even $L' + L + m_L' + m_L$, and finally even $m_L' + m_L$. From the properties of the first two Clebsch-Gordan coefficients in (3.1) we have $\nu' + m_L' = \nu + m_L$, from which we have $\nu' - \nu = m_L - m_L'$. Since ν', ν, m_L, and m_L' are whole numbers, the selection rule obtained can be expressed as follows: $\nu' + \nu$ must be an even number if the axis of quantization is chosen perpendicular to the plane of the reaction. In the important special case of completely unpolarized incident beam and target [in all coordinate systems all $\rho(\mathbf{n}_a, p_a; q_a\nu_a q_b\nu_b)$ other than $\rho(\mathbf{n}_a, p_a; 0000)$ are equal to zero] this rule states that only the $\rho(\mathbf{n}_c, p_c; q_c\nu_c q_d\nu_d)$ with even $\nu_c + \nu_d$ are nonvanishing.

In particular, the vanishing of $\rho'(\mathbf{n}_c, p_c; 1, \pm 1, 0, 0)$ and $\rho'(\mathbf{n}_c, p_c; 0, 0, 1, \pm 1)$ means that the polarization vector for each of the particles c and d must be perpendicular to the plane of the reaction if the incident beam and the target are unpolarized[1].

If in Eq. (2.11) we assume the initial state completely unpolarized and choose the usual coordinate system (z axis $\| \mathbf{n}_a$), then we can obtain one more selection rule. In this case $\rho'(\mathbf{n}, p; q_c\tau_c 00)$ [or $\rho'(\mathbf{n}, p; 00 q_d\tau_d)$] depends on τ_c owing to the following factors in the general term of the sum (*cf.* Eq. (8) in Ref. 3, with $D^J_{\varkappa\chi}$, $(\varphi_A, \vartheta_A, 0)$ replaced by $D^J_{\tau_c, 0}(-\pi, \vartheta, \pi - \varphi)$–*cf.* Sec. 2):

$$(-1)^{\tau_c} G_{\tau_c}(J_1 l_1' s_1'; J\ q_c;$$

$$J_2 l_2' s_2')\, D^J_{\tau_c, 0}(-\pi,\ \vartheta,\ \pi - \varphi),$$

or, taking into account the expression (3.3) of Ref. 2 for G_{τ_c} and the formula

$$D^J_{\tau, 0}(\varphi_2,\ \vartheta,\ \varphi_1)$$

$$= [4\pi/(2J+1)]^{1/2} (-1)^{\tau} Y_{J,\tau}(\vartheta, \pi - \varphi_2),$$

the factors in question are

$$(q_c J\tau_c - \tau_c \,|\, q_c J L' 0)\, Y_{J,\tau_c}(\vartheta,\ 0).$$

Similarly, $\rho'(\mathbf{n}_c, p_c; q_c - \tau_c 00)$ depends on $-\tau_c$ owing to the factors

$$(q_c J - \tau_c \tau_c \,|\, q_c J L' 0)\, Y_{J,-\tau_c}(\vartheta,\ 0).$$

From the law of conservation of the spatial parity of the system, and owing to the occurrence of the coefficients $(l_1' l_2' 00 \,|\, l_1' l_2' L' 0)$, $(l_1 l_2 00 \,|\, l_1 l_2 L 0)$, and $(0J00 \,|\, 0JL0)$ in G_{τ_c} and G^*_0, we have: $l_1 + l_2 + l_1' + l_2'$, $l_1' + l_2' + L'$, and $l_1 + l_2 + J$ are even numbers, from which it follows that $J + L'$ (and, of course, $J - L'$) must also be an even number. Therefore

$$(q_c J - \tau_c \tau_c \,|\, q_c J L' 0)$$

$$= (-1)^{q_c + J - L'} (q_c J\tau_c - \tau_c \,|\, q_c J L' 0)$$

$$= (-1)^{q_c} (q_c J\tau_c - \tau_c \,|\, q_c J L' 0).$$

Taking into account that

$$Y_{J,-\tau_c}(\vartheta, 0) = (-1)^{\tau_c} Y_{J,\tau_c}(\vartheta, 0),$$

we get

$$\rho'(\mathbf{n}, p; q_c, -\tau_c, 0, 0)$$

$$= (-1)^{q_c + \tau_c} \rho'(\mathbf{n}, p; q_c, \tau_c, 0, 0).$$

Taking into account now the Hermitian property of the c-tensors*, we conclude finally that if the initial state is completely unpolarized all the $\rho'(\mathbf{n}, p; q_c\, \tau_c 00)$ with even q_c are real, and those with odd q_c are purely imaginary†. This fact makes almost as great a simplification in the problem of finding the spin state of the system $c + d$ as the preceding selection rule. In particular, if the particle c is unstable, the selection rules that have been presented make it possible to simplify somewhat the description of the initial state of the reaction of its decay, without any sort of hypotheses about its production.

Similar selection rules can also be found for the

---

*One easily convinces oneself from (I.3) that to the Hermitian property of the density matrix, $(m_1 \,|\, \rho \,|\, m_2)^* = (m_2 \,|\, \rho \,|\, m_1)$ there corresponds the following property of the c-tensors: $\rho^*(q, \nu) = (-1)^{\nu} (q, -\nu)$.

†There exists a certain generalization of this selection rule: the contribution to $\rho'(\mathbf{n}, p; q\tau 00)$ from each c-tensor $\rho(\mathbf{n}_a, p_a; q_a 0 q_b 0)$ is real if $q + q_a + q_b$ is even, and purely imaginary if $q + q_a + q_b$ is odd.

reaction of the type $a \to c + d$ (directing the z axis respectively perpendicular and parallel to $\mathbf{n}_c$ and regarding particle a as completely unpolarized).

4. We now obtain some consequences that follow from Eq. (2.13) for the reaction $a \to c + d$ in the particular case $i_c = \frac{1}{2}$, $i_d = 0$, of which an important example is provided by the decay of the Λ^0 particle: $\Lambda^0 \to p + \pi^-$. First, for $i_d = 0$

$$X(i_c q_c i_c;\ s_1' q' s_2';\ 0 q_d 0) = (2i_c + 1)^{-1} (2q_c + 1)^{-1/2} \delta_{q_d 0} \delta_{q_c q'} \delta_{s_1' i_c} \delta_{s_2' i_c}.$$

Second, for $i_c = \frac{1}{2}$, from the triads $G_{\tau'}(sl_1' \tfrac{1}{2};\ q q_c;\ sl_2' \tfrac{1}{2})$ in Eq. (2.13) we have $l_1' = s \pm \frac{1}{2}$, $l_2' = s \pm \frac{1}{2}$, *i.e.*, l_1' and l_2' can differ only by unity. If the elements of the R matrix in Eq. (2.13) are nonvanishing only for transitions that conserve spatial parity, then l_1' and l_2' must have the same parity. We get the rule that $l_1' = l_2' = l' = s + \frac{1}{2}$ or else $l_1' = l_2' = l' = s - \frac{1}{2}$ depending on the unknown parity of particle a and the parities of c and d. In what follows it is assumed that the ensemble of particles a is a pure state with respect to the variable a [*i.e.*, $\rho_{\alpha_1, \alpha_2}(q\nu) = \rho(a;\ q\nu)\, \delta_{a\alpha_1} \delta_{a\alpha_2}$].

In Eq. (2.13) there then remains just one nonvanishing element of the R matrix, and if there are no alternative modes of decay of a, then from the unitary property of the S matrix it follows that

$$(\tfrac{1}{2}\, 0\, \tfrac{1}{2}\, l'\alpha' \mid R^{sE} \mid \alpha)\, (\tfrac{1}{2}\, 0\, \tfrac{1}{2}\, l'\alpha' \mid R^{sE} \mid \alpha)^* = 1. \tag{4.1}$$

If there are other decay schemes ($a \to c' + d'$), then on the right side of Eq. (4.1) we must put in place of unity the total probability w of the decay of a by the scheme $a \to c + d$ ($0 < w < 1$).

If now, furthermore, we integrate $\rho'(\mathbf{n}_c, p_c, a';\ q_c \tau_c 00)$ (with the weight factor $V/(2\pi h)^3$—*cf.* Appendix II) over the range of momenta $(p_c, p_c + \Delta p)$ containing momenta p_c that make $(p_c \mid E)$ equal to unity, and denote the resulting quantities by $T_{\tau_c}^{q_c}(\vartheta, \varphi)\, \Delta\Omega$ (index a' omitted), then from Eq. (2.13) we get

$$T_{\tau_c}^{q_c}(\vartheta, \varphi) = \frac{w\,(2s+1)^{-1/2}}{4\sqrt{2}\,\pi} \sum_{q\nu} (-1)^{q_c + \tau_c} G_{\tau_c}(sl' \tfrac{1}{2}, q\ q_c;\ sl' \tfrac{1}{2}) \times D_{\tau_c, \nu}^{q}(-\pi, \vartheta, \pi - \varphi)\, \rho(\alpha;\ q\nu). \tag{4.2}$$

On interchange of the upper and lower sets of arguments of the coefficient $G_{\tau_c}(sl' \tfrac{1}{2};\ q q_c;\ sl' \tfrac{1}{2})$, there must appear before G_{τ_c} the factor $(-1)^{2s+1+q+q_c}$ (*cf.* Ref. 2, page 38). But since these sets are identical, G_{τ_c} is not changed by this, and $2s + 1 + q + q_c$ must be an even number. Since the spin of particle a is half-integral, $2s + 1$ is an even number, and therefore $q + q_c$ must be even. The angular distribution of the decay products—$T_0^0(\vartheta, \varphi)$—is determined by only the even tensors of the initial state of particle a and the polarization of the decay protons (*i.e.*, the c-tensors T_0^1, $T_{\pm 1}^1$ are determined only by the odd ones. By measuring the angular distribution and polarization of particle c we obtain direct information about $\rho(q, \nu)$, the spin and parity of particle a, and, on the other hand, if these latter are known, we can predict all the c-tensors $T_{\tau_c}^{q_c}(\vartheta, \varphi)$.

By integrating the angular distribution $T_0^0(\vartheta, \varphi)$ with respect to ϑ or φ, we can obtain general formulas for distributions that are directly observed experimentally (for example, by integrating over ϑ we obtain the distribution in the angle between the plane of production of the Λ^0 and the plane of its disintegration)[16].

In conclusion it must be pointed out that a considerable part of the material presented here was developed by the writer in collaboration with A. M. Baldin (*cf.* Ref. 3), who is also to be thanked for discussions of some other points in the work. The writer also thanks Prof. M. A. Markov for his constant interest in the work and L. G. Zastavenko for discussion of a number of questions related to the theory of representations of the rotation group.

APPENDIX I

A quantum-mechanical state can be described not only by a wave function or a density matrix, but also by specifying the average values of a certain set of operators[12]. In particular, we shall describe in this way the spin state of a particle (and of a system of particles). We remark that also what is measured experimentally is not the probability of one or another value of the projection of a spin, but, for example, the average value of the spin vector operator (the so-called polarization of the particle).

Let $\hat{A}$ be an operator relating to the spin variables of a particle with spin i; the state of the particle is described by the density matrix $(m_1 \xi_1 \mid \rho \mid m_2 \xi_2)$, where m_1 and m_2 are magnetic

quantum numbers and ξ are all the other variables of the representation. We can find the average value of $\hat{A}$ in this state, if the matrix elements of $\hat{A}$ are known in the representation in which the density matrix is written

$$\bar{A} = \sum_{m_1 m_2 \xi_1 \xi_2} (m_2\xi_2 \mid \hat{A} \mid m_1\xi_1) \times (m_1\xi_1 \mid \rho \mid m_2\xi_2) = \mathrm{Sp}\,(A\rho). \tag{I.1}$$

We form from the components $\hat{\sigma}_x$, $\hat{\sigma}_y$, $\hat{\sigma}_z$ of the spin vector operator a tensor of rank q, transforming under three-dimensional rotations according to an irreducible representation of weight q, and denote its components by $\hat{A}^{q\nu}$. We remark that by its construction this operator is a contravariant tensor, like $\hat{\boldsymbol{\sigma}}$; *i.e.*, it transforms under rotations like $Y^*_{q\nu}(\mathbf{n})$, and not like $Y_{q\nu}(\mathbf{n})$. For example, the $\hat{A}^{1\nu}$ are simply the cyclic (or canonical[11]) components of $\hat{\boldsymbol{\sigma}}$; and transform like the vector $\mathbf{n}$, *i.e.*, like $Y^*_{1\nu}(\mathbf{n}) = (1\nu \mid \mathbf{n})$. The dependence of the matrix elements of $\hat{A}^{q\nu}$ on m_2 and m_1, according to the suitably modified (ν is a "contravariant" index!) Wigner-Eckart theorem[8], is given by:

$$(m_2\xi_2 \mid \hat{A}^{q\nu} \mid m_1\xi_1) = \sqrt{2i+1}\,(i\xi_1 \parallel \hat{A}^q \parallel i\xi_1)\,(\xi_1 \mid \xi_2)\,(-1)^{i-m_2}\,(iim_1 - m_2 \mid iq\nu) \tag{I.2}$$

(if the spin variables and the variables ξ are separable, then $(i\xi_1 \mid \hat{A}^q \mid i\xi_1)$ does not depend on ξ_1). Substituting (I.2) into (I.1), we see that to find $\overline{A^{q\nu}}$ one need not know the density matrix directly, but the quantity

$$\rho_{\xi_1,\xi_2}(q,\nu) = \sqrt{2i+1} \sum_{m_1, m_2} (-1)^{i-m_2}\,(iim_1 - m_2 \mid iq\nu)\,(m_1\xi_1 \mid \rho \mid m_2\xi_2), \tag{I.3}$$

proportional to $\overline{A^{q\nu}}$ (*cf.* also Ref. 12). From Eq. (I.3) it follows that the quantities $\rho(q, \nu)$, $q = 0, 1, \ldots, 2i$, $\nu = -q, -q+1, \ldots, q$ can characterize the spin state of the particle just as adequately as the density matrix. The inverse transformation from the q, ν representation to the m_1, m_2 representation has the form:

$$(m_1\xi_1 \mid \rho \mid m_2\xi_2) = (2i+1)^{-1/2} \sum_{q\nu} (-1)^{-i+m_2} \times (iim_1 - m_2 \mid iq\nu)\,\rho_{\xi_1,\xi_2}(q,\nu). \tag{I.4}$$

In the variables ξ, $\rho_{\xi_1,\xi_2}(q, \nu)$ is just the same sort of density matrix as is $(m_1\xi_2 \mid \rho \mid m_2\xi_2)$. From its origin, we can call $\rho_{\xi_1,\xi_2}(q\nu)$ the means or statistical means of the irreducible spin operators. Therefore we give them the name statistical tensors (abbreviated c-tensors) following Ref. 13 (page 735).

If we are interested only in the distribution of probabilities for the particle to have definite values of the variables ξ (for example, the angular distribution of the particles) in the state characterized by $(m_1\xi_1 \mid \rho \mid m_2\xi_2)$, then this will be described by the diagonal elements of the density matrix $\left[\sum_m (m\xi_1 \mid \rho \mid m\xi_2)\right]$. The transformation (I.3) is so chosen that

$$\sum_m (m\xi_1 \mid \rho \mid m\xi_2) = \rho_{\xi_1,\xi_2}(0,0),$$

and a beam of unpolarized particles would be described by the c-tensors $\rho_{\xi_1,\xi_2}(0,0)\,\delta_{q0}\delta_{\nu 0}$.

The c-tensors of the initial state, $\rho(q_a\nu_a q_b\nu_b)$, used in Sec. 2 are simply products of pairs of c-tensors $\rho(q_a\nu_a)$ and $\rho(q_b\nu_b)$ characterizing the separate spin states of particles a and b.

After the reaction, particles c and d are spatially separated, and consequently do not interact. It can be shown that just as the wave function of a system of two noninteracting particles separates as a product of the wave functions of the two particles, the density matrix and the c-tensors have a similar property:

$$\rho(q_c\nu_c q_d\nu_d) = \rho(q_c\nu_c 00)\,\rho(00\,q_d\nu_d)\,/\,\rho(0,0,0,0), \tag{I.5}$$

where $\rho(q_c\nu_c 00)$ are the c-tensors of particle c and $\rho(00 q_d\nu_d)$ are those of particle d. These c-tensors suffice to characterize completely the final spin of the system after the reaction, if c and d do not form a bound system.

We note that the "tensor moments" introduced in Ref. 3,

$$T^q_\nu = \sqrt{2i+1}\,\Sigma\,(-1)^{-i-m_1} \times (ii - m_1m_2 \mid iq\nu)\,(m_1 \mid \rho \mid m_2)$$

(there is a misprint in Eq. (5) of Ref. 3) are related to the $\rho(q, \nu)$ defined by Eq. (I.3) in the following way:

$$T_{\nu}^{q} = (-1)^{q+\nu} \rho(q, -\nu) = (-1)^{q} \rho^{*}(q, \nu).$$

APPENDIX II

We shall normalize all the wave functions (and the density matrix) of our problem in such a way that the system in the state η is located in the volume V (a three-dimensional sphere of radius R) at all times, with probability 1; in the x representation this condition is written

$$\int_{V} (x \mid \eta)^{*} (x \mid \eta) \, d^{3}x = 1. \tag{II.1}$$

The normalization of the wave function of the state η in other representations must correspond to this normalization.

The wave function $(\theta\Phi r \mid lm \mid \mathbf{k})$ ($\mathbf{k}$ is the wave vector) normalized in accordance with Eq. (II.1) has the form $g_{lk}(r) Y_{lm}(\theta, \Phi)$, where $g_{lk}(r)$ is given by Eq. (9) in Ref. 14. Furthermore, in accordance with the relation $(\vartheta\varphi k \mid l\mu k) = (\vartheta\varphi k \mid \theta\Phi r)(\theta\Phi r \mid l\mu k)$ (integration over θ, Φ, ϑ, and r is understood; ϑ, φ are the spherical angles of $\mathbf{k}$), we can obtain the correctly normalized wave function or transformation function $(\vartheta\varphi k \mid l\mu k)$. (We note that $(\vartheta\varphi k \mid \theta\Phi r)$ is equal to the expression (13) in Ref. 14, multiplied by $V^{-1/2}$). From these considerations we get:

$$(\vartheta\varphi p \mid l\mu E) = \frac{2\pi h \sqrt{2R}}{V\sqrt{V}} \frac{i^{-l}}{p} Y_{l\mu}(\vartheta, \varphi)(p \mid E), \tag{II.2}$$

where $(p \mid E)$ is defined analogously to $(\mathbf{p} \mid \mathbf{p}')$ (see below). The presence of the factor i^{-l} assures the invariance of the action of the time-reversal operator on wave functions with definite l and μ, in relation to the composition of angular momenta[15] (*i.e.*, the result of the action of this operator has the same form for $\psi_{l\mu}$ as for $\psi_{l_1\mu_1}$ and $\psi_{l_2\mu_2}$, if $\mathbf{l} = \mathbf{l}_1 + \mathbf{l}_2$). We note that

$$\begin{aligned} (l\mu E \mid \vartheta\varphi p) &= (\vartheta\varphi p \mid l\mu E)^{*} \\ &= (-1)^{-l+\mu} (\vartheta\varphi p \mid l, -\mu, E). \end{aligned} \tag{II.3}$$

Similarly it can be shown that $(\mathbf{p} \mid \mathbf{p}')$ has the form of Eq. (17) in Ref. 14 (*i.e.*, for $\mathbf{p} = \mathbf{p}'$, $(\mathbf{p} \mid \mathbf{p}') = 1$, and for $\mathbf{p} \neq \mathbf{p}'$, $(\mathbf{p} \mid \mathbf{p}') = 0$). If we require that, in accordance with the formalism of Dirac[5], $(\mathbf{p}'' \mid \mathbf{p})(\mathbf{p} \mid \mathbf{p}')$ be equal to $(\mathbf{p}'' \mid \mathbf{p}')$, then it turns out that the normalization (II.1) requires that the integration over $\mathbf{p}$ understood in $(\mathbf{p}'' \mid \mathbf{p})(\mathbf{p} \mid \mathbf{p}')$ be carried out with the weight factor $V/(2\pi h)^3$ (which is equivalent to a certain summation). According to Dirac (*cf.* Ref. 5, Sec. 24), this factor must be introduced into every formula in which integration over a momentum occurs.

In connection with the normalization (II.1) there arises the problem of obtaining from $\rho'(\mathbf{n}_c, p_c; q_c\nu_c q_d\nu_d)$ quantities that can be directly compared with the experimental results for the reaction $a + b \to c + d$. What is the meaning of $\rho'(\mathbf{p}_c; q_c\nu_c q_d\nu_d)$? There is a physical system consisting initially (at the time $-T$, where $T = R/v$, and v is the absolute value of the relative velocity of particles a and b: $v = |\mathbf{v}_a| + |\mathbf{v}_b|$) of the particles a and b existing in the volume V; its state is described by the quantities

$$((N \cdot \rho(\mathbf{p}_a; q_a\nu_a q_b\nu_b)(\mathbf{p}'_a \mid \mathbf{p}_a)(\mathbf{p}''_a \mid \mathbf{p}_a).$$

Then $\rho'(\mathbf{p}_c; 0, 0, 0, 0)$ is the probability of the appearance in the volume V at time $+T$ of particles c and d with momentum $\mathbf{p}_c$. The remaining ρ' with $q_c, q_d, \nu_c, \nu_d \neq 0$ are quantities proportional to the mean values of the corresponding spin operators (*cf.* Appendix I) in the ensemble of particles with that momentum.

For the comparison with experiment we need first of all to know how many of particles c and d will appear per second with momenta in the range $(\mathbf{p}_c, \mathbf{p}_c + \Delta\mathbf{p})$, if the constant incident current and the particle density of the target are prescribed (and not the number of particles a and b in a certain volume). To get this we must first divide $\rho'(\mathbf{p}_c; 0, 0, 0, 0)$ by $2T$ and integrate (with weight factor $V/(2\pi h)^3$) over the range $(\mathbf{p}_c, \mathbf{p}_c + \Delta\mathbf{p})$. If we further multiply the quantity obtained by V/v (normalization to unit current), we get the differential cross-section of the reaction, $\Delta\sigma(\mathbf{n}_c)$:

$$\begin{aligned} \Delta\sigma(\mathbf{n}_c) &= \frac{h^2}{4p_a^2} \frac{(4\pi)^2}{N} \rho'(\mathbf{n}_c, p'_c; 0, 0, 0, 0) \, \Delta\Omega, \\ N &= (2\pi h)^4 (p_c; p_a)^2 (2R)^2 [V^2 p_a^2 p_c^2]^{-1}; \end{aligned} \tag{II.4}$$

p'_c is the value of the modulus of the momentum $\mathbf{p}_c$ that is required by the law of conservation of energy. It is assumed that momenta with the absolute value p'_c exist in the range $(\mathbf{p}_c, \mathbf{p}_c + \Delta\mathbf{p})$; $\Delta\Omega$ is the solid angle of this range.

One could obtain quantities $\rho'_{\text{cur}}(\mathbf{p}_c; q_c\nu_c q_d\nu_d)$ normalized to unit current, and related to

$\rho'(\mathbf{p}_c;\ q_c \nu_c\, q_d \nu_d)$ in just the same way that $\Delta\sigma(\mathbf{n}_c)$ is related to $\rho'(\mathbf{n}_c,\ p_c;\ 0, 0, 0, 0)$. They would give the mean values of certain spin operators in an ensemble of particles with momenta in the range $(\mathbf{p}_c,\ \mathbf{p}_c + \Delta\mathbf{p})$. But the mean values so obtained would depend not only on the nature of the spin state, but also on the number of particles in the ensemble. Therefore the quantity used to characterize just the spin state is the mean value of the operator $\hat{A}^{q\nu}$ (for particle c, for example), calculated for one particle:

$$\overline{A^{q\nu}}(\mathbf{p}_c) = (i_c \| \hat{A}^q \| i_c)\, \rho_{n\tau}(\mathbf{n}_c,\ p_c';\ q, \nu, 0, 0) / \Delta\sigma(\mathbf{n}_c)$$
$$= (i_c \| \hat{A}^q \| i_c)\, \rho(\mathbf{n}_c,\ p_c;\ q\nu 00) / \rho(\mathbf{n}_c,\ p_c;\ 0, 0, 0, 0). \quad (\text{II}.5)$$

[1] A. Simon and T. Welton, Phys. Rev. **90**, 1036 (1953).

[2] A. Simon, Coll. Prob. Sovr. Fiz. (Problems of Contemporary Physics) **6**, 21 (1955); Phys. Rev. **92**, 1050 (1953); **93**, 1435 (1954).

[3] A. M. Baldwin and M. I. Shirokov, J. Exptl. Theoret. Phys. (U.S.S.R.) **30**, 784 (1956). Soviet Physics JETP **3**, 757 (1956).

[4] C. Møller, Kgl. Dansk. Mat. Fys. Medd. **23**, No. 1, Sec. 3 (1945).

[5] P. A. M. Dirac, *The Principles of Quantum Mechanics*.

[6] B. A. Lippmann and J. Schwinger, Phys. Rev. **79**, 473 (1950).

[7] D. I. Blokhintsev, *Principles of Quantum Mechanics*, Sec. 44. Moscow 1949.

[8] G. Racah, Phys. Rev. **62**, 438 (1942).

[9] Biedenharn, Blatt, and Rose, Rev. Mod. Phys. **24**, 249 (1952).

[10] Arima, Horie, and Tanabe, Prog. Theor. Phys. **11**, 143 (1954).

[11] I. M. Gel'fand and Z. Ia. Shapiro, Usp. Mat. Nauk **7**, 3 (1952).

[12] U. Fano, Phys. Rev. **90**, 577 (1953).

[13] L. C. Biedenharn and M. E. Rose, Rev. Mod. Phys. **25**, 735 (1953).

[14] J. Hamilton, Proc. Camb. Phil. Soc. **52**, No. 1, 97 (1956).

[15] R. Huby, Proc. Phys. Soc. **67A**, 1103 (1954).

[16] M. I. Shirokov, J. Exptl. Theoret. Phys. (U.S.S.R.) **31**, 734 (1956), Soviet Physics JETP **4**, 620 (1957).

Translated by W. H. Furry
220

SOVIET PHYSICS JETP VOLUME 5, NUMBER 5 DECEMBER, 1957

Electric Monopole Transitions of Atomic Nuclei

D. P. GRECHUKHIN

(Submitted to JETP editor March 28, 1956; resubmitted January 7, 1957)
J. Exptl. Theoret. Phys. (U.S.S.R.) **32**, 1036-1049 (June, 1957)

Processes arising in $E0$ transitions in nuclei are considered. Equations are derived for the probabilities of shell electron conversion, pair production, two-photon transitions, and electron scattering cross section involving excitation of the $E0$ nuclear transition. The calculations are carried out with Coulomb functions of the electron with allowance for the finite dimensions of the nucleus. The conversion probability in an $E0$ nuclear transition is compared with the competing $E2$ and $M1$ nuclear transitions. Some estimates are given for the $E0$ nuclear transition matrix element for various single-particle and collective nuclear models.

SINGLE-PHOTON NUCLEAR TRANSITIONS between states of zero spin are forbidden by the law of conservation of angular momentum. In this case the radiation transition occurs by emission of two (or more) quanta. A distinction is made between two types of transitions: the $M0$-transition, with a change in parity ($0^{\pm} \to 0^{\mp}$), and the $E0$ transition, in which parity remains unchanged ($0^{\pm} \to 0^{\pm}$). In the second case, shell electron conversion or pair production is possible in addition to the two-photon transition. The $E0$ conversion differs substantially from other multipole conversion processes in that the monopole potential is localized in the region of the nucleus, while in other conversion processes

the region of the nucleus makes a relatively small contribution. Since the Coulomb potential on the surface of the nucleus is approximately mc^2 even at low values of Z, the motion of the electron in the vicinity of the nucleus is essentially relativistic. The calculations must thus be made with relativistic electron functions. In addition, the field in the vicinity of the nucleus differs substantially from the field of a point charge, leading to a considerable local variation in the electron wave function compared with the functions in the field of a point charge. The calculations of the monopole conversion probability must therefore contain allowances for the finite dimensions of the nucleus (in the case of a point nucleus, the $E0$ conversion transition is strictly forbidden). $E0$ nuclear transitions with electron conversion and pair production were studied in many investigations[1-7]. However, Fowler's calculation[1] was made in a non-relativistic approximation, while the remaining works[2-7] are based on the Born approximation or fail to allow for the finite dimensions of the nucleus. It is interesing to find out how substantially the effect of the nuclear dimensions influence the results obtained. We shall give below the calculated values of the probabilities of many processes connected with the $E0$ nuclear transition. The nucleus is considered as a sphere of radius $R_0 = r_0 A^{1/3} = 1.2 \times 10^{-13} A^{1/3}$ cm, with a uniform volume charge density. The shielding effect of the atomic electrons is neglected. In the processes considered here the electrons do not have too high an energy, so that $kR_0 \ll 1$ (k is the electron wave vector), thus restricting the applicability of the results to electron energies $\varepsilon \lesssim 15$ Mev for heavy nuclei. Retardation is neglected. The calculations are in relativistic units. The wave functions of the electron in the continuous energy spectrum are normalized to a unity energy interval. The formalism of the spherical spinors, developed by Berestetskii *et al*[8], will henceforth be used everywhere. The initial state of the system is designated by the index 1, the final state by 2.

1. WAVE FUNCTION OF AN ELECTRON IN THE FIELD OF A FINITE NUCLEUS

Our calculations require wave functions of an electron in the field of a finite nucleus. These functions can be readily obtained by joining on the surface of the nucleus the regular solution of the Dirac equation for the region $r < R_0$ for each partial wave $(j, \lambda, l = j + \lambda)$, namely

$$\psi_{j\lambda\mu} = A_{j\lambda} \begin{cases} i\hat{Y}^{-\lambda}_{j\mu} F_{j\lambda}(r) \\ \hat{Y}^{\lambda}_{j\mu} G_{j\lambda}(r) \end{cases}$$

with the general solution to the equation in the region $r \geqslant R_0$, which is a superposition of the regular $\psi_{j\mu\lambda}(\gamma)$ and irregular $\psi_{j\mu\lambda}(\gamma)$ solutions of the Dirac equation for the field of a point charge (see Refs. 9–11). The constant $A_{j\lambda}$ is determined from the boundary conditions. The first to use this method to calculate the effect of the finite dimensions was Sliv[12]. Let us evaluate the constant $A_{j\lambda}$ with an accuracy to approximately $(kR_0)^2$:

$$A_{j\lambda} = \left\{ \frac{g_{j\lambda}(\gamma) f_{j\lambda}(-\gamma) - f_{j\lambda}(\gamma) g_{j\lambda}(-\gamma)}{G_{j\lambda} f_{j\lambda}(-\gamma) - F_{j\lambda} g_{j\lambda}(-\gamma)} \right\}_{r=R_0},$$

$$F_{j\lambda} = r^{j-\lambda}\Phi_1^{(2\lambda)}(x);\ G_{j\lambda} = r^{j+\lambda}\Phi_2^{(2\lambda)}(x);$$

$$x = r/R_0;\ \Phi_1^{(2\lambda)} = \sum_{\nu=0}^{\infty} a_\nu^{(2\lambda)} x^{2\nu};$$

$$\Phi_2^{(2\lambda)} = \sum_{\nu=0}^{\infty} b_\nu^{(2\lambda)} x^{2\nu}.$$

The series Φ_1 and Φ_2 converge rapidly and if an approximate accuracy of 5% is specified, one need merely take the following terms (at $x = 1$):

$$\lambda = +1/2:$$

$$\Phi_1^{(+)} = 1 - \omega^2/6 + Ze^2\omega/15 + \omega^4/120,$$

$$R_0\Phi_2^{(+)} = \omega/3 - Ze^2/10 - \omega^3/30;$$

$$\lambda = -1/2:$$

$$R_0\Phi_1^{(-)} = -\omega/3 + Ze^2/10 + \omega^3/30,$$

$$\Phi_2^{(-)} = 1 - \omega^2/6 + Ze^2\omega/15 + \omega^4/120.$$

Here $\omega = 1.5\ Ze^2 + \varepsilon R_0$, where ε is the total electron energy.

For further calculations it is convenient to normalize the functions $\psi_{j\lambda}(\gamma)$ so that the normalization coincides with that required for the analogous process in the point-charge representation. The functions $f_{j\lambda}(\pm\gamma, r)$ and $g_{j\lambda}(\pm\gamma, r)$ for the bound and free state of the electrons have been derived by many workers (see, for example, Refs. 9–11).

The constants $A_{j\lambda}$ for the continuous and dis-

crete spectrum are readily obtained by substituting the functions.

1) *Electron in bound state;* shell n, j, λ;

$$A_{j\lambda n} = N_{jn} R_0^{\gamma - j - 1/2} S_{j\lambda}(R_0);$$

here at $\lambda = -1/2$

$$S_{j\lambda} \approx \frac{(1-\varepsilon^2)^{1/2}[n'(n'+2\gamma) - (N-\varkappa)^2]}{(1-\varepsilon)^{1/2}[n'+2\gamma+N-\varkappa]\,\Phi_2^{(-)} + (1+\varepsilon)^{1/2} R_0 \Phi_1^{(-)}[N-2\gamma-n'-\varkappa]},$$

at $\lambda = +1/2$

$$S_{j\lambda} \approx \frac{(1-\varepsilon^2)^{1/2}[n'(n'+2\gamma) - (N-\varkappa)^2]}{(1-\varepsilon)^{1/2}[n'+2\gamma+N-\varkappa]\,R_0\Phi_2^{(+)} + (1+\varepsilon)^{1/2}\Phi_1^{(+)}[N-2\gamma-n'-\varkappa]},$$

$$N_{jn} = \left(\frac{\Gamma(2\gamma+1+n')}{n'!\,N(N-\varkappa)}\right)^{1/2} \frac{1}{\Gamma(2\gamma+1)} \left(\frac{2Ze^2}{N}\right)^{\gamma+1/2},$$

$$N = \sqrt{n^2 - 2n'(|\varkappa| - \gamma)}, \quad \varkappa = 2\lambda(j+1/2), \quad \gamma = \sqrt{\varkappa^2 - Z^2e^4}.$$

2) *Electron in continuous spectrum of energy* $\varepsilon > 0$:

$$A_{j\lambda} = C_j R_0^{\gamma - j - 1/2} S_{j\lambda}(\varepsilon R_0);$$

at $\lambda = -1/2$

$$S_{j\lambda}(\varepsilon R_0) = \left\{ \frac{(\varepsilon^2-1)^{1/2}[\mathrm{Re}\,Q_{j\lambda}(\gamma)\,\mathrm{Im}\,Q_{j\lambda}(-\gamma) - \mathrm{Re}\,Q_{j\lambda}(-\gamma)\,\mathrm{Im}\,Q_{j\lambda}(\gamma)]}{(\varepsilon-1)^{1/2}\Phi_2^{(-)}\mathrm{Im}\,Q_{j\lambda}(-\gamma) + (\varepsilon+1)^{1/2} R_0 \Phi_1^{(-)} \mathrm{Re}\,Q_{j\lambda}(-\gamma)} \right\}_{r=R_0},$$

at $\lambda = +1/2$

$$S_{j\lambda}(\varepsilon R_0) = \left\{ \frac{(\varepsilon^2-1)^{1/2}[\mathrm{Re}\,Q_{j\lambda}(\gamma)\,\mathrm{Im}\,Q_{j\lambda}(-\gamma) - \mathrm{Re}\,Q_{j\lambda}(-\gamma)\,\mathrm{Im}\,Q_{j\lambda}(\gamma)]}{(\varepsilon+1)^{1/2}\Phi_1^{(+)}\mathrm{Re}\,Q_{j\lambda}(-\gamma) + (\varepsilon-1)^{1/2} R_0 \Phi_2^{(+)} \mathrm{Im}\,Q_{j\lambda}(-\gamma)} \right\}_{r=R_0},$$

$$C_j = \frac{(2p)^\gamma\,|\,\Gamma(\gamma + iZe^2\varepsilon/p)\,|\,\exp(\pi Ze^2\varepsilon/2p)}{\sqrt{\pi p}\,\Gamma(2\gamma+1)}, \quad e^{2i\eta} = -\frac{\varkappa - iZe^2/p}{\hat{\gamma} + iZe^2\varepsilon/p},$$

$$Q_{j\lambda} = e^{i\eta}(\hat{\gamma} + iZe^2\varepsilon/p)\,{}_1F_1(\hat{\gamma}+1+iZe^2\varepsilon/p;\ 2\hat{\gamma}+1;\ 2ipR_0); \quad \hat{\gamma} = \pm\gamma.$$

3) *Electron at negative level of continous spectrum* $(-\varepsilon)$:

$$A_{j\lambda} = B_j R_0^{\gamma - j - 1/2} S_{j\lambda}(\varepsilon R_0);$$

at $\lambda = -1/2$

$$S_{j\lambda}(\varepsilon R_0) = \left\{ \frac{(\varepsilon^2-1)^{1/2}[\mathrm{Re}\,P_{j\lambda}(\gamma)\,\mathrm{Im}\,P_{j\lambda}(-\gamma) - \mathrm{Im}\,P_{j\lambda}(\gamma)\,\mathrm{Re}\,P_{j\lambda}(-\gamma)]}{(\varepsilon+1)^{1/2}\Phi_2^{(-)}\mathrm{Re}\,P_{j\lambda}(-\gamma) + (\varepsilon-1)^{1/2} R_0 \Phi_1^{(-)} \mathrm{Im}\,P_{j\lambda}(-\gamma)} \right\}_{r=R_0},$$

at $\lambda = +\frac{1}{2}$

$$S_{j\lambda}(\varepsilon R_0) = \left\{ \frac{(\varepsilon^2-1)^{1/2}[\mathrm{Re}\,P_{j\lambda}(\gamma)\,\mathrm{Im}\,P_{j\lambda}(-\gamma) - \mathrm{Im}\,P_{j\lambda}(\gamma)\,\mathrm{Re}\,P_{j\lambda}(-\gamma)]}{(\varepsilon-1)^{1/2}\Phi_1^{(+)}\,\mathrm{Im}\,P_{j\lambda}(-\gamma) + (\varepsilon+1)^{1/2}R_0\Phi_2^{(+)}\,\mathrm{Re}\,P_{j\lambda}(-\gamma)} \right\}_{r=R_0},$$

$$B_j = \frac{(2p)^\gamma\,|\,\Gamma(\gamma - iZe^2\varepsilon/p)\,|\exp(-\pi Ze^2\varepsilon/2p)}{\sqrt{\pi p}\,\Gamma(2\gamma+1)}, \quad e^{2i\eta} = \frac{\varkappa - iZe^2/p}{\hat{\gamma} - iZe^2\varepsilon/p},$$

$$P_{j\lambda}(\hat{\gamma}) = e^{i\eta}(\hat{\gamma} - iZe^2\varepsilon/p)_1F_1(\hat{\gamma}+1-iZe^2\varepsilon/p;\ 2\hat{\gamma}+1;\ 2ipR_0).$$

2. MATRIX ELEMENT OF ELECTRIC MONOPOLE

If retardation is neglected, the matrix element of the monopole assumes the form:

$$\langle 2\,|\,\hat{H}_{E0}\,|\,1\rangle = e^2\sum_{i=1}^{Z}\int \psi_2^+ u_2^+(\xi_i)\frac{1}{|\mathbf{r}-\xi_i|}\psi_1 u_1(\xi_i)\,(d\xi_i)\,(d\mathbf{r}),$$

where ψ_2 and ψ_1 are the electron wave functions, while u_2 and u_1 are the functions of the nucleus in the final and initial states respectively. Simple calculations yield for the matrix element of a transition of the type $(1, j\lambda) \to (2, j\lambda)$:

$$\langle 2\,|\,\hat{H}_{E0}\,|\,1\rangle = e^2 A_{j\lambda}(1)\,A^*_{j\lambda}(2)\,R_{j\lambda}R_0^{2j+1},$$

where $R_{j\lambda}$ is the nuclear matrix element. With an accuracy to quantities on the order of 0.03 and less, $R_{j\lambda}$ equals:

$$R_{j\lambda} \approx R_j = [(2j+1)(2j+2)]^{-1}\langle u_2^+\left|\sum_{i=1}^{Z}\left(\frac{\xi_i}{R_0}\right)^{2j+1}\right|u_1\rangle + \frac{(j+1)^{-1}\omega_1\omega_2 - \omega_1^2 - \omega_2^2}{4(j+1)(2j+3)(2j+4)} \times \langle u_2^+\left|\sum_{i=1}^{Z}\left(\frac{\xi_i}{R_0}\right)^{2j+3}\right|u_1\rangle + \ldots$$

The second term in R_j amounts to 0.1 of the first term even at $Z = 90$ and $\varepsilon \approx 30$. Hereinafter we shall denote

$$\langle u_2^+\left|\sum_{i=1}^{Z}\left(\frac{\xi_i}{R_0}\right)^{2j+1}\right|u_1\rangle = \rho_j.$$

3. PROBABILITIES OF $E0$ TRANSITIONS

Conversion of shell electron from state (n, j, λ).

$$W = \frac{2\pi e^4}{[(2j+1)(2j+2)]^2}C_j^2 N_{jn}^2\,|\,S_{j\lambda}(1)\,S_{j\lambda}(2)\,|^2\,R_0^{4\gamma}\rho_j^2.$$

In the case of the K, LI, and LII shells, the nuclear matrix elements are the same and the ratios of the corresponding values of W are independent of the properties of the nucleus:

$$\frac{W_K}{W_{LI}} = \frac{[2(\gamma+1)]^{\gamma+1}[(2+2\gamma)^{1/2}+1]}{2(2\gamma+1)}\left(\frac{P_K}{P_{LI}}\right)^{2\gamma-1} \times \exp\left(\pi Ze^2\left[\frac{\varepsilon_K}{P_K} - \frac{\varepsilon_{LI}}{P_{LI}}\right]\right)\left|\frac{S_K(1)\,S_K(2)}{S_{LI}(1)\,S_{LI}(2)}\right|^2,$$

$$\frac{W_{LI}}{W_{LII}} = \frac{\sqrt{2+2\gamma}-1}{\sqrt{2+2\gamma}+1}\left|\frac{S_{LI}(1)\,S_{LI}(2)}{S_{LII}(1)\,S_{LII}(2)}\right|^2.$$

The conversion of the $LIII$ shell electron is determined by the quantity $(Ze^2/N)^{2\gamma+1}p^{2\gamma-1}R_0^{4\gamma}$ and for $\gamma \sim 4$ it is approximately $10^8 - 10^{10}$ times smaller than the probability of the K-electron conversion. Numerical estimates of the probability of the L and K-electron conversion are given in the end of the article.

Paired Conversion of Monopole

The probability of the $E0$ conversion with pair production can be obtained by calculating the matrix element of an $E0$ transition with electron functions

$$\psi_{-\mathbf{p}_1\nu_1}(\mathbf{r}) = \sum_{j\mu\lambda} e^{i\pi(j-\lambda-1)/2} \times [\hat{Y}^\lambda_{j\mu}(-\mathbf{p}_1)]^*_{-\nu_1}\psi_{j\mu\lambda}(\mathbf{r}, -\varepsilon_1)\,e^{-i\delta_{j\lambda}(1)},$$

$$\psi_{\mathbf{p}_2\nu_2}(\mathbf{r}) = \sum_{j\mu\lambda} e^{i\pi(j-\lambda-1)/2} \times [\hat{Y}^\lambda_{j\mu}(\mathbf{p}_2)]^*_{-\nu_2}\psi_{j\mu\lambda}(\mathbf{r}, \varepsilon_2)\,e^{-i\delta_{j\lambda}(2)},$$

in the asymptotic approximation $\psi_{\mathbf{p}_2\nu_2}$ and $\psi_{\mathbf{p}_1\nu_1}$ contain plane and converging spherical waves (normalization of $\psi_{j\mu\lambda}$ by $\delta(\varepsilon-\varepsilon')\delta_{\mu\mu'}\delta_{jj'}\delta_{\lambda\lambda'}$). Considering that the contribution of waves with $j > 1/2$ is negligibly small, and taking only $j = 1/2$ into account, we obtain for the pair-production probability and for the angular correlation of the positron with the electron:

$$W_{\text{pair}} = \frac{2^{4\gamma-1}e^4R_0^{4\gamma}}{36\pi\,|\,\Gamma(2\gamma+1)|^4}\left(\int\sum_\lambda|\,S_\lambda(1)\,S_\lambda(2)\,|^2\,F(Z\Delta\varepsilon_1\varepsilon_2)\,\delta(\Delta-\varepsilon_1-\varepsilon_2)d\varepsilon_1\,d\varepsilon_2\right)\rho_j^2,$$

$$F(Z\Delta\varepsilon_1\varepsilon_2) = (p_1p_2)^{2\gamma-1}\exp\left(\pi Ze^2\left[\frac{\varepsilon_2}{p_2}-\frac{\varepsilon_1}{p_1}\right]\right)\left|\,\Gamma\left(\gamma+iZe^2\frac{\varepsilon_2}{p_2}\right)\Gamma\left(\gamma+iZe^2\frac{\varepsilon_1}{p_1}\right)\right|^2.$$

For Ca_{20}^{40}, Zr_{40}^{90}, and Po_{84}^{214} the integral was evaluated numerically to be 49, 1.2, and 0.017 respectively. The function of the angular correlation $N(\theta)$ of the positron with the electron at fixed energy $\varepsilon_1(\varepsilon_2)$ is determined by the square of the modulus of the elements:

$$N(\vartheta)\sim\sum_{\nu_1\nu_2}\left|\sum_{\mu\lambda}\exp\{i(\delta_{j\lambda}(2)-\delta_{j\lambda}(1))\}\,[\hat{Y}^\lambda_{j\mu}(\mathbf{p}_2)]_{-\nu_2}[\hat{Y}^\lambda_{j'\mu}(-\mathbf{p}_1)]^*_{-\nu_1}A_{j\lambda}(1)A^*_{j\lambda}(2)\right|^2.$$

From which we find: ($j = 1/2$) ($\lambda = \pm 1/2$)

$$N(\vartheta) = \frac{1}{2}\sum_\lambda|\,S_\lambda(1)\,S_\lambda(2)\,|^2 - [S_+(1)\,S_-(1)\,S_+(2)\,S_-(2)]\cos\varphi_1\cos\vartheta_{\mathbf{p}_1\mathbf{p}_2},$$

where the phase φ_1 is determined with accuracy to terms in $(pR_0)^2$ by the following equation

$$e^{i\varphi_1} = \left[\frac{(1-iZe^2/p_1)}{(1+iZe^2/p_1)}\,\frac{(1+iZe^2/p_2)}{(1-iZe^2/p_2)}\right]^{1/2}.$$

As $Z \to 0$, the equations for the conversion probability for the angular correlation become the known equations obtained in the Born approximations[9].

Inelastic Scattering of Electrons

Unlike the preceding case, the matrix element is calculated with the following electron functions

$$\psi_{\mathbf{p}_1\nu_1}(\mathbf{r}) = \sum_{j\mu\lambda}e^{i\pi(j-\lambda-1)/2}\,[\hat{Y}^\lambda_{j\mu}(\mathbf{p}_1)]^*_{-\nu_1}\psi_{j\mu\lambda}(\mathbf{r}\varepsilon_1)\,e^{i\delta_{j\lambda}(1)},$$

$$\psi_{\mathbf{p}_2\nu_2}(\mathbf{r}) = \sum_{j\mu\lambda}e^{i\pi(j-\lambda-1)/2}\,[\hat{Y}^\lambda_{j\mu}(\mathbf{p}_2)]^*_{-\nu_2}\psi_{j\mu\lambda}(\mathbf{r}\varepsilon_2)\,e^{-i\delta_{j\lambda}(2)},$$

and $\psi_{\mathbf{p}_1\nu_1}$ contains a plane wave and divergent waves in its asymptotic form. Restricting ourselves again to terms with $j = 1/2$, we obtain for the scattering cross section and for the angular distribution ($j = 1/2$; $\lambda = \pm 1/2$):

$$\sigma = \frac{\pi 2^{4\gamma}e^4R_0^{4\gamma}}{9\,|\,\Gamma(2\gamma+1)\,|^4}\,p_1^{2\gamma-3}p_2^{2\gamma-1}\,|\,\Gamma(\gamma+iZe^2\varepsilon_1/p_1)\,\Gamma(\gamma+iZe^2\varepsilon_2/p_2)\,|^2$$
$$\times\exp\left(\pi Ze^2\left[\frac{\varepsilon_1}{p_1}+\frac{\varepsilon_2}{p_2}\right]\right)\sum_\lambda|\,S_\lambda(1)\,S_\lambda(2)\,|^2\rho_j^2,$$

$$N(\vartheta) = \frac{1}{2}\sum_\lambda|\,S_\lambda(1)\,S_\lambda(2)\,|^2 + [S_+(1)\,S_-(1)\,S_+(2)\,S_-(2)]\cos\varphi_2\cos\vartheta_{\mathbf{p}_1\mathbf{p}_2},$$

where φ_2 is found with an accuracy to terms in $(pR_0)^2$ from

$$e^{i\varphi_2}\approx\left[\frac{(1-iZe^2/p_1)}{(1+iZe^2/p_1)}\,\frac{(1-iZe^2/p_2)}{(1+iZe^2/p_2)}\right]^{1/2}.$$

By way of illustration let us show the calculations of the cross sections for several elements at electron energies 10 and 20 mc^2. We shall represent the cross section as

$$\sigma = (\sigma_0/4\pi)\,(1+b\cos\theta)\,\rho_j^2\,10^{-30}\ (\text{cm}^2/\text{sterad}).$$

The values of b and σ_0 are given in Table 1.

TABLE I.

Nucleus	Energy 10 mc^2		Energy 20 mc^2	
	σ_0	b	σ_0	b^*
Ca_{20}^{40}	0.054	0.93	0.34	1
Ge_{32}^{72}	1.08	0.97	3.2	1
Zr_{40}^{90}	0.98	0.97	3.7	1
Pd_{46}^{106}	2.52	0.99	7.4	1
Po_{84}^{214}	67	0.98	190	1

*At an energy $E = 20$ it is important that the phase shift due to the finite dimensions of the nucleus be taken into account. This was not done in this estimate.

4. EFFECT OF FINITE NUCLEAR DIMENSIONS

It is interesting to determine to what extent results of calculations with the Coulomb functions of the point nucleus are charged by accounting for the finite dimensions of the nucleus. We obtain for the ratio of the probabilities, calculated for the point nucleus and finite nucleus:

$$\varkappa\left(\frac{\text{point}}{\text{finite}}\right)=\left[\frac{3}{\gamma(2\gamma+1)}\right]^2 F\left|\langle 2\left|\sum_{i=1}^{Z}\left(\frac{\xi_i}{R_0}\right)^{2\gamma}\right|1\rangle \Big/ \langle 2\left|\sum_{i=1}^{Z}\left(\frac{\xi}{R_0}\right)^{2}\right|1\rangle\right|^2;$$

For the conversion, scattering, and pair production processes, F assumes the following form: for the $(nj\lambda)$ shell electron conversion

$$F_\lambda \approx \frac{[(\varepsilon_1+1)^{1/2}(\varepsilon_2+1)^{1/2}(n'+\varkappa-N)\,\mathrm{Re}\,Q_{j\lambda}(\gamma 2)+(\varepsilon_2-1)^{1/2}(1-\varepsilon_1)^{1/2}(n'+N-\varkappa)\,\mathrm{Im}\,Q_{j\lambda}(\gamma 2)]^2}{[S_\lambda(1)\,S_\lambda(2)]^2},$$

for electron scattering ($\lambda = \pm \frac{1}{2}$)

$$F=\frac{\sum_\lambda [(\varepsilon_1+1)^{1/2}(\varepsilon_2+1)^{1/2}\mathrm{Re}\,Q_{j\lambda}(\gamma 1)\mathrm{Re}\,Q_{j\lambda}(\gamma 2)+(\varepsilon_1-1)^{1/2}(\varepsilon_2-1)^{1/2}\mathrm{Im}\,Q^*_{j\lambda}(\gamma 1)\mathrm{Im}\,Q_{j\lambda}(\gamma 2)]^2}{\sum_\lambda [S_\lambda(1)\,S_\lambda(2)]^2},$$

for pair production

$$F=\frac{\sum_\lambda |(\varepsilon_1+1)^{1/2}(\varepsilon_2-1)^{1/2}\mathrm{Re}\,P_{j\lambda}(\gamma 1)\,\mathrm{Im}\,Q_{j\lambda}(\gamma 2)+(\varepsilon_1-1)^{1/2}(\varepsilon_2+1)^{1/2}\,\mathrm{Im}\,P_{j\lambda}(\gamma 1)\mathrm{Re}\,Q_{j\lambda}(\gamma 2)|^2}{\sum_\lambda [S_\lambda(1)\,S_\lambda(2)]^2}$$

The corrections for the finite size of the nucleus, calculated for the case of conversion, are given at the end of the article. The values of $\varkappa$ for scattering and for $E = 10\ mc^2$ are:

Nucleus:	Ca_{20}^{40}	Ge_{32}^{72}	Zr_{40}^{90}	Pd_{46}^{106}	Po_{84}^{214}
$\varkappa$:	0,98	0,97	1,0	1,16	1,87

5. TWO-QUANTUM NUCLEAR TRANSITION

In the case of a 0–0 nuclear transition, radiation transition is possible only by emission of two or more photons simultaneously. The photon spectrum now becomes continuous. Similar two-quantum nuclear transitions were investigated earlier by Sachs[13], Schwinger[5], and Goldberger[14]. It was assumed in all these investigations that the nucleus emits quanta upon transition through one virtual state, the energy of which was chosen arbitrarily in the estimate. We shall give below a somewhat different estimate of the probability of a two-photon nucleus, taking into account a group of virtual states of the nucleus.

In recent studies of photo-nuclear processes, a gigantic maximum of the "resonance" type was observed in the cross sections of the (γn) and (γp) reactions at energies $\hbar\omega_{res} \approx 60\ A^{-1/3}$ Mev. The presence of such a nuclear "resonance" can be considered as a result of a sharp increase in the density of the "dipole" levels of the nucleus in the region of the "resonance" energy (by "dipole" levels we understand here levels reached by a nucleus, originally in the ground state, by absorption of a dipole quantum). It is natural to propose that in a nuclear transition with emission of two dipole quanta the greatest contribution is due to the virtual transitions at the levels near the "dipole resonance" of the nucleus.

Within the framework of these assumptions, we obtain for $W_{\gamma\gamma}$ and $dW_{\gamma\gamma}$:

$$dW_{\gamma\gamma} = 2\pi \sum_{\lambda_1\lambda_2} |\langle 2|\hat{H}_{\gamma\gamma}|1\rangle|^2 \rho_{\gamma_1}\rho_{\gamma_2}\delta(\Delta - k_1 - k_2)\,dk_1dk_2;$$

$$|\langle 2|\hat{H}_{\gamma\gamma}|1\rangle|^2 = \left|\sum_{\nu} \frac{\langle 2|\hat{H}_{\gamma}|\nu\rangle\langle\nu|\hat{H}_{\gamma}|1\rangle}{\Delta - k_1 - \varepsilon_{\nu}}\right|^2 \approx$$

$$\approx \frac{1}{(\varepsilon_{res} + k_1 - \Delta)^2}\left|\sum_{\nu}\langle 2|\hat{H}_{\gamma}|\nu\rangle\langle\nu|\hat{H}_{\gamma}|1\rangle\right|^2;$$

$\hat{H}_{\gamma}$ is the operator of interaction with the dipole quantum

$$\hat{H}_{\gamma} = \sum_i e\xi_i \mathbf{E}_{\lambda}; \quad \mathbf{E}_{\lambda} = ik\sqrt{2\pi/k}\,\varepsilon_{\lambda}\exp\{i\mathbf{k}\xi - i\omega t\},$$

ε_{λ} is the quantum polarization vector, and k is the wave number of the quantum;

$$dW_{\gamma\gamma} = \frac{8e^4k_1^3k_2^3R_0^4}{27\pi(\varepsilon_{res} + k_1 - \Delta)^2}|\langle 2|\sum_{i,j}^{Z}(\xi_i\xi_j/R_0^2)|1\rangle|^2\,\delta(\Delta - k_1 - k_2)\,dk_1dk_2,$$

$$W_{\gamma\gamma} = \frac{8e^4R_0^4}{27\pi}\left(\int\frac{k_1^3k_2^3\delta(\Delta - k_1 - k_2)}{(\varepsilon_{res} + k_1 - \Delta)^2}dk_1dk_2\right)|\langle 2|\sum_{i,j}(\xi_i\xi_j/R_0^2)|1\rangle|^2.$$

The integral can be calculated, but the end result is quite cumbersome. Taking it into account that $\varepsilon_{res} > \Delta$, it is easy to obtain the upper and lower estimates of the integral:

$$\int\frac{k_1^3k_2^3\delta(\Delta - k_1 - k_2)\,dk_1dk_2}{(\varepsilon_{res} + k_1 - \Delta)^2} = \frac{\Delta^5}{140}\left(\frac{\Delta}{\varepsilon_{res}}\right)^2 S,$$

where

$$\left\{1 + \frac{a}{2-a} - \frac{a^2}{2(2-a)^2}\right\} \leqslant S \leqslant \left\{1 + \frac{a}{1-a} - \frac{a^2}{(1-a)^2}\right\}, \quad a = \frac{\Delta}{\varepsilon_{res}}.$$

Thus

$$W_{\gamma\gamma} = \frac{2e^4 R_0^4}{945\pi} \Delta^5 \left(\frac{\Delta}{\varepsilon_{res}}\right)^2 S \,|\langle 2|\sum_{ij}(\xi_i\xi_j/R_0^2)|1\rangle|^2;$$

The matrix element of the transition can be broken up into two parts:

$$\langle 2\left|\sum_{i,j}(\xi_i\xi_j/R_0^2)\right|1\rangle = \langle 2\left|\sum_i(\xi_i/R_0)^2\right|1\rangle + \langle 2\left|\sum_{i>j}(\xi_i\xi_j/R_0^2)\right|1\rangle.$$

According to Levinger's calculation[15] we obtain for the diagonal matrix elements of such an operator

$$\langle 2\left|\sum_{i>j}\xi_i\xi_j\right|1\rangle \approx -\tfrac{1}{2}\langle 2\left|\sum_i \xi_i^2\right|1\rangle.$$

Assuming that this equation holds approximately also for the nondiagonal element, we obtain

$$W_{\gamma\gamma} \approx e^4 \frac{\Delta^5}{1890\pi}\left(\frac{\Delta}{\varepsilon_{res}}\right)^2 R_0^4 S \,|\langle 2|\sum_i(\xi_i/R_0)^2|1\rangle|^2.$$

The function of the quantum angular correlation $W(\theta)$ is identical with that obtained for two electric dipole quanta in the $0\to1\to0$ cascade and is of the form $W(\theta) = 1 + \cos^2\theta$, where θ is the angle between the wave vectors of the quanta.

6. RELATIVE CONTRIBUTION OF THE $M1$, $E2$, AND $E0$ TRANSITIONS OF THE NUCLEUS

In the case of a nuclear transition between states with equal spins and parities, it is possible to have a $E0$-transition along with $E2$ and $M1$ transitions. It would be interesting to compare the probabilities of the conversions of the shell electrons for various multipoles. We shall give below the calculated values of the ratios of the probabilities, W_{E0} to W_{M1} and to W_{E2}, for K-electron conversion.

To determine the conversion probability in the $E2$ transition we shall consider only the contribution of the charge of the transition. Actually, at energies on the order of $\lesssim Ze^2$ the contribution of the transition current is approximately $(Ze^2)^2$ of the corresponding contribution of the transition charge. At greater transition energies $k \gg Ze^2$ both terms are of the same order, but they have different signs (see Ref. 9). Thus, the estimate of the $E2$ transition made with the aid of the scalar potential differs in this case from the accurate value by a fact known not to exceed 4, a circumstance that can be allowed for in the estimate. Consequently

$$W_{E2} = 2\pi e^4 \frac{k^6}{225}\sum_{j_2\lambda_2}[IT_1 + IIT_2]\,|\langle 2\|E2\|1\rangle|^2;$$

$$T_1 = (2j_2+1)^{1/2}(2j_2-2\lambda_2+1)^{1/2}\omega\left(j_2\,\tfrac{1}{2}\,2j_1-\lambda_1;\ j_2-\lambda_2 j_1\right)C^{j_1-\lambda_1 0}_{j_2-\lambda_2 020},$$

$$T_2 = (2j_2+1)^{1/2}(2j_2+2\lambda_2+1)^{1/2}\omega\left(j_2\,\tfrac{1}{2}\,2j_1+\lambda_1;\ j_2+\lambda_2 j_1\right)C^{j_1+\lambda_1 0}_{j_2+\lambda_2 020},$$

$$I \approx \int_{R_0}^{\infty} g_{j_2\lambda_2}(r)\,g_{j_1\lambda_1}(r)\,F_2(kr)\,r^2dr,\quad II \approx \int_{R_0}^{\infty} f_{j_2\lambda_2}(r)\,f_{j_1\lambda_1}(r)\,F_2(kr)\,r^2dr,$$

where $F_L(kr)$ is the Hankel spherical function.

The integral of the $IIE2$ transition is always approximately proportional to $(Ze^2)^2$ also for all Z less than 1, and we can therefore disregard henceforth integral II in the estimate, without causing an error greater than 2. The reduced matrix element of the $E2$ transition is determined by the equation

$$\langle \Omega^{\Lambda+}_{IM_2}(2)\left|\sum_{i=1}^{Z}\xi_i^2\sqrt{4\pi}Y_{2M}(\theta_i\varphi_i)\right|\Omega^{\Lambda-}_{IM_1}(1)\rangle = C^{IM_2}_{IM_1 2M}\langle 2\|E2\|1\rangle.$$

We can denote analogously

$$\langle \Omega^{\Lambda+}_{1M} (2) \Big| \sum_{i=1}^{Z} \xi_i^2 \Big| \Omega^{\Lambda}_{1M} (1) \rangle = \langle 2 \| E0 \| 1 \rangle,$$

where $\Omega^{\Lambda}_{1M_2}(2)$ and $\Omega^{\Lambda}_{1M_1}(1)$ are the wave functions of the nucleus in the final and initial states respectively. In the case of an $E2$ multipole conversion on the K shell, two final states of the electron are possible:

$$(j = {}^3/_2,\ \lambda = +{}^1/_2,\ l = 2)$$

$$\text{and } (j = {}^5/_2,\ \lambda = -{}^1/_2,\ l = 2).$$

To compare the probability of the $E2$ transition with the probability W_{E0} of the monopole transition, we shall use the value of the probability for the first transition multiplied by two, thus overestimating the total probability of the $E2$ transition. For the $M1$ transition $(j_1\lambda_1 1) \to (j_1\lambda_1 2)$ we have

$$W_{M1} = 4\pi \frac{e^4 k^4}{9} [w (j_1 {}^1/_2\, 11;\ 1 j_1)]^2 \times (\mathrm{I} + \mathrm{II})^2 |\langle 2 \| M1 \| 1 \rangle|^2,$$

where the reduced matrix element is determined analogously:

$$\langle \Omega^{\Lambda+}_{1M_2} (2) \Big| \sum_i \sqrt{4\pi} \left\{ \left(\frac{\mu_i}{2M} + \xi_i^2 \frac{\delta_p \Phi(\xi_i)}{3} \right) \sqrt{2}\, (\sigma_i Y^{-1}_{1M}) + \frac{1}{M} (l_i Y^{-1}_{1M}) \right\} \Big| \Omega^{\Lambda}_{1M_1} (1) \rangle = C^{1\,M_2}_{1\,M_1 1M} \langle 2 \| M1 \| 1 \rangle.$$

The operator $\sqrt{2}(\xi^2/3)[\sigma_i Y^{-1}_{1M}(\theta_i\ \varphi_i)]$ takes into account the effect of the spin-orbital proton interaction in the $M1$ radiation, and this term plays an important role in the transitions of the type $1/2 + \to 1/2 +$; $\delta_p = 1$ for the proton and $\delta_p = 0$ for the neutron, while μ_i is the algebraic magnetic moment of the nucleon in the Bohr magneton, M is the nucleon mass (2×10^3), and σ are the Pauli matrices.

$$\mathrm{I} = \int_{R_0}^{\infty} f_{j_1\lambda_1}(2)\, g_{j_1\lambda_1}(1)\, F_1(kr)\, r^2\, dr,$$

$$\mathrm{II} = \int_{R_0}^{\infty} g_{j_1\lambda_1}(2)\, f_{j_1\lambda_1}(1)\, F_1(kr)\, r^2\, dr.$$

The integrals I and II of the conversion transitions can be readily estimated for two limiting values of the transition energy ($\Delta \equiv k$): $k \leqslant Ze^2$ and $k \gg Ze^2$.

If $k \lesssim Ze^2$, we employ the Bessel-function expansion

$$F_L(kr) = -i \frac{(2L)!}{2^L L!} (kr)^{-L-1},$$

and if $k \gg Ze^2$ we carry out the calculation in the Born approximation. As a result we obtain for $k \lesssim Ze^2$:

for the $E2$ transition:

$$\mathrm{I} \approx -3ik^{-3} (\varepsilon_2 + 1)^{1/2} (\varepsilon_1 + 1)^{1/2} N_{j_1}(1) \times C_{j_2}(2)\, R_0^{\gamma_1+\gamma_2-3} \operatorname{Re} \Phi(\gamma_2),$$

for the $M1$ transition:

$$\mathrm{I} \approx -ik^{-2} (\varepsilon_2 - 1)^{1/2} (\varepsilon_1 + 1)^{1/2} N_{j_1}(1)\, C_{j_1}(2)\, R_0^{2(\gamma_1-1)} \operatorname{Im} \Phi(\gamma_2),$$

$$\mathrm{II} \approx ik^{-2} (\varepsilon_2 + 1)^{1/2} (1 - \varepsilon_1)^{1/2} N_{j_1}(1)\, C_{j_1}(2)\, R_0^{2(\gamma_1-1)} \operatorname{Re} \Phi(\gamma_2),$$

where

$$\Phi(\gamma_2) = \frac{e^{i\pi_2} (\gamma_2 + iZe^2 \varepsilon_2 / p_2)}{Ze^2 + ip_2}\, {}_2F_1\left(\gamma_2 + 1 + \frac{iZe^2\varepsilon_2}{p_2};\ 1;\ 2\gamma_2 + 1;\ \frac{2ip_2}{Ze^2 + ip_2} \right).$$

We shall assume furthermore that $\operatorname{Re} \Phi(\gamma_2) \approx \operatorname{Im} \Phi(\gamma_2) \approx 1/Ze^2$. If $k \gg Ze^2$ we can neglect the integrals II, since they are approximately proportional to $(Ze^2)^2$ I. We obtain in this case for $E2$ and $M1$:

$$E2:\ \mathrm{I}=i\frac{2}{\sqrt{\pi}}\left[\frac{(\varepsilon_2+1)(\varepsilon_1+1)}{k}\right]^{1/2}N_{j_1}R_0^{\gamma_1-1}\left(\frac{p_2}{k}\right)^{5/2}\frac{1}{p_2^2-k^2},$$

$$M1:\ \mathrm{I}\approx i\frac{2}{\sqrt{\pi}}\left[\frac{(\varepsilon_2-1)(\varepsilon_1+1)}{k}\right]^{1/2}N_{j_1}R_0^{\gamma_1-1}\left(\frac{p_2}{k}\right)^{3/2}\frac{1}{p_2^2-k^2}.$$

Using the values obtained for the integrals I and II, we obtain for the ratios of the $E2$ and $M1$ probabilities to the $E0$ transition probability:

For $k \lesssim Ze^2$

$$\frac{W_{E0}}{W_{E2}} \geqslant 3{,}5\cdot 2^{2(\gamma_1-\gamma_2)}R_0^{2(\gamma_1+1-\gamma_2)}\frac{|S_\lambda(1)\,S_\lambda(2)|^2}{(\varepsilon_1+1)(\varepsilon_2+1)}\left|\frac{\Gamma(2\gamma_2+1)}{\Gamma(2\gamma_1+1)}\right|^2\frac{p_2^{2(\gamma_1-\gamma_2)}}{[\mathrm{Re}\,\Phi(\gamma_2)]^2}$$
$$\times\left|\frac{\Gamma(\gamma_1+iZe^2\varepsilon_2/p_2)}{\Gamma(\gamma_2+iZe^2\varepsilon_2/p_2)}\right|^2\left|\frac{\langle 2\|E0\|1\rangle}{\langle 2\|E2\|1\rangle}\right|^2,$$

For $k \gg Ze^2$

$$\frac{W_{E0}}{W_{E2}} \geqslant 2^{2\gamma_1+1}R_0^{2(\gamma_1-1)}(p_2^2-k^2)^2\,p_2^{2\gamma_1-6}\exp\left(\pi Ze^2\frac{\varepsilon_2}{p_2}\right)$$
$$\times\left|\frac{\Gamma(\gamma_1+iZe^2\varepsilon_2/p_2)}{\Gamma(2\gamma_1+1)}\right|^2\frac{|S_\lambda(1)\,S_\lambda(2)|^2}{(\varepsilon_1+1)(\varepsilon_2+1)}\left|\frac{\langle 2\|E0\|1\rangle}{\langle 2\|E2\|1\rangle}\right|^2.$$

Taking it into account that the two last factors are approximately equal to unity, we obtain in accordance with the above estimate for $p \lesssim Ze^2$

$$W_{E0}/W_{E2} \geqslant 144\,|\langle 2\|E0\|1\rangle/\langle 2\|E2\|1\rangle|^2.$$

At low energies this ratio depends little on Z and is close to unity, even if we assume a value of approximately 0.1 for the ratio of the matrix elements.

If the transition energy is higher, $\Delta \sim 1$, the ratio W_{E0}/W_{E2} depends greatly on the value of the nuclear charge. At small values of Z we have $W_{E2} \approx W_{E0}$, and at large values of Z ($Z > 60$) we have $W_{E0} \gg W_{E2}$, if the reduced matrix elements are equal.

Analogously, we obtain the ratio of W_{E0}/W_{M1} for the same limiting cases. (The transition ($j = 1/2$; $\lambda = -1/2$) → ($j = 3/2$; $\lambda = 1/2$) is taken into account by the factor 2.)

For $k \lesssim Ze^2$

$$\frac{W_{E0}}{W_{M1}} \geqslant \frac{4\,[S_\lambda(1)\,S_\lambda(2)]^2}{[(\varepsilon_2-1)^{1/2}(\varepsilon_1+1)^{1/2}\,\mathrm{Im}\,\Phi(\gamma_2)-(1-\varepsilon_1)^{1/2}(1+\varepsilon_2)^{1/2}\,\mathrm{Re}\,\Phi(\gamma_2)]^2}\left|\frac{\langle 2\|E0\|1\rangle}{\langle 2\|M1\|1\rangle}\right|^2$$

and for $k \gg Ze^2$

$$\frac{W_{E0}}{W_{M1}} \geqslant 2^{2\gamma_1-1}\frac{[S_\lambda(1)\,S_\lambda(2)]^2}{(\varepsilon_1+1)(\varepsilon_2-1)}\frac{[p_2^2-k^2]^2}{p_2^{4-2\gamma_1}}\frac{R_0^{2(\gamma_1-1)}\exp(\pi Ze^2\varepsilon_2/p_2)\,|\Gamma(\gamma_1+iZe^2\varepsilon_2/p_2)|^2}{[\Gamma(2\gamma_1+1)]^2}$$
$$\times\left|\frac{\langle 2\|E0\|1\rangle}{\langle 2\|M1\|1\rangle}\right|^2.$$

In this case the ratio W_{E0}/W_{M1} is also a rapidly-growing function of Z. If $Z \lesssim 50$, its approximate value is 10^{-2}. The estimates cited show that in the transition-energy region $k \lesssim Ze^2$ one can except a considerable inclusion of electric monopole in the K electron conversion in the case of nuclear transitions of the type $\mathrm{I}^{\pm} \to \mathrm{I}^{\pm}$. In the transition-energy region $k \gg Ze^2$, the contribution of the monopole may be substantial only for sufficiently large values of Z ($Z > 50$).

7. ESTIMATE OF THE NUCLEAR TRANSITION MATRIX ELEMENT

The monopole nuclear matrix element, like that of other multipoles, can be estimated at the present time only within the framework of definite model representations. We shall give below the results of the estimate of the $E0$ matrix element both for the single-particle model, as well as for several models with collective motion of the nucleons. The estimates of the monopole matrix element are also given by Schiff[16].

1) *Single-Particle Model*

In the limiting case, when the change in the state of the nucleus occurs by a transition of one particle from state $\Omega^{\Lambda}_{I\,M}(1)$ into the state $\Omega^{\Lambda}_{I\,M}(2)$, the matrix element $\langle 2|\sum \xi_i^2|1\rangle$ reduces to the single-particle matrix element:

$$\langle 2\Big|\sum_{i=1}^{Z}\xi_i^2\Big|1\rangle = \left(\frac{Z}{A^2}+\delta_p\right)\langle\Omega^{\Lambda}_{I\,M}(2)\,|\,\xi^2\,|\,\Omega^{\Lambda}_{I\,M}(1)\rangle.$$

The core, the field of which contains the "external" nucleon, is assumed invariant. The term proportional to Z/A^2 results from the allowance for the effect of the recoil of the core, while $\delta_p = 1$ for the proton transition and $\delta_p = 0$ for the neutron transition. As a rough estimate

$$\langle\Omega^{\Lambda+}_{I\,M}(2)|\xi^2\,|\,\Omega^{\Lambda}_{I\,M}(1)\rangle \leqslant 0{,}6\,R_0^2.$$

2) *Hydrodynamic Polarization Oscillations of the Nucleus*

The monopole nuclear matrix element can also be estimated by representing the nucleus as a drop of a charged two-component nuclear liquid. Such a drop may be subject not only to radially-symmetrical pulsating surface oscillations but also to polarization oscillations of the proton and neutron components of the liquid. The frequency of these oscillations is considerably smaller than the frequency of the oscillations connected with the compressibility of the nucleus.

Comparing the classical and quantum-theoretical polarizabilities of a drop acted upon by a small perturbation $V = \lambda r^2 e^{i\omega t}$, we obtain an integral singular equation for the square of the modulus of the matrix element. The solution of this equation leads to the estimate:

$$\Big|\langle 2\Big|\sum_i^Z \xi_i^2\Big|1\rangle\Big|^2 g(\Delta) = \frac{3\pi\Gamma E_0^2\, Z\Delta R_0^5}{(\Delta^2-E_0^2)^2+\Gamma^2\Delta^2}$$

$$\times\left\{1-\frac{5}{3}\,\mathrm{Im}\,F(x)+\frac{5}{3}\,\frac{\Delta^2-E_0^2}{\Gamma\Delta}\,\mathrm{Re}\,F(x)\right\},$$

$$F(x) = \frac{[(6-x^2)(x\cos x-\sin x)+2x^2\sin x]}{x^2(x\cos x-\sin x)},$$

$$x = (k_0R_0)\sqrt{\frac{\Delta^2}{E_0^2}-1+i\,\frac{\Gamma\Delta}{E_0^2}}, \qquad E_0 = \frac{MV_0A}{4\pi NZe^2},$$

$$V_0 = \frac{3}{4\pi}R_0^3;$$

$$(k_0R_0) \approx 2{,}08\left|\left[\frac{\varepsilon_{\mathrm{res}}^2}{E_0^2}-1-i\,\frac{\Gamma\varepsilon_{\mathrm{res}}}{E_0^2}\right]^{-1/2}\right|.$$

Here N is the number of neutrons in the nucleus, $A = N + Z$, M the nucleon mass, Γ and $\varepsilon_{\mathrm{res}}$ the width and "resonance" energy of the known dipole "resonance" appearing in (γn) and (γp) reactions, and $g(\Delta)$ the density of the nuclear levels that can be excited by the $E0$ transition of the nucleus at an energy Δ. The above estimate is correct for transition energies at which the spectrum of the nucleus becomes continuous.

3) *Surface Quadrupole Oscillations of the Nucleus*

Even-even nuclei with A ranging from 76 to 152 have apparently an energy spectrum corresponding to a hydrodynamic phonon nuclear excitation of the quadrupole type. This was first pointed out by Scharf-Goldhaber and Weneser[17]. However, another interpretation of the spectrum of these nuclei is possible. The problem can be solved by investigating the ratios of the photon-emission probabilities to the electron conversion probability for various nuclear transitions. Electric monopole transitions make possible still another clarification of the character of excitation of this group of nuclei. It would therefore be interesting, within the framework of this model, to estimate the matrix element of the $E0$ transition and to compare it with the matrix element of the $E2$ transition. We shall next describe the state of the nucleus by the following quantum numbers: ν – number of phonons, I, μ – spin and spin

projection on the OZ axis. The wave function of the nucleus is $\chi^{\nu}_{I\mu}$. Depending on the number of the phonons, the spin of the even-even nucleus can assume the following values $\nu = 0$, $I = 0$; $\nu = 1$, $I = 2$; $\nu = 2$, $I = 0$, 2, and 4. Experimentally one observes the following sequence in the values of the nuclear spin in the fundamental, first, and second excited states

$$[I = 0,\ I = 2,\ I = 0];$$
$$[I = 0,\ I = 2,\ I = 2]; \text{and } [I = 0,\ I = 2,\ I = 4].$$

In the case of the spectrum of the first and second types, $E0$ transitions with electron conversion can occur between the second and ground state and between the first and second states of the nucleus respectively. A simple calculation, under the assumption that these states are phonon excitations of the nucleus, yields the following values of the matrix elements of the $E2$ and $E0$ transitions ($\hat{E}2$ and $\hat{E}0$ operators of the $E2$ and $E0$ multipoles):

$$\langle \chi^{0+}_{00} | \hat{E0} | \chi^{2}_{00} \rangle = \frac{3}{4\pi} ZR_0^2 \sqrt{\frac{2}{5}} \left(\frac{\hbar\omega}{2c_2}\right),$$

$$\langle \chi^{1+}_{2\mu} | \hat{E0} | \chi^{2}_{2\mu} \rangle = \frac{3}{4\pi} ZR_0^2\, 6 \sqrt{\frac{5}{4\pi}}\, C^{20}_{2020} \left(\frac{\hbar\omega}{2c_2}\right)^{3/2},$$

$$\langle \chi^{0+}_{00} | (\hat{E2})_M | \chi'_{2\mu} \rangle = \frac{3}{4\pi} ZR_0^2 \left(\frac{\hbar\omega}{2c_2}\right)^{1/2} (-1)^M \delta_{\mu -M} \sqrt{\frac{4\pi}{5}},$$

$$\langle \chi^{0+}_{00} | (\hat{E2})_M | \chi^{2}_{2\mu} \rangle = \frac{3}{4\pi} ZR_0^2 \sqrt{8}\, C^{20}_{2020} \left(\frac{\hbar\omega}{2c_2}\right) \delta_{\mu -M}\, (-1)^M$$

$$\langle \chi^{1+}_{2\mu} | (\hat{E2})_M | \chi^{2}_{00} \rangle = \frac{3}{4\pi} ZR_0^2 \frac{2}{5} \left(\frac{\hbar\omega}{2c_2}\right)^{1/2} \delta_{\mu M} \sqrt{2\pi},$$

$$\langle \chi^{1+}_{2\mu_1} | (\hat{E2})_M | \chi^{2}_{2\mu_2} \rangle = \frac{3}{4\pi} ZR_0^2 \sqrt{\frac{8\pi}{5}}\, C^{2\mu_2}_{2\mu_1,\ 2-M} \left(\frac{\hbar\omega}{2c_2}\right)^{1/2} (-1)^M.$$

We obtain for the ratio of the matrix elements of the competing transitions:

$$\langle \chi^{0+}_{00} \| \hat{E0} \| \chi^{2}_{00} \rangle / \langle \chi^{1+}_{2\mu_1} \| \hat{E2} \| \chi^{2}_{00} \rangle \approx 0.1,$$

$$\langle \chi^{1+}_{2\mu} \| \hat{E0} \| \chi_{2\mu'} \rangle / \langle \chi^{1+}_{2\mu_1} \| \hat{E2} \| \chi_{2\mu_2} \rangle \leqslant 0.05.$$

It is assumed in the estimate that $(\hbar\omega/2c_2)^{1/2} \approx 0.18$ (see, for example, Refs. 18 and 19). For the matrix elements of the $E0$ transitions of two nuclei with different spectra we have

$$\langle \chi^{1+}_{2\mu} \| \hat{E0} \| \chi^{2}_{2\mu} \rangle / \langle \chi^{0+}_{00} \| \hat{E0} \| \chi^{2}_{00} \rangle \approx 0.5.$$

We obtain a numerical estimate of the order of magnitude of the matrix elements by putting $(\hbar\omega/2c_2)^{1/2} \approx 0.18$; then

$$\langle \chi^{0+}_{00} | \hat{E0} | \chi^{2}_{00} \rangle \approx 5 \cdot 10^{-3} ZR_0^2,$$

$$\langle \chi^{1+}_{2\mu} | \hat{E0} | \chi^{2}_{2\mu} \rangle \approx 2 \cdot 10^{-3} ZR_0^2.$$

8. CERTAIN RESULTS OF THE CALCULATIONS

By way of illustration let us give the calculated probabilities of the shell-electron conversion, pair conversion and $\gamma\gamma$ transition for the nuclei Ca^{40}_{20}, Ge^{72}_{32}, Zr^{90}_{40}, Pd^{106}_{46}, and Po^{214}_{84}.

Table 2 gives the values of the probabilities, divided by

$$|\langle 2 | \sum_i (\xi_i / R_0)^2 | 1 \rangle|^2 \text{ and } |\langle 2 | \sum_{i,\,j} (\xi_i \xi_j / R_0^2) | 1 \rangle|^2$$

for the $\gamma\gamma$ transition.

TABLE II.

Nucleus	$\frac{\Delta}{mc^2}$	$W_{\gamma\gamma}$	W_{pair}	W_K	$\frac{W_K}{W_{LI}}$	$\frac{W_{LI}}{W_{LII}}$	$\varkappa_K$	$\varkappa_{L\,II}$	$\varkappa_L$
Ca_{20}^{40}	6.7	$1.5\cdot10^9$	$\sim 4\cdot10^7$	$5{,}05\cdot10^8$	7.8	342	0.99	0.965	0.97
Ge_{32}^{72}	1.4	$5.5\cdot10^4$	0	$2{,}56\cdot10^8$	7.4	198	0.96	0.83	0.945
Zr_{40}^{90}	3.5	$5.7\cdot10^6$	$\sim 1.4\cdot10^6$	$1{,}16\cdot10^{10}$	7.6	102	0.87	0.88	0.88
Pd_{46}^{106}	2.27	$3.3\cdot10^6$	—	$3{,}54\cdot10^{10}$	6.9	71	0.88	0.87	0.87
Po_{84}^{214}	2.85	$5.6\cdot10^7$	$\sim 8.7\cdot10^6$	$8{,}45\cdot10^{12}$	5.3	19.6	0.68	0.77	0.75

All the values of the probabilities are given in the usual units, sec^{-1}.

Data concerning $E0$ transitions of even-nuclei with A ranging between 60 and 160 are of particular interest. A study of the $E0$ transitions for this range of A between levels of nuclei with spin $I: 0^+ \to 0^+$ and $2^+ \to 2^+$ would make it possible to establish the character of the excited states of the nuclei.

Note added in proof (April 27, 1957): After this article went to press, we became acquainted with the work by Church and Weneser [E. Church, J. Weneser, Phys. Rev. **103**, 1035 (1956)] which deals with the conversion of the shell electron in the $E0$ nuclear transition. They used numerical methods and took the screening effect into account. Since the calculated data are given in graphic form, direct comparison of the results is difficult. However, qualitative deductions and the values obtained in our work published for many nuclei are in good agreement with the values cited by Church and Weneser.

[1] R. H. Fowler, Proc. Roy. Soc. A129, 1 (1930).

[2] H. Yukawa and S. Sacata, Proc. Math. Soc. Japan **17**, 306 (1935).

[3] L. A. Sliv. J. Exptl. Theoret. Phys. (U.S.S.R.) **21**, 7 (1053).

[4] K. A. Ter-Martirosian, J. Exptl. Theoret. Phys. (U.S.S.R.) **20**, 925 (1950).

[5] J. R. Oppenheimer and J. Schwinger, Phys. Rev. **56**, 1066 (1939).

[6] R. H. Dalitz, Proc. Roy. Soc. **A206**, 521 (1951).

[7] J. R. Oppenheimer, Phys. Rev. **60**, 164 (1941).

[8] V. B. Berestetzkii, A. Z. Dolginov, K. A. Ter-Martirosian, J. Exptl. Theoret. Phys. (U.S.S.R.) **20**, 576 (1950).

[9] A. I. Akhiezer, and V. B. Berestetskii, *Quantum Electrodynamics*, 1955, pp 78-84

[10] H. Bethe, *Quantum Mechanics of Simplest Systems*, 1935, ONTI

[11] M. Rose, Phys. Rev. **51**, 484 (1937).

[12] L. A. Sliv, J. Exptl. Theoret. Phys. (U.S.S.R.) **17**, (1032) 1947.

[13] R. G. Sachs, Phys. Rev. **57**, 194 (1940).

[14] M. L. Goldberger, Phys. Rev. **72**, 1119 (1948)

[15] J. S. Levinger, Phys. Rev. **98**, 1281 (1955).

[16] L. Schiff, Phys. Rev. **95**, 418 (1954).

[17] G. Sharf-Goldhaber, J. Weneser, Phys. Rev. **98**, 212 (1955).

[18] F. J. Milford, Phys, Rev. **93**, 1297 (1954).

[19] O. Bohr, and B. Mottelson, Problemy sovr. fiziki **9** (1955).

Translated by J. G. Adashko
221

Investigation of a Model in Quantum Field Theory

V. G. SOLOV'EV

Institute of Nuclear Problems, Academy of Sciences of the U.S.S.R.

(Submitted to JETP editor May 15, 1956)

J. Exptl. Theoret. Phys. (U.S.S.R.) 32, 1050-1057 (May, 1957)

A model is considered in which a spinor field interacts with a pseudoscalar field, the classical pseudoscalar field being independent of the coordinates. Owing to the properties of the model the equations for the Green function are considerably simplified, and this makes it possible to find their exact solution. An investigation of the Green function is carried out.

IN VIEW OF the great difficulties in principle that stand in the way of the solution of the equations of quantum field theory, methodological interest attaches to the study of particular models for which exact solutions of the corresponding equations can be obtained. A large number of papers [1-9] have been devoted to the consideration of various models. The model of a renormalized field theory proposed by T. D. Lee [2] is studied in some papers [3,4], while others [5,6] consider generalizations of this model or use Lee's idea to construct a new model [7,8]. Consideration has been given to a model of a meson pair theory [9] and to a number of other theories.

The purpose of the present paper is the investigation of a new model, in which the equation for the Green function of the fermion can be solved exactly.

1. STATEMENT OF THE MODEL

We consider an interaction of pseudoscalar (for simplicity, neutral) bosons with fermions, which is characterized by the Lagrangian

$$L(x) = g : \overline{\Psi}(x)\gamma_5\Psi(x) : \varphi(x) + M(x), \qquad (1)$$

where $M(x)$ depends on the operator $\varphi(x)$ of the boson field and can include a "classical source" term $J(x)\varphi(x)$ and also counter-terms for renormalization. The model considered is such that the classical boson field does not depend on the coordinates.

Abrikosov and Khalatnikov [10] have examined the point interaction

$$g\overline{\Psi}(x)\Gamma\Psi(x)\varphi(x)$$

as the limit of the "smeared-out" interaction

$$g\int \overline{\Psi}(x)\Gamma\Psi(y)\varphi(z)K(x-y, x-z)\,dy\,dz$$

with limiting momenta λ_ψ and λ_φ satisfying the condition $\lambda_\psi \gg \lambda_\varphi$. In terms of this two-limit technique the model we have studied corresponds to the case in which the limiting momentum λ_φ of the boson is equal to zero and the limiting momentum λ_ψ of the fermion has gone to infinity.

To find the Green function of the fermion we employ the formulas obtained by Bogoliubov [11], which express the Green function $G(x, y|J)$ in terms of the Green function $G_{c1}(x, y|\varphi)$ of a single fermion in the classical field φ. In momentum space they have the following form [1]:

$$G(k|J) = \frac{\int \delta\varphi \exp\left\{-\frac{1}{2}\int dp\,\varphi(p)D^{-1}(p)\varphi(p)\right\} G_{c1}(k|\varphi)\times}{\int \delta\varphi \exp\left\{-\frac{1}{2}\int dp\,\varphi(p)D^{-1}(p)\varphi(p)\right\}\times}$$

$$\rightarrow \frac{\times \exp\left\{-\frac{1}{g}\int_0^1 d\beta \int dp\,dq\,\mathrm{Sp}\,\gamma_5\, G_{c1}(p-q, p|\beta\varphi)\varphi(q) + \int M(p)\,dp\right\}}{\times \exp\left\{-\frac{1}{g_0}\int_0^1 d\beta \int dp\,dq\,\mathrm{Sp}\,\gamma_5\, G_{c1}(p-q, p|\beta\varphi)\varphi(q) + \int M(p)\,dp\right\}}, \qquad (2)$$

$$(m + \gamma_\mu k_\mu) G_{c1}(k, k' | \varphi) - \bar{g} \gamma_5 \int dq\, G_{c1}(k - q, k | \varphi) \varphi(q) = \delta(k - k'), \tag{3}$$

$$\left[m + \gamma_\mu k_\mu + \int dp\, \gamma_\mu p_\mu \varphi(p) \frac{\delta}{\delta \varphi(p)} - \bar{g} \gamma_5 \int dp\, \varphi(p) \right] G_{c1}(k | \varphi) = 1. \tag{3'}$$

Here $\bar{g} = g(2\pi)^{-2}$, and the matrices γ and scalar products are defined as follows:

$$\gamma_k = \beta\alpha_k \quad (k = 1, 2, 3), \quad \gamma_4 = i\beta,$$

$$\gamma_5 = \gamma_1 \gamma_2 \gamma_3 \beta, \quad AB = A_4 B_4 + \mathbf{AB}.$$

In the model under consideration the limiting momentum λ_ϕ of the boson is equal to zero, *i.e.*, the boson is, so to speak, smeared over the entire x-space, and the limiting momentum λ_ψ of the fermion has gone to infinity, *i.e.*, the fermion is a point particle. If we study the behavior of the Green function of the fermion at momenta satisfying the condition $k^2 \gg \lambda_\phi^2$, our present model is the limiting case for $\lambda_\phi \to 0$.

In this model $\varphi(x)$ does not depend on x, so that we get the required formulas if we replace $\varphi(p)$ by $\varphi\delta(p)$, the variational derivative $\delta/\delta\varphi$ by the ordinary $\partial/\partial\varphi$, and the Feynman integral $\int \delta\varphi F(\varphi)$ by the integral over a single variable, $\int_{-\infty}^{\infty} d\varphi F(\varphi)$. Here also the Green function $D(p, p')$ of the free boson field goes over into $d \times \delta(p)\delta(p')$, where d is a constant. The equation for $G_{c1}(k, x; \varphi)$ now takes the simple form

$$(m + \gamma_\mu k_\mu - \bar{g} \gamma_5 \varphi) G_{c1}(k, x; \varphi) = 1. \tag{4}$$

The unrenormalized Green function $G(k; J)$ is then expressed in terms of $G_{c1}(k; \varphi)$ in the following way:

$$G(k; J) = \frac{\int_{-\infty}^{\infty} d\varphi e^{-\varphi^2/2d} G_{c1}(k; \varphi) \exp\left\{ \delta_\lambda \bar{g}' \int_0^1 d\beta \int_\Omega dp\, \mathrm{Sp}\, \gamma_5 G_{c1}(p, p; \beta\varphi) \varphi + M(\varphi; J) \right\}}{\int_{-\infty}^{\infty} d\varphi e^{-\varphi^2/2d} \exp\left\{ \delta_\lambda \bar{g}' \int_0^1 d\beta \int_\Omega dp\, \mathrm{Sp}\, \gamma_5 G_{c1}(p, p; \beta\varphi) \varphi + M(\varphi; J) \right\}}, \tag{5}$$

where

$$G_{c1}(k; \varphi) = (m - \gamma_\mu k_\mu + \bar{g} \gamma_5 \varphi) / (m^2 + k^2 + \bar{g}^2 \varphi^2), \tag{6}$$

and here $\lim_{\lambda \to \infty} \delta_\lambda = \delta(0)$, *i.e.*, the δ-function of zero; g' is the priming coupling constant. In Eq. (5) the integral with respect to p is taken over a finite four-dimensional region Ω, prior to carrying out the renormalization.

On the other hand, the expressions obtained in our model for the Green function of the fermion can be regarded as a sort of approximate Green function of the nucleon of quantum field theory, if we assume as a first approximation $\varphi(x) = \text{const}$. It was just this approximation that Feynman used to estimate the role of nucleon-antinucleon pairs.

2. ONE-PARTICLE APPROXIMATION

Let us consider the so-called one-particle approximation, which, in the language of Feynman diagrams, reduces to the neglect of closed fermion loops. In this approximation the Green function $G(k)$ is very simply related to the Green function $G_{c1}(k; \varphi)$ of a single fermion in the classical field φ, namely:

$$G(k) = (2\pi d)^{-1/2} \int_{-\infty}^{\infty} e^{-\varphi^2/2d} d\varphi\, G_{кл}(k; \varphi). \tag{7}$$

We use expression (6) and get

$$G(k) = 2(2\pi d)^{-1/2} \int_0^\infty d\varphi e^{-\varphi^2/2d} \frac{m - \gamma_\mu k_\mu}{m^2 + k^2 + \bar{g}^2 \varphi^2}. \tag{8}$$

The integral in Eq. (8), convergent in the region $k^2 \geq 0$, can be expressed in terms of the probability integral

$$\Phi(x) = \frac{2}{\sqrt{\pi}} \int_0^x dt e^{-t^2}.$$

On this basis we write the Green function $G(k)$ in the form

$$G(k) = \frac{m - \gamma_\mu k_\mu}{m^2 + k^2} \sqrt{2\pi} \left(\frac{\bar{g}^2 d}{m^2 + k^2} \right)^{-1/2} \exp\left\{ \frac{m^2 + k^2}{2\bar{g}^2 d} \right\} \left[1 - \Phi\left(\sqrt{\frac{m^2 + k^2}{2d\bar{g}^2}} \right) \right], \tag{9}$$

for $\bar{g}^2 \neq 0$.

Let us find out whether the function $G(k)$ can be represented as a converging series in powers of $\bar{g}^2$. For this purpose we write $G(k)$ in a different way, namely

$$G(k) = \frac{m - \gamma_\mu k_\mu}{\sqrt{m^2 + k^2}} \int_0^\infty dx e^{-x} (m^2 + k^2 + 2d\bar{g}^2 x)^{-1/2}. \tag{10}$$

Integrating by parts n times we get

$$G(k) = \frac{m - \gamma_\mu k_\mu}{m^2 + k^2} \left\{ 1 - \frac{\bar{g}^2 d}{m^2 + k^2} + 1 \cdot 3 \cdot \frac{\bar{g}^4 d^2}{(m^2 + k^2)^2} + \ldots \right.$$

$$\left. \ldots + (-1)^n (2n-1)!! \frac{d^n \bar{g}^{2n}}{(m^2 + k^2)^n} + \bar{g}^{2(n+1)} (2n+1)!! \sqrt{m^2 + k^2}\, d^{n+1} \right. \tag{10'}$$

$$\left. \times \int_0^\infty \frac{e^{-x} dx}{(m^2 + k^2 + 2d\bar{g}^2 x)^{(2n+3)/2}} \right\}.$$

Let S_n be the sum of the first $(n+1)$ terms of the expansion in power of g^2; then

$$\lim_{\bar{g}^2 \to 0} (\bar{g}^2)^{-n} [G(k) - S_n] = \lim_{\bar{g}^2 \to 0} \bar{g}^2 \frac{(2n+1)!!}{\sqrt{m^2 + k^2}} d^{n+1} \int_0^\infty \frac{e^{-x} dx}{(m^2 + k^2 + 2d\bar{g}^2 x)^{(2n+3)/2}} = 0.$$

From this it follows that $G(k)$ can be represented by the following asymptotic series

$$G(k) \sim \frac{m - \gamma_\mu k_\mu}{m^2 + k^2} \sum_{n=0}^\infty (-1)^n (2n-1)!! \bar{g}^{2n} \left(\frac{d}{m^2 + k^2} \right)^n. \tag{11}$$

This series is of the type summable by Borel's method[13,14]. This means that from the coefficients of the asymptotic expansion one can recover the original function by using the generalized Borel method. To show this, we represent unity in each term of the series (11) as

$$1 = \frac{2}{\sqrt{2\pi d}} \frac{1}{d^n} \frac{1}{(2n-1)!!} \int_0^\infty e^{-\varphi^2/2d} \varphi^{2n} d\varphi .$$

We interchange the order of summation and integration and obtain

$$G(k) \sim \frac{2}{\sqrt{2\pi d}} \frac{m - \gamma_\mu k_\mu}{m^2 + k^2} \int_0^\infty e^{-\varphi^2/2d} d\varphi \sum_{n=0}^\infty \bar{g}^{2n} \left(- \frac{\varphi^2}{m^2 + k^2} \right)^n . \tag{12}$$

We then write unity in each term of the series (12) in the form

$$1 = \frac{1}{n!} \int_0^\infty e^{-x} x^n dx,$$

interchange once more the order of summation and integration, and get the convergent series

$$G(k) = \frac{2}{\sqrt{2\pi d}} \frac{m - \gamma_\mu k_\mu}{m^2 + k^2} \int_0^\infty d\varphi e^{-\varphi^2/2d} \int_0^\infty e^{-x} dx \sum_{n=0}^\infty \frac{(-1)^n}{n!} x^n \bar{g}^{2n} \left(\frac{\varphi^2}{m^2 + k^2} \right)^n .$$

We thus recover the original function (8) from the asymptotic series (11) by using the generalized Borel method.

It must be remarked that in the case of the symmetric (not the neutral) theory the Green function of the fermion must be written as follows:

$$G(k) = \int_0^\infty dx (m - \gamma_\mu k_\mu) e^{-(m^2+k^2)x} (1 + 2d\bar{g}^2 x)^{-3/2} . \tag{13}$$

3. THE EXACT GREEN FUNCTION OF THE FERMION

For our model it is possible to find the exact Green function of the fermion, neglecting none of the Feynman diagrams.

First let us consider the nonrenormalized Green function $G(k)$. We substitute into Eq. (5) the function $G_{cl}(k; \varphi)$ in the form (6) and get

$$G(k) = \frac{\int_{-\infty}^{\infty} \frac{m - \gamma_\mu k_\mu}{m^2 + k^2 + \bar{g}^2\varphi^2} \exp\left\{ -4\bar{g}'^2 \delta_\lambda \int_0^1 \beta d\beta \int_\Omega \frac{\varphi^2 dp}{m^2 + p^2 + \bar{g}^2\varphi^2\beta^2} + M(\varphi) - \frac{\varphi^2}{2d} \right\} d\varphi}{\int_{-\infty}^{\infty} \exp\left\{ -4\bar{g}'^2 \delta_\lambda \int_0^1 \beta d\beta \int_\Omega \frac{\varphi^2 dp}{m^2 + p^2 + \bar{g}^2\varphi^2\beta^2} + M(\varphi) - \frac{\varphi^2}{2d} \right\} d\varphi} . \tag{14}$$

Since the model under consideration corresponds to a certain degree to the behavior of the nucleon Green function of pseudoscalar meson theory for large k^2, *i.e.*, very far from the pole $k^2 = m^2$, the mass of the fermion should be set equal to zero. But we do not do this, in order to avoid divergences of the type of the infrared catastrophe.

If we carry out the renormalization

$$\bar{g}^2 = \bar{g}'^2 \delta_\lambda m^4,$$

the Green function $G(k)$ degenerates into

$$G(k) = (m - \gamma_\mu k_\mu)/(m^2 + k^2),$$

i.e., into the Green function of the free fermion field. This occurs because of incorrect performance of the renormalization. In the carrying out of the renormalization there are certain peculiar features, owing to the nature of the model, *i.e.*, to the fact that all the virtual mesons transfer only zero momentum. Associated with this are divergences of the form $\delta(0)$. There are also divergences in those Feynman diagrams that involve fermion pairs, *i.e.*, in the boson self-energy diagrams, the diagrams of boson-boson scattering, and also the corresponding overlapping diagrams.

Owing to the presence of these two types of divergences we carry out the renormalization in two stages: first we renormalize the fermion Green function

$$G''(k) = (\delta_\lambda m^4)\, G(k)$$

and corresponding to this we renormalize the charge, and then, in the second stage, we remove the ordinary divergences associated with the fermion pairs.

To carry out the renormalization

$$G''(k) = (\delta_\lambda m^4)\, G(k)$$

one must either add to the Lagrangian a counterterm having the operator structure of the free fermion field, *i.e.*, a term of the form

$$L'(x) = -{}^1/_2\,[\delta_\lambda m^4 - 1] : \overline{\Psi}(x)$$

$$i(m - i\gamma_\mu \partial/\partial x_\mu)\,\Psi(x) : + \text{ compl. conj.}$$

or predetermine the pairing of two fermion operators in the following way:

$$\langle T\{\Psi(x)\,\overline{\Psi}(x')\}\rangle_0 = (\delta_\lambda m^4)^{-1} S_F(x - x').$$

In both cases this leads to the charge renormalization $g'' = (\delta_\lambda m^4)^{-1} g'$.

To carry out the second stage of the renormalization we use the counter-terms $B\varphi^4$ and $A\varphi^2$, where A and B are certain constants that go to infinity as the region of integration Ω is extended to the entire four-dimensional space. The term $B\varphi^4$ corresponds to the direct interaction of bosons; a counter-term of this form is necessary in carrying out the renormalization in pseudoscalar meson theory. In our case it is contained in $M'(\varphi)$. The counter-term $A\varphi^2$ is obtained by the predetermination of the T-product of two boson functions (*cf.* Ref. 15) and occurs in the expression for the fermion Green function in the form

$$\exp\{-\varphi^2(d^{-1} + A)/2\}.$$

The presence of these two counter-terms makes it possible to cancel from the integral

$$\int_\Omega dp\, \frac{\bar{g}^2 \varphi^2}{m^2 + p^2 + \bar{g}^2 \varphi^2 \beta^2}$$

the terms proportional to φ^2 and φ^4, which diverge for $\Omega \to \infty$, with the result having the appearance

$$\lim_{\Omega\to\infty} \int_\Omega dp \left\{ \frac{\bar{g}^2 \varphi^2}{m^2 + p^2 + \bar{g}^2 \varphi^2 \beta^2} - \frac{\bar{g}^2 \varphi^2}{m^2 + p^2} + \frac{\bar{g}^4 \varphi^4 \beta^2}{(m^2 + p^2)^2} \right\} = \int dp\, \frac{\bar{g}^6 \beta^4 \varphi^6}{(m^2 + p^2)^2 (m^2 + p^2 + \bar{g}^2 \varphi^2 \beta^2)}. \tag{15}$$

The divergent part of the coefficients A and B is uniquely determined, but in the determination of the finite parts there is a certain arbitrariness. As is well known, for the term $B\varphi^4$ this leads to the appearance of an additional coupling constant. The arbitrariness in the determination of the finite part of the coefficient A exists only in our model and is due to the absence of the condition

$$\lim_{\gamma_\mu k_\mu \to -m} G(k)(m + \gamma_\mu k_\mu) = 1.$$

imposed in field theory. In view of the presence of

this arbitrariness we can subtract from the expression (15) some finite function $N(\varphi) = a\varphi^2 + b\varphi^4$.

As the result of the renormalization, the Green function $G'(k)$ takes the following form

$$G'(k) = \frac{\int_{-\infty}^{\infty} \frac{m - \gamma_\mu k_\mu}{m^2 + k^2 + \bar{g}^2\varphi^2} \exp\left\{-\frac{\bar{g}^6}{m^4}\int_0^1 \beta^5 d\beta \int \frac{\varphi^6 dp}{(m^2+p^2)^2(m^2+p^2+\bar{g}^2\varphi^2\beta^2)} - N(\varphi) - \frac{\varphi^2}{2d}\right\} d\varphi}{\int_{-\infty}^{\infty} \exp\left\{-\frac{\bar{g}^6}{m^4}\int_0^1 \beta^5 d\beta \int \frac{\varphi^6 dp}{(m^2+p^2)^2(m^2+p^2+\bar{g}^2\varphi^2\beta^2)} - N(\varphi) - \frac{\varphi^2}{2d}\right\} d\varphi} \tag{16}$$

We evaluate the integral in the exponential function and obtain the final expression

$$G'(k) = \frac{\int_0^{\infty} e^{-\varphi^2/2d} d\varphi \frac{m - \gamma_\mu k_\mu}{m^2 + k^2 + \bar{g}^2\varphi^2} \exp\left\{f_1\left(\frac{\varphi}{m}\right)^4 + f_2\left(\frac{\varphi}{m}\right)^2\right\}\left(1 + \bar{g}^2\frac{\varphi^2}{m^2}\right)^{-\pi^2(1+\bar{g}^2\varphi^2/m^2)^2}}{\int_0^{\infty} e^{-\varphi^2/2d} d\varphi \exp\left\{f_1\left(\frac{\varphi}{m}\right)^4 + f_2\left(\frac{\varphi}{m}\right)^2\right\}\left(1 + \bar{g}^2\frac{\varphi^2}{m^2}\right)^{-\pi^2(1+\bar{g}^2\varphi^2/m^2)^2}}, \tag{17}$$

where f_1 and f_2 are arbitrary constants. The integrals over φ converge for $k^2 \geq 0$, and the values of the constants f_1 and f_2 cannot affect the convergence of these integrals.

From these considerations it can be seen that the renormalization procedure can be carried out consistently without the use of perturbation theory.

The properties of the propagation functions of fermions and bosons and of the renormalization constants have been studied by Lehmann [16], Gell-Mann and Low [17], and Källen [18].

Lehmann considered a neutral pseudoscalar field $\varphi(x)$ interacting with a spinor field $\Psi(x)$. Without making any special assumptions about the form of the interaction, but assuming that the theory is relativistically invariant and that the energy operator possesses a smallest eigenvalue, which is normalized to zero, he obtained the conditions that must be satisfied by the elements of the suitably written propagation functions and renormalization constants.

It is of interest to write our fermion Green function $G'(k)$ in the form given by Lehmann and examine whether these conditions are satisfied. If we take into account our notations and the properties of the model considered (absence of a discrete level at $k^2 = m^2$), Lehmann's formulas can be written in the following way: the fermion Green function has the form

$$G'(k) = \int_{m^2}^{\infty} d(\varkappa^2) \frac{(\varkappa - \gamma_\mu k_\mu)\rho_1(\varkappa^2) - \rho_2(\varkappa^2)}{k^2 + \varkappa^2}, \tag{18}$$

where $\rho_1(\varkappa^2)$ and $\rho_2(\varkappa^2)$, defined for positive values of the argument, must satisfy the inequalities

$$\rho_1(\varkappa^2) \geqslant 0, \quad 2\varkappa\rho_1(\varkappa^2) \geqslant \rho_2(\varkappa^2) \geqslant 0. \tag{19}$$

The renormalization constants have the form

$$Z_2^{-1} = \int_{m^2}^{\infty} \rho_1(\varkappa^2)\, d(\varkappa^2),$$

$$\delta m = Z_2 \int_{m^2}^{\infty} [(m - \varkappa)\rho_1(\varkappa^2) + \rho_2(\varkappa^2)]\, d(\varkappa^2), \tag{20}$$

where Z_2 must satisfy the inequality

$$Z_2 \geqslant 0. \tag{21}$$

In order to get $G'(k)$ in the form (18), we make in Eq. (17) the change of variable $\varkappa^2 = m^2 + \bar{g}^2\varphi^2$, valid for $\bar{g}^2 \neq 0$; then

$$G'(k) = \frac{\int\limits_{m^2}^{\infty} \frac{d(\varkappa^2)}{\sqrt{\varkappa^2 - m^2}} \frac{(\varkappa - \gamma_\mu k_\mu) - (\varkappa - m)}{\varkappa^2 + k^2} \left(\frac{\varkappa^2}{m^2}\right)^{-\pi^2(\varkappa^2/m^2)^2} e^{-\varkappa^2/2\bar{g}^2 d}}{\int\limits_{m^2}^{\infty} \frac{d(\varkappa^2)}{\sqrt{\varkappa^2 - m^2}} \left(\frac{\varkappa^2}{m^2}\right)^{-\pi^2(\varkappa^2/m^2)^2} e^{-\varkappa^2/2\bar{g}^2 d}}, \tag{22}$$

here $\varkappa_\Lambda = (\varkappa^2)^{1/2}$ and, for simplicity, $f_1 = f_2 = 0$. Comparing Eqs. (22) and (18), we get

$$\rho_1(\varkappa^2) = \frac{\frac{1}{\sqrt{\varkappa^2 - m^2}} \left(\frac{\varkappa^2}{m^2}\right)^{-\pi^2(\varkappa^2/m^2)^2} e^{-\varkappa^2/2\bar{g}^2 d}}{\int\limits_{m^2}^{\infty} \frac{d(\varkappa^2)}{\sqrt{\varkappa^2 - m^2}} \left(\frac{\varkappa^2}{m^2}\right)^{-\pi^2(\varkappa^2/m^2)^2} e^{-\varkappa^2/2\bar{g}^2 d}}, \quad \rho_2(\varkappa^2) = (\varkappa - m)\rho_1(\varkappa^2). \tag{23}$$

It can easily be seen that $\rho_1(\varkappa^2)$ and $\rho_2(\varkappa^2)$ satisfy the conditions (19). Substituting the values (23) for ρ_1 and ρ_2 into Eq. (20), we get

$$Z_2 = 1, \quad \delta m = 0. \tag{24}$$

The fulfillment of the conditions (19) and (21) shows that our model is free from internal contradictions.

It has been shown by Lehmann that if

$$\int\limits_{m^2}^{\infty} \rho_1(\varkappa^2)\, d(\varkappa^2) < \infty,$$

then at large momenta the exact Green functions exhibit the same behavior as the free Green functions. In our model this integral is equal to unity, so that the fermion Green function $G'(k)$ behaves like $1/\gamma k$ at very large momenta.

From the consideration of the fermion Green function $G'(k)$, taken in the form (17), it can be seen that $G'(k)$ cannot be represented as a convergent series in powers of g^2. Moreover, neither in the numerator nor in the denominator of (17) can the integrand be expanded in convergent power series in g^2. It turns out to be impossible to introduce a finite number of supplementary integrations over the parameters in such a way that the integrand could be represented in the form of a convergent series in powers of the interaction constant g^2. This suggests that the series of perturbation theory cannot serve as the basis for carrying out any investigations in pseudoscalar meson theory.

We proceed further to write $G'(k)$ in the form

$$G'(k) = \frac{\int\limits_{m^2}^{\infty} \frac{d(\varkappa^2)}{\sqrt{\varkappa^2 - m^2}} \frac{m - \gamma_\mu k_\mu}{\varkappa^2 + k^2} \left(\frac{\varkappa^2}{m^2}\right)^{-\pi^2(\varkappa^2/m^2)^2} e^{-\varkappa^2/2\bar{g}^2 d}}{\int\limits_{m^2}^{\infty} \frac{d(\varkappa^2)}{\sqrt{\varkappa^2 - m^2}} \left(\frac{\varkappa^2}{m^2}\right)^{-\pi^2(\varkappa^2/m^2)^2} e^{-\varkappa^2/2\bar{g}^2 d}}, \tag{25}$$

valid for $\bar{g}^2 \neq 0$. From this expression it can be seen that both in the numerator and in the denominator the integrands can be expanded in series of inverse powers of the coupling constant. These series under the sign of integration over $\varkappa^2$ are convergent, and even if one carries out the integration term by term each term of the series obtained will be finite.

It must be remarked that the contribution from the polarization of the vacuum is included in the first term of the expansion in inverse powers of the coupling constant; the vacuum polarization does not occur in the perturbing term.

If in the case of the one-particle approximation one expands the integrand in a series of inverse powers of the coupling constant, then after integration each term of the series, except the first, will be infinite. This leads to the conclusion that the inclusion of the vacuum polarization decidedly strengthens the coupling. Moreover, it follows from

a consideration of Eqs. (17) and (25) that the strong-coupling approximation is in better correspondence with the nature of the interaction of the type γ_5 than the weak-coupling approximation.

The model we have considered gives an idea of the behavior of the Green function of the nucleon in pseudoscalar meson theory in the region $k^2 \gg m^2$, *i.e.*, far from the pole $k^2 = m^2$. Feynman[12] calculated the polarization of the vacuum in the approximation $\varphi(x) = \text{const}$; on the basis of the study of our model it can be said that his conclusion about the large part played by the polarization of the vacuum relates only to the region $k^2 \gg m^2$.

In conclusion I express my deep gratitude to Academician N. N. Bogoliubov for direction and help in the work, and also to S. M. Bilen'kii, N. P. Klepikov, L. I. Lapidus, and N. A. Chernikov for interesting discussions.

[1] V. G. Solov'ev, Dokl. Akad. Nauk SSSR **108**, 1041 (1956).

[2] T. D. Lee, Phys. Rev. **95**, 1329 (1954).

[3] G. Källen and W. Pauli, Kgl. Dansk. Mat. Fys. Medd. **30**, No. 7 (1955). Y. Munakata, Prog. Theoret. Phys. **13**, 455, (1955).

[4] N. N. Bogoliubov and D. V. Shirokov, Dokl. Akad. Nauk SSSR **105**, 685 (1955).

[5] H. Umezawa and A. Visconti, Nuclear Physics **1**, 20 (1956).

[6] K. Tanaka, Phys. Rev. **99**, 676 (1955).

[7] B. Bosko and R. Stroffolini, Nuovo cimento **2**, 133 (1955); **3**, 662 (1956).

[8] S. Machida, Prog. Theoret. Phys. **14**, 407 (1955).

[9] W. Thirring, Helv. Phys. Acta **28**, 344 (1955).

[10] A. A. Abrikosov and I. M. Khalatnikov, Dokl. Akad. Nauk SSSR **103**, 993 (1955).

[11] N. N. Bogoliubov, Dokl. Akad. Nauk SSSR **99**, 225 (1954).

[12] R. Feynman, Proc. Fifth Rochester Conf. (1955).

[13] E. T. Whittaker and G. N. Watson, *A Course of Modern Analysis*, Part I.

[14] G. Hardy, *Divergent Series*.

[15] N. N. Bogoliubov and D. V. Shirkov, Prog. Phys. Sci. **55**, 148; **57**, 3 (1955).

[16] H. Lehmann, Nuovo cimento **11**, 342, (1954).

[17] M. Gell-Mann and F. Low, Phys. Rev. **95**, 1300 (1954).

[18] G. Källen, Kgl. Dansk. Mat. Fys. Medd. **27**, No. 12 (1953); Helv. Phys. Acta **25**, 417 (1952).

Translated by W. H. Furry
222

SOVIET PHYSICS JETP VOLUME 5, NUMBER 5 DECEMBER, 1957

Extension of the Spin-Wave Model to the Case of Several Electrons Surrounding Each Site

IU. A. IZIUMOV
Ural' State University

(Submitted to JETP editor December 5, 1956)
J. Exptl. Theoret. Phys. **32**, 1058-1064 (May, 1957)

The energy of a weakly excited state of a ferromagnetic or antiferromagnetic crystal in which each site is surrounded by several electrons is calculated by the method of approximate second quantization, applied to a system consisting of two types of interacting Fermi particles. It is found that besides the usual excitations of the ferromagnon-antiferromagnon type, some additional excitations, which depend weakly on the quasi-momentum, appear in these systems. A physical interpretation of these excitations is proposed.

1. THE PICTURE OF a weakly excited state of a ferromagnetic or antiferromagnetic crystal, when there is only one magnetically active electron at each lattice site, is now fairly well understood. In the approximations of the spin-wave model it is possible to approximate the energy of a weakly-excited state of these crystals by the energy of an ideal gas of separate Bose-type quasi-particles—ferromagnons[1] antiferromagnons[2, 3, 4] obeying the dispersion laws

$$E_\mu = {}^1/_2 c J (a\mu)^2, \quad E_\mu = {}^1/_2 c J (a\mu) \qquad (1)$$

respectively for ferromagnets and antiferromagnets, whereupon two independent branches of excitations are obtained for antiferromagnets. Here μ is the quasi-momentum, J the exchange integral between nearest neighbors, and c the number of these nearest neighbors.

According to the model of Bloch [1], each of these quasi-particles corresponds to the motion of an inverted electron spin through the ordered array of the remaining spins. This simplified homeopolar model leads to qualitative results which agree with experiment. Real ferromagnetic or antiferromagnetic crystals, however, have several electrons with uncompensated spins at each site.

The first attempt to allow for the existence of several electrons per atom in a ferromagnetic crystal was made in a very approximate form by Möller[5], who considered all the electrons of the atom to be in a single state. This approach was so crude that Möller was not able to obtain any new qualitative results.

Recently Kondorskii and Pakhomov[6] have carried out a more accurate calculation of the energy of a ferromagnetic crystal with several electrons per atom. In this paper we will solve the analogous problem for antiferromagnetic crystals. Since the spectra of ferromagnets and antiferromagnets have a great many regularities in common, it is expedient to study them together within a single mathematical scheme. For this purpose we will consider a Hamiltonian of fairly general type which describes a system consisting of two types of interacting Fermi particles, and determine its lowest eigenvalues by the method of approximate second quantization of Bogoliubov and Tiablikov[7,8] which they developed for a system made up of identical particles.

By considering the electrons of the individual sublattices in an antiferromagnet as particles of different kinds, we can imagine the Hamiltonian of an antiferromagnet to be a special case of our general Hamiltonian; the Hamiltonian of a ferromagnet will be contained in it automatically. We will thus be able to solve the problem for ferromagnets and antiferromagnets at the same time.

2. We will consider a crystalline system at the nodes of which there are two different types of Fermi particles, but with only one particle at each node. In addition to the principal S-state of the isolated atom there will be other states with large degeneracy. Let us say that the wave function of these states will be $\varphi_{f\nu}(q, s)$, where ν runs through a finite set of values. We will suppose that the interatomic spacings are sufficiently large to guarantee that there will be little overlapping of the electronic orbits. In the representation of second quantization the Hamiltonian of such a system is written in the form:

$$\begin{aligned}\hat{H} = {} & \sum A (f_1 \nu_1 \nu_1') a^+_{f_1\nu_1} a_{f_1\nu_1'} + \sum C(g_1 \nu_1 \nu_1') c^+_{g_1\nu_1} c_{g_1\nu_1'} \\ & + \tfrac{1}{2} \sum B (f_1 f_2 \nu_1 \nu_2 \nu_1' \nu_2') a^+_{f_1\nu_1} a^+_{f_2\nu_2} a_{f_2\nu_2'} a_{f_1\nu_1'} \\ & + \tfrac{1}{2} \sum{}' D (g_1 g_2 \nu_1 \nu_2 \nu_1' \nu_2') c^+_{g_1\nu_1} c^+_{g_2\nu_2} c_{g_2\nu_2'} c_{g_1\nu_1'} \\ & + \sum E (f_1 g_2 \nu_1 \nu_2 \nu_1' \nu_2') a^+_{f_1\nu_1} a_{f_1\nu_1'} c^+_{g_2\nu_2} c_{g_2\nu_2'},\end{aligned} \qquad (2)$$

(each term is summed over all indices), in which

$$\sum_\nu a^+_{f\nu} a_{f\nu} = 1, \quad \sum_\nu c^+_{g\nu} c_{g\nu} = 1. \qquad (3)$$

Here the indices f and g designate the sites at which the Fermi particles of respective types are located: $a_{f\nu}$ and $c_{g\nu}$ are self-commuting Fermi-operators.

Following the basic idea of the method of approximate second quantization, we select two system functions $\theta_\omega(f\nu)$ and $\Phi_\omega(g\nu)$ such that

$$\begin{aligned}\sum_\nu \theta^*_\omega (f\nu)\, \theta_{\omega'} (f\nu) &= \delta (\omega - \omega'), \\ \sum_\nu \Phi^*_\omega (g\nu)\, \Phi_{\omega'} (g\nu) &= \delta (\omega - \omega')\end{aligned} \qquad (4)$$

(where ω takes the same values as ν) and require that $\theta_0(f\nu)$ and $\Phi_0(g\nu)$ yield a minimum for Eq. (2) under the condition (3), if the operators in these expressions are replaced by the usual c-numbers.

We now consider a canonical transformation

$$a_{f\nu} = \sum_\omega \theta_\omega (f\nu)\, a_{f\omega}, \quad c_{g\nu} = \sum_\omega \Phi_\omega (g\nu)\, c_{g\omega} \qquad (5)$$

of the Fermi operators $a_{f\nu}$ and $c_{f\nu}$ to new Fermi operators $a_{f\omega}$ and $c_{g\omega}$. We determine the functions $\theta_\omega(f\nu)$ and $\Phi_\omega(g\nu)$ for $\omega \neq 0$ by requiring that they obey the equations:

$$\sum_{\nu_1'} A(f_1\nu_1\nu_1')\,\theta_\omega(f_1\nu_1') + \sum_{f_2(\neq f_1)\nu_2\nu_1'\nu_2'} B(f_1 f_2\nu_1\nu_2\nu_1'\nu_2')\,\theta^*(f_2\nu_2)\,\theta(f_2\nu_2')\,\theta_\omega(f_1\nu_1')$$
$$+ \sum_{g_2\nu_2\nu_1'\nu_2'} E(f_1 g_2\nu_1\nu_2\nu_1'\nu_2')\,\theta_\omega(f_1\nu_1')\,\Phi^*(g_2\nu_2)\,\Phi(g_2\nu_2') = \lambda_\omega(f_1)\,\theta_\omega(f_1\nu_1).$$
$$\sum_{\nu_2'} C(g_2\nu_2\nu_2')\,\Phi_\omega(g_2\nu_2') + \sum_{g_1(\neq g_2)\nu_1\nu_2'\nu_1'} D(g_1 g_2\nu_1\nu_2\nu_1'\nu_2')\,\Phi_\omega(g_2\nu_2')\,\Phi(g_1\nu_1')$$
$$\times\,\Phi^*(g_1\nu_1) + \sum_{f_1\nu_1\nu_1'\nu_2'} E(f_1 g_2\nu_1\nu_2\nu_1'\nu_2')\,\theta^*(f_1\nu_1)\,\theta(f_1\nu_1')\,\Phi_\omega(g_2\nu_2') = \lambda_\omega(g_2)\,\Phi_\omega(g_2\nu_2), \tag{6}$$

where $\lambda_\omega(f\nu)$ and $\lambda_\omega(g\nu)$ are undetermined Lagrangian multipliers.

These equations make it possible for us to eliminate from the Hamiltonian, expressed in the new Fermi operators, those terms which contain only one non-zero index ω. Retaining first-order terms (those with two non-zero indices ω) in the Hamiltonian, we find that we can introduce new operators constructed from Fermi operators in the following way:

$$b_{f\omega} = a_{f0}^+ a_{f\omega},\quad d_{g\omega} = c_{g0}^+ c_{g\omega},$$
$$b_{f\omega}^+ = a_{f\omega}^+ a_{f0},\quad d_{g\omega}^+ = c_{g\omega}^+ c_{g0}. \tag{7}$$

As it turns out, the operators (7) satisfy Bose commutation relations approximately if we consider the weak interactions of the system. It is easy to show that the original Hamiltonian (2) is represented in this approximation by a quadratic form in the Bose operators $b_{g\omega}$ and $d_{f\omega}$.

The diagonalization of the quadratic form obtained above can be carried out by the usual methods.[7,8] For the energy of the system which we are studying we obtain:

$$E = E_0 + \sum_j \sum_\mu E_\mu^j\, n_\mu^j, \quad n_\mu^j = 0, 1, 2, \ldots, \tag{8}$$

where E_μ^j is determined from the characteristic equation of the system of homogeneous linear equations:

$$\Phi^-(f\omega)\,c_{1\mu}(\omega) + \sum_{\omega_2}\{q(f\omega\omega_2)\,c_{1\mu}(\omega_2) + p(f\omega\omega_2)\,c_{2\mu}(\omega_2) + k^*(f\omega\omega_2)\,c_{3\mu}(\omega_2)$$
$$+ t(f\omega\omega_2)\,c_{4\mu}(\omega_2)\} = 0.$$
$$\overset{*}{\Phi}{}^+(f\omega)\,c_{2\mu}(\omega) + \sum_{\omega_2}\{p(f\omega\omega_2)\,c_{1\mu}(\omega_2) + q^*(f\omega\omega_2)\,c_{2\mu}(\omega_2) + t^*(f\omega\omega_2)\,c_{3\mu}(\omega_2)$$
$$+ k(f\omega\omega_2)\,c_{4\mu}(\omega_2)\} = 0.$$
$$\Phi^-(g\omega)\,c_{3\mu}(\omega) + \sum_{\omega_2}\{k(g\omega_2\omega)\,c_{1\mu}(\omega_2) + t(g\omega_2\omega)\,c_{2\mu}(\omega_2) + q(g\omega\omega_2)\,c_{3\mu}(\omega_2)$$
$$+ p(g\omega\omega_2)\,c_{4\mu}(\omega_2)\} = 0. \tag{9}$$
$$\overset{*}{\Phi}{}^+(g\omega)\,c_{4\mu}(\omega) + \sum_{\omega_2}\{t^*(g\omega_2\omega)\,c_{1\mu}(\omega_2) + k(g\omega_2\omega)\,c_{2\mu}(\omega_2) + p(g\omega\omega_2)\,c_{3\mu}(\omega_2)$$
$$+ q^*(g\omega\omega_2)\,c_{4\mu}(\omega_2)\} = 0,$$

in which the following matrices have been introduced

$$q(f\omega_1\omega_2) = \sum_{f_2}{}' e^{i\mu(f_2-f)} \sum_{\nu_1\nu_2\nu_1'\nu_2'}{}' B(ff_2\nu_1\nu_2\nu_1'\nu_2')\,\theta^*_{\omega_1}(f\nu_1)\,\theta^*(f_2\nu_2)\,\theta_{\omega_2}(f_2\nu_2')\,\theta(f\nu_1').$$

$$p(f\omega_1\omega_2) = \sum_{f_2} e^{i\mu(f_2-f)} \sum_{\nu_1\nu_2\nu_1'\nu_2'} B(ff_2\nu_1\nu_2\nu_1'\nu_2')\,\theta^*_{\omega_1}(f\nu_1)\,\theta^*_{\omega_2}(f_2\nu_2)\,\theta(f_2\nu_2')\,\theta(f\nu_1').$$

$$k(f\omega_1\omega_2) = \sum_{g_2}{}' e^{i\mu(g_2-f)} \sum_{\nu_1\nu_2\nu_1'\nu_2'} E(fg_2\nu_1\nu_2\nu_1'\nu_2')\,\theta^*_{\omega_1}(f\nu_1)\,\theta(f\nu_1')\,\Phi^*_{\omega_2}(g_2\nu_2)\,\Phi(g_2\nu_2'). \qquad (10)$$

$$t(f\omega_1\omega_2) = \sum_{g_2} e^{i\mu(g_2-f)} \sum_{\nu_1\nu_2\nu_1'\nu_2'} E(fg_2\nu_1\nu_2\nu_1'\nu_2')\,\theta^*(f\nu_1)\,\theta_{\omega_2}(f\nu_1')\,\Phi^*_{\omega_1}(g_2\nu_2)\,\Phi(g_2\nu_2').$$

$$\Phi^{\mp}(f\omega) = \lambda_\omega(f) - \lambda_0(f) \mp E_\mu.$$

3. We now allow for the existence of several electrons per site and look into the two possibilities.

1. *Ferromagnetism.* According to Bogoliubov[8], the Hamiltonian of a ferromagnetic crystal with allowance for the electronic excited states is written in the form:

$$\hat{H} = U_0 - \frac{1}{2} \sum_{f_1\lambda_1 \neq f_2\lambda_2\sigma_1\sigma_2} J(f_1\lambda_1 f_2\lambda_2)\, a^+_{f_1\lambda_1\sigma_1} a^+_{f_2\lambda_2\sigma_2} a_{f_2\lambda_2\sigma_1} a_{f_1\lambda_1\sigma_2} \qquad (11)$$

together with the conditions of homeopolarity

$$\sum_\sigma a^+_{f\lambda\sigma} a_{f\lambda\sigma} = 1, \qquad (12)$$

according to which there is at the node f only one electron in the state λ; $\lambda = 1, 2 \ldots z$, where z is the number of occupied states (the number of electrons per site).

For a positive exchange integral $J(f_1\lambda_1 f_2\lambda_2) > 0$ the solution of the system of equations (6) can be put in the form

$$\theta_\omega(f\lambda\nu) = \delta(\nu - \omega), \quad \Phi_\omega(g\lambda\nu) \equiv 0,$$

$$\nu = \sigma + {}^1/_2 = 0; 1.$$

It is easy to show that in this case the basic equations (10) agree with the equations of Kondorskii and Pakhomov[6].

By applying the method of "perturbations" to the equations obtained above we can find that for small values of the quasi-momentum μ the solution of the system has the following structure:

$$E^1_\mu = (c/2z)(a\mu)^2 \sum_{ij} J_{ij},$$

$$E^2_\mu = E^{(0)}_{\mu 2} + E^{(1)}_{\mu 2}(a\mu)^2, \ldots \qquad (13)$$

$$E^z_\mu = E^{(0)}_{\mu z} + E^{(1)}_{\mu z}(a\mu)^2,$$

where the last $z - 1$ quantities are determined by the mutual relations between the exchange integrals. If it is assumed that the exchange integrals between different states are $J_{ij} = J$; $J^0_{ij} = J^0$, which seems to be approximately true for real crystals, then the solutions of (13) are

$$E^1_\mu = {}^1/_2\, czJ(a\mu)^2, \quad E^k_\mu = z(J^0 + cJ), \quad k = 2, 3, \ldots, z. \qquad (14)$$

Comparing Eqs. (13) and (14) we see that in a ferromagnet only one of the z branches of the spectrum depends quadratically on the quasi-momentum. For the other $z - 1$ branches the large constant term overlaps the small one which depends on the quasi-momentum and which all but disappears if the exchange integrals differ little for different states.

2. *Antiferromagnetism.* We take for the Hamiltonian of an antiferromagnet

$$\hat{H} = E_0 - \frac{1}{2} \sum_{f_1\lambda_1 g_2\lambda_2\sigma_1\sigma_2} J(f_1\lambda_1 g_2\lambda_2)\, a^+_{f_1\lambda_1\sigma_1} a_{f_1\lambda_1\sigma_2} c^+_{g_2\lambda_2\sigma_2} c_{g_2\lambda_2\sigma_1} \qquad (15)$$

with the conditions

$$\sum_\sigma a^+_{f\lambda\sigma} a_{f\lambda\sigma} = 1; \quad \sum_\sigma c^+_{g\lambda\sigma} c_{g\lambda\sigma} = 1.$$

Now the solution of the system of equations (6) will be

$$\theta_\omega(f\lambda\nu) = \delta(\nu - \omega), \quad \Phi_\omega(g\lambda\nu) = \delta(\nu + \omega - 1).$$

Under these conditions, after approximations analogous to those made for a ferromagnet, the secular equation of the system of equations (9) has $2z$ positive solutions:

$$E_\mu^1 = {}^1/_2\, zcJ(a\mu), \qquad \text{multiplicity } 2$$

$$E_\mu^i = z(J^0 + cJ/2), \quad \text{multiplicity } 2(z-1).$$

Thus it is found that when there are z electrons per atom a ferromagnet has z independent branches of Bose-type excitations, while an antiferromagnet has $2z$ branches.

In addition to the usual excitations of ferromagnon-antiferromagnon type some new excitations arise, which depend weakly on the quasi-momentum and vanish for $z = 1$.

4. In order to explain the physical meaning of these special excitations which depend weakly on the quasi-momentum, we consider still another subsidiary problem: let us find the energy of a weakly excited state of a ferromagnetic crystal with one electron per site, in which, in addition to the S-state, there are other excited states, designated by the index λ, which arbitrarily assume the values 0, 1, ... $(z-1)$. In all there will be $2z$ different electronic states per atom, since for each "orbit" the electron can have two spin directions. If it is assumed that an electron with a given spin direction is in its ground state, then all told there will be $2z - 1$ different excited states possible for the electrons inside each atom.

From Bogoliubov's general scheme[8] it is a simple matter to obtain an expression for the Hamiltonian of this system. If we require that the following condition be satisfied:

$$\sum_{\lambda\sigma} a^+_{f\lambda\sigma} a_{f\lambda\sigma} = 1, \tag{16}$$

then the Hamiltonian takes the form

$$\hat{H} = \sum_{f\lambda\lambda'\sigma} L(f\lambda f\lambda')\, a^+_{f\lambda\sigma} a_{f\lambda'\sigma} + \frac{1}{2} \sum_{(f\lambda)\sigma_1\sigma_2} F(f_1\lambda_1 f_2\lambda_2 f_1\lambda_1' f_2\lambda_2')\, a^+_{f_1\lambda_1\sigma_2} a^+_{f_2\lambda_2\sigma_1}$$
$$\times a_{f_2\lambda_2'\sigma_2} a_{f_1\lambda_1'\sigma_1} - \frac{1}{2} \sum_{(f\lambda)\sigma_1\sigma_2}{}^{\cdot} F(f_1\lambda_1 f_2\lambda_2 f_2\lambda_2' f_1\lambda_1')\, a^+_{f_1\lambda_1\sigma_1} a^+_{f_2\lambda_2\sigma_2} a_{f_2\lambda_2'\sigma_1} a_{f_1\lambda_1'\sigma_2}. \tag{17}$$

Now let us renormalize the quantity σ and assume that it takes the values 0, 1: this change will not affect our results. Since $\nu = (\lambda\sigma)$, then $\omega = (\Lambda\Sigma)$. If we take the functions

$$\theta_{\Lambda\Sigma}(f\lambda\sigma) = \delta(\lambda - \Lambda)\,\delta(\sigma - \Sigma), \quad \Phi_{\Lambda\Sigma}(g\lambda\sigma) \equiv 0,$$

as solutions of Eq. (6), it is not difficult to show that the non-zero coefficients in Eq. (10) will be

$$p_\mu(f\Lambda 0\Lambda_2 0) = \sum_{f_2(\neq f)} e^{i\mu(f_2 - f)}\, \mathrm{Re}\,[F(f\Lambda f_2\Lambda_2 f 0 f_2 0) - F(f\Lambda f_2\Lambda_2 f_2 0 f 0)],$$

$$q_\mu(f\Lambda 0\Lambda_2 0) = \sum_{f_2(\neq j)} e^{i\mu(f_2 - f)}\,[F(f\Lambda f_2 0 f 0 f_2\Lambda_2) - F(f\Lambda f_2 0 f_2\Lambda_2 f 0)], \tag{18}$$

$$q_\mu(f\Lambda 1\,\Lambda_2 1) = -\sum_{f_2(\neq f)} e^{i\mu(f_2 - f)}\, F(f\Lambda f_2 0 f_2\Lambda_2 f 0).$$

For the problem at hand the characteristic equation of the system (9) breaks up into three equations:

$$\det\|\, q_\mu(f\Lambda\, 1\,\Lambda_2\, 1) + \Phi^-(f\Lambda\, 1)\,\delta_{\Lambda\Lambda_2}\| \cdot \det\|\, q^*_\mu(f\Lambda\, 1\,\Lambda_2\, 1) + \overset{*}{\Phi}{}^+(f\Lambda 1)\,\delta_{\Lambda\Lambda_2}\| = 0,$$

$$\det \left\| \begin{array}{c|c} q_\mu(f\Lambda 0\Lambda_2 0) + \Phi^-(f\Lambda 0)\,\delta_{\Lambda\Lambda_2} & p_\mu(f\Lambda 0\Lambda_2 0) \\ \hline p_\mu(f\Lambda 0\Lambda_2 0) & q^*_\mu(f\Lambda 0\Lambda_2 0) + \overset{*}{\Phi}{}^+(f\Lambda 0)\,\delta_{\Lambda\Lambda_2} \end{array} \right\| = 0. \tag{19}$$

The first two equations in (19) are each of order z; the third, of order $2z - 1$. It is not difficult to show that if E_μ is a root of Eq. (19), then $-E_\mu$ will also be a root, so that there will be $2z - 1$ positive solutions.

In the determinants of the matrices on the left hand side of Eq. (19) there appear only matrix elements with $\Sigma = 0$ or with $\Sigma = 1$; consequently we conclude that the group of eigenvalues of the Hamiltonian (17) can be split up into two independent subgroups—one with spin excitations, one without. The equations of order z describe the spin excitations of the crystal. For the case $z = 2$ they are easily solved and yield two positive solutions:

$$E_\mu^- = {}^1/_2\,\Delta_{10} + 2cJ_{10} + {}^1/_4\,(J_{00} + J_{11} - 2J_{10})\,c\,(a\mu)^2,$$
$$E_\mu^+ = {}^1/_2\,\Delta_{10} + {}^1/_4\,(J_{00} + J_{11} + 2J_{10})\,c\,(a\mu)^2, \quad (20)$$

where $J_{\Lambda_1\Lambda_2} = F(f\Lambda_1 f_2 0 f_2 \Lambda_2 f\,0)$ are the exchange integrals between two electrons Λ_1 and Λ_2 of neighboring atoms, occupying either the ground state or excited states. Δ_{10} is just the difference between the levels of the electrons in an atom of the crystal.

We now turn our attention to a deep analogy which exists between Eqs. (20) and the equations of Kondorskii and Pakhomov[6]. The latter describe the spin excitations which arise out of nearest-neighbor interactions of atoms, each of which has two electrons fixed in their "orbits." Equations (20), however, describe the analogous excitations for a system in which each atom has one electron in the lower state, so that in order to transfer the electron to the next "orbit" it is necessary to supply it with an energy Δ_{10}. Consequently Eqs. (20) describe the spin excitations after part of the electrons has already gone into the excited state. We will not investigate the excitations without spin here.

We have carried out an analysis of the solution for $z = 2$. Great technical difficulties arise for the other cases. We assume that the exchange integrals J_{ji} are identical for different pairs of states (ji).

In this case the first equation of (19) yields

$$E_\mu^i = f\,(\Delta_{ij}) + czJ, \quad (z - 1); \quad E_\mu^1 = A\,(a\mu)^2, \quad (21)$$

where $f(\Delta_{ij})$ is some function of Δ_{ij}, the difference between energy levels, which vanishes when $\Delta_{ij} = 0$. Equation (20) now becomes identical with Eq. (14) for a ferromagnet with z electrons per atom. Thus we come to the conclusion that in a system with several electrons per atom, the appearance of the new excitations which depend weakly on the quasi-momentum is connected with the possibility of exchange between electrons separated by energy gaps.

We still have to explain the significance of the solutions which depend on the quasi-momentum:

$$E_\mu^1 = {}^1/_2\,czJ\,(a\mu)^2. \quad (22)$$

In the ground state at each site there are up to z electrons with their spins directed, say, to the left. The total spin at this node will be $-z/2$. If at a site there were just one particle with spin $s = z/2$, instead of z electrons with spins $s = 1/2$, the number of possible orientations of this spin would be $2s + 1 = z + 1$. Such particles could have z excited states. The solution of the problem for these particles would be

$$E_\mu^j = {}^1/_2\,cJ\,(a\mu)^2, \quad j = 1, 2, \ldots z.$$

If we compare this expression with the first equation of (1), we come to the conclusion that each such excitation has to correspond to a change of the spin projection by unity. Then a change of the spin projection by z units has to correspond to the energy

$$E_\mu = {}^1/_2\,zc\,J\,(a\mu)^2, \quad (23)$$

whereupon the spin projection becomes equal to $z/2$, *i.e.*, the spin flips over. But Eq. (23) agrees with (22), so that latter ought to correspond to a change of the spin projection by z units, *i.e.*, the entire group of spins surrounding the atom flips over as a whole. We did not find any other excitations of the system which depend on the quasi-momentum in the same way, so we conclude that in a ferromagnetic crystal (containing up to z magnetically active electrons per atom) spin waves are propagated in which a whole group of spins at the site acts as a unit. This is a natural extension of the idea of a ferromagnon to the case of z electrons surrounding the site.

For antiferromagnets the interpretation of the elementary excitations has to be analogous.

In conclusion I take the opportunity to express sincere appreciation to Professor S. V. Vonsovskii and to G. G. Taluts for valuable discussions.

[1] F. Bloch, Z. Physik 74, 295 (1932).
[2] P. W. Anderson, Phys. Rev. 86, 694 (1952).
[3] R. Kubo, Phys. Rev. 87, 568 (1952).
[4] J. Tessman, Phys. Rev. 88, 1132 (1952).
[5] C. Möller, Z. Physik 82, 559 (1933).
[6] E. Kondorskii and A. Pakhomov, Dokl. Akad. Nauk SSSR 93, 431 (1953).
[7] N. N. Bogoliubov and S. V. Tiablikov, J. Exptl. Theoret. Phys. (U.S.S.R.) 19, 256 (1949).
[8] N. N. Bogoliubov, *Lectures in Quantum Statistics*, 1949.
[9] S. V. Tiablikov, Fiz. Metallov i Metallovedenie 2, 193 (1956).

Translated by W. M. Whitney
223

SOVIET PHYSICS JETP VOLUME 5, NUMBER 5 DECEMBER, 1957

Equations with Variational Derivatives in Statistical Equilibrium Theory

I. P. BAZAROV
Moscow State University

(Submitted to JETP editor April 18, 1956)
J. Exptl. Theoret. Phys. (U.S.S.R.) 32, 1065-1077 (May, 1957)

Equations with variational derivatives for correlation functions have been derived. A method is developed for solving these for various systems in statistical equilibrium. A "superposition" theorem is derived for obtaining the correlation functions when the interaction between the particles of the system can be described as the sum of long and short range forces.

THE BEHAVIOR OF A statistical system of interacting particles is determined by the corresponding distribution functions of these particles $F_s(x_1, x_2, \ldots, x_s)$ $(s = 1, 2, 3, \ldots)$. Bogoliubov[1] has shown that the functions F_s can be represented by variational derivatives of the functional introduced by him, and the series of equations for the determination of these distribution functions were first obtained by him. As Bogoliubov also pointed out[2], his functional does not have a direct physical interpretation; he therefore pointed out a method in Ref. 2 for the construction of other functionals, based on the idea of the inclusion of the external field, in a manner similar to that employed in the Schwinger theory of the Green function.

In the present work, starting out from a functional for the free energy of a system of M types of particles in an external field $\varphi(x)$, closed equations are found with variational derivatives for the unitary distribution function for different forms of the functional argument; with the help of these derivatives, a method of determining the correlation functions has been deduced for systems of particles with different interactions: Coulombic $\Phi_0(r)$, an interaction decreasing rapidly with distance, $\Phi_1(r)$, and an interaction of the form $\Phi(r) = \Phi_0(r) + \Phi_1(r)$.

1. FREE ENERGY AS A FUNCTIONAL. DISTRIBUTION FUNCTIONS. EQUATIONS WITH VARIATIONAL DERIVATIVES

Let us consider a system of M types N_a molecules of the ath type. Let this system be located in an external field $\varphi(\mathbf{r})$. The probability density function of the position of the molecules is determined by the Gibbs function:

$$D = \frac{1}{Q}\exp\left\{-\frac{1}{\Theta}\left(U_N + \sum_{a,i}\varphi_a(\mathbf{r}_i)\right)\right\},$$
$$Q = \int \exp\left\{-\frac{1}{\Theta}\left(U_N + \sum_{a,i}\varphi_a(\mathbf{r}_i)\right)\right\} d\tau, \quad (1)$$
$$U_N = \sum \Phi_{ab}(|\mathbf{r}_{ai} - \mathbf{r}_{bj}|),$$

where U_N is the potential energy of interaction of the particles with each other; $\mathbf{r}_{ai}$ determines the position of the ith molecule of the ath type, while the summation is taken over all different pairs of

molecules; Q is the configuration integral of the system; the mutual potentials Φ_{ab} are assumed to be symmetric functions relative to a, b; $\Theta = kT$.

The free energy of such a system,

$$F = -\Theta \ln Q =$$
$$-\Theta \ln \int \exp\left\{-\frac{1}{\Theta}\left(U_N + \sum_{a,i} \varphi_a(\mathbf{r}_i)\right)\right\} d\tau \qquad (2)$$

is a functional of the external field $\varphi(\mathbf{r})$. The distribution functions of complex particles $F_{a_1, \ldots, a_s}(\mathbf{r}_1, \ldots, \mathbf{r}_s)$ which are so normalized that $V^{-s} F_{a_1, \ldots, a_s}\, d\mathbf{r}_1 \ldots d\mathbf{r}_s$ defines the probability that s particular molecules of types $a_1, \ldots, a_s$ having specified coordinates in the volume V, can be expressed by variational derivatives of the functional (2).

Actually, we have from (2) (we shall denote the $\mathbf{r}_i$ as $x, y, \ldots$):

$$\delta F / \delta \varphi_a(x) = N_a\, E_a(x \mid \varphi)/Q, \qquad (3)$$

$$F_a(x \mid \varphi) = (V/N_a)\, \delta F / \delta \varphi_a(x), \qquad (4)$$

where

$$E_a(x \mid \varphi) = \exp\left\{-\frac{1}{\Theta}\left(U_N + \overline{\sum_{a,i} \varphi_a(x_i)}^{\,x_{a_1} = x}\right)\right\},$$

$$F_a(x \mid \varphi) = \overline{VD} = V \frac{E_a(x \mid \varphi)}{Q},$$

F_a is the distribution function of a single particle (the number density of particles of the ath type) in the presence of the external field $\varphi(x)$. (Here the bar over quantities denotes integration over all variables $\{x_{a,i}\}$ except $x_{a_1} = x$.) It is easy to find the distribution function of a pair of particles $F_{ab}(x, y \mid \varphi)$ by taking the functional derivative of (3). We then get:

$$\frac{\delta^2 F}{\delta \varphi_a(x)\, \delta \varphi_b(y)} = \frac{N_a}{\Theta}\left\{-(N_b - \delta_{ab})\frac{E_{ab}(x, y \mid \varphi)}{Q} - \frac{E_a(x \mid \varphi)}{Q} + N_b \frac{E_a(x \mid \varphi)}{Q}\frac{E_b(y \mid \varphi)}{Q}\right\} \qquad (5)$$

or

$$\frac{\delta^2 F}{\delta \varphi_a(x)\, \delta \varphi_b(y)} = -\frac{N_a(N_b - \delta_{ab})}{\Theta V^2} F_{ab}(x, y \mid \varphi) - \frac{N_a}{\Theta V} F_a(x \mid \varphi)\, \delta(x - y) + \frac{N_a N_b}{\Theta V^2} F_a(x \mid \varphi)\, F_b(y \mid \varphi), \qquad (6)$$

where

$$E_{ab}(x, y \mid \varphi) = \overline{\exp\left\{-\frac{1}{\Theta}\left(U_N + \sum_{a,i} \varphi_a(x_i)\right)\right\}}^{\,x_{a_1} = x,\ x_{b_2} = y},$$

and δ_{ab} is the Kronecker delta. From (6) we obtain

$$F_{ab}(x, y \mid \varphi) = \frac{N_b}{N_b - \delta_{ab}} F_a(x \mid \varphi)\, F_b(y \mid \varphi) - \frac{V}{N_b - \delta_{ab}} F_a(x \mid \varphi)\, \delta(x - y) - \frac{\Theta V^2}{N_a(N_b - \delta_{ab})} \frac{\delta^2 F}{\delta \varphi_a(x)\, \delta \varphi_b(y)} \qquad (7)$$

or

$$F_{ab}(x, y \mid \varphi) = \frac{N_b}{N_b - \delta_{ab}} F_a(x \mid \varphi)\, F_b(y \mid \varphi) - \frac{V}{N_b - \delta_{ab}} F_a(x \mid \varphi)\, \delta(x - y) - \frac{\Theta V}{N_b - \delta_{ab}} \frac{\delta F_a(x \mid \varphi)}{\delta \varphi_b(y)}. \qquad (8)$$

It is then obvious that the pair correlation function is entirely expressed in terms of unitary functions with the help of variational derivatives.

If, just as we did with Eq. (3), we continue to take functional derivatives of Eq. (5), then we find the value of the third functional derivative and the four-particle distribution function $F_{abc}(x, y, y \mid \varphi)$ which, similar to $F_{ab}(x, y \mid \varphi)$ is also entirely expressed in terms of unitary distribution functions with variational derivatives.

Thus, finding the correlation functions $F_s(x_1, x_2, \ldots, x_s)$ $(s = 2, 3, \ldots)$ reduces to the determination of the unitary distribution function and the corresponding variational derivatives.

Beginning with the determination of the unitary distribution function

$$F_a(x \mid \varphi) = \overline{VD}^{\,x_{a_1} = x}, \qquad (9)$$

it is easy to find a closed differential equation with variational derivatives. Actually, differentiating the Gibbs distribution with respect to $x^{\alpha}_{a_1}$, we get

$$\frac{\partial D}{\partial x^{\alpha}_{a_1}} + \frac{1}{\Theta}\frac{\partial \varphi_{\alpha}(x)}{\partial x^{\alpha}_{a_1}} D + \frac{1}{\Theta}\frac{\partial U_N}{\partial x^{\alpha}_{a_1}} D = 0 \quad (\alpha = 1, 2, 3).$$

Multiplying by V and integrating, we have

$$\frac{\partial F_a(x\,|\,\varphi)}{\partial x^{\alpha}} + \frac{1}{\Theta}\frac{\partial \varphi_a(x)}{\partial x^{\alpha}} F_a(x\,|\,\varphi) + \frac{1}{\Theta V}\sum_{b=1}^{M}(N_b - \delta_{ab}) \times \int \frac{\partial \Phi_{ab}(|x-y|)}{\partial x^{\alpha}} F_{ab}(x, y\,|\,\varphi)\, dy = 0.$$

Substituting (7), and carrying out the transition to the limit $N \to \infty$, $V \to \infty$ for the finite ratios $V/N = v$, $N_a/N = n_a$ $(a = 1, 2, \ldots, M)$ we obtain a closed equation for $F_a(x|\varphi)$ with variational derivatives:

$$\frac{\partial F_a(x\,|\,\varphi)}{\partial x^{\alpha}} + \frac{1}{\Theta}\frac{\partial \psi_a(x)}{\partial x^{\alpha}} F_a(x/\varphi) = 0, \qquad (10)$$

$$\psi_a(x) = \varphi_a(x) + \sum_{b=1}^{M}\int \Phi_{ab}(|x-y|)\left\{\frac{n_b}{v} F_b(y\,|\,\varphi) - \delta(x-y) - \Theta\frac{\delta}{\delta\varphi_b(y)}\right\} dy \qquad (11)$$

or an equation in variational derivatives of the functional $F(\varphi)$:

$$\frac{\partial}{\partial x^{\alpha}}\frac{\delta F}{\delta \varphi_a(x)} + \frac{1}{\Theta}\frac{\partial \varphi_a(x)}{\partial x^{\alpha}}\frac{\delta F}{\delta \varphi_a(x)} + \frac{1}{\Theta}\sum_{b=1}^{M}\int \frac{\partial \Phi_{ab}(|x-y|)}{\partial x^{\alpha}} \times \left\{\frac{\delta F}{\delta \varphi_a(x)}\frac{\delta F}{\delta \varphi_b(y)} - \frac{\delta F}{\delta \varphi_a(x)}\delta(x-y) - \Theta\frac{\delta^2 F}{\delta\varphi_a(x)\,\delta\varphi_b(y)}\right\} dy = 0. \qquad (12)$$

It is evident from (10) that the equation for the distribution function $F_a(x|\varphi)$ is the same form of an equation as in the case of the motion of two particles of an ideal gas in a given external field $\psi_a(x)$. A real interaction between the particles is expressed by the fact that $\psi_a(x)$ is not the usual field but an operator one.

Let us now analyze the method of finding the correlation functions, starting out from Eq. (10), with variational derivatives of the unitary distribution function, for the case of a different sort of system.

2. SYSTEM WITH COULOMBIC INTERACTION BETWEEN THE PARTICLES

We consider a system of electrically charged particles interacting according to Coulomb's law. The operator field in which the particles of the system are placed has the form (11). If the second and third terms in the integral of this operator field are small in comparison with the first term, we then have the ordinary field

$$\psi_a(x) = \varphi_a(x) + \sum_{b=1}^{M}\int \Phi_{ab}(|x-y|)\frac{n_b}{v} F_b(y\,|\,\varphi)\, dy. \qquad (13)$$

Neglect of these terms corresponds to ignoring the short-range interaction forces between the particles.

Equation (10) for the distribution function $F_a(x|\varphi)$ of a system of particles between which only long-range forces act (for example, Coulomb forces) will then be

$$\frac{\partial F_a(x\,|\,\varphi)}{\partial x^{\alpha}} + \frac{1}{\Theta}\frac{\partial \varphi_{\alpha}(x)}{\partial x^{\alpha}} F_a(x\,|\,\varphi) + \frac{1}{\Theta} F_a(x\,|\,\varphi)\sum_{b=1}^{M}\int \frac{\partial \Phi_{ab}(|x-y|)}{\partial x^{\alpha}}\frac{n_b}{v} F_b(y|\varphi)\, dy = 0. \qquad (14)$$

Let the total charge of the system be zero and let the different particles differ only in charge. We denote the charge of the particles of type a by the symbol e_a; there are M types. Then

$$\sum_{a=1}^{M} n_a = 1, \quad \sum_{a=1}^{M} n_a e_a = 0. \qquad (15)$$

For Coulombic interaction $\Phi_{ab} = e_a e_b/\varepsilon r$, where ε is the dielectric constant of the medium. In our case, this includes electrolytes phenomenologically.

In looking for a quantity which serves as the small parameter in powers of which we shall expand $F_a(x|\varphi)$, we can, following Bogoliubov[1], transform to dimensionless quantities, taking the Debye radius r_d as the unit of length:

$$r_d^2 = \Theta\varepsilon v / 4\pi \sum_{a=1}^{M} n_a e_a^2. \qquad (16)$$

Then for the case of the Debye theory of electro-

lytes at low concentration, when the interaction energy at distances of the order of r_d is much smaller than the thermal energy ($e_a e_b / \varepsilon r_d \ll \Theta$), the volume per particle in dimensionless units is our small parameter:

$$v^* = v / r_d^3 = \mu = 4\pi \sum_a n_a e_a^2 / \Theta \varepsilon r_d \ll 1.$$

In this case, introducing variables of the order of unity

$$\lambda_a = e_a \Big/ \sqrt{4\pi \sum_a n_a e_a^2},$$

we note that $\Phi_{ab}(r)/\Theta = \mu \lambda_a \lambda_b / r^*$. Keeping this in mind, we shall not transform to dimensionless units but immediately expand $F_a(x|\varphi)$ in powers of v, remembering that $\Phi_{ab}(r)/\Theta$ is proportional to v:

$$\Phi_{ab}(r) / \Theta = v\psi_{ab}(r), \qquad \psi_{ab}(r) = \lambda_a \lambda_b / r_d^2 r. \quad (17)$$

Thus, we shall solve Eq. (14) with the help of the expansion

$$F_a(x|\varphi) = F_a^0(x|\varphi) + vF_a^1(x|\varphi) + v^2 F_a^2(x|\varphi) + \ldots \quad (18)$$

with the normalization condition

$$\lim_{V\to\infty} \frac{1}{V} \int F_a(x|\varphi)\, dx = 1,$$

i.e.,

$$\lim_{V\to\infty} \frac{1}{V} \int F_a^0(x|\varphi)\, dx = 1, \qquad \lim_{V\to\infty} \frac{1}{V} \int F_a^1(x|\varphi)\, dx = 0. \quad (19)$$

Substituting (18) in (14) and setting the sum of terms of a given power of v equal to zero, we obtain the equations for the approximation:

$$\frac{\partial F_a^0(x|\varphi)}{\partial x^\alpha} + \frac{1}{\Theta} \frac{\partial \varphi_a(x)}{\partial x^\alpha} F_a^0(x|\varphi) + F_a^0(x|\varphi) \sum_{b=1}^{M} \int \frac{\partial \psi_{ab}(|x-y|)}{\partial x^\alpha} n_b F_b^0(y|\varphi)\, dy = 0, \quad (20)$$

$$\frac{\partial F_a^1(x|\varphi)}{\partial x^\alpha} + \frac{1}{\Theta} \frac{\partial \varphi_\alpha(x)}{\partial x^\alpha} F_a^1(x|\varphi) + F_a^0(x|\varphi) \sum_{b=1}^{M} \int \frac{\partial \psi_{ab}(|x-y|)}{\partial x^\alpha} n_b F_b^1(y|\varphi)\, dx + F_a^1(x|\varphi) \sum_{b=1}^{M} \int \frac{\partial \psi_{ab}(|x-y|)}{\partial x^\alpha} n_b F_b^0(y|\varphi)\, dy = 0. \quad (21)$$

Setting the external field $\varphi_a(x) = 0$, we get equations for the approximation in the absence of such a field. We note that, according to (15), the following condition holds:

$$\sum_{b=1}^{M} \psi_{ab}(r)\, n_b = (e_a / \Theta \varepsilon v r) \sum_{b=1}^{M} n_b e_b = 0. \quad (22)$$

By virtue of the normalization condition, Eq. (20) has, at $\varphi_a(x) = 0$, the obvious solution

$$F_a^0(x) = 1. \quad (23)$$

From Eq. (21) [at $\varphi_a(x) = 0$], we get $F_a^1(x) = 0$ by taking (22), (23), and (29) into account. Solution of the equation for subsequent approximations similar to the solution of Eq. (21), gives [for $\varphi_a(x) = 0$]: $F_a^i(x) = 0$, $i = 1, 2, \ldots$. Thus, in the absence of an external field, in a system of charged particles in the approximation in which the second and third terms in the operator field (11) are small in comparison with the first term, the distribution function for a single particle $F_a(x)$ has a value exactly equal to unity:

$$F_a(x) = F_a^0(x) = 1, \quad (24)$$

which corresponds to a spatially homogeneous distribution of the particles.

The correlation pair function in the absence of field will be, by Eq. (8):

$$F_{ab}(x, y) = F_a(x) F_b(y) - (v/n_b) F_a(x) \delta(x-y) - (v\Theta/n_b) (\delta F_a(x|\varphi) / \delta \varphi_b(y))_{\varphi=0}$$

or

$$F_{ab}(x, y) = 1 - (v/n_b) \delta(x-y) - (v\Theta/n_b) (\delta F_a(x|\varphi) / \delta \varphi_b(y))_{\varphi=0}.$$

In the first approximation,

$$F_{ab}(x, y) = 1 - (v/n_b)\,\delta(x-y) - (v\Theta/n_b)\,(\delta F_a^0(x\,|\,\varphi)/\delta\varphi_\beta(y))_0. \quad (25)$$

We find the variational derivative here by taking the functional derivative of Eq. (20) with respect to $\varphi_b(y)$ and assuming $\varphi(x) = 0$, taking Eqs. (22) and (24) into account. We then obtain

$$\left(\frac{\delta F_a^0(x\,|\,\varphi)}{\delta\varphi_b(y)}\right)_0 + \frac{1}{\Theta}\,\delta(x-y) + \sum_{c=1}^{M}\int \psi_{ac}(|x-z|)\,n_c\left(\frac{\delta F_c^0(z\,|\,\varphi)}{\delta\varphi_b(y)}\right)_0 dz = 0,$$

or, on the basis of Eq. (25):

$$1 - F_{ab}(x, y) + \sum_{c=1}^{M}\int \psi_{ac}(|x-z|)\,n_c\left((1 - F_{bc}(y, z) - \frac{v}{n_b}\,\delta(y-z)\right)dz = 0,$$

$$1 - F_{ab}(x, y) - v\psi_{ab}(|x-y|) + \sum_{c=1}^{M}\int \psi_{ac}(|x-z|)\,n_c\,(1 - F_{bc}(y, z))\,dz = 0$$

Writing $(F_{ab}(x, y) - 1)/v = g_{ab}(x, y)$, we get the equation

$$g_{ab}(x, y) + \sum_{c=1}^{M}\int \psi_{ac}(|x-z|)\,n_c g_{cb}(z, y)\,dz = -\psi_{ab}(|x-y|), \quad (26)$$

the solution of which is well known[1]:

$$g_{ab}(x, y) = g_{ab}(|x-y|) = g_{ab}(r) = -\lambda_a\lambda_b r_d^{-2}\exp(-r/r_d)/r$$

and, consequently,

$$F_{ab}(r) = 1 - v\lambda_a\lambda_b r_d^{-2}\exp(-r/r_d)/r. \quad (27)$$

The variational derivatives of F_a^1, F_a^2, *etc.*, are equal to zero, as is not difficult to show by taking functional derivatives of Eq. (21). So also is the equation for the other approximations.

Thus the solution of Eq. (10) with variational derivative reduces in our approximation (for Coulomb forces) to the value of the binary distribution function $F_{ab}(x, y)$, which coincides with the first approximation for this function, which was first found by Bogoliubov[1] and which is well known in the Debye theory of electrolytes.

Determination of the pair distribution function by starting out from the exact Eq. (10) for Coulomb forces, reduces to finding the variational derivatives $(\delta F_a^0(x\,|\,\varphi)/(\delta\varphi_b(y))_0$, $(\delta F_a^1(x\,|\,\varphi)/\delta\varphi_b(y))_0$, *etc.*, from the corresponding equations for the aproximation in the expansion of the unitary distribution functions in powers of v. This is the procedure that we have already carried out. In Sec. 3, we shall consider the details of finding these derivatives for systems of particles with short-range interaction forces.

3. SYSTEM OF PARTICLES WITH SHORT-RANGE INTERACTION FORCES

Suppose that we have a molecular system (of weak concentration) of identical particles whose mutual interaction falls off rapidly with distance, so that r_0^3/v is a small parameter (r_0 = effective action radius of the molecule). We can find the correlation function of such a system by starting from Eq. (10) with variational differentiation with the aid of an expansion in powers of the density $n = 1/v$. In order to determine the coefficients of this expansion for the correlation function, it is advantageous to replace the functional argument $\varphi(x)$ by $u(x)$ in Eq. (12) for one type of particle ($M = 1$), using the formula

$$\varphi(x) = -\Theta\ln(1 + vu(x)) \quad (28)$$

and then represent the correlation functions by the variational derivatives of the new functional with another argument. In such a substitution of the functional argument, we have:

$$\frac{\partial\varphi(x)}{\partial x^\alpha} = -\frac{v\Theta}{1+vu(x)}\frac{\partial u(x)}{\partial x^\alpha},$$

$$\frac{\delta F}{\delta\varphi(x)} = \int\frac{\delta F}{\delta u(y)}\frac{\delta u(y)}{\delta\varphi(x)}dy = -\int\frac{\delta F}{\delta u(y)}\frac{1+vu(y)}{v\Theta}\delta(x-y)\,dy = -\frac{1+vu(x)}{v\Theta}\frac{\delta F}{\delta u(x)}, \tag{29}$$

$$\frac{\delta^2 F}{\delta\varphi(x)\,\delta\varphi(y)} = \frac{(1+vu(y))(1+vu(x))}{v^2\Theta^2}\frac{\delta^2 F}{\delta u(x)\,\delta u(y)} + \frac{1}{v\Theta^2}\delta(x-y)\frac{\delta F}{\delta u(x)}(1+vu(x)).$$

Substituting (29) in (12) (for $M = 1$), we find that the new functional $F(u)$ satisfies the following equation in variational derivatives:

$$-\frac{\partial}{\partial x^\alpha}\frac{\delta F}{\partial u_x} + \frac{1}{\Theta^2}\int\frac{\partial\Phi(|x-y|)}{\partial x^\alpha}(n+u_y)\left(\frac{\delta F}{\delta u_x}\frac{\delta F}{\delta u_y} - \Theta\frac{\delta^2 F}{\delta u_x\delta u_y}\right)dy = 0 \tag{30}$$

[here we write $u(x) = u_x$ for brevity].

We introduce the functions

$$g_s(x_1, x_2, \ldots, x_s) = \delta^s F/\delta u_{x_1}\ldots\delta u_{x_s}, \tag{31}$$

which are connected with the distribution functions in the following way:

$$F_1(x_1/\varphi) = \frac{V}{N}\frac{\delta F}{\delta\varphi_{x_1}} = -\frac{1+vu_{x_1}}{\Theta}\frac{\delta F}{\delta u_{x_1}}, \qquad F_1(x_1) = -\frac{1}{\Theta}\left(\frac{\delta F}{\delta u_{x_1}}\right)_{u=0} = -\frac{1}{\Theta}g_1(x_1) \tag{32}$$

and on the basis of Eqs. (7) and (29):

$$F_2(x_1, x_2\,|\,\varphi) = \frac{N}{N-1}F_1(x_1\,|\,\varphi)F_1(x_2\,|\,\varphi) - \frac{V}{N-1}\delta(x_1-x_2)F_1(x_1\,|\,\varphi)$$

$$-\frac{V\Theta}{N-1}\frac{\delta F_1(x_1\,|\,\varphi)}{\delta\varphi_{x_2}} = \frac{V^2}{N(N-1)}\left\{\frac{\delta F}{\delta\varphi_{x_1}}\frac{\delta F}{\delta\varphi_{x_2}} - \delta(x_1-x_2)\frac{\delta F}{\delta\varphi_{x_1}} - \Theta\frac{\delta^2 F}{\delta\varphi_{x_1}\delta\varphi_{x_2}}\right\}$$

$$= \frac{V^2}{N(N-1)}\frac{(1+vu_x)(1+vu_y)}{v^2\Theta^2}\left\{\frac{\delta F}{\delta u_{x_1}}\frac{\delta F}{\delta u_{x_2}} - \Theta\frac{\delta^2 F}{\delta u_{x_1}\delta u_{x_2}}\right\},$$

and in the limiting case ($V, N\to\infty$, $N/V = n$) and for $u = 0$, we get

$$F_2(x_1, x_2) = \Theta^{-2}\{g_1(x_1)\,g_1(x_2) - \Theta\delta g_1(x_1)/\delta u_{x_2}\}. \tag{33}$$

Similarly we can represent the other F_s in terms of g_s. Using Eq. (31), we can put Eq. (30) in the form

$$-\frac{\partial g_1(x\,|\,u)}{\partial x^\alpha} + \frac{1}{\Theta^2}\int\frac{\partial\Phi(|x-y|)}{\partial x^\alpha}(n+u_y)\left\{g_1(x\,|\,u)\,g_1(y\,|\,u) - \Theta\frac{\delta g_1(x\,|\,u)}{\delta y_y}\right\}dy. \tag{34}$$

We expand $g_1(x\,|\,u)$ in a power series in the density $n = 1/v$:

$$g_1(x\,|\,u) = g_1^0(x\,|\,u) + ng_1^1(x\,|\,u) + n^2 g_1^2(x\,|\,u) + \cdots, \tag{35}$$

Substituting this expression in Eq. (34), we get equations with variational derivatives for determining the expansion coefficients

$$-\frac{\partial g_1^0(x\mid u)}{\partial x^\alpha}+\frac{1}{\Theta^2}\int\frac{\partial\Phi(\mid x-y\mid)}{\partial x^\alpha}u_y\left\{g_1^0(x\mid u)\,g_1^0(y\mid u)-\Theta\frac{\delta g_1^0(x\mid u)}{\delta u_y}\right\}dy=0, \tag{36}$$

$$-\frac{\partial g_1^1(x\mid u)}{\partial x^\alpha}+\frac{1}{\Theta^2}\int\frac{\partial\Phi(\mid x-y\mid)}{\partial x^\alpha}\left\{g_1^0(x\mid u)\,g_1^0(y\mid u)-\Theta\frac{\delta g_1^0(x\mid u)}{\delta u_y}\right.$$

$$\left.+u_y\left(g_1^0(x\mid u)\,g_1^1(y\mid u)+g_1^0(y\mid u)\,g_1^1(x\mid u)\right)-\Theta\frac{\delta g_1^1(x\mid u)}{\delta u_y}\right\}dy=0. \tag{37}$$

Setting $u=0$, we get from Eq. (36): $\partial g_1^0(x)/\partial x^\alpha=0$, whence $g_1^0(x)=\text{const}$, since g_1^0 is symmetric relative to x, y, z.

We have from Eqs. (32) and (19):

$$g_1^0(x)=-\Theta \tag{38}$$

and consequently,

$$F_1^0(x)=-g_1^0(x)/\Theta=1. \tag{39}$$

We find the following approximation for $F_1(x)$. By substitution of $u=0$ in Eq. (37), we determine $F_1^1(x)=-g_1^1(x)/\Theta$:

$$-\frac{\partial g_1^1(x)}{\partial x^\alpha}+\int\frac{\partial\Phi(\mid x-y\mid)}{\partial x^\alpha}\left(1-\frac{1}{\Theta}\frac{\delta g_1^0(x)}{\delta u_y}\right)dy=0. \tag{40}$$

The expressions under the integral in this equation can be found by functional differentiation of (36) with respect to u_{x_2} and subsequent equating of u to zero:

$$-\frac{\partial}{\partial x^\alpha}\frac{\delta g_1^0(x)}{\delta u_{x_2}}+\frac{1}{\Theta^2}\frac{\partial\Phi(\mid x-x_2\mid)}{\partial x^\alpha}\left(g_1^0(x)\,g_1^0(x_2)-\Theta\frac{\delta g_1^0(x)}{\delta u_{x_2}}\right)$$

$$+\frac{1}{\Theta^2}\int\frac{\partial\Phi(\mid x-y\mid)}{\partial x^\alpha}u_y\left(g_1^0(x)\frac{\delta g_1^0(y)}{\delta u_{x_2}}+g_1^0(y)\frac{\delta g_1^0(x)}{\delta u_{x_2}}-\Theta\frac{\delta^2 g_1(x)}{\delta u_y\delta u_{x_2}}\right)dy=0. \tag{41}$$

Employing (38) and setting $u=0$, we get, upon integration

$$\delta g_1^0(x)/\delta u_y=\Theta\left(1-c_1\exp\left\{-\frac{1}{\Theta}\Phi(\mid x-y\mid)\right\}\right). \tag{42}$$

Substituting (41) in (40), and making use of (19), we find

$$g_1^1(x)=0 \tag{43}$$

and, consequently, $F_1^1(x)=0$. Similarly, the following approximations are determined:

$$F_1^2(x)=F_1^3(x)=\cdots=0.$$

Thus

$$F_1(x) = 1, \tag{44}$$

which corresponds to a uniform spatial distribution of particles with short-range interaction forces in statistical equilibrium.

We now determine the pair distribution function. If we substitute the expansion (35) for $g_1(x)$ in Eq.(39), we obtain an expansion of the function $F_2(x_1, x_2)$ in powers of the density of the form:

$$F_2(x, y) = F_2^0(x, y) + nF_2^1(x, y) + n^2F_2^2(x, y) + \cdots,$$

where

$$F_2^0(x_1, x_2) = \frac{1}{\Theta^2}\left\{g_1^0(x_1)\, g_1^0(x_2) - \Theta\, \frac{\delta g_1^0(x_1)}{\delta u_{x_2}}\right\} = 1 - \frac{1}{\Theta}\, \frac{\delta g_1^0(x_1)}{\delta u_{x_2}} = c_1 \exp\left\{-\frac{1}{\Theta}\, \Phi(|x_1 - x_2|)\right\},$$

or

$$F_2^0(x_1, x_2) = \exp\left\{-\frac{1}{\Theta}\, \Phi(|x_1 - x_2|)\right\}, \tag{45}$$

since, from the boundary condition:

$$F_2^0(x_1, x_2) \to F_1(x_1)\, F_1(x_2) = 1 \quad \text{at} \quad |x_1 - x_2| \to \infty$$

it follows that the constant $c_1 = 1$;

$$F_2^1(x_1, x_2) = \Theta^{-2}\{g_1^0(x_1)\, g_1^1(x_2) + g_1^1(x_1)\, g_1^0(x_2) - \Theta\delta g_1^1(x_1)/\delta u_{x_2}\} = -\Theta^{-1}\delta g_1^1(x_1)/\delta u_{x_2}, \tag{46}$$

$$F_2^2(x_1, x_2) = -\Theta^{-1}\delta g_1^2(x_1)/\delta u_{x_2}, \ldots \tag{47}$$

As is evident from (46), $F_2^1(x_1, x_2)$ is proportional to the variational derivative $\delta g_1^1(x_1)/\delta u_{x_2}$. We can find this derivative by functional differentiation of Eq. (37) with respect to u_{x_2} and setting $u = 0$. We then get, taking Eqs. (38), (42) and (43) into account:

$$-\frac{\partial}{\partial x_1^\alpha}\, \frac{\delta g_1^1(x_1)}{\delta u_{x_2}} + \int \frac{\partial \Phi(|x_1 - y|)}{\partial x_1^\alpha}\left\{\exp\left[-\frac{1}{\Theta}\,(\Phi(|x_1 - x_2|) + \Phi(|x_2 - y|))\right]\right.$$
$$\left. - 2 - \frac{1}{\Theta}\, \frac{\delta^2 g_1^0(x_1)}{\delta u_y \delta u_{x_2}}\right\} dy - \frac{1}{\Theta}\, \frac{\partial \Phi(|x_1 - x_2|)}{\partial x_1^\alpha}\, \frac{\delta g_1^1(x_1)}{\delta u_{x_2}} = 0. \tag{48}$$

We find the derivative of g_1^0 here from Eq. (41) by functional differentiation with respect to u_y and substitution of $u = 0$, and also, making use of Eqs. (38) and (42). We then get:

$$\delta^2 g_1^0(x_1)/\delta u_y \delta u_{x_2} = \Theta\left\{\exp\left[-\frac{1}{\Theta}\,(|x_2 - y|)\right] + \exp\left[-\frac{1}{\Theta}\,\Phi(|x_1 - x_2|)\right]\right.$$
$$\left. + \exp\left[-\frac{1}{\Theta}\,\Phi(|x_1 - y|)\right] - 2\right\} \tag{49}$$
$$+ c_2 \exp\left\{-\frac{1}{\Theta}\left[\Phi(|x_1 - x_2|) + \Phi(|x_1 - y|) + \Phi(|x_2 - y|)\right]\right\}.$$

The constant c_2 is determined similarly to c_1, and is equal to unity.

Substituting Eq. (49) in (48) for $c_2 = 1$, we get the equation

$$\frac{\partial}{\partial x^\alpha}\frac{\delta g_1^1(x_1)}{\delta u_{x_2}} + \frac{1}{\Theta}\frac{\partial \Phi(|x_1 - y|)}{\partial x_1^\alpha}\frac{\delta g_1^1(x_1)}{\delta u_{x_2}} = \exp\left\{-\frac{1}{\Theta}\Phi(|x_1 - x_2|)\right\}\int \frac{\partial \Phi(|x_1 - y|)}{\partial x_1^\alpha}$$
$$\times \exp\left\{-\frac{1}{\Theta}[\Phi(|x_1 - y|) + \Phi(|x_2 - y|)]\right\} dy. \tag{50}$$

Moreover, since

$$\frac{\partial \Phi(|x_1 - y|)}{\partial x_1^\alpha}\exp\left\{-\frac{1}{\Theta}[\Phi(|x_1 - y|) + \Phi(|x_2 - y|)]\right\} = -\Theta\frac{\partial}{\partial x^\alpha}\{(1 + f(|x_1 - y|))(1 + f(|x_2 - y|))\},$$

where

$$f(r) = \exp\{-\Phi(r)/\Theta\} - 1,$$

then, taking (46) into consideration, we get the following equation for $F_2^1(x_1, x_2)$:

$$\frac{\partial F_2^1}{\partial x_1^\alpha} + \frac{1}{\Theta}\frac{\partial \Phi(|x_1 - x_2|)}{\partial x_1^\alpha}F_2^1 = \exp\left\{-\frac{1}{\Theta}\Phi(|x_1 - x_2|)\right\}\frac{\partial}{\partial x_1^\sigma}\int f(|x_1 - y|) f(|x_2 - y|)\, dy. \tag{51}$$

Looking for a solution of this equation in the form

$$F_2^1(x_1, x_2) = \psi(|x_1 - x_2|)\exp\left\{-\frac{1}{\Theta}\Phi(|x_1 - x_2|)\right\},$$

we get (after substitution):

$$F_2^1(|x_1 - x_2|) = F_2^1(|x|) = \exp\left\{-\frac{1}{\Theta}\Phi(|x|)\right\}\int f(|x - x'|) f(|x'|)\, dx'. \tag{52}$$

Similarly, we can find the other terms of the expansion of F_2^2, F_2^3, etc.

Thus the pair distribution function of a system of particles with short-range interaction is equal, with accuracy up to terms of second order, to

$$F_2(x_1, x_2) = F_2(|x|) = \exp\left\{-\frac{1}{\Theta}\Phi(|x|)\right\}\left(1 + n\int f(|x - x'|) f(|x'|)\, dx'\right). \tag{53}$$

Other correlation functions are found by the method of variational derivatives in the same way as the pair functions.

4. SUPERPOSITION THEOREM

In Secs. 2 and 3 we developed a method for finding the correlation functions for systems of particles corresponding to the Coulomb interaction potential $\Phi_0(r)$, and to a potential $\Phi_1(r)$ which falls off rapidly with distance. In the first case, these functions are found by an expansion in powers of v; in the second case, by an expansion in powers of $n = 1/v$. Here, the first approximation for the pair distribution function (27) loses its applicability for small r, and finding higher approximations would be senseless since they diverge even more strongly for small r.[1]

Real interaction between charged particles consists of Coulomb forces ($r > r_0$) and short-range forces, such that the potential of this interaction has the form $\Phi_0(r) + \Phi_1(r)$. However, as Bogoliubov pointed out in Ref. 1, the problem is open at the present time of the construction of expansions by

which we could find the correlation functions for systems with interaction including both Coulomb and short-range forces; such a construction would make it possible to obtain asymptotic formulas for any approximation.

In the present Section, making use of variational derivatives, we establish a "superposition theorem", *i.e.*, we set forth a method of investigation of a system with interaction of the form

$$\Phi(r) = \Phi_0(r) + \Phi_1(r). \tag{54}$$

Let the total energy of interaction of a system of N particles in the potential (54) be equal to

$$U = U_0 + \sum_{1 \leqslant i < j \leqslant N} \Phi_1(|x_i - x_j|),$$

where U_0 is the part of the interaction energy of the system of particles which corresponds to the potential $\Phi_0(r)$. Moreover, if our system is located in an external field $\varphi(x)$, then the configurational integral of the system is

$$\begin{aligned} Q &= \int \exp\left\{-\frac{1}{\Theta} U - \frac{1}{\Theta} \sum_{1 \leqslant i \leqslant N} \varphi(x_i)\right\} dx_1 \ldots dx_N \\ &= \int \exp\left\{-\frac{1}{\Theta} U_0 - \frac{1}{\Theta} \sum_{1 \leqslant i \leqslant N} \varphi(x_i)\right\} \prod_{1 \leqslant i < j \leqslant N} (1 + f(x_i, x_j))\, dx_1 \ldots dx_N, \end{aligned} \tag{55}$$

where

$$f(x_i, x_j) = \exp\{-\Phi_1(|x_i - x_j|)/\Theta\} - 1.$$

The free energy of the system is equal to $F = -\Theta \ln Q$. Both the configurational integral (55) and the free energy are themselves functionals of the external field $\varphi(x)$ and the interaction energy $f(x_i, x_j)$. The correlation functions of the system $F_1(x_1 \mid \varphi \mid f)$, $F_2(x_1, x_2 \mid \varphi \mid f)$, etc., are expressed in terms of the variational derivatives of the functional F with respect to $\varphi(x)$ according to Eqs. (4) and (7).

In Secs. 2 and 4, we found $F_1(x_1 \mid \varphi)$ from the corresponding equations with variational derivatives with the help of well known expansions. We now proceed otherwise. We shall show that the functional $F(\varphi \mid f)$ can be expressed by the correlation functions of the system for a potential $\Phi_0(r)$, so that, for finding the variational derivatives of $F(\varphi \mid f)$ with respect to $\varphi(x)$ and, consequently, the correlation functions $F_s(x_1, \ldots, x_s \mid \varphi \mid f)$, it is not necessary to construct and solve the differential equations for these functions; it is necessary to know them only for the potential $\Phi_0(r)$, the determination of which was carried out in Sec. 2.

With this end in view, we expand the function $F(\varphi \mid f)$ in a series

$$F(\varphi \mid f) = F_{f=0} + \int f(x, y) \left(\frac{\delta F}{\delta f_{x,y}}\right)_{f=0} dx\, dy + \frac{1}{2} \int f(x, y) f(x', y') \left(\frac{\delta^2 F}{\delta f_{x,y} \delta f_{x',y'}}\right)_{f=0} dx\, dy\, dx'\, dy' + \ldots \tag{56}$$

and find expressions for the variational derivatives therein: On the one hand, we have from (55):

$$\begin{aligned} \delta Q &= \int \exp\left\{-\frac{1}{\Theta} U_0 - \frac{1}{\Theta} \sum_{1 \leqslant j \leqslant N} \varphi(x_j)\right\} \sum_{1 \leqslant r < j \leqslant N} \delta f(x_i, x_j) \\ &\quad \times \left[\prod_{1 \leqslant r < s \leqslant N} (1 + f(x_r, x_s))/(1 + f(x_i, x_j))\right] dx_1 \ldots dx_N, \\ (1 + f(x, y)) \frac{\delta Q}{\delta f_{x,y}} &= \frac{N(N-1)}{2} \int \exp\left\{-\frac{1}{\Theta} U_0 - \frac{1}{\Theta} \sum_j \varphi(x_j)\right\} \\ &\quad \times \prod_{1 \leqslant r < s \leqslant N} (1 + f(x_r, x_s))\, dx_3 \ldots dx_N \end{aligned} \tag{57}$$

(here we have set $x_1 = x$, and $x_2 = y$), and on the other hand:

$$\frac{\delta Q}{\delta \varphi_x} = -\frac{N}{\Theta}\int \exp\left\{-\frac{1}{\Theta}U_0 - \frac{1}{\Theta}\sum_j \varphi(x_j)\right\} \prod_{1\leqslant r<s\leqslant N}(1+f_{r,s})\,dx_2\ldots dx_N, \tag{58}$$

$$\frac{\delta^2 Q}{\delta\varphi_x\delta\varphi_y} = \frac{N(N-1)}{\Theta^2}\int \exp\left\{-\frac{1}{\Theta}U_0 - \frac{1}{\Theta}\sum_j \varphi(x_j)\right\} \prod_{1\leqslant r<s\leqslant N}(1+f_{r,s})\,dx_3\ldots dx_N$$
$$+\frac{N}{\Theta^2}\delta(x-y)\int \exp\left\{-\frac{1}{\Theta}U_0 - \frac{1}{\Theta}\sum_j \varphi(x_j)\right\} \prod_{1\leqslant r<s\leqslant N}(1+f_{r,s})\,dx_2\ldots dx_N. \tag{59}$$

Comparing (57) with (58) and (59), we find

$$(1+f_{x,y})\frac{\delta Q}{\delta f_{x,y}} = \frac{\Theta^2}{2}\left\{\frac{\delta^2 Q}{\delta\varphi_x\delta\varphi_y} - \frac{\delta(x-y)}{\Theta}\frac{\delta Q}{\delta\varphi_x}\right\}, \tag{60}$$

and since $Q = e^{-F/\Theta}$, then, substituting the values of the corresponding variational derivatives in Eq. (60), we get

$$(1+f_{x,y})\frac{\delta F}{\delta f_{xy}} = \frac{\Theta^2}{2}\left\{\frac{\delta^2 F}{\delta\varphi_x\delta\varphi_y} - \frac{1}{\Theta}\frac{\delta F}{\delta\varphi_x}\frac{\delta F}{\delta\varphi_y} + \frac{\delta(x-y)}{\Theta}\frac{\delta F}{\delta\varphi_x}\right\}. \tag{61}$$

Again taking functional derivatives of this equation with respect to $f_{x'y'}$, we find an expression for the second derivative. The right side of (61), in accord with Eqs. (8) and (4), is equal to

$$-{}^1/_2\Theta N(N-1)V^{-2}F_2(x, y|\varphi|f),$$

therefore

$$(1+f_{xy})\,\delta F/\delta f_{xy} = -{}^1/_2 n^2\Theta F_2(x, y|\varphi|f). \tag{62}$$

Setting $f_{xy} = 0$, we get

$$(\delta F/\delta f_{xy})_{f=0} = -{}^1/_2 n^2\Theta F_2(x, y|\varphi|0),$$

i.e., this variational derivative is expressed by the pair distribution function for the potential $\Phi_0(r)$. Therefore, in first approximation, and in accord with (56), the free energy of the system for the potential (54) is equal to

$$F(\varphi|f) = F_{f=0} - n^2\frac{\Theta}{2}\int f(x, y)\,F_2(x, y|\varphi)\,dx\,dy. \tag{63}$$

Knowing $F_2(x, y|\varphi)$, taking the functional derivative of (63) with respect to $\varphi(x)$, we can find the correlation functions $F_1(x|\varphi|f)$, $F_2(x, y|\varphi|f)$ *etc.*, and then setting $\varphi = 0$, we find $F_1(x|f)$, $F_2(x, y|f)$ etc. for our system.

A calculation carried out by the method of correlation functions of a system for the concrete case $\Phi_0(r)$ and $\Phi_1(r)$ will form the subject of another paper.

In conclusion, I express my deep gratitude to Academician N. N. Bogoliubov under whose direction this research was carried out.

---

[1] N. N. Bogoliubov, *Problems of Dynamical Theory in Statistical Physics*, Gostekhizdat, 1946.

[2] N. N. Bogoliubov, Vestnik, Moscow State Univ. Nos. 4–5, 115 (1955).

Translated by R. T. Beyer
224

Bremsstrahlung of Polarized Electrons

G. L. VISOTSKII, A. A. KRESNIN, AND L. N. ROZENTSVEIG
Physico-Technical Institute, Academy of Sciences, U.S.S.R.

(Submitted to JETP editor May 3, 1956)
J. Exptl. Theoret. Phys. 32, 1078-1082 (May, 1957)

The polarization properties of the bremsstrahlung arising when a polarized electron beam strikes a target are considered. It is shown that in this case the bremsstrahlung contains a circularly polarized component. For highly relativistic electrons which are completely polarized in the direction of motion, the circular polarization near the upper limit of the spectrum amounts to as much as 25%; multiple scattering of electrons in the target has practically no effect on this value. Equations have been derived for the polarization of bremsstrahlung photons produced by electrons of arbitrary energy.

THE POLARIZATION PROPERTIES of bremsstrahlung have been studied in detail in a series of papers [1,2,3,4] on the assumption that the electron beam striking the target is not polarized. In this case the bremsstrahlung contains a linearly polarized component in addition to the unpolarized part. If an integration is carried out over the direction of the final momentum of the electron, the bremsstrahlung turns out to be partly polarized along the normal to the plane of emission. At high energies the effective polarization falls off strongly as a result of multiple scattering of electrons in the target.

In connection with the possibility mentioned by one of the authors[5] of obtaining an intense beam of polarized electrons, the following question arose: what properties would the bremsstrahlung have if the electron beam striking the target had arbitrary polarization? It has already been pointed out by Zel'dovich[6] that polarization of the incident electrons leads to circular polarization of the bremsstrahlung photons. The present paper is devoted to a quantitative investigation of this question.

In order to describe the polarization properties of the beam of photons we will make use of density matrices[7,8]

$$\rho_{\text{ph}} = \frac{1}{2}(1 + \xi\Omega), \tag{1}$$

where Ω is a "matrix vector" with components

$$\Omega_1 = \begin{pmatrix} 1 & 0 \\ 0 & -1 \end{pmatrix}, \quad \Omega_2 = \begin{pmatrix} 0 & 1 \\ 1 & 0 \end{pmatrix}, \quad \Omega_3 = \begin{pmatrix} 0 & -i \\ i & 0 \end{pmatrix}, \tag{2}$$

ξ_1, ξ_2, ξ_3 are Stokes parameters. We recall that the set of values $\xi_1 = 1$ ($\xi_1 = -1$), $\xi_2 = \xi_3 = 0$ designates linear polarization along the OX (OY) axis; the set $\xi_2 = 1$ ($\xi_2 = -1$), $\xi_1 = \xi_3 = 0$ designates linear polarization at an angle of 45° with respect to the OX(OY) axis; and the set $\xi_3 = 1$ ($\xi_3 = -1$), $\xi_1 = \xi_2 = 0$ designates clockwise (counterclockwise) circular polarization. The quantities ξ_i are not components of a vector and under a rotation of the coordinate axes they are transformed according to a different law. The vector symbol ξ has to be understood in a strictly formal sense; in particular, $\xi\Omega$ is an abbreviation for the sum $\xi_1\Omega_1 + \xi_2\Omega_2 + \xi_3\Omega_3$.

If the electron beam striking the target is not polarized, the bremsstrahlung parameters ξ_i are determined by the expression

$$\xi\Omega = {}_{\lambda'\lambda''}\,\text{Sp}\,(S_{\lambda'}S_{\lambda'}^{+}) \,/\, \text{Sp}\,(S_{\lambda}S_{\lambda}^{+}), \tag{3}$$

where S_λ is the element of the scattering matrix corresponding to the emission of a bremsstrahlung photon with polarization vector e_λ ($\lambda = 1, 2$; $e_\lambda e_{\lambda'} = \delta_{\lambda\lambda'}$, $e_\lambda k = 0$); we assume that the corresponding operators of the projection are already included in S_λ, and it is possible to write down the "spurs" at once.

We define $Q_{\lambda\lambda'} = \text{Sp}(S_\lambda S_{\lambda'}^{+})$. Calculations yield

$$\begin{aligned} q^4 Q_{\lambda\lambda'} \sim\ & 4\left(\frac{\varepsilon_0}{\varkappa_0}\mathbf{p} + \frac{\varepsilon}{\varkappa}\mathbf{p}_0,\ \mathbf{e}_\lambda\right)\left(\frac{\varepsilon_0}{\varkappa_0}\mathbf{p} + \frac{\varepsilon}{\varkappa}\mathbf{p}_0,\ \mathbf{e}_{\lambda'}\right) \\ & - q^2\left(\frac{\mathbf{p}}{\varkappa_0} + \frac{\mathbf{p}_0}{\varkappa},\ \mathbf{e}_\lambda\right)\left(\frac{\mathbf{p}}{\varkappa_0} + \frac{\mathbf{p}_0}{\varkappa},\ \mathbf{e}_{\lambda'}\right) \\ & - \frac{\delta_{\lambda\lambda'}}{\varkappa_0\varkappa}[\mathbf{p} - \mathbf{p}_0,\ \mathbf{k}]^2 \end{aligned} \tag{4}$$

[we have ignored factors which play no role when $Q_{\lambda\lambda'}$ is substituted into equation (3)]; here

$$\varkappa_0 = -\frac{2\varepsilon\omega}{m^2}(1 - v\cos\vartheta),$$
$$\varkappa = \frac{2\varepsilon_0\omega}{m^2}(1 - v_0\cos\vartheta_0), \tag{5}$$

$\mathbf{p}_0$, $\mathbf{p}$ are the initial and final momenta of the electron, $\mathbf{k}$ the momentum of the photon, ε_0, ε and ω the corresponding energies, θ_0, θ the angles between $\mathbf{k}$ and $\mathbf{p}_0$, $\mathbf{p}$; $\mathbf{q}$ the momentum transferred to the nucleus ($\mathbf{q} = \mathbf{p} + \mathbf{k} - \mathbf{p}_0$).

Except for a factor, the denominator of the right hand side of equation (3) agrees with the bremsstrahlung cross-section[9]:

$$q^4(Q_{11} + Q_{22}) \sim q^4 Q(\mathbf{p}_0, \mathbf{p}, \mathbf{k})$$
$$= \frac{4}{\omega^2}\left[\mathbf{k}, \frac{\varepsilon_0}{\varkappa_0}\mathbf{p} + \frac{\varepsilon}{\varkappa}\mathbf{p}_0\right]^2 - \frac{q^2}{\omega^2}\left[\mathbf{k}, \frac{\mathbf{p}}{\varkappa_0} + \frac{\mathbf{p}_0}{\varkappa}\right]^2$$
$$- \frac{2}{\varkappa_0\varkappa}[\mathbf{k}, \mathbf{p} - \mathbf{p}_0]^2. \tag{6}$$

As coordinate axes we select mutually perpendicular vectors $\mathbf{e}_1$, $\mathbf{e}_2$, and $\mathbf{k}/\omega$. The choice of $\mathbf{e}_1$ and $\mathbf{e}_2$ is arbitrary; for definiteness in what follows we set $\mathbf{e}_1 = \mathbf{n} \equiv [\mathbf{p}_0\mathbf{k}]/|[\mathbf{p}_0\mathbf{k}]|$, $\mathbf{e}_2 = \mathbf{l} \equiv [\mathbf{kn}]/\omega$. Since $Q_{12} = Q_{21}$, the third Stokes parameter is equal to zero; *i.e.*, the bremsstrahlung is linearly polarized:

$$\xi_1 = \frac{Q_{11} - Q_{22}}{Q_{11} + Q_{22}}$$
$$= \frac{2(4\varepsilon_0^2 - q^2)(\mathbf{pn})^2 - 2\frac{\varkappa_0}{\varkappa}[\mathbf{p} - \mathbf{p}_0, \mathbf{k}]^2}{\varkappa_0^2 q^4 Q(\mathbf{p}_0, \mathbf{p}, \mathbf{k})} - 1, \tag{7}$$

$$\xi_2 = \frac{2Q_{12}}{Q_{11} + Q_{22}}$$
$$= \frac{2(\mathbf{pn})}{\varkappa_0 q^4 Q}\left(\frac{4\varepsilon_0^2 - q^2}{\varkappa_0}\mathbf{p} + \frac{4\varepsilon_0\varepsilon - q^2}{\varkappa}\mathbf{p}_0, \mathbf{l}\right), \tag{8}$$

$$\xi_3 = i(Q_{12} - Q_{21})/(Q_{11} + Q_{22}) = 0. \tag{9}$$

In Eqs. (7)–(9) the direction of $\mathbf{p}$ is fixed. Since it does not interest us, we have to multiply $\boldsymbol{\xi}$ by the probability of a given direction $\mathbf{p}$, which is equal to

$$w(\mathbf{p})\, do_{\mathbf{p}} = Q(\mathbf{p}_0, \mathbf{p}, \mathbf{k})\, do_{\mathbf{p}} \Big/ \int Q(\mathbf{p}_0, \mathbf{p}', \mathbf{k})\, do_{\mathbf{p}'},$$

and integrate over all directions $\mathbf{p}$:

$$\bar{\boldsymbol{\xi}} = \int \Omega_{\lambda\lambda'} Q_{\lambda'\lambda}\, do_{\mathbf{p}} \Big/ \int Q\, do_{\mathbf{p}'}. \tag{10}$$

The integral of equation (8) gives zero (as was to be expected from symmetry considerations), and for the single non-vanishing parameter $\bar{\xi}_1$ we obtain a result well-known from previous work[2, 4].

The state of polarization of electrons with momentum $\mathbf{p}_0$ is described by a four-row density matrix[7, 10]

$$\rho_e = \eta_l^{(+)}(\mathbf{p}_0)\frac{1}{2}(1 + \zeta\Sigma\gamma_4)\eta_l^{(+)}(\mathbf{p}_0), \quad \Sigma = \begin{pmatrix}\sigma & 0\\ 0 & \sigma\end{pmatrix}, \tag{11}$$

where $\eta^{(+)}(\mathbf{p}_0)$ is an operator of the projection onto a state with positive energy $\varepsilon_0 = \sqrt{m^2 + \mathbf{p}_0^2} > 0$

$$\eta_l^{(+)}(\mathbf{p}_0) = \frac{1}{2\varepsilon_0}(m - i\hat{p}_0)\gamma_4, \quad \hat{p}_0 = p_{0\mu}\gamma_\mu, \tag{12}$$

and the vector $\boldsymbol{\zeta}$, characterizing the polarization, is equal to

$$\zeta = \zeta_t^0 + \frac{\varepsilon_0}{m}\zeta_l^0; \tag{13}$$

$\boldsymbol{\zeta}^0$ is the polarization vector in the coordinate system in which the electrons are at rest, $\boldsymbol{\zeta}_t^0(\boldsymbol{\zeta}^{0t})$ is its component perpendicular (parallel) to the vector $\mathbf{p}_0$.

When the electron beam is polarized [matrix density of Eq. (11)] the Stokes parameters of the bremsstrahlung are equal to

$$\frac{\xi = \Omega_{\lambda'\lambda''}\,\mathrm{Sp}\{S_{\lambda''}[1 + (\zeta\Sigma)\gamma_4]S_{\lambda'}^+\}}{\mathrm{Sp}[S_\lambda(1 + \zeta\Sigma\gamma_4)S_\lambda^+]}; \tag{14}$$

where for brevity, as in (3), we do not write out the factors $\eta^{(+)}(\mathbf{p}_0)$, $\eta^{(+)}(\mathbf{p})$, taking them to be included in S_λ, *i.e.*,

$$S_\lambda = \eta_l^{(+)}(\mathbf{p})\, S_\lambda^{(0)} \eta_l^{(+)}(\mathbf{p}_0),$$

where $S_\lambda^{(0)}$ is the scattering matrix in the usual sense.

We define $R_{\lambda\lambda'} = \mathrm{Sp}(S_\lambda\zeta\Sigma\gamma_4 S_{\lambda'}^+)$. It is easily shown that $R_{11} + R_{22} = 0$, and the denominator $\mathrm{Sp}[S_\lambda(1 + \zeta\Sigma\gamma_4)S_\lambda^+] = Q$ in (14) is the same as in (3). Consequently the polarization of the electrons has no effect on the bremsstrahlung cross-section, as calculated from the Born approximation. Analogously, $R_{11} - R_{22} = R_{12} + R_{21} = 0$. *i.e.*, the second component in ρ_e makes no contribution to ξ_1 and ξ_2, which as before are determined

by Eqs. (7) and (8). But the parameter ξ_3, which was equal to zero for unpolarized electrons, now does not vanish:

$$\xi_3 = i(R_{12} - R_{21})/(Q_{11} + Q_{22})$$
$$= \frac{m}{2\varepsilon_0\omega^2 q^4 Q}\left\{\left(\frac{p_0}{\varkappa} + \frac{p}{\varkappa_0},\ [k[k,\ p_0 - p]]\right)\left(\zeta,\ \frac{p_0 + \varepsilon_0 k}{\varkappa_0} + \frac{\omega p_0 - \varepsilon_0 k}{\varkappa}\right)\right. \quad (15)$$
$$\left. + \frac{1}{2}m^2\omega\left[\frac{\varkappa_0}{\varkappa} - \frac{\varkappa}{\varkappa_0} + \frac{4\omega}{m^2}\left(\frac{\varepsilon_0}{\varkappa_0} + \frac{\varepsilon}{\varkappa}\right)\right]\left(\zeta,\ \frac{\varepsilon}{\varkappa}(\omega p_0 - \varepsilon_0 k) + \frac{\varepsilon_0}{\varkappa_0}(\omega p - \varepsilon k)\right)\right\}.$$

We introduce the unit vectors $a = p_0/p_0$ and $b = [an]$. Clearly

$$\bar{\xi}_3 = i\int (R_{12} - R_{21})\, do_p \Big/ \int Q\, do_{p'} = \Lambda_a(\zeta^0 a) + \Lambda_b(\zeta^0 b), \quad (16)$$

that is, the projection of the polarization vector of the electrons in the direction of the normal n vanishes when the integration is performed.

In the limiting case of non-relativistic energies Eqs. (7), (8) and (15) simplify greatly:

$$\xi_1 = 2\omega^2 (pn)^2 [k,\ p - p_0]^{-2} - 1,\ \xi_2 = 2\omega^2 (pn)(p - p_0,\ 1)[k,\ p - p_0]^{-2},\ \xi_3 = (\zeta k)/4m. \quad (17)$$

In the opposite limiting case of extreme relativistic energies it is necessary to take account of the screening effect. The approximate expression for the parameter $\bar{\xi}_1$ in this case has been given in Ref. 2. If in the expressions $R_{12} - R_{21}$ and Q under the integral in Eq. (16) we replace q^{-4} by $(q^2 + g^2)^{-2}$, where $g = mZ^{1/3}/137$ and carry out an integration over the directions of the vector p, with the approximation

$$m^2 x_0 \equiv \varepsilon_0^2 \sin^2\vartheta_0,\ m^2 x \equiv \varepsilon^2 \sin^2\vartheta \ll \varepsilon_0^2,\ \varepsilon^2,\ \omega^2, \quad (18)$$

then we obtain corresponding expressions for Λ_a and Λ_b:

$$\Lambda_a = \gamma\Phi^{-1}\left\{\frac{1}{4}[(1 + x_0)^2 + (1 - \gamma)(1 - x_0)^2]\left(\ln\frac{1 + x_0}{f} - 1\right) + \frac{1}{8}\gamma(1 + x_0)^2 + x_0(1 - \gamma)\right\},$$
$$\Lambda_b = -\gamma\Phi^{-1}(1 - \gamma)(1 - x_0)\sqrt{x_0}\left(\frac{1}{2}\ln\frac{1 + x_0}{f} - 1\right), \quad (19)$$

$$\Phi = 2\left[\left(1 - \gamma + \frac{1}{2}\gamma^2\right)(1 + x_0)^2 - 2(1 - \gamma)x_0\right]\ln\frac{1 + x_0}{f} - \frac{1}{2}\gamma^2(1 + x_0)^2 - 2(1 - \gamma)(1 - x_0)^2;$$
$$\gamma = \omega/\varepsilon_0,\ f^2 = q_{\min}^2 + g^2 \approx (m^2\omega/2\varepsilon_0\varepsilon)^2 + g^2. \quad (20)$$

The dependence of $\bar{\xi}_3$ on x_0 and γ for a beam of completely polarized, highly relativistic electrons is shown in the figure. For ζ^0 parallel to a, the quantity $\bar{\xi}_3$ depends weakly on x_0; for photons with energy* $\omega \sim 0.9\,\epsilon_0$ with $|\zeta^0| = 1$ we have $\bar{\xi}_3 \sim 25\%$.

* We note that Eq. (19) loses its applicability in the immediate vicinity of the limit of the spectrum, where the condition (18) is not satisfied.

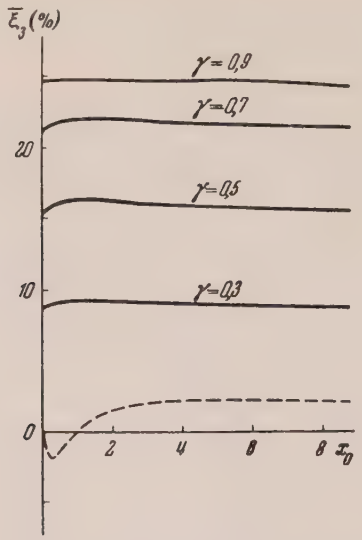

Circular polarization of the bremsstrahlung of highly relativistic electrons, averaged over the directions of the final moments of the electrons, shown as a function of $x_0 = (\epsilon_0/m)^2 \sin^2\theta_0$ for fixed values of $\gamma = \omega/\epsilon_0$: solid curve--electron beam totally polarized along $\mathbf{p}_0$; dotted curve--electron beam totally polarized in the plane of emission perpendicular to the vector $\mathbf{p}_0$, $\gamma = 0.5$, $Z = 13$.

Because of the weak dependence of Λ_a on θ_0, multiple scattering of electrons in the target of the beam has little effect on that part of $\bar{\xi}_3$ which is determined by the projection of the vector ζ^0 onto **a**. The other part of $\bar{\xi}_3$, corresponding to the projection of ζ^0 onto **b**, is small, and for targets of ordinary thickness ($t \sim 10^{-2} t_0$, where t_0 is the radiation unit of length), practically disappears because of the multiple scattering of electrons preceding the emission. Only for very thin targets ($t \sim 10^{-4} t_0$) can the effect connected with Λ_b become noticeable*.

In the general case of arbitrary energy we obtain rather cumbersome expressions for Λ_a and Λ_b:

$$2\Gamma\Lambda_a = -\gamma v_0^2 [v_0(1+\gamma^2+v_0^2) - (1+\gamma)(\gamma+2v_0^2)\cos\vartheta_0 + 3\gamma v_0\cos^2\vartheta_0] L_1 + (\gamma/2v_0)\Delta_0^{-2}\{v_0[1-3\gamma+v_0^2(1+2\gamma)] + [4\gamma - v_0^2(2+5\gamma) + 2\gamma v_0^4]\cos\vartheta_0 + v_0[6\gamma - v_0^2(3+5\gamma) + v_0^4]\cos^2\vartheta_0 - [6\gamma - 2v_0^2(1+3\gamma) + \gamma v_0^4]\cos^3\vartheta_0\} L_2 + v(1-\gamma)\Delta_0^{-2}\{v_0(1-3\gamma+2\gamma v_0^2) + 2[2\gamma - v_0^2(1+2\gamma)]\cos\vartheta_0 + v_0[6\gamma + v_0^2(1-3\gamma)]\cos^2\vartheta_0 - 2\gamma(3-2v_0^2)\cos^3\vartheta_0\} - v_0^2 v(1-\gamma)(v_0 - \gamma\cos\vartheta_0) T^{-2}, \quad (21)$$

$$-2(\gamma\sqrt{1-v_0^2}\sin\vartheta_0)^{-1}\Gamma\Lambda_b = v_0^2[3\gamma\Delta_0 + v^2(1-\gamma)^2] L_1 + (1/2v_0)\Delta_0^{-2}\{\gamma + v_0^2(1-2\gamma) + 2v_0[3\gamma - v_0^2(2+\gamma)]\cos\vartheta_0 + [-6\gamma + v_0^2(2+3\gamma) + v_0^4]\cos^2\vartheta_0\} L_2 + v(1-\gamma)\Delta_0^{-2}[1 - 2v_0^2 + 6v_0\cos\vartheta_0 - (6-v_0^2)\cos^2\vartheta_0] + v_0^2 v(1-\gamma) T^{-2}, \quad (22)$$

$$\Gamma = v_0^2[(2-3\gamma\Delta_0 - 2v_0^2) T^2 - \gamma(v_0^2-\gamma^2)\Delta_0] L_1 + v_0^{-1}\{2(1-v_0^2)\Delta_0^{-2}[3\gamma - v_0^2(1+2\gamma)]\sin^2\vartheta_0 + \gamma^2 - 5\gamma + v_0^2(3+\gamma+\gamma^2) + v_0^4 + \gamma\Delta_0(1-\gamma+v_0^2)\} L_2 - 2v_0^2\Delta_0 L_3 + v(1-\gamma)\{4(1-v_0^2)(3-v_0^2)\Delta_0^{-2}\sin^2\vartheta_0 - 10 + 2\gamma + 3v_0^2 + 2(1-\gamma)\Delta_0 + v_0^2(\gamma^2 - v_0^2) T^{-2}\}, \quad (23)$$

*See the analogous considerations of May[2] concerning the influence of multiple scattering on the effective value of the parameter $\bar{\xi}_1$.

where

$$L_1 = T^{-3} \ln \frac{T + v(1-\gamma)}{T - v(1-\gamma)}, \quad L_2 = \ln \frac{v_0^2 + v_0 v(1-\gamma) - \gamma}{v_0^2 - v_0 v(1-\gamma) - \gamma}, \quad L_3 = \ln \frac{1+v}{1-v}; \tag{24}$$

$$T^2 = \gamma^2 + v_0^2 - 2\gamma v_0 \cos\vartheta_0, \quad \Delta_0 = 1 - v_0 \cos\vartheta_0. \tag{25}$$

Equations (21)–(23) are valid for values of ε_0 which are not too large ($\varepsilon_0 \ll 137\, mZ^{1/3}$) and for values of γ which are not too small, for which the screening effect is unimportant.

[1] M. May and G. C. Wick, Phys. Rev. **81**, 628 (1951).
[2] M. M. May, Phys. Rev. **84**, 265 (1951).
[3] Gluckstern, Hull, and Breit, Phys. Rev. **90**, 1026 (1953).
[4] R. L. Gluckstern and M. H. Hull, Jr., Phys. Rev. **90**, 1030 (1953).
[5] L. N. Rosentsveig, J. Exptl. Theoret. Phys. (U.S.S.R.) **31**, 520 (1956), Soviet Physics JETP **4**, 455 (1957).
[6] Ia. B. Zel'dovich, Dokl. Akad. Nauk SSSR **83**, 63 (1952).
[7] F. W. Lipps and H. A. Tolhoek, Physica **20**, 85 (1954).
[8] W. H. McMaster, Am. J. Phys. **22**, 351 (1954).
[9] A. I. Akhiezer and V. B. Berestetskii, *Quantum Electrodynamics*, Moscow, 1953.
[10] A. A. Kresnin and L. N. Rosenzweig, J. Exptl. Theoret. Phys. (U.S.S.R.) **32**, 353 (1957), Soviet Phys. JETP **5**, 288 (1957).

Translated by W. M. Whitney
225

SOVIET PHYSICS JETP VOLUME 5, NUMBER 5 DECEMBER, 1957

Theory of Kinetic Phenomena in Liquid He^3

A. A. ABRIKOSOV AND I. M. KHALATNIKOV
Institute for Physical Problems, Academy of Sciences, U.S.S.R.

(Submitted to JETP editor May 9, 1956)
J. Exptl. Theoret. Phys. (U.S.S.R.) **32**, 1083-1091 (May, 1957)

The kinetic coefficients of liquid He^3 have been computed on the basis of the theory of a Fermi liquid by Landau. The temperature dependences of the coefficients and their numerical order of magnitude have also been computed.

IN THE PRESENT WORK, which is based on the theory of a Fermi liquid developed by Landau[1], we shall consider the problem of the viscosity and thermal conductivity of He^3. In accord with the Landau theory, the excitation energy in a Fermi liquid is a functional of the distribution function n. At temperatures close to $T = 0$, where the diffuse region of the Fermi function is not large, we can, according to the Landau theory, represent this functional dependence in the form of a decomposition in the deviation of the distribution function from its equilibrium value at $T = 0$. Limiting ourselves to terms up to first order of smallness, we have

$$\varepsilon = \varepsilon(p) + \int f(\mathrm{p}, \mathrm{p}')\, \nu d\tau', \qquad d\tau = 2dp_x dp_y dp_z / (2\pi\hbar)^3, \tag{1}$$

where ν is the difference between the actual distribution function and its value at $T = 0$.

It is most natural to consider that the distribution is the Fermi sphere at $T = 0$. Then at not too high temperatures the excitation energy will be described by the expression

$$\varepsilon(p) = a + p_0(p - p_0)/m, \tag{2}$$

where p_0 is the limiting momentum and a and m are constants (in the ideal gas case, this expression becomes $\varepsilon = p^2/2m$). By Ref. 2, it follows from the measurement of the density and entropy of He^3 that $p_0/\hbar = 0.76 \times 10^8$ cm^{-1}, $m = 1.43\, m_{He^3}$. In view of the fact that the energy ε enters into the Fermi distribution in the combination $\varepsilon - \mu$, the constant a

can be added to μ; as we shall see, it is inconsequential in the calculation of the kinetic coefficients.

As was shown in Ref. 2, it is possible that the temperature dependence of thermodynamical quantities in He^3 is better explained if we take as the ground state not the Fermi sphere but a thin spherical shell, such that the excitation spectrum has the form

$$\varepsilon(p) = a + (p - p_0)^2/2m. \tag{3}$$

We shall discuss the results which follow from such a form of the spectrum in Sec. 4.

1. THE KINETIC (BOLTZMANN) EQUATION

Let the motion in the liquid under consideration take place with a slightly inhomogeneous (in the coordinates) velocity u and let there be a small temperature gradient. In this case the distribution function will differ but slightly from its equilibrium value

$$n = n_0 + \delta n, \tag{4}$$

where

$$n_0 = \left[\exp\left\{\frac{\varepsilon - \mathbf{pu} - \mu}{kT}\right\} + 1\right]^{-1}, \quad |\delta n| \ll n_0. \tag{5}$$

The quantity δn is found from the kinetic or Boltzmann equation

$$\frac{\partial n}{\partial t} + \frac{\partial n}{\partial \mathbf{r}}\frac{\partial \varepsilon}{\partial \mathbf{p}} - \frac{\partial n}{\partial \mathbf{p}}\frac{\partial \varepsilon}{\partial \mathbf{r}} = I(n). \tag{6}$$

As usual, we must substitute the function n_0 on the left side of the Boltzmann equation. In this case, we shall consider that at the point in the liquid being considered, $\mathbf{u} = 0$. Substituting (5) in Eq. (6), we get

$$\begin{aligned} &\frac{\partial n_0}{\partial t} - \frac{1}{3}\frac{\partial n_0}{\partial \varepsilon}\mathbf{p}\frac{\partial \varepsilon}{\partial \mathbf{p}}\operatorname{div}\mathbf{u} \\ &- \frac{1}{2}\frac{\partial n_0}{\partial \varepsilon}\left(p_i\frac{\partial \varepsilon}{\partial p_k} - \frac{1}{3}p_l\frac{\partial \varepsilon}{\partial p_l}\delta_{ik}\right) \\ &\times\left(\frac{\partial u_i}{\partial x_k} + \frac{\partial u_k}{\partial x_i} - \frac{2}{3}\delta_{ik}\frac{\partial u_l}{\partial x_l}\right) \\ &- \frac{\partial n_0}{\partial \varepsilon}\left(\frac{\varepsilon - \mu}{T} - s\right)\frac{\partial \varepsilon}{\partial \mathbf{p}}\nabla T = I(n), \end{aligned} \tag{7}$$

where s is the entropy per particle, and in all terms except $\partial n_0/\partial t$, we take $\varepsilon = \varepsilon(p)$, since they contain only small values for the velocity and temperature gradients.

We now transform $\partial n_0/\partial t$ and shall show that this expression no longer depends on the term with f in Eq. (1). In accord with Eq. (5), we can write

$$\delta n_0 = \frac{\partial n_0}{\partial \varepsilon}\left(\delta\varepsilon - \delta\mu - \frac{\varepsilon - \mu}{T}\delta T\right) \tag{8}$$

(in the variation, we consider the rate of n to be fixed). But, as is well known, the derivative $\partial n/\partial\varepsilon$ is different from zero in a small circle about the point $\varepsilon = \mu$, where it is a rapidly changing function. Therefore, we can consider the quantities in the bracket relative to this point [corrections will have the relative order $(kT/\mu)^2$]. In this variation, $\delta\varepsilon$ and $\delta\mu$ are arbitrary and are not equal to each other. We note incidentally that the second term in the energy ε of (1) is of importance only in $\delta\varepsilon$. On the other hand, following the Landau theory, the distribution function is normalized by the relation

$$\int n_0 d\tau = N, \tag{9}$$

where N is the number of atoms per unit volume. Differentiating this relation, we find

$$\begin{aligned} \delta N &= \int \frac{\partial n_0}{\partial \varepsilon}\left(\delta\varepsilon - \delta\mu - \frac{\varepsilon - \mu}{T}\delta T\right)d\tau \\ &\approx -\left[(\delta\varepsilon - \delta\mu)\frac{d\tau}{d\varepsilon}\right]_{\varepsilon=\mu}, \end{aligned} \tag{10}$$

since $\int (\partial n_0/\partial\varepsilon)\, d\varepsilon = -1$. Comparing Eqs. (8) and (10), we get

$$\frac{\partial n_0}{\partial t} = -\frac{\partial N}{\partial t}\frac{\partial n_0}{\partial \varepsilon}\left(\frac{d\varepsilon}{d\tau}\right)_{\varepsilon=\mu}.$$

Thus we have succeeded in eliminating $\delta\varepsilon$, while in the remaining terms, and therefore in the last equation, we can consider $\varepsilon = \varepsilon(p)$.

The number of atoms N satisfies the continuity equation

$$(\partial N/\partial t) + N\operatorname{div}\mathbf{u} = 0. \tag{11}$$

Thus the term with $\partial n_0/\partial t$ gives the contribution to the term with div u and as a result this term takes the form:

$$-\frac{\partial n_0}{\partial \varepsilon}\left(\frac{1}{3}\mathbf{p}\frac{\partial \varepsilon}{\partial \mathbf{p}} - N\left(\frac{d\varepsilon}{d\tau}\right)_{\varepsilon=\mu}\right)\operatorname{div}\mathbf{u}. \tag{12}$$

The collision integral appears on the right side of Eq. (7):

$$I(n) = -\int w\,[n_1 n_2 (1-n_1')(1-n_2') - (1-n_1)(1-n_2)(n_1' n_2')] \times \delta(\mathbf{p}_1 + \mathbf{p}_2 - \mathbf{p}_1' - \mathbf{p}_2') \times \delta(\varepsilon_1 + \varepsilon_2 - \varepsilon_1' - \varepsilon_2')\, d\tau_2 d\tau_1' d\mathbf{p}_2'. \quad (13)$$

Introducing the function

$$\delta n = -n_0(1-n_0)\,\psi = kT\,(\partial n_0/\partial\varepsilon)\,\psi \quad (14)$$

and neglecting quadratic terms, we can rewrite it in the form

$$I(n) = \int w n_{01} n_{02} (1-n_{01}')(1-n_{02}') \times (\psi_1 + \psi_2 - \psi_1' - \psi_2')\,\delta(\mathbf{p}_1 + \mathbf{p}_2 - \mathbf{p}_1' - \mathbf{p}_2') \times \delta(\varepsilon_1 + \varepsilon_2 - \varepsilon_1' - \varepsilon_2')\, d\tau_2 d\tau_1' d\mathbf{p}_2'. \quad (15)$$

The collision probability w depends, generally speaking, on all four momenta. However, in this temperature region, where Eq. (1) is generally valid, the momenta whose absolute magnitude is close to the bounding value on the Fermi surface are of interest. Therefore, we can consider that w depends only on θ—the angle between $\mathbf{p}_1$ and $\mathbf{p}_2$ and φ—the angle formed by the planes $(\mathbf{p}_1, \mathbf{p}_2)$ and $(\mathbf{p}_1', \mathbf{p}_2')$.

We can put the function ψ in a different form depending on which of the kinetic coefficients is being calculated, *i.e.*, which of the terms on the left side we keep. However, independently of this, we apply only one method of transformation of the integrals. We make use of the fact that the momenta of the particles in the basic region of integration differ slightly in absolute magnitude from the limiting momentum p_0. If we turn the plane of the vectors $(\mathbf{p}_1, \mathbf{p}_2)$ relative to the axis, directed along $\mathbf{p}_1 + \mathbf{p}_2$, through the angle φ, so that this plane coincides with the plane $(\mathbf{p}_1, \mathbf{p}_2)$, then we get the diagram shown in the Figure. It is clear that the vector $\mathbf{f}$ will be small in absolute magnitude, and the

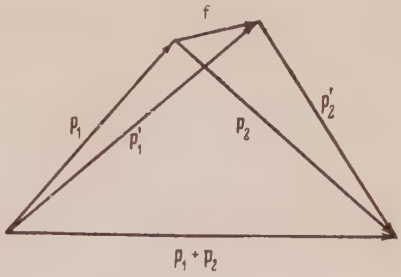

angles between all the momenta and the $\mathbf{p}_1 + \mathbf{p}_2$ axis will be approximately equal to $\theta/2$ or to $-\theta/2$. Then we obtain

$$p_1' \approx p_1 + f_z \cos\frac{\theta}{2} + f_r \sin\frac{\theta}{2},$$
$$p_2' \approx p_2 - f_z \cos\frac{\theta}{2} + f_r \sin\frac{\theta}{2}, \quad (16)$$

where f_z is the component of $\mathbf{f}$ along the $\mathbf{p}_1 + \mathbf{p}_2$ axis, while f_r is the perpendicular component. Integrating over $d\mathbf{p}_2'$, we solve the δ-function of the momenta, while we replace the integral over $d\tau_1'$ by an integral over $df_r\, df_z\, d\varphi$, introducing cylindrical coordinates with axis along $\mathbf{p}_1 + \mathbf{p}_2$:

$$d\tau_1' = 2p_0 \sin(\theta/2)\, df_r df_z d\varphi / (2\pi\hbar)^3. \quad (17)$$

We now introduce the following notation:

$$x = (\varepsilon_1' - \mu)/kT, \quad y = (\varepsilon_2' - \mu)/kT, \quad t = (\varepsilon - \mu)/kT, \quad \varkappa = \mu/kt \quad (18)$$

with ε from (2). Transformation from the variables f_r, f_z, to x and y is easily accomplished with the help of Eq. (16). We then obtain

$$d\tau_1' \int d\tau_2 \delta(\varepsilon) = \frac{m^3 (kT)^2\, dx\, dy\, (d\Omega/2\pi)\, (d\varphi_2/2\pi)}{8\pi^4\hbar^6 \cos(\theta/2)}, \quad (19)$$

where $d\Omega$ denotes the solid angle differential $\sin\theta d\theta d\varphi$ on which $w(\theta, \varphi)$ depends. We note that, in view of the indistinguishability of particles, the angle φ changes only within the limits 0 to π.

2. COEFFICIENT OF VISCOSITY

We begin with the calculation of the viscosity coefficient. In this case, the tensor term on the left side of Eq. (7) is dominant. From symmetry considerations, it is evident that ψ must have the form

$$\psi = \frac{1}{2} q(t) \left(p_i \frac{\partial\varepsilon}{\partial p_k} - \frac{1}{3} p_l \frac{\partial\varepsilon}{\partial p_l} \delta_{ik}\right)\left(\frac{\partial u_l}{\partial x_k} + \frac{\partial u_k}{\partial x_l} - \frac{2}{3}\delta_{ik}\frac{\partial u_m}{\partial x_m}\right). \quad (20)$$

Upon substitution of this expression in the collision integral, the second factor can be transformed by the addition theorem of spherical functions. After integration over the angle $d\varphi_2$, only the first terms are left, *i.e.*,

$$P_2(\theta_1+\theta_2)\to P_2(\theta_1)\,P_2(\theta_2),\ \text{where}\ P_2(\theta)=\tfrac{3}{2}\cos^2\theta-1.$$

As a result, we get the following equation for q from Eq. (7):

$$n_0(t)\,[1-n_0(t)]=\frac{(mkT)^3}{8\pi^4\hbar^6\cos(\theta/2)}\int\frac{d\Omega}{2\pi}\int\limits_{\substack{-\infty\\ x+y>t-\infty}}^{\infty}dx\int\limits_{-\infty}^{\infty}dy\,w(\theta,\varphi) \tag{21}$$

$$\times\, n_0(t)\,n_0(x+y-t)\,[1-n_0(x)]\,[1-n_0(y)]\,[q(t)+q(x+y-t)\,P_2(\theta)-q(x)\,P_2(\theta_1')-q(y)\,P_2(\theta_2')].$$

In view of the fact that, in the temperature region we have considered, only the values of x, y, and t much smaller than $\varkappa$ are important, we can consider the lower limit in Eq. (21) to be $-\infty$. Under these conditions, and assuming that q is a symmetric function (this is verified by the result), we are easily convinced that all terms with different q can be put in the same form in the sense of its dependence on x and y. Thus the bracketed expression can be put in the form:

$$q(t)+q(x)\,[P_2(\theta)-P_2(\theta_1')-P_2(\theta_2')].$$

Expressions for the spherical functions in terms of the angles θ and φ are easily obtained with the aid of the Figure. Integrating over the variable y, on which q no longer depends, we get the following expression after some transformations:

$$\frac{8\pi^4\hbar^6}{(mkT)^3}=\overline{\frac{w(\theta,\varphi)}{\cos(\theta/2)}\left[\frac{3}{4}(1-\cos\theta)^2\sin^2\varphi-1\right]}$$
$$\times\left\{\int_0^\infty\frac{dx\,x\,[q(x+t)+q(x-t)]}{e^x-1}+2\int_0^\infty\frac{dx\,xq(x)}{e^x+1}\right.$$
$$\left.+\int_0^t dx\,xq(x-t)\right\}+\overline{\frac{w(\theta,\varphi)}{\cos(\theta/2)}}\,q(t)\,\frac{\pi^2+t^2}{2}, \tag{22}$$

where the bar denotes averaging over the solid angle.

This expression is very complicated. However, analysis shows that for arbitrary assumptions concerning the form of $w(\theta,\varphi)$, the error in the viscosity coefficient will be less than 10% if we simply take it into account that the values we need are $t^2\ll\pi^2$. In this case, q turns out to be constant, equal to

$$q=\frac{64\pi^2\hbar^6}{3(mkT)^3}\left[\overline{\frac{w(\theta,\varphi)}{\cos(\theta/2)}(1-\cos\theta)^2\sin^2\varphi}\right]^{-1}. \tag{23}$$

In accordance with Landau's theory[1], the momentum flux is equal to

$$\Pi_{ik}=\int p_i\frac{\partial\varepsilon}{\partial p_k}n\,d\tau+\delta_{ik}\left(\int n\varepsilon\,d\tau-E\right). \tag{24}$$

However, it is necessary to recall that the energy is also a functional of the distributing function. Substituting Eqs. (4) and (11) with $\nu=\delta n$, we get

$$\Pi_{ik}=\int p_i\frac{\partial\varepsilon(p)}{\partial p_k}\delta n\,d\tau$$
$$-\int\delta n\,f(\mathbf{p},\ \mathbf{p}')\frac{\partial n'}{\partial\varepsilon'}\,p_i'\frac{\partial\varepsilon(p')}{\partial p_k'}\,d\tau\,d\tau'. \tag{25}$$

Substituting δn in accordance with Eqs. (14), (20) and (23), we find the value of the viscosity coefficient, defining it as the coefficient of proportionality between Π_{ik} and $(\delta u_i/\delta x_k)+(\delta u_k/\delta x_i)-\frac{2}{3}\,\delta u_l/\delta x_l$ with opposite sign:

$$\eta=\frac{64}{45}(kT)^{-2}\frac{\hbar^3p_0^5}{m_4}\left[1+\overline{f(\theta)\,P_2(\theta)}\,\frac{p_0m}{\pi^2\hbar^3}\right]$$
$$\times\left[\overline{\frac{w(\theta,\varphi)}{\cos(\theta/2)}(1-\cos\theta)^2\sin^2\varphi}\right]^{-1}. \tag{26}$$

Thus, it is shown that $\eta\sim T^{-2}$. This dependence was predicted earlier by Pomeranchuk[3] on the basis of qualitative considerations. So far as the numerical value of the viscosity is concerned, this depends on the definite form of averaging $f(\theta)$ and $w(\theta,\varphi)$, and therefore cannot be determined precisely. However, with the help of Eq. (26), we can estimate the order of magnitude. We shall assume that $w(\theta,\varphi)$ does not depend upon the angle φ, and make use of the fact that, from Landau's theory,

$$w(\theta,\ 0)=2\pi f^2(\theta)/\hbar. \tag{27}$$

If we consider the quantity f to be approximately given by $f_0 + f_1 \cos\theta$, we can find the coefficients f_0 and f_1 from experimental data on the compressibility (4) and the relation between m and m_{He^3}. This gives

$$(mp_0/\pi^2\hbar^3) f = 5{,}4 + 1{,}3\cos\theta. \tag{28}$$

We then obtain the following expression for the order of magnitude of the viscosity:

$$\eta \sim 1\cdot 10^{-6} T^{-2} \text{ poise}. \tag{29}$$

Simple analysis shows that the second viscosity is a quantity of much higher order of smallness than η. Actually, taking into account that the collision integral for both cases is approximately identical, we can compare both coefficients, taking the corresponding integrals from the tensor term on the left side of Eq. (7), and from Eq. (12). Recalling that $p_0^3/3\pi^2\hbar^3 = N$, we find that the terms of zeroth order for the second viscosity vanish. Thus $\zeta/\eta \sim (kT/\mu)^2$.

3. COEFFICIENT OF THERMAL CONDUCTIVITY

We now proceed to the thermal conductivity. The function ψ has in this case the form

$$\psi = q\left(\frac{\varepsilon(p)-\mu}{kT}\right)\left(\frac{\partial\varepsilon}{\partial p}\nabla T\right). \tag{30}$$

In place of Eq. 12, we get here the same equation but with $\cos\theta$ in place of $P_2(\theta)$ in the collision integral, and the factor $(\epsilon-\mu)/T - s$ on the left side. The presence of such a factor shows that the desired function ought to contain both symmetric and anti-symmetric parts, namely,

$$q(t) = q_s(t) + q_a(t). \tag{31}$$

Substitution in the collision integral gives two equations

$$\frac{8\pi^4\hbar^6}{(mkT)^3} s = \overline{\frac{w(\theta,\varphi)}{\cos(\theta/2)}}\left[q_s(t)\frac{\pi^2+t^2}{2} - \int_0^\infty dx\,\frac{x[q_s(x+t)+q_s(x-t)]}{e^x-1} - 2\int_0^\infty \frac{dx\,xq_s(x)}{e^x+1} - \int_0^\infty dx\,xq_s(x-t)\right], \tag{32}$$

$$\frac{8\pi^4\hbar^6 k}{(mkT)^3} t = \overline{\frac{w(\theta,\varphi)(1+2\cos\theta)}{\cos(\theta/2)}}\left[\int_0^\infty dx\,\frac{x[q_a(x-t)-q_a(x+t)]}{e^x-1}\right.$$

$$\left. + 2t\int_0^\infty \frac{dx\,q_a(x)}{e^x+1} + \int_0^t dx\cdot xq_a(x-t)\right] + \overline{\frac{w(\theta,\varphi)}{\cos(\theta/2)}} q_a(t)\frac{\pi^2+t^2}{2}. \tag{33}$$

However, in the given case, the Boltzmann equation does not define the complete solution of the problem. To it must be added an additional condition which expresses the conservation of the total momentum of the system, which reduces to the equality $\int \mathbf{p}\delta n\, d\tau = 0$ or, in other words,

$$\int \frac{\partial n}{\partial\varepsilon}\left(\mathbf{p}\frac{\partial\varepsilon}{\partial\mathbf{p}}\right) q(t)\, d\tau = 0. \tag{34}$$

To find the odd part $q_a(t)$, it suffices to solve Eq. (33), in the same way as was done in considering the viscosity. So far as the even part $q_s(t)$ is concerned, the situation is quite different. In the first place we must note that $q_s = \text{const}$ makes the right side of Eq. (32) identically equal to zero. Therefore we must determine the constant term $q_s(0)$ not from this equation, but from Eq. (34). Here it is easy to show that the additional terms in $q_s(t)$, namely, $a_2t^2 + a_4t^4 + \ldots$, generally do not contribute to the thermal conductivity. Actually, the appearance of such a term, for example, $a_m t^{2m}$, should change the constant term in $q_s(t)$ by an amount a_m^0 so that

$$\int \frac{\partial n}{\partial\varepsilon}\mathbf{p}\frac{\partial\varepsilon}{\partial\mathbf{p}}[a_m t^{2m} + a_m^0]\, d\tau = 0$$

From this condition, we get

$$a_m^0 = -a_m(2m)!\, R_m, \qquad R_m = \int_0^\infty \frac{z^{2m-1}}{e^z+1} dz.$$

In the calculation of the energy flow, we must compute integrals of the type

$$\int \frac{\partial n}{\partial\varepsilon} F(\varepsilon)(a_m t^{2m} + a_m^0)\, d\tau$$

$$= \left(F\frac{d\tau}{d\varepsilon}\right)_{\varepsilon=\mu}[a_m(2m)!\, R_m + a_m^0] = 0.$$

We thus come to the conclusion that, to find the thermal conductivity, we need only solve Eq. (33), and select the constant term in q_s in order to satisfy the condition (34). In practice, as in the viscosity case, it suffices to find a solution under the assumption $t^2 \ll \pi^2$. Here we obtain

$$q = \frac{24\pi^2\hbar^6 k}{(mkT)^3}\left(t - \frac{\pi^2 kTm}{p_0^2}\right)\left[\overline{\frac{w(\theta, \varphi)(1-\cos\theta)}{\cos(\theta/2)}}\right]^{-1} \tag{35}$$

The energy flow is equal to (see Ref. 1):

$$\mathbf{Q} = \int \varepsilon \frac{\partial \varepsilon}{\partial \mathbf{p}} n d\tau. \tag{36}$$

Substituting (4), we have

$$\mathbf{Q} = \int \varepsilon(p) \frac{\partial \varepsilon(\mathbf{p})}{\partial \mathbf{p}} \delta n d\tau - \int \delta n f(\mathbf{p}, \mathbf{p}') \frac{\partial n'}{\partial \varepsilon'} \varepsilon(\mathbf{p}') \frac{\partial \varepsilon(\mathbf{p}')}{\partial \mathbf{p}'} d\tau d\tau'. \tag{37}$$

Substituting δn in accord with (14), (30) and (35), we determine the value of the coefficient of thermal conductivity:

$$\varkappa = \frac{8}{3}\frac{\pi^2\hbar^3 p_0^3}{m^4 T}\left(1 + \frac{p_0^3 m}{2\pi^2\hbar^3}\frac{\partial}{\partial p}\left[\overline{\frac{f(p, p_0)\cos\theta}{p}}\right]_{p=p_0}\right)\left[\overline{\frac{w(\theta, \varphi)(1-\cos\theta)}{\cos(\theta/2)}}\right]^{-1}. \tag{38}$$

Thus the temperature dependence of the coefficient of thermal conductivity is expressed by a T^{-1} law, which also coincides with the qualitative prediction of Pomeranchuk[3].

Estimating the numerical value of $\varkappa$ in a fashion similar to what was done in the viscosity case, we obtain the relation*

$$\varkappa \sim (40/T) \text{ erg/cm-sec-deg}. \tag{39}$$

4. LIMITS OF APPLICABILITY

The resulting expressions for the coefficients of viscosity and thermal conductivity in each case cease to be valid in the temperature region $kT \sim \mu$. However, in addition there exists a limitation which moves back the region of applicability of the theory in the direction of much lower temperatures. It consists in the fact that the energy interval of excitation of order kT of interest to us must be much greater than the quantum uncertainty in the energy arising from the collisions, *i.e.*,

$$\tau \gg \hbar/kT, \tag{40}$$

where τ is the time between collisions. We note that fulfillment of condition (40) is required not only for the calculation of the kinetic coefficients, as was the case earlier, but also for the validity of the entire theory of the Fermi liquid[1].

We can determine the collision time for He^3 from the Boltzmann equation if we write it in the form

$$Dn = -\delta n/\tau,$$

where Dn denotes the left side of the equation. Comparing this expression with Eqs. (7), (14), (20), (30), we get

$$\tau \sim qkT. \tag{41}$$

For the different processes which we have considered, the functions q are different, but for an estimate, we can make use of any one q, for example, the one obtained in the determination of the viscosity. In this case, condition (40), with consideration of the numerical values of the coefficients, gives:

$$T < 0{,}05°. \tag{42}$$

It is possible that such a small value is connected with the inaccuracy of our estimate, in the first degree arising from the replacing of $w(\theta, \varphi)$ by $w(\theta, 0)$. However, it is sufficiently clear that even in the best case one can hardly expect that the theory would be suitable at temperatures higher than 0.1–0.2°. This completely corresponds to the fact that the theoretical curve computed in Ref. 2 for the entropy or thermal capacity ceases to correspond to the experimental data above 0.3° K.

Now let us consider briefly what would be obtained in the case of a spectrum of type (3). It is not difficult to see that in this case the tempera-

*In the estimate, we pick out the term with f in Eq. (35). An argument in support of this is the fact that if we take into account

$$\frac{\partial}{\partial p}\left[\frac{f(p, p_0)}{p}\right]_{p_0} \sim \frac{f}{p_0^2},$$

then the term with f adds about 0.2 to the expression in round brackets.

ture dependences of the kinetic coefficients would remain the same as for a spectrum of type (2). With regard to the numerical values of the coefficients, it turns out that in the given case they depend on a large number of unknown quantities, such as df/dp and the higher terms of the expansion of the energy in $p - p_0$. In view of this, calculation of these coefficients is of no interest. The estimates of the order of magnitude that we have made show that in all probability, the coefficients will be of an order larger than in the case of a spectrum of type (2).

As was shown by us in Ref. 2, for a spectrum of type (3), we must consider not only the low temperature range but also the Boltzmann region. This is quite easy, as in this region, the kinetic coefficients ought to depend on the temperature. Actually, in this case, the situation is the same as for the rotons in He II. In accord with the calculations of Landau and Khalatnikov[5], the roton viscosity does not depend on the temperature. Thus in the Boltzmann region, we must expect $\eta = \text{const}$. To find the coefficient of thermal conductivity, we must make use of the relation $\varkappa/\eta \sim c/m^*$, where c is the heat capacity for a single particle, and m^* is the effective mass of the excitation. But the effective mass of the roton, as is well known (see Ref. 6) is equal to $p_0^2/3kT$. Thus in this case we must expect $\varkappa \sim T$. In other words, the curve $\varkappa(T)$ will have a minimum.

If we apply limitation (40) to the case under examination, it then appears that the calculations in the Boltzmann region can be valid if the temperature is higher than some limit. An estimate shows that this limit corresponds to several degrees. Hence the theory which pertains to the Boltzmann region can, in the best case, indicate a definite tendency in the temperature dependence of a quantity, but cannot delineate this dependence exactly. The same applies to the calculation of thermodynamic quantities carried out in Ref. 2.

Therefore, on the basis of data on thermodynamic quantities and the coefficients η and $\varkappa$ we cannot select any definite spectra. The fact is that in the case of a spectrum of type (3), the second viscosity ζ ought to have a value comparable with the first. We can convince ourselves of this, just as before, by taking the corresponding interval from Eq. (12). In zeroth order, the integral does not vanish, in contrast to the case of a spectrum of type (2). Thus, whenever the second viscosity is finally measured in the region of very low temperatures (for example, by sound absorption), we can expect more or less of a verification of the form of the He^3 spectrum.

In conclusion, we note that there are lacking at the present time any sort of measurements which could be compared with the theory developed above. Measurements of viscosity recently carried out by Zinov'eva* apply to the temperature region from 1 to 3° K. In this region, the viscosity is slightly temperature dependent and changes approximately from 2.2×10^{-5} to 1.7×10^{-5} poise. If we compare this with Eq. (29), an impression is created that the spectrum of type (2) leads to too small a value of the viscosity, although naturally Zinov'eva's data refer to a very remote temperature region, and the accuracy of the estimate of the coefficient in Eq. (29) is not large. On the other hand, such a slow change in the coefficient of viscosity and its magnitude is not in bad agreement with the results for spectrum (3). However, because of what was pointed out above, this cannot be considered as proof of the correctness of such a spectrum.

In conclusion, the authors express their gratitude to Acad. L. D. Landau for discussion of the results of the research.

[1] L. D. Landau, J. Exptl. Theoret. Phys. (U.S.S.R.) **30**, 1058 (1956); Soviet Phys. JETP **3**, 920 (1957).

[2] I. M. Khalatnikov and A. A. Abrikosov, J. Exptl. Theoret. Phys. (U.S.S.R.) **32**, 915 (1957); Soviet Phys. JETP **5**, 745 (1957).

[3] I. Ia. Pomeranchuk, J. Exptl. Theoret. Phys. (U.S.S.R.) **20**, 919 (1950).

[4] G. K. Walters and W. M. Fairbanks, Phys. Rev. **103**, 263 (1956).

[5] L. D. Landau and I. M. Khalatnikov, J. Exptl. Theoret. Phys. (U.S.S.R.) **19**, 637, 709 (1949).

[6] E. M. Lifshitz, Uspekhi Fiz. Nauk **34**, 512 (1948).

Translated by R. T. Beyer
226

* The authors are grateful to K. N. Zinov'eva for a report on the viscosity data prior to publication.

Remarks on the Theory of the Electron Plasma in Semiconductors

V. L. BONCH-BRUEVICH
Moscow State University

(Submitted to JETP editor May 12, 1956)
J. Exptl. Theoret. Phys. (U.S.S.R.) 32, 1092-1097 (May, 1957)

The scattering of current carriers by charged impurities is considered on the basis of the many-electron theory of semiconductors. In addition, the ionization energy of impurity centers of the third and fifth groups in germanium type semiconductors is calculated. It is shown that plasma screening produces an essential change in the character of the scattering at low temperatures. The ionization energy of impurity centers is found to be dependent on concentration, and to decrease when the latter increases.

1. INTRODUCTION

AS HAS BEEN SHOWN previously[1, 2], the qualitative statements of the zone theory of homopolar semiconductors can be justified by using the picture of elementary excitations of a many-electron system. The "conduction electrons" and "holes", whose behavior is investigated in experiments, are actually excitations of the Fermi type; unlike the other electrons, they actually behave like independent particles, and it is legitimate to apply to them all the statements concerning the energy spectrum which are usually made in the zone theory. In particular, it is precisely their spectrum which is investigated in experiments on cyclotron resonance, etc. However, we must emphasize that the distinction between these excitations and "real" electrons is not merely a verbal distinction, but makes itself felt in various special features, of which the following two are of importance for us here:

a) the interaction of the fermions with an external field and with one another is screened; its Fourier expansion contains only wave numbers $k > k_0$, where k_0 is a certain limiting value;

b) in addition to the fermions, there is also a Bose branch of the spectrum[3], consisting of oscillations of the plasma type with wave numbers $k < k_0$. (We note that the effective charge of a plasma phonon is zero.)

The second item listed is essential in the theory of recombination of current carriers[2]; the first must be taken into account in the theory of local levels and, in particular, in studying the scattering of current carriers by charged impurities. (It is easy to see that the screening which is automatically obtained in the many-electron theory of semiconductors gives precisely that cutoff of the Rutherford scattering at small angles which, in the one-electron approximation, has to be introduced in more or less artificial *ad hoc* fashion[4]). In the present paper we shall consider the last two problems, and also the question of the estimate of the limiting wave number k_0.

2. EVALUATION OF k_0*

As shown in Ref. 2, the Hamiltonian of the many-electron system in a crystal can be brought to the form

$$H = H_1 + H_2 + H' + H'' + H''' + E_0, \quad (2.1)$$

where H_1 and H_2 are the energy operators of the non-interacting fermions and bosons, H', H'', H''' contain their various interactions with one another (and are treated as small perturbations), and E_0 is a constant.

We shall consider a semiconductor with current carriers of a single type, and for brevity we shall refer to them simply as electrons. This means, in particular, that we neglect the intrinsic conductivity. Thus in our case the plasma is made up of electrons (or holes) supplied by the impurity, and the positively (or negatively) charged impurity ions. The concentration, n, of electrons is then constant and equal to the concentration of impurities. We emphasize that this quantity in general does not coincide with the concentration of free current carriers, since some of the fermions may be localized near impurities.

In this case[2]

* The author is very grateful to L. E. Gurevich, D. N. Zubarev, V. V. Tolmachev and S. V. Tiablikov for discussion of this question.

$$H_1 = \sum_{r,\sigma} E_r A^*_{r,\sigma} A_{r,\sigma}, \qquad (2.2)$$

$$H_2 = \sum_{\mathbf{k},k<k_0} W(k)\, B^*(\mathbf{k})\, B(\mathbf{k}), \qquad (2.3)$$

Here A^*, A and B^*, B are the Fermi and Bose operators of second quantization, σ is the spin quantum number, r denotes the remaining quantum numbers characterizing the electrons (which, for states in the band is simply the quasi-momentum $\hbar\mathbf{f}$),

$$W(k) = \sqrt{W_0^2 + (\hbar^2 k^2/2m)^2}, \qquad (2.4)$$

$$W_0 = \hbar\sqrt{4\pi n e^2/\varepsilon m'}, \qquad (2.5)$$

and m' is the effective mass of the electron.*

The eigenvalues E_r are determined from the "one-particle" Schroedinger equation for the fermion, with the Hamiltonian

$$H_{\text{ind}} = -\frac{\hbar^2}{2m}\nabla^2 + \sum_{\mathbf{k},k>k_0} \frac{b(\mathbf{k})}{V} e^{-i\mathbf{kr}}, \qquad (2.6)$$

where $b(\mathbf{k})$ is the Fourier coefficient of the external field, V is the normalization volume (the usual periodicity conditions are imposed on the vector $\mathbf{k}$). In describing the fermions we shall use the method of effective masses (and regard the mass as isotropic).

For the determination of k_0 we should, strictly speaking, minimize the free energy of the whole system (including the perturbation terms describing the interactions of the various types of excitations). However, we shall limit ourselves to evaluating the limiting admissible values of k_0. In the first place, the screened interaction between fermions must be small; this gives the obvious condition $k_0 \gg n^{1/3}$. Secondly, the coupling between fermions and bosons must be small. This coupling is contained in one of the perturbation terms, and also in the supplementary condition which is imposed when the "superfluous" variables are introduced. (*Cf.* Ref. 3.) This coupling shows itself in particular in the fact that a certain electrical current is associated with the plasma quanta. But it is clear that the effective charge of a plasma quantum must be equal to zero. In an exact treatment of the problem, the current carried by the bosons becomes zero automatically. We take the supplementary condition into account approximately by requiring that this current be negligibly small.* This gives a second inequality: $k_0^4 \ll 16\pi n m e^2/\hbar^2$. Thus the approximate condition for the applicability of our computation is

$$n^{1/3} \ll k_0 < 2(\pi n m e^2/\hbar^2)^{1/4}. \qquad (2.7)$$

This proves to be adequate for the evaluation of the magnitude of the effects we are interested in. Actually we shall use the lower bound, thus obtaining somewhat reduced values for the "plasma" effects.

3. SCATTERING BY CHARGED IMPURITIES INCLUDING THE EFFECT OF PLASMA SCREENING

In accordance with (2.6), the motion of a current carrier in the field of a defect with charge Ze ($b(k) = 4\pi Ze/\epsilon k^2$; the values of Z may be either positive or negative) is described by a "one-particle" Schroedinger equation with the Hamiltonian

$$H_{\text{ind}} = -\frac{\hbar^2}{2m^*}\nabla^2 + \frac{Ze^2}{\varepsilon r}\left(\frac{2}{\pi}\int_{k_0 r}^{\infty} \frac{\sin u}{u}\, du\right). \qquad (3.1)$$

The actual mass of the electron is here replaced by the effective mass of the fermion, taking into account the effect of the periodic field of the lattice. (In general, the effective mass does not coincide with m'.)

Obviously, the presence of the screening factor (the factor in brackets) in the potential energy results in: a) the elimination of the logarithmic divergence in the reciprocal relaxation time which is characteristic for pure coulomb scattering; b) a drastic change in the character of the scattering when the average thermal momentum p of the electron becomes of the order of or less than $\hbar k_0$.

This last situation occurs if

$$T \sim \hbar^2 k_0^2/m^* \varkappa.$$

Thus at helium temperatures we should expect significant deviations from the usual Conwell-Weisskopf formula because of plasma screening. (This remark retains its validity even when we take into account modifications introduced when we include the interference of waves scattered by different defects[5]. We also emphasize that, unlike the Debye screening, the plasma screening is purely mechanical.) To illustrate the type of dependence obtained, we shall treat the scattering

* Strictly speaking, because of exchange effects, the interaction potential between the "excess" electrons is not purely a Coulomb interaction, so that we should write in (2.4) $v(k) = 4\pi e^2/k^2 + f(k)$, $f(0) \neq \infty$. However, this will not change the result.

* L. E. Gurevich pointed out to the author that in general this approximate treatment is inadequate. However, it can apparently be used for the problem treated in the present paper.

from the screened potential in (3.1) by means of the Born approximation.*

Then the probability of scattering per unit time with momentum change $\mathbf{p} - \mathbf{p}'$ is equal to

$$P(\mathbf{p}, \mathbf{p}') = \frac{2\pi^3\hbar^3 e^4 N Z^2}{\varepsilon^2 p^4 \sin^4(\theta/2)} \delta(E_p - E_{p'}) f\left(\frac{2p}{\hbar}\sin\frac{\theta}{2} - k_0\right), \tag{3.2}$$

where θ is the angle between the vectors $\mathbf{p}$ and $\mathbf{p}'$, N is the concentration of scattering centers,

$$f(z) = \begin{cases} 1 & \text{for } Z > 0 \\ 0 & \text{for } Z < 0. \end{cases}$$

Thus the scattering is actually "cut off" at $\theta/2 = \arcsin(\hbar k_0/2p)$. For the reciprocal relaxation time, $1/\tau$, we get (*cf.* Ref. 7).

$$\frac{1}{\tau}\frac{p^2(dp/dE)}{(2\pi)^2\hbar^3}\int_0^\pi \sin\theta(1-\cos\theta)P(\theta)\,d\theta = \frac{2\pi N e^4 Z^2}{\sqrt{2m^*}\,\varepsilon^2} E_p^{-3/2} \ln\left(\frac{2p}{\hbar k_0}\right) f\left(1 - \frac{\hbar k_0}{2p}\right). \tag{3.3}$$

Thus there is no scattering when $p < \hbar k_0/2$. Of course this result should not be taken too literally: it is changed if we take into account both the correction to the Born approximation and the small term H' which was dropped in (2.6) and (3.1). However there is no doubt about the fact (which is obvious beforehand) that there is a marked decrease in scattering for $p \sim \hbar k_0$. Under these circumstances we must take account of other possible scattering mechanisms, the most important of which (at low temperatures) is scattering by uncharged impurities. The corresponding relaxation time was calculated in Ref. 8 (without including screening). Since in the present case the forces are short range, the plasma screening is unimportant, so that we can use the formula of Ref. 8 for our estimate:

$$1/\tau_0 = 20\varepsilon\hbar^3 N_0 / m^{*2} e^2 \tag{3.4}$$

(The subscript 0 refers to quantities characterizing neutral impurity centers.)

Remembering the illustrative nature of our computation, we may assume that only one scattering mechanism acts for each value of p, (on charged impurities for $p < \hbar k_0/2$, and on uncharged impurities for $p > \hbar k_0/2$). Then we get for the microscopic mobility μ, the Hall coefficient R, and the Hall mobility μ_H.

$$\mu = \frac{8e\tau_0}{3m^*\sqrt{\pi}}\chi(u_0) + \frac{4\varepsilon^2\varkappa^{3/2}\psi(u_0)T^{3/2}e^{-u_0^2/2}}{\sqrt{m^*}\,\pi^{3/2}e^2 N \ln(2\sqrt{7m^*\varkappa T}/\hbar k_0)},$$

$$R = R'\frac{64}{945\sqrt{\pi}}\frac{\varphi(u_0)e^{-u_0^2/2} + \tau_0^2\alpha^{-2}(\varkappa T)^{-3}\chi(u_0)}{[\psi(u_0)e^{-u_0^2/2} + {}^1/_3\tau_0\alpha^{-1}(\varkappa T)^{-3/2}\chi(u_0)]^2}, \tag{3.5}$$

$$\mu_H = \mu_H'\frac{64}{945\sqrt{\pi}}\frac{\varphi(u_0)e^{-u_0^2/2} + \tau_0^2\alpha^{-2}(\varkappa T)^{-3}\chi(u_0)}{\psi(u_0)e^{-u_0^2/2} + {}^1/_3\tau_0^2\alpha^{-1}(\varkappa T)^{-3/2}\chi(u_0)},$$

where R' and μ_H' are the values obtained from the Cornell-Weisskopf formula, neglecting the scattering by uncharged impurities ($R' = 1.93/n_e ec$, n_e is the concentration of current carriers),

$$\alpha = \sqrt{2m^*}\,\varepsilon^2/2\pi N e^4 Z^2 \ln\frac{2\sqrt{7m^*\varkappa T}}{\hbar k_0},$$

$$\varphi(u_0) = \frac{945\sqrt{\pi}}{64}\left[1 - \operatorname{erf}\left(\frac{u_0}{\sqrt{2}}\right)\right]e^{u_0^2/2} + \frac{u_0}{32\sqrt{2}}(u_0^8 + 9u_0^6 + 63u_0^4 + 315u_0^2 + 945), \tag{3.6}$$

*Strictly speaking, the Born approximation is not applicable under the conditions of interest to us; it can nevertheless give us a description of the true state of affairs. In addition, it hardly makes sense to carry out exact calculations of the scattering and then to use a kinetic equation whose criterion of applicability[6] is rather poorly satisfied at those temperatures and impurity concentrations of interest to us.

$$\psi(u_0) = 1 + u_0^2/2 + u_0^4/8 + u_0^6/48,$$

$$\chi(u_0) = \frac{3\sqrt{\pi}}{8}\,\mathrm{erf}\left(\frac{u_0}{\sqrt{2}}\right) - \frac{u_0}{4\sqrt{2}}\,e^{-u_0^2/2}\,(u_0^2+3),$$

and $u_0^2 = \hbar^2 k_0^2/8\,m^* \varkappa T$.

From Eq. (3.5) it is clear that for $u_0^2/2 \ll 1$ the plasma screening plays no part ($R \to R'$, $\mu_H \to \mu_H'$); however if the temperature is sufficiently low (of the order of 1° K for $n \sim 10^{15}$ cm^{-3}), the scattering has nothing in common with the Conwell-Weisskopf scattering. Thus, for example, if we determine the concentration of current carriers, n_c, from measurements of the Hall constant in the usual way ($n_c \sim 1/Rec$), then what is actually determined is the effective concentration

$$n_{\mathrm{eff}} = n_c \frac{945\sqrt{\pi}}{64}\,\frac{[\psi(u_0)\,e^{-u_0^2/2} + {}^1/_3\,\tau_0 a^{-1}(\varkappa T)^{-3/2}\chi(u_0)]^2}{\varphi(u_0)\,e^{-u_0^2/2} + \tau_0^2\,a^{-2}(\varkappa T)^{-3}\,\chi(u_0)}. \tag{3.7}$$

When $u_c \gtrsim 1$ this quantity has nothing in common with n_c; under suitable conditions, the factor multiplying n_c can even increase exponentially with temperature (for $N/N_0 \sim 10^{-2}$). Possibly this is one of the causes of the (apparent) decrease in activation energy which is observed for high concentrations of impurities ($n \sim 10^{18}$ cm^{-3}). In this latter case the plasma screening becomes particularly important, and its inclusion is apparently necessary not only at helium, but also at hydrogen temperatures.*

4. LOCAL LEVELS WHEN PLASMA SCREENING IS INCLUDED

The deviation of the potential of the interaction between the fermion and the impurity center from the Coulomb form naturally shows itself not only in scattering but also in the structure of the local levels produced by the center. Within the realm of the so-called "hydrogen-like" model, the energy of the local level (measured from the bottom of the zone) is determined by a wave equation with the Hamiltonian (3.1) with $Z = -1$. For not too large values of k_0 it is natural to represent the potential energy in (3.1) in the form

$$-\frac{e^2}{\varepsilon r} + \frac{e^2}{\varepsilon r}\left\{1 - \frac{2}{\pi}\int_{k_0 r}^{\infty}\frac{\sin u}{u}\,du\right\}$$

and to treat the second term as a perturbation. We then find for the ground state energy E_0 in first approximation:

$$E_0 = -\frac{m^* e^4}{2\varepsilon^2\hbar^2}\left\{1 - 2\left[\frac{1}{\pi}\,\frac{k_0 a_0}{1+(k_0 a_0/2)^2} + 1 - \frac{2}{\pi}\tan^{-1}\frac{2}{k_0 a_0}\right]\right\}, \tag{4.1}$$

where

$$a_0 = \varepsilon\hbar^2/m^* e^2.$$

For small values of $k_0 a_0$ (which are the only values for which the use of perturbation theory is meaningful), (4.1) becomes

$$E_0 = -(m^* e^4/2\varepsilon^2\hbar^2)\{1 - (4\varepsilon\hbar^2 k_0/\pi m^* e^2)\}, \tag{4.2}$$

or, using the lower limit in (2.7) for a rough estimate,

$$E_0 = -\frac{m^* e^4}{2\varepsilon^2\hbar^2} + \Delta E, \quad \Delta E = \frac{2e^2 k_0}{\pi\varepsilon} \gtrsim \frac{2e^2}{\pi\varepsilon}\,n^{1/3}. \tag{4.3}$$

We get the well-known[9] relation $\Delta E = \text{const.}\ n^{1/3}$, with a reasonable value for the constant ($\sim 10^8$ if ΔE is measured in electron volts and n in cm^{-3}). We emphasize that the "plasma" level shift treated here should occur not only at high impurity concentrations, but also at low concentrations if the concentration of carriers forming the plasma is raised by some other means. This should make it possible experimentally to distinguish the "plasma" mechanism for shift of the levels from the effect of formation of impurity bands.

Summarizing, we must recognize that "plasma" effects already become significant for current carrier concentrations $\sim 10^{15} - 10^{16}$ cm^{-3}; for still higher concentrations (and also at low temperatures), their inclusion is absolutely essential.

* However, one should remember that the use of the kinetic equation for these values of impurity concentration is already entirely inadmissible.

[1] V. L. Bonch-Bruevich, Fizich. sb. L'vovskovo un-ta (Physics Reports of the Lvov Univ.), 1 (6), 1955.
[2] V. L. Bonch-Bruevich. Report to the 8th All-Union Congress on the Physics of Semiconductors, 1955, Izv. Akad. Nauk SSSR, ser. fiz., 21, 87 (1957).
[3] D. N. Zubarev, J. Exptl. Theoret. Phys. (U.S.S.R.) 25, 548 (1953).
[4] E. M. Conwell, V. F. Weisskopf, Phys. Rev., 77, 388 (1950).
[5] P. P. Debye, E. M. Conwell, Phys. Rev., 93, 693 (1954).
[6] L. E. Gurevich, *Fundamentals of Physical Kinetics*, Gostekhizdat, 1940.
[7] F. Seitz, Modern Theory of Solids.
[8] Cavid Erginsoy, Phys. Rev., 79, 1013 (1950).
[9] G. L. Pearson, J. Bardeen, Phys. Rev., 75, 865 (1949).

Translated by M. Hamermesh
227

SOVIET PHYSICS JETP VOLUME 5, NUMBER 5 DECEMBER, 1957

On the Dependence of the Motion of Bodies in a Gravitational Field on Their Mass

I. G. FIKHTENGOL'TS
Leningrad Institute of Precision Mechanics and Optics

(Submitted to JETP editor March 12, 1956)
J. Exptl. Theoret. Phys. (U.S.S.R.) 32, 1098-1101 (May, 1957)

The Lagrangian function for the motion of a body of small mass, in the fixed field of n other bodies of finite mass, is derived to the second approximation of gravitational theory. This function is compared with the Lagrangian function for the motion of a body of finite mass in the gravitational field of all $n + 1$ bodies. It is found that in the approximation under consideration, the Lagrangian function for the motion of a finite mass depends in an essential way on the value of that mass.

IN ACCORDANCE WITH the principle of the geodesic line, the motion of a body in a fixed gravitational field* is determined by the requirement that

$$\delta \int \mathcal{L}\, dt = 0, \tag{1}$$

where

$$\mathcal{L} = mc^2\left(1 - \frac{1}{c}\sqrt{g_{00} + 2g_{0i}\dot{x}_i + g_{ik}\dot{x}_i\dot{x}_k}\right) \tag{2}$$

is the Lagrangian function of the mechanical problem. Here m is the mass of the body under consideration, $x_i(t)$ the Cartesian coordinates of the center of mass of m at the instant t and g_{00}, g_{0i}, g_{ik} the components of the fundamental tensor as determined by the Einstein equations of gravitation; the Latin indices i, k take the values 1, 2, 3 and summation over a repeated index is understood. A superior dot indicates a time derivative.

In order to find an approximate expression for the Lagrangian function $\mathfrak{L}$ for the motion of a small mass in the fixed field of n other finite (not small) masses, we shall use an approximate solution of the Einstein equations of gravitation, obtained by Fock[1].

We consider spherically symmetric, nonrotating bodies, whose linear dimensions are much smaller than the distances between them; and we retain only quantities of order v^2/c^2, where v^2 is the square of the velocity of translational motion of one of the bodies. We then obtain the following expressions for the components of the fundamental tensor:

$$g_{00} = c^2 - 2U + (2U^2 - 2S^*)/c^2, \quad g_{0i} = 4U_i/c^2,$$
$$g_{ik} = -(1 + 2U/c^2)\,\delta_{ik}. \tag{3}$$

* The field of a system of bodies is regarded as fixed, with respect to a given body, if the motion of each of the bodies of the system that produces the field is supposed independent of the motion of the given body.

Here

$$U = \sum_a \frac{\gamma m_a}{|\mathbf{r}-\mathbf{a}|}\left\{1 + \frac{1}{2c^2}(\mathbf{v}_a^2 - U^{(a)}(\mathbf{a}))\right\} + \frac{1}{2c^2}\frac{\partial^2}{\partial t^2}\sum_a \gamma m_a |\mathbf{r}-\mathbf{a}|,$$

$$U^{(a)}(\mathbf{r}) = \sum_b{}' \frac{\gamma m_b}{|\mathbf{r}-\mathbf{b}|}, \qquad U_i = \sum_a \frac{\gamma m_a \dot{a}_i}{|\mathbf{r}-\mathbf{a}|}, \quad (b \neq a)$$

$$S^* = \sum_a \frac{\gamma m_a \mathbf{v}_a^2}{|\mathbf{r}-\mathbf{a}|} - \frac{1}{2}\sum_{\substack{a,b \\ (a\neq b)}} \frac{\gamma^2 m_a m_b}{|\mathbf{r}-\mathbf{a}|\cdot|\mathbf{a}-\mathbf{b}|}. \quad (4)$$

In these formulas, the radius vectors of the centers of mass of m, m_a, m_b, ... at the instant t are denoted respectively by $\mathbf{r}(x_1, x_2, x_3)$, $\mathbf{a}(a_1, a_2, a_3)$, $\mathbf{b}(b_1, b_2, b_3)$, ... ; $\mathbf{v}_a^2$ is the square of the velocity of mass m_a; a prime on a summation is a reminder that the summation index takes all values except one from 1 to n.

Upon substituting the expressions (3) for the components of the fundamental tensor in the Lagrangian function $\mathfrak{L}$, we find that, in our approximation

$$\mathscr{L} = \frac{m\dot{\mathbf{r}}^2}{2} + \frac{m\dot{\mathbf{r}}^4}{8c^2} + mU - \frac{mU^2}{2c^2} + \frac{mS^*}{c^2} - \frac{4mU_i\dot{x}_i}{c^2} + \frac{3mU\dot{\mathbf{r}}^2}{2c^2},$$

or by use of (4),

$$\mathscr{L} = \frac{m\dot{\mathbf{r}}^2}{2} + \frac{m\dot{\mathbf{r}}^4}{8c^2} + m\sum_a \frac{\gamma m_a}{|\mathbf{r}-\mathbf{a}|}\left\{1 - \frac{1}{c^2}(\dot{\mathbf{r}}\cdot\dot{\mathbf{a}}) + \frac{3}{2c^2}(\dot{\mathbf{r}}-\dot{\mathbf{a}})^2 - \frac{1}{2c^2}\sum_b \frac{\gamma m_b}{|\mathbf{r}-\mathbf{b}|} - \frac{1}{c^2}\sum_b{}' \frac{\gamma m_b}{|\mathbf{a}-\mathbf{b}|}\right\} + \frac{m}{2c^2}\frac{\partial^2}{\partial t^2}\sum_a \gamma m_a |\mathbf{r}-\mathbf{a}|. \quad (5)$$

The dependence of the Lagrangian function (5) on the accelerations of the finite masses m_a is not an essential feature of the problem; it can easily be removed, thanks to the fact that the variables a_i (and likewise $\dot{a}_i$ and $\ddot{a}_i$) are independent of the variables x_i.

Remembering that

$$\frac{\partial}{\partial t}\sum_a \gamma m_a |\mathbf{r}-\mathbf{a}| = -\sum_a \frac{\gamma m_a}{|\mathbf{r}-\mathbf{a}|}(\dot{\mathbf{a}}\cdot(\mathbf{r}-\mathbf{a})),$$

we get

$$\frac{\partial^2}{\partial t^2}\sum_a \gamma m_a |\mathbf{r}-\mathbf{a}| = \frac{d}{dt}\frac{\partial}{\partial t}\sum_a \gamma m_a |\mathbf{r}-\mathbf{a}| + \sum_a \frac{\gamma m_a}{|\mathbf{r}-\mathbf{a}|}(\dot{\mathbf{r}}\cdot\dot{\mathbf{a}}) - \sum_a \frac{\gamma m_a}{|\mathbf{r}-\mathbf{a}|}(\dot{\mathbf{r}}\cdot(\mathbf{r}-\mathbf{a}))(\dot{\mathbf{a}}\cdot(\mathbf{r}-\mathbf{a})).$$

Consequently

$$\mathscr{L} = \frac{m\dot{\mathbf{r}}^2}{2} + \frac{m\dot{\mathbf{r}}^4}{8c^2} + m\sum_a \frac{\gamma m_a}{|\mathbf{r}-\mathbf{a}|}\left\{1 - \frac{1}{2c^2}(\dot{\mathbf{r}}\cdot\dot{\mathbf{a}}) - \frac{1}{2c^2}\frac{(\dot{\mathbf{r}}(\mathbf{r}-\mathbf{a}))(\dot{\mathbf{a}}(\mathbf{r}-\mathbf{a}))}{|\mathbf{r}-\mathbf{a}|^2} + \frac{3}{2c^2}(\dot{\mathbf{r}}-\dot{\mathbf{a}})^2 - \frac{1}{2c^2}\sum_b \frac{\gamma m_b}{|\mathbf{r}-\mathbf{b}|} - \frac{1}{c^2}\sum_b{}' \frac{\gamma m_b}{|\mathbf{a}-\mathbf{b}|}\right\} + \frac{d}{dt}f(t, x_1, x_2, x_3); \quad (6)$$

$$f(t, x_1, x_2, x_3) = -\frac{m}{2c^2}\sum_a \frac{\gamma m_a}{|\mathbf{r}-\mathbf{a}|}(\dot{\mathbf{a}}\cdot(\mathbf{r}-\mathbf{a})).$$

An expression of the form df/dt, where $f(t, x_1, x_2, x_3)$ is an arbitrary differentiable function of its arguments, reduces Lagrange's equations to identities; therefore we may drop the last term in the Lagrangian function (6).

Before writing the final expression for the Lagrangian function of the mechanical problem under consideration, we shall change to a slightly different notation. Denoting the radius vectors of the centers of mass of m and m_k ($k = 1, 2, \ldots n$) by $\mathbf{r}(x, y, z)$ and $\mathbf{r}_k(x_k, y_k, z_k)$ respectively, and the Lagrangian function without the term df/dt by L^*, we have

$$L^* = \frac{m\dot{\mathbf{r}}^2}{2} + \frac{m\dot{\mathbf{r}}^4}{8c^2} + m\sum_k \frac{\gamma m_k}{|\mathbf{r}-\mathbf{r}_k|}\left\{1 - \frac{1}{2c^2}(\dot{\mathbf{r}}\cdot\dot{\mathbf{r}}_k) - \frac{1}{2c^2}\frac{(\dot{\mathbf{r}}\cdot(\mathbf{r}-\mathbf{r}_k))(\dot{\mathbf{r}}_k\cdot(\mathbf{r}-\mathbf{r}_k))}{|\mathbf{r}-\mathbf{r}_k|^2} + \frac{3}{2c^2}(\dot{\mathbf{r}}-\dot{\mathbf{r}}_k)^2 - \frac{1}{2c^2}\sum_l \frac{\gamma m_l}{|\mathbf{r}-\mathbf{r}_l|} - \frac{1}{c^2}\sum_l{}' \frac{\gamma m_l}{|\mathbf{r}_k-\mathbf{r}_l|}\right\}. \quad (7)$$

The equations of motion corresponding to the Lagrangian function $\mathfrak{L}$ (or equivalently L^*) actually do not contain the value of the mass m; they indicate nondependence of the motion of a body (of small mass), in a fixed gravitational field, upon the value of its mass.

In the case of motion of a body of finite mass, it is not permissible to treat the field as fixed with respect to this body. A finite mass, even in the first (Newtonian) approximation, affects the motion of the other masses, changing it; and this change in turn has an influence on the motion of the mass under consideration. However, the dependence of the motion of a body upon its mass, in the first approximation, still does not affect the form of the Lagrangian function.

The situation changes in an essential way when we go on to a consideration of the motion of finite masses in a higher approximation than the first (the Newtonian). In this case, in the derivation of the equations of motion it is necessary to start directly from the Einstein equations of gravitation. The equations of motion that emerge from them, for a system of finite masses, can also be expressed in Lagrangian form; but the Lagrangian function of this more general problem* has the form[2]

$$L = \sum_i L_{0i} - V, \quad L_{0i} = {}^1/_2\, m_i \dot{\mathbf{r}}_i^2 + m_i \dot{\mathbf{r}}_i^4 / 8c^2,$$

$$V = -\frac{1}{2} \sum_{\substack{i,\,k \\ (i \neq k)}} \frac{\gamma m_i m_k}{|\mathbf{r}_i - \mathbf{r}_k|} \Big\{ 1 - \frac{1}{2c^2} (\dot{\mathbf{r}}_i \cdot \dot{\mathbf{r}}_k) - \frac{1}{2c^2} \frac{(\dot{\mathbf{r}}_i \cdot (\mathbf{r}_i - \mathbf{r}_k))\,(\dot{\mathbf{r}}_k \cdot (\mathbf{r}_i - \mathbf{r}_k))}{|\mathbf{r}_i - \mathbf{r}_k|^2} + \frac{3}{2c^2} (\dot{\mathbf{r}}_i - \dot{\mathbf{r}}_k)^2 - \frac{1}{c^2} \sum_l{}' \frac{\gamma m_l}{|\mathbf{r}_i - \mathbf{r}_l|} \Big\}. \tag{8}$$

It follows that when we examine the motion of the ith mass in the gravitational field of all the bodies (in the present case the number of bodies is supposed equal to $n + 1$), the Lagrangian function of the appropriate mechanical problem can be reduced to the following form:

$$L_i = \frac{m_i \dot{\mathbf{r}}_i^2}{2} + \frac{m_i \dot{\mathbf{r}}_i^4}{8c^2} + m_i \sum_k{}' \frac{\gamma m_k}{|\mathbf{r}_i - \mathbf{r}_k|} \Big\{ 1 - \frac{1}{2c^2} (\dot{\mathbf{r}}_i \cdot \dot{\mathbf{r}}_k) - \frac{1}{2c^2} \frac{(\dot{\mathbf{r}}_i \cdot (\mathbf{r}_i - \mathbf{r}_k))\,(\dot{\mathbf{r}}_k \cdot (\mathbf{r}_i - \mathbf{r}_k))}{|\mathbf{r}_i - \mathbf{r}_k|^2} + \frac{3}{2c^2} (\dot{\mathbf{r}}_i - \dot{\mathbf{r}}_k)^2 - \frac{1}{2c^2} \sum_l{}' \frac{\gamma m_l}{|\mathbf{r}_i - \mathbf{r}_l|} - \frac{1}{c^2} \sum_{\substack{l \\ (l \neq k,\ l \neq i)}}{}'' \frac{\gamma m_l}{|\mathbf{r}_k - \mathbf{r}_l|} - \frac{1}{2c^2} \frac{\gamma m_i}{|\mathbf{r}_i - \mathbf{r}_k|} \Big\}. \tag{9}$$

In order to compare the functions L_i of (9) and L^* of (7), we set

$$L^*|_{m=m_i,\,\mathbf{r}=\mathbf{r}_i} = L_i^*, \tag{10}$$

then

$$L_i - L_i^* = -\frac{m_i^2}{2c^2} \sum_k{}' \frac{\gamma^2 m_k}{|\mathbf{r}_i - \mathbf{r}_k|^2}. \tag{11}$$

Consequently, the Lagrangian function L_i differs from L_i^* by an expression proportional to the square of the mass m_i (whereas L_i^* is proportional to the first power of m_i). Only when the mass m_i is small does the function L_i in fact agree with L_i^*.

Thus in a treatment of the motion of a body of finite mass, with quantities of order v^2/c^2 taken into account, the dependence of this motion on the value of the mass expresses itself in an essential way, in the actual form of the Lagrangian function.

Note added in proof (April 12, 1957). In a recently published article[3], Shirokov and Brodovskii attempt to prove that "the center of inertia of any body (not necessarily of small mass–I. F.) of the system moves along a geodesic line in the gravitational field of the other bodies," and that the equations of motion derived by the principle of the geodesic line agree with the equations of motion of a system of bodies obtained by Petrova[4] by Fock's method.

From relation (11) of the present article, it follows that both these assertions made are incorrect (for more details on this, *cf.* Ref. 5, p. 34).

*We consider only translational motion of the bodies, and we take no account of the dependence of this motion on their shape and on other parameters.

[1] V. A. Fock, J. Exptl. Theoret. Phys. (U.S.S.R.) 9,

375 (1939). *Cf.* also: V. A. Fock, *Theory of Space, Time, and Gravitation*, GTTI, 1955.

[2] I. G. Fikhtengol'ts, J. Exptl. Theoret. Phys. (U.S.S.R.) **20**, 233 (1950).

[3] M. F. Shirokov and V. B. Brodovskii, J. Exptl. Theoret. Phys. (U.S.S.R.) **31**, 1027 (1956). Soviet Phys. **4**, 904 (1957).

[4] I. M. Petrova, J. Exptl. Theoret. Phys. (U.S.S.R.) **19**, 989 (1949).

[5] I. G. Fikhtengol'ts, *Dissertation*, Leningrad State Univ., 1952.

Translated by W. F. Brown, Jr.
228

SOVIET PHYSICS JETP VOLUME 5, NUMBER 5 DECEMBER, 1957

On Magnetohydrodynamic Waves and Magnetic Tangential Discontinuities in Relativistic Hydrodynamics

I. M. KHALATNIKOV

Institute for Physical Problems, Academy of Sciences, U.S.S.R.

(Submitted to JETP editor June 8, 1957)

J. Exptl. Theoret. Phys. (U.S.S.R.) **32**, 1102-1107 (May 1957)

The problem of magnetohydrodynamic waves in relativistic hydrodynamics is discussed. Equations are derived for the velocity of these waves in the presence of a magnetic field making an arbitrary angle with the direction of propagation of the waves in a medium with an arbitrary equation of state. The properties of purely magnetic tangential discontinuities in relativistic hydrodynamics are also discussed.

AN INVESTIGATION by Hoffman and Teller[1] was devoted to problems of relativistic magnetohydrodynamics. In the present note we consider in more detail the problem of magnetohydrodynamic waves in relativistic hydrodynamics. In contrast to Ref. 1 where the absence of a magnetic field along the direction of wave propagation was supposed, we shall assume the presence of a magnetic field whose direction makes an arbitrary angle with the direction of wave propagation. Furthermore, we shall not assume, as was done in Ref. 1, that the ultrarelativistic equation of state $\varepsilon = 3p$ applies. We shall conduct the entire investigation for an arbitrary equation of state. Also, we shall consider the question of purely magnetic tangential discontinuities in relativistic hydrodynamics where the thermodynamic quantities remain continuous.

MAGNETOHYDRODYNAMIC WAVES IN RELATIVISTIC HYDRODYNAMICS

The energy momentum tensor in relativistic hydrodynamics has the following form

$$T_k^{i\,\mathrm{h}} = wnu_iu_k + p\delta_{ik}. \tag{1}$$

Here w is the heat function referred to one particle, n the density of the number of particles, p the pressure, u_i the 4-velocity component ($u_i^2 = -1$). The speed of light is $c = 1$.

We next denote the energy momentum tensor of the electromagnetic field by

$$T_{\alpha\beta}^{\mathrm{em}} = \frac{1}{4\pi}\left\{-H_\alpha H_\beta - E_\alpha E_\beta + \frac{1}{2}\delta_{\alpha\beta}(\mathbf{H}^2 + \mathbf{E}^2)\right\},$$
$$T_{\alpha 4}^{\mathrm{em}} = \frac{i}{4\pi}[\mathbf{EH}]_\alpha; \quad T_{44}^{\mathrm{em}} = -\frac{1}{8\pi}(\mathbf{E}^2 + \mathbf{H}^2). \tag{2}$$

We consider a medium with an infinite conductivity σ. For such a medium there follows from Ohm's law

$$\mathbf{j} = \sigma(\mathbf{E} + [\mathbf{vH}]) \tag{3}$$

a relationship between the electric and magnetic fields

$$\mathbf{E} = -[\mathbf{vH}]. \tag{4}$$

For one-dimensional motion, all quantities are functions of one spatial coordinate (x_1) and of the time ($x_4 = it$).

The conditions at the discontinuity for such a motion may be written in the form of continuity of the corresponding components of the total energy-

momentum tensor, which constitutes the sum of the tensors T_{ik}^{h} and T_{ik}^{em} [Eqs. (1) and (2)]:

$$T_{ik} = T_{ik}^{h} + T_{ik}^{em}. \tag{5}$$

All components of the total tensor having the subscript 1 must remain continuous. This follows directly from the condition

$$\partial T_{ik} / \partial x_k = 0. \tag{6}$$

We thus have the following conditions at the discontinuity (we shall designate the difference between the values of a given quantity on the discontinuity by braces)

$$\left\{ wnu_1^2 + p + \frac{1}{8\pi}(H_\tau^2 - H_1^2 + E_\tau^2 - E_1^2) \right\} = 0, \tag{7}$$

$$\left\{ wnu_1 \mathbf{u}_\tau - \frac{1}{4\pi}(H_1 \mathbf{H}_\tau + E_1 \mathbf{E}_\tau) \right\} = 0, \tag{8}$$

$$\left\{ wnu_1 u_4 + \frac{i}{4\pi}(H_3 E_2 - H_2 E_3) \right\} = 0. \tag{9}$$

Here we denote a vector in the $2-3$ plane by the subscript τ ($\mathbf{u}_\tau$ has the components u_2 and u_3, etc.)

Let us also take account of the first pair of Maxwell's equations [the second pair is contained in Eq. (6)].

$$\operatorname{curl} \mathbf{E} = -\partial \mathbf{H} / \partial t, \quad \operatorname{div} \mathbf{H} = 0. \tag{10}$$

These equations lead to the two conditions

$$\{\mathbf{E}_\tau\} = 0, \tag{11}$$

$$\{H_1\} = 0. \tag{12}$$

Finally, we also must write the condition for the particle density

$$\{nu_1\} = 0, \tag{13}$$

resulting from the equation of continuity

$$\partial nu_1 / \partial x_1 = 0. \tag{14}$$

The conditions (7) – (9) can be somewhat simplified, using (11), (12), and (4), to read

$$\left\{ wnu_1^2 + p + \frac{1}{8\pi}(\mathbf{H}_\tau^2 - E_1^2) \right\} = 0, \tag{15}$$

$$\{wnu_1 \mathbf{u}_\tau\} = \frac{1}{4\pi} H_1 \{\mathbf{H}_\tau\} + \frac{1}{4\pi} \mathbf{E}_\tau \{E_1\}, \tag{16}$$

$$\left\{ wnu_1 u_4 + \frac{i}{4\pi} v_1 \mathbf{H}_\tau^2 \right\} = \frac{iH_1}{4\pi} \{\mathbf{v}_\tau \mathbf{H}_\tau\}. \tag{17}$$

Taking (4) into account, we may write the condition (11) in the form

$$\{\mathbf{v}_\tau\} H_1 = \{v_1 \mathbf{H}_\tau\}. \tag{18}$$

The relationships (12), (13), and (15) – (18) constitute the complete system of conditions on the discontinuity.

Making use of these conditions, we shall consider the problem of magnetohydrodynamic waves in relativistic hydrodynamics. Magnetohydrodynamic waves can be regarded as the limiting case of discontinuities of very small intensity. The components v_2 and v_3 in the hydrodynamic wave may be regarded as small. As to v_1, however, that quantity cannot be regarded as small since under relativistic conditions the wave can move along the axis l at a speed approaching the speed of light.

In a magnetohydrodynamic wave all quantities are functions of one parameter. Moreover, in view of the infinitesimal smallness of the jumps, the ratio of the jumps may be replaced by derivatives. We choose the velocity v_1 as the independent variable. Derivatives with respect to this variable will be denoted by primes. Thus we have, for instance

$$p' = \{p\} / \{v_1\} = W' \partial p / \partial W. \tag{19}$$

Below, we shall denote the derivative $\partial p / \partial W$ by a^2. With the aid of the known relationship between the thermodynamic quantities

$$W = \varepsilon + p; \quad W = wn \tag{20}$$

we find the connection between the quantity a^2 and the speed of sound

$$c^2 = \partial p / \partial \varepsilon. \tag{21}$$

By simple differentiation we obtain

$$c^2 = a^2 / (1 - a^2). \tag{22}$$

We introduce also the symbol

$$\overline{W} = W / (1 - v_1^2). \tag{23}$$

Considering all this, we can, after eliminating v_τ', reduce, without difficulty, the system of conditions (15) – (18) to the following form

$$\overline{W}(1-a^2)\,2v_1 + [v_1^2 + a^2(1-v_1^2)]\,\overline{W}' + \mathbf{H}_\tau \mathbf{H}_\tau'/4\pi = 0, \tag{24}$$

$$\overline{W} + v_1\overline{W}' + v_1\mathbf{H}_\tau\mathbf{H}_\tau'/4\pi = 0, \tag{25}$$

$$\overline{W}H_2v_1 = (H_1^2/4\pi - v_1^2H_3^2/4\pi - \overline{W}v_1^2)\,H_2' + v_1^2H_2H_3H_3'/4\pi, \tag{26}$$

$$\overline{W}H_3v_1 = (H_1^2/4\pi - v_1^2H_2^2/4\pi - \overline{W}v_1^2)\,H_3' + v_1^2H_2H_3H_2'/4\pi. \tag{27}$$

Let us multiply Eq. (26) by H_2 and Eq. (27) by H_3 and add the products. We obtain, as a result, the quantity $\mathbf{H}_\tau\mathbf{H}_\tau'$ entering into Eqs. (24) and (25).

$$\mathbf{H}_\tau\mathbf{H}_\tau' = \overline{W}v_1\mathbf{H}_\tau^2/(H_1^2 - 4\pi\overline{W}v_1^2). \tag{28}$$

We next substitute the expression obtained into (24) and (25) and eliminate the derivative $\overline{W}'$ from these equations. In this way we obtain

$$\left[v_1^2 - \frac{a^2}{1-a^2}\right] + \frac{\mathbf{H}_\tau^2 v_1^2}{H_1^2 - 4\pi\overline{W}v_1^2}(1-v_1^2) = 0, \tag{29}$$

which determines the velocity of the magnetohydrodynamic waves.

Taking (22) and (23) into account, we rewrite (29) as

$$(v_1^2 - c^2)\left(\frac{v_1^2}{1-v_1^2} - \frac{H_1^2}{4\pi W}\right) = (1-v_1^2)\frac{\mathbf{H}_\tau^2 v_1^2}{4\pi W}. \tag{30}$$

Here W is the heat function per unit volume in a reference system in which the given volume element is at rest, and $\mathbf{H}_1$, $\mathbf{H}_\tau$ are components of a field in a reference system that moves together with the wave front. The index zero denotes the field components in the reference system that is at rest together with the fluid. We then have

$$H_1 = H_{10}; \quad \mathbf{H}_\tau = \mathbf{H}_{\tau_0}/\sqrt{1-v_1^2}. \tag{31}$$

Having expressed in (30) the field $\mathbf{H}$ by $\mathbf{H}_0$, we obtain

$$(v_1^2 - c^2)\left(\frac{v_1^2}{1-v_1^2} - \frac{H_{10}^2}{4\pi W}\right) = v_1^2\mathbf{H}_{\tau_0}^2/4\pi W. \tag{32}$$

Hoffman and Teller[1] considered the special case where an ultrarelativistic equation of state applies and $H_{10} = 0$. In this case

$$\varepsilon = 3p, \quad c^2 = \partial p/\partial\varepsilon = 1/3, \quad W = 4\varepsilon/3, \tag{33}$$

and Eq. (32) leads to the result of Hoffman and Teller

$$(v_1^2 - 1/3)/(1-v_1^2) = 3\mathbf{H}_{\tau_0}^2/16\pi\varepsilon. \tag{34}$$

In the general case, however, the velocity of propagation v_1 of the front of a magnetohydrodynamic wave is determined by the biquadratic equation (32), the roots of which are equal to

$$v_1^2 = \frac{c^2(1+r_{10}^2) + r_0^2 \pm \sqrt{[c^2(1+r_{10}^2) - r_0^2]^2 + 4c^2r_{\tau_0}^2}}{2(1+r_0^2)}, \tag{35}$$

$$r_0^2 = H_0^2/4\pi W, \quad r_{10}^2 = H_{10}^2/4\pi W, \quad r_{\tau_0}^2 = H_{\tau_0}^2/4\pi W.$$

In the general case, two waves can thus propagate at different speeds; the sum of their velocities is equal to

$$(v_1^{(1)})^2 + (v_1^{(2)})^2 = [c^2(1+r_{10}^2) + r_0^2]/(1+r_0^2). \tag{36}$$

In the case where the external field is longitudinal, $\mathbf{H}_\tau = 0$, and Eq. (32) breaks up into two. The first root $v_1^2 = c^2$ corresponds to hydrodynamic waves not connected with a magnetic field, *i.e.*, to ordinary sound. The second root

$$v_1^2 = \frac{H_{10}^2}{4\pi W}\Big/\left(1 + \frac{H_{10}^2}{4\pi W}\right) \tag{37}$$

determines the velocity of the magnetohydrodynamic wave.

For an arbitrary direction of the field $\mathbf{H}$ there follows from Eqs. (19) and (27) that the existence of special purely magnetic waves is possible. The velocities of these waves are found in the following manner. We multiply Eq. (26) by $\mathbf{H}_3$, Eq. (27) by $\mathbf{H}_2$

and subtract the results; in this way we obtain

$$(H_1^2 - v_1^2 H_\tau^2 - 4\pi\overline{W} v_1^2)(H_2' H_3 - H_3' H_2) = 0. \quad (38)$$

Hence follows an equation for the wave velocity v_1:

$$H_1^2 - v_1^2 H_\tau^2 - 4\pi\overline{W} v_1^2 = 0. \quad (39)$$

Solving this equation with respect to v_1^2 and using (25) and (31), we find

$$v_1^2 = H_{10}^2 / (H_0^2 + 4\pi W). \quad (40)$$

So far we used the equation of continuity for the density of the particles. In the ultrarelativistic case, at high temperatures, processes of particle formation are possible. In this case the law of particle conservation no longer holds. However, in all cases the entropy is continuous simply as the result of Eq. (6). As has been shown in our report on relativistic hydrodynamics[2], results for the ultrarelativistic case are obtained from the above equations by substituting the temperature T for the heat function W.

ON TANGENTIAL DISCONTINUITIES

The properties of purely magnetic tangential discontinuities may be easily obtained from the conditions (13) and (15) – (18). We shall now consider such tangential discontinuities in which the thermodynamic quantities are continuous. We then have from (13)

$$\{u_1\} = \{v_1 / \sqrt{1 - v^2}\} = 0, \quad (41)$$

and since $\{v_1\} = 0$,

$$\{v_\tau^2\} = 0. \quad (42)$$

Next, we introduce the symbol

$$nu_1 = j, \quad (43)$$

take $\{v_\tau\}$ from (18), and substitute it into the condition (16); thus we obtain

$$4\pi j^2 (w/n)\{\mathbf{H}_\tau\} = H_1^2\{\mathbf{H}_\tau\} + H_1 \mathbf{E}_\tau \{E_1\}. \quad (44)$$

We express the jump $\{E_1\} = \{-v_2 H_3 + v_3 H_2\}$, with the aid of (18), in terms of the jump $\{H_\tau\}$:

$$\{E_1\} = -\mathbf{E}_\tau \{\mathbf{H}_\tau\} / H_1. \quad (45)$$

Substituting this expression into (44), we obtain an equation

$$4\pi j^2 (w/n)\{\mathbf{H}_\tau\} = H_1^2\{\mathbf{H}_\tau\} - \mathbf{E}_\tau(\mathbf{E}_\tau\{\mathbf{H}_\tau\}). \quad (46)$$

which is homogeneous with respect to $\{\mathbf{H}_\tau\}$. The condition of compatability of the two components of Eq. (46) leads to the following equation for the velocity j of the tangential discontinuities under consideration:

$$\left\{4\pi j^2 \frac{w}{n} - (H_1^2 - E_2^2)\right\}\left\{4\pi j^2 \frac{w}{n} - (H_1^2 - E_3^2)\right\} = E_2^2 E_3^2. \quad (47)$$

This equation has two solutions

$$j^2 = \frac{n}{4\pi w}\begin{cases} H_1^2 \\ H_1^2 - E_\tau^2 \end{cases}. \quad (48)$$

The quantity j^2 is connected with the velocity of the discontinuity v_p^2 by the obvious relationship

$$j^2 / n^2 = v_p^2 / (1 - v_p^2). \quad (49)$$

Let us dwell briefly on the relationships between the jumps of the fields in the tangential discontinuities. According to (15), we have

$$\{H_\tau^2\} = \{E_1^2\} \quad (50)$$

It may easily be shown that each of these jumps is equal to zero.

In fact, according to (17) and (18)

$$v_1\{H_\tau^2\} = H_1(H_\tau v_\tau\}, \quad (51)$$

$$\{v_\tau H_1 - v_1 H_\tau\} = 0. \quad (52)$$

The square of the quantity in braces in (52) is also continuous, as is the quantity itself

$$\{v_\tau^2\} H_1^2 + v_1^2\{H_\tau^2\} - 2v_1 H_1\{v_\tau H_\tau\} = 0. \quad (53)$$

Eliminating the quantity $\{v_\tau H_\tau\}$ from (51) and (53) and taking (42) and (50) into consideration, we obtain

$$\{H_\tau^2\} = \{E_1^2\} = (H_1 / v_1)^2\{v_\tau^2\} = 0. \quad (54)$$

It follows from (47) and (54) that in tangential discontinuities of the type considered the absolute values of the velocity and magnitude of the magnetic field do not change on the discontinuity. All that occurs on the discontinuity is the rotation of those vectors, without a change in their length. We choose axis 2 in such a manner that the component H_2 is not changed by rotation of the vector $\mathbf{H}_\tau$. Then $\{H_2\} = 0$ and $\{v_2\} = 0$, $\{v_3\} = \frac{v_1}{H_1}\{H_3\}$. It can be seen from the figure that thereby the components v_3 and H_3 on the discontinuity change their sign. From the expression for $E_1 = -v_2H_3 + v_3H_2$ it follows that as a result E_1 also changes its sign on the discontinuity.

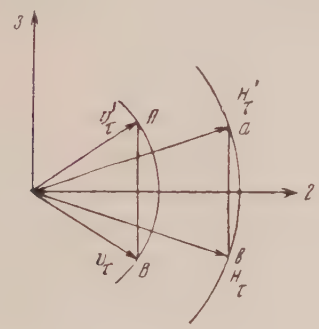

$$v_3 \to -v_3, \quad H_3 \to -H_3, \quad E_1 \to -E_1.$$

[1] F. Hoffman and E. Teller, Phys. Rev. 80, 692 (1950).
[2] I. M. Khalatnikov, J. Exptl. Theoret. Phys. (U.S.S.R.) 27, 529 (1954).

Translated by Mary L. Mahler
229

SOVIET PHYSICS JETP VOLUME 5, NUMBER 5 DECEMBER, 1957

Theory of Diffusion and Thermal Conductivity for Dilute Solutions of He^3 in Helium II

I. M. KHALATNIKOV AND V. N. ZHARKOV
Institute of Physical Problems, Academy of Sciences, U.S.S.R.
(Submitted to JETP editor June 8, 1956)
J. Exptl. Theoret. Phys. (U.S.S.R.) 32, 1108-1125 (May, 1957)

The phenomena of diffusion and thermal conductivity are investigated for dilute solutions of He^3 in helium II, on the basis of the theory of superfluidity proposed by Landau for helium II. A solution is found for the system of kinetic equations for the elementary excitations in the case of non-zero temperature and concentration gradients within the solution. The temperature dependence of the effective thermal conductivity for the solution is determined. A comparison with experiment is made.

1. INTRODUCTION

THE PROBLEM of the kinetic coefficients for solutions of foreign particles in helium II has been investigated by one of the authors [1]. From phenomenological considerations it was demonstrated that in addition to the single coefficient of first viscosity η, the three coefficients of second viscosity, ζ_1, ζ_2, ζ_3, and the coefficient of thermal conductivity $\varkappa$ existing in pure helium II[2] two further kinetic coefficients appear in the case of solutions: the diffusion coefficient D and the thermal diffusion coefficient Dk_T, where k_T is the thermal diffusion ratio. The diffusion of an admixture of the isotope He^3 has been investigated experimentally by Beenakker, *et al*[3], who determined the temperature dependence of the diffusion coefficient in the temperature range from 1.2° K to the λ-point for a concentration $c \sim 10^{-4}$. In the present paper we consider the phenomena of diffusion, thermal diffusion, and thermal conductivity for dilute solutions of He^3 in helium II.

According to Landau's theory[4], liquid helium in the temperature region below the λ-point (helium II) is to be regarded as a weakly-excited quantum system. This implies that thermal energy of helium II may be represented as a gas of elementary excita-

tions—phonons and rotons[5]. The phonon energy ε_p is a linear function of the momentum

$$\varepsilon_p = sp, \tag{1.1}$$

where s is the velocity of sound in helium II.

The roton energy ε_r depends upon the momentum p in the following way

$$\varepsilon_r = \Delta_r + (p - p_0)^2/2\mu_r, \tag{1.2}$$

where Δ_r, p_0, and μ_r are parameters of the theory; μ_r represents the effective mass of the roton. From the most recent data[6]

$$\Delta_r / k = 8{,}9^\circ\,\mathrm{K},\quad p_0/\hbar = 1{,}95\cdot 10^8\ \mathrm{cm}^{-1},$$
$$\mu_r = 1{,}7\cdot 10^{-24}\ \mathrm{g}. \tag{1.3}$$

As has been shown by Landau and Pomeranchuk[7], all foreign particles (including He^3 atoms) dissolved in helium II combine with the normal component of the helium II, and do not participate in the superfluid motion.

From the experiments of Lynton and Fairbank[8], who determined the velocity of second sound in mixtures of He^3 in helium II, it may be concluded[9] that the excitations associated with the He^3 atoms in helium II have the following spectrum:

$$\varepsilon_i = (p^2/2\mu) + \Delta, \tag{1.4}$$

where $\mu = 8.5\ m_1$ (m_1 is the proton mass).

In order to find the dependence of the kinetic coefficients for a solution upon temperature and concentration it is essential to determine the distribution function describing the behavior of gases of elementary excitations when non-zero gradients of temperature T, concentration c, and velocity $\mathbf{v}_n$ are present within the system. The distribution functions are determined by solution of a kinetic equation which we shall now derive.

2. THE KINETIC EQUATION

Non-zero temperature and concentration gradients within the solution give rise to motion of the normal and superfluid components of the helium II, leading to the appearance of additional terms on the left-hand side of the kinetic equation. We shall derive these additional terms by means of the method employed in Ref. 2.

The kinetic equation determining the distribution function n for the elementary excitations in a solution of He^3 in helium II has the form

$$\frac{\partial n}{\partial t} + \frac{\partial H}{\partial \mathbf{p}}\frac{\partial n}{\partial \mathbf{r}} - \frac{\partial H}{\partial \mathbf{r}}\frac{\partial n}{\partial \mathbf{p}} = I(n), \tag{2.1}$$

where $n = n(\mathbf{r}, \mathbf{p}, t)$ is the distribution function, $\mathbf{r}$ and $\mathbf{p}$ are the radius and momentum for the excitation, H is the Hamiltonian for the excitation, and $I(n)$ is the collision integral. When superfluid motion of velocity $\mathbf{v}_s$ takes place in the solution, the Hamiltonian has the form

$$H = \varepsilon(\rho, \mathbf{p}) + \mathbf{p}\mathbf{v}_s, \tag{2.2}$$

where $\varepsilon(\rho, \mathbf{p})$ is the energy of an elementary excitation in the coordinate system for which $\mathbf{v}_s = 0$.

The equilibrium distribution functions for the excitations in a solution in which there is uniform normal fluid motion with velocity $\mathbf{v}_n$ and superfluid motion with velocity $\mathbf{v}_s$ have the form[2]:

$$n = \left(\exp\left\{\frac{\varepsilon_p - \mathbf{p}(\mathbf{v}_s - \mathbf{v}_n)}{kT}\right\} - 1\right)^{-1} \text{(phonons)}; \tag{2.3}$$

$$N = \exp\left\{-\frac{\varepsilon_r - \mathbf{p}(\mathbf{v}_n - \mathbf{v}_s)}{kT}\right\} \quad \text{(rotons)}; \tag{2.4}$$

$$N_i = A(c, T)\exp\left\{-\frac{\varepsilon_i - \mathbf{p}(\mathbf{v}_n - \mathbf{v}_s)}{kT}\right\} \text{(impurities)};$$
$$A(c, T) = N_3(2\pi\mu kT)^{-3/2} = (c\rho/m_3)(2\pi\mu kT)^{-3/2}, \tag{2.5}$$

ρ is the solution density, $c = N_3m_3/(N_3m_3 + N_4m_4)$ is the concentration, N_3 and N_4 are the numbers of atoms of He^3 and He^4 per unit volume, and m_3 and m_4 are the atomic masses of He^3 and He^4. For dilute solutions

$$c = N_3m_3/\rho = N_3m_3/N_4m_4 = \varepsilon m_3/m_4, \tag{2.6}$$

where ε is the molar concentration.

If ∇c and ∇T are small, $\mathbf{v}_n$ and $\mathbf{v}_s$ are also small, and are proportional to a linear combination of ∇c and ∇T. Taking this into consideration, it is possible to linearize the hydrodynamic equations for the solution[10,11] which take the form

$$\dot\rho = -\operatorname{div}\mathbf{j};\quad \dot\sigma = -\operatorname{div}\sigma\mathbf{v}_n;\quad \frac{\partial \mathbf{j}}{\partial t} + \nabla p = 0,$$
$$\frac{\partial}{\partial t}(\rho c) = -\operatorname{div}(\rho c\mathbf{v}_n);$$
$$\dot{\mathbf{v}}_n - \dot{\mathbf{v}}_s = -\left(1 + \frac{\rho_s}{\rho_n}\right)\left(\dot\sigma_0 + \frac{kc}{m_3}\right)\nabla T - \left(1 + \frac{\rho_s}{\rho_n}\right)\frac{kT}{m_3}\nabla c, \tag{2.7}$$

where ρ_n is the density of the normal component of the solution, $\rho_n = \rho_{n0} + \rho_{ni}$; ρ_s is the density of the superfluid component; σ is the entropy per unit mass of the solution; σ_0 is the entropy per unit mass for pure helium II; ρ_{n0} is the fraction of the normal density which is associated with the phonons and rotons; and $\rho_{ni} = (\rho c/m_3)\mu$ is the fraction of the normal density associated with the impurities.

We can then obtain the form of the additional terms in the kinetic equation (2.1) by substituting into the left-hand side of Eq. (2.1) the distribution functions (2.3)–(2.5) and determining $\mathbf{v}_n$ and $\mathbf{v}_s$ from (2.7). We obtain, as a result, the kinetic equation for the impurity excitations in a dilute solution of He^3 in helium II:

$$
\begin{aligned}
D(N_i) &= N_i + \frac{\partial N_i}{\partial \mathbf{r}}\frac{\partial H}{\partial \mathbf{p}} - \frac{\partial N_i}{\partial \mathbf{r}}\frac{\partial H}{\partial \mathbf{r}} \\
&= -\frac{N_{i0}}{kT}\left\{\operatorname{div}(\mathbf{j}-\rho\mathbf{v}_n)\left[\frac{3}{2}k\left(\frac{c}{\rho}\frac{\partial T}{\partial c}-\frac{\partial T}{\partial \rho}\right)+\frac{\varepsilon_i}{T}\left(\frac{\partial T}{\partial \rho}-\frac{c}{\rho}\frac{\partial T}{\partial \rho}\right)-\frac{\partial \varepsilon_i}{\partial \rho}\right]\right. \\
&\quad + \operatorname{div}\mathbf{v}_n\left[\left(\frac{\varepsilon_i}{T}-\frac{3}{2}k\right)\left(\frac{\partial T}{\partial s}s+\frac{\partial T}{\partial \rho}\rho\right)+kT-\frac{\partial \varepsilon_i}{\partial \rho}\rho-\frac{1}{3}\frac{\partial \varepsilon_i}{\partial \mathbf{p}}\mathbf{p}\right] \\
&\quad + \left(\frac{\partial \varepsilon_i}{\partial p_l}p_k-\frac{1}{3}\delta_{lk}\frac{\partial \varepsilon_i}{\partial \mathbf{p}}\mathbf{p}\right)\left(\frac{\partial v_{nk}}{\partial x_l}+\frac{\partial v_{nl}}{\partial x_k}-\frac{2}{3}\delta_{lk}\frac{\partial v_{ni}}{\partial x_i}\right) \\
&\quad + \left[\frac{\rho}{\rho_n}\frac{kT}{m_3}\mathbf{p}+\frac{kT}{c}\frac{\partial \varepsilon_i}{\partial \mathbf{p}}\right]\nabla c \\
&\quad \left.+\left[\frac{\rho}{\rho_n}\left(\sigma_0+\frac{kc}{m_3}\right)\mathbf{p}+\frac{3}{2}k\frac{\partial \varepsilon_i}{\partial \mathbf{p}}-\frac{\varepsilon_i}{T}\frac{\partial \varepsilon_i}{\partial \mathbf{p}}\right]\nabla T-\frac{kT}{\rho}\frac{\partial \varepsilon_i}{\partial \mathbf{p}}\nabla\rho\right\}. \\
&= I(N_i)
\end{aligned}
\tag{2.8}
$$

Neglecting the terms in (2.8) which are associated with the first and second viscosity of the solution, we obtain the kinetic equation in which we are interested:

$$
-\frac{N_{0i}}{kT}\left\{\left(\frac{\rho}{\rho_n}\frac{kT}{m_3}\mathbf{p}-\frac{kT}{c}\frac{\partial \varepsilon_i}{\partial \mathbf{p}_i}\right)\nabla c+\left[\frac{\rho}{\rho_n}\left(\sigma_0+\frac{kc}{m_3}\right)\mathbf{p}_i+\frac{3}{2}k\frac{\partial \varepsilon_i}{\partial \mathbf{p}_i}-\frac{\varepsilon_i}{T}\frac{\partial \varepsilon_i}{\partial \mathbf{p}_i}\right]\nabla T\right\} = I(N_i). \tag{2.9}
$$

In a similar manner we can derive the equations for the rotons and phonons; these equations have the form

$$
\frac{n'}{kT}\left\{\frac{\rho}{\rho_n}\frac{kT}{m_3}\mathbf{p}\nabla c+\left[\frac{\rho}{\rho_n}\left(\sigma_0+\frac{kc}{m_3}\right)\mathbf{p}-\frac{\varepsilon_i}{T}\frac{\partial \varepsilon}{\partial \mathbf{p}}\right]\nabla T\right\} = I(n). \tag{2.10}
$$

Here, n' is the distribution function for the rotons or phonons, differentiated with respect to the argument $(\varepsilon - \mathbf{p}\mathbf{v}_n + \mathbf{p}\mathbf{v}_s)/kT$. In (2.10), as in (2.9), the terms associated with the viscosity of the helium have been omitted. In order to solve this system of kinetic equations it is necessary to know how the elementary excitations interact with one another. The scattering of phonons by phonons and rotons and of rotons by rotons has already been computed by Landau and Khalatnikov[5] in treating the viscosity of helium II. We shall consider below, therefore, the scattering of phonons by impurities and the scattering of impurities by impurities and rotons.

3. COLLISIONS BETWEEN ELEMENTARY EXCITATIONS

Impurity–Roton Scattering

The impurity–roton interaction law is not known. In selecting the impurity–roton interaction energy, therefore, we shall proceed from the same considerations as those used by Landau and Khalatnikov[5] in treating roton–roton scattering. In order to ascertain the temperature dependence of the kinetic coefficients for the solution it will suffice, in accordance with Ref. 5, to determine the impurity–roton scattering probability as a function of temperature accurately to within some constant multiplier.

This probability is insensitive to the choice of distribution function for the interaction of the impurity–roton system.

Taking the impurity–roton interaction energy to be a δ-function of the separation, we shall treat it as a perturbation.

$$v = v_{01}\delta(\mathbf{r} - \mathbf{r}_1) \tag{3.1}$$

where $\mathbf{r}$ and $\mathbf{r}_1$ are the radius vectors for the impurity and the roton, respectively, and v_{01} is a constant whose value may be determined from experiments on the diffusion of He^3 in helium II containing the He^3 as an impurity. We shall designate the energy and momentum of the impurity and the roton, by E, $\mathbf{p}$ and E_1, $\mathbf{p}_1$, respectively; for the state prior to the collision we shall use unprimed quantities, and for that following the collision, primed. The probability of a transition from the state $A(\mathbf{p}, \mathbf{p}_1)$ to the state $F(\mathbf{p}', \mathbf{p}_1')$ is determined from the perturbation theory formula

$$dw = (2\pi/\hbar)\,|v_{AF}|^2\,\delta(E + E_1 - E' - E_1') \times (2\pi\hbar)^{-6} d\mathbf{p}' d\mathbf{p}_1' \Omega^2, \tag{3.2}$$

where Ω is the normalization volume.

Taking the wave functions for the system in the form of plane waves normalized over the volume, the matrix element for the transition v_{AF} can be readily computed and integrated over the impurity momentum. We obtain as a result

$$d\sigma_{ip} = (2\pi\mu/\hbar p)\,|v_{01}|^2\,\delta(E + E_1 - E' - E_1') \times (2\pi\hbar)^{-3} d\mathbf{p}_1', \tag{3.3}$$

assuming the roton to be at rest prior to the collision and taking the total momentum $\mathbf{Q} = \mathbf{p} + \mathbf{p}_1 = \mathbf{p}' + \mathbf{p}_1'$ along the polar axis, we integrate (3.3) over $\mathbf{p}_1'$:

$$I = \int \delta(E + E_1 - E_1' - E_1')\, dp_1' p_1'^2 \sin\vartheta d\vartheta d\varphi = 4\pi\mu\, \mathrm{R} \int_{(A-B)/L}^{(A+B)/L} \frac{2L^2y^2 - L^2}{B\sqrt{y^2-1}}\, dy, \tag{3.4}$$

where ϑ is the angle made by $\mathbf{p}_1'$ with the total momentum $\mathbf{Q}$;

$$M = \frac{\mu\mu_r}{\mu + \mu_r}, \quad A = \frac{p_0}{1 + \mu_r/\mu}, \quad B = \frac{Q\mu_r/\mu}{1 + \mu_r/\mu};$$

$$L^2 = \frac{p_0^2 + \mu_r Q^2/\mu - 2\mu_r E}{1 + \mu_r/\mu}, \quad y = (A + B\cos\vartheta)/L.$$

The symbol R in front of the integral sign indicates that the integration is carried out only over the region in which the integral assumes a real value. It can easily be shown, with the aid of the conservation laws, that I in (3.4) has a real value only for integration over the region $1 \le y \le (A + B)/L$. Carrying out the computation and expanding B and L in terms of p/p_0 we obtain

$$\sigma_{ir}(\cos\vartheta) = \frac{1}{\pi}\frac{|v_{01}|^2}{\hbar^4}\frac{\mu\mu_r}{\mu + \mu_r}\mu\left(\frac{\mu_r}{\mu}\right)^{-1/2}\left(1 + \frac{\mu_r}{\mu} - \cos^2\vartheta\right)^{1/2}. \tag{3.5}$$

Averaging over the directions of the incident momentum for the impurity we find

$$\sigma_{ir} = (|v_{01}|^2\,\mu/2\pi\hbar^4)\,\mu\mu_r/(\mu + \mu_r). \tag{3.6}$$

An absolute value for σ_{ir} may be obtained from experimental data[3] on the diffusion of He^3 in helium II. It turns out to be

$$\sigma_{ir} = 2.1 \cdot 10^{-14}\ \mathrm{cm}^2. \tag{3.7}$$

The impurity–roton interaction constant may be determined from (3.6) and (3.7)

$$|v_{01}| \approx 8 \cdot 10^{-38}\ \mathrm{erg\text{-}cm}^3.$$

Impurity–Impurity Scattering

The interaction law for the impurity particles is not known. Following, therefore, the considerations cited above in the treatment of impurity–roton collisions, we select an interaction energy in the form of a δ-function

$$v = v_{02}\delta(\mathbf{r}_1 - \mathbf{r}_2), \tag{3.8}$$

where $\mathbf{r}_1$ and $\mathbf{r}_2$ are the radius vectors of the impurities, and v_{02} is some constant whose value can be determined experimentally.

It can easily be seen that the computation of the total effective cross-section σ_{ii} for impurity–impurity scattering is completely analagous to the compu-

tation for the scattering of slow neutrons by nuclei [12], with the single difference that since the impurity particles are identical it is accordingly necessary to symmetrize the wave functions. As a result, we obtain for σ_{ii}

$$\sigma_{ii} = |v_{02}|^2\mu^2 / 4\pi\hbar^4. \tag{3.9}$$

To obtain an approximate value we take

$$|v_{02}|^2 \sim 10^{-76} \text{ erg-cm}^3,$$

whence

$$\sigma_{ii} = 1{,}4 \cdot 10^{-15}\alpha \text{ cm}^2, \tag{3.10}$$

where the constant α is included to take account of the fact that $|v_{02}|$ is not actually known.

In collisions of impurities with impurities and with rotons there can also take place, in addition to scattering, an emission of phonons due to deceleration. Calculation shows, however, that the probability for such processes is small, and hence they need not be considered in the phenomena which we shall treat below.

Phonon–Impurity Scattering

We shall treat the impurity as a particle in a phonon field. From this standpoint the internal structure of the impurity is of no significance, since the phonon wavelength is much greater than the de Broglie wavelength for the impurity. Thus it may be shown, as in Ref. 2, that the total perturbation energy for the case under consideration is

$$v = -\tfrac{1}{2}(\mathbf{pv} + \mathbf{vp}) + \frac{\partial\Delta}{\partial\rho}\rho' + \tfrac{1}{2}\frac{\partial^2\Delta}{\partial\rho^2}\rho'^2 + \frac{p^2}{2\mu}(a\rho' + \tfrac{1}{2}b\rho'^2), \tag{3.11}$$

where Δ is the zero-point energy of the impurity excitation, ρ' the deviation of the density of the solution from its equilibrium value due to the presence of a phonon, v the macroscopic velocity of the medium associated with the presence of a phonon, and $\mathbf{p} = -i\hbar\nabla$ the momentum operator for the impurity.

Calculations show that the last term in (3.11) is much smaller than the first. The terms involving derivatives of Δ with respect to ρ, however, cannot be evaluated, since the functional form of $\Delta = \Delta(\rho)$ is not known. We write the excitation energy in the final form

$$v = -\tfrac{1}{2}(\mathbf{pv} + \mathbf{vp}) + \frac{\partial\Delta}{\partial\rho}\rho' + \tfrac{1}{2}\frac{\partial\Delta}{\partial\rho^2}\rho'^2. \tag{3.12}$$

Further, on carrying out computations of the type performed in Ref. 5, we obtain for the differential effective phonon–impurity cross-section σ_{pi} the expression

$$d\sigma_{pi} = (Pp^2/4\pi\hbar\rho s)^2\{\mathbf{m}(\mathbf{n}+\mathbf{n}')(\mathbf{nn}') + \frac{P}{\mu s}[(\mathbf{mn})(\mathbf{mn}')(\mathbf{nn}') + \mathbf{m}(\mathbf{n}+\mathbf{n}')(\mathbf{mn})] + A + B\}^2 dO', \tag{3.13}$$

in which P is the impurity momentum, p the phonon momentum, s the velocity of sound, $\mathbf{m} = \mathbf{P}/P$, $\mathbf{n} = \mathbf{p}/p$, $\mathbf{n}' = \mathbf{p}'/p'$ is the direction of the phonon momentum following the collision, and

$$A = \frac{\rho^2}{Ps}\left(\frac{\partial\Delta}{\partial\rho}\right)^2\frac{1}{\mu s^2}(\mathbf{nn}') + \frac{\rho^2}{Ps}\left(\frac{\partial\Delta}{\partial\rho}\right)\frac{1}{\rho^2}\left[(1-\mathbf{nn}')\frac{s^2}{\rho} - \frac{\partial s^2}{\partial\rho}\right], \qquad B = \frac{\rho^2}{Ps}\frac{\partial^2\Delta}{\partial\rho^2}. \tag{3.14}$$

Averaging (3.13) over the angles of the incident and scattered impurity particles, we obtain

$$d\sigma_{pi}(P, p, \psi) = \left(\frac{Pp^2}{4\pi\hbar^2\rho s}\right)^2\left\{\tfrac{2}{3}(1+\cos\psi)\cos^2\psi + \frac{P}{3\mu s}(A+B)(1+2\cos\psi) + (A+B)^2\right\}dO', \tag{3.15}$$

where $\cos\psi = (\mathbf{n}'\mathbf{n})$. Integrating (3.15) over all scattering angles we find for the total effective cross-section for scattering of a phonon of momentum p by an impurity particle

$$\sigma_{pi} = (Pp/\hbar^2\rho s)^2\delta'/4\pi. \tag{3.16}$$

$$\delta' = \tfrac{2}{9} + \tfrac{1}{3}(P/\mu s)\overline{A(1+2\cos\psi)} + \tfrac{2}{9}(P/\mu s)B + \bar{A}^2 + 2\bar{A}B + B^2,$$

the bar indicating an average over the angles. Substituting into (3.16) the numerical values of all of the known parameters, we obtain

$$\sigma_{pi} = 4.7 \cdot 10^{-20} \delta' (yT) (xT)^4. \quad (3.17)$$

Here x is the phonon momentum in units of kT/s, and y is the energy of the impurity in units of $3kT/2$, so that

$$p = xkT/s \text{ and } p^2/2\mu = 3ykT/2.$$

4. TEMPERATURE DEPENDENCE OF THE DIFFUSION COEFFICIENT

We shall treat first the diffusion of the impurity. The kinetic equations for the impurities and the thermal excitations have been derived above (2.9), (2.10); when a non-zero concentration gradient is present in the system they have the form

$$\frac{n_{0i}}{kT} \frac{\rho}{\rho_n} \frac{kT}{m_3} \frac{\rho_{n0}}{\rho_{ni}} \mathbf{p}_i \nabla c = I_{ie} + I_{ii}; \quad (4.1)$$

$$\frac{n'}{m_3} \frac{\rho}{\rho_n} \mathbf{p} \nabla c = I_{ee} + I_{ei}. \quad (4.2)$$

The collision integrals in (4.1) and (4.2) refer to the following processes: I_{ie}—scattering of impurities by excitations; I_{ii}—scattering of impurities by impurities; I_{ei}—scattering of excitations by impurities; I_{ee}—scattering of excitations by excitations.

The solution of the kinetic equations for the general case involves extremely tedious computations. For this reason we will consider four limiting cases; the results for the intermediate regions may then be obtained by interpolation. Elementary calculations show that for concentrations of impurity excitations $c < 10^{-6}$ deviations from the equilibrium values of the roton and impurity distribution functions are determined by the scattering of rotons and impurities by one another. Roton—phonon and impurity—phonon collisions need, therefore, not be considered for $c < 10^{-6}$ in connection with the establishment of equilibrium in the impurity and roton gases.

On the other hand, the momentum transfer is determined at high temperatures, as can be seen from what follows, by the scattering of impurities by rotons, and at low temperatures by the scattering of phonons by impurities. In view of these circumstances we shall consider first the high-temperature region, in which the diffusion of the impurities may be regarded as taking place in a pure roton gas. We shall then consider the low-temperature region, in which the diffusion of the impurities may be regarded as taking place in a pure phonon gas. The expression for the diffusion coefficients in the general case is obtained by joining the solutions obtained at high temperatures with the solutions for the case of low temperatures. The temperature which in a given instance divides the high- and low-temperature regions depends upon the concentration of the impurity excitations in the solution and will be determined below.

It follows from the symmetry of the problem that deviations of the distribution functions from their equilibrium values may be sought in the form

$$\delta n_i = a_i(\varepsilon) (\mathbf{p}_i \nabla c) n_i, \quad (4.3)$$

$$\delta n = a_r(\varepsilon) (\mathbf{p} \nabla c) n (n + 1). \quad (4.4)$$

It is essential here that the function a be angle-independent.

The High-Temperature Region

Under these conditions the fundamental role in the thermodynamics as well as in kinetic phenomena is played by the rotons. Detailed analysis shows that the phonons play no part in transport processes at temperatures above 0.6° K. In this temperature region we shall consider two limiting cases.

1) The relative number of impurity particles is much smaller than the number of excitations. The probability for collisions between impurity particles is small and such collisions may be ignored. The concentration region for which these conditions hold is determined from the condition $t_{ir} \ll t_{ii}$; *i.e.*, the time characterizing impurity—roton collisions is much smaller than that characterizing collisions between impurities. In this case the kinetic equation for the impurities is highly simplified.

The deviations of the roton distribution function, as a simple calculation shows, are much smaller than the deviations of the impurity functions. The roton gas may thus be taken to be in equilibrium. Impurity particles colliding with a roton are scattered elastically. From these considerations we obtain

$$n_i \frac{\rho}{\rho_n m_3} \frac{\rho_{n0}}{\rho_{ni}} (\mathbf{p} \nabla c) = I_{ir} = -\int a (\mathbf{p} \nabla c) \sigma^*_{ir} v_i n_r d\tau_r n_i. \quad (4.5)$$

Here σ^*_{ir} is the transport cross-section for scattering of an impurity by a roton.

$$\sigma^*_{ir} = {}^1/_2 \int \sigma_{ir} (1 - \cos\psi) d\cos\psi. \quad (4.6)$$

Further, from (3.5), σ_{ir}^* is independent of the energy of the colliding particles. From (4.5), therefore, it follows that

$$a = -(\rho/\rho_n m_3)(\rho_{n0}/\rho_{ni})/N_r \sigma_{ir}^* v_i. \quad (4.7)$$

We now compute the impurity current

$$\mathbf{g} = \int a(\mathbf{p}_i \nabla c)\, \mathbf{p}_i d\tau_i = -\frac{\rho\rho_{n0}}{3\rho_n\rho_{ni}m_3 N_r} \int \frac{p_i^2 n_i d\tau_i}{\sigma_{ir}^* v_i} \nabla c.$$

Equating the current $\mathbf{g}$ to the quantity $-\rho D\nabla c$ we obtain an expression for the diffusion coefficient

$$D = \frac{\rho_{n0}}{\rho_n} \frac{kT}{N_p m_3} \overline{(1/\sigma_{ir}^* v_i)}, \quad (4.8)$$

where

$$\overline{(1/\sigma_{ir}^* v_i)} = \int \frac{1}{\sigma_{ir}^* v_i} p_i^2 n_i d\tau_i / \int p_i^2 n_i d\tau_i. \quad (4.9)$$

Under the present conditions $\rho_{ni} \ll \rho_{n0}$, and the factor ρ_{n0}/ρ_n in (4.8) is equal to unity. Thus the temperature variation of the diffusion coefficient is largely determined by the temperature dependence of the number of rotons N_r, which falls exponentially with temperature. Under these conditions the diffusion coefficient rises with falling temperature as $e^{\Delta/T}$.

2) The number of impurities exceeds the number of thermal excitations (rotons). More precisely, the time characterizing collisions between impurities is much smaller than that for impurity–roton collisions. In this case the distribution function for the impurities may be taken to have its equilibrium form. Since the differences between the roton energy Δ and between the momentum and p_0 are slight, the factor a in Eq. (4.4) can be regarded as energy-independent. For the impurity kinetic equation in this limiting case we write

$$n_i \frac{\rho_{n0}\rho}{\rho_{ni}\rho_n m_3} (\mathbf{p}\nabla c) = I_{ir} + I_{ii}. \quad (4.10)$$

We now multiply both sides of this equation by the momentum $\mathbf{p}$ and integrate over the phase volume for the impurity $d\tau_i$. Since for impurity–impurity collisions the total impurity momentum is unchanged, the integral

$$\int p_i I_{ii} d\tau_i$$

is equal to zero. Performing the indicated integration we obtain

$$\rho_{n0}\rho/\rho_{ni}\rho_n m_3 = a_r \overline{\sigma_{ir}^* v_i} N_r. \quad (4.11)$$

Here

$$\overline{\sigma_{ir}^* v_i} = \int \sigma_{ir}^* v_i p_i^2 n_i d\tau_i / \int p_i^2 n_i d\tau_i. \quad (4.12)$$

Solving this relation for a_r, we now calculate the roton current

$$\mathbf{g}_r = \int a_r (\mathbf{p}_r \nabla c)\, n_r \mathbf{p}_r d\tau = \frac{p_0^2 \rho_{n0}\rho}{3\rho_{ni}\rho_n m_3 \overline{\sigma_{ir}^* v_i}} \nabla c. \quad (4.13)$$

On the other hand, the total momentum of the liquid does not change when diffusion is present, and the sum of the diffusion currents of the rotons and impurities is equal to zero

$$\mathbf{g}_r + \mathbf{g}_i = 0. \quad (4.14)$$

Consequently

$$\mathbf{g}_r = \rho D \nabla c. \quad (4.15)$$

Comparing (4.15) and (4.13), we obtain for D the expression

$$D = \frac{\rho_{n0} p_0^2}{3\rho_{ni}\rho_n m_3} \Big/ \overline{\sigma_{ir}^* v_i} = \frac{(\rho_{n0})^2 kT}{\rho_{ni}\rho_n m_3 N_r} \Big/ \overline{\sigma_{ir}^* v_i}. \quad (4.16)$$

In this limiting case ($\rho_n = \rho_{ni}$) the temperature variation of the diffusion coefficient is determined by the variation of the normal density, which decreases exponentially in this temperature region.

According to (3.5) σ_{ir}^* is independent of the energy of the impurity. Performing the elementary integrations in (4.9) and (4.12) we obtain

$$\overline{\frac{1}{\sigma_{ir}^* v_i}} = \frac{1}{\sigma_{ir}^*} \cdot \frac{\overline{1}}{v_i} = \frac{1}{\sigma_{ir}^* \bar{v}_i} \frac{32}{9\pi}; \quad \bar{v}_i = \frac{8}{3}\left(\frac{2kT}{\pi\mu}\right)^{1/2}. \quad (4.17)$$

Thus the quantities $\overline{(1/\sigma_{ir}^* v_i)}$ and $1/\overline{\sigma_{ir}^* v_i}$ appearing in Eqs. (4.8) and (4.16) differ only by the factor $32/9\pi$, which is very near to unity. This makes it

possible to write an interpolation formula for the diffusion coefficient which covers the whole high-temperature region:

$$D = (\rho_{n0}/\rho_n)^2 (kT/m_3) / N_r \sigma_{ir}^* v_i. \qquad (4.18)$$

For the case in which $t_{ir} \ll t_{ii}$, $\rho_{n0} \approx \rho_n \gg \rho_{ni}$ Eq. (4.18) reduces to Eq. (4.8). In the other limiting case $t_{ir} \gg t_{ii}$, $\rho_{n0} \ll \rho_{ni} \approx \rho_n$ and Eq. (4.18) reduces to Eq. (4.16). Equation (4.18) may also be rewritten in the form

$$D = (\rho_{n0}/\rho_n)^2 (kT/m_3)\, t_{ir}, \qquad (4.19)$$

where the time t_{ir} characterizes the scattering of impurities by rotons:

$$\frac{1}{t_{ir}} = N_r \sigma_{ir}^* \bar{v}_i = \sigma_{ir}^* N_r \frac{8}{3}\left(\frac{2kT}{\pi\mu}\right)^{1/2};$$
$$N_r = \frac{2p_0^2 (\mu_r kT)^{1/2} e^{-\Delta/kT}}{(2\pi)^3 \hbar^3}. \qquad (4.20)$$

Making use of the experimental values for the diffusion coefficient we can with the aid of (4.19) find σ_{ir}^* and, consequently, the unknown impurity–roton interaction constant in Eq. (3.8). Thus we find

$$1/t_{ir} = 1.0 \cdot 10^{13} T e^{-\Delta/kT}. \qquad (4.21)$$

Inserting this value into Eq. (4.19) we obtain an expression for the diffusion coefficient.

$$D = 2.8 \cdot 10^{-6} e^{-\Delta/kT} (\rho_{n0}/\rho_n)^2,$$
$$\rho_{n0} = \rho_{nr} = p_0^2 N_r / 3kT, \qquad (4.22)$$

which is applicable over the whole high-temperature region, in which the phonons play no role.

As regards the time t_{ii}, which characterizes collisions between two impurities, this cannot be obtained from the experimental data. Extremely crude estimates for this time yield

$$\frac{1}{t_{ii}} = \overline{\sigma_{ii} v_i} N_i = \frac{1}{\pi} \frac{|v_{02}|^2 m^2}{\hbar^4} \sqrt{\frac{kT}{\pi\mu}}\, N_i$$
$$= 3 \cdot 10^{11} \cdot T^{1/2} c \qquad (4.23)$$

(v_{02} is taken equal to 10^{-38} erg/cm^3, approximately the same rate as for the interaction between two rotons). The concentration for which the times t_{ir} and t_{ii} become comparable in order of magnitude is

$$c \sim 10^2 T^{1/2} e^{-\Delta/kT}.$$

The Low-Temperature Region

In this temperature region the part played by the rotons, both in transport processes and in the thermodynamics, is negligible. These phenomena are now governed entirely by the phonon portion of the excitation spectrum. As in the high-temperature region, we shall consider two limiting cases.

1) The case in which there are few phonons as compared with the number of impurities. More precisely, the time t_{ii} between collisions of two impurities is small as compared with the phonon–impurity collision time t_{ip}. Evaluation of the times t_{ii} and t_{ip} with the aid of (3.9) and (3.18) shows that the inequality $t_{ii} \ll t_{ip}$ limits the region of applicability to that indicated by the inequality

$$c > 10^{-5} T^{7.5}. \qquad (4.24)$$

This condition (4.24) indicates that in solving the kinetic equations for the present case the impurity excitations may be taken to be in equilibrium for concentrations down to $c > 10^{-6}$. The phonons, however, are scattered elastically, and their distribution does not change (the phonons form a light gas, the impurities a heavy gas). Calculation shows that, despite the low phonon concentration, phonon–phonon collisions are extremely important in the establishment of equilibrium with regard to energy in the phonon gas. The time required to establish energy equilibrium in a phonon gas has been calculated[5] and is

$$1/t_p = 10^5 T^7 x (x+6)^3 \qquad (4.25)$$

($x = \varepsilon/kT$ is the phonon energy in units of kT). The time t_{pi} characterizing the scattering of a phonon by the impurity gas is

$$\frac{1}{t_{pi}} = \frac{6! s N_i}{8\pi} \left[\frac{(3\mu kT)^{1/2} (kT/s)^2}{\hbar^2 \rho s}\right]^2 \delta,$$
$$\delta = \frac{8}{45} + L_0 + \frac{L_{-2}}{3\mu kT}, \qquad (4.26)$$

δ is a complicated function of the parameters describing the impurity energy spectrum; in our calculations it will be taken of order unity (*cf.* Sec. 3). In transport processes the important phonons are those having energies on the order of 6 to 7 kT. For such phonons the inequality $t_p < t_{pi}$ assumes the form

$$T^2/c > 1.$$

This latter inequality shows that at temperatures down to 0.1° K for concentrations $c < 10^{-2}$ equilibrium with respect to energy will be established rapidly as compared with the scattering of phonons by impurities. As regards the time θ_p for establishment of equilibrium with respect to the number of phonons (for a more detailed discussion, *cf.* Ref. 5), this will in the region of interest be comparable with the time t_{ip}. Taking values for θ_p from the expression $\theta_p = 2 \times 10^8 T^9$ we obtain

$$t_{pi}/\theta_p \sim T^4/15\, c. \qquad (4.26')$$

The solution of the kinetic equation for this limiting case follows a procedure completely analogous to that involved in the calculation of the phonon viscosity[5]. Omitting the simple computations, we give directly the expression for δn_p

$$\delta n_p = n_p (n_p + 1) \frac{\rho}{\rho_n} \frac{kT}{m_3} \frac{t_{pi}}{s} \frac{31.2 - (ps/kT)(3.5 - 3{,}7\, t_{pi}/\theta_p)\, p\nabla c}{(1 + 8 t_{pi}/\theta_p)\, p}. \qquad (4.27)$$

The time t_{pi} for scattering of phonons by the impurity is determined from Eq. (4.26). Further, with the aid of (4.27) we compute the diffusion component of the phonon current

$$\mathbf{g}_p = \int \mathbf{p} \delta n_p d\tau_p$$

and, using the fact that $\mathbf{g}_i = -\mathbf{g}_p = -\rho D \nabla c$, we find the diffusion coefficient to be

$$D = 5.1 \frac{\rho_{np}}{\rho_n} \frac{kT}{m_3} t_{pi} \left\{ \frac{1 + 0.75\, t_{pi}/\theta_p}{1 + 8 t_{pi}/\theta_p} \right\}. \qquad (4.28)$$

Inasmuch as the temperature dependence of ρ_{np} is given by a T^4 law, the product $\rho_{np} k T t_{pi}$ is, in view of (4.26), temperature-independent. In this region, therefore, the diffusion depends only weakly upon temperature. The entire temperature dependence is embodied in the factor enclosed in the braces.

We shall now treat the final limiting case.

2) The number of impurities is small compared with the number of phonons. Here only collisions between impurities and phonons are significant; collisions of the impurities with one another are not important. Simple analysis shows that in this case the deviations of the phonon distribution functions from their equilibrium values are small and may be neglected in the kinetic equation.

The deviation of the impurity distribution function from its equilibrium value due to the presence of a concentration gradient can be written in the form

$$\delta n_i = a_i(\varepsilon)(\mathbf{p}_i \nabla c) n_i \qquad (4.29)$$

The quantity a_i depends upon the energy of the impurity. We can also write down the kinetic equations for the impurities and phonons

$$(n_i \rho / \rho_{ni} m_3)(\mathbf{p}_i \nabla c) = I_{ip}, \qquad (4.30)$$

$$(n(n+1)\rho/\rho_n m_3)(\mathbf{p}_p \nabla c) = I_{pi} + I_{pp}. \qquad (4.31)$$

We multiply the second of these equations by $\mathbf{p}_p$ and integrate over the phonon phase volume; taking account of the fact that in collisions between two phonons the total phonon momentum does not change we obtain

$$-(\rho kT/m_3)\nabla c = \int \mathbf{p}_p I_{pi} d\tau_p. \qquad (4.32)$$

In what follows we shall disregard the weak dependence of the scattering cross-section σ_{pi} upon the phonon scattering angle. Further, it follows from the conservation of energy

$$p_i^2/2\mu + s p_p = p_i'^2/2\mu + s p_p'$$

that the change in the energy of an impurity resulting from a collision will be small compared with the magnitude of the energy ε_i

$$\Delta\varepsilon = \varepsilon_i' - \varepsilon_i = \mathbf{p}_i(\mathbf{p}_p - \mathbf{p}_p')/\mu + (\mathbf{p}_p - \mathbf{p}_p')^2/2\mu.$$

This is connected with the fact that the momentum of a phonon is small compared with that of the impurity. We expand the difference $a_i' \mathbf{p}_i' - a_i \mathbf{p}_i$ appearing in the collision integral in a power series to terms of the second order of $\Delta\varepsilon$. After a simple integration over angle the integral equation (4.30) assumes the following form:

$$\frac{\rho}{\rho_{ni}m_3}$$

$$= \left(\frac{5}{3}\frac{\partial a_l}{\partial \varepsilon} + \frac{2}{3}\frac{\partial^2 a_i}{\partial \varepsilon^2}\varepsilon\right)\int d\tau_{\mathbf{p}} n_{\mathbf{p}}(n_{\mathbf{p}}+1)\,\sigma_{\mathbf{p}i}s_{\mathbf{p}}\frac{p_{\mathbf{p}}^2}{\mu}. \tag{4.33}$$

We thus reduce our problem to one of solving a differential equation of the Fokker-Planck type.

The relation (4.32) yields a condition which must be satisfied by the functions a_i; this condition has the form

$$-\frac{\rho kT}{m_3} = \iint \sigma_{\mathbf{p}i}s\left(a_i + \frac{2}{3}\frac{\partial a_i}{\partial \varepsilon}\varepsilon\right) n_{\mathbf{p}} d\tau_{\mathbf{p}} \frac{p_{\mathbf{p}}^2}{3} n_i d\tau_i. \tag{4.34}$$

The cross-section $\sigma_{\mathbf{p}i}$ depends linearly upon ε_i. The solution of Eq. (4.33) is readily found

$$a_i = A\ln\varepsilon + \left(B - \frac{2}{3}A\right) + C\varepsilon^{-1/2}, \tag{4.35}$$

where

$$A = \frac{\mu\rho}{\rho_{ni}m_3}\Big/\int\left(\frac{\sigma}{\varepsilon}\right)p_{\mathbf{p}}^2 n_{\mathbf{p}}(n_{\mathbf{p}}+1)\,d\tau_{\mathbf{p}} = \mu\rho\Big/2\rho_{ni}m_3\rho_{np}\sigma_{\mathbf{p}i}s, \tag{4.36}$$

$$\overline{\sigma_{\mathbf{p}i}s} = \frac{s\int \sigma_{\mathbf{p}i}n_{\mathbf{p}}(n_{\mathbf{p}}+1)\,p_{\mathbf{p}}^2\,d\tau_{\mathbf{p}}n_i d\tau_i}{\int p_{\mathbf{p}}^2 n_{\mathbf{p}}(n_{\mathbf{p}}+1)\,d\tau_{\mathbf{p}}n_i d\tau_i}. \tag{4.37}$$

The characteristic time previously introduced can be expressed in terms of the quantities of (4.37) by means of

$$1/t_{\mathbf{p}i} = 0.47\,\overline{\sigma_{\mathbf{p}i}s}N_i, \tag{4.38}$$

B and C are constants of integration. The constant C must necessarily be set equal to zero, since the number of phonons moving in any given direction must be finite. The constant B is determined by the condition (4.32)

$$\overline{\sigma_{\mathbf{p}i}s}\int(A\ln\varepsilon + B)\,\varepsilon n_i d\tau = -\rho kT/m_3\rho_{n0}. \tag{4.39}$$

From this we obtain

$$B = -2A - A\,\overline{\ln\varepsilon},$$
$$\overline{\ln\varepsilon} = \int \ln\varepsilon\cdot\varepsilon n_i d\tau_i\Big/\int \varepsilon n_i d\tau_i. \tag{4.40}$$

We now compute the impurity diffusion current

$$\mathbf{g}_i = -\rho D\nabla c = \int A\left(\ln\varepsilon - \overline{\ln\varepsilon} - \frac{8}{3}\right)\mathbf{p}_i(\mathbf{p}_i\nabla c)\,n_i d\tau_i. \tag{4.41}$$

From this, taking (4.40) into account, we obtain

$$D = 8AkT\rho_{ni}/3\rho = 4\rho_{ni}kT/3m_3\rho_{n0}N_i\overline{\sigma_{\mathbf{p}i}s}. \tag{4.42}$$

Thus we have, to within a factor of order unity

$$D = (\rho_{ni}kT/\rho_{n0}m_3)/\overline{N_i\sigma_{\mathbf{p}i}s}. \tag{4.43}$$

The coefficient D thus obtained increases with falling temperature according to a T^{-8} law.

An interpolation formula embracing both limiting cases at low temperatures may readily be written. For this we rewrite Eq. (4.28), which holds in the region $\rho_{n\mathbf{p}} \ll \rho_n \approx \rho_{ni}$, in the following form:

$$D = 11\left(\frac{\rho_{n\mathbf{p}}}{\rho_{ni}}\right)^2\frac{kT}{m_3}\frac{1}{\overline{\sigma_{\mathbf{p}i}s}N_{\mathbf{p}}(4kT/\mu s^2)}\frac{1+0.75\,t_{\mathbf{p}i}/\theta_{\mathbf{p}}}{1+8\,t_{\mathbf{p}i}/\theta_{\mathbf{p}}}. \tag{4.43'}$$

Here we make use of the relation (4.38) and the following well-known formulas:

$$\rho_{n\mathbf{p}} = 4E_{\mathbf{p}}/3s^2 \approx (4kT/s^2)\,N_{\mathbf{p}}, \quad \rho_{ni} = \mu N_i. \tag{4.44}$$

Equation (4.43), which holds for the region in which $\rho_n = \rho_{\mathbf{p}} \gg \rho_{ni}$, may likewise be rewritten in the form

$$D = \frac{kT}{m_3}\Big/\overline{\sigma_{\mathbf{p}i}s}N_{\mathbf{p}}\frac{4kT}{\mu s^2}. \tag{4.45}$$

We note further that in this region the impurity concentrations are extremely small, and, in accordance with (4.26′),

$$t_{\mathbf{p}i}/\theta_{\mathbf{p}} \gg 1.$$

It is now readily seen that Eqs. (4.43) and (4.45) can be combined into a single equation

$$D = \left(\frac{\rho_{n\mathbf{p}}}{\rho_n}\right)^2\frac{kT}{m_3}\frac{1}{\overline{\sigma_{\mathbf{p}i}s}\,N_{\mathbf{p}}(4kT/\mu s^2)}\frac{11+8\,t_{\mathbf{p}i}/\theta_{\mathbf{p}}}{1+8\,t_{\mathbf{p}i}/\theta_{\mathbf{p}}}. \tag{4.46}$$

Comparing Eq. (4.18), which applies in the high-temperature region, with Eq. (4.46), applying in the

low-temperature region, we note that both of these equations may be combined into a single expression

$$D = (\rho_{n0}/\rho_n)^2 (kT/m_3)\, t_i, \tag{4.47}$$

in which the time t_i characterizes the collisions of the impurity with the thermal excitations is given by

$$t_i = \left\{ \overline{\sigma_{ir} v_i} N_r + \overline{\sigma_{ip} s} N_p \frac{4kT}{\mu s^2} \frac{1 + 8t_{pi}/\theta_p}{11 + 8t_{pi}/\theta_p} \right\}^{-1} \tag{4.48}$$

In the limit of high temperatures, for which the gas of thermal excitations consists principally of rotons, $\rho_{n0} = \rho_{np}$, and all of the terms due to phonons may be neglected. We obtain as a result Eq. (4.18). In the low-temperature region, on the other hand, we neglect the rotons, and obtain Eq. (4.46).

Making use now of Eqs. (4.21), (4.26) and (4.38), we obtain an expression for t_i in a form convenient for numerical calculation:

$$t_i = \left\{ 1 \cdot 10^{13} T e^{-\Delta/kT} + 1.2 \cdot 10^6 T^9 \frac{1 + T^4/15c}{11 + T^4/15c} \right\}^{-1}. \tag{4.49}$$

It should be noted that the second term in (4.49), due to the phonons, becomes important in this equation at temperatures below 0.5° K. This can easily be understood if we recall that in the thermodynamic treatment the phonon component of the normal density predominates only for $T < 0.5°$ K. From the kinetic standpoint the times characterizing scattering of the impurity by rotons t_{ir} and by the phonon gas t_{ip} are comparable only for $T \sim 0.5°$ K. For temperatures higher than 0.5° K, $t_{ir} \ll t_{ip}$, and, as a consequence, the diffusion is in this case determined by scattering of impurities by rotons. Thus for $T > 0.5°$ K we may limit ourselves to the first term in Eq. (4.49) at all concentrations:

$$1/t_i = 10^{13} T e^{-\Delta/kT}. \tag{4.50}$$

5. THERMAL DIFFUSION

In general, when non-zero temperature and concentration gradients exist in a solution (under constant pressure) the impurity current g is defined by the expression

$$\mathbf{g} = -\rho D [\nabla c + (k_T/T) \nabla T], \tag{5.1}$$

where D is the diffusion coefficient as calculated above (4.38), and k_T is the thermal diffusion ratio. Simple calculation shows that the thermal diffusion contribution to the diffusion current is neglible when the number of impurity excitations is small compared with the number of thermal excitations.

1) The case for which the number of impurities greatly exceeds the number of rotons. Following a procedure completely analogous to that used in calculating the diffusion coefficient in the second limiting case, we find for the thermal diffusion ratio

$$k_T = c(1 - \rho_{ni} \sigma_0 m_3/\rho_{n0} kc). \tag{5.2}$$

2) The case of low temperatures, for which the momentum is transported by the phonons and the contribution of the rotons to the diffusion process may be neglected. In this limiting case, the thermal diffusion ratio is

$$k_T = c(1 + \sigma_0 m_3/kc - \rho_n \sigma_p m_3/\rho_{np} kc). \tag{5.3}$$

For sufficiently low temperatures ($T \ll 0.6°$ K), $\rho_{n0} \sim \rho_{np}$ and $\sigma_0 \sim \sigma_p$, and the thermal diffusion ratio takes on the simpler form

$$k_{Tp} = c(1 - \rho_{ni} \sigma_p m_3/\rho_{np} kc) = c(1 - \mu s^2/kT). \tag{5.3'}$$

Comparison of k_T for the roton region (5.2) with k_T for the deep phonon region (5.3′) shows that Eq. (5.2) can serve as a useful interpolation formula for the thermal diffusion ratio of the solution over the whole range of temperatures and concentrations:

$$k_T = c(1 - \rho_{ni} \sigma_0 m_3/\rho_{n0} kc). \tag{5.4}$$

6. THERMAL CONDUCTIVITY

The mechanism for thermal transport in the solution can be twofold. On one hand, heat can be transferred due to motion of the normal component of the helium. On the other hand, the presence within the solution of a non-zero temperature gradient leads to an additional thermal current which arises, as in ordinary condensed media, from the transfer of heat by diffusion of thermal excitations. This thermal current is characterized by a definite thermal conductivity coefficient. The thermal conductivity coefficient for a solution of He^3 in helium II is defined in such a way that for zero impurity diffusion current g = 0 the heat current q will be

$$-\mathbf{q} = \varkappa \nabla T. \tag{6.1}$$

The thermal conductivity coefficient $\varkappa$ for the solution is a sum of roton, phonon and impurity components. Calculations analogous to those carried out for the thermal conductivity of helium II[6] yield the following result:

$$\varkappa = \varkappa_r + \varkappa_p + \varkappa_i, \tag{6.2}$$

$$\varkappa_r = t_r \frac{\Delta_r^2 N_r}{3T\mu_r}\left[1 - \frac{3\sigma_0\sigma_r T^2 \mu_r \rho^2}{\Delta_r^2 N_r \rho_{n0}}\right]. \tag{6.3}$$

$$\varkappa_p = 1.7\theta N_p s^2 k \frac{11 + 8\theta/\theta_p}{1 + 8\theta/\theta_p}\left\{1 - \frac{\sigma_0 T \rho}{\rho_{n0} s^2}\right\}, \tag{6.4}$$

$$\varkappa_i = \frac{c\rho}{\mu} t_i \frac{kT}{m_3} \frac{5}{2} k, \tag{6.5}$$

where s is the velocity of sound, σ_0 is the entropy per unit mass for pure helium II, and σ_r is the entropy per unit mass of the roton gas. The effective time θ is determined by the expression

$$1/\theta = 1/t_{pr} + 1/t_{pi},$$

$$\frac{1}{t_{pr}} = 0{,}85 \frac{N_r 6!}{4\pi s}\left[\frac{p_0 (kT/s)^2}{\rho\hbar^2}\right]^2, \tag{6.6}$$

$$\frac{1}{t_{pi}} = \frac{6! N i}{8\pi s}\left[\frac{(3\mu kT)^{1/2}(kT/s)^2}{\rho\hbar^2}\right]^2 \delta.$$

In the transition to the pure helium II case $c \to 0$, and $\varkappa_r$ and $\varkappa_p$ go over into the corresponding quantities for helium II as computed in Ref. 6.

It can easily be seen that for concentrations $c > 10^{-6}$, $\varkappa_i \ll \varkappa_r + \varkappa_p$ over the whole temperature range. Substituting numerical values for the quantities in (6.3)–(6.5) and dropping the negligible second term in $\varkappa_r$ we obtain

$$\varkappa = \frac{2.0 \cdot 10^3}{T} \frac{1}{1 + 0.2ce^{8.9/T}} \tag{6.7}$$

$$+ \frac{7.6 \cdot T^{-3/2} e^{8.9/T}}{1 + \delta \cdot 2.8 \cdot 10^{-2} T^{1/2} ce^{8.9/T}} \frac{11 + 8\theta/\theta_p}{1 + 8\theta/\theta_p}\left[1 - \frac{\sigma_0 T \rho}{\rho_{n0} s^2}\right].$$

The temperature dependence of $\varkappa$ for various concentrations is illustrated in Fig. 1.

7. EFFECTIVE THERMAL CONDUCTIVITY OF SOLUTIONS

Experiment gives a direct determination not of the diffusion coefficient, but of the effective thermal conductivity coefficient

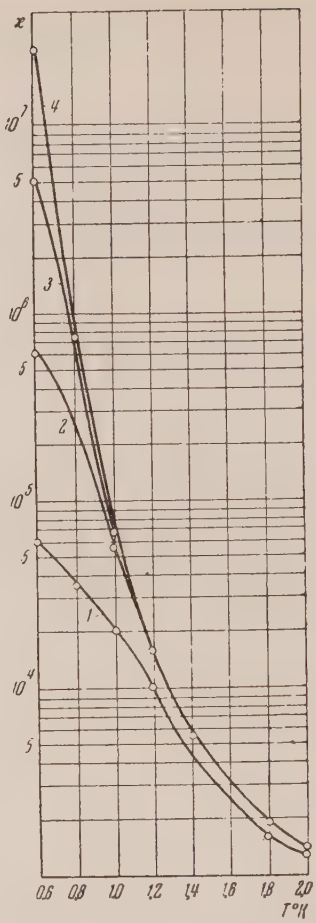

FIG. 1. Dependence of the thermal conductivity coefficient for a solution of He^3 in He^4 on the temperature T and the concentration c [Eq. (6.7)]: 1—$c = 10^{-2}$, 2—$c = 10^{-3}$, 3—$c = 10^{-4}$, 4—$c = 10^{-5}$.

$$\mathbf{Q} = -\varkappa_m \nabla T, \tag{7.1}$$

where $\mathbf{Q}$ is the heat flow through the solution per unit area. The diffusion coefficient D is directly related to $\varkappa_m$. We shall derive an expression for $\varkappa_m$ under the restriction that the experiment be performed under stationary conditions. The heat current per unit area $\mathbf{Q}$ in the solution is[8]:

$$\mathbf{Q} = Zc\mathbf{v}_n + \sigma\rho T\mathbf{v}_n + \mathbf{q}' = -\varkappa_m \nabla T, \tag{7.2}$$

where $\mathbf{v}_n$ is the velocity of the normal component of the solution, $Z = \rho(\mu_3/m_3 - \mu_4/m_4)$, and μ_3 and μ_4 are the chemical potentials of the pure He^3 and He^4 isotopes. In (7.2) the thermal current $\mathbf{q}'$ has the form

$$\mathbf{q}' = T^2\left[\frac{k_T}{T}\frac{\partial}{\partial c}\frac{Z}{\rho T} - \frac{\partial}{\partial T}\frac{Z}{\rho T}\right]\mathbf{g} - \varkappa\nabla T, \tag{7.3}$$

where $\varkappa$ is the thermal conductivity coefficient for the solution and g is taken from (5.11). Under stationary conditions there follows from the constancy of the potential Φ the equation

$$\frac{\partial}{\partial c}\left(\frac{Z}{\rho}\right)\nabla c = c\,\frac{\partial}{\partial c}\left(\frac{\sigma}{c}\right)\nabla T, \qquad (7.4)$$

the equation of motion for the impurities being given by the expression

$$\mathbf{g} + \rho c \mathbf{v}_n = 0. \qquad (7.5)$$

Using the thermodynamic relations which follow from $d\Phi = (dp/\rho) - \sigma dT + (Z/\rho)dc$ and solving simultaneously Eqs. (7.2)–(7.5), we can determine the effective thermal conductivity coefficient

$$\varkappa_m = \varkappa + \left(\rho DT \Big/ \frac{\partial}{\partial c}\frac{Z}{\rho}\right)\left\{c\,\frac{\partial}{\partial c}\left(\frac{\sigma}{c}\right) + \frac{k_T}{T}\frac{\partial}{\partial c}\left(\frac{Z}{\rho}\right)\right\}. \qquad (7.6)$$

For a weak solution

$$c\,\frac{\partial}{\partial c}\left(\frac{\sigma}{c}\right) = -\frac{\sigma_0}{c} - \frac{k}{m_3}, \qquad \frac{\partial}{\partial c}\frac{Z}{\rho} = \frac{kT}{m_3 c}.$$

If we also introduce into (7.6) the value of the thermal diffusion ratio from (5.4) we obtain the simpler expression

$$\varkappa_m = (\rho D m_3 \sigma_0^2 / kc)\,(\rho_n / \rho_{n0})^2 + \varkappa, \qquad (7.7)$$

where D is the diffusion coefficient determined from Eq. (4.52). Setting Eq. (4.47) in place of D, we obtain

$$\varkappa_m = \rho T \sigma_0^2 t_i / c + \varkappa. \qquad (7.8)$$

As we have already noted, the time t_i is practically independent of the concentration of the solution. Thus the first term in Eq. (7.8) depends upon the concentration as $1/c$. As regards the second term—the thermal conductivity coefficient for the solution—this, in accordance with (6.7), depends in a rather complicated fashion upon the concentration of the solution. As can be seen from the graph (Fig. 2), the second term in (7.8) is negligible in the high temperature region for sufficiently low concentrations. We then have ($\rho_n \approx \rho_{n0}$)

$$\varkappa_m = \rho T \sigma_0^2 t_i / c. \qquad (7.9)$$

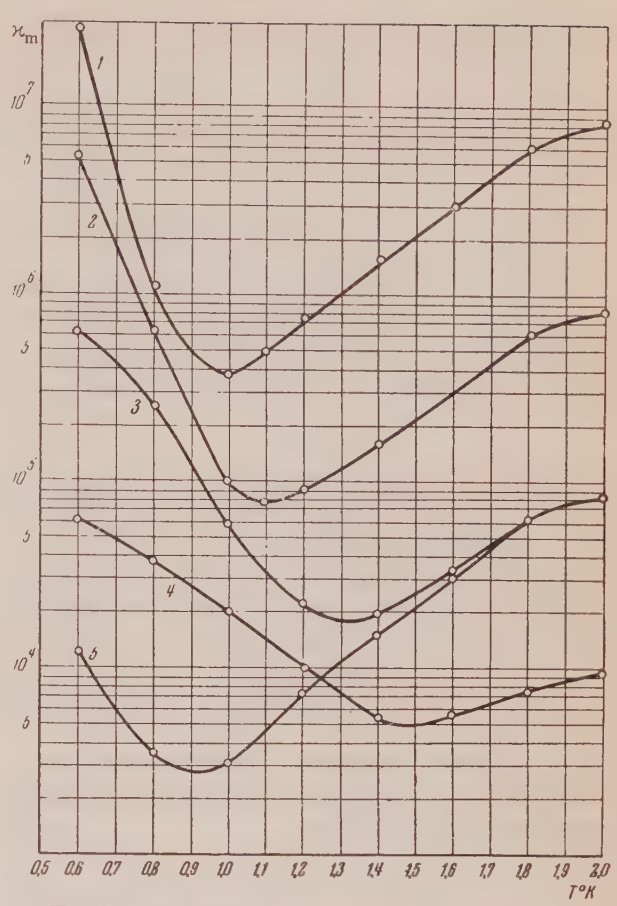

FIG 2. Dependence of the effective thermal conductivity for a solution of He^3 in He^4 on the temperature T and concentration c [Eq. (7.9)]: $\varkappa_m = K(T)/c + \varkappa$; 1—$c = 10^{-5}$, 2—$c = 10^{-4}$, 3—$c = 10^{-3}$, 4—$c = 10^{-2}$, 5—$c = K \times 10^{-3}$.

The temperature distribution in a weak solution of He^3 in He^4 in the presence of a thermal current is determined as follows. We write the expression for the thermal current (taking the one-dimensional case for simplicity)

$$q = -\varkappa_m \partial T / \partial x \qquad (7.10)$$

and the condition that the potential Φ be constant along the solution

$$\Phi_0 - ckT/m_3 = \text{const} \qquad (7.11)$$

(Φ_0 is the solvent potential, that for helium II, which depends upon temperature but is independent of the concentration c). Further, we express the concentration c from (7.11) in terms of the temperature and an unknown constant. We substitute this

expression into the equation for $\varkappa_m$ and integrate Eq. (7.10)

$$x = -\frac{1}{q}\int_{T_0}^{T} \varkappa_m dT, \qquad (7.12)$$

T_0 is the temperature at the cold end of the vessel ($x = 0$). We then find, with the aid of (7.12) and (7.11), the dependence of the concentration c upon the coordinate x. This dependence includes an unknown constant, which can be determined from the condition that the impurities must be conserved.

$$c_0 = \frac{1}{d}\int_0^d c dx, \qquad (7.13)$$

We shall illustrate this procedure, taking as our example an extremely weak solution, for which Eq. (7.10) is applicable; we write the latter in the form [with $K(T)$ a function of temperature]

$$\varkappa_m = K(T)/c. \qquad (7.14)$$

It is essential here to bear in mind that for sufficiently weak solutions it follows from the condition (7.11) ($kc/m_3 \ll \sigma_0$) that:

$$\sigma_T \nabla T = -(kT/m_3)\nabla c. \qquad (7.15)$$

Thus

$$|\nabla c/c| \gg |\nabla T/T|,$$

and, consequently, under these conditions the temperature varies only slightly along the helium, while the concentration changes quite appreciably. Integrating (7.15), we obtain

$$c = -(m_3/kT)\sigma_0 (T - T_c), \qquad (7.16)$$

where T_c is a constant of the integration. Equation (7.15) represents an alternative form for the condition (7.11). We now integrate Eq. (7.10), taking (7.14) and (7.16) into account, and obtain

$$x = -\frac{1}{q}\int_{T_0}^{T}\frac{K(T)\,dT}{c} = \frac{1}{m_3 q}\int_{T_0}^{T}\frac{kTK(T)\,dT}{\sigma_0 (T - T_c)}$$

$$= \frac{kTK(T)}{m_3 q \sigma_0}\ln\frac{T - T_c}{T_0 - T_c}. \qquad (7.17)$$

Since the temperature variation is small, the coefficient preceding the logarithm in (7.17) can be computed for the mean temperature of the helium. From (7.17) we obtain the temperature

$$T = T_c + (T_0 - T_c)e^{x/x_0},$$
$$1/x_0 = kTK(T)/m_3 q \sigma_0. \qquad (7.18)$$

Further, using (7.16) we express the concentration c as

$$c = -(m_3/kT)\sigma_0 (T_0 - T_c)e^{x/x_0}, \qquad (7.19)$$

and, finally, we obtain the constant of integration T_c from the condition (7.13)

$$-(T_0 - T_c) = c_0 \frac{d}{x_0}\frac{kT}{m_3\sigma_0}\frac{1}{e^{d/x_0} - 1}. \qquad (7.20)$$

Ultimately, we obtain from (7.18) and (7.20) the formula for temperature distribution along the solution:

$$T - T_0 = \frac{c_0 d}{x_0}\frac{kT}{m_3\sigma_0}\frac{e^{x/x_0} - 1}{e^{d/x_0} - 1}. \qquad (7.21)$$

Beenakker *et al.*[3] obtained experimental values of the diffusion coefficient for the impurities in a solution. In analyzing their results, however, the authors used in place of the entropy σ appearing in Eq. (7.21) another quantity f, which they took from the results of unpublished experiments. We have recalculated the data of these authors, using known data for the value of the entropy. This recalculation changes the value of the diffusion coefficient somewhat. Under the conditions of the experiment—$T \geq 1.20°$, $c \sim 10^{-4}$—the part played by the phonons was negligible (the quantity $\varkappa$ could also be neglected), and the diffusion of the impurities was determined solely by their interactions with the rotons. The unknown impurity–roton interaction constant was determined from the experimental value of the diffusion coefficient at $T = 1.5°$ K. The effective time t_{ir} then takes the value given by Eq. (4.20).

It should be emphasized that in experiments conducted under stationary conditions diffusion of the impurities cannot be considered alone. What is actually determined experimentally, in accordance with (7.7), is a certain effective thermal conductivity coefficient for the solution, representing a com-

bination of the diffusion and thermal conductivity coefficients and the thermal diffusion ratio.

The results obtained in the present work are correct for the temperature region $T \leq 1.6 - 1.8°$ K, in which the rotons may be regarded as constituting an ideal gas. At low temperatures the applicability of the theory is limited by the mean free paths of the excitations associated with the transport phenomena. As usual, the mean free paths must be much shorter than the characteristic dimensions of the containers. For high impurity concentrations, for which the mean free paths are short down to the lowest temperatures, the theory is applicable down to the temperatures at which the Fermi degeneracy of the impurities becomes significant.

In conclusion, the authors wish to express their deep indebtedness to Academician L. D. Landau for his helpful discussions.

[1] I. M. Khalatnikov, J. Exptl. Theoret. Phys. (U.S.S.R.) **23**, 265 (1952).

[2] I. M. Khalatnikov, J. Exptl. Theoret. Phys. (U.S.S.R.) **23**, 8 (1952).

[3] Beenakker, Taconis, Lynton, Dokoupil, and Van Soest, Physica **18**, 433 (1952).

[4] L. D. Landau, J. Exptl. Theoret. Phys. (U.S.S.R.) **11**, 592 (1941).

[5] L. D. Landau and I. M. Khalatnikov, J. Exptl. Theoret. Phys. (U.S.S.R.) **19**, 637, 709 (1949).

[6] I. M. Khalatnikov, J. Exptl. Theoret. Phys. (U.S.S.R.) **23**, 21 (1952).

[7] L. D. Landau and I. Ia. Pomeranchuk, Dokl. Akad. Nauk SSSR **53**, 661 (1948).

[8] E. A. Lynton and H. A. Fairbank, Phys. Rev. **80**, 1043 (1950).

[9] I. M. Khalatnikov, Dokl. Akad. Nauk SSSR **79**, 57 (1951).

[10] I. Ia. Pomeranchuk, J. Exptl. Theoret. Phys. (U.S.S.R.) **19**, 42 (1949).

[11] I. M. Khalatnikov, J. Exptl. Theoret. Phys. (U.S.S.R.) **23**, 169 (1952).

[12] L. D. Landau and E. M. Lifshitz, *Quantum Mechanics*; GITTL, 1948, L. D. Landau and E. M. Lifshitz, *Mechanics of Continuous Media*; GITTL, 1944.

Translated by S. D. Elliott
230

SOVIET PHYSICS JETP VOLUME 5, NUMBER 5 DECEMBER, 1957

Shock Waves of Large Amplitude in Air

IA. B. ZEL'DOVICH
Institute of Chemical Physics, Academy of Sciences, U.S.S.R.

(Submitted to JETP editor June 10, 1956)
J. Exptl. Theoret. Phys. (U.S.S.R.) **32**, 1126-1135 (May, 1957)

The state of air compressed by strong shock waves is examined by taking dissociation and ionization into account. Approximate expressions are given for the density and temperature in this region. The radiation from the front of the shock wave is considered. With increasing shock-wave amplitude, the observed surface temperature passes through a maximum, owing to the formation of an opaque layer of air, preheated by the radiation, ahead of the front of the wave. A proof is given of the non-existence of a continuous solution and of the unavoidability of discontinuities in the velocity, density, and temperature in a strong shock wave with radiative heat exchange. The wave structure is investigated in a strongly-ionized gas with allowances for the slow energy transfer between the ions and electrons.

PHENOMENA OCCURRING in strong shock waves are very interesting from many points of view. In practice we encounter shock waves during explosions and during the motion of bodies at supersonic speeds. The principal interest lies in the peculiarities of the compression in the shock wave: the compression occurs rather rapidly, is accompanied by a sharp increase in the gas entropy, and is irreversible. Gas compression in a shock wave produces high temperatures, considerably higher than adiabatic compression to the same pressure.

It was already noted by Muraour[1] that the glow observed in an explosion is neither the chemiluminescence reaction of the decomposition of the ex-

ploding substance nor thermal glow of the explosion products. What really glows is the air, compressed by the explosion shock wave around the explosion substance.

O. I. Leipunskii and the author[2] observed rather high temperatures in a shock wave produced by the motion of a bullet in mercury vapor. Extensive investigations of strong shock waves are being carried at the present time in the U.S. with the aid of a so-called shock tube[3], in which a diaphragm separates the high-pressure gas from the low-pressure gas, and the wave is produced by rupture of the diaphragm* or with the aid of explosive substances[4].

The high temperatures of the strong shock waves are accompanied by new physical phenomena, such as dissociation, ionization, and emission of light. The influence of these phenomena on the properties of air compressed by a shock wave and on the structure of the wave is the subject of this article.

Ionization and radiation in a shock wave was considered in detail in an article by Prokof'ev[7], using compressed monatomic hydrogen as an example. Let us note that we are not in agreement with Prokof'ev's conclusions concerning the structure of the wave (see Sec. 5).

1. DISSOCIATION AND IONIZATION IN SHOCK WAVE

The temperatures reached at shock-wave pressures of 200–600 atmos are 5,000–10,000°, at which strong dissociation of the oxygen and the nitrogen molecules takes place[8,9]. The compressed air becomes monatomic. Because of the large amount of energy required to break up the molecule, the gas pressure is substantially less than 2/3 the energy density (subtracted from the molecule energy at 0°K). The density of the air compressed in the shock-wave therefore does not diminish to $4\rho_0$, but, to the contrary, increases to $9-12\ \rho_0$ at the above pressure and temperature ranges.

With increasing pressure, the dissociation energy, which is a constant term, becomes less and less important. However, noticeable ionization of the atoms occurs even before the dissociation is complete†. The pressure range, in which the density is on the order of $10\ \rho_0$, is therefore quite extensive. Substituting into the Sach equation the electron density corresponding to almost complete ionization of air compressed ten times atmospheric density, we obtain the following numerical expression for the average number of K-electrons (electrons of the innermost shell of the nucleus) in equilibrium at a temperature T:

$$n_K = 2/[1+60\,T^{3/2}e^{-E/T}], \tag{1}$$

where T and E are given in electron volts, E being the binding energy, which is 650 ev for nitrogen and 850 ev for oxygen. The detachment of the K-electrons occurs not at $T \sim E$, but at $T \sim E/\ln(60\,T^{3/2}) \approx E/10$. The energy consumed in the ionization therefore constitutes a large component in the energy balance of the shock wave.

The density reaches its limiting value $4\ \rho_0$ quite slowly, in accordance with the equation

$$\rho = 4\rho_0/(1 - 2Q\rho_0/p), \tag{2}$$

where Q is the total ionization and dissociation energy, $2Q\ \rho_0 = 4\times 10^{11}$ dyne/cm², so that, for example, $\rho = 6\rho_0$ is reached at $p = 10^{12}$ (10^6 atmos), when $T = 230$ ev $= 2.5\times 10^6$ degrees.

One can roughly estimate that a ten-fold compression is reached in the shock-wave over the entire range $T = 1$–100 ev of interest to us; the speed of the shock-wave is then (D–cm/sec, p–dyne/cm²)

$$D = 28\sqrt{p} \tag{3}$$

and the temperature (ev) is

$$T = 10^{-6.75}\,p^{3/4}. \tag{4}$$

A 100 ev temperature is reached at approximately 4.5×10^{11} pressure, after which the temperature increases linearly with the pressure. The above equations and relationships are obtained by interpolating the results of actual numerical calculations.

2. RADIATION OF SHOCK-WAVE

The ionization of the gas results in a continuous spectrum of emission and absorption of light. A layer of compressed air of sufficient thickness becomes opaque and radiates as a black body. For a first estimate of the role of radiation, let us compare the work required to compress the air with the radiation

* Gershanik, Rozlovskii, and the author[5] studied the chemical reactions using the compression shock wave produced in a shock tube setup, while Shluapintokh and the author[6] studied the compression in the shock wave of a bullet.

† Ionization of hydrogen and argon was treated by Prokof'ev.[7]

energy, both quantities being taken per square centimeter of front surface and per second.

The work of compression, or more accurately that portion of the work that is converted into heat energy, is $W = pu/2 = 13\,p^{3/2}$ (all CGS quantities). If T is given in ev, the black-body radiation is $S = 10^{12}T^4$ in accordance with the Stefan-Boltzmann law.

Substituting the expression for T we obtain the radiation flux

$$S = 10^{-15}\,p^3. \tag{5}$$

The ratio of the radiation flux to the compression work is $S/w = 8 \times 10^{-17}\,p^{3/2}$. This ratio becomes unity at $p = 5.5 \times 10^{10}$ and $T = 20$ ev. A conclusion suggests itself that the energy carried away by radiation in strong shock-waves can play a substantial role. An elementary calculation for the case of a strong point-source explosion, considered by Sedov[10], leads to a divergent integral. In Sedov's solution the radius of the spherical wave is $r \sim t^{2/5}$, and the pressure on the front is $p \sim r^{-3} \sim t^{-6/5}$, from which it follows that the total energy radiated

$$\int Sr^2\,dt \sim \int p^3 r^2\,dt \sim \int t^{-11/5}\,dt \tag{6}$$

diverges at small values of t, *i.e.*, in the initial stage, when the temperature is high, if expression (5) is used for S.

It must be borne in mind that actually the air ahead of the wave front is transparent only to visible light and to the adjacent portion of the spectrum. Quanta with energies 7–10 ev and higher experience very strong absorption even in cold air. Consequently, the radiation flux of the shock-wave increases as K^4 only as long as the temperature does not exceed 2–3 ev. At higher temperatures, the Wien maximum occurs already in the region of the spectrum absorbed by the cold air ahead of the front.

If the wave front has a high temperature (above 8–10 ev) the radiation energy in the transparent region for cold air increases as T, according to the Rayleigh-Jeans law. The ratio of the thermal losses of the shock-wave front to the work of compression actually passes through a maximum not exceeding 1%.

3. STRUCTURE OF WAVE WITH ALLOWANCE FOR RADIATION

The energy emitted by the wave front and absorbed by the air ahead of the front does not enter into the equation for the final state of the air compressed by the shock wave. However, the radiation heat exchange exerts a substantial effect on the structure of the wave.

The structure of the wave with allowance for radiation was considered in detail by Prokof'ev[7] who derived equations, determined transparency coefficients (using atomic hydrogen as an example), and examined the structure of the wave in monatomic hydrogen and argon. His treatment of the structure of the wave contains disagreements with our work, which will be discussed in detail below in Sec. 5. We shall give here qualitatively, without equations, our ideas concerning the structure of the wave.

The radiation emitted by the wave front heats the air ahead of the front. This heating is accompanied by increased pressure. The shock wave in the narrow sense of the word—the discontinuity in pressure and density—now propagates in heated gas.

As is known, the compression in a shock wave occurs in a zone whose thickness is on the order of the mean free path of the molecules and atoms. A layer of gas of this thickness is transparent at all temperatures. Thus, the compression follows the classical Hugoniot adiabatic line. Radiant cooling of the gas and asymptotic assumption of the final state occur only behind the compression, at a distance on the order of the path length of the radiation.

The structure of the front is shown schematically in Fig. 1, which shows the temperature distribution, and in Fig. 2, where it is shown in the (p, v) plane. The indices 1, A, B, and 2 of Figs. 1 and 2 pertain to identical states. From the condition that the entire pattern of Fig. 1 has a stationary propagation with equal velocity it follows that all points of Fig. 2 lie on a straight line. What is remarkable in Fig. 1 is the temperature peak B. At a given wave velocity, the compression of the heated gas A leads to a state B, in which the temperature is higher than in the final state 2, which is reached by compressing cold gas 1. An entirely different diagram is obtained if the radiant heat exchange is set approximately equal to the heat conduction (Fig. 3), and is an isothermal density jump appears at the origin. Actually, the narrow temperature peak, drawn in Fig. 3 dotted from the point $T3$, should appear also at high temperatures, when the heat conduction approximation would seem permissible. The presence of a temperature peak at Figs. 1 and 3 is closely related to the finite range of the radiation and to the fact that in the case of abrupt changes

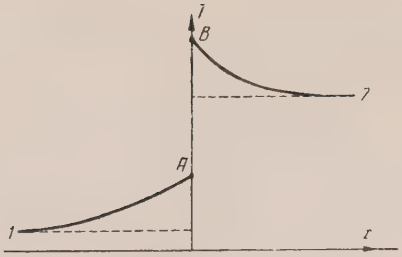

FIG. 1

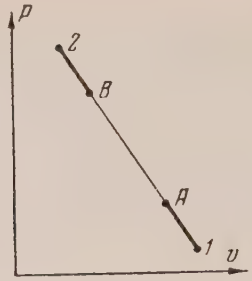

FIG. 2

of state, at distances less than the free path length, the differential equation of heat conductivity is not applicable. This will be treated in greater detail at the end of Sec. 5.

When we estimated the heat flux in the end of Sec. 2 we remarked on the absorption of ultraviolet by the cold air ahead of the front. In the visible portion of the spectrum, the cold air is transparent and the temperature of the wave can therefore be determined optically. However, as the temperature rises, the heating of the air ahead of the wave front, according to Fig. 1, causes the boundary of air absorption to shift towards the long-wave region; when the air ahead of the front becomes opaque, the visible temperature diminishes.

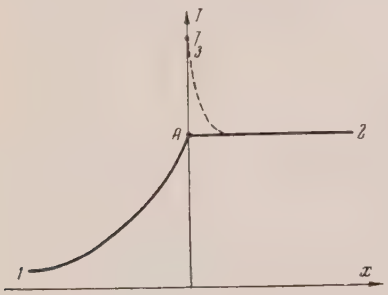

FIG. 3

Thus, in a monotonic increase of the shock wave temperature, the optically-measured temperature first coincides with the true temperature of the front and increases together with it, and then begins to lag the true temperature and passes through a maximum. These phenomena were observed by Model' in investigations[11] carried out in connection with our ideas. Similar phenomena were observed earlier by Vul'fson and his associates[14]. A quantitative examination of the theory of air radiation was made by Raizer[12].

4. ELECTRONIC HEAT CONDUCTION

Peculiar effects occur in strong shock waves with high ionization when allowances are made for the great difference between the electron and ion masses.

On one hand, the small mass of the electron means a high velocity of sound in the electron gas taken by itself. The shock wave is subsonic and slow relative to the electron gas. The electron and ion gases are bound to each other by electrostatic forces. The heat conduction of the electron gas is large, but the energy exchange between the electrons and ions is slow. If we specify the medium to be electrically neutral, we are left with finding density distribution at two different temperatures, T_i of the ions and T_e of the electrons.

Assuming the energy exchange between the electrons and ions to be the slowest process, we arrive in the limit at a following situation: at first the ions in the front of the shock wave heat up rapidly, and the electrons remain cold. The temperature is then gradually equalized in the compressed air—the ions become cooler and the electrons hotter. The ion temperature T_i is at first higher than the final temperature assumed by the ions and electrons after equalization (without heat losses).

If the energy exchange between electrons and ions is faster, we obtain the temperature distribution shown in Fig. 4. The front of the shock wave, *i.e.*, the density discontinuity, is at the origin. The electron temperature T_e is shown dotted, the ion temperature T_i is shown solid, with a discontinuity at the ordinate.

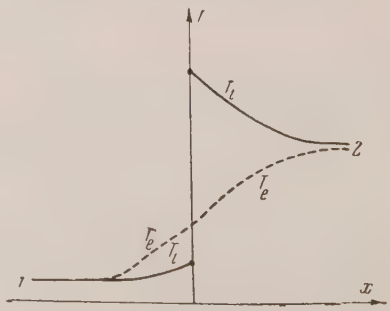

FIG. 4

The heating ahead of the front is due to the energy transferred by the electron heat conduction, while the electrons in turn heat the gases, so that $T_i < T_e$ at $x < 0$. The density discontinuity is accompanied by a sharp jump in the ion temperature T_i. The energy equation (in which the flow of heat transferred by the electron heat conduction must be allowed for) gives the connection between the sums of the electron and ion energies before and after the explosion. To make the system of equations complete, it is necessary to make use of the fact that the compression in a shock wave is slow relative to the electron gas.

Thanks to the electron heat conduction, T_e is not discontinuous on the density discontinuity surface. The work of compression of the electrons at the density discontinuity is given by the known expression $T_e \ln(\rho_2/\rho_1)$ (for one electron), and the equation of energy for the electron gas alone remains continuous

$$\lambda \frac{dT_e}{dx}\Big|_{\text{bef. raref.}} = \lambda \frac{dT_e}{dx}\Big|_{\text{aft. raref.}} + n_0 D T_e \ln \frac{\rho_2}{\rho_1}. \tag{7}$$

Here λ is the heat conduction, $\lambda dT_e/dx$ the heat flux, n_0 the electron density in the initial matter, and D the velocity of the wave. The energy equation for the ions is obtained by subtracting the equation for the electrons from the complete energy-balance equation. This results in a complete system of equations.

The substance remains electrically neutral because of electric fields that are particularly strong near the discontinuity. The potential difference is on the order of the temperature in the wave (T_e); a characteristic length is a quantity well known in electrochemistry, namely the thickness of the double layer, on the order of $\sqrt{T_e/n_0 e^2}$, from which we estimate the field to be $\sqrt{T_e n_0 e^2}$, where e is the electron charge. If $T_e = 300$ ev and $n_0 \sim 4 \times 10^{20}$ (ionized air), we obtain a thickness of 2×10^{-6} cm, and a field on the order of $1\text{–}2 \times 10^8$ v/cm.

The role of electrons pertains only to the extreme limiting case of shock waves of such intensity, that the ionization energy can be considered small. Only in this case is it possible to disregard the ionization process itself and the air prior to compression—evidently not ionized—can be considered as a mixture of cold electrons and ions. In this work we do not consider the considerably more complicated case of actual shock waves, in which the temperature is of the same order or lower than the ionization energy (see, for example, Ref. 3).

5. RIGOROUS THEORY OF WAVE STRUCTURE WITH ALLOWANCE FOR RADIATION

The previously cited article by Prokof'ev contains rigorous equations for the change in state of the substance in the wave front, and we shall make use of these equations. Let us remark immediately that the conclusions we reached by analysis of this equation differ from Prokof'ev's conclusions when it comes to the most important qualitative aspect of the problem. Prokof'ev proposes that in the presence of radiation the state of the gas varies continuously, whereas in our opinion a strong wave with radiation contains discontinuities in density, velocity, and temperature (see Figs. 1–4).

Using Prokof'ev's premises and notations, and using a coordinate system in which the wave is at rest, we have

$$\rho u = m, \quad p + \rho u^2 = p + mu = n, \tag{8}$$

$$m(\varepsilon_T + {}^1/_2 u^2) + pu + H = \tag{9}$$

$$m\varepsilon_I + nu - {}^1/_2 mu^2 + H = l,$$

where m, n, and l are constants, representing the flow of material, momentum, and energy, respectively. In the last equation ε_T is the internal (thermal) energy per unit mass of substance—a known single-valued function of p and ρ. H is the energy flux carried by the radiation. With the aid of the first two equations of (8) any two of the three quantities (u, p, ρ) can be expressed algebraically and uniquely in terms of the third.

In the absence of viscosity, all the intermediate states are represented as points on a straight line in the plane p, $v = 1/\rho$, the same as in the case of the detonation waves[13].

Prokof'ev chooses as his variable the dimensionless velocity $\tilde{u} = u/u_1$. It is evident that $\tilde{u} = v/v_1$.

The quantity H, *i.e.*, the thermal flux needed to effect any one of the intermediate states, can be expressed in terms of $\tilde{u}$ through the third equation of (9). The thermodynamic equation of state gives the temperature T as a function of $\tilde{u}$. The typical form of the dependences $H(\tilde{u})$ and $T(\tilde{u})$, shown in Fig. 5, is based on Fig. 11 of Prokof'ev's article.

The fact that $H \leq 0$ when $\tilde{u}_2 < \tilde{u}_1 < 1$ and $H = 0$ when $\tilde{u} = 1$ and $\tilde{u}_1 = \tilde{u}_2$ is a general property of shock waves. The presence of a temperature maxi-

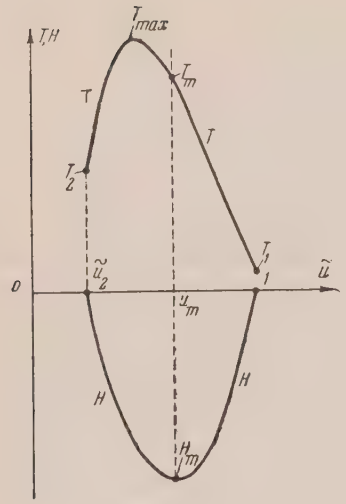

FIG. 5

mum is a characteristic of strong shock waves. Let us note that T reaches a maximum for a value of $\tilde{u}$ less than the value of $\tilde{u}$ corresponding to minimum H.

An examination of the emission and absorption of radiation yields the dependence of H on the temperature distribution; averaging over the frequencies and denoting $\sigma T^4 = \Theta$ (σ is the Stefan-Boltzmann-law constant) we can write down Eq. (20) of Ref. 7 [for the meaning of E_2 see Eq. (11) below] as

$$H = 2\int_{-\infty}^{\tau} \Theta(\zeta)\, E_2(\tau-\zeta)\, d\zeta - 2\int_{\tau}^{\infty} \Theta(\zeta)\, E_2(\zeta-\tau)\, d\zeta. \tag{10}$$

The coordinate x is replaced here by the optical thickness τ, $d\tau = \varkappa dx$, where $\varkappa$ is the coefficient of absorption.

The equation expresses the radiation flux through the τ plane as a sum of fluxes from individual layers $d\xi$, taken with a plus sign if $\xi < \tau$, and with a minus sign if $\xi > \tau$. The fraction of the transmitted flux is given by the function

$$2E_2(\tau-\zeta) = 2\int_1^{\infty} s^{-2} e^{-(\tau-\zeta)s}\, ds, \tag{11}$$

obtained by integrating the contribution of the oblique rays over all the angles. The assumptions under which it is possible to go from the integral expression for H to the differential equation (2) (Ref. 7), namely,

$$\frac{d^2H}{d\tau^2} = \frac{H}{\alpha^2} + \frac{2}{\alpha}\frac{d\Theta}{dx}, \tag{12}$$

are fully equivalent to replacing the function $2E_2(\xi)$ by the exponent $\exp(-\xi/\alpha)/\alpha$, where α is a dimensionless number that differs little from unity.

To prove this, let us write the corresponding approximate expression

$$H = F - G;\quad F = \int_{-\infty}^{\tau} \Theta(\zeta)\frac{1}{\alpha} e^{(\zeta-\tau)/\alpha}\, d\zeta,$$
$$G = \int_{\tau}^{\infty} \Theta(\zeta)\frac{1}{\alpha} e^{(\tau-\zeta)/\alpha}\, d\zeta. \tag{13}$$

We obtain

$$dF/d\tau = \Theta/\alpha - F/\alpha;\quad dG/d\tau = -\Theta/\alpha + G/\alpha, \tag{14}$$

$$\frac{d^2F}{d\tau^2} = \frac{1}{\alpha}\frac{d\Theta}{d\tau} - \frac{\Theta}{\alpha^2} + \frac{F}{\alpha^2};$$

$$\frac{d^2G}{d\tau^2} = -\frac{1}{\alpha}\frac{d\Theta}{d\tau} + \frac{G}{\alpha^2} - \frac{\Theta}{\alpha^2}, \tag{15}$$

$$\frac{d^2H}{d\tau^2} = \frac{d^2F}{d\tau^2} - \frac{d^2G}{d\tau^2} = \frac{2}{\alpha}\frac{d\Theta}{d\tau} + \frac{1}{\alpha^2}H. \tag{16}$$

Let us note that α in the two terms of Eq. (16) must be the same, so that the radiation from a half space uniformly heated to a temperature T and adjacent to a vacuum is identically equal to $\Theta = \sigma T^4$.

One can notice that the expression H with the exponents (13) is the Green function of differential equation (12). It is evident from Eq. (13) that H is continuous and cannot experience finite jumps; in particular, if T and Θ are discontinuous, the first derivatives $dF/d\tau$, $dG/d\tau$, and $dH/d\tau$ become discontinuous, but not the quantities F, G, and H themselves.

It is further evident that the quantity H_{max} determined from Eqs. (10) or (13) satisfies the inequality $|H| < \Theta_{max}$, where Θ_{max} corresponds to the maximum temperature T_{max}. Consequently, at low temperatures, when $\Theta_{max} < |H_m|$ where H_m is the extremum of the flux of H as determined from Eq. (9), the equation $H(u) = F - G$ cannot be satisfied for all values of u and a discontinuity in the solution [a discontinuity in the function $u(\tau)$] is unavoidable. At low temperatures, this situation in unavoidable, since $H_{max} \sim T$ and $\Theta_{max} \sim T^4$.

In this respect, the case of small radiation differs from the case of low viscosity: if the viscosity μ is low, the curve $u(x)$ is continuous, decreasing u decreases the width of the zone, and $du/dx \sim 1/\mu$, but

if μ is finite the derivative du/dx is everywhere finite.

In the case of a small but finite radiation, when $\Theta_{max} < |H_m|$, the solution must have an infinitesimally thin discontinuity, if we disregard other dissipative factors (viscosity).

Let us now consider the general case, when Θ_{max} is not small. Let us introduce the quantity

$$K = (F + G)/2. \tag{17}$$

From the definition of integrals F and G it follows that K, like H, is continuous; in addition

$$\begin{aligned} &\text{at} \quad \tau = -\infty, \ H = 0, \ K = \Theta_1 = \sigma T_1^4, \\ &\text{at} \quad \tau = +\infty, \ H = 0, \ K = \Theta_2 = \sigma T_2^4. \end{aligned} \tag{18}$$

From Eqs. (13)–(15) we get

$$dH/d\tau = 2(\Theta - K)/\alpha, \quad dK/d\tau = -H/2\alpha. \tag{19}$$

Dividing one by the other we eliminate τ and obtain an equation that can be investigated in the "phase plane" H, K (see Fig. 6):

$$dK/dH = H/4(K - \Theta). \tag{20}$$

From the integral definitions of H and K it follows that neither can be discontinuous.

A feature of the investigation is that H does not vary monotonically: if a continuous solution exists, H varies in the wave from zero in the initial state to H_m somewhere in the middle (region I), and then from H_m to 0 (region II).

Since $H(u)$ and $\Theta(u)$ are functions of a single parameter u, an expression can be found for $\Theta(H)$. This relationship, however, is not unique, and the curve $\Theta(H)$ has two branches with respect to the two regions of the variation of H.

We denote this curve by $\Theta_a(H)$ in the first region (between the initial state and the extremum H_m) and by $\Theta_b(H)$ in the second region (between the minimum and the final state). In particular, $\Theta_a(0) = \Theta_1$, $\Theta_b(0) = \Theta_2$, and $\Theta_a(A_m) = \Theta_b(A_m) = \Theta_m$.* Graphically, $\Theta(H)$ for a strong wave is shown solid in Fig. 6. In the K, H plane the line $K = \Theta(H)$ is the isocline of infinity. The differential equation (20) should be written separately for each region

$$\begin{aligned} dK_a/dH &= H/4(K_a - \Theta_a), \\ dK_b/dH &= H/4(K_b - \Theta_b) \end{aligned} \tag{21}$$

with boundary conditions (argument of function H):

$$K_a(0) = \Theta_1 = \Theta_a(0), \ K_b(0) = \Theta_2 = \Theta_b(0). \tag{22}$$

The surface of Fig. 6 is thus bifoliate with a common intersection along the vertical $H = H_m$.

If a solution exists in which all the quantities in the wave vary continuously, the transition from one branch to the other should occur at $H = H_m$.

$$K_a(H_m) = K_b(H_m) \tag{23}$$

should be satisfied for the values of K_a and K_b satisfying Eqs. (21) and (22).

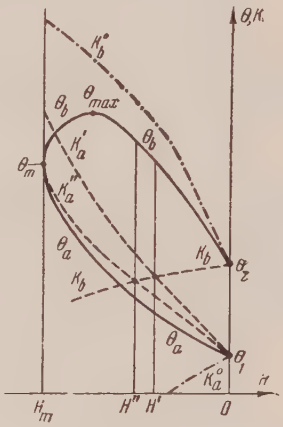

FIG. 6

An examination of the signs of the derivatives affords a ready qualitative picture of the field of the isoclines and of the behavior of the integral curves K_a and K_b. If $H = 0$, the equation has a saddle-point singularity in both cases (regions I and II). Two integral curves emerge from each saddle point.

The value of K is determined from Eqs. (17) and (13) and can be rewritten as a single integral

$$K(x) = \frac{1}{2}\int_{-\infty}^{\infty} \Theta(\zeta)\, e^{-|x-\zeta|/\alpha}\, \frac{d\zeta}{\alpha}, \tag{24}$$

from which it follows, by the theorem of the mean, that

$$\Theta_{min} < K < \Theta_{max}. \tag{25}$$

On this basis, it is possible to discard immediately the lower integral curve emerging from point Θ_1 in region I, shown in Fig. 6 by dash-dot lines, and

* Let us remark that the value of Θ at $H = H_m$, denoted Θ_m, is somewhat smaller than the maximum value of Θ reached in region II, denoted Θ_{max}.

marked K_a^0, since $K < \Theta_1 = \Theta_{min}$ on this curve. One can analogously discard the upper dash-dot integral curve in region II (K_b^0) emerging from the point $\Theta = \Theta_2$ on the $H = 0$ axis, for this curve is in its entirety above the line $\Theta_b(H)$; consequently, we obtain on the upper curve $K > \Theta_{max}$ in contradiction with condition (25).

The solution should therefore consist of an upper line K_a and a lower line K_b. The upper line K_a may reach the vertical line $H = H_m$ either at $\Theta > \Theta_m$ (see Fig. 6, K_a') or else at the point $\Theta = \Theta_m$ itself (see Fig. 6, K_a''), which is a singular point.

The realization of any one particular case depends on the numerical values of the function Θ. In any case, the only line K_a that can emerge from the saddle point $H = 0$, $\Theta = \Theta_1$ cannot intersect the line $\Theta_a(H)$, so that

$$K_a(H_m) \geqslant \Theta_m. \tag{26}$$

Exactly the same way, the line K_b chosen in accordance with condition (25) does not intersect the corresponding line Θ_b

$$K_b(H) < \Theta(H), \quad H_m < H < 0. \tag{27}$$

But in this case it follows from the differential equation (20) that $dK/dH > 0$, and we obtain a stronger condition

$$K_b(H) < \Theta_2 = \Theta_b(0). \tag{28}$$

A plot of K_b is also shown in Fig. 6.

Since $\Theta_2 < \Theta_m$ for strong shock waves, it follows from inequalities (26) and (28) that $K_a(H_m)$ and $K_b(H_m)$ cannot coincide, and consequently no solution exists in which H varies continuously from 0 to H_m on one branch and then from H_m to 0 on the other branch.

Actually H varies from 0 to H' or H'' along the lines K_a' or K_a'' and then (at the point of intersection with line K_b) there is a transition to line K_b and the value of H varies back from H' or H'' to zero.

The transition from line K_a to line K_b at the intersection point represents a shock wave in a limited sense of the word—a discontinuity of ρ, u, and Θ—the width of which is no longer dependent on the radiation (see above). H and K are conserved in this discontinuity. The conservation of H denotes that the quantities ρ, u, and Θ to the left and to the right of the discontinuity are related by the ordinary Hugoniot equation. The values of Θ to the left and to the right of the discontinuity are given by the intersection points of the curves Θ_a and Θ_b with the vertical $H = H'$ or $H = H''$ (see Fig. 6).

As can be seen from the inequalities and from Fig. 6

$$\Theta_2 > K_b(H') = K_a'(H') > \Theta(H'), \tag{29}$$

i.e., the temperature, to which the gas can be heated by radiation ahead of the discontinuity front cannot exceed the final gas temperature $\Theta(H') < \Theta_2$ (the same result is obtained when K_a'' is realized also on the discontinuity $H = H''$).

This result is not as trivial as it appears at first glance, for behind the discontinuity front there is a temperature peak, in which $\Theta_b > \Theta_2$ (see Fig. 1).

How were the continuous solutions obtained in Prokof'ev's work? It can be shown that in the continuous solution proposed by him, at the point where $H = H_m$, $dH/d\tau$ experiences a discontinuity and H has a cusp. According to the initial equation (12), a discontinuity in $dH/d\tau$ is possible only in the point where the quantity Θ and the gas temperature uniquely related with it experience a discontinuity. Yet in Prokof'ev's solution the temperature is continuous.

The continuous solution derived by Prokof'ev is thus unacceptable.

Let us remark, finally, that replacing E_2 by the exponent [see Eqs. (10), (11), and (13)] (*i.e.*, a rough allowance for the oblique rays) is a poor approximation in the presence of a temperature discontinuity. One can assume that precise analysis will show that the fact itself that discontinuities are unavoidable when $\Theta_b > \Theta_2$ will remain in force*, but that the temperature discontinuities will be accompanied by singularities in the derivatives to the left and to the right of each discontinuity.

I take this opportunity to thank N. A. Dmitriev, the late S. P. D'iakov, A. S. Kompaneets, L. D. Landau, I. Sh. Model', V. A. Prokof'ev, and Iu. P. Raizer for valuable discussions.

---

[1] H. Muraour and M. Levy, Compt. rend. 198, 825, 1499, 1760, 2091 (1934).

[2] Ia. B. Zel'dovich and O. I. Leipunskii, J. Exptl. Theoret. Phys. (U.S.S.R.) 13, 183 (1943).

---

* Actually, if there is no discontinuity, the absence of a solution again becomes valid proof of a smooth distribution of temperature.

[3] Resler, Lin, and Kantrowitz, J. Appl. Phys. **23**, 1390 (1952); A. Kantrowitz, Sci. American **191**, 132 (1954).
[4] R. H. Christian and F. L. Yarger, J. Chem. Phys. **23**, 2042 (1955).
[5] Gershanik, Zel'dovich, and Rozlovskii, Zhur. Fiz. Khim. **24**, 85 (1950).
[6] Ia. B. Zel'dovich and I. Ia. Shliapintokh, Dokl. Akad. Nauk SSSR **65**, 871 (1949).
[7] V. A. Prokof'ev, Uch. zap. MGU (Sci. Records of Moscow State Univ.) **172**, Mechanics, p 79 (1954).
[8] D. R. Davies, Proc. Phys. Soc. **61** (B), 105 (1948).
[9] Christian, Duff, and Yarger, J. Chem. Phys. **23**, 2045 (1955).
[10] L. I. Sedov, *Similarity and Dimensionality Methods in Mechanics*, 3rd Ed., Moscow, GTTI (1954).
[11] I. Sh. Model', J. Exptl. Theoret. Phys. (U.S.S.R.) **32**, 714 (1957); Soviet Physics JETP **5**, 589 (1957).
[12] Iu. P. Raizer, J. Exptl. Theoret. Phys. (U.S.S.R.) **32**, 1528 (1957); Soviet Physics JETP, **5** (in press).
[13] Ia. B. Zel'dovich, J. Exptl. Theoret. Phys. (U.S.S.R.) **10**, 550 (1940).
[14] Vul'fson, Libin, and Charnaia, Izv. Akad. Nauk SSSR, ser. fiz. **19**, 61 (1955).

Translated by J. G. Adashko
231

SOVIET PHYSICS JETP VOLUME 5, NUMBER 5 DECEMBER, 1957

Resonant Pion-Nucleon Interaction and Production of Pions by Nucleons

L. M. SOROKO

(Submitted to JETP editor June 11, 1956)
J. Exptl. Theoret. Phys. (U.S.S.R.) **32**, 1136-1142 (May, 1957).

The production of pions by nucleons is studied in an attempt to take approximate account of the strong pion-nucleon interaction. The calculation is based on the assumption that the probability of the process $N + N \to \pi + N + N'$ is determined by the energy of the created pion relative to one of the nucleons. Using experimental values for the matrix elements of the pion-nucleon interaction, we calculate the spectrum of pions and nucleons in the reaction $N + N \to \pi + N + N'$, and also the intensity of pion emission as a function of the angle between pion and nucleon. The results are compared with experiment.

IT IS NOW firmly established that the pion-nucleon interaction is strong in the P-state with total angular momentum $J = 3/2$ and isotopic spin $T = 3/2$. Upon this fact is based the hypothesis of a nucleon isobar state, formulated by Brueckner[1] and by Tamm and his collaborators[2]. To compare the consequences of this hypothesis with experiment, several properties of the production of pions by nucleons have been calculated[3]. Belen'kii and Nikishov[4] evaluated the relative magnitudes of single and multiple pion production, including both direct production and production through an intermediate isobar state. Many authors, for example Aitken *et al.*[5], have calculated pion production by nucleons taking the strong pion-nucleon interaction into account explicitly.

Instead of making such direct calculations, one can establish a phenomenological correspondence between two processes. Assuming that the matrix element for the process

$$N + N \to \pi + N + N', \tag{1}$$

depends only on the relative energy of the pion and one nucleon, the magnitude and the energy-dependence of the production cross-section can be obtained from the experimental values of the total cross-section for pion-nucleon scattering. In order that the strong pion-nucleon interaction shall appear in the process (1), it is only necessary[6] that the isotopic spin of the two nucleons in the initial state should be $T = 1$.

1. THE PION-NUCLEON INTERACTION MATRIX ELEMENT IN STATES WITH $T = 3/2$

The cross-section for a reaction

$$A + b \to C + d \tag{2}$$

is completely determined by a matrix element H according to the formula

$$d\sigma(\vartheta)/d\Omega = (2\pi/\hbar)\,|H(\vartheta)|^2\,p^2/2\pi^2\hbar^3\,(v_C + v_d)\,v_{Ab}, \qquad (3)$$

where p is the momentum of particles C and d, v_c and v_d are their respective velocities in the center-of-mass system, and v_{Ab} is the relative velocity of collision of particles A and b. The total cross-section, apart from irrelevant constant factors, is given by

$$\sigma = |H_t|^2\,p^2/(v_C + v_d)\,v_{Ab}. \qquad (4)$$

The matrix element of the pion-nucleon interaction was deduced[7] from experimental values of the total cross-section for pion-proton scattering in the energy range from 30 to 400 Mev. Figure 1 shows the values we have used for the total cross-section, agreeing satisfactorily with a resonance curve[6]. Figure 2 shows the dependence of the squared matrix element on pion energy; this curve is the basis of the subsequent calculations. In Fig. 3 we show the total cross-section for photo-production of neutral pions in hydrogen, deduced from the matrix element plotted in Fig. 2. From the agreement of the

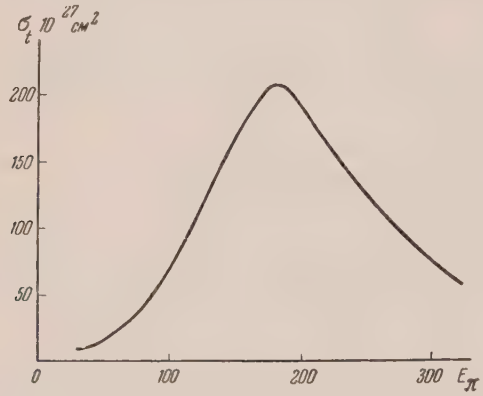

FIG. 1

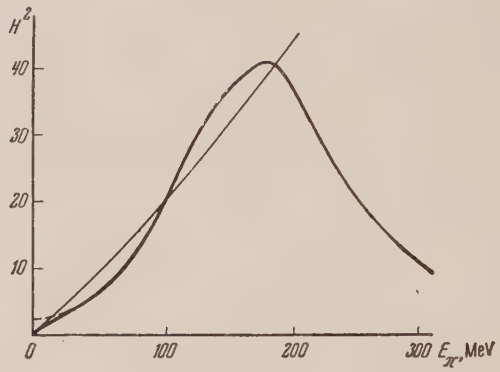

FIG. 2

FIG. 1. Total $\pi^+ - p$ scattering cross-section given by the formula $\sigma_t(\pi^+ p) = 2\pi\lambda^2\Gamma^2/[(E - E_0)^2 + \Gamma^2/4]$; $\Gamma = 2b\,(a/\lambda)^3/[1 + (a^2/\lambda)^2]$; $a = 1.4\hbar/\mu c$, $b = 75$ Mev. $E_0 = 154$ Mev, E_π is the pion energy in the center-of-mass system.

FIG. 2. The squared pion-nucleon interaction matrix element in the state with isotopic spin $T = 3/2$, as a function of pion energy. The lighter curve shows the result of a p^2 dependence in the center-of-mass system.

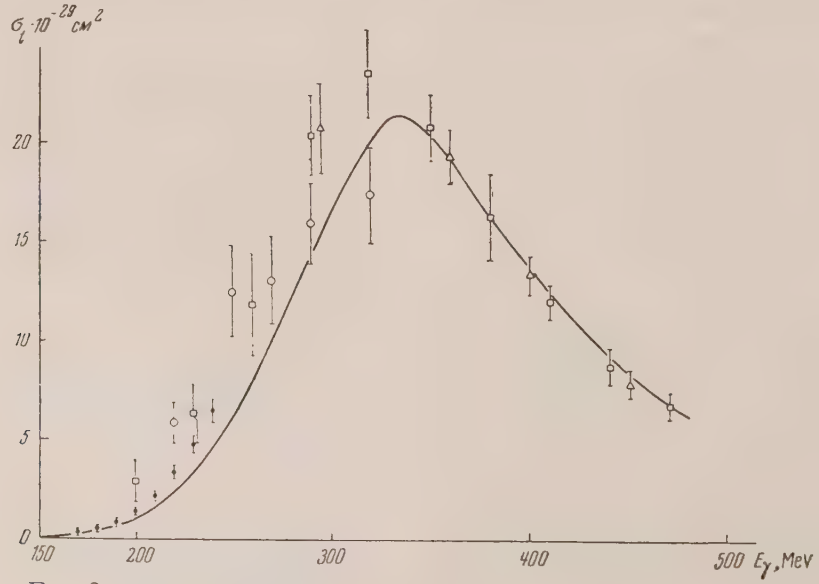

FIG. 3. Total π^0 photoproduction cross-section as a function of photon energy. Experimental points, ●—Ref. 12, □—Ref. 13, ○—Ref. 14, △—Ref. 15.

calculated curve with the experimental points[12–15], one may conclude that the processes $\pi^+ + p \to \pi^+ + p$ and $\gamma + p \to \pi^0 + p$ proceed through the same matrix element.

2. PION SPECTRUM IN THE PROCESS $N + N \to \pi + N' + N$.

The vector diagram of the momenta of three particles (Fig. 4) forms a closed triangle. The position of the vertex A of the triangle is fixed by energy conservation[8], thus

$$(p_1^2 + p_2^2)/2M + \sqrt{p^2 + m^2} = W. \tag{5}$$

Here W is the combined kinetic energy of the two colliding nucleons in the center-of-mass system, m and M are the pion and nucleon masses, and p, p_1, p_2 are their momenta. In this approximation, the locus of the vertex A of the vector triangle is a sphere in momentum space with radius

$$R = [M(W - \sqrt{p^2 + m^2}) - {}^1/_4 p^2]^{1/2}. \tag{6}$$

The probability for emitting a pion of momentum p is

$$1/\tau = |H|^2 R(p;\ W)\, p^2 dp, \tag{7}$$

and the differential cross-section is

$$d\sigma/dp = v_{NN}^{-1} |H|^2 R(p;\ W)\, p^2. \tag{8}$$

If H is independent of energy and angle, then

$$d\sigma/dp = (p^2/v_{NN})\, R(p;\ W). \tag{9}$$

For given pion momentum and auxiliary angle θ (see Fig. 4), the energy of the pion relative to a nucleon at rest is

$$E_{\pi N}(p,\ \theta;\ W) = \sqrt{p^2 + m^2}\ \sqrt{1 + (R^2 + {}^1/_4 p^2 - Rp\cos\theta)/M^2} - pR\cos\theta/M + p^2/2M - m. \tag{10}$$

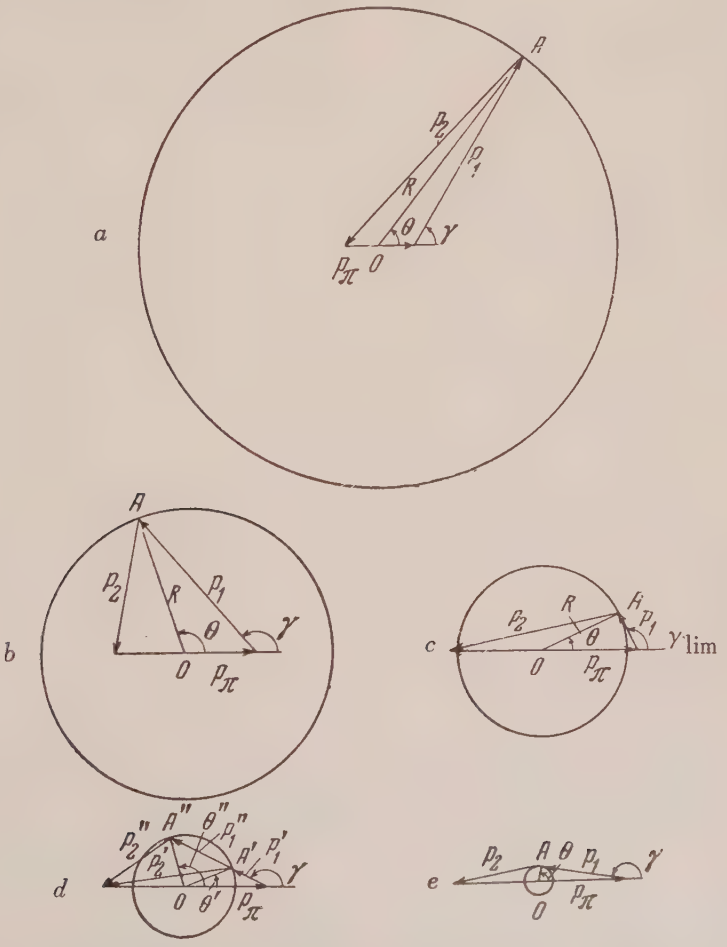

FIG. 4. Vector diagrams for the three particle momenta in the reaction $N + N \to \pi + N + N'$ center-of-mass system. The pion momentum p_π is 100, 200, 232, 240, 248 Mev/c in the five diagrams.

Equation (10) implies that a fixed pion momentum corresponds to a certain range of values for $E_{\pi N}$. The pion spectrum is finally given by

$$\frac{d\sigma}{dp} = \frac{p^2}{v_{NN}(W)} R(p;W) \int_{-1}^{+1} d\cos\theta \{H[E_{\pi N}(p, \theta; W)]\}^2. \quad (11)$$

Calculations have been made for a total energy $W = 300$ Mev, corresponding to an incident proton energy $E_p = 650$ Mev. Figure 5 compares the averaged matrix element $H(p_\pi)$ defined by the expression

$$H(p_\pi) = \left[\int_{-1}^{+1} d\cos\theta \{H[E_{\pi N}(p, \theta; W = 300)]\}^2\right]^{1/2}, \quad (12)$$

with the empirical matrix element

$$H_e = \left[\frac{d^2\sigma}{dp d\omega} \frac{1}{p^2 R(p; W)}\right]^{1/2},$$

derived from production experiments[9].

Figure 5 shows that the graph of $H(p_\pi)$ does not start at the origin but has a finite intercept on the vertical axis. This is a consequence of the motion of the nucleons, which have rather large momenta even for $p_\pi = 0$. It is also remarkable that $H(p_\pi)$ has no maximum, although the pion energy in the center-of-mass system can go up to 150 Mev. The cause of this "sluggishness" is the averaging over energy which occurred in the definition of the matrix element. Calculations show that a maximum appears in the graph of $H(p_\pi)$ at an incident energy $E_p \sim 750$ Mev.

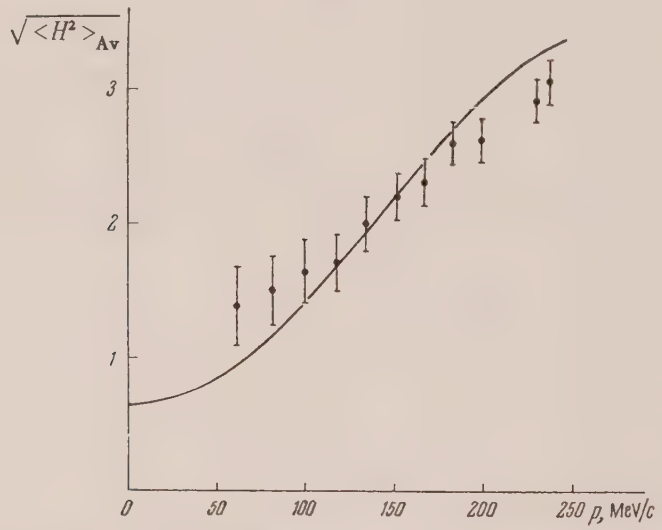

FIG. 5. Dependence of $\sqrt{\langle H^2\rangle_{Av}}$ on pion momentum in center-of-mass system. Experimental points taken from Ref. 9 at $E_p = 657$ Mev.

3. NUCLEON SPECTRUM IN THE PROCESS $N + N \to \pi + N' + N$.

The vector diagram of the momenta which determine the nucleon spectrum has the property that the locus of the vertex A is not a circle with center at O, so that the distance $OA = \rho(\theta_1)$ is a function of the angle θ_1.

If the momentum p_1 of one nucleon and the angle θ_1 are fixed, the relative energy of the pion and nucleon is

$$E_{\pi N}(p_1, \theta_1; W) = [(1 + p_1^2/M^2)(m^2 + \rho^2 + p_1^2/4 - \rho p_1 \cos\theta_1)]^{1/2} + p_1^2/2M - p_1 \rho \cos\theta_1 / M - m, \quad (13)$$

and the differential cross-section has the form

$$\frac{d\sigma}{dp_1} = \frac{p_1^2}{v_{NN}(W)} \times \int_{-1}^{+1} \rho(p_1, \theta_1; W) \{H[E_{\pi N}(p_1, \theta_1; W)]\}^2 d\cos\theta. \quad (14)$$

with the function $\rho = \rho(p_1, \theta_1; W)$ defined by the parametric representation

$$\rho^2 + {}^1/_4 p_1^2 - p_1 \rho \cos\theta_1 = p^2,$$
$$p_1^2 + 2p_1 \rho \cos\theta_1 = 2M(W - \sqrt{p^2 + m^2}) - p^2, \quad (15)$$

where the parameter p is in fact the pion momentum.

Figure 6 shows the nucleon spectra, calculated at energy $E_p = 650$ Mev, for the case of a resonant interaction H and for the case of an interaction whose matrix element is constant. The spectra differ significantly only near the upper limit, where the resonant interaction gives a less steep descent to zero. The results apply only to σ_{i0} transitions in which the nucleon isotopic spin changes from 1 to 0. The proton spectra experimentally observed[10] at energy $E_p = 650$ Mev include not only σ_{i0} but also σ_{i1} transitions, and the latter occur with triple weight because of the existence of the process $p + p \to \pi^0 + p + p$. The spectrum of σ_{i1} transitions has not been calculated, and therefore a decisive comparison with the experimental results cannot be made. Still it seems that the σ_{i0} and σ_{i1} spectra should not differ essentially in the immediate neighborhood of the upper limit.

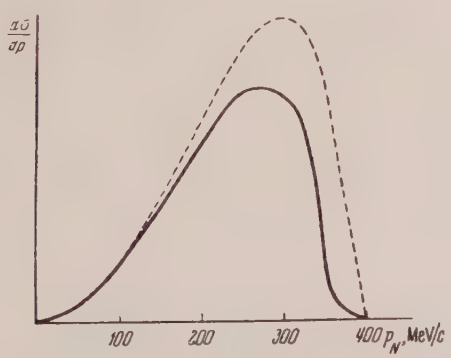

FIG. 6. Nucleon spectra from the reaction $N+N \to \pi + N + N$ at $E_p = 657$ Mev; σ_{i0} transitions only.

4. PION-NUCLEON ANGULAR CORRELATIONS

The dependence of the cross-section for reaction (1) upon the angle γ between the pion and one nucleon has some peculiarities arising from energy and momentum conservation alone. Figure 4 shows vector diagrams of the momenta corresponding to various regions of the pion spectrum. When the pion momentum is large, the angle between pion and nucleon becomes concentrated into the region $\gamma > 90°$. For $p_\pi > 230$ Mev/c and $W = 300$ Mev, angles $\gamma < 90°$ cannot occur.

The probability $W(\gamma)$ can be expressed in terms of the pion momentum and the matrix element $H(E_{\pi N})$. We find

$$W(\gamma, p)\, d\gamma\, dp = |H|^2 p^2 R(p; W) \times \frac{d\cos\theta}{d\cos\gamma} \sin\gamma\, d\gamma\, dp. \quad (16)$$

The quantity $(d\cos\theta/d\cos\gamma)$ is obtained from the geometrical relations

$$p_1^2 = R^2 + {}^1/_4 p^2 - Rp\cos\theta,$$
$$R\cos\theta = {}^1/_2 p + p_1 \cos\gamma, \quad (17)$$

hence the final expression for $W(\gamma)$ is

$$\frac{W(\gamma, p)}{\sin\gamma} d\gamma dp = |H|^2 p^2 R(p; W) \left\{\left[1 - \left(\frac{p}{2R}\right)^2 \sin^2\gamma\right]^{1/2} + \left(\frac{p}{2R}\right)^2 \cos^2\gamma \left[1 - \left(\frac{p}{2R}\right)^2 \sin^2\gamma\right]^{-1/2} - \frac{p}{R}\cos\gamma\right\} d\gamma\, dp. \quad (18)$$

Equation (18) shows that $W(\gamma) \approx \sin\gamma$ only for pion momenta close to zero. In the region $p > 2R$, angles $\gamma < 90°$ are forbidden.

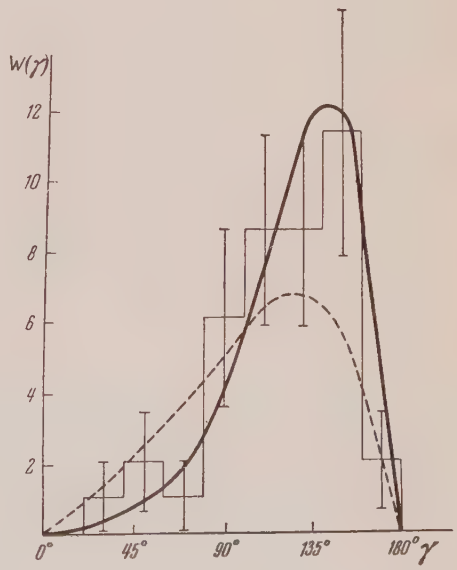

FIG. 7. Pion production probability as a function of angle γ between pion and nucleon in center-of-mass system. Experimental histogram from Ref. 11.

Figure 7 shows the functions $W(\gamma)$ calculated for a resonant H (full curve) and for a constant H (dotted curve). Also shown is the experimental histogram obtained[11] at a proton energy of 650 Mev. Although the statistics are not very good, it is clear from Fig. 7 that the experiment agrees better with a resonant than with a constant interaction.

The author thanks M. G. Meshcheriakov, B. S. Neganov, V. P. Zrelov, I. K. Vzorov, and A. F. Shabudin for information about their experimental results, and also L. M. Lapidus for valuable advice and criticism.

[1] K. Brueckner, Phys. Rev. **86**, 106 (1952).
[2] Tamm, Gol'fand and Fainberg, J. Exptl. Theoret. Phys. (U.S.S.R.) **26**, 649 (1954).
[3] D. C. Peaslee, Phys. Rev. **94**, 1085 (1954).
[4] S. Z. Belen'kii and A. I. Nikishov, J. Exptl. Theoret. Phys. (U.S.S.R.) **28**, 744 (1955); Soviet Phys. **1**, 593 (1955).
[5] Aitken, Mahmoud, Henley, Ruderman and Watson, Phys. Rev. **93**, 1349 (1954).
[6] M. Gell-Mann and K. M. Watson, Annual Rev. Nucl. Sci. **4**, 219 (1954).
[7] H. A. Bethe and F. DeHoffmann, *Mesons and Fields* [Row, Peterson (Evanston 1955)] Vol. **2**, 130.
[8] I. L. Rozental', J. Exptl. Theoret. Phys. (U.S.S.R.) **28**, 118 (1955); Soviet Phys. **1**, 166 (1955).
[9] Meshcheriakov, Zrelov, Neganov, Vzorov and Shabudin, J. Exptl. Theoret. Phys. (U.S.S.R.) **31**, 45 (1956); Soviet Phys. **4**, 60 (1957).
[10] Meshcheriakov, Neganov, Zrelov, Vzorov and Shabudin, Dokl. Akad. Nauk SSSR, **109**, 499 (1956); Soviet Phys. "Doklady," **1**, 447 (1957).
[11] L. Riddiford, *Proton-proton interaction at 650 Mev*, Report to Liverpool Conference (1955).
[12] F. E. Mills and L. J. Koester, Phys. Rev. **98**, 210 (1955).
[13] Watson, Keck, Tollestrup and Walker, Phys. Rev. **101**, 1159 (1956).
[14] Goldschmidt-Clermont, Osborne and Scott, Phys. Rev. **97**, 188 (1955).
[15] D. C. Oakley and R. L. Walker, Phys. Rev. **97**, 1283 (1955).

Translated by F. J. Dyson
232

SOVIET PHYSICS JETP VOLUME 5, NUMBER 5 DECEMBER, 1957

Model of a Semi-transparent Nucleus with a Diffuse Boundary, II

P. E. NEMIROVSKII

(Submitted to JETP editor June 12, 1956)
J. Exptl. Theoret. Phys. (U.S.S.R.) **32**, 1143-1149 (May, 1957)

A new method is presented for calculating nuclear interaction cross-sections for low energy neutrons. Assuming that no absorption occurs in the surface layer, it is shown that the energy dependence of the cross-section at low energy is the same for a potential with diffuse boundary as for a rectangular well. The capture cross-section is larger for the diffuse than for the sharp boundary. Values of the parameters and of the nuclear potential are found which give satisfactory agreement with experiment over a wide range of nuclear weights and energies.

IN AN EARLIER PAPER[1] we reported results of calculations of cross-sections for a semi-transparent nuclear model with diffuse boundary. We found good agreement of the capture of cross-sections transparent nuclear model with diffuse boundary. We found good agreement on the capture of cross-sections with experiment, up to an energy of a few million volts, with the following values of the parameters:

$$V(r) = 20\,\text{MeV} \quad \text{for} \quad r \leqslant r_0,$$

$$V(r) = 20 \exp\{-(r - r_0)/1.4 \cdot 10^{-13}\} \quad \text{for} \quad r \geqslant r_0,$$

$$r_0 + 1.4 \cdot 10^{-13} = 1.25 \cdot 10^{-13} A^{1/3}\ \text{cm}.$$

The imaginary part $\zeta V(r)$ of the potential was variable. However, it has since been reported[2] that the potential $V(r)$ should be 42 Mev. Also it seems appropriate to compare the calculated results with a

wider range of experimental data, in order to test the diffuse-boundary model and to choose the most satisfactory set of parameters to describe nuclear matter. Therefore we decided to carry out calculations of total cross-sections for the diffuse-boundary model at low energies. We found some devices which allow us to simplify the calculation to the point where numerical computations are avoided.

1. CALCULATION OF PHASE-SHIFT

Suppose $V = V(r_0)$ for $r \leq r_0$. A boundary condition must be satisfied at $r = r_0$. The internal wave-function at $r = r_0$ is evidently

$$\Psi_l^{(i)} = (X + i\xi)^{-1/2} J_{l+1/2}(X + i\xi), \qquad (1)$$

with $X = K_0 r_0$, $\xi = \varkappa r_0$, where K and $\varkappa$ are the real and imaginary parts of the wave-number. We write

$$d \ln \Psi_l^{(i)}/dX = (K/K_0) A_l. \qquad (2)$$

Then the boundary condition is

$$A_l = \frac{1}{\Psi_l^{(a)}} \frac{d\Psi_l^{(a)}}{dx} \quad \text{for} \quad r = r_0 \qquad (3)$$

where $x = kr$, and $X_l^{(a)}$ is the wave-function for $r \geq r_0$. But

$$\Psi_l^{(a)} = \Psi_l^{\mathrm{II}} + \eta_l \Psi_l^{\mathrm{I}},$$

where Ψ_l^{I} represents an outgoing wave at $x = \infty$, and Ψ_l^{II} an ingoing wave. Substituting (3a) into (3), we obtain

$$A_l = \left(\frac{d\Psi_l^{\mathrm{II}}}{dx} + \eta_l \frac{d\Psi_l^{\mathrm{I}}}{dx} \right) / (\Psi_l^{\mathrm{II}} + \eta_l \Psi_l^{\mathrm{I}}), \qquad (4)$$

and hence

$$\eta_l = \left(A_l \Psi_l^{\mathrm{II}} - \frac{d\Psi_l^{\mathrm{II}}}{dx} \right) \Big/ \left(\frac{d\Psi_l^{\mathrm{I}}}{dx} - A_l \Psi_l^{\mathrm{I}} \right) \qquad (5)$$

Obviously, Ψ_l^{I} and Ψ_l^{II} can be written in the form

$$\begin{aligned} \Psi_l^{\mathrm{I}} &= x^{-1/2} H_{l+1/2}^{(1)}(x)\, v_l^{(1)}(x), \quad \Psi_l^{\mathrm{II}} \\ &= x^{-1/2} H_{l+1/2}^{(2)}(x)\, v_l^{(2)}(x), \end{aligned} \qquad (6)$$

with $v_l^{(1)} = v_l^{(2)} = 1$ for $x \to \infty$. From Eqs. (6) and (5) we obtain

$$\eta_l = \frac{x^{1/2} v_l^{(2)} H_{l+1/2}^{(2)}(x) \left[A_l - \frac{1}{v_l^{(2)}} \frac{dv_l^{(2)}}{dx} - \frac{d \ln x^{1/2} H_{l+1/2}^{(2)}}{dx} \right]}{x^{1/2} v_l^{(1)} H_{l+1/2}^{(1)}(x) \left[\frac{1}{v_l^{(1)}} \frac{dv_l^{(1)}}{dx} - A_l + \frac{d \ln x^{1/2} H_{l+1/2}^{(1)}}{dx} \right]}. \qquad (7)$$

Introducing

$$S_l^{(2)} = d \ln v_l^{(2)}/dx, \quad S_l^{(1)} = d \ln v_l^{(1)}/dx,$$

$$f_l = d \ln x^{1/2} H_{l+1/2}^{(1)}/dx,$$

we find

$$\frac{\sigma_a^{(l)}}{(2l+1)\pi\lambda^2} = 1 - |\eta_l|^2 = 1 - \frac{|v_l^{(2)}|^2 |A_l - S_l^{(2)} - f_l^*|^2}{|v_l^{(1)}|^2 |A_l - S_l^{(1)} - f_l|^2}, \qquad (8)$$

$$\frac{\sigma_e^{(l)}}{(2l+1)\pi\lambda^2} = |1 - \eta_l|^2 = \left| 1 + \frac{H_{l+1/2}^{(2)}(x)\, v_l^{(2)} (A_l - S_l^{(2)} - f_l^*)}{H_{l+1/2}^{(1)}(x)\, v_l^{(1)} (A_l - S_l^{(1)} - f_l)} \right|^2. \qquad (9)$$

When $v_l^{(2)} = v_l^{(1)} = 1$ and $S_l^{(2)} = S_l^{(1)} = 0$, Eqs. (8) and (9) reduce to the formulas for a sharp boundary.

The case in which $V(r)$ is real for $r \geq r_0$ is particularly simple. Then $v_l^{(2)} = v_l^{(1)} = v_l$,

$$1 - |\eta_l|^2 = - \frac{4 \operatorname{Im} A_l [\operatorname{Im} S_l + h_l]}{|A_l - S_l - f_l|^2}, \qquad (10)$$

$$|1 - \eta_l|^2 = \left| 1 + e^{-2i\psi - 2i\varphi} \frac{A_l - S_l^* - f_l^*}{A_l - S_l - f_l} \right|^2, \qquad (11)$$

$$\begin{aligned} f_l &= g_l + i h_l, \quad v_l = |v_l| e^{-i\varphi}, \\ H_{l+1/2}^{(2)} &= |H_{l+1/2}^{(2)}| e^{-i\psi}. \end{aligned} \qquad (12)$$

The function S_l satisfies the equation

$$dS_l/dx + S_l^2 + 2 f_l S_l + (K_0/k)^2 V(x) = 0, \qquad (13)$$

with $V(x_0) = 1$. Separating the real and imaginary parts $S_l = a_l + i b_l$ in Eq. (13), we have

$$\frac{da_l}{dx} + a_l^2 - b_l^2 + 2 g_l(x)\, a_l - 2 h_l(x)\, b_l + \frac{K_0^2}{K^2} V(x) = 0 \qquad (14a)$$

$$\frac{db_l}{dx} + 2 a_l b_l + 2 g_l(x)\, b_l + 2 h_l(x)\, a_l = 0. \qquad (14b)$$

By means of Eq. (14b) we can express b_l in terms of a_l. The Hankel functions satisfy here the identity

$$2\int_x^\infty g_l(x')\,dx' = \ln h_l(x).$$

Hence the general solution of the homogeneous part of Eq. (14b) is

$$b_l = Ch_l(x)\exp\left(2\int_x^\infty a_l(x')\,dx'\right),$$

and the solution of the inhomogeneous equation is

$$b_l = h_l\exp\left\{2\int_x^\infty a_l(x')\,dx'\right\} \times\int_x^\infty \exp\left\{-2\int_x^\infty a_l(x'')\,dx''\right\} 2a_l(x')\,dx'.$$

which reduces to

$$b_l = h_l(x)\left[\exp\left(2\int_x^\infty a_l(x')\,dx'\right)-1\right]. \qquad (15)$$

Thus Eq. (10) can be written

$$1-|\eta_{il}|^2 = -\frac{4\,\mathrm{Im}\,A_l h_l \exp\left\{2\int_x^\infty a_l(x')\,dx'\right\}}{[\mathrm{Re}\,A_l - a_l - g_l(x)]^2+\left[\mathrm{Im}\,A_l - h_l\exp\left\{2\int_x^\infty a_l(x')\,dx'\right\}\right]^2} \qquad (16)$$

and a similar expression holds for $|1-\eta_l|^2$.

At low energy, the quantities b_l^2 and $h_l b_l$ are small and Eq. (14a) can be solved independently of (14b). The resulting value of a_l can then be used to determine b_l.

The function $\exp\left\{2\int_x^\infty a_l\,dx\right\}$ varies slowly with radius and with energy. Hence we can interpolate between values of the function calculated at the ends of a wide interval. The main energy-dependence of the cross-section comes from the factor $h_l(x)$, which is a known rational function of the energy. Also at low energy, when $kr_0 < l$, the capture cross-section becomes proportional to x^{2l-1}, as for a rectangular well. But it may happen that the capture cross-section for a diffuse boundary is greater than for a rectangular well with the same depth and coefficient of absorption.

2. COMPARISON WITH EXPERIMENT

Detailed calculations of cross-sections were made with a boundary of exponential shape. With a well-depth $V(0) = 45$ Mev and a boundary shape $e^{-\alpha(r-r_0)}$ where $1/\alpha = 1\times10^{-13}$ cm, the calculated total cross-sections at 1 Mev were much larger than the experimental values, and had too sharp maxima as functions of r_0. The imaginary part of the potential was taken to be 0.03 $V(r)$. The calculated cross-sections $\sigma_t(r_0)$ and $\sigma_a(r_0)$ are shown graphically in Figs. 1 and 2. Consequently the later calculations were made with the value $\alpha = K_0 = 1.43\times10^{13}$ cm^{-1}.

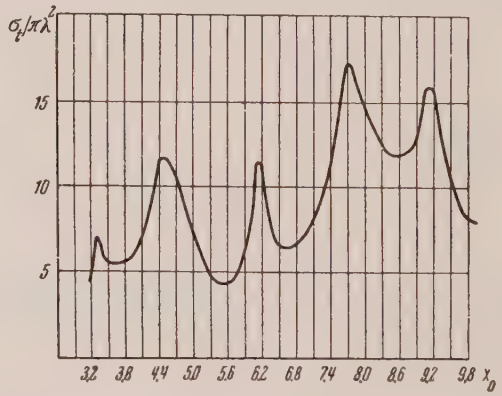

FIG. 1. Total cross-section as a function of r_0 for neutron energy 1 Mev. Parameters $1/\alpha = 10^{-13}$ cm, $\zeta = 0.03$.

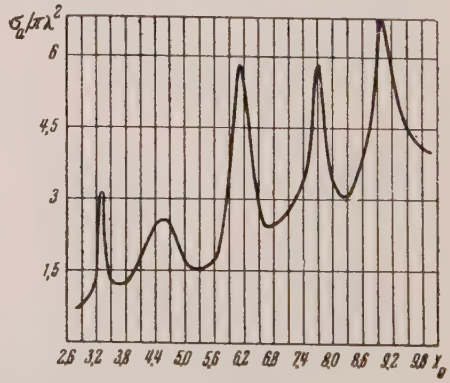

FIG. 2. Capture cross-section as a function of r_0 for neutron energy 1 Mev. Parameters $1/\alpha = 10^{-13}$ cm, $\zeta = 0.03$.

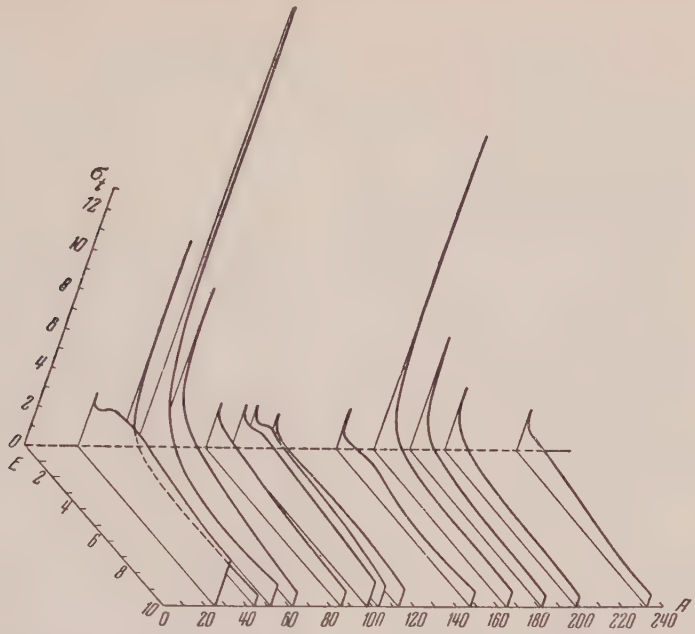

FIG. 3. Total nuclear cross-sections. The x axis represents atomic weight, the y axis neutron energy in units of 0.1 Mev, the z axis $\sigma_t/\pi R^2$.

With this value of a we constructed surfaces showing the total cross-section as a function of energy and atomic weight (see Fig. 3). The imaginary fraction of the potential was taken to be 0.05 for $r \leq r_0$ and zero for $r \geq r_0$. The calculations with $1/a = 1 \times 10^{-13}$ cm had shown that the vanishing of the imaginary part of the potential in the surface layer did not significantly change the behavior of the cross-sections.

Satisfactory agreement with experiment was found with $V(0) = 44$ Mev and $r_0 = 1.25 \times 10^{-13} A^{1/3}$ cm. The minimum of the cross-section at 1 Mev for elements with $A \sim 200$ is clearly visible, as is the maximum for elements with $A \sim 90$–100. The maximum at 1 Mev in the region of titanium is apparently missing, and the cross-sections for $A = 150$–180 are bigger and less energy-dependent than the theoretical values. The latter discrepancy is probably connected with the non-spherical shapes of nuclei in this region.

Capture cross-sections were also calculated at various energies. Unfortunately the experimental data at 1 Mev (see Fig. 4) are inconclusive. Elastic scattering through compound nucleus states is small for silver and gold, and $\sigma_a \sim 2$ barns. The theory gives 2 barns for gold and 1.7 for silver. For iron the capture cross-section is probably greater than 1 barn, since the scattering into the spin-2 level at 860 kev is 0.4 barn and the compound nucleus decays predominantly into the elastic channel. The theory gives 1.8 barns for iron. Thus there is no contradiction with experiment.

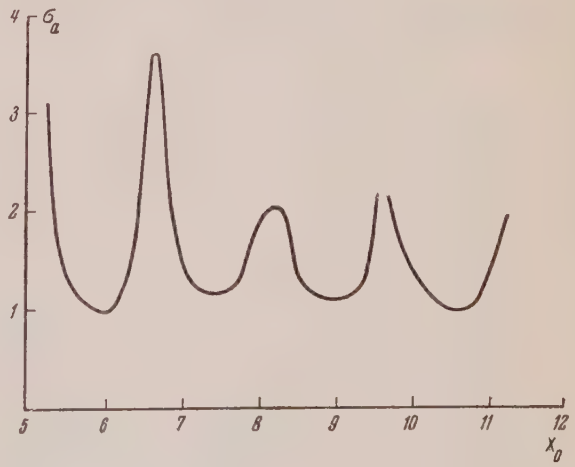

FIG. 4. Neutron capture cross-section in units of $\pi(r_0 + 1/a)^2$ as a function of r_0 for energy 1 Mev. Parameters $1/a = 0.71 \times 10^{-13}$ cm, $\zeta = 0.05$.

At low energy one can compare with experiment the quantity (Γ_n/D). This comparison allows one to determine one relation between the real part of the potential and the nuclear radius. Fig. 5 shows the value of (Γ_n/D) for the indicated values of the parameters $V(r)$, r_0, $(1/a)$ and ζ. The maximum of (Γ_n/D) at $A \sim 51$ is evidently displaced to the right

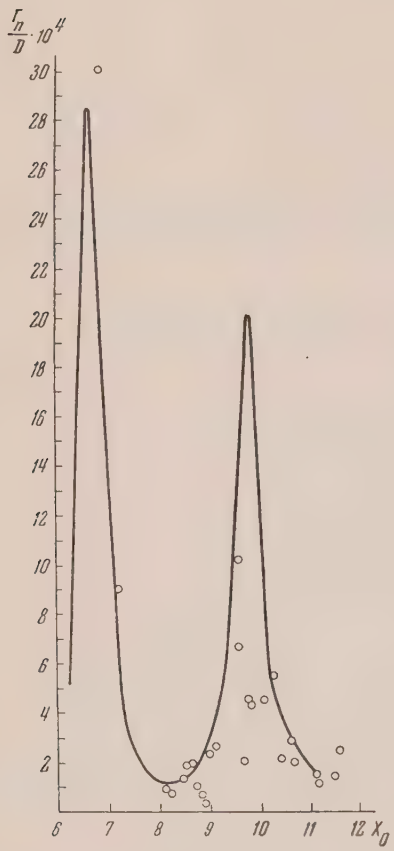

FIG. 5. Ratio of reduced neutron width to level spacing. Parameters $1/\alpha = 0.71 \times 10^{-13}$ cm, $\zeta = 0.05$.

of its theoretical position. But the data are very inaccurate. The height of the maximum does not disagree with the theory. In the region of the minimum at $A \sim 90$–120 the agreement is also satisfactory. The lowering of the second maximum is attributable to non-spherical nuclei. For non-spherical nuclei the position of the maximum is a function of two parameters, the major axis and the eccentricity of the ellipsoid. Since the eccentricity varies abruptly from nucleus to nucleus, the position of exact resonance may never be reached. For $A \sim 200$–230 the experimental values of (Γ_n/D) also agree with the theory.

Nuclei in the range $A = 90$–100 should have some peculiar features. In such nuclei the p-wave maximum should be visible in the cross-sections for forming a compound nucleus even in the energy-region 3–10 kev.

In this region an increase in level density by a factor of 3 or 4 should be observable. There ought to be many weak levels, with neutron widths increasing rapidly with energy like $E^{3/2}$. The observation of these levels seems to lie just at the limit of the resolving power of present-day neutron spectroscopy.

3. SOME CHARACTERISTIC ANGULAR DISTRIBUTIONS

The most interesting angular distributions occur for rather slow neutrons with energies from 0.1 to 0.5 Mev. In this energy-range inelastic scattering is unimportant, and the cross-sections for radiative capture in elements at the middle of the periodic table are small (at 0.5 Mev not greater than 0.2 barn). At these energies, the main interaction of a neutron with nuclei is therefore elastic scattering. The elastic-scattering cross-section σ_s is equal to $\sigma_t - \sigma_r \sim \sigma_t$. However, the angular distribution will be completely different for the two components of σ_t. We have calculated the angular distribution of the optical component with the same values for the parameters as were used in calculating the total cross-section. Figs. 6, 7, 8 show the results for energies 0.11 and 0.44 Mev at $A = 100$ and for energy 0.44 Mev at $A = 84$. In each case the angular distribution is strongly anisotropic. In Fig. 7 there is a peculiar secondary maximum at 180°, which is absent in Fig. 8. Since the calculation of angular distributions of elastic scattering proceeding through compound nucleus formation is not equally reliable, we have nothing to say here about this component. It should be possible to make statements about the compound nucleus component after investigating the distributions in various special cases.

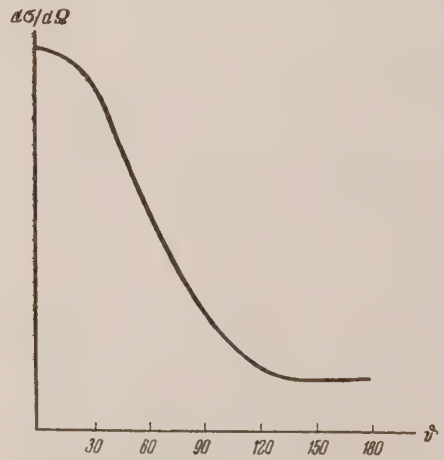

FIG. 6. Angular distribution of optical elastic scattering. Parameters $1/\alpha = 0.71 \times 10^{-13}$ cm, $E = 0.11$ Mev, $A = 100$.

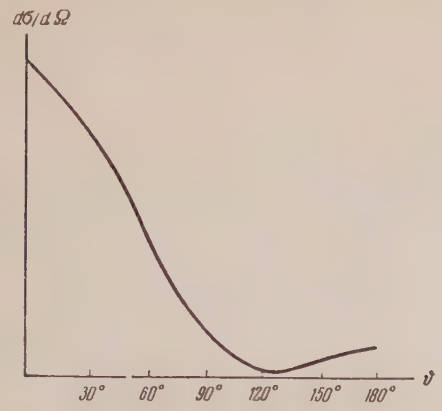

FIG. 7. Angular distribution of optical elastic scattering. Parameters $1/\alpha = 0.71 \times 10^{-13}$ cm, $E = 0.44$ Mev, $A = 100$.

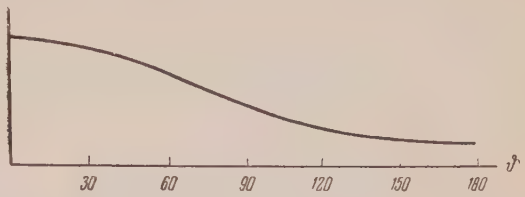

FIG. 8. Angular distribution of optical elastic scattering. Parameters $1/\alpha = 0.71 \times 10^{-13}$ cm, $E = 0.44$ Mev, $A = 84$.

[1] P. E. Nemirovskii, J. Exptl. Theoret. Phys. (U.S.S.R.) 30, 551 (1956); Soviet Phys. JETP, 3, 484 (1956).
[2] R. K. Adair, Phys. Rev. 94, 737 (1954).

Translated by F. J. Dyson
233

SOVIET PHYSICS JETP VOLUME 5, NUMBER 5 DECEMBER, 1957

Contribution to the Theory of the Molecular Generator

IU. L. KLIMONTOVICH AND R. V. KHOKHLOV
Moscow State University

(Submitted to JETP editor June 29, 1956)
J. Exptl. Theoret. Phys. (U.S.S.R.) 32, 1150-1155 (May, 1957)

Processes of resonance interaction between an electromagnetic field and a molecular beam and also auto-oscillation processes in a molecular generator are examined in the present paper. Unlike other papers, the case of a beam of monochromatic (with respect to velocity) molecules is considered in detail and the peculiarities of this case are elucidated. The result obtained by taking into account non-monochromatic molecules in the beam is discussed qualitatively.

INCREASED STABILITY requirements have led to the development of a molecular generator in which the electromagnetic oscillations in the resonator are excited by radiation of excited gas molecules passing through the resonator. The possibility of such a generator was indicated in 1952 by Basov and Prokhorov[1, 2]. The molecular generator was almost simultaneously developed by a group of American physicists [3, 4] and by Basov and Prokhorov in the U.S.S.R. Even before the experimental success of the molecular generator, Basov and Prokhorov suggested a theory of its operation[5-7], which in essence consists of the following. Using the theory of dispersion, and taking account of saturation effects, the dielectric constant of the molecular beam passing through the resonator is determined. They then examine oscillatory processes in a circuit with a capacitor whose dielectric has the same constant as the molecular beam. The dielectric constant depends on the square of the electric field. Therefore this oscillatory process is described by a non-linear differential equation whose solution determines the amplitudes and frequencies of the oscillation. The theoretical method used by Basov and Prokhorov is not sufficiently complete and makes difficult an analysis of more complicated processes connected with the operation of a molecular generator. We therefore give in the present work a more rigorous statement of the problem, on the basis of which a thorough examination of molecular generator operation in the stationary state is made. We first examine the case of a single-velocity molecular beam ($v = v_0$) and afterwards give a qualitative evaluation of the effect of molecules with speeds other than v_0.

1. In analysis of the operation of a molecular generator it suffices to examine two energetic states

of the molecules, which we shall call E_1 and E_2. Then for the description of the molecular beam state in the resonator we shall use the density matrix:

$$\begin{vmatrix} C_{11}(x,t) & C_{12}(x,t) \\ C_{21}(x,t) & C_{22}(x,t) \end{vmatrix}. \tag{1}$$

For definiteness we assume that $E_2 > E_1$. The matrix elements C_{11} and C_{22} determine at point x and at time t the density of molecules in states 1 and 2 moving with velocity v_0. The matrix elements C_{12} and C_{21} determine the polarization vector P of the molecular beam, which polarization is due to molecular transitions between states 1 and 2 as a consequence of the action of the field.

$$P(x,t) = p_{12}(t)\,C_{21} + p_{21}(t)\,C_{12}, \tag{2}$$

where $p_{12}(t)$ and $p_{21}(t)$ are the matrix elements of the molecular dipole moment. Let us denote by

$$D(x,t) = C_{22}(x,t) - C_{11}(x,t) \tag{3}$$

the difference in density of molecules of velocity v in states 2 and 1 at the point x at the instant t. For D, C_{12} and C_{21} we have the following equations:

$$\partial D/\partial t + v\,\partial D/\partial x = -(2/ih)\,[p_{21}(t)\,C_{12} - p_{12}(t)\,C_{21}]\,E(t), \tag{4}$$

$$\partial C_{12}/\partial t + v\,\partial C_{12}/\partial x = -(1/ih)\,p_{12}(t)\,DE(t), \tag{5}$$

$$\partial C_{21}/\partial t + v\,\partial C_{21}/\partial x = (1/ih)\,p_{21}(t)\,DE(t). \tag{6}$$

The x axis is directed along the axis of the resonator. Equations (4)–(6) are obtained from the general equations for the density matrix $C_{ik}(x, t)$, in which account is taken of the kinetic energy of the molecules. We assume that the molecular beam does not interact with itself and that the interactions of the separate molecules with the field are determined by the expression $-(\hat{\mathbf{p}}\mathbf{E})$, where $\hat{\mathbf{p}}$ is the dipole moment operator of the separate molecule, and $\mathbf{E}$ is electric field intensity of that normal component, whose frequency ω_p is close to the transition frequency $\omega_{21} = (E_2 - E_1)/n$. This normal oscillation has a homogeneous distribution of the electric field along the resonator. The direction of the E field is along the x axis. If the molecular-generator resonator is replaced by an equivalent circuit with a capacitance shunted by a resistance, then the equation for E has the following form:

$$\frac{d^2E}{dt^2} + \frac{\omega_p}{Q}\frac{dE}{dt} + \omega_p^2 E = -4\pi\frac{d^2\bar{P}}{dt^2}. \tag{7}$$

Here Q is the quality of the resonator and $\bar{P}$ the average polarization along the x axis.

If the generator resonator is replaced by a circuit with a series resistance as was done in Refs. 6 and 7, we must add to the right half of Eq. 7 the term $-4\pi(\omega_p/Q)d\bar{P}/dt$. However, if we limit our examination to an accuracy of Q^{-2}, we can ignore this term. Thus it is first necessary to find an expression for the polarization P of the molecular beam, and then substitute this expression into (7) to analyze the resulting solution.

2. The beam polarization $P(x, t)$, according to (2), is expressed in terms of the solutions of the system (4)–(6). Let us examine the solutions of this system in the case that oscillations are already established, assuming that the electric field strength is $E = E_0 \cos \omega t$. In the steady state the distribution of the molecules does not depend explicitly on time. We therefore set $\partial D/\partial t = 0$. If the expression for E is substituted into Eqs. (4)–(6), terms appear on the right which are rapidly varying in time (with a frequency $\omega + \omega_{21}$), and slowly varying in time (with a frequency $\omega_{21} - \omega = \delta$). Neglecting on the right hand side of the equations for D, C_{12} and C_{21} the terms which are rapidly varying in time and assuming that $\partial D/\partial t = 0$, we obtain the following system of equations:

$$v\,\partial D/\partial x = -(1/ih)\,[p_{21}e^{i\delta t}\,C_{12} - p_{12}e^{-i\delta t}\,C_{21}]\,E_0, \tag{8}$$

$$\partial C_{12}/\partial t + v\,\partial C_{12}/\partial x = -(1/2\,ih)\,p_{12}e^{-i\delta t}\,DE_0, \tag{9}$$

$$\partial C_{21}/\partial t + v\partial C_{21}/\partial x = (1/2\,ih)\,p_{21}e^{i\delta t}\,DE_0. \tag{10}$$

In equations (8)–(10) we take it into account that $p_{ik}(t) = p_{ik}e^{i\omega_{ik}t}$. These relationships will be solved with the boundary conditions:

$$D = D_0; \quad C_{12} = C_{21} = 0 \quad \text{for} \quad x = 0. \tag{11}$$

The solutions of equations (9) and (10) satisfying the boundary conditions (11) have the form

$$C_{12}(x,t) = -\frac{p_{21}E_0}{2ihv}\int_0^x \exp\left\{-i\delta\left[t - \frac{1}{v}(x-x')\right]\right\} D(x')\,dx', \tag{12}$$

$$C_{21}(x, t) = \frac{p_{21}E_0}{2ih\upsilon}\int_0^x \exp\left\{i\delta\left[t - \frac{1}{\upsilon}(x - x')\right]\right\} D(x')\,dx'. \quad (13)$$

Substituting (12) and (13) into Eq. (8), we obtain an equation for $D(x)$

$$\frac{dD}{dx} = -\frac{p^2E_0^2}{h^2\upsilon^2}\int_0^x \cos\frac{\delta}{\upsilon}(x - x')\,D(x')\,dx'. \quad (14)$$

The solution of Eq. (14) satisfying the boundary conditions has the form

$$D(x) = D_0\left[\frac{p^2E_0^2}{\Omega^2h^2}\cos kx + \frac{\delta^2}{\Omega^2}\right], \quad (15)$$

$$\Omega^2 = p^2E_0^2/h^2 + \delta^2; \quad k = \Omega/\upsilon. \quad (16)$$

Expression (15) describes the level distribution of the constant-velocity beam molecules moving along the resonator, as a function of the detuning δ and of other parameters. It follows from this that for a small detuning δ there is a resonance action on the molecular beam: almost all molecules go from the upper level to the lower and back again as they move along the resonator. For large detuning the indicated transition is made only by a small part of the beam molecules: the function $D(x)$ is almost constant along the resonator.

We now calculate the polarization vector of the molecular beam. Substituting the expressions (12), (13) for C_{12} and C_{21} into expression (2) for the polarization vector P, and using expression (15) for $D(x)$, we find

$$P(x, t) = -D_0(p^2E_0/h\Omega^2)[\Omega\sin kx\sin\omega t + \delta(1 - \cos kx)\cos\omega t]. \quad (17)$$

From expression (17) we find the average polarization along the resonator of the beam molecules moving with constant velocity.

$$\bar{P}(t) = -D_0\frac{p^2E_0\tau}{h}\left[\frac{1 - \cos\Omega\tau}{\Omega^2\tau^2}\sin\omega t + \delta\tau\frac{1 - \sin\Omega\tau/\Omega\tau}{\Omega^2\tau^2}\cos\omega t\right], \quad (18)$$

where $\tau = L/v$ is the transit time through a resonator of length L.

3. Let us now proceed to analyze solution of the equation for the electric field in the case of a molecular beam which is monochromatic in velocity. Using expressions (18) for $\bar{P}(t)$, we write Eq. (7) for E in the form

$$\frac{d^2E}{dt^2} + \frac{\omega_p}{Q}\frac{dE}{dt} + \omega_p^2E = -B\omega^2\frac{1 - \cos\Omega\tau}{\Omega^2\tau^2}E_0\sin\omega t - B\omega^2\delta\tau\frac{1 - \sin\Omega\tau/\Omega\tau}{\Omega^2\tau^2}E_0\cos\omega t. \quad (19)$$

Here $B = 4\pi D_0p^2\tau/h$. Putting $E = E_0\cos\omega t$ and equating the sine and cosine coefficients to zero, we obtain a transcendental equation for the amplitude and frequency of the steady-state oscillations

$$1/QB = (1 - \cos\Omega\tau)/\Omega^2\tau^2, \quad (20)$$

$$\omega^2 - \omega_p^2 = B\omega^2\delta\tau\frac{1 - \sin\Omega\tau/\Omega\tau}{\Omega^2\tau^2}. \quad (21)$$

Expression (21) can be written in the following manner:

$$\omega_p - \omega_{21} = (\omega - \omega_{21}) + \frac{B}{2}\omega\tau(\omega - \omega_{21})\frac{1 - \sin\Omega\tau/\Omega\tau}{\Omega^2\tau^2}. \quad (22)$$

From (22) it follows that when the resonance frequency ω_p equals the frequency ω_{21} of the transition in the molecule, the detuning is $\delta = \omega_{21} - \omega = 0$ and therefore the generator frequency coincides exactly with the frequency ω_{21}. In expression (22), for very large values of $\Omega\tau$ the second term is larger than the first. We therefore have approximately

$$\omega_p - \omega_{21} = -\frac{B}{2}\tau\delta\frac{1 - \sin\Omega\tau/\Omega\tau}{\Omega^2\tau^2}. \quad (23)$$

Let us introduce the notation

$$F(x) = \frac{1 - \cos x}{x^2}, \quad \Phi(x) = \frac{1}{x^2}\cdot\left(1 - \frac{\sin x}{x}\right), \quad \Delta = \omega_p - \omega_{21}. \quad (24)$$

Then

$$1/QB = F(\Omega\tau), \quad \Delta = -{}^1/_2B\omega_{21}\tau\Phi(\Omega\tau)\delta. \quad (25)$$

The functions $F(x)$ and $\Phi(x)$ are plotted in Figs. 1 and 2. Figure 1 shows that for a molecular beam which is monochromatic in velocity there exist values of the transit phase $\Omega\tau$ for which oscillation is impossible for any value of the coefficient QB. These transit phases have the values $2\pi n$, where n is an integer. In these cases there is no transfer of energy during the passage of the molecular beam through the resonator and all the active molecules entering the resonator leave it. For all other values of transit phase, self-oscillation is possible for sufficiently large values of the coefficient QB. From Figs. 1 and 2 it is seen that slightly above

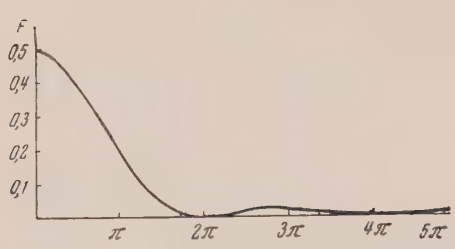

FIG. 1

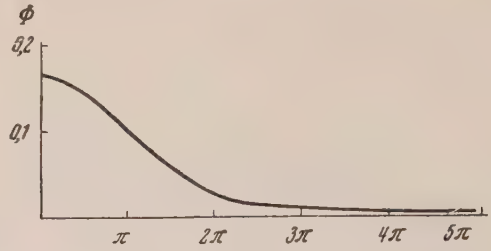

FIG. 2

the self-excitation threshold*, when $1/QB \lesssim 1/2$, self-oscillations are possible corresponding to small values of $\Omega\tau$ that are negligible compared with 2π. The generator frequency which is determined with the aid of Fig. 2 and relationship (23) is close in this case to the value $\omega = \omega_{21} + 6Q\Delta/\omega_{21}\tau$ and approaches ω_{21} with an increasing margin above the self-excitation threshold. When the coefficient QB becomes sufficiently large that the inequality $1/QB \lesssim 0.024$ is satisfied, we have the possibility of generation for transit phases in the region $2\pi < \Omega\tau < 4\pi$. It is essential to note that values of the transit phase corresponding to increasing branches of $F(x)$ determine unstable regions of self-oscillation, and therefore cannot be realized. For large increase in the intensity of a beam that is monochromatic in velocity, it becomes possible to generate in the transit phase region $4\pi < \Omega\tau < 6\pi$.

So far we have been examining the case of a beam that is monochromatic in velocity. In reality the molecules have some velocity distribution. For a properly selected length of level-sorting quadrupole capacitor and for a small entrance aperture to the resonator, the molecular velocities concentrate more or less closely about the values v_0, $v_0/3$, $v_0/5$ *etc.* If we limit ourselves to examination of the velocities v_0, $v_0/3$, $v_0/5$ in the molecular beam the following changes will take place in the above derivations. Equation (25) takes on the form

$$1/Q = d_1 B(\tau_0) F(\Omega\tau_0) + d_3 B(3\tau_0) F(3\Omega\tau_0) + \ldots, \quad (26)$$

where $d_1, d_3, \ldots$ are the relative molecular concentrations with velocities v_0, $v_0/3$, ... The presence of velocities $v_0/3$, $v_0/5$, *etc.*, which differ from v_0 by 3, 5, *etc.*, times, results in a somewhat different effective value for the expression $\widetilde{B}\,\widetilde{F}$. However, the new function $\widetilde{F}$ has almost the same characteristics as the function F for a beam monochromatic in velocity. In particular, when the argument of $\widetilde{F}$ is equal to $2\pi n$ this function vanishes. Between these values of the argument the function $\widetilde{F}$ is different from zero. Therefore there exist various isolated regions of transit phase for which oscillation is possible. The second relationship in (25) can also be rewritten in a form analogous to (26). We obtain in this case instead of (24) a new function $\widetilde{\Phi}$ which qualitatively does not differ from the old one. Thus the existence of the several indicated molecular velocities in the beam does not cause a qualitative change in the basic relationships (25) which determine the self-oscillatory process in the generator. Taking account of the small spread in the velocities around v_0, $v_0/3$, $v_0/5$, *etc.*, leads to a smearing of the function F: its minima increase and the maxima decrease; the function $\widetilde{F}$ will no longer vanish for values of the argument $2\pi n$. However, for small velocity spreads the function $\widetilde{F}$ retains its important characteristic—the existence of various isolated regions of transit phase values for which oscillations are possible. For a considerably larger spread of velocities all regions of transit phase which allow generation merge into one region. It should be noted that for small transit angles even a considerable spread in velocity has little effect on the function $F(x)$ and it is therefore unnecessary in this case to take account of this spread.

4. Let us now evaluate the importance of various accidental factors on the stability of molecular-generator operation. Let us first evaluate the order of magnitude which characterizes the oscillations in the molecular generator. Let $Q = 10^4$, $\Delta = 10^3$ sec^{-1}, $\omega_{21} = 1.5\times10^{11}$, $\tau = 10^{-4}$ sec. For these values of the parameters the oscillation frequency for a slight margin above the self-excitation threshold is determined by the equation $\omega = \omega_{21} + 6Q\Delta/\omega_{21}\tau$ and is $\omega = \omega_{21} + 5$. With increasing beam intensity, the oscillation frequency approaches ω_{21}. The oscillation amplitude can be evaluated from Eq. (19). We have for a transit phase $\Omega\tau \approx 1$, $E = h\Omega/p = 10^5$ CGS electrostatic units. The order of magni-

* The conditions for self-excitation differ from those developed in reference (2) by an unimportant constant coefficient, which is the result of a different averaging of the beam polarization vector.

tude of the output power is determined by the relationship $W = E^2\omega_{21}\theta/2Q$ where θ is the volume of the resonator which is in order of magnitude 10 cm^3. Substituting here the given quantities we have $W = 7 \times 10^{-3}$ erg/sec. To produce self-oscillation it is essential that $B > 2/Q$. Let us take therefore a value $B = 10^{-3}$. Then from Eq. (19) we have $D_0 = Bh/4\pi p^2\tau \approx 10^9$ cm^{-3}. The number of molecules falling on an area of 1 cm^2 is $D_0 v = 4 \times 10^{13}$ cm^{-2} sec^{-1}. It should be noted that in real operating conditions the molecules are concentrated in a narrow beam whose area is significantly smaller than the transverse area of the resonator. The value that has been used above is characteristic of an average molecular density in the resonator. The total number of molecules which enter the resonator in a unit time is $N = D_0 vS \approx 10^{14}$ sec^{-1} where S is the transverse area of the resonator. The order of magnitude of the power emitted by the molecule is the same as the input power of the generator $Nh\omega/2 = 7 \times 10^{-3}$ erg/sec. This value agrees with the value obtained above.

Let us evaluate the effect of a varying resonator temperature on the generator stability. The order of magnitude of resonator frequency variation due to unconstant temperature is determined by the following relationship:

$$\Delta\omega_p / \omega_p = \Delta R / R = \alpha \Delta T, \qquad (27)$$

where α is the linear expansion coefficient, R the radial dimension of the resonator, and ΔT is the accuracy with which the resonator temperature is maintained. For example for invar we have $\alpha = 1.5 \times 10^{-6}$. For small values of transit phase

$$\Delta\omega = \Delta\omega_p (6Q / \omega_{21}\tau) \approx 4 \cdot 10^{-3} \Delta\omega_p. \qquad (28)$$

From (27) and (28) it follows that in order to maintain a stability of 5×10^{-11} near the self-oscillation threshold it is essential to maintain the temperature constant with an accuracy of 10^{-2}. With an increase in beam intensity, the accuracy with which it is necessary to maintain the temperature can be decreased by one order of magnitude.

[1] N. G. Basov and A. M. Prokhorov, Paper at All-Union Radiospectroscopy Conference, May, 1952.

[2] N. G. Basov and A. M. Prokhorov, J. Exptl. Theoret. Phys. (U.S.S.R.) **27**, 431 (1954).

[3] Gordon, Zeiger, and Townes, Phys. Rev. **95**, 282 (1954).

[4] Gordon, Zeiger, and Townes, Phys. Rev. **99**, 1253 (1955).

[5] N. G. Basov and A. M. Prokhorov, Dokl. Akad. Nauk SSSR **101**, 47 (1955).

[6] N. G. Basov and A. M. Prokhorov, Usp. Fiz. Nauk **57**, 485 (1955).

[7] N. G. Basov and A. M. Prokhorov, J. Exptl. Theoret. Phys. (U.S.S.R.) **30**, 560 (1956), Soviet Phys. JETP **3**, 426 (1956).

Translated by G. L. Gerstein
234

SOVIET PHYSICS JETP VOLUME 5, NUMBER 5 DECEMBER, 1957

On the Nonlinear Generalization of the Meson and Spinor Field Equations

D. F. KURDGELAIDZE
Moscow State University

(Submitted to JETP editor August 29, 1956)
J. Exptl. Theoret. Phys. (U.S.S.R.) **32**, 1156-1162 (May, 1957)

Exact periodic solutions of the nonlinear generalized Klein-Gordon and Dirac equations are considered. The energy of the nonlinear classical meson field is compared with that derived from quantum theory.

THE NECESSITY for nonlinear generalizations of scalar, spinor, and other field equations, as well as the possible importance of the nonlinearities in specific effects, makes desirable detailed examinations of this problem. Here we consider a purely classical unquantized scalar or pseudo-scalar neutral meson field. We make use of the exact solution of nonlinear wave equations in terms of

elliptic functions, which are used to calculate the total energy and momentum of the field. Further, the expression obtained is expanded in a series in terms of a small parameter of nonlinearity. We can consider also the case in which this parameter is large. It is of interest to compare the expressions obtained in the case of weak nonlinearity with the results of a perturbation-theory treatment of the nonlinear quantum field.

We also consider the nonlinear spinor equation.

1. NONLINEAR MESODYNAMICS

Let us take

$$L = -\tfrac{1}{2}\{(\nabla\varphi)^2 - \varphi_t^2 + \Phi(\varphi)\}, \qquad (1.1)$$

to be the fundamental Lagrangian of a nonlinear scalar field, where the nonlinearity of the problem is given by the arbitrary function $\Phi(\varphi)$. We attempt to find a solution of the corresponding nonlinear equation

$$\varphi_{tt} - \varphi_{nn} + F(\varphi) = 0, \quad F(\varphi) = \frac{1}{2}\frac{d}{d\varphi}\Phi(\varphi) \qquad (1.2)$$

in the form

$$\varphi = \varphi(\sigma), \quad \sigma = k_\mu x_\mu, \quad (k_4 = i\omega, \ x_4 = it, \ c \equiv 1). \qquad (1.3)$$

We shall restrict our considerations to periodic $\varphi(\sigma)$, which are known to exist at least if $\Phi(\varphi)$ is a polynomial of no higher than fourth order.

We shall find the time-average of the energy and momentum densities

$$\overline{H} = \frac{1}{2T}\int_0^T \{(\nabla\varphi)^2 + \varphi_t^2 + \Phi(\varphi)\}\, dt,$$

$$\mathbf{G} = -\frac{1}{T}\int_0^T (\nabla\varphi)\,\varphi_t\, dt. \qquad (1.4)$$

After inserting (1.3) into (1.2) and (1.4), we obtain

$$\overline{H} = a(k^2 + K_0^2)/\omega, \qquad \mathbf{G} = a\mathbf{k}, \qquad (1.5)$$

$$(\omega^2 - k^2)\,\varphi_\sigma^2 + \Phi(\varphi) = h \equiv \text{const},$$

$$K_0^2 = h\omega/2a, \quad a = (\omega/T)\int_0^T \varphi_\sigma^2\, dt. \qquad (1.6)$$

Let us apply the general expressions obtained to certain specific cases

$$F(\varphi) = k_0^2\varphi, \qquad (1.7)$$

$$F(\varphi) = k_0^2\varphi + \alpha\varphi^2, \qquad (1.8)$$

$$F(\varphi) = k_0^2\varphi + \beta\varphi^3. \qquad (1.9)$$

For the linear case (1.7) we have

$$\varphi = \varphi_0\begin{pmatrix}\cos(\sigma - \sigma_0)\\ \sin(\sigma - \sigma_0)\end{pmatrix}, \quad \varphi_0 = \text{const}, \qquad (1.10)$$

where σ is given by (1.3), and $\omega^2 - k^2 = k_0^2$. This leads to

$$a = \varphi_0^2\omega/2, \quad h = k_0^2\varphi_0^2, \quad K_0 = k_0,$$
$$\overline{H} = a\omega, \quad \mathbf{G} = a\mathbf{k}. \qquad (1.11)$$

Similarly, in the nonlinear case (1.8) we obtain

$$\varphi = \varphi_0\begin{pmatrix}\mathrm{cn}^2(\sigma - \sigma_0)\\ \mathrm{sn}^2(\sigma - \sigma_0)\end{pmatrix} + \varphi_1; \quad \varphi_0, \varphi_1 \equiv \text{const}, \qquad (1.12)$$

where

$$\omega^2 - k^2 = \left(\frac{k_0}{2}\right)^2\left[\frac{\varepsilon}{3}\left(\frac{\alpha\varphi_0}{k_0^2}\right) + \sqrt{1 - \frac{1}{3}\left(\frac{\alpha\varphi_0}{k_0^2}\right)^2}\right],$$

$$\varphi_1 = -\frac{k_0^2}{2\alpha}\left[\left(1 + \frac{\alpha\varphi_0}{k_0^2}\right) - \sqrt{1 - \frac{1}{3}\left(\frac{\alpha\varphi_0}{k_0^2}\right)^2}\right],$$

$$k_1^2 = \varepsilon\frac{\alpha\varphi_0}{6(\omega^2 - k^2)}, \quad \varepsilon = \begin{pmatrix}+1\\ -1\end{pmatrix},$$

$$h = k_0^2\left[1 + \frac{2}{3}\left(\frac{\alpha\varphi_1}{k_0^2}\right)\right]\varphi_1^2,$$

$$a = l\frac{\omega\varphi_0^2}{2}, \quad K_0^2 = k_0^2\left[1 + \frac{2}{3}\left(\frac{\alpha\varphi_1}{k_0^2}\right)\right]\left(\frac{\varphi_1}{\varphi_0}\right)^2\frac{1}{l},$$

$$l = \frac{8}{15}\left\{(2k_1^2 - 1)\left(\frac{k_1'}{k_1}\right)^2 + \left[3k_1'^2 + \frac{(1 - 2k_1^2)^2}{k_1^2}\right]\left[\frac{E(k_1)}{K(k_1)} - k_1'\right]\frac{2}{k_1^2}\right\}.$$

In the nonlinear case (1.9) we have, analogously,

$$\varphi = \varphi_0\begin{pmatrix}\mathrm{cn}(\sigma - \sigma_0)\\ \mathrm{sn}(\sigma - \sigma_0)\end{pmatrix}, \varphi_0 = \text{const}, \qquad (1.13)$$

where

$$\omega^2 - k^2 = \begin{pmatrix} k_0^2 + \beta\varphi_0^2 \\ k_0^2 + \tfrac{1}{2}\beta\varphi_0^2\end{pmatrix}, \quad k_1^2 = \varepsilon\frac{\beta\varphi_0^2}{2(\omega^2 - k^2)}.$$

Here the functions (1.5), (1.6) become

$$h = k_0^2(1 + \beta\varphi_0^2/2k_0^2)\,\varphi_0^2,\quad a = l\omega\varphi_0^2/2(\omega^2 - k^2),$$
$$l = \frac{2}{3}\left\{2 - (1 + k_1^2)\,\frac{1}{k_1^2}\left[1 - \frac{E(k_1)}{K(k_1)}\right]\right\},\qquad (1.14)$$
$$K_0^2 = k_0^2[1 + \beta\varphi_0^2/2k_0^2]\,l^{-1},$$

where $K(k_1)$, $E(k_1)$ are the complete elliptic integrals of the first and second kind, k_1 is the elliptic-function modulus*, and

$$k_1^2 + k_1'^2 = 1.$$

Let us now expand the expressions obtained in power series in the small parameters a and β, respectively, considering the nonlinearity to be weak. Then in case (1.8) the average energy of the two solutions is

$$\overline{H}_\alpha = {}^1/_2(\overline{H}_{\varepsilon=1} + \overline{H}_{\varepsilon=-1})_\alpha \qquad (1.15)$$
$$= a\omega_0\left\{1 - \frac{2}{9}\left[1 + \frac{17}{15}\left(\frac{\omega_0}{k_0}\right)^2\right]\frac{\alpha}{\omega_0^2}\,\frac{a}{\omega_0} + \ldots\right\}$$

and when $k = 0$ (writing $\omega_0^2 = k^2 + k_0^2$), we have

$$\overline{H}_\alpha^0 = \frac{1}{2}(\overline{H}_{\varepsilon=1}^0 + \overline{H}_{\varepsilon=-1}^0)_\alpha$$
$$= ak_0\left\{1 - \frac{5}{12}\,\frac{67}{60}\,\frac{102}{100}\left(\frac{\alpha}{k_0^2}\right)^2\left(\frac{a}{k_0^2}\right) + \ldots\right\}.$$

Similarly, for case (1.9) we have

$$\overline{H}_\beta = {}^1/_2(\overline{H}_{\varepsilon=1} + \overline{H}_{\varepsilon=-1})_\beta = a\omega_0\left\{1 + \frac{3}{8}\left(\frac{\beta a}{\omega_0^3}\right)\right.$$
$$\left. - \frac{3}{4}\left[1 - \frac{23}{48}\left(\frac{\omega_0}{k_0}\right)^2\right]\left(\frac{\beta a}{\omega_0^3}\right)^2 + \ldots\right\},\qquad (1.16)$$

and when $k = 0$,

$$\overline{H}_\beta^0 = {}^1/_2(\overline{H}_{\varepsilon=1}^0 + \overline{H}_{\varepsilon=-1}^0)_\beta$$
$$= ak_0\left\{1 + \frac{4}{5}\left[\frac{3}{8}\,\frac{5}{4}\left(\frac{\beta a}{k_0^3}\right) - 0.49\left(\frac{\beta a}{k_0^3}\right)^2\right] + \ldots\right\}.$$

We may consider more general cases in which the nonlinearity is given by a sum of terms such as (1.8) and (1.9). Then in the first approximation, the correction to the energy will be given by the sum of the corrections from each nonlinear term, namely,

$$\overline{H}^0 = \overline{H}_\alpha^0 + \overline{H}_\beta^0 = ak_0\left\{1 + \frac{4}{5}\left[\frac{3}{8}\,\frac{5}{4}\left(\frac{\beta a}{k_0^3}\right) - 0.49\left(\frac{\beta a}{k_0^3}\right) - \frac{5}{12}\,\frac{67}{60}\left(1.02\cdot\frac{5}{4}\right)\left(\frac{\alpha}{k_0^2}\right)\left(\frac{a}{k_0}\right)\right] + \ldots\right\}.\qquad (1.17)$$

Let us now consider the quantum theory of the scalar nonlinear field, which is usually treated by perturbation theory in a way similar to an anharmonic oscillator. This makes it possible to find an approximate expression for the energy in the form of a power series in the parameter of nonlinearity. In particular, by supplementing known results[1,2], we obtain a correction term proportional to β^2 for the energy, namely

$$H_q = k_0\left\{\left(n + \frac{1}{2}\right) + \frac{3\beta}{8k_0^3}\left[n^2 + n + \frac{1}{2}\right] - \frac{5}{12}\left(\frac{\alpha}{k_0^2}\right)^2\frac{1}{k_0}\left[n^2 + n + \frac{11}{30}\right]\right.$$
$$- \left(\frac{\beta}{k_0^3}\right)^2 2^{-10}\left[2\left(\sqrt{n^2(n+1)(n+2)} + \sqrt{(n+1)^3(n+2)}\right.\right.\qquad (1.18)$$
$$\left.\left. + \sqrt{(n+2)^3(n+1)} + \sqrt{(n+3)^3(n+1)}\right)^2\right.$$
$$\left. + (n+1)(n+2)(n+3)(n+4)\right] + \ldots\right\}$$

*It is interesting to note that the solution of the nonlinear equation in case (1.9) can also be written in a form similar to the well-known Euler expression

$$\varphi = \varphi_0\begin{pmatrix} e_n(\sigma - \sigma_0) \\ e_n^*(\sigma - \sigma_0)\end{pmatrix},\quad e_n(z) = \operatorname{cn} z + i\operatorname{sn} z$$

$\omega^2 - k^2 = k_0^2 + \beta\varphi_0^2$, $k_1^2 = 2\beta\varphi_0^2/(\omega^2 - k^2)$, $\varphi_0 \equiv$ const

As $\beta \to 0$, we obtain the ordinary Euler expression $e_n(z) \to e^{iz}$.

and the amplitude a is related to the quantum number n by $a = n + {}^1/_2$.

Thanks to this relation, we can compare H_q with $\overline{H}^0$. It is not difficult to see that they do not coincide for arbitrary a, although comparing (1.17) for $a = 1$ with the expression

$$H_q = k_0\left\{1 + \frac{3}{8}\frac{5}{4}\frac{\beta}{k_0^3} - 0{,}51\left(\frac{\beta}{k_0^3}\right)^2 - \frac{5}{12}\frac{67}{60}\left(\frac{\alpha}{k_0^2}\right)\frac{1}{k_0^2} + \ldots\right\},$$

obtained from (1.18) by setting $a = 1$ (that is, $n = \frac{1}{2}$), we get

$$(\overline{H}^0 - k_0) \approx {}^4/_5\,(H_q - k_0). \tag{1.19}$$

It should be emphasized that the classical and quantum results coincide only for a single amplitude, and that other values of the amplitude cause sharp differences. This leads to the evident conclusion that the nonlinear equations correspond to treating a single particle. We note again[3] that if we consider N similar particles whose total energy is N times the energy of each particle, then to make the energy expression and the equation itself have the same form as that for a single particle, the parameter of nonlinearity must be replaced by

$$\lambda_n' = \lambda_n / N^{(n/2-1)}, \tag{1.20}$$

where λ_n is the coefficient of φ^n in the polynomial $\Phi(\varphi)$.

2. SOLUTION OF THE NONLINEAR SPINOR EQUATION

The nonlinear generalization of the spinor equation previously proposed by Ivanenko, Heisenberg, and Mirianashvili[5,1,7] is of particular interest in view of the possibility of using it as the basis of a general particle theory. In this section we establish the relation between the nonlinear Dirac and Klein-Gordon equations and find several of their exact solutions in terms of elementary functions.

Let us consider the nonlinear Dirac equation

$$[(\gamma_\mu\,\partial/\partial x_\mu) + a(\bar{\psi},\psi)]\,\psi = 0, \tag{2.1}$$

where $a(\bar{\psi}, \psi)$ is an arbitrary scalar function of $\bar{\psi}$, ψ, and γ_μ. Let us restrict ourselves to the case in which $a(\bar{\psi}, \psi)$ is independent of the γ_μ matrices. We then have

$$a(\bar{\psi}, \psi) = a(\rho), \quad \rho = \bar{\psi}\psi = \bar{\psi}^\alpha\psi^\alpha. \tag{2.2}$$

Further, let us assume that the equation is separable in terms of the spin and space coordinates in the form

$$\psi(s, x_\mu) = \chi(s)\,\Phi(x_\mu), \quad \overline{\chi}(s)\,\chi(s) = 1, \tag{2.3}$$

where $\chi(s)$ is a constant unit spinor, and $\Phi(x_\mu)$ is a real function of the coordinates.* Then (2.1) becomes

$$\begin{gathered}(\gamma_\mu\,\partial\Phi/\partial x_\mu + A(\Phi))\,\chi(s) = 0,\\ A(\Phi) = a(\rho)\,\Phi.\end{gathered} \tag{2.4}$$

Applying the operator[4] $\gamma_\nu\,\partial/\partial x_\nu$ to equation (2.4), we obtain the nonlinear Klein-Gordon equation for $\Phi(x_\mu)$[3,5,6]

$$\begin{gathered}\partial^2\Phi/\partial x_\mu^2 - B(\Phi) = 0,\\ B(\Phi) = A(\Phi)\,dA(\Phi)/d\Phi.\end{gathered} \tag{2.5}$$

Since $\Phi(x_\mu)$ is a real function, it follows from (2.5) that $B(\Phi)$ must also be a real function of Φ. After determining $\Phi(x_\mu)$ from (2.5), the spin part $\chi(s)$ is determined from (2.4). This should be done by considering only such solutions of (2.5) which lead to $\chi(s)$ independent of x_μ.

Thus the set (2.1) of first-order equations can be considered a linearization of the second-order equations (2.5) in the sense that (2.1) has a solution of the type given by (2.3) [with condition (2.2)] whose spatial part satisfies (2.5).

If Eq. (2.5) is given, its linearization reduces to finding $A(\Phi)$ from the equation

$$\begin{gathered}A(\Phi) = \pm\sqrt{h + 2\int_0^\Phi B(\Phi)\,d\Phi},\\ h = \text{const}.\end{gathered} \tag{2.6}$$

As we see, the transition from (2.4) to (2.5) is unique, although the inverse transition is not unique (in view of the ± in front of the radical and the arbitrary constant h in (2.6)). To be specific we can, for instance, choose the positive sign and set

$$h = 0 \ [i.e., A(0) = 0]. \tag{2.7}$$

We shall attempt to find a solution of (2.4) of the form†

*It is not particularly difficult to find complex solutions, and they will be published in the immediate future.

†Equation (2.1) has the following particular solutions: the function $\psi = c\exp(ik_\mu x_\mu)$, $c = \text{const}$, with $k_\mu^2 = a^2$, and the constant spinor $= \psi_0$, which is a solution of the algebraic equation $a(\bar{\psi}_0\psi) = 0$.

$$\Phi(x_\mu) = \Phi(\sigma), \quad \sigma = k_\mu x_\mu, \tag{2.8}$$

so that Eqs. (2.4) and (2.5) become

$$(\gamma_\mu k_\mu \, d\Phi/d\sigma + A(\Phi))\chi(s) = 0, \tag{2.9}$$

$$(k_\mu^2 \, d^2\Phi/d\sigma^2 - B(\Phi)) = 0. \tag{2.10}$$

It follows from this that in order for $\chi(s)$ to be independent of x_μ, it is necessary that

$$A(\Phi) = \lambda d\Phi/d\sigma, \tag{2.10'}$$

where λ is a constant that causes the determinant of the coefficients of Eq. (2.4) to vanish.

On the other hand, the first integral of (2.10) is of the form

$$\sqrt{k_\mu^2}\frac{d\Phi}{d\sigma} = \left[h' + 2\int_0^\Phi B(\Phi)\,d\Phi\right]^{1/2}, \quad h \equiv \text{const}. \tag{2.11}$$

According to (2.6), putting $h' = h$ makes (2.11) coincide with (2.10') if

$$\lambda = \pm M \quad M = \sqrt{k_\mu^2}. \tag{2.11'}$$

For the spin part we obtain

$$(\gamma_\mu k_\mu + M)\chi(s) = 0, \tag{2.12}$$

whose solution is known[5]. We have thus shown that when condition (2.2) is satisfied, Eq. (2.1) has a solution of the type given by (2.3), (2.8).

Let us consider some examples; since the spin part $\chi(s)$ is always given by Eq. (2.12), we shall consider only the spatial part $\Phi(x_\mu)$.

Let us consider the nonlinear equation[1]

$$(\gamma_\mu \partial/\partial x_\mu + a\bar{\psi}\psi)\psi = 0, \tag{2.13}$$

whose solution of type (2.3), (2.7) is given, in view of (2.5), by the solution of

$$(\partial^2/\partial x_\mu^2 - b\Phi^4)\Phi = 0, \quad b = 3a^2; \tag{2.14}$$

when (2.7) is satisfied, we have

$$\Phi = (k_\mu x_\mu + c)^{-1/2}, \quad c = \text{const}, \tag{2.15}$$

$$k_\mu^2 = (2a)^2 = M^2.$$

Similarly, the spatial part of the solution of[7]

$$(\gamma_\mu \partial/\partial x_\mu) + a_0 + a_1\bar{\psi}\psi)\psi = 0, \tag{2.16}$$

is given by the solution of

$$(\partial^2/\partial x_\mu^2 - b_0 - b_1\Phi^2 - b_2\Phi^4)\Phi = 0,$$

$$b_0 = a_0^2, \quad b_1 = 4a_0a_1, \quad b_2 = 3a_1^2; \tag{2.17}$$

when condition (2.7) is satisfied, we obtain

$$\Phi = \sqrt{-a_0/2a_1}\exp[{}^1\!/_4(k_\mu x_\mu + c)]\{\sinh[{}^1\!/_2(k_\mu x_\mu + c)]\}^{1/2}$$

$$k_\mu^2 = (2a_0)^2 = M^2, \quad a_0 \neq 0, \quad a_1 \neq 0. \tag{2.18}$$

Let us now consider the inverse problem. The equation

$$(\partial^2/\partial x_\mu^2 - b_0 - b_1\Phi^2)\Phi = 0 \tag{2.19}$$

can be linearized. In particular, according to (2.6), we have

$$\left(\gamma_\mu \partial\Phi/\partial x_\mu + \sqrt{h + \left(b_0 + \tfrac{1}{2}b_1\Phi^2\right)\Phi^2}\right)\chi(s) = 0,$$

$$\psi = \chi(s)\Phi(x_\mu), \quad \bar{\chi}(s)\chi(s) = 1. \tag{2.20}$$

The spatial part of the solution of (2.20) is given by the solution of (2.19)[8]

$$\Phi = \Phi_0 Z(\sigma), \quad \Phi_0 = \text{const}, \tag{2.21}$$

where $Z(\sigma)$ is an elliptic function.

In particular, when condition (2.7) is satisfied, Eq. (2.21) leads to

$$\Phi = \sqrt{-b_0/2b_1}\,[\cos(k_\mu x_\mu + c)]^{-1},$$

$$k_\mu^2 = b_0^2 = M^2. \tag{2.22}$$

When $b_1 = 0$, we obtain the linear equation

$$(\partial^2/\partial x_\mu^2 - b_0)\Phi = 0 \tag{2.23}$$

and the analogue, in the sense of the above linearization, of the Dirac equation

$$(\gamma_\mu \partial\Phi/\partial x_\mu + \sqrt{h + b_0\Phi^2})\chi(s) = 0. \tag{2.24}$$

The spatial part of (2.24) is

$$\Phi = c_1\cos\sigma + c_2\sin\sigma. \tag{2.25}$$

Here $h = -b_0(c_1^2 + c_2^2)$. In particular, when condition (2.7) is satisfied, we have

$$c_2 = \pm ic_1, \quad \Phi = ce^{i\sigma} + c^* e^{i\sigma} \qquad (2.26)$$

which gives the solution to the ordinary Dirac equation.

It is also of interest to investigate the nonlinear generalization of the Duffin-Kemmer equation

$$(\beta_\mu \partial / \partial x_\mu - c(\overline{\varphi}, \varphi))\varphi = 0, \qquad (2.27)$$

where the β_μ are Kemmer-Duffin matrices, and $c(\overline{\varphi}, \varphi)$ is an arbitrary scalar function.

I consider it my duty to express my deep gratitude to Professor D. D. Ivanenko for constant attention to the work and to Professor Kh. Ia. Khristov for valuable comments.

[1] W. Heisenberg, Gott. Nachr. 8, 11 (1953).

[2] L. D. Landau and E. M. Lifshitz, *Quantum Mechanics*, Part 1, 1948, p. 163.

[3] D. Ivanenko and D. Kurdgelaidze, Dokl. Akad. Nauk SSSR 88, 39 (1954).

[4] W. Pauli, *Relativistic Field Theory of Elementary Particles*, M., 1947.

[5] A. Sokolov and D. Ivanenko, *Quantum Field Theory*, M.-L., 1952.

[6] L. Shiff, Phys. Rev. 84, 61 (1951); J. Malenka, Phys. Rev. 85, 685 (1952); W. Thyrring, Helv. Phys. Acta 26, 33 (1953).

[7] D. Ivanenko, M. Mirianashvili, Dokl. Akad. Nauk SSSR 106, 413 (1956).

[8] D. Kurdgelaidze, Vestn. MGU (News of Moscow State Univ.) 8, 81 (1954).

Translated by E. J. Saletan
235

SOVIET PHYSICS JETP VOLUME 5, NUMBER 5 DECEMBER, 1957

Statistical Theory of Systems of Charged Particles With Account of Short Range Forces of Repulsion

I. P. BAZAROV
Moscow State University

(Submitted to JETP editor July 5, 1956)
J. Exptl. Theoret. Phys. (U.S.S.R.) 32, 1163-1170 (May, 1957)

The free energy of an electrically neutral system of charged particles (ions) has been found by taking into account the repulsive forces between them. The general expression obtained for the free energy of such systems is applied to its calculation for a concrete form of "long-range" and "short-range" forces.

THE EQUILIBRIUM STATE of each statistical system of N particles is entirely determined by a knowledge of the Gibbs distribution function D or the equivalent aggregate distribution function $F_s(x_1, x_2, \ldots, x_s)$ $(s = 1, 2, \ldots)$[1]. For example, the pair distribution function $F_s(x_1, x_2)$ permits us to find the thermodynamic potential of the system, knowing which we can solve any problem pertaining to the state of thermodynamic equilibrium.

Ways of finding the correlation functions of systems of particles both with Coulomb (slowly decreasing with distance) potential of interaction $\Phi^0(r)$, and with molecular (rapidly decreasing with distance) interaction $\Phi^1(r)$, were first developed by Bogoliubov[1]. However, the problem of the construction of an expansion by which we could find the correlation functions in the case of a system with an interaction containing both Coulomb and short-range forces, remained unsolved.

Making use of an equation with variational derivatives, we[2] succeeded in outlining a method of finding the correlation functions both for systems with interaction $\Phi^0(r)$ or $\Phi^1(r)$, and for the "additive" interaction $\Phi(r) = \Phi^0(r) + \Phi^1(r)$ which contains, in the terminology of Vlasov[3], both "short-range" and "long-range" forces. In this paper, following Ref. 2, we define as the thermodynamic potential the free energy $F(\Phi)$ of a system of charged particles with explicit account of the short-range repulsive forces between them, which enables us to de-

velop the entire thermodynamics of such a type of system.

1. FREE ENERGY OF A SYSTEM OF CHARGED PARTICLES

Let us consider a system of M types of different charged particles (for example, a solution of strong electrolytes) with numbers N_a and charges e_a ($a = 1, 2, \ldots, N$) of particles of each type, and with interaction potentials

$$\Phi_{ab}(r) = \Phi^0_{ab}(r) + \Phi^1_{ab}(r), \tag{1}$$

where $r = r_{ab}$ = distance between particular particles of types a and b. Let the system as a whole be electrically neutral and the various particles differ only in charge; then

$$\sum_a N_a e_a = 0 \quad \text{or} \quad \sum_a n_a e_a = 0, \tag{2}$$

where $n_a = N_a/N$ = concentration of particles of the ath type and $N = N_a$ is the total number of particles in a system of volume V. If this system is found in an external field $\varphi(\mathbf{r})$, then the configuration integral of such a system is equal to*

$$Q = \int \exp\left\{-\frac{1}{\theta}\, U - \frac{1}{\theta}\sum_{i,a}\varphi_a(\mathbf{r}_i)\right\} d\tau, \tag{3}$$

where

$$U = \sum_{\substack{a<b\\ i,j}} \Phi_{ab}(|\mathbf{r}_{a,i} - \mathbf{r}_{b,j}|) = \sum \Phi^0_{ab}(|\mathbf{r}_{a,i} - \mathbf{r}_{b,j}|) + \sum \Phi^1_{ab}(|\mathbf{r}_{a,i} - \mathbf{r}_{b,j}|)$$
$$= U^0 + \sum \Phi^1_{ab}(|\mathbf{r}_{a,i} - \mathbf{r}_{b,j}|)$$

is the potential energy of interaction of the particles with one another, $\mathbf{r}_{a,i}$ defines the position of the ith molecule of the ath type (below, we shall call $\mathbf{r}_i$, or any set r_{ix}, r_{iy}, r_{iz}, by the letter x_i), $d\tau$ is the element of phase volume of the system and $\theta = kT$.

We can also put the configuration integral in the form

$$Q = \int \exp\left\{-\frac{1}{\theta}U^0 - \frac{1}{\theta}\sum_{a,i}\varphi_a(x_i)\right\} \prod_{\substack{a<b\\ i,j}} (1 + f_{ab}(x_i, x_j))\, d\tau, \tag{4}$$

$$f_{ab}(x_i, x_j) = \exp\left\{-\frac{1}{\theta}\Phi^1_{ab}(|x_i - x_j|)\right\}. \tag{5}$$

The free energy of our system, $F(\varphi\,|\,\Phi) = F(\varphi\,|\,\Phi^0 + \Phi^1)$, is a functional of the external field and the interaction potential between the particles and is equal to

$$F(\varphi\,|\,\Phi) = -\theta \ln Q(\varphi\,|\,\Phi). \tag{6}$$

As for an arbitrary functional,

$$F(\varphi\,|\,\Phi^0\,|\,f) = F(\varphi\,|\,\Phi^0) + \sum_{a,b}\int f_{ab}(x, y)\left(\frac{\delta F}{\delta f_{ab}(x, y)}\right)_{f=0} dxdy +$$
$$+ \frac{1}{2}\sum_{a,b}\sum_{a',b'}\int f_{ab}(x, y)\, f_{a'b'}(x', y')\left(\frac{\delta^2 F}{\delta f_{ab}(x, y)\,\delta f_{a'b'}(x'y')}\right)_{f=0} dxdydx'dy' + \ldots \tag{7}$$

Determining the different variational derivatives of F from Eq. (6), and comparing them, we find

$$(1 + f_{ab}(x, y))\frac{\delta F}{\delta f_{ab}(x, y)} = \frac{\theta^2}{2}\left\{\frac{\delta F}{\delta\varphi_a(x)\,\delta\varphi_b(y)} - \frac{1}{\theta}\frac{\delta F}{\delta\varphi_a(x)}\frac{\delta F}{\delta\varphi_b(y)}\right.$$
$$\left. - \frac{\delta(x-y)}{\theta}\frac{\delta F}{\delta\varphi_a(x)}\right\} = -\frac{\theta}{2}\frac{N_a(N_b - \delta_{ab})}{V^2}F_{ab}(x, y\,|\,\Phi^0 + \Phi^1), \tag{8}$$

* Sums of products over a, b, c, ... run everywhere from 1 to M. The sums over i and j run, respectively, from 1 to N_a and from 1 to N_b (if not stated otherwise).

whence

$$\left(\frac{\delta F}{\delta f_{ab}(x, y)}\right)_{f=0} = -\frac{\theta}{2}\frac{N_a(N_b-\delta_{ab})}{V^2}F_{ab}(x, y \mid \Phi^0), \tag{9}$$

where $F_{ab}(x, y \mid \Phi^0)$ is the pair distribution function of the system for the potential $\Phi^0(r)$, and δ_{ab} is the Kronecker symbol. If we set the external field $\varphi(x)$ in Eq. (7) equal to zero, then we can find the value of the free energy of the system of charged particles for the potential $\Phi(r) = \Phi^0(r) + \Phi^1(r)$. For the free energy of such a system, we get, with accuracy up to the second term in the expansions of (7) and (9):

$$F(\Phi) = F(\Phi^0) - \frac{\theta}{2}\sum_{a,b}\frac{N_a(N_b-\delta_{ab})}{V^2}\int f_{ab}(x, y)\,F_{ab}(x, y \mid \Phi^0)\,dxdy\,. \tag{10}$$

We can represent the free energy $F(\Phi^0)$ of a system of particles with an interaction potential $\Phi^0(r)$ by a pair distribution function $F_{ab}(x, y \mid \Phi^0)$ for this system.

Thus Eq. (10) gives the possibility of calculating the free energy of a system of charged particles with consideration of short-range repulsive forces between them if the pair distribution function $F_{ab}(x, y \mid \Phi^0)$ is known for the $\Phi^0(r)$ potential of "long-range" forces.

2. PAIR DISTRIBUTION FUNCTIONS AND THE FREE ENERGY OF A SYSTEM OF PARTICLES FOR THE POTENTIAL

The first approximation for the pair distribution function for a Coulomb interaction potential between ions:

$$\Phi^0_{ab}(r) = e_a e_b/\varepsilon r, \tag{11}$$

was first found by Bogoliubov[1] by the method of equations with variational derivatives[2]; it corresponds to the well-known[4] Debye-Hückel self-consistent potential

$$V(r) = (e_a/\varepsilon)\,e^{-\varkappa r}/r \tag{12}$$

and is equal to

$$F^1_{ab}(r) = -(e_a e_b/\varepsilon\theta v)\,e^{-\varkappa r}/r, \tag{13}$$

where ε is the dielectric constant of the solution, and the quantity

$$\frac{1}{\varkappa} = r_d = \left(\frac{\varepsilon\theta v}{4\pi\sum_a n_a e_a^2}\right)^{1/2} = \left(\frac{\varepsilon\theta}{4\pi n\sum_a n_a e_a^2}\right)^{1/2} \tag{14}$$

determines the mean radius of the ionic cloud which surrounds the given ion (and is known as the Debye radius), $v = V/N$ is the volume per particle, and $n = N/V$ is the concentration of the solution.

The pair function $F_{ab}(x, y \mid \Phi^0)$ for the potential (11) is, in first approximation (*i.e.*, with accuracy to quantities of second order of smallness):

$$F_{ab}(r) = 1 + v\,F^1_{ab}(r) = 1 - (e_a e_b/\varepsilon\theta)\,e^{-\varkappa r}/r. \tag{15}$$

As is evident from (13) and (15), the first approximation of the pair distribution function for the potential (11) diverges when $r \to 0$, which demonstrates the invalidity of the extrapolation of the Coulomb potential to a distance of the order of the particle radius, and the necessity of considering short-range repulsive forces. The second approximation for $F_{ab}(x, y \mid \Phi^0)$ in the case of a system with Coulomb interaction was found in Ref. 5, where, as was also pointed out in Ref. 1, this approximation becomes even more divergent for small r.

This difficulty with the divergence (at zero) of the pair distribution function in the use of the Coulomb potential of interaction between particles can be avoided as Kramers[6,4] bypassed the difficulty in the case of a purely statistical derivation of the free energy of an electrolyte, in which, in place of the energy of a solution with Coulomb interaction between the particles

$$U = \sum_{1\leqslant i<j\leqslant N}\frac{e_i e_j}{\varepsilon r_{ij}}$$

he used an expression of the form

$$U_1 = \sum_{1\leqslant i<j\leqslant N}\frac{e_i e_j}{\varepsilon r_{ij}}G_{ij}\,,$$

where

$$G_{ij} = \frac{1}{r_{ij}}(1 - e^{-\lambda h_{ij}}), \quad h_{ij} \to r_{ij}\,,$$

λ is a constant quantity. From the physical point of view, the introduction of the functions G_{ij} denotes implicit account of the short-range forces of repulsion between the ions. A qualitative account of repulsive forces of such a nature, which reduces to relieving the divergence (at zero) of the pair distribution function $F_{ab}(x, y \mid \Phi^0)$, was carried out in Refs. 7–9, in which, in place of the Coulomb potential (11), the interaction between the particles is determined by the potential

$$\Phi^0_{ab}(r) = (e_a e_b / \varepsilon r)(1 - e^{-\lambda r}). \tag{16}$$

In accord with Ref. 9, the pair distribution function for the potential $\Phi^0(r)$ with accuracy up to quantities of third order of smallness, is equal to

$$F_{ab}(r) = 1 + vF^1_{ab}(r) + v^2 \frac{1}{2}\{F^{1^2}_{ab}(r) + \sum n_c \int [F^{1^2}_{ac}(r_1) F^1_{cb}(r_2) + F^1_{ac}(r_1) F^{1^2}_{cb}(r_2)]\, dx_c + \sum_c \sum_d n_c n_d \int F^1_{ac}(r_1) F^{1^2}_{cd}(r_3) F^1_{db}(r_4)\, dx_c dx_d, \tag{17}$$

where $F^1_{ab}(r)$ is the first approximation of the pair distribution function determined in Ref. 9 for the potential (16). In the present research we shall find the free energy (10) of a system of charged particles with explicit account of the short-range forces of repulsion, taking for the potentials $\Phi^0(r)$ and $\Phi^1(r)$ functions of the form

$$\Phi^0(r) = \begin{cases} 0 & \text{for } r < \sigma \\ \dfrac{e_a e_b}{\varepsilon r} & \text{for } r > \sigma, \end{cases} \tag{18}$$

$$\Phi^1(r) = \begin{cases} \infty & \text{for } r < \sigma \\ 1 & \text{for } r > \sigma, \end{cases} \tag{19}$$

where σ is the diameter of the particle (for an ion, $\sigma \sim 10^{-8}$ cm). We find the first approximation of the pair distribution function $F_{ab}(x, y \mid \Phi^0)$ for a potential (18) from the Bogoliubov equation for the first approximation [1]:

$$F^1_{ab}(x, x') + \sum_c n_c \int \psi_{ac}(|x - x''|) F^1_{cb}(x''_1 x')\, dx'' = -\psi_{ab}(|x - x'|), \tag{20}$$

where

$$\psi_{ab}(r) = \frac{1}{\theta v} \Phi^0_{ab}(r) = \begin{cases} 0 & \text{for } r < \sigma, \\ e_a e_b / \varepsilon \theta v r & \text{for } r > \sigma. \end{cases} \tag{21}$$

Substituting the Fourier transform into Eq. (20):

$$F^1_{ab}(x, x') = \int L_{ab}(\nu, x) \exp\{i(\nu x')\}\, d\nu, \tag{22}$$

$$\psi_{ab}(|x - x'|) = \frac{1}{4\pi} \int Y_{ab}(|\nu|) \exp\{i(\nu, x - x')\}\, d\nu = \frac{1}{r} \int_0^\infty \nu \sin \nu r Y_{ab}(|\nu|)\, d\nu, \tag{23}$$

we get a system of linear algebraic equations

$$L_{ab}(\nu, x') + 2\pi^2 \sum_c n_c Y_{ac}(|\nu|) L_{cb}(\nu, x') = -\frac{1}{4\pi} Y_{ab}(|\nu|) \exp\{-i(\nu, x')\}. \tag{24}$$

Setting

$$L_{ab}(\nu, x') = K_{ab} \exp\{-i(\nu x')\} \tag{25}$$

we get

$$K_{ab} + 2\pi^2 \sum_c n_c Y_{ac}(|\nu|) K_{cb} = -\frac{1}{4\pi} Y_{cb}(|\nu|). \tag{26}$$

Since, from (21) and (23),

$$Y_{ab}(|\nu|) = \frac{1}{2\pi^2} \int \psi_{ab}(|x - x'|) \exp\{-i(\nu, x - x')\}\, dx' = \frac{2}{\pi\nu^2} \frac{e_a e_b}{\varepsilon\theta v} \cos \sigma\nu, \tag{27}$$

then the solution of the system (26) can be written in the form

$$K_{ab} = -\frac{\lambda_a \lambda_b}{2\pi^2} \frac{\cos \sigma\nu}{\nu^2 r_d^2 + \cos \sigma\nu},$$

$$\lambda_a = e_a \left(4\pi \sum_a n_a e_a^2\right)^{-1/2}.$$

We see from (22) and (25) that $F^1_{ab}(|x - x'|)$ is a radially symmetric function and is equal, according to the inversion formula of the Fourier integral, to

$$F^1_{ab}(r \mid \Phi^0) = \frac{4\pi}{r} \int_0^\infty \nu K_{ab}(|\nu|) \sin r\nu\, d\nu = -\frac{2 e_a e_b}{\pi r \varepsilon \theta v} r_d^2 I, \tag{28}$$

where

$$I = \int_0^\infty \frac{\nu \cos \sigma\nu \sin r\nu}{\nu^2 r_d^2 + \cos \sigma\nu}\, d\nu. \tag{29}$$

It is not difficult to see that at $\sigma = 0$ we get the expression (13) for $F^1_{ab}(r \mid \Phi^0)$.

In accord with (17), the second approximation of the function $F_{ab}(x_1, x_2 \mid \Phi^0)$ consists of three components, of which the latter two determine the effect of all the remaining particles of the system on the probability of finding two particular particles a and b at the points x_1 and x_2. Therefore, for small concentrations, in which the collective interaction between the particles is small, both these components are small (the third is smaller than the second) and the principal term is the first component $\frac{1}{2}F^{1^2}_{ab}(r)$; in case of symmetric solutions, the second approximation is exactly equal to this first term, since the two remaining terms are identically equal to zero, because of the neutrality of the system.

Thus, with account only of the principal term of the second approximation, the pair distribution function $F_{ab}(r \mid \Phi^0)$ is, in the second approximation for the potential (18), equal to

$$F_{ab}(r \mid \Phi^0) = 1 + vF^1_{ab}(r) + v^2 \frac{1}{2} F^{1^2}_{ab}(r)$$
$$= 1 - \frac{2e_a e_b}{\pi r \varepsilon \theta} r_d^2 I + 2\left(\frac{e_a e_b r_d^2}{\pi r \varepsilon \theta}\right)^2 I^2. \qquad (30)$$

Knowing $F_{ab}(r \mid \Phi^0)$, it is easy to calculate the free energy $F(\Phi^0)$ for the potential $\Phi^0(r)$ by the Gibbs-Helmholtz equation, and then, in accord with Eq. (10), we also calculate the free energy of the system of charged particles with consideration of short-range forces of repulsion. Actually, integrating the Gibbs-Helmholtz equation $F = E + T(dF/dT)_v$, we get for the free energy corresponding to the interaction of particles with the potential $\Phi^0(r)$ the expression

$$F(\Phi^0) = -T \int T^{-2} E(\Phi^0)\, dT. \qquad (31)$$

The average energy of interaction of the particles $E(\Phi^0)$ for the potential $\Phi^0(r)$ is equal to

$$E(\Phi^0) = \int U^0 D d\tau$$
$$= \int \sum_{\substack{a<b \\ i,j}} \Phi^0_{ab}(|x_{ai} - x_{bi}|) \cdot D dx_1 \ldots dx_N$$
$$= \sum_{a<b} N_a N_b \int \Phi^0_{ab}(|x_1 - x_2|)\, dx_1 dx_2 \int D dx_3 \ldots dx_N$$

or

$$E(\Phi^0) = \frac{2\pi}{V} \sum_{a,b} N_a N_b \int \Phi^0_{ab}(r)\, F_{ab}(r \mid \Phi^0)\, r^2 dr. \qquad (32)$$

Substituting (18) and (30), and taking into account the neutrality condition (2), we get

$$E(\Phi^0) = -\frac{4}{V} \sum_{a,b} N_a N_b$$
$$\times \int_\sigma^\infty \frac{e_a e_b}{\varepsilon r}\left(\frac{e_a e_b r_d^2}{\varepsilon \theta r} I - \frac{e_a^2 e_b^2 r_d^4}{\pi \varepsilon^2 \theta^2 r^2} I^2\right) r^2 dr. \qquad (33)$$

For symmetric solutions, $\sum_a N_a e_a^3 = 0$; therefore, the integral of the second term in (33) is equal to zero* and $E(\Phi^0)$ for such solutions will be

$$E(\Phi^0) = -\frac{\sum N_a e_a^2}{\pi \varepsilon} \int_0^\infty \frac{\cos^2 \sigma v}{v^2 r_d^2 + \cos \sigma v}\, dv. \qquad (34)$$

The integral here does not reduce to finite form; limiting ourselves to the first term of the asymptotic expression of this integral, we get

$$E(\Phi^0) = -\left(\sum N_a e_a^2 / 2\varepsilon\right) \cdot \varkappa / \sqrt{1 - \tfrac{1}{2}\sigma^2 \varkappa^2}, \qquad (35)$$

or

$$E(\Phi^0) = -\frac{\sum N_a e_a^2}{2\varepsilon} \varkappa \left(1 + \frac{1}{4}\sigma^2 \varkappa^2 + \frac{3}{32}\sigma^4 \varkappa^4 + \ldots\right). \qquad (36)$$

In the case of vanishingly small concentrations, where

$$\sigma \varkappa \ll 1, \qquad (37)$$

Equation (36) gives the Debye value for the energy of solution of a strong electrolyte[4]:

$$E = -(\varkappa / 2\varepsilon) \sum N_a e_a^2.$$

Equation (35) for the energy of solution, being a function of the variables T, V, N_a, is not a thermodynamic potential, and consequently does not permit us to develop the thermodynamics of strong electrolytes. Therefore, we must calculated the free energy, which is precisely the potential in these variables. For this purpose, we substitute (36) in (31). After integration we obtain the free energy of the system of charged particles for an interaction potential in the form of (18):

* In the case of non-symmetric solutions, the second term in (33) is not equal to zero, as a consequence of which, $E(\Phi^0)$ diverges logarithmically for $\sigma \to 0$.

$$F(\Phi^0) = -\frac{\varkappa}{3\varepsilon}\sum_a N_a e_a^2\left(1+\frac{3}{20}\sigma^2\varkappa^2+\frac{9}{224}\sigma^4\varkappa^4+\cdots\right) \quad (38)$$

For very small concentrations, in which the condition (37) of the applicability of the Debye theory is satisfied, we get from (38) the value given by this theory for the free energy of a strong electrolyte*:

$$F = -\frac{\varkappa}{3\varepsilon}\sum_a N_a e_a^2.$$

3. FINAL RESULTS. FURTHER IMPROVEMENT IN ACCURACY

Knowing the free energy $F(\Phi^0)$ of a system of particles for the potential $\Phi^0(r)$ of "long-range" forces, we can calculate the free energy $F(\Phi)$ of a system of charged particles with account of short-range forces of repulsion.

According to Eq. (10), $F(\Phi^0)$ is equal to

$$F(\Phi) = F(\Phi^0) - \frac{\theta}{2V}\sum_{a,b} N_a(N_b-\delta_{ab})\int_0^\infty\left[\exp\left\{-\frac{1}{\theta}\Phi^1_{ab}(r)\right\}-1\right]\times F_{ab}(r\mid\Phi^0)\,4\pi r^2\,dr.$$

For the potential of "short-range" forces in the form (19) and for the value of $F(\Phi^0)$ determined by (38), the free energy of a system of charged particles [keeping only the first approximation in $F_{ab}(r\mid\Phi^0)$] will be:

$$F(\Phi) = -\frac{\varkappa}{3\varepsilon}\sum_a N_a e_a^2\left(1+\frac{3}{20}\sigma^2\varkappa^2+\cdots\right)+\frac{2\pi\sigma^3\theta}{3V}\sum_{a,b}N_a(N_b-\delta_{ab}). \quad (39)$$

The expression obtained for the free energy is the thermodynamic potential and therefore permits the determination of both the thermal and the caloric properties of the system: the osmotic pressure (more precisely, the change in the osmotic pressure relative to the pressure in ideal solutions), the activity coefficients f_a of ions of the ath type, *etc.* We shall not determine these quantities, inasmuch as their computation reduces merely to differentiation of (39) with respect to V, T and N_a.

The free energy (39), and also Eqs. (35) and (38), were obtained for symmetric solutions with the exact value of the second approximation of the pair distribution function. In the case of asymmetric solutions, the expression for the pair distribution function (30) takes account only of the principal term of the second approximation of this function, which applies to solutions of low concentration. Upon increase in the concentration, the collective interactions between particles increase, and the value of the second and third terms in the expression of the second approximation of the pair distribution function (17) increase. Inasmuch as both these terms are expressed by the function $F^1_{ab}(r\mid\Phi^0)$, the value of which is given by Eq. (8), then even in this case we can compute the free energy of the system of charged particles with account of repulsive forces, similarly to what was done above.

In conclusion, I express my deep gratitude to Academician N. N. Bogoliubov for discussions on the results and for valued advice.

* The expression found in Ref. 8 for the first approximation of the free energy of a symmetric solution for the potential (16) [Eq. (2.4) of Ref. 8], diverges for $\sigma\to 0$, but does not go over into the Debye form, which points out the error of this expression. The correct value of the free energy of a symmetric solution, for the potential (16), is

$$F = -\frac{1}{12\,\varepsilon\varkappa^2\sigma^3}\left(\sqrt{1+2\varkappa\sigma}-1\right)^3\left(\sqrt{1+2\varkappa\sigma}+3\right).$$

[1] N. N. Bogoliubov, *Problems of Dynamical Theory in Statistical Physics*, Gostekhizdat, 1946.

[2] I. P. Bazarov, J. Exptl. Theoret. Phys. (U.S.S.R.) **32**, 1065 (1957); Soviet Phys. JETP **5**, 946 (1957).

[3] A. A. Vlasov, *Theory of Many Particles*, GITTL, 1950.

[4] V. K. Semenchenko, *Physical Theory of Solutions*, Gostekhizdat, 1941.

[5] E. A. Strel'tsova, J. Exptl. Theoret. Phys. (U.S.S.R.) **26**, 173 (1954).

[6] H. A. Kramers, Proc. Amsterdam Acad. **30**, 145 (1927).

[7] A. E. Glauberman, Dokl. Akad. Nauk SSSR **78**, 883 (1951).

[8] A. E. Glauberman and I. P. Iukhnovskii, J. Exptl. Theoret. Phys. (U.S.S.R.) 22, 562 (1952).
[9] I. P. Iukhnovskii, J. Exptl. Theoret. Phys. (U.S.S.R.) 27, 690 (1954).

Translated by R. T. Beyer
236

SOVIET PHYSICS JETP VOLUME 5, NUMBER 5 DECEMBER, 1957

Relation Between Scattering and Multiple Particle Production

S. Z. BELEN'KII
P. N. Lebedev Institute of Physics, Academy of Sciences, U.S.S.R.

(Submitted to JETP editor July 5, 1956)
J. Exptl. Theoret. Phys. (U.S.S.R.) 32, 1171-1175 (May 1957)

According to Fermi's theory, the multiple production of particles in high-energy collisions should be determined by the statistical weight of the respective states. In the present investigation, the statistical weight is calculated while taking into account the mutual interaction of pairs of particles, and it is shown that in this case the phase shift of the interacting particles is involved as a characteristic of the interaction. In resonance scattering, the effect of the scattering reduces to the appearance of an intermediate "isobaric" state which should be included in the statistical theory.

THE STATISTICAL THEORY of multiple production as originally suggested by Fermi[1] is well known to be in disagreement with experiments. In neutron-proton collisions, at energies around 2 Bev, the production of two mesons is considerably more probable than predicted by the theory[2].

Theoretical and experimental results disagree by a factor of 20. It was suggested by Nikishov and the author[3] to modify Fermi's theory according to the following considerations. The cross section of the scattering of π-mesons against nucleons has a strong maximum at a center-of-mass energy of about 160 Mev. This maximum corresponds to a P-state and isotopic spin $3/2$. These experiments indicate the presence of a strong interaction between π-mesons and nucleons in these circumstances. Such an interaction must also manifest itself in multiple particle production. It is evidently not taken into account in the original form of Fermi's theory.

A strong interaction between mesons and nucleons may be described qualitatively through the presence of an intermediate, rapidly decaying state of the meson-nucleon system with spin $3/2$ and isotopic spin $3/2$.

This concept of a so-called "isobaric" state was used in a number of articles[5,6], including also the work of Tamm and his collaborators[7]. We have suggested (see Ref. 3) that this isobaric state should be included in the statistical theory of multiple production, thus effectively allowing for the strong interaction between the particles. It was suggested that in a collision between two nucleons or a nucleon and a meson, there may appear "quasi-particles" (isobaric states of the system) of mass $1.32\,M_0$, where M_0 is the nucleon mass, having isotopic spin $3/2$ and ordinary spin $3/2$, and rapidly decaying into a nucleon and a meson. It was also suggested that the probability for the production of such "particles" may be determined from their statistical weight. A comparison was made between the modified Fermi theory and experimental results on the multiple production of mesons in nucleon-meson and meson-nucleon collisions in the energy range of 1.4 to 5 Bev (see Refs. 3 and 8). Comparison shows that the theory agrees with experiments regarding the probability of various multiple production processes, and also regarding the energy distribution of secondary particles.

In the present article we want to bring up certain theoretical considerations regarding the relation between resonance scattering and multiple particle production.

First we shall introduce the following example suggested by Landau. We shall consider the statistical sum of the states of a non-ideal gas. In the first approximation we shall assume an ideal gas,

and in the second we shall include only two-particle interactions (see Ref. 9). Uhlenbeck and Beth[10] have shown that the additional term appearing in the sum over the states when two-particle interaction is included, may be represented in the following form:

$$Z = Z_1 + Z_2, \tag{1}$$

where Z_1 is the sum over states of the discrete spectrum of the two particles, and Z_2 is the sum over the continuous spectrum including two-particle interaction:

$$Z_2 = \frac{1}{\pi} \sum_l \int_0^\infty (2l+1) \frac{\partial \eta_l}{\partial p} e^{-p^2/mT} dp, \tag{2}$$

where $\eta_l(p)$ is the phase shift, p the momentum of the particle in the center-of-mass system, l the orbital angular momentum, T the temperature, and m the mass of the particle. If the scattering shows resonance character for some value of l, then

$$\eta_l = \eta_l^0 + \tan^{-1} \frac{\Gamma}{E_0 - E}, \tag{3}$$

where η_l^0 is the phase shift due to resonance. The phase changes by π when going through resonance. If the resonance is sufficiently sharp, then the expression for Z_2 reduces to

$$Z_2 = (2l+1) e^{-p_0^2/mT}, \tag{4}$$

where p_0 is the momentum at which maximum scattering takes place. Expression (4) corresponds to an extra "discrete" state of positive energy for the two-particle system.

Now, we shall turn directly to the problem of interest and consider a π-meson-nucleon collision. According to the statistical theory, the production of n mesons as a result of the collision is proportional to the statistical weight of the system consisting of one nucleon and n mesons.

Excluding the interaction of secondary particles, the statistical weight is computed by the following formula

$$S_0(W, n, M_0) = \left[\frac{\Omega}{(2\pi\hbar)^3}\right]^n \frac{1}{n!} \int \prod_{i=1}^{n} d\mathbf{p}_i d\mathbf{p} \, \delta(W - \Sigma W_i - W_M) \, \delta(\Sigma \mathbf{p}_i + \mathbf{p}). \tag{5}$$

W is here the energy of the system, M_0 the nucleon mass (in energy units), Ω the effective volume (a quantity of the order of $(4\pi/3)(\hbar/\mu c)^3$, where μ is the meson mass), $\mathbf{p}_i$ the momentum of the ith meson, $\mathbf{p}$ the momentum of the nucleon, W_i the energy of the ith meson, W_M the energy of the nucleon, and the δ-function insures conservation of energy and momentum. The integration is to be carried out over the momentum space of all the mesons and of the nucleon.

Now let us compute the statistical weight including the interaction of the nucleon with the mesons. We shall assume two-particle interaction. First let us single out in Eq. 5 a pair of particles, say a nucleon and a meson. We transform to the variables $\mathbf{p}_c$ and $\mathbf{p}'$, where $\mathbf{p}_c$ is the momentum of the center of mass of the nucleon-meson system, and $\mathbf{p}'$ is the momentum of the meson (or the nucleon) in the center-of-mass system. The formula for the statistical weight may then be written in the following form:

$$S^{(1)}(W, n, M_0) = \sum_{\mathbf{p}'} \left[\frac{\Omega}{(2\pi\hbar)^3}\right]^{n-1} \frac{1}{n!} \int \prod_{i=1}^{n-1} d\mathbf{p}_i d\mathbf{p}_c \delta\left(W - \sum_{i=1}^{n-1} W_i - W_c - W'\right) \delta\left(\sum_{i=1}^{n-1} \mathbf{p}_i + \mathbf{p}_c\right). \tag{6}$$

W_c is here the kinetic energy of the center of mass of the two particles, and W' is their total energy in the system where their center of mass is at rest.

We shall sum over all possible states of the nucleon-meson system in the same fashion as this was done for a non-ideal gas (see Ref. 9). At large distances, the wave function for the state with orbital angular momentum l and momentum p' has the following well-known asymptotic form

$$\psi = \frac{\text{const}}{r} \sin\left(\frac{p'}{\hbar} r - \frac{l\pi}{2} + \eta_l\right). \tag{7}$$

The phase shift η_l depends on the specific form of the particle interaction. Let the range of r be limited to some large but finite radius R_0. The possible values of the momentum are then determined by the condition

$$R_0 p'/\hbar - l\pi/2 + \eta_l = s\pi, \tag{8}$$

where s is an integer. If R_0 is sufficiently large, one may assume that s varies continuously and transform the summation in Eq. 6 to an integral

$$S^{(1)}(W, n, M_0) = \sum_{p'} S_{p'}^{(1)} = \int \sum_{l} (2l+1) S_{p'}^{(1)} \frac{1}{\pi} \left(\frac{R_0}{\hbar} + \frac{\partial \eta_l}{\partial p'} \right) dp' , \tag{9}$$

where $S_{p'}^{(1)}$ is the expression appearing in Eq. 6 after the summation sign; the factor $(2l + 1)$ and the sum over l is related to the angular momentum degeneracy. The first term in Eq. 9 gives the statistical weight exclusive of the interaction, *i.e.*, it leads to Eq. 5; the second term which includes the two-particle interaction reduces to the following expression:

$$S^{(2)} = \sum_{l} \frac{2l+1}{\pi} \left[\frac{\Omega}{(2\pi\hbar)^3} \right]^{n-1} \frac{1}{n!} \int \prod_{i=1}^{n-1} d\mathbf{p}_i d\mathbf{p}_c \delta \left(W - \sum_{i=1}^{n-1} W_i - W_c - W' \right) \times \delta \left(\sum_{i=1}^{n-1} \mathbf{p}_i + \mathbf{p}_c \right) \frac{\partial \eta_l}{\partial W'} dW' . \tag{10}$$

We have transformed here from the variable p' to the variable W' (W' is the total energy in the center-of-mass system), which is uniquely related to p'. Equation 10 should be multiplied by n to allow for the presence of the n mesons. The resulting expression for the statistical weight including two-particle interaction between nucleon and mesons is written as follows:

$$S(W, n, M_0) = S_0(W, n, M_0) + \sum_{l} \frac{2l+1}{\pi} \int S_0(W, n-1, W') \frac{\partial \eta_l}{\partial W'} dW' . \tag{11}$$

The formula for $S_0(W, n, M_0)$ is obtained here from Eq. 5, and $S_0(W, n - 1, W')$ is the statistical weight for n non-interacting particles: $n - 1$ mesons and one heavy "particle" of mass W'. Let us assume that the scattering exhibits a resonance character for some value of l. If the resonance is sufficiently sharp, the function $S_0(W, n - 1, W')$ may be removed from under the integral sign and its value taken at the point $W' = W_0$ corresponding to the maximum of $\partial\eta_l/\partial W'$, and the integral $\int(\partial\eta_l/\partial W')dW' = \pi$. If we substitute for the second term of Eq. 11 just the term corresponding to resonance scattering, we obtain

$$S(W, n, M_0) = S_0(W, n, M_0) + (2l+1) S_0(W, n-1, W_0), \tag{12}$$

where $W_0 = M_0 + \mu + E_0$, and E_0 is the kinetic energy of the nucleon and the meson for the case of resonance.

Thus the second term of Eq. 12 which includes the meson-nucleon interaction formally corresponds exactly to a system of $n - 1$ mesons and a nucleon in an "isobaric" state. At the same time, Eq. 12 gives the statistical weight for the production of one nucleon and n mesons. It should be noted that it is not clear whether the interaction may generally be limited to a two-particle type of interaction. This is a natural assumption, however, for the case of the specially strong two-particle interaction which corresponds to resonance scattering. Similarly, if we consider the collision between two nucleons, it is necessary to include the simultaneous interaction of the two nucleons with the mesons. Augmenting Eq. 12, we obtain

$$S_{NN} = \sum_{l'} \frac{2l'+1}{\pi} \sum_{l} \frac{2l+1}{\pi} \times \iint S_0(W, n-2, W', W'') \frac{\partial \eta_l}{\partial W'} \frac{d\eta'}{\partial W''} dW' dW'' . \tag{13}$$

$S_0(W, n - 2, W', W'')$ is here the statistical weight for n non-interacting particles: $n - 2$ mesons and two "heavy particles" of mass W' and W''. If the scattering exhibits resonance character for some value of l, Eq. 13 reduces to the following expression:

$$S_{NN} = (2l+1)^2 S_0(W, n-2, W_0, W_0). \tag{14}$$

This expression formally corresponds to the statistical weight for a system consisting of $n - 2$ mesons and two nucleons in an "isobaric" state. If it turns out that the scattering of π-mesons against π-mesons exhibits resonance character at certain energy values (there is an indication of this in the literature [12]), it will be necessary to include analogously the π-meson interaction in computing the statistical weight.

Let us consider the following example. We shall compute the statistical weight corresponding to the

production of a system of one nucleon and two mesons as a result of a meson-nucleon collision.

This statistical weight is determined by the following expression:

$$S(W, 2, M_0) = S_0(W, 2, M_0) + \sum_l \frac{2l+1}{\pi} \int S_0(W, 1, W') \frac{\partial \eta_l}{\partial W'} dW'. \quad (15)$$

The formula for $S_0(W, 1, W')$ has a simple analytical form (see for example Ref. 3):

$$S_0(W, 1, W_1) = C(W^2 - \mu^2 - W_1^2)(1 - (W_1^2 - \mu^2)^2 / W^4). \quad (16)$$

C is here a coefficient which is independent of $W_1 \equiv W'$. If $(W_1/W)^4 < 1$, the second term in parenthesis is practically equal to 1. We shall assume that this condition is satisfied. Indeed, when $W_1 = 1.23$ Bev and $W = 2$ Bev, the ratio $(W_1/W)^4$ is on the order of 12 percent. Let us assume that the scattering shows resonance character for some value of l, and the phase shift is obtained from Eq. 3. We shall assume the quantity Γ is independent of the energy; we find, then

$$\partial \eta_l / \partial W_1 = \partial \eta_l / \partial E_1 = \Gamma / [\Gamma^2 + (E_0 - E_1)^2], \quad (17)$$

where $E_1 = W_1 - M_0 - \mu$.

The second term of Eq. 15 may now be written as follows:

$$S_2 = \frac{C_1}{\pi} \int_0^{E_{\max}} [W^2 - \mu^2 - (M_1 + E_1)^2] \frac{\Gamma dE_1}{\Gamma^2 + (E_0 - E_1)^2}, \quad (18)$$

where C_1 is a constant, and

$$M_1 = M_0 + \mu, \quad E_{\max} = \sqrt{W^2 - \mu^2} - M_1.$$

Let us transform to the variable $\varepsilon = E_1 - E_0$; the integration is then easily carried out, and we obtain the following result:

$$S_2 = \frac{C_1}{\pi} [(W^2 - \mu^2 - M_2^2) \left(\tan^{-1} \frac{\sqrt{W^2 - \mu^2} - M_2}{\Gamma} - \tan^{-1} \left(-\frac{E_0}{\Gamma} \right) \right) - \Gamma M_2 \log \frac{\Gamma^2 + (\sqrt{W^2 - \mu^2} - M_2)^2}{\Gamma^2 + E_0^2} - \Gamma (\sqrt{W^2 - \mu^2} - M_2) + \Gamma^2 \left(\tan^{-1} \frac{\sqrt{W^2 - \mu^2} - M_2}{\Gamma} - \tan^{-1} \left(-\frac{E_0}{\Gamma} \right) \right). \quad (19)$$

$M_2 = M_0 + \mu + E_0$ is here the mass of the nucleon in the "isobaric" state. It is easily seen that as Γ tends to zero, $S_2 = C_0(W^2 - \mu^2 - M_2^2)$. This expression corresponds to the statistical weight of a system of two particles having respectively mass μ (meson) and M_2 ("isobaric" state of the nucleon). Let us assume now that $\Gamma = E_0/2$ and $E_0 = 160$ Mev. These values are close to the values obtained from experiments on the scattering of π-mesons against nucleons (see Ref. 13). Γ is given here the value it had at an energy of E_0. Actually it turns out to be a function of E_1. We shall evaluate Eq. 19 for $W = 1.9$ Bev. This corresponds, in the laboratory system, to an incident π-meson energy of 1.37 Bev. We find that the value of S_2 for $\Gamma = E_0/2$ is 0.78 times the value for S_2 for $\Gamma = 0$. In this case the computation of the level width leads to a correction which it is hardly worth considering in view of the approximate nature of the whole theory. This correction is even smaller at higher energies.

An attempt to compute the nucleon-meson interaction in the framework of the statistical theory was also made by Kovacs [14]. That analysis, however, introduces, along with statistical notions, certain matrix elements which are evaluated by applying a specific type of meson theory. The computations are extremely difficult. It seems to us that it is inconsistent to combine a statistical theory of phenomenological character with computations based on a certain variant of meson theory which appears doubtful itself.

In conclusion, the author wishes to express his gratitude to L. D. Landau for a discussion of the subjects considered in this article.

[1] E. Fermi, Progr. Theoret. Phys. 5, 570 (1950); Phys. Rev. 92, 452 (1953); 93, 1434 (1954).

[2] Fowler, Shutt, Thorndike and Whittemore, Phys. Rev. 95, 1026 (1954).

[3] S. Z. Belen'kii and A. I. Nikishov, J. Exptl. Theoret. Phys. (U.S.S.R.) 28, 744 (1955); Soviet Phys. JETP 1, 593 (1955).

[4] H. A. Bethe and F. de Hoffmann, *Mesons and Fields*, Vol. 2, Row, Peterson and Co., New York (1955).

[5] K. A. Brueckner, Phys. Rev. 86, 106 (1952).

[6] F. J. Belinfante, Phys. Rev. 92, 145 (1953); D. C. Peasly, Phys. Rev. 94, 1085 (1954); R. Gatto, Nuovo cimento 1, 159 (1955).

[7] Tamm, Gol'fand and Fainberg, J. Exptl. Theoret. Phys. (U.S.S.R.) 26, 649 (1954).

[8] A. I. Nikishov, J. Exptl. Theoret. Phys. (U.S.S.R.) 29, 246 (1955); Soviet Phys. JETP 29, 161 (1956); 30, 601 (1956); Soviet Phys. JETP 3, 634 (1956); 30, 990 (1956); Soviet Phys. JETP 3, 783 (1956); V. M. Maksimenko and A. I. Nikishov, J. Exptl. Theoret. Phys. (U.S.S.R.) 31, 727 (1956); Soviet Phys. JETP 4, 614 (1957).

[9] L. Landau and E. Lifshitz, *Statistical Physics*, GITTL (1951), § 75.

[10] G. E. Uhlenbeck and E. Beth, Physica 3, 729 (1936); 4, 915 (1937).

[11] R. H. Milburn, Rev. Mod. Phys. 27, 1 (1955); I. L. Rozental', J. Exptl. Theoret. Phys. 28, 118 (1955); Soviet Phys. JETP 1, 166 (1955).

[12] F. J. Dyson, Phys. Rev. 99, 1037 (1955); G. Takeda, Phys. Rev. 100, 440 (1955).

[13] J. Orear, Phys. Rev. 100, 288 (1955).

[14] J. S. Kovacs, Phys. Rev. 101, 397 (1956).

Translated by M. A. Melkanoff
237

SOVIET PHYSICS JETP VOLUME 5, NUMBER 5 DECEMBER, 1957

Contribution to the Theory of Transport Processes in a Plasma Located in a Magnetic Field

E. S. FRADKIN

P. N. Lebedev Institute of Physics, Academy of Sciences, U.S.S.R.

(Submitted to JETP editor July 5, 1956)

J. Exptl. Theoret. Phys. (U.S.S.R.) 32, 1176-1187 (May, 1957)

The mean statistical characteristics (velocity, heat current, stress tensor, etc.) have been determined for transport phenomena in a plasma located in a magnetic field.

THE PRESENT ARTICLE develops the theory of a plasma located in electric and magnetic fields (a brief account of the principal results of the author's analysis[1] is presented here). A method of approximations is used to solve the Boltzmann equation. The essence of this method lies in computing the terms of the distribution function, expanded in powers of some small parameter characteristic of the specific problem. One thus finds a so-called "local" distribution function which must be understood in the following sense: the complete distribution function is a function of 6 variables (3 coordinates and 3 velocity components) while the "local" distribution function depends explicitly upon the velocity only, and its dependence upon the coordinates enters only through the externally-acting forces and the mean statistical characteristics (temperature, density, and in general, velocity of the center of mass), which play the role of parameters. The dependence of these characteristics upon the coordinates is obtained by solving a certain system of equations which also arise from the Boltzmann equation. These equations represent a generalization of the well-known hydrodynamical equations.

1. As is well known[2], the Boltzmann equation for particles of type s, mixed with particles of other types, has the following form in the presence of magnetic and electric fields (the notation is that used by Chapman and Cowling):

$$\frac{\partial f_s}{\partial t} + \mathbf{v}_i \frac{\partial f_s}{\partial x_i} + \frac{e_s}{m_s}\left\{\mathbf{E} + \frac{1}{c}[\mathbf{vH}]\right\}_i \frac{\partial f_s}{\partial \mathbf{v}_i} = -\sum_{n=1} J_{sn}(f_s, f_n). \tag{1}$$

It will later be found convenient to rewrite the Boltzmann equation (1) in terms of a new set of independent variables; specifically, we transform the velocity of particles of a given type into their velocity with respect to the center of mass. The latter is given by the following formula:

$$\mathbf{v}_0 = \sum_{s=1}^{n} \int m_s \mathbf{v} f_s d\mathbf{v} \Big/ \sum_s \int m_s f_s d\mathbf{v}. \tag{2}$$

Eq. (1) takes the following form in terms of the new variables (henceforth, we write v for v^{rel}):

$$\frac{Df_s}{Dt} + v_i \frac{\partial f_s}{\partial x_i} + \left\{ \frac{e_s}{m_s} \left(\mathbf{E} + \frac{1}{c} [\mathbf{v}_0 \mathbf{H}] \right) - \frac{D\mathbf{v}_0}{Dt} \right\}_i \frac{\partial f_s}{\partial v_i}$$

$$+ \frac{e_s}{m_s c} [\mathbf{v}\mathbf{H}] \frac{\partial f_s}{\partial \mathbf{v}} - \frac{\partial v_s}{\partial v_i} v_k \frac{\partial v_{0i}}{\partial x_k} = - \sum_n J_{sn}(f_s, f_n), \tag{3}$$

where $D/Dt = \partial/\partial t + v_{0i}\partial/\partial x_i$.

As an approximate method for solving the system of equations (1), we expand the solution as a power series in a small parameter of the problem. In the case of axial symmetry, the following parameters are available: L, the dimension of the system, l, the mean free path, and R, the Larmor radius. Depending upon the relations between these three parameters, the general problem may be divided into three cases: 1) strong magnetic field ($\nu/\omega \ll 1$), where ν is the collision frequency, and ω the Larmor frequency, $R/l \ll 1$; 2) weak magnetic field ($\nu/\omega \gg 1$) $R/l \gg 1$; 3) intermediate region $R/l \sim 1$.

Formally, however, it is convenient to seek the distribution function as a series in the dimensional parameter

$$f = \sum \lambda^m f^{(m)}, \tag{4}$$

where it follows from our exposition that the parameter λ turns out to be $\lambda = 1/\omega$ in a strong magnetic field, $\lambda = 1/\nu$ in a weak magnetic field, and $\lambda = 1/L$ in the intermediate case.

The equations for each term $f^{(m)}$ are easily obtained in the usual fashion. One must also include the fact that the Boltzmann equation must satisfy certain integral conditions of solubility:

$$\int D f_s d\mathbf{v} = 0, \tag{5a}$$

$$\sum_{s=1}^{n} \int D f_s m_s \mathbf{v} d\mathbf{v} = 0, \tag{5b}$$

$$\sum_{s=1}^{n} \int D f_s \frac{m_s v^2}{2} d\mathbf{v} = 0. \tag{5c}$$

These equations are the equations of hydrodynamics, generalized to include a plasma in the presence of magnetic and electric fields, and can be written explicitly as follows:

a) equation of continuity for particles of type s

$$DN_s/Dt + N_s \operatorname{div} \mathbf{v}_0 + \operatorname{div}(N_s \tilde{\mathbf{v}}_s) = 0, \tag{6a}$$

b) equation of motion

$$\rho \frac{Dv_{0i}}{Dt} = \sum_{s=1}^{n} e_s N_s \left(\mathbf{E} + \frac{1}{c} [\mathbf{v}_0 \mathbf{H}] \right)_i - \frac{\partial \Pi_{ik}}{\partial x_k} + \frac{1}{c} [\mathbf{j}\mathbf{H}]_i, \tag{6b}$$

c) equation of conservation of energy for all the particles

$$D\mathcal{E}/Dt + \mathcal{E} \operatorname{div} \mathbf{v}_0 + \operatorname{div} \mathbf{q} + \Pi_{ik} \partial v_{0i}/\partial x_k$$

$$- \mathbf{j} \left(\mathbf{E} + \frac{1}{c} [\mathbf{v}\mathbf{H}] \right) = 0, \tag{6c}$$

where we have introduced the following notation:

$$\int f_s d\mathbf{v} = N_s, \quad \int f_s \mathbf{v} d\mathbf{v} = N_s \tilde{v}_s, \quad \mathbf{q} = \sum_{s=1}^{n} \int \frac{m_s v^2}{2} \mathbf{v} f_s d\mathbf{v},$$

$$\Pi_{ik} = \sum_{s=1}^{n} \int m_s v_i v_k f_s d\mathbf{v}, \quad \mathbf{j} = \sum e_s N_s \tilde{\mathbf{v}}_s, \quad \rho = \sum N_s m_s, \quad \mathcal{E} = \sum \frac{m_s v^2}{2} f_s d\mathbf{v}.$$

It will be found convenient in later analyses to be certain that Eqs. (5a) and (5c) are identically satisfied. The following system of equations may easily be shown to fulfill this requirement

$$\frac{Df_s}{Dt} + v_i \frac{\partial f_s}{\partial x_i} + \left\{ \frac{e_s}{m_s} \left(\mathbf{E} + \frac{1}{c} [\mathbf{v}_0 \mathbf{H}] - \frac{D\mathbf{v}_0}{Dt} \right\}_i \frac{\partial f_s}{\partial v_i} - \frac{\partial f_s}{\partial v_i} v_k \frac{\partial v_{0i}}{\partial x_k}$$

$$+ \frac{e_s}{m_s c} [\mathbf{v}\mathbf{H}] \frac{\partial f_s}{\partial \mathbf{v}} - \sum_{r=1}^{n} \left\{ \frac{DN_r}{Dt} + N_r \operatorname{div} \mathbf{v}_0 + \operatorname{div}(N_r \tilde{\mathbf{v}}_r) \right\} \frac{\partial f_s}{\partial N_r}$$

$$- \left(2/3 \sum_{r=1}^{n} N_r k \right) \left\{ \frac{3}{2} \sum_{r=1}^{n} N_r k \frac{DT}{Dt} - \frac{3}{2} kT \sum_{r=1}^{n} \operatorname{div}(N_r \tilde{\mathbf{v}}_r) + \operatorname{div} \mathbf{q} \right.$$

$$\left. + \Pi_{ik} \partial v_{0i}/\partial x_k - \mathbf{j} \left(\mathbf{E} + \frac{1}{c} [\mathbf{v}_0 \mathbf{H}] \right) \right\} \partial f_s / \partial T = - \sum_n J_{sn}(f_s, f_n), \tag{7}$$

where instead of using the total interval energy $\mathcal{E}$ of the plasma, we have introduced the "effective" temperature of the plasma (the word "effective" will be omitted hereinafter), *i.e.*,

$$\mathcal{E} = \frac{3}{2} \sum_{s=1}^{n} N_s kT.$$

Note that in expanding the mean quantities in terms of a small parameter, it may be assumed that the zero approximation completely determines N_s and T.

2. We shall now consider a stationary problem with axial symmetry, a mixture of two charged gases in a strong magnetic field. Let N_1, $-e$, m, and f_1 be the density, charge, mass, and distribution function of the electrons, and N_2, Ze, M, and f_2 be the corresponding properties of the ions.

In this case the system of equations (1) has the form:

$$v_{0x} \frac{\partial f_1}{\partial x} + v_x \frac{\partial f_1}{\partial x} - \left\{ \frac{e}{m} \left(\mathbf{E} + \frac{1}{c} [\mathbf{v}_0 \mathbf{H}] \right) + v_{0x} \frac{\partial \mathbf{v}_0}{\partial x} \right\} \frac{\partial f_1}{\partial \mathbf{v}} -$$

$$- \frac{\partial f_1}{\partial v_i} v_x \frac{\partial v_{0i}}{\partial x} - \frac{e}{mc} [\mathbf{v}\mathbf{H}] \frac{\partial f_1}{\partial \mathbf{v}} = - \{ J_{11}(f_1, f_1) + J_{12}(f_1, f_2) \}, \tag{8}$$

$$v_{0x} \frac{\partial f_1}{\partial x} + v_x \frac{\partial f_2}{\partial x} + \left\{ \frac{eZ}{M} \left(\mathbf{E} + \frac{1}{c} [\mathbf{v}_0 \mathbf{H}] - v_{0x} \frac{\partial \mathbf{v}_0}{\partial x} \right\} \frac{\partial f_2}{\partial \mathbf{v}} - \right.$$

$$- \frac{\partial f_2}{\partial v_i} v_x \frac{\partial v_{0i}}{\partial x} + \frac{eZ}{Mc} [\mathbf{v}\mathbf{H}] \frac{\partial f_2}{\partial \mathbf{v}} = - \{ J_{22}(f_2, f_2) + J_{21}(f_2, f_1) \}, \tag{9}$$

where the z-axis is taken along $\mathbf{H}$.*

In this case the gradients of the concentration and the electric field have no z-components, and if the system is sufficiently large in the z-direction, $L_z \gg l$, the distribution will be Maxwellian, and we shall assume that $v_{0z} = 0$.

Expanding the distribution function and the mean quantities (except N_2 and T) as series in the parameter $1/\omega$ and equating coefficients of equal power, we obtain equations which may be used for computing successive approximations to the distribution function. We thus obtain the following equations for $f_s^{(0)}$ and $f_s^{(1)}$

$$- \frac{e}{mc} [\mathbf{v}\mathbf{H}] \frac{\partial f_1^{(0)}}{\partial \mathbf{v}} = 0, \quad \frac{eZ}{Mc} [\mathbf{v}\mathbf{H}] \frac{\partial f_0^{(2)}}{\partial \mathbf{v}} = 0, \tag{10}$$

$$- \frac{e}{mc} [\mathbf{v}\mathbf{H}] \frac{\partial f_1^{(1)}}{\partial \mathbf{v}} + v_x \frac{\partial f_1^{(0)}}{\partial x} - \left\{ \frac{e}{m} \left(\mathbf{E} + \frac{1}{c} [\mathbf{v}_0 \mathbf{H}] \right) \right\} \frac{\partial f_1^{(0)}}{\partial \mathbf{v}} = - \{ J_{11} + J_{12} \}, \tag{11}$$

$$\frac{eZ}{Mc} [\mathbf{v}\mathbf{H}] \frac{\partial f_2^{(1)}}{\partial \mathbf{v}} + v_x \frac{\partial f_2^{(0)}}{\partial x} + \left\{ \frac{eZ}{M} \left(\mathbf{E} + \frac{1}{c} [\mathbf{v}_0 \mathbf{H}] \right) \right\} \frac{\partial f_2^{(0)}}{\partial \mathbf{v}} = - \{ J_{22} + J_{21} \}. \tag{12}$$

All the equations which are used for computing successive approximations may be symbolically written as follows:

$$[\mathbf{v}\omega_s] \partial f_s^{(m)} / \partial \mathbf{v} = F_s(v, x); \quad \omega_s = (eZ_s/m_s c) \mathbf{H}. \tag{13a}$$

It is evident that the solution to this equation makes sense only when the result of the integration does not depend on the contour of integration. In order for this to be true, it is sufficient that the following relation hold:

$$\operatorname{curl} \{ [\mathbf{u}\omega_s] F_s(u, x) / [\mathbf{u}, \omega_s]^2 \} = 0. \tag{13b}$$

* Since the problem is solved locally, we replace the cylindrical coordinates with cartesian coordinates having the x-axis along the radius r and the axis $x_2 = y$ along the θ-direction.

The significance of condition (13b) becomes clearer when the solution to Eq. (13) is written in terms of new variables

$$f_s^{(m)} = \frac{1}{\omega_s}\int_0^{\alpha} F_s(\mathbf{v}, x)\, d\alpha.\ \cot\alpha = v_x/v_y. \quad (13c)$$

Condition (13b) becomes in these variables a periodicity condition, $f_s^{(m)}(\alpha) = f_s^{(m)}(\alpha + 2\pi)$, for which it is necessary and sufficient that the following hold:

$$\int_0^{2\pi} F_s(v, x)\, d\alpha = 0. \quad (13d)$$

Condition (13d) together with the requirement that the temperature and density be wholly obtainable from the zero approximation, completely determine the solution to the equations for $f_s^{(m)}$. Computations yield the following results

$$f_n^{(0)} = N_n\pi^{-3/2}\beta_n^3 \exp(-\beta_n^2 v^2),\ \beta_1 = (m/2kT)^{1/2},$$

$$\beta_2 = (M/2kT)^{1/2}$$

$$f_1^{(1)} = \frac{1}{\omega_{el}}[\mathbf{A}_1\mathbf{n}_0]\,\mathbf{v}f_1^{(0)};\ f_2^{(1)} = -\frac{1}{\omega_{ion}}[\mathbf{A}_2\mathbf{n}_0]\,\mathbf{v}f_2^{(0)}, \quad (14)$$

$$\mathbf{A}_n = \frac{\nabla N_n}{N_n} + \frac{\nabla T}{T} + \frac{e\mathbf{E}}{kT} + \frac{e}{ckT}[\mathbf{v}_0^{(1)}\mathbf{H}] - \left(\frac{5}{2} - \beta_n v^2\right)\frac{\nabla T}{T};$$

$$n_0 = \mathbf{H}/H;\ \omega_{el} = eH/mc;\ \omega_{ion} = eZH/Mc. \quad (15)$$

The relative velocities $\mathbf{v}_n$ and heat currents $\mathbf{q}_n$ for each type of particle are found to be

$$\tilde{\mathbf{v}}_1^{(1)} = \frac{kT}{m\omega_{el}}\left[\left(\frac{\nabla N_1}{N_1} + \frac{\nabla T}{T} + \frac{e\mathbf{E}}{kT} + \frac{1}{\omega_{el}}[\mathbf{v}_0\mathbf{n}_0]\right), \mathbf{n}_0\right], \quad (16)$$

$$\tilde{\mathbf{v}}_2^{(1)} = -\frac{kT}{M\omega_{ion}}\left[\left(\frac{\nabla N_2}{N_2} + \frac{\nabla T}{T} + \frac{e\mathbf{E}}{kT} - \frac{1}{\omega_{ion}}[\mathbf{v}_0\mathbf{n}_0]\right),\ \mathbf{n}_0\right], \quad (17)$$

$$\mathbf{v}_0^{(1)} = -\frac{kT}{M\omega_{ion}}\left[\frac{\frac{\nabla N_2}{N_2} + \frac{\nabla T}{T} - \frac{eZ\mathbf{E}}{kT} - \frac{N_1 mZ}{N_2 M}\left(\frac{\nabla N_1}{N_1} + \frac{\nabla T}{T} + \frac{e\mathbf{E}}{kT}\right)}{1 + N_1 m_1/N_2 M}, \mathbf{n}_0\right], \quad (18)$$

$$\mathbf{q}_1^{(1)} = \frac{5}{2}\frac{N_1(kT)^2}{m\omega_{el}}\left[\frac{\nabla T}{T}\mathbf{n}_0\right] + \frac{5}{2}N_1 kT\tilde{\mathbf{v}}_2, \quad (19)$$

$$\mathbf{q}_{tot}^{(1)} = \mathbf{q}_1^{(1)} + \mathbf{q}_2^{(1)} = \frac{5N_1(kT)^2}{2m\omega_{el}}\left[\frac{\nabla T}{T}\mathbf{n}_0\right]\left(1 - \frac{N_2}{N_1 Z}\right) + \frac{5}{2}kT(N_1\tilde{\mathbf{v}}_2 + N_2\tilde{\mathbf{v}}_2). \quad (20)$$

In this approximation, the addition to the stress tensor Π_{ik} is zero. Since a complete solution of the problem requires knowledge of the addition to the stress tensor, it is necessary to obtain a higher approximation to the distribution function. Instead of solving the Boltzmann equation in higher approximations, it is more convenient to use it for finding a system of equations for the mean quantities of interest, and solve these equations directly. Thus, obtaining in the second approximation the equations for $\tilde{v}_n^{(2)}$, $q_n^{(2)}$ and $\Pi_{ik}^{(2)}$, and solving them (to the order m/M), we find

$$\tilde{\mathbf{v}}_{0,x}^{(2)} = -\frac{N_1 kT\nu_{el}}{N_2 Zm\omega_{el}^2}\left\{\frac{N_1'}{N_1} + \frac{N_2'}{ZN_2} + \frac{T'}{T}\left(\frac{1}{Z} - \frac{1}{2}\right)\right\},\ \tilde{v}_1^{(2)} = -\frac{N_2 M}{N_1 m}\tilde{v}_2^{(2)}, \quad (21)$$

$$\tilde{v}_{1x} = -\frac{\nu_{el}kT}{m\omega_{el}^2}\left(1 - \frac{N_1}{N_2 Z}\right)\left\{\frac{N_2'}{N_2 Z} + \frac{N_1'}{N_1} + \frac{T'}{T}\left(\frac{1}{Z} - \frac{1}{2}\right)\right\}, \quad (22)$$

$$q_{1x}^{(2)} = -\frac{N_1(kT)^2\nu_{el}}{m\omega_{el}^2}\left\{\left(\frac{7}{4} - \frac{3}{2Z} + \sqrt{2}\frac{N_1}{N_2 Z^2}\right)\frac{T'}{T} - 1.5\left(\frac{N_1'}{N_1} + \frac{N_2'}{N_2 Z}\right)\right\} + \frac{5}{2}N_1 kT\tilde{v}_{2x}, \quad (23)$$

$$q^{(2)}_{\text{tot}\,x} = -\frac{N_2 (kT)^2 \nu_{\text{el}}}{m\omega^2_{\text{el}}}\left\{\left(\sqrt{2}\left(\frac{M}{m}\right)^{1/2} + \frac{7N_1}{4N_2} - \frac{3N_1}{2N_2 Z} + \frac{15N_1}{2N_2 Z^2} + \frac{\sqrt{2}N_1^2}{Z^2 N_2^2}\right)\frac{T'}{T}\right.$$

$$\left. + 1.5\left(\frac{N_1'}{N_1} + \frac{N_2'}{ZN_2}\right)\frac{N_1}{N_2}\right\} + \frac{5}{2} N_1 kT \tilde{v}^{(2)}_{1x}, \tag{24}$$

$$\Pi^{(2)}_{xx} = -\frac{N_2}{2}\frac{(kT)^2}{M\omega^2_{\text{ion}}}\left\{\frac{N_2''}{N_2} + 1.2\frac{T''}{T} + 0.8\frac{N_2' T'}{N_2 T} - \frac{eE'}{kT} - \left(\frac{N_2'}{N_2}\right)^2\right.$$

$$\left. + 0.9\left(\frac{T'}{T}\right)^2 - \frac{H'}{H}\left(\frac{N_2'}{N_2} + 1.2\frac{T'}{T} - \frac{eE}{kT}\right)\right\}, \tag{25}$$

$$\Pi^{(2)}_{yy} = \frac{N_2 (kT)^2}{2M\omega_{\text{ion}}}\left\{\frac{N_2''}{N_2} + \frac{2.8T''}{T} + 3.2\frac{N_2' T'}{N_2 T} - \frac{eE'}{kT} - \left(\frac{N_2'}{N_2}\right)^2\right.$$

$$\left. + 1{,}1\left(\frac{T'}{T}\right)^2 - \frac{H'}{H}\left(\frac{N_2'}{N_2} + 3.8\frac{T'}{T} - \frac{eE}{kT}\right)\right\}, \tag{26}$$

$$\Pi_{zz} = -\Pi_{xx} - \Pi_{yy}, \tag{27}$$

where

$$N' = \frac{dN}{dx},\quad N'' = \frac{d^2N}{dx^2},\quad \text{etc.} \qquad \nu_{\text{el}} = \frac{4\sqrt{2\pi}}{3m^{1/2}} N_2 \frac{(Ze^2)^2}{(kT)^{3/2}} \ln\left(\frac{3(kT)^{3/2}}{2e^3\pi^{1/2}(N_1+N_2)^{1/2}}\right).$$

The remaining components are zero in this approximation (note that the expression for Π_{ik} is obtained in the approximation $Z \ll (M/m)^{1/2}$. As for Π_{xy}, it only starts to differ from zero in the third approximation and is found to be

$$\Pi^{(3)}_{xy} = -\frac{\sqrt{\pi}8eZc^3(kT)^{1/2}}{15H^3} N_2^2 M^{3/2} \ln\left(\frac{3(kT)^{3/2}}{2e^3\pi^{1/2}(N_1+N_2)^{1/2}}\right)\left\{\frac{7N_2' T'}{2N_2 T} + \frac{47T''}{16T}\right.$$

$$\left. - \frac{7}{8}\left(\frac{T'}{T}\right)^2 - \frac{47H'T'}{16HT} + \frac{3}{4}\left[\frac{N_2''}{N_2} - \left(\frac{N_2'}{N_2}\right)^2 - \frac{H'}{H}\left(\frac{N_2'}{N_2} - \frac{eE'}{kT}\right)\right]\right\}. \tag{28}$$

3. In this section we shall investigate the existence of transport phenomena in a mixture of electrons and ions, for a stationary case with arbitrary symmetry, when $\nu/\omega \sim 1$. The expansion parameters are in this case R/L and l/L. Formally, this leads to the fact that the collision integral and the magnetic term $\mathbf{v} \times \mathbf{H}\, \partial f/\partial \mathbf{v}$ must be considered on equal footing in the Boltzmann equation. The zero approximation for f_n is obtained from the system of equations

$$+\frac{e}{mc}[\mathbf{vH}]\frac{\partial f_1^{(0)}}{\partial \mathbf{v}} = J_{11}(f_1^{(0)}, f_1^{(0)}) + J_{12}(f_1^{(0)}, f_2^{(0)}),\quad -\frac{eZ}{Mc}[\mathbf{vH}]\frac{\partial f_2^{(0)}}{\partial \mathbf{v}} = J_{22}(f_2^{(0)}, f_2^{(0)}) + J_{21}(f_2^{(0)}, f_1^{(0)}). \tag{29}$$

It is easily seen that solution (14) satisfies the system (29). We also obtain the following system of equations for $f_n^{(1)}$:

$$(\mathbf{Av})\, f_1^{(0)} - \frac{e}{mc}[\mathbf{vH}]\frac{\partial f_1^{(1)}}{\partial \mathbf{v}} = -\sum_{n=1}^{2}\{J_{1n}(f_1^{(0)}, f_n^{(0)}) + J_{1n}(f_1^{(0)}, f_n^{(0)}),$$

$$(\mathbf{A}_2\mathbf{v})\, f_2^{(0)} + \frac{eZ}{Mc}[\mathbf{vH}]\frac{\partial f_2^{(1)}}{\partial \mathbf{v}} = -\sum_{n=1}^{2}\{J_{2n}(f_2^{(0)}, f_n^{(0)}) + J_{2n}(f_2^{(0)}, f_n^{(0)}); \tag{30}$$

$$\mathbf{A}_1 = \frac{\nabla N_1}{N_1} + \frac{\nabla T}{T} + \frac{e\mathbf{E}}{kT} + \frac{e}{ckT}[\mathbf{v}_0^{(1)}\mathbf{H}] - \left(\frac{5}{2} - \beta_1^2 v^2\right)\frac{\nabla T}{T},$$
$$\mathbf{A}_2 = \frac{\nabla N_2}{N_2} + \frac{\nabla T}{T} - \frac{eZ\mathbf{E}}{kT} - \frac{eZ}{ckT}[\mathbf{v}_0^{(1)}\mathbf{H}] - \left(\frac{5}{2} - \beta_1^2 v^2\right)\frac{\nabla T}{T}. \tag{31}$$

Considering the form of the free terms, it is natural to seek solutions of the form $f_n^{(1)} = \mathbf{h}\cdot\mathbf{v} f_n^{(0)}$, and to seek $\mathbf{h}$ in the form of a series of Laguerre polynomials to the $^3/_2$ power,

$$\mathbf{h}_n = \sum \mathbf{p}_n^{(r)} L_r^{3/2}(\beta_n^2 v^2).$$

From (30), the following system of algebraic equations* may be obtained for the coefficients $\mathbf{p}_n^{(r)}$

$$\mathbf{A}_1^{(1)}\delta_{0s} - \frac{5}{2}\frac{\nabla T}{T}\delta_{1s} - [\omega_{e1}\mathbf{p}_1^{(s)}]\frac{\Gamma(s+5/2)}{\Gamma(s+1)\Gamma(5/2)} + \sum_{r=0}^{\infty}\{\mathbf{p}_1^{(r)}H_{rs}^{1} + \mathbf{p}_2^{(r)}H_{rs}^{(12)}\} = 0,$$
$$\mathbf{A}_2^{(1)}\delta_{0s} - \frac{5}{2}\frac{\nabla T}{T}\delta_{1s} + [\omega_{ion}\mathbf{p}_2^{(s)}]\frac{\Gamma(s+5/2)}{\Gamma(s+1)\Gamma(5/2)} + \sum_{r=0}^{\infty}\{\mathbf{p}_2^{(r)}H_{rs}^{II} + \mathbf{p}_2^{(r)}H_{rs}^{(21)}\} = 0, \tag{32}$$

where $R = N_1/N_2Z^2$,

$$H_{rs}^{I} = \nu_{el}\begin{vmatrix} 1 & \frac{3}{2} & \frac{15}{8} & \cdots \\ \frac{3}{2} & \frac{13}{4}+\sqrt{2}R & \frac{3\sqrt{2}}{4}R+\frac{69}{16} & \cdots \\ \frac{15}{8} & \frac{3\sqrt{2}}{4}R+\frac{69}{16} & \frac{45\sqrt{2}}{16}R+\frac{433}{64} & \cdots \\ \cdots & \cdots & \cdots & \end{vmatrix};$$

$$H_{rs}^{(12)} = -\frac{m_1}{M}\nu_{el}\begin{vmatrix} 1 & \frac{3}{2} & \frac{15}{8} & \cdots \\ 0 & 0 & 0 & \cdots \\ 0 & 0 & 0 & \cdots \\ \cdots & \cdots & \cdots & \end{vmatrix};$$

$$H_{rs}^{(21)} = -\frac{N_1}{N_2}\nu_{el}\begin{vmatrix} 1 & 0 & \cdots \\ \frac{3}{2} & 0 & \cdots \\ \frac{15}{8} & 0 & \cdots \\ \cdots & \cdots & \end{vmatrix};$$

$$H_{rs}^{II} = \frac{N_1 m}{N_2 M}\nu_{el}\begin{vmatrix} 1 & 0 & 0 & \cdots \\ 0 & \frac{15}{2}+\sqrt{2}\left(\frac{M}{m}\right)^{1/2}R^{-1}; & \frac{3\sqrt{2}}{4}\left(\frac{M}{m}\right)^{1/2}R^{-1} & \cdots \\ 0 & \frac{3\sqrt{2}}{4}\left(\frac{M}{m}\right)^{1/2}R^{-1}; & \frac{175}{8}+\frac{45\sqrt{2}}{16}\left(\frac{M}{m}\right)^{1/2}R^{-1} & \cdots \end{vmatrix}.$$

* The system of equations (32) was also solved by Landshoff[3], who obtained numerical values of the transport coefficient for certain values of the ratio ω/ν and for $Z = 1, 2, 3$; we are interested in the explicit form of the dependence of the transport coefficient upon Z, M, and ω/ν, as derived below.

It is easily seen that

$$\tilde{\mathbf{v}}_n^{(1)} = \frac{kT}{M_n}\mathbf{p}_n^{(0)}, \quad \mathbf{q}_n = \frac{5(kT)^2 N_n}{2M_n}(\mathbf{p}_n^{(0)} - \mathbf{p}_n^{(1)}).$$

The condition that the sum of the relative momenta be zero yields

$$\mathbf{p}_2^{(0)} = -N_1\mathbf{p}_1^{(0)}/N_2.$$

We shall consider later the case when the concentration gradients are perpendicular to the magnetic field (transport phenomena in the H direction are the same as if there were no magnetic field); in addition we set $N_1 \approx N_2 Z$ (quasineutral gas). Omitting a rather cumbersome computation, we obtain with sufficient accuracy the following expressions for the quantities of interest (we omit the expression for Π_{ik} as being too cumbersome):

$$\tilde{\mathbf{v}}_1^{(1)} = -\frac{kT}{m\omega_{\text{el}}}\left\{\left(\frac{\nabla N_2}{ZN_2} + \frac{\nabla N_1}{N_1}\right)\alpha_1 + \frac{\nabla T}{T}\alpha_2\right\}\left(1 - \frac{N_1}{N_2 Z}\right)$$
$$+ \frac{kT}{m\omega_{\text{el}}}\left[\left(\frac{\nabla N_2}{ZN_2} + \frac{\nabla N_1}{N_1} + \frac{\nabla T}{T}\frac{1-Z}{Z}\right), \mathbf{n}_0\right], \quad \mathbf{j} \approx -eN_1\tilde{\mathbf{v}}_1^{(1)}, \tag{34}$$

$$\tilde{\mathbf{v}}_0^{(1)} = \frac{kT}{m\omega_{\text{el}}}\left\{\left(\frac{\nabla N_2}{ZN_2} + \frac{\nabla N_1}{N_1}\right)\alpha_1 + \frac{\nabla T}{T}\alpha_2 - \left[\left(\alpha_3\left(\frac{\nabla N_1}{N_1} + \frac{\nabla N_2}{ZN_2}\right) + \alpha_4\frac{\nabla T}{T}\right.\right.\right.$$
$$\left.\left.\left. + \frac{1}{Z}\left(\frac{\nabla N_2}{ZN_2} + \frac{\nabla T}{T} - \frac{eZ\mathbf{E}}{kT}\right)\right), \mathbf{n}_0\right]\right\}, \tag{35}$$

$$\tilde{\mathbf{v}}_2^{(1)} = -\tilde{\mathbf{v}}_1^{(1)}N_1 m/N_2 M, \tag{36}$$

$$\mathbf{q}_{\text{tot}}^{(1)} = \frac{5N_1(kT)^2}{2m\omega_{\text{el}}}\left\{\frac{15}{4a}\left(\frac{\nabla N_2}{ZN_2} + \frac{\nabla N_1}{N_2}\right)\left(\frac{\omega}{\nu}\right)_{\text{el}} + \alpha_5\frac{\nabla T}{T} + \left[\left(\alpha_6\frac{\nabla T}{T} - \alpha_7\left(\frac{\nabla N_2}{ZN_2} + \frac{\nabla N_1}{N_1}\right)\right), \mathbf{n}_0\right]\right\}, \tag{37}$$

where

$$a = 10.56 + \frac{9.1}{Z} + \frac{2}{Z^2} + \frac{25}{4}\left(\frac{\omega}{\nu}\right)_{\text{el}}^2, \quad \alpha_1 = -\left(\frac{\nu}{\omega}\right)_{\text{el}}\left(1 - \frac{7.3 + 3.17/Z}{a}\right),$$
$$\alpha_2 = \frac{1+Z}{Z}\alpha_1 + \frac{75}{8a}\left(\frac{\omega}{\nu}\right)_{\text{el}}, \quad \alpha_3 = \frac{5{,}6}{a}, \quad \alpha_4 = -\frac{6{,}6}{a},$$
$$\alpha_5 = -\frac{35}{8a} - \frac{2N_2(\sqrt{2}(M/m)^{1/2} + 15/2Z)(\omega/\nu)_{\text{el}}}{5N_1(\omega/\nu)_{\text{el}}^2 + \frac{4}{25}(15N_1/2ZN_2 + (2M/m)^{1/2}Z)^2},$$
$$\alpha_6 = \frac{1}{a}\left\{\frac{5}{2}\left(\frac{\omega}{\nu}\right)_{\text{el}}^2 + \left(4.88 + 2.1\frac{1}{Z}\right)\left(1 + \frac{1}{Z}\right)\right\} + 1 + \frac{1}{Z}$$
$$- \frac{(\omega/\nu)^2 N_2/ZN_1}{(\omega/\nu)_{\text{el}}^2 + \frac{4}{25}(15N_1/2ZN_2 + (2M/m)^{1/2}Z)^2},$$
$$\alpha_7 = 1 + \frac{4.88 + 2.1/Z}{a}, \quad \mathbf{n}_0 = \mathbf{H}/H.$$

4. We shall consider here transport phenomena in a mixture of electrons and ions located in a weak magnetic field, and in order to be more general, we shall consider a non-stationary problem (the center of mass

has arbitrary velocity). In this case it is convenient to alter somewhat the system of equations (3) in such a way that the process of successive approximation does not apply to v_0, and that the conditions of solubility (5) are automatically satisfied. In order to do this, it is sufficient to replace Dv_0/Dt in Eq. (3) by the right-hand term of the equation of motion [see (6b)]. Omitting a rather laborious development, we present the final results for this case

$$\widetilde{\mathbf{v}}_1^{(1)} = \frac{kT}{m\nu_{el}} \frac{(4.5R^2+13.35R+3.4)(\nabla N_1/N_1+\nabla T/T+eE/kT+(e/ckT)[\mathbf{v}_0\mathbf{H}])+(5.1+9.9R)\nabla T/T}{4.5R^2+5.4R+1} \tag{38}$$

$$\mathbf{q}_{tot}^{(1)} = -\frac{N_1(kT)^2}{m\nu_{el}} \frac{(11.25R^2+43.3R+13.5)\{\nabla N_1/N_1+(e/kT)(\mathbf{E}+c^{-1}[\mathbf{v}_0\mathbf{H}])\}}{4.5R^2+5.4R+1}$$

$$+\frac{(11.25R^2+93.3R+46.5)(\nabla T/T)}{4.5R^2+5.4R+1}. \tag{39}$$

The diffusion coefficient is

$$D = (kT/m\nu_{el})(4.5R^2+13.35R+5.4)/(4.5R^2+5.41R+1.01), \quad R = N_1/N_2Z^2. \tag{40}$$

The thermal diffusion coefficient is

$$D_T = (kT/m\nu_{el})(4.5R^2+23.3R+8.5)/(4.5R^2+5.41R+1.01). \tag{41}$$

The electrical conductivity is

$$\sigma_e = De^2N_1/kT. \tag{42}$$

The viscosity is
a) for $(N_1/N_2)(M/m)^{1/2}Z^{-2} \gg 1$

$$\eta_{l1} = 5(kT)^{5/2}M^{1/2}/8\pi^{1/2}e^4Z^4 \ln L; \tag{43}$$

b) for $(N_1/N_2)(M/m)^{1/2}Z^{-2} \ll 1$ (for heavy elements)

$$\eta_{l2} = 5\sqrt{2}(kT)^{5/2}N_1m^{1/2}/8\pi^{1/2}e^4Z^2N_2 \ln L; \quad L = 3(kT)^{3/2}/2e^3\pi^{1/2}(N_1+N_2)^{1/2}. \tag{44}$$

Note that in the latter case the Boltzmann equation can be solved exactly without expansion in series of Laguerre polynomials, and yields the following expressions whose values are close to those obtained above:

$$D^{ex} = 32kT/3\pi m\nu_{el}, \; D_T = {}^5/_2D^{ex}; \; \eta_l^{ex} = 32\sqrt{2}m^{1/2}(kT)^{5/2}N_1/15\pi^{3/2}Z^2N_2e^4 \ln L. \tag{45}$$

Note, in conclusion, that in the case of strong temperature gradients, it is not enough to restrict oneself to the dependence of the stress tensor Π_{ik} on the gradients of v_0, and for heavy elements we find

$$\Pi_{ik} = (N_1+N_2)kT\delta_{ik} - \eta_{l2}\left(\frac{\partial v_{0i}}{\partial x_k}+\frac{\partial v_{0k}}{\partial x_i}-\frac{2}{3}\operatorname{div}\mathbf{v}_0\delta_{ik}\right)+\frac{2}{5N_1kT}\left(\frac{\partial q_i}{\partial x_k}+\frac{\partial q_k}{\partial x_i}-\frac{2}{3}\operatorname{div}\mathbf{q}\delta_{ik}\right). \tag{46}$$

5. a) Of special interest is the case when the plasma is located in a strong magnetic field deviating slightly from axial symmetry, *i.e.*, when

$$\frac{R}{L}\frac{l}{L}\frac{\Delta H}{H} \ll 1$$

(ΔH is the variation in the magnetic field due to deviation from axial symmetry). In this case we obtain the following final results:

$$\mathbf{q}_{\text{tot}} = \frac{5N_2(kT)^2}{2m\omega_{\text{el}}}\left[\left(\frac{\nabla N_1}{N_1}+\frac{\nabla N_2}{ZN_2}+\frac{\nabla T}{T}\left(2+\frac{1}{Z}-\frac{N_2}{N_1Z}\right)\right),\mathbf{n}_0\right]$$
$$-\frac{kT}{M(\nu\omega)_{\text{ion}}}[(0.8\nabla\,\text{div}\,\mathbf{q}_2^{(1)}+1.80\nabla\,\text{div}\,\mathbf{v}_0),\mathbf{n}_0]$$
$$+\frac{e}{m\omega_{\text{el}}\nu_{\text{ion}}}\left[(\mathbf{E}+\frac{1}{c}[\mathbf{v}_0^{(1)}\mathbf{H}]),\mathbf{n}_0\right](0.46\,\text{div}\,\mathbf{q}_2^{(1)}+0.64\,\text{div}\,\mathbf{v}_0^{(1)})$$
$$-\frac{N_2(kT)^2\nu_{\text{el}}}{m\omega_{\text{el}}^2}\frac{\nabla T}{T}\left\{\sqrt{2}\left(\frac{M}{m}\right)^{1/2}+\frac{7N_1}{4N_2}-\frac{3N_1}{2ZN_2}+\frac{15N_1}{2N_2Z^2}+\frac{\sqrt{2}N_1^2}{N_2^2Z^2}\right\}, \tag{47}$$

$$\tilde{\mathbf{v}}_1=\frac{kT}{m\omega_{\text{el}}}\left[\left(\frac{\nabla N_1}{N_1}+\frac{\nabla N_2}{ZN_2}+\frac{\nabla T}{T}\left(1+\frac{1}{Z}\right)\right),\mathbf{n}_0\right]-$$
$$-\left(\frac{\nu}{\omega^2}\right)_{\text{el}}\frac{kT}{m}\left\{\frac{\nabla N_1}{N_1}+\frac{\nabla N_2}{ZN_2}+\frac{\nabla T}{T}\left(\frac{1}{Z}-\frac{1}{2}\right)\right\}\left(1-\frac{N_1}{N_2Z}\right)$$
$$-\frac{[(0.46\,\nabla\,\text{div}\,\mathbf{q}_2^{(1)}+0.64\,\nabla\,\text{div}\,\mathbf{v}_0^{(1)}),\mathbf{n}_0]}{N_2M(\omega\nu)_{\text{ion}}}, \tag{48}$$

$$\mathbf{v}_0=-\frac{kT}{M\omega_{\text{ion}}}\left[\left(\frac{\nabla N_2}{N_2}+\frac{\nabla T}{T}-\frac{e\mathbf{Z}\mathbf{E}}{kT}\right),\mathbf{n}_0\right]-\frac{\nu_{\text{el}}N_1kT}{N_2Zm\omega_{\text{el}}^2}\left\{\frac{\nabla N_1}{N_1}+\frac{\nabla N_2}{ZN_2}\right.$$
$$\left.+\frac{\nabla T}{T}\left(\frac{1}{Z}-\frac{1}{2}\right)\right\}+\frac{[(0.46\,\nabla\text{div}\,\mathbf{q}_2^{(1)}+0.64\,\nabla\text{div}\,\mathbf{v}_0^{(1)}),\mathbf{n}_0]}{N_2M(\omega\nu)_{\text{ion}}}, \tag{49}$$

where

$$\mathbf{v}_0^{(1)}=-\frac{kT}{M\omega_{\text{ion}}}\left[\left(\frac{\nabla N_2}{N_2}+\frac{\nabla T}{T}-\frac{e\mathbf{Z}\mathbf{E}}{kT}\right),\mathbf{n}_0\right],\quad \mathbf{q}_2^{(1)}=-\frac{5}{2}\frac{N_2(kT)^2}{M\omega_{\text{ion}}}\left[\frac{\nabla T}{T}\mathbf{n}_0\right], \tag{50}$$
$$\nabla=\mathbf{i}\partial/\partial x+\mathbf{j}\partial/\partial y,\quad \nu_{\text{ion}}=8\pi^{1/2}N_2e^4Z^4\ln L/3\,(kT)^{3/2}M^{1/2}.$$

b) To conclude this section, we shall consider the case of a plasma consisting of electrons and ions in the presence of an electromagnetic field which varies in space (both in magnitude and direction) and in time. We shall restrict ourselves to the case when the time variations of all the quantities that characterize the plasma during the periods between collisions are smaller than the quantities themselves (*i.e.*, $\partial f/\partial t \ll \nu f$ where ν is the collision frequency. In this case (as in Sec. 4), it is convenient, in order to obtain the local distribution function, to transform the Boltzmann equation in such a way as to satisfy identically the conditions of solubility (5), independently of the values of N, T, or $\mathbf{v}_0$. Here the space and time variation of these quantities need not be expanded in power series in a small parameter, but their values will be obtained by solving the complete system of generalized hydrodynamical equations. Omitting the computations, we present here the final results. In this case:

$$\tilde{\mathbf{v}}_1^{(1)}=\frac{kT}{m\nu_{\text{el}}}\left\{\alpha_1[[\mathbf{A}_1\mathbf{n}_0]\mathbf{n}_0]+\alpha_2\left[\frac{\nabla T}{T}\mathbf{n}_0\right]+\alpha_3[\mathbf{A}_1\mathbf{n}_0]\right.$$
$$\left.+\alpha_4\left[\frac{\nabla T}{T}\mathbf{n}_0\right]+\alpha_5\frac{\nabla T}{T}+\alpha_6\mathbf{A}_2\right\};\quad \mathbf{j}^{(1)}=-eN_1\tilde{\mathbf{v}}_1^{(1)}, \tag{51}$$

$$\mathbf{q}_{\text{tot}}=\frac{5N_1(kT)^2}{2m\nu_{\text{el}}}\left\{\beta_1\left[[\mathbf{A}_1\mathbf{n}_0]\mathbf{n}_0\right]+\beta_2\left[\left[\frac{\nabla T}{T}\mathbf{n}_0\right]\mathbf{n}_0\right]+\beta_3[\mathbf{A}_1\mathbf{n}_0]+\beta_4\left[\frac{\nabla T}{T}\mathbf{n}_0\right]+\beta_5\mathbf{A}_1+\beta_6\frac{\nabla T}{T}\right\}, \tag{52}$$

where

$$\mathbf{A}_1 = \frac{\nabla N_1}{N_1} + \frac{\nabla T}{T} + \frac{e}{kT}\left(\mathbf{E} + \frac{1}{c}[\mathbf{v}_0\mathbf{H}]\right); \quad a = 1 + 2R^2 + \frac{25}{4}\left(\frac{\omega}{\nu}\right)_{el}^4 +$$

$$+ \left(\frac{\omega}{\nu}\right)_{el}^2 (28 + 2R^2 + 9.2R),$$

$$b = 4.5R^2 + 5.4R + 1; \quad \alpha_2 = \frac{15}{4a}\left\{1 + 2R - \frac{5}{2}\left(\frac{\omega}{\nu}\right)_{el}^2\right\} - \frac{5.1 + 10R}{b};$$

$$\alpha_1 = \frac{1}{a}\left(\frac{13}{4} + \frac{17\sqrt{2}R}{4} + \frac{25}{4}\left(\frac{\omega}{\nu}\right)_{el}^2 + 2R^2\right) - \frac{1}{b}(4.5R^2 + 13.35R + 5.4);$$

$$\alpha_4 = \frac{15}{4a}\left(\frac{\omega}{\nu}\right)_{el}\left(\frac{23}{4} + \sqrt{2}R\right),$$

$$\alpha_3 = \frac{1}{a}\left\{\frac{25}{4}\left(\frac{\omega}{\nu}\right)_{el}^3 + \left(\frac{\omega}{\nu}\right)_{el}\left(\frac{259}{16} + \frac{13}{2}\sqrt{2}R + 2R^2\right)\right\}; \quad \alpha_5 = -(5.1 + 10R)/b;$$

$$\alpha_6 = -(4.5R^2 + 13.4R + 3.4)/b; \quad \beta_2 = -\frac{13.2 + 20R}{b} +$$

$$+ \frac{5}{2a}\left\{\frac{5}{2} + \frac{5}{2}\sqrt{2}R + \left(\frac{\omega}{\nu}\right)_{el}^2\left(\sqrt{2}R - \frac{1}{2}\right)\right\} + \frac{0.4\,(7.5Z^{-2} + \sqrt{2M/m}N_2/N_1)}{8MZ^2/25m + (\omega/\nu)_{el}^2};$$

$$\beta_1 = -\frac{1}{b}(4.5R^2 + 17.3R + 5.4) + \frac{1}{a}\left(\frac{19}{4} + \frac{23}{4}\sqrt{2}R + \frac{5}{2}\left(\frac{\omega}{\nu}\right)_{el}^2 + 2R^2\right);$$

$$\beta_3 = \frac{1}{a}\left\{\frac{25}{4}\left(\frac{\omega}{\nu}\right)_{el}^3 + \left(\frac{\omega}{\nu}\right)_{el}(24.8 + 8\sqrt{2}R + 2R^2)\right\};$$

$$\beta_4 = \frac{5}{2}\left(\frac{\omega}{\nu}\right)_{el}\frac{1}{a}\left\{13.4 + 1.5\sqrt{2}R + 2.5\left(\frac{\omega}{\nu}\right)_{el}^2\right\} - \left(\frac{\omega}{\nu}\right)_{el}\frac{N_2}{N_1 Z}\Big/\left(\frac{8Z^2M}{25m} + \left(\frac{\omega}{\nu}\right)_{el}^2\right);$$

$$\beta_5 = -\frac{1}{b}(4.5R^2 + 17.3R + 5.4); \quad \beta_6 = -\frac{1}{b}(13.2 + 20R).$$

6. Up to now we have found the quantities of interest in each concrete case as averaged out by a "local" distribution function. Space and time dependence enter only through the externally acting forces and the mean statistical characteristics, and are obtained by solving the generalized hydrodynamical equations (6a–c). The complete solution of the problem of plasma motion requires, in addition to the given initial (and boundary) conditions for j, Π_{ik}, $\tilde{v}$ and q through T, v_0, N, also the Maxwell equations for the electromagnetic field

$$\operatorname{div} E = 4\pi\sum e_s N_s; \quad \operatorname{curl}\mathbf{E} = -\frac{1}{c}\frac{\partial\mathbf{H}}{\partial t}, \qquad \operatorname{curl}\mathbf{H} - \frac{1}{c}\frac{\partial\mathbf{E}}{\partial t} = \frac{4\pi}{c}(\mathbf{j} + \sum N_s e_s \mathbf{v}_0). \tag{53}$$

As an example, we shall consider a plasma in a strong magnetic field (stationary case with axial symmetry). It follows, in this case, from the equation of continuity that

$$v_{0r} = \tilde{v}_r = j_r = 0. \tag{54}$$

From (21)–(22), we have:

$$\frac{1}{N_1}\frac{dN_1}{dr} + \frac{1}{ZN_2}\frac{dN_2}{dr} + \left(\frac{1}{Z} - \frac{1}{2}\right)\frac{dT}{Tdr} = 0, \tag{55}$$

from which it follows that

$$N_1 N_2^{1/Z} = N_{01} N_{02}^{1/Z}\,(T/T_0)^{-(2+Z)/2Z}, \tag{56}$$

where N_0, T_0 are the initial values of the density and the temperature. If, in particular, the gas is almost quasi-neutral, we have*:

$$N_1 = N_2 Z = \text{const}\, T^{(Z-2)/2(1+Z)}.$$

We obtain next a generalized equation for the conservation of momentum in a magnetic field from the equation for the radial component of the momentum

$$H^2/8\pi + (N_1 + N_2)\, kT + \int eE\,(ZN_2 - N_1)\, dr = \text{const}. \tag{57}$$

In this case the equation of conservation of energy, to a good approximation (including sources), takes the form

$$-\frac{1}{r}\frac{d}{dr}\left\{\frac{rN_2 (kT)^2 \nu_{el}}{m\omega_{el}^2}\left(\sqrt{2} + \frac{15}{2Z} + Z + \sqrt{\frac{2M}{m}}\right)\frac{dT}{dr}\right\} = S, \tag{58}$$

where S is the heat source.

Including the equations of the electromagnetic field and the equation of motion in the θ-direction, we have 5 equations for the 5 quantities N_1, N_2, E, T, and H, and accordingly the given boundary conditions completely determine the solution.

In conclusion, the author wishes to express his profound gratitude to Academician I. E. Tamm and to Prof. V. L. Ginzburg for valuable advice and discussion of the results.

[1] E. S. Fradkin, Otchet (Report) FIAN, 1950-1951.

[2] S. Chapman and T. G. Cowling, *The Mathematical Theory of Non-uniform Gases*, Cambridge (1939).

[3] R. Landshoff, Phys. Rev. **76**, 904 (1949).

Translated by M. A. Melkanoff
238

* If, in particular, the plasma consists primarily of electrons and ions of $Z = 1$ amongst a mixture of ions of various types, one may obtain the following law for the density distribution: $N_{el} = N_{Z=1} = \text{const}\, T^{-1/4}$; $N_{Z_1} = \text{const}\, T^{-[(M_Z(3Z+4)-M_1(3Z+2)]/4(M_1+M_Z)}$, where M_Z is the mass of an ion of charge Z.

Thermal Conductivity and Thermoelectric Phenomena in Metals in a Magnetic Field

M. IA. AZBEL', M. I. KAGANOV, AND I. M. LIFSHITZ
Physico-Technical Institute, Academy of Sciences, Ukraine SSR
(Submitted to JETP editor July 9, 1956)
J. Exptl. Theoret. Phys. (U.S.S.R.) **32**, 1188-1192 (May, 1957)

Asymptotic expressions for the tensors of the thermal conductivity and Thomson coefficients in a strong magnetic field have been found. No special assumptions on the dispersion law or collision integral are made in the derivations.

IT IS KNOWN that the magnetic field changes not only the resistivity of a metal but also the heat conduction, the Thomson and Peltier coefficients, *etc.*[1] Using the techniques developed earlier[2], the dependence of the kinetic coefficients on a strong magnetic field can be determined. As in Ref. 2, we will not take into account quantization of the electron motion in the magnetic field. The limits of the applicability of such a classical analysis are indicated in the reference cited.

To find the kinetic coefficients, it is necessary to calculate the current density j_i and the energy flow w_i due to the electric field E_i, and the temperature gradient $\partial T/\partial x_i$. If the addition to the equilibrium Fermi distribution function $f_0 = (e^{(\varepsilon-\zeta)/T} + 1)^{-1}$ [$\varepsilon = \varepsilon(\mathbf{p})$ is the electron energy, $\mathbf{p}$ the quasi-momentum; $\zeta = \zeta(T)$ the chemical potential of the electron gas, and $\zeta(0) = \zeta_0$ the limiting Fermi energy] is denoted by f_1, then

$$j_i = 2e(2\pi\hbar)^{-3}\int v_i f_1 (d\mathbf{p}); \qquad w_i = 2(2\pi\hbar)^{-3}\int \varepsilon v_i f_1 (d\mathbf{p}). \tag{1}$$

The function f_1 satisfies the linearized kinetic equation which we write schematically

$$\left(\frac{\partial f_1}{\partial t}\right)_{\text{field}} + \left(\frac{\partial f_1}{\partial t}\right)_{\text{st}} = -\frac{\partial f_0}{\partial \varepsilon} e v_i \left\{E_i + \frac{T}{e}\frac{\partial}{\partial T}\left(\frac{\varepsilon-\zeta}{T}\right)\frac{\partial T}{\partial x_i}\right\}. \tag{2}$$

Here, the first term on the left describes the change in the distribution function in a constant and homogeneous magnetic field. In the notation of Ref. 2,

$$(\partial f_1/\partial t)_{\text{field}} = t_0^{-1}\partial f_1/\partial\tau.$$

However, this form will not need suit us later. One need merely bear in mind that if φ is a function of the energy only then $(\partial\varphi/\partial t)_{\text{field}} \equiv 0$.

Now, let us put

$$f_1 = -\frac{\partial f_0}{\partial \varepsilon}\left\{eE_k\psi_k + T\frac{\partial}{\partial T}\left(\frac{\varepsilon-\zeta}{T}\right)\frac{\partial T}{\partial x_k}\varphi_k\right\}. \tag{3}$$

Then

$$j_i = \sigma_{ik}^{(0)}E_k + s_{ik}^{(0)}\partial T/\partial x_k; \qquad w_i = \sigma_{ik}^{(1)}E_k + s_{ik}^{(1)}\partial T/\partial x_k, \tag{4}$$

where

$$\sigma_{ik}^{(n)} = -e^2\int_0^\infty \varepsilon^n \frac{\partial f_0}{\partial\varepsilon} A_{ik}(\varepsilon)\, d\varepsilon;$$

$$es_{ik}^{(n)} = -Te^2\int_0^\infty \varepsilon^n \frac{\partial}{\partial T}\left(\frac{\varepsilon-\zeta}{T}\right)\frac{\partial f_0}{\partial\varepsilon} B_{ik}(\varepsilon)\, d\varepsilon = -e^2\int_0^\infty \varepsilon^n \frac{\partial f_0}{\partial T} B_{ik}(\varepsilon)\, d\varepsilon, \tag{5}$$

and

$$A_{ik}(\varepsilon) = \frac{2}{(2\pi\hbar)^3}\int_{\varepsilon(\mathbf{p})=\varepsilon}\frac{v_i\psi_k}{v}\, dS, \qquad B_{ik}(\varepsilon) = \frac{2}{(2\pi\hbar)^3}\int_{\varepsilon(\mathbf{p})=\varepsilon}\frac{v_i\varphi_k}{v}\, dS. \tag{6}$$

The functions Ψ_k and φ_k are the solutions of the following equations

$$\left(\frac{\partial\psi_k}{\partial t}\right)_{\text{field}} + \left(\frac{\partial f_0}{\partial\varepsilon}\right)^{-1}\left(\frac{\partial}{\partial t}\right)_{\text{st}}\left(\frac{\partial f_0}{\partial\varepsilon}\psi_k\right) = v_k, \qquad \left(\frac{\partial\varphi_k}{\partial t}\right)_{\text{field}} + \left(\frac{\partial f_0}{\partial T}\right)^{-1}\left(\frac{\partial}{\partial t}\right)_{\text{st}}\left(\frac{\partial f_0}{\partial T}\varphi_k\right) = v_k, \tag{7}$$

which differ from each other only in the form of the component describing the change in the distribution function because of collisions.

If the collision operator is an energy δ-function, we see from (6) and (7) that

$$A_{ik}(\varepsilon) \equiv B_{ik}(\varepsilon). \tag{8}$$

This holds in two cases: a) at temperatures high in comparison with the Debye temperature, when the collision integral is f_1/t_0 (t_0 is the relaxation time) and b) for very low temperatures (the criterion depends on the purity of the metal) when elastic collisions between electrons and impurities play a fundamental part.

To express the experimentally-measurable coefficients (resistivity, heat conduction, Thomson coefficient) in terms of $\sigma_{ik}^{(n)}$ and $s_{ik}^{(n)}$, let us write the law of conservation of energy for an electron gas.

If Q denotes the internal energy of the electrons, then evidently

$$(\partial Q/\partial t) + (\partial w_i/\partial x_i) = E_i j_i. \tag{9}$$

We easily obtain from (4) and (9)

$$\frac{\partial Q}{\partial t} = \sigma_{ik}^{(0)-1} j_i j_k - \left\{\sigma_{il}^{(0)-1} s_{lk}^{(0)} + \frac{1}{e}\frac{\partial}{\partial T}(\sigma_{kl}^{(1)}\sigma_{li}^{(0)-1})\right\} j_i \frac{\partial T}{\partial x_k} - \frac{1}{e}\frac{\partial}{\partial x_i}\left\{[s_{ik}^{(1)} - \sigma_{il}^{(1)}\sigma_{lm}^{(0)-1}s_{mk}^{(0)}]\frac{\partial T}{\partial x_k}\right\}.$$

Hence, it is seen that

$$\sigma_{ik}^{(0)-1} = \rho_{ik} \tag{10}$$

is the resistivity tensor, whose asymptotic form in a strong magnetic field was studied in Ref. 2;

$$-e^{-1}\{s_{ik}^{(1)} - \sigma_{ip}^{(1)}\sigma_{pq}^{(0)-1}s_{qk}^{(0)}\} = \varkappa_{ik} \tag{11}$$

is the tensor of the heat conduction coefficient*; and

$$\sigma_{il}^{(0)-1}s_{lk}^{(0)} + \frac{1}{e}\frac{\partial}{\partial T}(\sigma_{kp}^{(1)}\sigma_{pi}^{(0)-1}) = \mu_{ik} \tag{12}$$

is the Thomson coefficient tensor.

Let us note that relations (10)–(12) are always valid and are not related to the presence or absence of a magnetic field (see for example Ref. 3).

All the kinetic coefficients depend on the temperature for two reasons: First, because the collision integral depends on the temperature; second, because of the temperature dependence of the electron equilibrium distribution function f_0. Since the electron gas is always strongly degenerate ($T \ll \zeta_0$), a calculation of the first non-vanishing terms of the expansion of these coefficients in powers of the small parameter T/ζ_0 is of interest.

We will use the well known formula[4]:

$$\int_0^\infty \varphi(\varepsilon) f_0(\varepsilon)\, d\varepsilon = \int_0^{\zeta} \varphi(\varepsilon)\, d\varepsilon + \frac{\pi^2}{6} T^2 \frac{\partial \varphi}{\partial \varepsilon}\Big|_{\varepsilon=\zeta} + \cdots \tag{13}$$

[$\varphi(\varepsilon)$ is an arbitrary function of the energy]. This expression can be considered as an expansion in powers of the temperature if it is recognized that the chemical potential of the electrons ζ is constant. However, the number of electrons n is constant. Consequently, the ζ-function of the temperature, which can be found from the normalization condition

$$2(2\pi\hbar)^{-3}\int f_0(\varepsilon)\,(d\mathbf{p}) = 2(2\pi\hbar)^{-3}\int_0^\infty f_0(\varepsilon)\, g(\varepsilon)\, d\varepsilon = n$$

(n is the electron density), where

$$g(\varepsilon) = \oint_{\varepsilon(\mathbf{p})=\varepsilon} dS/v$$

is the density of the levels in the energy interval $d\varepsilon$. Denoting $\zeta(T) - \zeta_0$ by Δ, we obtain, using (13)

$$\Delta = -(\pi^2 T^2/6)\, g'(\zeta_0)/g(\zeta_0). \tag{14}$$

We have from (13) and (14)

$$\int_0^\infty \varphi(\varepsilon) f_0(\varepsilon)\, d\varepsilon = \int_0^{\zeta_0} \varphi(\varepsilon)\, d\varepsilon + \frac{\pi^2 T^2}{6}\left[\varphi' - \varphi\frac{g'(\varepsilon)}{g(\varepsilon)}\right]_{\varepsilon=\zeta_0} + \cdots$$

Using the expressions obtained, we easily find

$$\sigma_{ik}^{(0)} = e^2\left\{A_{ik}(\zeta_0) - \frac{\pi^2T^2}{6}\left[A'_{ik}(\zeta_0)\frac{g'(\zeta_0)}{g(\zeta_0)} - A''(\zeta_0)\right]\right\};$$

$$\sigma_{ik}^{(1)} = e^2\left\{A_{ik}(\zeta_0)\zeta_0 - \left[\frac{\partial}{\partial\zeta_0}(\zeta_0 A_{ik}(\zeta_0)\left(\frac{g'(\zeta_0)}{g(\zeta_0)} - \frac{\partial^2}{\partial\zeta_0^2}(\zeta_0 A_{ik}(\zeta_0)\right)\right]\frac{\pi^2T^2}{6}\right\}.$$

$$s_{ik}^{(0)} = e\left\{\frac{\partial}{\partial T}\int_0^{\zeta_0} B_{ik}(\varepsilon)\, d\varepsilon - \frac{\pi^2 T}{3}\left[B'_{ik}(\zeta_0) - B_{ik}(\zeta_0)\frac{g'(\zeta_0)}{g(\zeta_0)}\right]\right\}. \tag{15}$$

* As is known, the heat conduction of a metal is determined not only by electrons but also by other "quasi-particles" in the metal (phonons, spin waves, etc.). Hereinafter we shall understand $\varkappa_{ik}$ to mean only the electron part of the heat conduction.

In obtaining the last formulas, we used the fact that $A_{ik}(\varepsilon)$ and $B_{ik}(\varepsilon)$ are smooth functions of ε. The latter follows from (6) and (7). It can be shown that this is not so because Eqs. (7) contain derivatives of the Fermi function. However, if the general form of the linearized collision integral is taken into account [see for example (8.18) of Ref. 1], it is easy to show that ψ_k and φ_k do not have singularities at $\varepsilon = \varepsilon_0$ (as $T \to 0$).

Using formulas (15), the first non-vanishing terms of the expansion in powers of T/ζ_0 can be obtained for the quantities of interest to us:

$$\sigma_{ik} = e^2 A_{ik}(\zeta_0), \quad \varkappa_{ik} = {}^1/_3 \pi^2 k^2 T B_{ik}(\zeta_0),$$
$$\mu_{ik} = \frac{\pi^2 k^2 T}{3e} \left\{ (2A_{li}^{-1} A'_{kl} - A_{il}^{-1} B'_{lk}) - (\delta_{ik} - A_{il}^{-1} B_{lk}) \frac{g'(\zeta_0)}{g(\zeta_0)} \right\} + \frac{1}{e} A_{il}^{-1} \frac{\partial}{\partial T} \int_0^{\zeta_0} B_{lk}(\varepsilon)\, d\varepsilon. \tag{16}$$

The last term in the expression for μ_{ik} can be omitted, as a rule, since electron scattering by impurities, which is practically independent of the temperature, plays a fundamental part at low temperatures (which are of greatest interest).

When condition (8) is satisfied, the expressions obtained are simplified considerably

$$\sigma_{ik} = e^2 A_{ik}(\zeta_0), \quad \varkappa_{ik} = {}^1/_3 \pi^2 k^2 T A_{ik}(\zeta_0),$$
$$\mu_{ik} = (\pi^2 k^2 T / 3e)(2A_{li}^{-1} A'_{kl} - A_{il}^{-1} A'_{lk}). \tag{17}$$

As is seen, the Wiedemann-Franz law, independent of the magnitude and direction of the magnetic field (see Ref. 3), holds here for each of the components of the conductivity and heat conduction tensors.

The asymptotic form of the conductivity tensor σ_{ik} [*i.e.*, $A_{ik}(\zeta_0)$] was analyzed in Ref. 2 in a strong magnetic field, where it was shown that this asymptotic form is independent of the kind of collision integral and is determined only by the topology of the equal-energy surfaces. Since the equations for φ_k and Ψ_k differ only in the kind of collision integral, evidently the asymptotic expression for the tensor $B_{ik}(\zeta_0)$ differs from that for the tensor $A_{ik}(\zeta_0)$ only by those factors of the corresponding powers of the magnetic field which depend on the kind of collision integral (see Sec. 3 of Ref. 2). Hence, the asymptotic form of the heat conduction tensor $\varkappa_{ik}(H)$ is similar to that of the tensor $\sigma_{ik}(H)$. If the z axis is directed along the magnetic field, then

$$\varkappa_{ik}(H) \sim \begin{pmatrix} \frac{a_{xx}}{H^2} & \frac{1}{3}\left(\frac{\pi k}{e}\right)^2 T \frac{ec(n_1 - n_2)}{H} & \frac{a_{xz}}{H} \\ -\frac{1}{3}\left(\frac{\pi k}{e}\right)^2 T \frac{ec(n_1 - n_2)}{H} & \frac{a_{yy}}{H^2} & \frac{a_{yz}}{H} \\ \frac{a_{zx}}{H} & \frac{a_{zy}}{H} & a_{zz} \end{pmatrix}.$$

Here n_1 (or n_2) is the number of electrons (or "holes")[2]. The expansion of the matrices a_{ik} in powers of $1/H$ starts with the zero term. If $n_1 = n_2$, then $\varkappa_{xy} \sim 1/H^2$.

Let us note that the *Wiedemann-Franz law* is always satisfied [independently of condition (8)] *for asymptotic values* of the $\varkappa_{xy}$ and σ_{xy} components independent of the kind of collision integral *for unequal numbers* of electrons and "holes." A comparison of the results of the present analysis concerning heat conduction with experiment is difficult. This is because of the scantiness of experimental data on simultaneous measurements of resistivity and heat conduction in strong magnetic fields and because the total heat conduction (which does not equal the electron heat conduction) is always measured. However, the latter difficulty is automatically avoided if the following quantity is measured

$$[\varkappa_{xy}(H) - \varkappa_{xy}(-H)] / [\sigma_{xy}(H) - \sigma_{xy}(-H)]\, T,$$

which must be asymptotically equal to the Lorentz number ${}^1/_3(\pi k/e)^2$ for $n_1 \neq n_2$. Here, the phonon part of the heat conduction (which evidently is independent of the magnetic field) drops out.

As we saw, the asymptotic forms of the tensors $\varkappa_{ik}$ and σ_{ik} differ substantially in those cases when $n_1 \neq n_2$ and $n_1 = n_2$. It is seen from (16) that the asymptotic form of the Thomson-coefficient tensor is also related to the topology of the equal-energy surfaces. Generally speaking, its components depend on the kind of the collision integral. However, if $n_1 \neq n_2$, then

$$\mu_{xx} \approx \mu_{yy} \approx (\pi^2 k^2 / 3e)\, TV'(\zeta_0) / V(\zeta_0).$$

Here $V(\zeta_0) = V_1(\zeta_0) - V_2(\zeta_0)$; $V_1(\zeta_0)$ is the volume in momentum space occupied by the electrons; $V_2(\zeta_0)$ is the volume "occupied" by the "holes."

As is seen, μ_{xx} and μ_{yy} depend in this case on the angles between the field and the crystallographic axes and are determined exclusively by the energy spectrum. If the open surfaces are substantial[2], then μ_{xx} and μ_{yy} are functions of the angles. If $n_1 = n_2$ [hence $V(\zeta_0) = V_1(\zeta_0) - V_2(\zeta_0) = 0$ and $V'(\zeta_0) \neq 0$]*, then the asymptotic form of the tensor μ_{ik} is as follows: the $\mu_{\alpha\beta}$ increase linearly with the magnetic field ($\alpha, \beta = x, y$), and the μ_{iz} approach saturation. Hence, a study of the asymptotic form of the Thomson coefficient tensor in a strong magnetic field affords an additional possibility of investigating the topology of the equal-energy surfaces of the conduction electrons.

* There is no foundation for the assumption $V'(\zeta_0) = 0$. For example, in the case of a quadratic isotropic dependence:

$$V'(\zeta_0) = 2\pi (3V_{1,2}/4\pi)^{1/3} [(2m_1)^{1/2} + (2m_2)^{1/2}],$$

$m_1(m_2)$ is the effective mass of the electrons ("holes").

[1] A. H. Wilson, *The Theory of Metals*, Cambridge, 1954.
[2] Lifshitz, Azbel', and Kaganov, J. Exptl. Theoret. Phys. (U.S.S.R.) **30**, 220 (1956), **31**, 63 (1956); Soviet Phys. JETP **3**, 143 (1956), **4**, 41 (1957).
[3] M. Kohler, Ann. Phys. **6**, 18 (1949).
[4] L. Landau and E. Lifshitz, *Statistical Physics*, Moscow-Leningrad, Gostekhizdat, 1951.

Translated by M. D. Friedman
239

SOVIET PHYSICS JETP VOLUME 5, NUMBER 5 DECEMBER, 1957

Quantum States of Particles Coupled to a Harmonically Oscillating Continuum with Arbitrarily Strong Interaction, I. Case of Absence of Translational Symmetry

V. M. BUIMISTROV AND S. I. PEKAR
Physics Institute of the Ukrainian Academy of Sciences

(Submitted to JETP editor July 16, 1956)
J. Exptl. Theoret. Phys. (U.S.S.R.), **32**, 1193-1199 (May, 1957)

The ground-state energy is calculated by a variational method for the system defined by Hamiltonian (1). The trial wave-function is given by Eq. (3). The results are applied to the special cases of F and F'-centers. In the limits of weak and strong coupling, the calculated energy agrees with the exact results of second-order perturbation theory and of the adiabatic treatment respectively. The calculation can be regarded as an interpolation through the intermediate coupling region. It is valid when the effective size of the localized electron state is large, and when the conditions of the continuum model of F and F' centers are fulfilled.

WE CONSIDER systems described by a Hamiltonian of the form

$$H = -\sum_{i=1}^{N} \frac{\hbar^2}{2m_i} \Delta_i + \sum_{\varkappa, t} {}^1/_2 \hbar\omega_{\varkappa t} \left(q_{\varkappa t}^2 - \frac{\partial^2}{\partial q_{\varkappa t}^2} \right) + \sum_{\varkappa i t} c_{\varkappa t}^i q_{\varkappa t} \chi_{-\varkappa}(\mathbf{r}_i) + V(\mathbf{r}_1, \ldots, \mathbf{r}_N). \quad (1)$$

Here $\mathbf{r}_i$ is the radius-vector of the ith particle, m_i is its mass, $\omega_{\varkappa t}$ is the vibration frequency of the continuum corresponding to a wave-vector $\varkappa$ and to branch number t of the energy-surface, $q_{\varkappa t}$ is the normal coordinate of the same vibration, $e_{\varkappa t}^i$ is the coupling-constant between this vibration and the ith particle, $V(\mathbf{r}_1, \ldots, \mathbf{r}_N)$ is the potential of the interaction of the particles with each other and with external fields, and

$$\chi_{+\varkappa}(\mathbf{r}_i) = \sqrt{\frac{2}{V}} \sin\left(\varkappa \mathbf{r}_i + \frac{\pi}{4}\right)$$
$$\varkappa_j = \frac{2\pi}{L} \nu_j; \quad j = 1, 2, 3; \quad (2)$$
$$\nu_j = 0 \pm 1, \pm 2, \ldots \quad V = L^3$$

Thus the $\chi_{\pm\varkappa}$ are a complete system of functions normalized in a volume V, comprising a cube of side L. In Eq. (1), the first term is the kinetic energy of the particles, the second is the energy of free vibration of the continuum, and the third is the interaction between particles and continuum. Such Hamiltonians occur in many physical situations. For example, the conduction electrons in a crystal have an interaction with the lattice vibrations which reduces to the form of Eq. (1) after the effective-mass approximation is made. The same is true of electrons localized around an impurity center, whose effect is included in the term $V(\mathbf{r}_1, \ldots, \mathbf{r}_N)$. The same type of Hamiltonian describes an exciton of large radius, in which the electron and hole move as two interacting quasi-particles. A similar Hamiltonian arises in the problem of a particle interacting with a quantized field.

The particular forms of $\omega_{\varkappa t}$, $c^i_{\varkappa t}$ and $V(\mathbf{r}_1, \ldots, \mathbf{r}_N)$ will be chosen later when particular applications are considered. Initially we develop a general approximation method which applies to all values of these quantities. The energy levels will be calculated by a direct variational method which is valid for any strength of coupling. The results obtained go over, in the limits of weak and strong coupling, into the well-known results of perturbation theory and of strong-coupling theory. In this paper we consider the case of particles localized in a potential well produced by an external field. There is no translational symmetry. A following paper will deal with the case of translational symmetry.

I. CHOICE OF APPROXIMATE WAVE-FUNCTION AND DETERMINATION OF ITS VIBRATIONAL PART

One of the authors [1,2] showed earlier that the strong-coupling limit represents the particle as following adiabatically the comparatively slow oscillations of the continuum. The adiabatic approximation[3] consists in assuming for the system a wave-function of the form

$$\Psi = \psi(\mathbf{r}_i, q_{\varkappa t})\, \Phi(q_{\varkappa t}),$$

with ψ varying much slower than Φ as a function of $q_{\varkappa t}$. We showed further[1,2] that in $\psi(\mathbf{r}_i, q_{\varkappa t})$ one may replace the coordinates $q_{\varkappa t}$ by a self-consistent set of mean values, with an error which becomes smaller as the coupling becomes stronger. Consequently, as the coupling strength tends to infinity, the multiplicative approximation

$$\Psi = \psi(\mathbf{r}_1, \ldots, \mathbf{r}_N)\, \Phi(\ldots q_{\varkappa t} \ldots)$$

becomes exact. This is explained by observing that the particle moves so fast in its potential well that the slowly moving continuum feels only the average field of the ψ-cloud of the particle. Thus the continuum moves as if it were subjected to a given external force. The field of the ψ-cloud produces a displacement in the equilibrium positions of the continuum coordinates $q_{\varkappa t}$. The equilibrium values of these coordinates are functionals of ψ. If the coupling is weakened, the particle motion becomes slower and the continuum begins to feel the instantaneous field of the particle. Then the equilibrium positions $q^0_{\varkappa t}$ of the coordinates become functions of the particle positions $\mathbf{r}_i$, $q^0_{\varkappa t} = q^0_{\varkappa t}(\mathbf{r}_1 \ldots \mathbf{r}_N)$. We thus approximate the wave-function of the system by the expression

$$\Psi^* = \psi(\mathbf{r}) \prod_{\varkappa} \Phi_\varkappa(q'_\varkappa), \quad q'_\varkappa = q_\varkappa - q^0_\varkappa(\mathbf{r}), \qquad (3)$$

where $\mathbf{r}$ denotes the totality of particle coordinates $\mathbf{r}_i$. We number the normal vibrations by a single index $\varkappa$ instead of the pair of indices $\varkappa, t$. The double indices can be reintroduced in the final results. The approximation (3) is a generalization of the multiplicative approximation mentioned earlier. We minimize the functional

$$\overline{H} = \int \Psi^* \hat{H} \Psi d\mathbf{r} dq, \quad dq = \prod_{\varkappa} dq_\varkappa$$

with the supplementary condition that Ψ be normalized. To do this we transform from the variables $\mathbf{r}_i \ldots q_\varkappa$ to the variables $\mathbf{r}_i \ldots q'_\varkappa$. The Jacobian of the transformation is unity. The energy-operator in terms of the new variables is

$$\hat{H} = -\sum_{i=1}^{N} \frac{\hbar^2}{2m_i}\Big[\Delta_i - 2\sum_{\varkappa}\Big(\nabla_i q^0_\varkappa,\ \nabla_i \frac{\partial}{\partial q'_\varkappa}\Big) + \sum_{\varkappa,\,\varkappa_1} (\nabla_i q^0_\varkappa,\ \nabla_i q^0_{\varkappa_1}) \frac{\partial^2}{\partial q'_\varkappa \partial q'_{\varkappa_1}}$$

$$-\sum_{\varkappa} (\Delta_i q^0_\varkappa) \frac{\partial}{\partial q'_\varkappa}\Big] + \sum_{\varkappa} \frac{\hbar\omega_\varkappa}{2}\Big[(q^0_\varkappa + q'_\varkappa)^2 - \frac{\partial^2}{\partial q'^2_\varkappa}\Big] + \sum_{\varkappa i} c^i_\varkappa (q^0_\varkappa + q'_\varkappa)\chi_{-\varkappa}(\mathbf{r}_i) + V(\mathbf{r}). \qquad (4)$$

Without loss of generality we may suppose that each of the functions ψ, $\Phi_\varkappa$ is normalized. We also suppose these functions to be real. Then, using the identity

$$\int \Phi_\varkappa \frac{\partial \Phi_\varkappa}{\partial q'_\varkappa} dq'_\varkappa = 0$$

and writing $\overline{\varphi} = \int \varphi(\mathbf{r}) |\psi(\mathbf{r})|^2 d\mathbf{r}$, we find

$$\begin{aligned} \overline{H[\Psi]} = &\sum_{i=1}^{N} \frac{\hbar^2}{2m_i} \int |\nabla_i \psi|^2 d\mathbf{r} + \sum_\varkappa \frac{\hbar\omega_\varkappa}{2} \overline{q_\varkappa^{02}} + \sum_{\varkappa i} c_\varkappa^i \overline{q_\varkappa^0(\mathbf{r}) \chi_{-\varkappa}(\mathbf{r}_i)} + \overline{V(\mathbf{r}_1, \ldots, \mathbf{r}_N)} \\ &+ \sum_\varkappa \frac{\hbar\omega_\varkappa}{2} \int \Phi_\varkappa \left(-\alpha_\varkappa \frac{\partial^2}{\partial q_\varkappa'^2} + q_\varkappa'^2 \right) \Phi_\varkappa dq'_\varkappa + \sum_\varkappa \hbar\omega_\varkappa \beta_\varkappa \int q'_\varkappa \Phi_\varkappa^2 dq'_\varkappa, \qquad (5) \\ &\alpha_\varkappa = 1 + \sum_i \frac{\hbar}{m_i \omega_\varkappa} \overline{(\nabla_i q_\varkappa^0)^2}, \quad \beta_\varkappa = q_\varkappa^0 + \frac{1}{\hbar\omega_\varkappa} \sum_i c_\varkappa^i \overline{\chi_{-\varkappa}(\mathbf{r}_i)}. \end{aligned}$$

We minimize this functional with respect to $\Phi_\varkappa$ for fixed ψ, and obtain the Euler equation

$$-\alpha_\varkappa (\partial^2 \Phi_\varkappa / \partial q_\varkappa'^2) + q_\varkappa'^2 \Phi_\varkappa + 2q'_\varkappa \beta_\varkappa \Phi_\varkappa = (2\lambda_\varkappa / \hbar\omega_\varkappa) \Phi_\varkappa.$$

Here $\lambda_\varkappa$ is a Lagrange multiplier introduced by the minimization. The Euler equation has the solution

$$\begin{aligned} &\Phi_\varkappa \equiv \Phi_{n_\varkappa} = A_{n_\varkappa} e^{-x_\varkappa^2/2} H_{n_\varkappa}(x_\varkappa), \quad \lambda_\varkappa \equiv \lambda_{n_\varkappa} = \frac{\hbar\omega_\varkappa}{2} [\alpha_\varkappa^{1/2}(2n_\varkappa + 1) - \beta_\varkappa^2], \\ &x_\varkappa = \alpha_\varkappa^{-1/4}(q'_\varkappa + \beta_\varkappa), \end{aligned} \qquad (6)$$

where $H_{n_\varkappa}$ is a Chebyshev-Hermite polynomial and $n_\varkappa = 0, 1, 2, \ldots$. Substitution of this result into Eq. (5) gives

$$\begin{aligned} \overline{H[\Psi]} = Q[\psi \ldots q_\varkappa^0] = &J[\psi] + \sum_\varkappa \hbar\omega_\varkappa (n_\varkappa + 1/2) + \sum_{\varkappa, i} \frac{\hbar^2}{2m_i} \overline{(\nabla_i q_\varkappa^0)^2} (n_\varkappa + 1/2) \\ &+ \sum_\varkappa 1/2 \hbar\omega_\varkappa (\overline{q_\varkappa^{02}} - \overline{q_\varkappa^0}^2) + \sum_{\varkappa, i} c_\varkappa^i [\overline{q_\varkappa^0 \chi_{-\varkappa}(\mathbf{r}_i)} - \overline{q_\varkappa^0}\, \overline{\chi_{-\varkappa}(\mathbf{r}_i)}], \qquad (7) \end{aligned}$$

$$J[\psi] \equiv \sum_{i=1}^{N} \frac{\hbar^2}{2m_i} \int \nabla_i \psi^2 d\mathbf{r} - \sum_\varkappa \frac{1}{2\hbar\omega_\varkappa} \left(\sum_i c_\varkappa^i \overline{\chi_{-\varkappa}(\mathbf{r}_i)} \right)^2 + \overline{V(\mathbf{r})}. \qquad (8)$$

In deriving Eq. (7) we suppose that $q_\varkappa^0(\mathbf{r}) \sim V^{-1/2}$ and pass to the limit $V \to \infty$. In this case we can write

$$\alpha_\varkappa^{1/2} = 1 + \sum_i \frac{\hbar}{2m_i\omega_\varkappa} \overline{(\nabla_i q_\varkappa^0)^2}.$$

The functional (8) differs only in notation from the functional $J[\psi]$ appearing in the earlier papers, where the multiplicative approximation was used. See Eq. (29) of Ref. 2, or for F and F' centers Eqs. (23.11) and (26.10) of Ref. 1.

We shall next minimize the functional Q, varying $q_\varkappa^0(\mathbf{r})$ for fixed $\psi(\mathbf{r})$. The resulting Euler equation looks complicated and has not been solved in the general case. We solved it in the limits of weak and strong coupling and found that in both cases the solution can be written in the form

$$q_\varkappa^0 = \sum_i a_\varkappa^i \chi_{-\varkappa}(\mathbf{r}_i) \qquad (9)$$

with a suitable choice of the coefficients $a_\varkappa^i$. We

therefore use the approximation (9) for $q^0_\varkappa(\mathbf{r})$ in the general case, and use the variational method to determine the $a^i_\varkappa$. Substituting Eq. (9) into (7), we obtain

$$\begin{aligned} Q[\psi \ldots a^i_\varkappa \ldots] &= J[\psi] + \sum_\varkappa \hbar\omega_\varkappa (n_\varkappa + {}^1/_2) \\ &+ \sum_{\varkappa, i} \frac{\hbar^2}{2m_i}\, a^{i^2}_\varkappa \overline{[\nabla_i \chi_{-\varkappa}(\mathbf{r}_i)]^2}(n_\varkappa + {}^1/_2) \\ &+ \sum_{\varkappa, i, i_1} \left[\frac{\hbar\omega_\varkappa}{2}\, a^i_\varkappa a^{i_1}_\varkappa + c^i_\varkappa a^{i_1}_\varkappa\right] \\ &\times \left[\overline{\chi_{-\varkappa}(\mathbf{r}_i)\chi_{-\varkappa}(\mathbf{r}_{i_1})} - \overline{\chi_{-\varkappa}(\mathbf{r}_i)}\,\overline{\chi_{-\varkappa}(\mathbf{r}_{i_1})}\right]. \end{aligned} \tag{10}$$

2. THE GROUND STATE

We obtain the energy of the ground state as the absolute minimum of the functional (10), in which we should set all $n_\varkappa = 0$ since this removes positive terms from the functional. The minimum is then found by a direct variational method.

If we take $\psi = \text{const} = V^{-1/2}$, which corresponds to the case $V(\mathbf{r}) = 0$ in the limit of weak coupling ($c^i_\varkappa \to 0$), then

$$\begin{gathered} \overline{\chi_{-\varkappa}(\mathbf{r}_i)} = 0; \quad \overline{\chi_{-\varkappa}(\mathbf{r}_i)\chi_{-\varkappa}(\mathbf{r}_{i_1})} = \frac{\delta_{ii_1}}{V}, \\ \overline{[\nabla_i \chi_{-\varkappa}(\mathbf{r}_i)]^2} = \frac{\varkappa^2}{V}, \quad J[\psi] = 0. \end{gathered} \tag{11}$$

When Eq. (11) is substituted into (10) and the result is minimized with respect to the $a^i_\varkappa$, the ground-state energy becomes

$$E_0 = -\frac{1}{2V} \sum_{\varkappa, i=1}^{N} \frac{c^{i^2}_\varkappa}{(\hbar^2\varkappa^2/2m_i) + \hbar\omega_\varkappa}. \tag{12}$$

This coincides with the energy calculated by second-order perturbation theory. The last term in Eq. (1) is treated as the perturbation. In particular, in the polaron problem which has $N = 1$, $\omega_\varkappa = \omega$ independent of $\varkappa$, and

$$c^1_\varkappa = -e\sqrt{4\pi\hbar\omega c}/|\boldsymbol{\varkappa}|, \; c = 1/n^2 - 1/\varepsilon, \tag{13}$$

the energy is given by

$$E_{0p} = -\alpha\hbar\omega, \quad \alpha = e^2 c h^{-3/2}(m/2\omega)^{1/2}. \tag{14}$$

Here ε is the static dielectric constant of an ionic crystal, n is the refractive index, and m is the effective mass of a conduction electron in the crystal, assuming the ions to be fixed and motionless. Eq. (14) was obtained earlier by Fröhlich[4] using perturbation theory, and by Gurari[5] and Lee, Low and Pines[6] using variational methods.

From the other side, the approximation (3) also gives the correct ground-state energy in the strong-coupling limit, since even the less general multiplicative approximation, as we mentioned earlier, gives the right result in that limit. Knowing that the approximation (3) gives accurate results in both weak and strong coupling limits, we may hope that it also allows us to make a reasonable calculation in the intermediate coupling range.

In problems where $\psi(\mathbf{r})$ is symmetric in the particle coordinates, for example for the ground-state of an F'-center, and in various other cases, we may use for $\psi(\mathbf{r})$ the approximation

$$\psi(\mathbf{r}) = \prod_{i=1}^{N} \psi_i(\mathbf{r}_i) \tag{15}$$

If we also assume $\psi^2_i(\mathbf{r}_i) = \psi^2_i(-\mathbf{r}_i)$, we find

$$\begin{aligned} &\overline{[\nabla_i \chi_{-\varkappa}(\mathbf{r}_i)]^2} = \varkappa^2/V, \; \overline{[\chi_{-\varkappa}(\mathbf{r}_i)]^2} \\ &= 1/V, \; \overline{\chi_{-\varkappa}(\mathbf{r}_i)} = V^{-1/2}\,\overline{\cos \boldsymbol{\varkappa}\mathbf{r}_i}. \end{aligned} \tag{16}$$

When these values are substituted into Eq. (10) and the result is minimized with respect to the $a^i_\varkappa$, we obtain

$$a^i_\varkappa = -\frac{c^i_\varkappa (1 - \overline{\cos \boldsymbol{\varkappa}\mathbf{r}_i})}{(\hbar^2\varkappa^2/2m_i) + \hbar\omega_\varkappa (1 - \overline{\cos \boldsymbol{\varkappa}\mathbf{r}_i})}, \tag{17}$$

$$Q = J[\psi] - \frac{1}{2V} \sum_{\varkappa i} \frac{c^{i^2}_\varkappa (1 - \overline{\cos \boldsymbol{\varkappa}\mathbf{r}_i})^2}{(\hbar^2\varkappa^2/2m_i) + \hbar\omega_\varkappa (1 - \overline{\cos \boldsymbol{\varkappa}\mathbf{r}_i})}. \tag{18}$$

In the subsequent calculations we must specify the form of the functions $\psi_i(\mathbf{r}_i)$. For many applications the following choice gives a good approximation:

$$\psi_i(\mathbf{r}_i) = (2\beta_i/\pi)^{3/4} \exp(-\beta_i \mathbf{r}_i^2). \tag{19}$$

In this case

$$\overline{\cos \boldsymbol{\varkappa}\mathbf{r}_i} = \exp(-\varkappa^2/8\beta_i)$$

and Eq. (18) gives

$$Q = J[\psi] - \frac{1}{2V} \sum_{\varkappa, i} \frac{c^{i^2}_\varkappa (1 - \exp(-\varkappa^2/4\beta_i))^2}{(\hbar^2\varkappa^2/2m_i) + \hbar\omega_\varkappa (1 - \exp(-\varkappa^2/4\beta_i))}. \tag{20}$$

In the F-center problem there is only one electron ($N = 1$), $V = -ze^2/\varepsilon r$, $c_\varkappa$ is given by Eq. (13), and one may neglect the dispersion of longitudinal optical vibrations of the ions by setting $\omega_\varkappa = \omega$. Then, replacing sums by integrals according to the rule

$$\sum_\varkappa f(\varkappa) = (2\pi)^{-3} V \int f(\varkappa)\, d\varkappa_1 d\varkappa_2 d\varkappa_3,$$

we obtain

$$Q_F = J(\beta) - \frac{2c^2 c V\sqrt{3}}{\pi} \int_0^\infty \frac{(1-e^{-x^2})^2\, dx}{bx^2 + 1 - e^{-x^2}},$$

$$x = \frac{\varkappa}{2\sqrt{\beta}}, \qquad b = \frac{2\beta\hbar}{m\omega}, \tag{21}$$

$$J(\beta) = \frac{3\hbar^2\beta}{2m} - \frac{e^2}{\sqrt{\pi}}\sqrt{\beta}\,(c + z2^{3/2}/\varepsilon). \tag{22}$$

The ground-state energy of the F-center is the minimum of Eq. (21) with respect to β.

In the strong-coupling limit we shall see that β is large. Thus $J(\beta)$, which contains terms of order β and $\beta^{1/2}$, is considerably larger than the second term in Eq. (21) which is of order $\beta^{-1/2}$. Hence the extremum of Q_F can be found approximately by minimizing the term $J(\beta)$ alone. This minimization was carried out in our earlier paper[7], with the result

$$\beta = (m^2e^4/9\pi\hbar^4)\,(c + 2^{3/2}z/\varepsilon)^2. \tag{23}$$

This value of β gives

$$E_F = -\frac{me^4}{6\pi\hbar^2}\left(c + \frac{2^{3/2}z}{\varepsilon}\right)^2 - \frac{2e^4mc\,(c + 2^{3/2}z/\varepsilon)}{3\hbar^2\pi^{3/2}} \int_0^\infty \frac{(1-e^{-x^2})^2 dx}{b_F x^2 + 1 - e^{-x^2}}, \tag{24}$$

$$b_F = (2me^4/9\pi\hbar^3\omega)\,(c + 2^{3/2}z/\varepsilon)^2.$$

In the denominator of the integrand in Eq. (24) we neglect $(1 - e^{-x^2})$ in comparison with the large term $b_F x^2$. The final result is then

$$E_F = -\frac{me^4}{6\pi\hbar^2}\left(c + \frac{2^{3/2}z}{\varepsilon}\right)^2 - 1{,}76\hbar\omega \Big/ \left(1 + \frac{2^{3/2}z}{\varepsilon c}\right). \tag{25}$$

We can go from the F-center to the polaron problem by setting $z = 0$. Eq. (24) then gives for the ground-state energy of the polaron

$$E_{0p} = -\frac{me^4c^2}{6\pi\hbar^2} - \frac{2c^4mc^2}{3\hbar^2\pi^{3/2}} \int_0^\infty \frac{(1-e^{-x^2})^2\, dx}{b_p x^2 + 1 - e^{-x^2}},$$

$$b_p = 2me^4c^2/9\pi\hbar^3\omega. \tag{26}$$

If here we neglect $(1 - e^{-x^2})$ compared with $b_p x^2$ in the denominator of the integrand, we obtain

$$E_{0p} = -(0.106\alpha^2 + 1.76)\,\hbar\omega. \tag{27}$$

This is the polaron ground-state energy in the strong-coupling limit.

It is interesting to see that Eq. (26) also gives the correct result (14) for the energy in the weak-coupling limit when β is small. The reason for this is that as $c \to 0$, $\beta \to 0$ too and hence $\psi \to$ const. A constant ψ, as we saw earlier, gives the perturbation-theory result. Hence Eq. (26) gives a single analytic expression for the polaron ground-state energy which is correct in both weak and strong coupling limits. It is reasonable to use it as an interpolation formula for the energy in the intermediate coupling region. But Eq. (26) was obtained from Eq. (21) by substituting the value of β from Eq. (23). This value of β was found by minimizing Eq. (21) in the strong-coupling limit. If we minimize Eq. (21) in the intermediate coupling range, we shall find a value of β differing from Eq. (23), and this will give a more accurate result (a lower value for E_{0p}) than Eq. (26).

A shortcoming of the approximations (3) and (19) as applied to the polaron problem is their lack of translational invariance. Only in the case of weak coupling, when ψ = const, is the correct translational symmetry preserved by the approximations. This shortcoming will be removed in a following paper, in which problems with translational symmetry will be considered separately and the correct approximations to use in such problems will be developed. We shall then find a lower value for the polaron ground-state energy.

The above criticism does not apply to problems of localized electron states where $V(\mathbf{r})$ contains a potential well binding the electron by means of external forces, for example the problems of F and F' centers, for in these cases there is no translational symmetry.

If we compare the formula (25) for the F-center ground-state energy with the corresponding result of the multiplicative approximation[8], we see that

the second term of Eq. (25) is new and is always negative. Thus our approximation (3) gives a lower ground-state energy. The lowering of the energy is particularly large for crystals with a high dielectric constant.

In the case of an F'-center there are two electrons ($N = 2$) attached to a positively charged crystal defect.

$$V = -\frac{ze^2}{\varepsilon}\left(\frac{1}{r_1}+\frac{1}{r_2}\right)+\frac{e^2}{n^2|\mathbf{r}_1-\mathbf{r}_2|},$$
$$c_\varkappa^1 = c_\varkappa^2 = c_\varkappa,$$

and $c_\varkappa$ is given by Eq. (13). Then Eq. (20) gives

$$Q_{F'}(\beta) = J_{F'}(\beta) - \frac{4ce^2\sqrt{\beta}}{\pi}\int_0^\infty \frac{(1-e^{-x^2})^2\,dx}{bx^2+1-e^{-x^2}}, \quad (28)$$

$$J_{F'}(\beta) = \frac{3\beta\hbar^2}{m} - \frac{2e^2}{\sqrt{\pi}}\left(c'+\frac{2^{3/2}z}{\varepsilon}\right)\sqrt{\beta},$$
$$c' = 2c - \frac{1}{n^2}. \quad (29)$$

We minimize $Q_{F'}$ with respect to β by going to the strong-coupling range and minimizing only the main term $J_{F'}(\beta)$, just as we did for the F-center. This gives

$$\beta = (m^2e^4/9\pi\hbar^4)(c'+2^{3/2}z/\varepsilon)^2, \quad (30)$$

$$E_{F'} = -\frac{me^4}{3\pi\hbar^2}\left(c'+\frac{2^{3/2}z}{\varepsilon}\right)^2 - \frac{4ce^4m(c'+2^{3/2}z/\varepsilon)}{3\pi^{3/2}\hbar^2}\int_0^\infty \frac{(1-e^{-x^2})^2\,dx}{b_{F'}x^2+1-e^{-x^2}},$$

$$b_{F'} = 2me^4(c'+2^{3/2}z/\varepsilon)^2/9\pi\hbar^3\omega. \quad (31)$$

In the strong-coupling range we keep only the term $b_{F'}x^2$ in the denominator of the integrand, and obtain

$$E_{F'} = -\frac{me^4}{3\pi\hbar^2}\left(c'+\frac{2^{3/2}z}{\varepsilon}\right)^2 - \frac{3{,}52c\hbar\omega}{c'+2^{3/2}z/\varepsilon}. \quad (32)$$

This expression likewise differs from the result of the multiplicative approximation[9] only by the appearance of the second term on the right.

We have also studied the excited states of F-centers, for which the corrections to the results of the multiplicative approximation are significantly larger. These results were published elsewhere[10].

[1] S. I. Pekar, *Studies in the Electronic Theory of Crystals*, (Gostekhizdat, 1951), (German Translation, Akademie-Verlag, Berlin 1954).

[2] S. I. Pekar, J. Exptl. Theoret. Phys. (U.S.S.R.), **22**, 641 (1952).

[3] M. Born and J. R. Oppenheimer, Ann. Phys. **84**, 457 (1927).

[4] Fröhlich, Pelzer and Zienau, Phil. Mag. **41**, 221 (1950).

[5] M. Gurari, Phil. Mag. **44**, 329 (1953).

[6] Lee, Low and Pines, Phys. Rev. **90**, 297 (1953).

[7] S. I. Pekar and M. F. Deigen, J. Exptl. Theoret. Phys. (U.S.S.R.), **18**, 481 (1948).

[8] S. I. Pekar, J. Exptl. Theoret. Phys. (U.S.S.R.), **20**, 510 (1950).

[9] S. I. Pekar, and O. F. Tomasevich, J. Exptl. Theoret. Phys. (U.S.S.R.) **21**, 1218 (1951).

[10] V. M. Buimistrov and S. I. Pekar, Ukrain. Phys. Journ. **2**, 2 (1957).

Translated by F. J. Dyson
240

Minami Transformation for Nucleon-Nucleon Scattering

R. M. RYNDIN AND IA. A. SMORODINSKII
United Institute for Nuclear Studies

(Submitted to JETP editor July 12, 1956)
J. Exptl. Theoret. Phys. (U.S.S.R.) 32, 1200-1205 (May, 1957)

It is shown that for the case of nucleon-nucleon scattering there is no analog of the transformation of phases which, in the case of scattering of pions by nucleons, leaves the scattering cross section invariant. In the case of nucleon-nucleon scattering, a transformation consisting of a rotation of the spins does not yield a new set of phases which are physically meaningful.

INTRODUCTION

IN THE CASE of scattering of spin ½ particles by spinless particles, there are two sets of phases[1-3] which cannot be distinguished except by means of polarization experiments (or by investigating the energy dependence of the scattering cross section at low energies). These sets of phases are obtained from one another by a simultaneous interchange of the phases referring to a given value of the total angular momentum. If δ_l^j denotes the phase of the scattered wave for given values of j and l, then the transformation is

$$\delta^j_{j-1/2} \rightleftarrows \delta^j_{j-1/2} \quad \text{(for all } j \text{ simultaneously)} \qquad \text{(I)}$$

In a paper by the authors [4] it was shown that the existence of this transformation is a consequence of the obvious invariance of the cross section for scattering of an unpolarized beam with respect to rotation of the spin through an angle of $\pm\pi$ around the direction $\boldsymbol{\nu}$ of the wave vector of the scattered particles. The transformation (I) is easily generalized to the case of rotation of the spin through an arbitrary angle γ, and then takes the form:

$$\begin{aligned} E^j_{j-1/2} &\to i\cos\tfrac{\gamma}{2}\,E^j_{j-1/2} - \sin\tfrac{\gamma}{2}\,E^j_{j+1/2}, \\ E^j_{j+1/2} &\to i\cos\tfrac{\gamma}{2}\,E^j_{j+1/2} - \sin\tfrac{\gamma}{2}\,E^j_{j-1/2}. \end{aligned} \qquad \text{(II)}$$

E_l^j here denotes the quantity $\exp(2i\delta_l^j) - 1$. The existence of this transformation is proven most simply by applying to the scattering amplitude the operator $i\exp(-i\sigma\boldsymbol{\nu}\gamma/2)$, which is proportional to the operator for rotation of the spin through angle γ about the direction $\boldsymbol{\nu}$. The scattering cross section can be expressed in the form:*

$$d\sigma/d\omega = f^+_{1/2}f_{1/2},$$

where $f_{1/2}$ denotes the scattering amplitude when the projection of the total angular momentum along the direction of the incident beam is ½. It is obvious that the cross section is invariant under replacement of $f_{1/2}$ by $f'_{1/2} = i\exp(-i\sigma\boldsymbol{\nu}\gamma/2)f_{1/2}$. By using the standard rules for quantum-mechanical addition of angular momenta, the amplitude $f_{1/2}$ is expressed in terms of the eigenfunctions $Y^{1/2}_{j,\,l,\,1/2}(\boldsymbol{\nu})$ of the operators $\mathbf{j}^2$, $\mathbf{l}^2$, $\mathbf{s}^2$ and s_z:

$$f_{1/2} = \frac{\pi^{1/2}}{ik}\sum_{j=1/2}^{\infty}(j+1/2)^{1/2}\{E^j_{j-1/2}Y^{1/2}_{j,j-1/2,1/2}(\boldsymbol{\nu}) - E^j_{j+1/2}Y^{1/2}_{j,j+1/2,1/2}(\boldsymbol{\nu})\}. \qquad \text{(III)}$$

If we now use the relation[5]

$$\sigma\boldsymbol{\nu}Y^{1/2}_{j,l,1/2}(\boldsymbol{\nu}) = Y^{1/2}_{j,l',1/2}(\boldsymbol{\nu}),$$

$$l' = 2j - l = \begin{cases} j+1/2 & \text{for } l = j-1/2 \\ j-1/2 & \text{for } l = j+1/2, \end{cases}$$

the amplitude $f'_{1/2}$ can be put in the form

$$f'_{1/2} = \frac{\pi^{1/2}}{ik}\sum_{j=1/2}^{\infty}(j+1/2)^{1/2}\Big\{\Big(i\cos\tfrac{\gamma}{2}E^j_{j-1/2} - \sin\tfrac{\gamma}{2}E^j_{j+1/2}\Big)Y^{1/2}_{j,\,j-1/2,\,1/2}(\boldsymbol{\nu}) - \Big(i\cos\tfrac{\gamma}{2}E^j_{j+1/2} - \sin\tfrac{\gamma}{2}E^j_{j-1/2}\Big)Y^{1/2}_{j,\,j+1/2,\,1/2}(\boldsymbol{\nu})\Big\}. \qquad \text{(IV)}$$

Comparing (III) and (IV), we see that the amplitude $f'_{1/2}$ can be obtained from $f_{1/2}$ by means of the transformation (II), and consequently the cross section is in fact invariant under this transformation. The new

*As a consequence of the invariance of the interaction Hamiltonian with respect to rotations and reflections, the relation $f^+_{1/2}f_{1/2} = f^+_{-1/2}f_{-1/2}$ holds. Because of this the amplitude $f_{-1/2}$ does not appear explicitly in the expression for the scattering cross section for an unpolarized beam.

phases will be complex for all values of γ except the values $\gamma = \pm\pi$ considered by Minami. Therefore the transformation (II) with $\gamma \neq \pm\pi$ cannot be considered in the phase analysis of data on scattering of spin ½ particles by spinless particles.

It is of interest to investigate the question of the existence of a similar type of invariance in the case of nucleon-nucleon scattering. We shall show that such a transformation does exist. However, this transformation does not satisfy the physical conditions of the problem. The symmetry of the system demands that the phases be independent of the magnetic quantum number m. But the phases obtained from the transformation we are considering turn out to depend on $|m|$. Consequently, in contradiction to our earlier expectation[4], there is no ambiguity of the phases of the type which occurs in a system with total spin ½.

We shall limit ourselves to considering proton-proton scattering, since the more general case of neutron-proton scattering gives nothing essentially new.

1. AMPLITUDES AND DIFFERENTIAL SCATTERING CROSS SECTION

In this section we give a brief presentation of the method for describing the collision of identical particles with spin ½, and express the amplitudes for proton-proton scattering in a form which is convenient for investigating their behavior under spin rotations.

The wave function of two protons moving along the z axis before the collision can be written in the center of mass system (c.m.s.) in the form

$$\psi_{sm} \sim (e^{ikz} - (-1)^{s+1} e^{-ikz})\,\chi_{sm} + F_{sm}(\boldsymbol{\nu})\, e^{ikr}/r. \tag{1.1}$$

Here χ_{sm} are spin functions ($s = 0$ and $s = 1$ in singlet and triplet states, respectively; m is the projection of the total spin on the z axis), k is the wave number, while $\boldsymbol{\nu}$ is a unit vector along the direction of motion of the scattered particles.

The scalar product* $\langle F_{sm}, F_{sm} \rangle$ determines the differential scattering cross section $d\sigma_{sm}(\boldsymbol{\nu})$ for given initial spin s and spin projection m. The cross section for scattering of an unpolarized beam is gotten by averaging the cross section $d\sigma_{sm}(\boldsymbol{\nu})$ over all possible initial spin states:

$$d\sigma(\boldsymbol{\nu})/d\omega = \tfrac{1}{4}\Big\{\langle F_{00}(\boldsymbol{\nu}),\, F_{00}(\boldsymbol{\nu})\rangle + \sum_{m=-1}^{+1} \langle F_{1m}(\boldsymbol{\nu}),\, F_{1m}(\boldsymbol{\nu})\rangle\Big\}. \tag{1.2}$$

Using the standard methods for investigating the asymptotic behavior of wave functions (*cf.* for example, the paper of Blatt and Biedenharn[5]), one can easily obtain explicit expressions for the amplitudes $F_{sm}(\boldsymbol{\nu})$ in terms of the elements of the scattering matrix S and the functions $Y^{m}_{j,l,s}$. The singlet scattering in a state with given j is described by means of the single matrix element $S'_j = \exp(2i\Delta_j)$, where Δ_j denotes the corresponding phase. The description of the triplet scattering is much more complicated. Here we have to distinguish two groups of states, with $j = l$ and $j \pm 1 = l$ respectively. In the first group ($j = l$) are the states with odd j, while the second contains states with even j. In the states of the first group, as in the singlet states, the orbital angular momentum is conserved, so that the scattering is again described by a single matrix element $T'_j = \exp(2i\delta_j)$. In states of the second group the orbital angular momentum is not conserved, and transitions are possible between states with $l = j + 1$ and $l' = j - 1$ (*e.g.*, the states ${}^3P_2$ and ${}^3F_2$). Consequently the scattering in states with a given j is described by a two-by-two matrix. In the example of the states ${}^3P_2$ and ${}^3F_2$, its matrix elements are given by the transition probabilities ${}^3P_2 \to {}^3P_2$, ${}^3P_2 \to {}^3F_2$, ${}^3F_2 \to {}^3P_2$, and ${}^3F_2 \to {}^3F_2$. This matrix is symmetric (the equality of the transition amplitudes for ${}^3P_2 \to {}^3F_2$ and ${}^3F_2 \to {}^3P_2$ is a consequence of the invariance of the interaction Hamiltonian under time reversal), and is unitary. We shall label the matrix elements of the scattering matrix in states with a given j according to the scheme:

l \ l'	$j-1$	$j+1$
$j-1$	A'_j	C_j
$j+1$	C_j	B'_j

The unitarity condition enables us to express[6,7] the three complex parameters A'_j, B'_j and C_j in terms of three independent real parameters consisting of the two phases δ^{I}_j and δ^{II}_j and a mixing parameter ε_j, by means of the relations:

---

* By the scalar product of two linear combinations of spin functions

$$a = \sum_{s'}\sum_{m'} a_{s'm'}\chi_{s'm'} \quad \text{and} \quad b = \sum_{s''}\sum_{m''} b_{s''m''}\chi_{s''m''}$$

we mean the quantity

$$\langle a, b\rangle = \sum_{s}\sum_{m} a^{*}_{sm} b_{sm}.$$

$$A_j' = \cos^2\varepsilon_j \exp(2i\delta_j^{\mathrm{I}}) + \sin^2\varepsilon_j \exp(2i\delta_j^{\mathrm{II}}),$$
$$B_j' = \sin^2\varepsilon_j \exp(2i\delta_j^{\mathrm{I}}) + \cos^2\varepsilon_j \exp(2i\delta_j^{\mathrm{II}}), \quad (1.3)$$
$$C_j = {}^1/_2 \sin 2\varepsilon_j (\exp(2i\delta_j^{\mathrm{I}}) - \exp(2i\delta_j^{\mathrm{II}})).$$

The mixing parameter is associated with the tensor forces and vanishes if they are absent.

The scattering amplitudes are given by:

$$F_{00}(\boldsymbol{\nu}) = \frac{(4\pi)^{1/2}}{ik}\sum_j (2j+1)^{1/2} S_j Y^0_{j,j,0}(\boldsymbol{\nu}),$$
$$F_{1,1}(\boldsymbol{\nu}) = \frac{(2\pi)^{1/2}}{ik}\sum_j \{[(j+1)^{1/2}A_j + j^{1/2}C_j]\, Y^1_{j,j-1,1}(\boldsymbol{\nu}) - (2j+1)^{1/2}\, T_j Y^1_{j,j,1}(\boldsymbol{\nu})$$
$$+ [j^{1/2}B_j + (j+1)^{1/2}C_j]\, Y^1_{j,j+1,1}(\boldsymbol{\nu})\},$$
$$F_{1,0}(\boldsymbol{\nu}) = \frac{(4\pi)^{1/2}}{ik}\sum_j \{[j^{1/2}A_j - (j+1)^{1/2}C_j]\, Y^0_{j,j-1,1}(\boldsymbol{\nu}) +$$
$$+ [-(j+1)^{1/2}B_j + j^{1/2}C_j]\, Y^0_{j,j+1,1}(\boldsymbol{\nu})\}, \quad (1.4)$$
$$F_{1,-1}(\boldsymbol{\nu}) = \frac{(2\pi)^{1/2}}{ik}\sum_j \{[(j+1)^{1/2}A_j + j^{1/2}C_j]\, Y^{-1}_{j,j-1,1}(\boldsymbol{\nu}) +$$
$$+ (2j+1)^{1/2} T_j Y^{-1}_{j,j,1}(\boldsymbol{\nu}) + [j^{1/2}B_j + (j+1)^{1/2}C_j]\, Y^{-1}_{j,j+1,1}(\boldsymbol{\nu})\}.$$

S_j, T_j, A_j and B_j denote the quantities $S_j' - 1$, $T_j' - 1$, $A_j' - 1$ and $B_j' - 1$. The summation in the singlet scattering amplitude is taken only over even j in accordance with the Pauli principle. In the triplet scattering amplitude, the summation is taken over odd j for states with $j = l$ and over even j for states with $j \pm 1 = l$.

2. BEHAVIOR OF SCATTERING AMPLITUDES UNDER SPIN ROTATIONS

We now proceed to investigate the transformation of the scattering amplitudes $F_{sm}(\boldsymbol{\nu})$ under rotations of the total spin and the spins of the individual protons, and find substitutions on the elements of the scattering matrix which lead to the same transformations of the amplitudes.

We start by studying rotations of the total spin $\boldsymbol{s} = (\boldsymbol{\sigma}_1 + \boldsymbol{\sigma}_2)/2$, where the $\boldsymbol{\sigma}_i$ are the Pauli spin operators for the two protons. The operator for rotation of the spin s through angle γ around the axis $\boldsymbol{\nu}$ is given by the direct product of the operators for rotation of the proton spins through the same angle:

$$R(\boldsymbol{\nu}, \gamma) = \exp(-i\mathbf{s}\boldsymbol{\nu}\gamma) = \cos^2\frac{\gamma}{2}$$
$$- i\mathbf{s}\boldsymbol{\nu}\sin\gamma + \sin^2\frac{\gamma}{2}(1 - 2(\mathbf{s}\boldsymbol{\nu})^2). \quad (2.1)$$

The effect of $R(\boldsymbol{\nu}, \gamma)$ on singlet spin functions is the same as that of the unit operator, since the projection of the total spin on any direction is zero in the singlet state.

We note first of all that, in the case of identical particles (two protons), rotations of the total spin $\boldsymbol{s}$ through an arbitrary angle γ cannot lead to physically admissible substitutions on the elements of the scattering matrix, since the amplitudes $F'_{sm} = R(\boldsymbol{\nu}, \gamma) F_{sm}$ which result from this transformation do not satisfy the Pauli principle. On the one hand the rotation operator $R(\boldsymbol{\nu}, \gamma)$ commutes with the square of the total spin $\mathbf{s}^2$, and consequently leaves the spin parity of the state unchanged. On the other hand, rotation through an arbitrary angle γ changes a state with a definite orbital parity into a linear combination of states with different parities. The exception is the case of $\gamma = \pm\pi$, when the rotation operator becomes $1 - 2(\mathbf{s}\cdot\boldsymbol{\nu})^2$, which does not change the parity of the state.

One can show that the amplitudes $F'_{sm}(\boldsymbol{\nu})$, corresponding to a total spin s rotated through the angle $\pm\pi$, have the form

$$F'_{0,0}(\boldsymbol{\nu}) = R(\boldsymbol{\nu}, \pm\pi) F_{0,0}(\boldsymbol{\nu}) = F_{0,0}(\boldsymbol{\nu}),$$
$$F'_{1,1}(\boldsymbol{\nu}) = R(\boldsymbol{\nu}, \pm\pi) F_{1,1}(\boldsymbol{\nu}) = \frac{(2\pi)^{1/2}}{ik}\sum_j \Big\{-\frac{1}{2j+1}[(j+1)^{1/2}A_j + j^{1/2}(2j+3)C_j +$$

$$+ (j+1)^{1/2} 2jB_j] Y^1_{j,j-1,1}(\nu) + (2j+1)^{1/2} T_j Y^1_{j,j,1}(\nu) - \frac{1}{2j+1} [j^{1/2} 2(j+1) A_j$$

$$+ (j+1)^{1/2} (2j-1) C_j - j^{1/2} B_j] Y^1_{j,j+1,1}(\nu)\Big\},$$

$$F'_{1,0}(\nu) = R(\nu, \pm\pi) F_{1,0}(\nu) = \frac{(4\pi)^{1/2}}{ik} \sum_j \Big\{ - \frac{1}{2j+1} [j^{1/2} A_j + (j+1)^{1/2} (2j-1) C_j$$

$$- j^{1/2} 2(j+1) B_j] Y^0_{j,j-1,1}(\nu) - \frac{1}{2j+1} [(j+1)^{1/2} 2jA_j - j^{1/2} (2j+3) C_j \tag{2.2}$$

$$+ (j+1)^{1/2} B_j] Y^0_{j,j+1,1}(\nu)\Big\},$$

$$F'_{1,-1}(\nu) = R(\nu, \pm\pi) F_{1,-1}(\nu) = \frac{(2\pi)^{1/2}}{ik} \sum_j \Big\{ - \frac{1}{2j+1} [(j+1)^{1/2} A_j + j^{1/2} (2j+3) C_j$$

$$+ (j+1)^{1/2} 2jB_j] Y^{-1}_{j,j-1,1}(\nu) - (2j+1)^{1/2} T_j Y^{-1}_{j,j,1}(\nu) - \frac{1}{2j+1} [j^{1/2} 2(j+1) A_j$$

$$+ (j+1)^{1/2} (2j-1) C_j - j^{1/2} B_j] Y^{-1}_{j,j+1,1}(\nu)\Big\}.$$

This transformation of the amplitudes is equivalent to their transformation by the following substitutions on the triplet elements of the scattering matrix:

$$m = \pm 1 \begin{cases} (j+1)^{1/2} A_j + j^{1/2} C_j \to \\ \to - \frac{1}{2j+1} [(j+1)^{1/2} A_j + j^{1/2} (2j+3) C_j + (j+1)^{1/2} 2jB_j], \\ j^{1/2} B_j + (j+1)^{1/2} C_j \to \\ \to - \frac{1}{2j+1} [j^{1/2} 2(j+1) A_j + (j+1)^{1/2} (2j-1) C_j - j^{1/2} B_j], \\ T_j \to - T_j, \end{cases} \tag{2.3a}$$

$$m = 0 \begin{cases} j^{1/2} A_j - (j+1)^{1/2} C_j \to \\ \to - \frac{1}{2j+1} [j^{1/2} A_j + (j+1)^{1/2} (2j-1) C_j - j^{1/2} 2(j+1) B_j], \\ - (j+1)^{1/2} B_j + j^{1/2} C_j \to \\ \to - \frac{1}{2j+1} [(j+1)^{1/2} 2jA_j - j^{1/2} (2j+3) C_j + (j+1)^{1/2} B_j], \\ T_j \to - T_j. \end{cases} \tag{2.3b}$$

The cross section $d\sigma(\nu)$ remains invariant when we replace $F_{sm}(\nu)$ by $F'_{sm}(\nu) = R(\nu, \pm\pi) F_{sm}(\nu)$ because of the unitarity of the operator $R(\nu, \pm\pi)$. This means that $d\sigma(\nu)$ is also invariant with respect to the substitutions (2.3). However, substitution (2.3a), which gives the desired transformation of the amplitudes $F_{1,\pm 1}(\nu)$ differs from (2.3b), which gives the transformation of $F_{1,0}(\nu)$. The substitutions do not depend on the sign of the projection m of the total angular momentum, but they do depend on its absolute value. The difference between the substitutions (2.3a) and (2.3b) is seen most simply in the case where tensor forces are absent ($C_j = 0$; this does not result in disappearance of polarization effects, since a nuclear spin-orbit interaction between nucleons may still be present). In this case the substitutions (2.3) become a determined set of substitutions on a pair of parameters and take the form:

$$m = \pm 1: \quad A_j \to - \frac{1}{2j+1} [A_j + 2jB_j],$$

$$B_j \to - \frac{1}{2j+1} [2(j+1) A_j - B_j],$$

$$T_j \to - T_j; \tag{2.4a}$$

$$m = 0: \quad A_j \to - \frac{1}{2j+1} [A_j - 2(j+1) B_j],$$

$$B_j \to + \frac{1}{2j+1} [2jA_j + B_j], \quad T_j \to - T_j. \tag{2.4b}$$

The difference between (2.4a) and (2.4b) is obvious. The reason for this difference is the difference in the weights with which the angular wave functions $Y^m_{j,l,s}$ with different values of $|m|$ enter into the expansion of the initial plane waves [the first term in (1.1)]. The distinction between the substitutions (2.3a) and (2.3b) in the general case follows directly from the incompatibility of the system of four equations for the three elements of the new scattering matrix S', which do not depend on the value of the projection. These equations are obtained from (2.3a) and (2.3b) by replacing the $\to$ by an equality sign and replacing A_j, B_j and C_j on the left sides of the equations by the elements $S' - 1$.

The difference in the substitutions corresponding to different values of $|m|$ means that the elements of the scattering matrix become dependent on $|m|$ after we carry out the indicated substitution. This fact is not compatible with the symmetry of the system and consequently we cannot, by means of rotations of the total spin, construct a physically admissible set of scattering matrix elements from the set obtained by analysis of data on the scattering of unpolarized protons.

We can attack the problem of investigating the transformation of the scattering amplitudes under rotations of the spin of one of the protons by a similar method. These transformations, like the amplitude transformations for rotations of the total spin, do not give physically admissible substitutions on the elements of the scattering matrix. In the first place, the amplitude resulting from the transformation by a rotation of one of the spins corresponds to a scattering matrix with non-zero elements for singlet-triplet transitions (the operator $\sigma_i \cdot \nu$ does not commute with the square of the total spin $\mathbf{s}^2$), and consequently does not satisfy the Pauli principle. Secondly, the substitutions leading to the required amplitude transformation depend on $|m|$, as in the case of rotations of the total spin. However, in the special case when only $^1S_0$ and $^3P_0$ states (with zero projection of the total angular momentum) contribute to the scattering, we find the well-known invariance of the cross section with respect to interchange of the phases $\delta(^1S_0)$ and $\delta(^3P_0)$, which occurs for a rotation of the spin of one of the protons through $\pm\pi$.

Finally, we note that a treatment of the collision of non-identical particles, for which the limitations imposed by the Pauli principle are absent, gives nothing new beyond what was found for proton-proton scattering. Moreover, the results of the investigation of the behavior of the scattering amplitudes under rotation of the total spin of the two-nucleon system can be taken over directly to the case of scattering of deuterons by spin zero particles.

The only system (for the case of non-relativistic particles), for which the spin rotation leads to an ambiguity of phases in the analysis of data on scattering of unpolarized particles is the system with total spin $\frac{1}{2}$, since in this case there is only value of $|m|$.

[1] S. Minami, Progr. Theor. Phys. 11, 213 (1954).

[2] S. Hayakawa *et al.*, Progr. Theor. Phys. 11, 332 (1954).

[3] N. Fukuda *et al.*, Progr. Theor. Phys. 12, 79 (1954).

[4] R. M. Ryndin and Ia. A. Smorodinskii, Dokl. Akad. Nauk SSSR 103, 69 (1955).

[5] A. I. Akhiezer and V. B. Berestetskii, *Quantum Electrodynamics*, Moscow, 1953, p. 67; H. Bethe and F. de Hoffman, Mesons and Fields, Vol. II, New York, 1955, p. 72.

[6] J. M. Blatt and L. C. Biedenharn, Rev. Mod. Phys. 24, 258 (1952).

[7] J. M. Blatt and L. C. Biedenharn, Phys. Rev. 86, 399 (1952).

Translated by M. Hamermesh
241

Magnetic Interaction of Electrons and Anomalous Diamagnetism

B. T. GEILIKMAN
Moscow State Pedagogical Institute
(Submitted to JETP editor July 13, 1956)
J. Exptl. Theoret. Phys. (U.S.S.R.) 32, 1206-1211 (May, 1957)

It is shown that the taking into account of magnetic interaction, within the framework of perturbation theory for an ideal electron gas, does not lead to anomalous diamagnetism.

IN THE PRESENT WORK the diamagnetism of electrons in a metal is studied with the magnetic interaction of the electrons taken into account. Some considerations regarding the importance of magnetic interaction of electrons for superconductivity were presented by Welker[1]. However, in view of the complete absence there of quantitative calculations, the question remained open.

It is possible to point out more convincing arguments than those in Ref. 1 in favor of the possible importance of magnetic interaction for anomalous diamagnetism. It is not difficult to see that the energy of a system in a magnetic field, for arbitrary specification of the vector potential A, must have the following form:

$$E = \sum_{\mathbf{q}} [(\mathbf{A}_{\mathbf{q}}, \mathbf{A}_{-\mathbf{q}}) - q^{-2}(\mathbf{q}, \mathbf{A}_{\mathbf{q}})(\mathbf{q}, \mathbf{A}_{-\mathbf{q}})]\,\varphi(q^2)$$
$$\mathbf{A}_{\mathbf{q}} = \frac{1}{V}\int e^{-i(\mathbf{qr})/\hbar}\mathbf{A}(\mathbf{r})\,d\mathbf{r}. \qquad (1)$$

Relation (1) follows from the equation of continuity; one can easily check this by using the expression for the current density $\mathbf{j}_s = -c\,\delta E/\delta \mathbf{A}$. In the case of a slowly changing field, φ can be expanded in a series,

$$\varphi(q^2) = \varphi_0 + \varphi_1 q^2 + \ldots$$

Anomalous diamagnetism is possible only when the term of zero order, φ_0, differs from zero. In fact, in this case we get for the current London's equation

$$\mathbf{j}_{\mathbf{q}} \approx -c\varphi_0(\mathbf{A}_{\mathbf{q}} - q^{-2}(\mathbf{q}, \mathbf{A}_{\mathbf{q}})\mathbf{q}),$$

i.e., $\operatorname{curl}\,\mathbf{j} = -c\varphi_0\mathbf{H}$.

Thus in order that London's equation may be obtained (for $\operatorname{div}\mathbf{A} \neq 0$), there must be a pole of type q^{-2} in the expression for E or $\mathbf{j}_{\mathbf{q}}$. Schafroth has shown that interaction of electrons with the lattice vibrations, within the framework of perturbation theory, gives no poles of this type[2]. But Coulomb interaction of the electrons, at first glance, might give such a pole. In fact, the correction to the energy in the third approximation of perturbation theory (the second with respect to the interaction of electrons with a magnetic field, is

$$-(e/2mc)\sum_i [\mathbf{p}_i\mathbf{A}_i + \mathbf{A}_i\mathbf{p}_i]$$

and the first with respect to the Coulomb interaction is $\frac{1}{2}\sum e^2/r_{ij}$) has the form (the factor q^{-2} is characteristic of an interaction of the type $1/r$):

$$\left(\frac{e}{mc}\right)^2 \sum_{\mathbf{p}_1,\mathbf{p}_2,\mathbf{q}} \frac{(\mathbf{p}_1 + \mathbf{q}/2, \mathbf{A}_{\mathbf{q}})(\mathbf{p}_2 - \mathbf{q}/2, \mathbf{A}_{-\mathbf{q}})}{(E_0 - E_1)(E_0 - E_2)} \frac{4\pi\hbar^2 e^2}{q^2 V},$$
$$\mathbf{q} = \mathbf{p}_1' - \mathbf{p}_1 = \mathbf{p}_2 - \mathbf{p}_2'. \qquad (2)$$

However, as was shown by Schafroth, Coulomb interaction in perturbation theory does not lead to anomalous diamagnetism, because the summation over $\mathbf{p}_1$ and $\mathbf{p}_2$, which enters to the first power in the numerator, gives zero. In the case of magnetic interaction, there is an additional factor $(\mathbf{p}_1\mathbf{p}_2 - \frac{1}{2}\mathbf{p}_1\mathbf{q} + \frac{1}{2}\mathbf{p}_2\mathbf{q})$ in the numerator, thanks to which expression (2) will not reduce to zero. But in this case the Hamiltonian contains other terms that are likewise capable of giving an energy correction quadratic in A. It will be shown below that magnetic interaction of the electrons similarly does not lead to anomalous diamagnetism, within the framework of perturbation theory.

In the nonrelativistic approximation, the Hamiltonian contains a rather large number of terms that depend on A; it therefore proves more convenient to use the relativistic Hamiltonian for electrons interacting with a quantized electromagnetic field. In this formulation the interaction of the electrons, either Coulomb or magnetic, is not introduced ex-

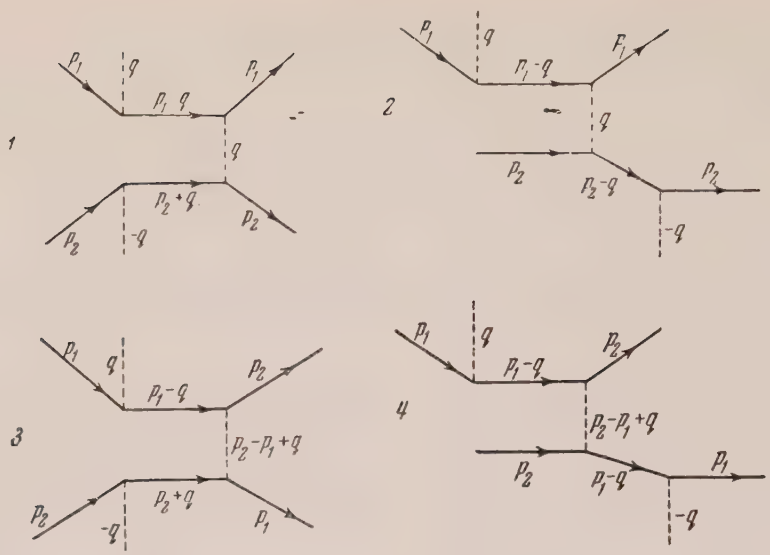

plicitly but is a consequence of the exchange of virtual photons (longitudinal and transverse). Then the first nonvanishing energy correction quadratic in A is obtained in the fourth approximation of perturbation theory, *viz.*, in the second with respect to the external potential and in the second with respect to the radiation field. To this correction correspond eight diagrams: the four shown in the figure and four obtained from them by reversal of the directions of the electron paths. The contributions to the energy from two diagrams that differ only in the directions of the electron paths are exactly equal; it is therefore possible to consider only the four diagrams shown in the figure, by doubling the energy correction that corresponds to these diagrams.

We write the matrix elements for the first and second diagrams (the notation is the same as in Ref. 4):

$$S_1 = \frac{e^4 i}{(2\pi)^4}\int \bar{u}(p_2)\,\gamma_\nu \frac{i(\hat{p}_2+\hat{q})-m}{(p_2+q)^2+m^2}\,\hat{a}(-q)\,u(p_2)\,\frac{1}{q^2}\;\bar{u}(p_1)\,\gamma_\nu \frac{i(\hat{p}_1-\hat{q})-m}{(p_1-q)^2+m^2}\,\hat{a}(q)\,u(p_1)\,d^4q;$$

$$S_2 = \frac{e^4 i}{(2\pi)^4}\int \bar{u}(p_2)\,\hat{a}(-q)\,\frac{i(\hat{p}_2-\hat{q})-m}{(p_2-q)^2+m^2}\,\gamma_\nu u(p_2)\,\frac{1}{q^2}\;\bar{u}(p_1)\,\gamma_\nu \frac{i(\hat{p}_1-\hat{q})-m}{(p_1-q)^2+m^2}\,\hat{a}(q)\,u(p_1)\,d^4q.$$

It is evident that in the case of the third and fourth diagrams, the factor q^{-2} is replaced by $(p_2 - p_1 + q)^{-2}$. Because of the absence of a pole of type q^{-2}, these diagrams cannot give anomalous diamagnetism; we shall therefore not consider them.

We calculate S_1 and S_2 according to the general rules:

$$S_1 = \frac{ie^4}{(2\pi)^4}\int \frac{4/m^2}{q^2(-2(p_1q)+q^2)(2(p_2q)+q^2)}\,[2(p_1a(q))\,p_{1\nu} - (p_1a(q))\,q_\nu$$
$$-(qa(q))\,p_{1\nu} + (p_1q)\,a_\nu(q)]\,[2(p_2a(-q))\,p_{2\nu} + (p_2a(-q))\,q_\nu +$$
$$+(qa(-q))\,p_{2\nu} - (p_2q)\,a_\nu(-q)]\,d^4q; \qquad (3)$$

$$S_2 = \frac{ie^4}{(2\pi)^4}\int \frac{4/m^2}{q^2(-2(p_1q)+q^2)(-2(p_2q)+q^2)}\,[2(p_1a(q))\,p_{1\nu} -$$
$$-(p_1a(q))\,q_\nu - (qa(q))\,p_{1\nu} + (p_1q)\,a_\nu(q)]\,[2(p_2a(-q))\,p_{2\nu} - (p_2a(-q))\,q_\nu$$
$$-(qa(-q))\,p_{2\nu} + (p_2q)\,a_\nu(-q)]\,d^4q. \qquad (4)$$

Henceforth we shall suppose that $a_4 = 0$ and that A is independent of time. Then

$$\mathbf{a}(q) = \int \mathbf{A}(\mathbf{r})\, e^{-i(qx)}\, d^4x = \mathbf{A}_\mathbf{q} \int e^{iq_4 x_4}\, dx_4.$$

Since all the terms in (3) and (4) contain $a(q)\, a(-q)$, it is appropriate to replace $a_\mu(q)\, a_\nu(-q)$ everywhere by the product

$$A_\mu(\mathbf{q})\, A_\nu(-\mathbf{q})\, 2\pi\delta(q_4)\, \Delta t$$

(Δt is a normalizing interval). As is well known, the energy correction $\Delta\varepsilon$ is connected with the matrix element by the relation[4] $S = -i\Delta t\, \Delta\varepsilon$.

Thus for $\Delta\varepsilon_1$ and $\Delta\varepsilon_2$ we get the same expressions (3) and (4), except that the integration must be carried out only over the three-dimensional volume $d\mathbf{q}$, not over d^4q, and the four-dimensional vectors q and $a(q)$ in all the terms must be replaced by the three-dimensional vectors $\mathbf{q}$ and $\mathbf{A}_\mathbf{q}$.

Upon adding S_1 and S_2 and taking account of the fact that $(p_1p_2) = \mathbf{p}_1\mathbf{p}_2 - \varepsilon_1\varepsilon_2$, we get ($\mathbf{p}_2$ has been replaced by $-\mathbf{p}_2$ in S_1):

$$\begin{aligned}\Delta\varepsilon = \frac{i}{\Delta t}(S_1 + S_2) = \frac{-2e^4}{(2\pi)^3 m^2}\int \frac{1}{q^2(-\mathbf{p}_1\mathbf{q} + q^2/2)(-\mathbf{p}_2\mathbf{q} + q^2/2)}\,[4(\mathbf{p}_1\mathbf{a})(\mathbf{p}_2\mathbf{a}_-)(\mathbf{p}_1\mathbf{p}_2)\\ -2(\mathbf{p}_1\mathbf{a})(\mathbf{p}_2\mathbf{a}_-)(\mathbf{p}_1\mathbf{q}) - 2(\mathbf{p}_1\mathbf{a})(\mathbf{q}\mathbf{a}_-)(\mathbf{p}_1\mathbf{p}_2) + 2(\mathbf{p}_1\mathbf{a})(\mathbf{p}_2\mathbf{q})(\mathbf{p}_1\mathbf{a}_-)\\ -2(\mathbf{p}_1\mathbf{a})(\mathbf{p}_2\mathbf{a}_-)(\mathbf{p}_2\mathbf{q}) + 2(\mathbf{p}_1\mathbf{q})(\mathbf{p}_2\mathbf{a}_-)(\mathbf{p}_2\mathbf{a}) - 2(\mathbf{q}\mathbf{a})(\mathbf{p}_2\mathbf{a}_-)(\mathbf{p}_1\mathbf{p}_2)\\ +(\mathbf{p}_1\mathbf{a})(\mathbf{p}_2\mathbf{a}_-)q^2 + (\mathbf{q}\mathbf{a})(\mathbf{q}\mathbf{a}_-)(\mathbf{p}_1\mathbf{p}_2) - (\mathbf{q}\mathbf{a})(\mathbf{p}_2\mathbf{q})(\mathbf{p}_1\mathbf{a}_-)\\ -(\mathbf{p}_1\mathbf{q})(\mathbf{q}\mathbf{a}_-)(\mathbf{p}_2\mathbf{a}) + (\mathbf{p}_1\mathbf{q})(\mathbf{p}_2\mathbf{q})(\mathbf{a}\mathbf{a}_-)]\,d\mathbf{q};\end{aligned} \tag{5}$$

here $\mathbf{a} = \mathbf{A}_\mathbf{q}$, $\mathbf{a}_- = \mathbf{A}_{-\mathbf{q}}$.

To get the correction ΔE to the energy of the whole system, $\Delta\varepsilon$ must be summed over $\mathbf{p}_1$ and $\mathbf{p}_2$. We integrate first over angles in $\mathbf{p}_1$- and $\mathbf{p}_2$-space, *i.e.*, we find

$$\begin{aligned}\Delta\varepsilon' &= \int \Delta\varepsilon \sin\vartheta_1\, d\vartheta_1 \sin\vartheta_2\, d\vartheta_2\, d\varphi_1\, d\varphi_2\\ &= \int \Delta\varepsilon\, d\Omega_1\, d\Omega_2.\end{aligned}$$

We point the z axis for $\mathbf{p}_1$ and $\mathbf{p}_2$ along $\mathbf{q}$. The integration of all the twelve terms that enter in (5) reduces to the calculation of the following three integrals, which are to be understood as principal values:

$$J_1 = \int_0^\pi \frac{\sin\vartheta\, d\vartheta}{-pq\cos\vartheta + q^2/2} = \frac{1}{pq}\int_{-1}^{1}\frac{d\mu}{\mu + q/2p}$$

$$= \frac{1}{pq}\ln\left|\frac{1+q/2p}{1-q/2p}\right| \approx \frac{1}{p^2}\left(1 + \frac{q^2}{12p^2} + \ldots\right);$$

$$J_2 = \int_0^\pi \frac{\cos\vartheta\sin\vartheta\, d\vartheta}{-pq\cos\vartheta + q^2/2} = -\frac{2}{pq}$$

$$+\frac{qJ_1}{2p} \approx -\frac{2}{pq}\left(1 - \frac{q^2}{4p^2} + \ldots\right); \tag{6}$$

$$J_3 = \int_0^\pi \frac{\cos^2\vartheta\sin\vartheta\, d\vartheta}{-pq\cos\vartheta + q^2/2} = -\frac{1}{p^2}$$

$$+\left(\frac{q}{2p}\right)^2 J_1 \approx -\frac{1}{p^2}\left(1 - \frac{q^2}{4p^2} + \ldots\right);$$

here $p^2 = \mathbf{p}^2$.

To clarify the problem of anomalous diamagnetism, it is sufficient to consider merely the term of zero order, φ_0, in the expression (1). In this case only terms quadratic in q need to be retained in the expansions of J_1, J_2, and J_3.

We calculate the first term $\Delta\varepsilon'_1$ in the expression $\Delta\varepsilon'$:

$$\Delta\varepsilon'_1 = 4b\int\frac{d\mathbf{q}}{q^2}\int(\mathbf{p}_2\mathbf{a}_-)\,p_1^2 a p_2 \frac{[\cos\vartheta_1\cos\theta + \sin\vartheta_1\sin\theta\cos(\varphi_1 - \Phi)]}{(-p_1q\cos\vartheta_1 + q^2/2)(-p_2q\cos\vartheta_2 + q^2/2)} \times$$

$$\times[\cos\vartheta_1\cos\vartheta_2 + \sin\vartheta_1\sin\vartheta_2\cos(\varphi_1 - \varphi_2)]\sin\vartheta_1\, d\vartheta_1\, d\varphi_1\, d\Omega_2 =$$

$$= 4b(2\pi)\,p_1^2 a p_2\,(\mathbf{p}_2, \mathbf{a}_-)\int\frac{d\mathbf{q}}{q^2}\int\frac{[\cos^2\vartheta_1\cos\theta\cos\vartheta_2 + {}^1/_2\sin^2\vartheta_1\sin\theta\sin\vartheta_2\cos(\varphi_2 - \Phi)]}{(-p_1q\cos\vartheta_1 + q^2/2)(-p_2q\cos\vartheta_2 + q^2/2)}$$

$$\times\sin\vartheta_1^1\, d\vartheta_1\, d\Omega_2 \approx 8\pi b p_2^2 a a_- \int\frac{d\mathbf{q}}{q^2}\int\left[-\left(1 - \frac{q^2}{4p_1^2}\right)\cos\theta\cos\vartheta_2 +\right.$$

$$\left.+\left(1 - \frac{q^2}{12p_1^2}\right)\sin\theta\sin\vartheta_2\cos(\varphi_2 - \Phi)\right]\frac{[\cos\vartheta_2\cos\theta_- + \sin\vartheta_2\sin\theta_-\cos(\varphi_2 - \Phi_-)]}{(-p_2q\cos\vartheta_2 + q^2/2)}\sin\vartheta_2\, d\vartheta_2\, d\varphi_2$$

$$= 4b(2\pi)^2\int\frac{d\mathbf{q}}{q^2}\left[(\mathbf{a}\mathbf{a}_-)\left(1 - \frac{q^2}{12p_1^2} - \frac{q^2}{12p_2^2}\right) - \frac{(\mathbf{a}\mathbf{q})(\mathbf{a}_-\mathbf{q})}{6}\left(\frac{1}{p_1^2} + \frac{1}{p_2^2}\right)\right];$$

$$b = -2e^4/(2\pi)^2 m^2; \quad \mathbf{a} = \{a, \theta, \Phi\}; \ \mathbf{a}_- = \{a_-, \theta_-, \Phi_-\}.$$

In the same way we calculate the remaining terms:

$$\frac{1}{4b\pi^2}\Delta\varepsilon'_2 \approx -4\int (\mathbf{aq})(\mathbf{a}_-\mathbf{q})\frac{d\mathbf{q}}{q^4}\left(1-\frac{q^2}{4p_1^2}-\frac{q^2}{4p_2^2}\right); \ \Delta\varepsilon'_3 \approx \Delta\varepsilon'_2;$$

$$\frac{1}{4b\pi^2}\Delta\varepsilon'_4 = -4\int\frac{d\mathbf{q}}{q^2}\left[\left(1-\frac{q^2}{12p_1^2}\right)(\mathbf{aa}_-)-\frac{(\mathbf{aq})(\mathbf{a}_-\mathbf{q})}{q^2}\left(2-\frac{q^2}{3p_1^2}\right)\right]\left(1-\frac{q^2}{4p_2^2}\right);$$

$$\Delta\varepsilon'_5 \approx \Delta\varepsilon'_2; \ \frac{1}{4b\pi^2}\Delta\varepsilon'_6 \approx -4\int\frac{d\mathbf{q}}{q^2}\left[\left(1-\frac{q^2}{12p_2^2}\right)(\mathbf{aa}_-)-\right.$$

$$\left.-\frac{(\mathbf{aq})(\mathbf{a}_-\mathbf{q})}{q^2}\left(2-\frac{q^2}{3p_2^2}\right)\right]\left(1-\frac{q^2}{4p_1^2}\right); \ \Delta\varepsilon'_7 \approx \Delta\varepsilon'_2;$$

$$\Delta\varepsilon'_8 \approx \Delta\varepsilon'_9 \approx -\Delta\varepsilon'_2; \ \Delta\varepsilon'_{10} \approx \Delta\varepsilon'_{11} \approx \Delta\varepsilon'_2;$$

$$\frac{1}{4b\pi^2}\Delta\varepsilon'_{12} \approx 4\int\frac{d\mathbf{q}}{q^2}(\mathbf{a}_-\mathbf{a})\left(1-\frac{q^2}{4p_1^2}-\frac{q^2}{4p_2^2}\right).$$

Adding, we find

$$\Delta\varepsilon' = \sum_{i=1}^{12}\Delta\varepsilon'_i = 0.$$

Thus the magnetic interaction (likewise the Coulomb interaction, since we have also taken account of exchange via longitudinal photons) gives no anomalous diamagnetism. The neglected terms of higher order in q^2 give a correction to the ordinary diamagnetism. There is no point in considering higher approximations of perturbation theory in the case of magnetic interaction, *i.e.*, the sixth (of fourth order in the radiation field), *etc.*, since the fourth approximation, already considered, would give for the London constant in the case of anomalous diamagnetism an extra factor of order 1/137, the sixth would give one of order $(1/137)^2$ and so on.

We point out that the application of perturbation theory to magnetic interaction is apparently justified. In fact, the mean interaction energy of a single pair of electron is

$$U_{\text{Av}} \approx (e/mc)^2 p_{\text{Av}}^2/r_{\text{Av}} \approx (e/mc)^2 p_0^3/\hbar;$$

p_0 is the maximum momentum.

The mean kinetic energy of the electrons is $T_{\text{Av}} \approx p_0^2/m$;

$$U_{\text{Av}}/T_{\text{Av}} \approx (e^2/\hbar c)\, p_0/mc = p_0/137\,mc \ll 1.$$

In conclusion, I express my gratitude to I. M. Polievktov-Nikoladze for an interesting discussion.

APPENDIX

In the appendix we present a simple proof of the absence of anomalous diamagnetism in the case of a system of free electrons within the framework of perturbation theory [2].

The Hamiltonian of a single free electron in a magnetic field has the form

$$H = H_0 + H'; \ H_0 = \frac{p^2}{2m}; \ .$$

$$H' = -\frac{e}{2mc}[\mathbf{Ap}+\mathbf{pA}] + \frac{e^2}{2mc^2}A^2.$$

The correction to the energy of the electron, quadratic in A, in the second approximation of perturbation theory, is evidently equal to

$$\Delta\varepsilon = \Delta\varepsilon^{(1)} + \Delta\varepsilon^{(2)}; \quad \Delta\varepsilon^{(1)} = \frac{e^2}{2mc^2V}\int A^2 d\mathbf{r} = \frac{e^2}{2mc^2}\sum_{\mathbf{q}}(\mathbf{A}_{\mathbf{q}}\mathbf{A}_{-\mathbf{q}});$$

$$\Delta\varepsilon^{(2)} = \left(\frac{e}{mc}\right)^2\sum_{\mathbf{q}}\frac{(\mathbf{p}+\mathbf{q}/2, \mathbf{A}_{\mathbf{q}})(\mathbf{p}+\mathbf{q}/2, \mathbf{A}_{-\mathbf{q}})}{[p^2-(\mathbf{p}+\mathbf{q})^2]/2m} = -\frac{e^2}{mc^2}\sum_{\mathbf{q}}\frac{1}{\mathbf{pq}+q^2/2}\Big[(\mathbf{pA}_{\mathbf{q}})(\mathbf{pA}_{-\mathbf{q}}) \qquad (A.1)$$

$$+\frac{1}{2}(\mathbf{pA}_{\mathbf{q}})(\mathbf{qA}_{-\mathbf{q}})+\frac{1}{2}(\mathbf{pA}_{-\mathbf{q}})(\mathbf{qA}_{\mathbf{q}})+\frac{1}{4}(\mathbf{qA}_{\mathbf{q}})(\mathbf{qA}_{-\mathbf{q}})\Big] \equiv \sum_{i=1}^{4}\Delta\varepsilon_i^{(2)}.$$

In the summation over all electrons, *i.e.*, over p, we first carry out the integration over angles in p-space. In this step the calculation of $\Delta\varepsilon' = \int \Delta\varepsilon d\Omega$ reduces again to the calculation of the integrals J_1, J_2, and J_3, in which we limit ourselves to terms quadratic in q. According to (6),

$$\Delta\varepsilon_1^{(2)'} = -(e^2/mc^2)\,2\pi \sum [(\mathbf{A_q}\,\mathbf{A_{-q}}) - 2q^{-2}(\mathbf{A_q q})(\mathbf{A_{-q} q})];$$

$$\Delta\varepsilon_2^{(2)'} = \Delta\varepsilon_3^{(2)'} = -(e^2/mc^2)\,2\pi \sum_{\mathbf{q}} (\mathbf{A_q q})(\mathbf{A_{-q} q})/q^2,$$

and $\Delta\varepsilon_4^{(2)'}$, it is easily seen, has the form $\sim \Sigma(\mathbf{qA_q})(\mathbf{qA_{-q}})$, *i.e.*, in general gives no anomalous diamagnetism.

Thus the sum becomes

$$\sum_{\mathbf{p}} \sum_{i=1}^{4} \Delta\varepsilon_i^{(2)} = \sum_{\mathbf{p}} \Delta\varepsilon^{(2)} = -\frac{Ne^2}{2mc^2} \sum_{\mathbf{q}} (\mathbf{A_q A_{-q}}),$$

i.e., it is equal to the sum $\Sigma\Delta\varepsilon^{(1)}$ with the sign reversed. Consequently, anomalous diamagnetism is absent. This proof relates to an arbitrary system of free electrons with an isotropic distribution in p-space and with momenta p different from zero, *i.e.*, to a Fermi gas and to a Bose gas not in a state of condensation. In the case of a charged Bose gas in a state of condensation, this result retains its validity for electrons with momenta $\mathbf{p} \neq 0$. For electrons with $\mathbf{p} = 0$ (let their number be N_s), the energy in a magnetic field may be found directly from formula (A.1) by setting $\mathbf{p} = 0$. Then

$$\Delta E = \frac{N_s e^2}{2mc^2} \left\{ \sum_{\mathbf{q}} \mathbf{A_q A_{-q}} - \sum_{\mathbf{q}} (\mathbf{A_q q})(\mathbf{A_{-q} q})/q^2 \right\}. \tag{A.2}$$

We see that (A.2) agrees with expression (1) for $\varphi_0 = N_s e^2/2mc^2$; that is, a Bose gas in a state of condensation possesses anomalous diamagnetism[5-7]

[1] H. Welker, Z. Physik **114**, 525 (1939); Physik. Z. **44**, 134 (1943).

[2] M. Schafroth, Helv. Phys. Acta 24, 645 (1951).

[3] M. Schafroth, Nuovo cimento **9**, 291 (1952).

[4] A. Akhiezer and V. Berestetskii, *Quantum Electrodynamics* (1953).

[5] V. Ginzburg, Usp. fiz nauk **48**, 25 (1952).

[6] B. Geilikman, *Statistical Theory of Phase Transformations* (1954), p. 104.

[7] M. Schafroth, Phys. Rev. **96**, 1149 (1954); **100**, 463 (1955).

Translated by W. F. Brown Jr.
242

Paramagnetic Resonance and Polarization of Nuclei in Metals*

M. IA. AZBEL', V. I. GERASIMENKO AND I. M. LIFSHITZ
Physico-Technical Institute, Academy of Sciences, Ukrainian SSR

(Submitted to JETP editor July 14, 1956)
J. Exptl. Theoret. Phys. (U.S.S.R.) 32, 1212-1225 (May, 1957)

A theory of paramagnetic resonances in metals is constructed, based on the simultaneous solution of Maxwell's equations and the kinetic equation for the density operator. The resultant nuclear polarization is determined. It is shown that this polarization varies very slowly with depth, decreasing exponentially up to depths of 10^{-3} to 1 cm, which is the mean distance traversed by an electron between collisions involving spin reversal. It is found that paramagnetic resonance brings about selective transparency of metallic films.

1. STATEMENT OF THE PROBLEM. A COMPLETE SET OF EQUATIONS

AS IS WELL KNOWN[1], paramagnetic resonance of of the conduction electrons takes place in metals placed in a constant magnetic field H_0 and a variable electromagnetic field of frequency $\omega = \Omega_0 \equiv 2\mu H_0/\hbar$ (μ is the magnetic moment of the electron).

As Overhauser has shown[2], this resonance is accompanied by polarization of the nuclei of the metal; in this case such polarization takes place as if the nuclei possessed an effective magnetic moment μ_{eff}, equal to

$$\mu_{\text{eff}} = \mu_{\text{nu}} + \mu\alpha T_{\text{ff}} / (1 + \alpha T_{\text{ff}}) \qquad (1)$$

(μ_{nu} true magnetic moment of the nucleus; T_{ff} is the time of free flight of the electrons between collisions involving spin reversal; $a = (4\mu^2 H_1^2/\hbar^2) T_{\text{ff}}$ is the probability of spin reversal of an electron per unit time in a variable magnetic field $2H_1 \cos \omega t$). However, it is easily seen that Eq. (1) is applicable only for very thin metallic samples, the thickness d of which is of the same order as, or small in comparison with, the thickness of the skin layer: 10^{-4} to 10^{-5} cm. In fact, the resonance probability of spin reversal per unit time can be introduced only when the electron is found in an almost homogenous field for a time interval significantly exceeding the period of the field. In the case of a large sample ($d \gg \delta$), this condition is satisfied for $\delta/v \gg 2\pi/\omega$, which corresponds to the frequencies

$$\omega \gg (2\pi v / c) \sqrt{2\pi\sigma / t_0} \sim 10^{13} \text{ sec}^{-1}$$

and in a magnetic field $H_0 = \hbar\omega/2\mu \gg 10^6$ Oe, which is practically unobtainable at the present time. Therefore, the polarization of nuclei by the Overhauser method takes place only in small particles of micron diameter, in which the electrons always move in a practically homogenous field[3].

At the same time, it can be shown that the Overhauser method permits polarization of the nuclei in layers whose thickness is tens and hundreds of times greater than that of the skin layer. In accord with Ref. 2, the degree of polarization P of the nuclei is determined only by the relative depolarization of the electrons along the direction x of the constant magnetic field:

$$P = \frac{1}{I}\left\{\left(I + \frac{1}{2}\right)\coth\left(I + \frac{1}{2}\right)\bar{w}_z - \frac{1}{2}\coth\frac{1}{2}\bar{w}_z\right\}; \quad \bar{w}_z = \frac{\chi H_0 - M_z}{\chi H_0}, \qquad (1a)$$

where M is the spin magnetic moment of the electrons, I = nuclear spin. Polarization of the electron at a given point is determined by all the values of the magnetic field H_1 which it experiences along the path (up to the given point) from the previous collision involving spin reversal. Therefore, the magnetic moment at the given point is connected with the values of the magnetic field at all points within distances of the order of δ_{eff} passed by the electron between two successive collisions with spin reversal. Since the time T_{ff} between such collisions is much greater than the usual times of free flight t_0 of the electron, the diffusion length is $\delta_{\text{eff}} \approx v\sqrt{t_0 T_{\text{ff}}/3} \sim 10^{-3} - 1$ cm (v = velocity of the electron). Consequently, beginning with the low frequencies $\omega \gtrsim c^2/2\pi\sigma\delta_{\text{eff}}^2$, when $\delta_{\text{eff}} > \delta$ (for

*A preliminary note on this research has already been published[10].

$t_0 \sim 10^{-11}$ sec and $T_{ff} \sim 10^{-6}$ sec, $\omega \gtrsim 10^3$ sec^{-1}), a peculiar "anomalous skin effect" for the magnetic moment takes place; the coupling between the magnetic moment M and the variable magnetic field H_1 is an integral, in which the integration is carried out over a region with radius of the order δ_{eff}. This leads to a slow change in the magnetic moment with depth; the "depth of skin layer" for the magnetic moment is equal to δ_{eff}.

There then follow two important physical consequences:

1) Polarization of nuclei in the metal can take place in layers of thickness of the order $\delta_{eff} \sim 10^{-3}$ to 1 cm. This gives the possibility of obtaining rather thick polarized nuclear targets*.

2) The slow attenuation of the magnetic moment leads, in accord with Maxwell's equations, to the presence in E and H_1 of small, but slowly vanishing parts. In the case of a film of thickness $d \gg \delta$, just this part will determine the transmission coefficient for electromagnetic waves through the film in the vicinity of resonance. Consequently, for paramagnetic resonance, not only resonance absorption appears, but also resonance transmission of the film, in which the transmission coefficient can increase by many orders of magnitude. Thus, for low temperatures, the transmission coefficient of the wave through a film of about 0.1 mm thickness (at resonance) can have the order 10^{-9} to 10^{-13}, while away from resonance, it has the order of 10^{-40} to 10^{-50}. (We note that such a phenomenon occurs at all temperatures.)

The present research was also devoted to the determination of the degree of polarization of nuclei in metals and the transmission coefficient of metallic films with account of the spin diffusion†.

This problem is solved by use of the Maxwell equations

$$\operatorname{curl} \mathbf{E} = -\frac{1}{c}\frac{\partial \mathbf{B}}{\partial t}; \qquad \operatorname{curl} \mathbf{H} = \frac{4\pi}{c}\mathbf{j}; \quad \mathbf{B} = \mathbf{H}_1 + 4\pi\mathbf{M} \tag{2}$$

and the Boltzmann equation for the density operator of the electrons*:

$$\frac{\partial \hat{f}}{\partial t} + \mathbf{v}\frac{\partial \hat{f}}{\partial \mathbf{r}} + \frac{\partial \hat{f}}{\partial \mathbf{p}}\left\{e\mathbf{E} + \frac{e}{c}[\mathbf{vB}]\right\} + \frac{i}{\hbar}[\hat{\mathcal{H}}, \hat{f}] + \left(\frac{\partial \hat{f}}{\partial t}\right)_{col} = 0, \tag{3}$$

$$\hat{\mathcal{H}} = \mu\hat{\sigma}\mathbf{B}; \quad \mathbf{B} = \mathbf{B}_0 + \mathbf{B}_1(\mathbf{r}, t); \quad \mathbf{v} = \nabla_{\mathbf{p}}\varepsilon(\mathbf{p}).$$

Here ε, p and v are the energy, quasi-momentum and velocity of the electrons; $\hat{\sigma}$ is the spin operator:

$$\hat{\sigma}_x = \begin{pmatrix} 0 & 1 \\ 1 & 0 \end{pmatrix}, \quad \hat{\sigma}_y = \begin{pmatrix} 0 & -i \\ i & 0 \end{pmatrix}, \quad \hat{\sigma}_z = \begin{pmatrix} 1 & 0 \\ 0 & -1 \end{pmatrix},$$

the z-axis is chosen along the direction $\mathbf{H}_0$; $(\partial\hat{f}/\partial t)_{col}$ is the collision integral for the electrons.

It remains to write down the boundary condition for $\hat{f}$. Describing the reflection of the electrons from the surface $\zeta = 0$ semi-phenomenologically[6], and considering that the electron spin does not change in collisions with the surface, we have (for $\zeta = 0$†):

$$\hat{f}(v_\zeta) = (1 - q)\,\bar{\hat{f}} + q\hat{f}(-v_\zeta), \quad v_\zeta > 0 \tag{4}$$

(the bar denotes averaging over the momenta).

Solution of the Boltzmann equation permits us to determine the relation between the current density j and the direction of the electric field E, and between the spin magnetic moment M and the direction of the variable magnetic field $\mathbf{H}_1$:

$$\mathbf{j} = \frac{e}{h^3}\int \mathbf{v}\,\mathrm{Sp}\hat{f}\,d\tau_{\mathbf{p}}; \qquad \mathbf{M} = \frac{\mu}{h^3}\int \mathrm{Sp}(\hat{\sigma}\hat{f})d\tau_{\mathbf{p}}; \quad d\tau_{\mathbf{p}} = dp_x\,dp_y\,dp_z. \tag{5}$$

Equations (2), (3) and (5) form the complete system of equations for the problem under consideration.

2. REDUCTION OF THE EQUATION TO CANONICAL FORM

We set

$$\hat{f} = \hat{f}^0 + \hat{f}', \tag{6}$$

where $\hat{f}^0$ is a function which at each given moment corresponds to the equilibrium state for E = 0.

*As Rozentsveig and Fogel' noted, nuclei of adsorbed hydrogen can be polarized in this manner.

†We note that determination of the power absorbed in paramagnetic resonance in a metal in the case of a constant magnetic field, perpendicular to the surface of the metal, and a weak electromagnetic field (when saturation of resonance is absent), was carried out by Dyson[4] on the basis of a study of the diffusion of electrons. The polarization of nuclei and selective transparency of a film was not considered at all by Dyson.

*After completion of this research, a paper appeared[5], in which the same equation was used.

† In Ref. 5, this condition was written for $q = 1$. Evidently, $q \approx 0$ almost always.

Evidently, in a system of coordinates in which the direction of the magnetic induction $\mathbf{B}$ coincides with the axis ξ, $\hat{f}^0$ has the form

$$\hat{f}^0 = \begin{pmatrix} f_0(\varepsilon_0 - \mu B) & 0 \\ 0 & f_0(\varepsilon_0 + \mu B) \end{pmatrix} = \frac{1}{2}\left[f_0(\varepsilon_0 - \mu B) + f_0(\varepsilon_0 + \mu B)\right]\hat{I} + \\ + \frac{1}{2}\hat{\sigma}_\xi [f_0(\varepsilon_0 - \mu B) - f_0(\varepsilon_0 + \mu B)] = \frac{1}{2}[f_0(\varepsilon_0 + \mu B) + f_0(\varepsilon_0 - \mu B)]\hat{I} \\ - \frac{1}{2}[f_0(\varepsilon_0 + \mu B) - f_0(\varepsilon_0 - \mu B)]\mu \mathbf{H}\hat{\boldsymbol{\sigma}} = f_1^0 \hat{I} + \mathbf{f}^0 \hat{\boldsymbol{\sigma}}. \tag{7}$$

For $\mu H \ll kT$,

$$\hat{f}^0 = f_0(\varepsilon)\hat{I} - \mu \hat{\boldsymbol{\sigma}}\mathbf{B} f_0'(\varepsilon), \quad f_0(x) = \{e^{(x-\varepsilon_0)/kT} + 1\}^{-1}. \tag{8}$$

Here f_0 is the equilibrium Fermi function, $\hat{I}$ is a unit operator.

Taking as variables ζ – the direction of the normal to the surface of the metal (which does not coincide, generally speaking, with the direction z of the constant magnetic field), the energy ε, the projection of the momentum p_z, and the dimensionless time $\tau = (1/2\pi m_0)\partial S_\tau / \partial \varepsilon$ of rotation of the electron about the orbit (S_τ is the area of the sector in the intersection of the plane $\mathcal{E}(\mathbf{p}) = \varepsilon$ with the plane $p_z = \text{const}$ – see Ref. 8), we get for the zeroth approximation in E,

$$\frac{\partial \hat{f}'}{\partial t} + \frac{\partial \hat{f}'}{\partial \zeta} v_\zeta + \frac{1}{T_0}\frac{\partial \hat{f}'}{\partial \tau} + \frac{i}{\hbar}[\mu \hat{\boldsymbol{\sigma}}\mathbf{B}, \hat{f}'] \\ + \left(\frac{\partial \hat{f}'}{\partial t}\right)_{\text{col}} = -\frac{\partial \hat{f}^0}{\partial t} - \frac{\partial \hat{f}^0}{\partial \varepsilon} e\mathbf{v}\mathbf{E}. \tag{9}$$

(Here we have assumed that $(\partial \hat{f}^0/\partial t)_{\text{col}} = 0$ and that $[\hat{f}, \hat{\mathcal{H}}] = 0$, where $\hat{\mathcal{H}}$ is the Hamiltonian operator for $\mathbf{E} = 0$). The term $(i/\hbar)[\mu \hat{\boldsymbol{\sigma}}\mathbf{B}, \hat{f}']$ in this equation describes the change in the operator of the electron density in the magnetic field, connected with the presence of electron spins. This change is brought about for two reasons: first, the variable magnetic field leads to the equalization of the electron densities in states with spins oriented parallel and antiparallel to the constant magnetic field $\mathbf{H}_0$ (see, for example, Ref. 2), and second, in an inhomogeneous magnetic field, forces act on the spin which are proportional to $\partial H_1/\partial \zeta$. The first reason leads to resonance reversal of spins and it itself determines the degree of depolarization of the electrons at resonance. The second reason leads only to "fine tuning" of the electrons according to the direction of the total magnetic induction $\mathbf{B}$ (the latter is accounted for mainly by the form of the operator $\hat{f}^0$). It is natural that in the determination of the depolarization of the electrons and the polarization of the nuclei, it does not have to be considered. (The same is also done in Ref. 10.) In order to demonstrate this fact, we note that

$$\frac{i}{\hbar}[\hat{\boldsymbol{\sigma}}\mathbf{B}, \hat{f}'] = \frac{i}{\hbar}[\hat{\boldsymbol{\sigma}}, \hat{f}']\mathbf{B} + \hat{\boldsymbol{\sigma}}\frac{i}{\hbar}[\mathbf{B}, \hat{f}'],$$

or, in the quasi-classical approximation,

$$\frac{i}{\hbar}[\mu \hat{\boldsymbol{\sigma}}\mathbf{B}, \hat{f}'] = \frac{i}{\hbar}[\hat{\boldsymbol{\sigma}}, \hat{f}']\mathbf{B} - \hat{\boldsymbol{\sigma}}\frac{\partial \boldsymbol{B}}{\partial \zeta}\frac{\partial f'}{\partial p_\zeta}. \tag{10}$$

The first term on the right leads to spin reversal, the second corresponds to the classical force acting on the spin.

We now set

$$\hat{f}' = f_1' \hat{I} + \mathbf{f}' \hat{\boldsymbol{\sigma}}, \quad \hat{f}^0 = f_1^0 \hat{I} + \mathbf{f}^0 \boldsymbol{\sigma}. \tag{11}$$

From (9) and (10) we get, taking into account the commutation law for $\hat{\boldsymbol{\sigma}}$:

$$\frac{\partial f_1'}{\partial t} + \frac{\partial f_1'}{\partial \zeta} v_\zeta + \frac{1}{T_0}\frac{\partial f_1'}{\partial \tau} + \left(\frac{\partial f_1'}{\partial t}\right)_{\text{col}} \\ - \mu \frac{\partial \mathbf{B}}{\partial \zeta}\frac{\partial \mathbf{f}'}{\partial p_\zeta} = -\frac{\partial f_1^0}{\partial t} - \frac{\partial f_1^0}{\partial \varepsilon} e\,\mathbf{v}\,\mathbf{E},$$

$$\frac{\partial \mathbf{f}'}{\partial t} + \frac{\partial \mathbf{f}'}{\partial \zeta} v_\zeta + \frac{1}{T_0}\frac{\partial \mathbf{f}'}{\partial \tau} + [\mathbf{f}'\boldsymbol{\Omega}] + \left(\frac{\partial \mathbf{f}'}{\partial t}\right)_{\text{col}} \\ - \mu \frac{\partial \mathbf{B}}{\partial \zeta}\frac{\partial f_1'}{\partial p_\zeta} + i\mu\left[\frac{\partial \mathbf{B}}{\partial \zeta}, \frac{\partial \mathbf{f}'}{\partial p_\zeta}\right] \\ = -\frac{\partial \mathbf{f}^0}{\partial t} - \frac{\partial \mathbf{f}^0}{\partial \varepsilon} e\,\mathbf{v}\mathbf{E}, \quad \boldsymbol{\Omega} = 2\mu\,\mathbf{B}/\hbar.$$

We can show, using direct estimates, that we can neglect all terms pertaining to the second component in (10). Here the equations take the form

$$\frac{\partial f_1'}{\partial t}+\frac{\partial f_1'}{\partial \zeta}v_\zeta+\frac{1}{T_0}\frac{\partial f_1'}{\partial \tau}+\left(\frac{\partial f_1'}{\partial t}\right)_{col}=-\frac{\partial f_0}{\partial \varepsilon}e\mathbf{vE},$$

$$\frac{\partial \mathbf{f}'}{\partial t}+\frac{\partial \mathbf{f}'}{\partial \zeta}v_\zeta+\frac{1}{T_0}\frac{\partial \mathbf{f}'}{\partial \tau}+[\mathbf{f}'\Omega]+\left(\frac{\partial \mathbf{f}'}{\partial t}\right)_{col}=-\frac{\partial \mathbf{f}^0}{\partial t}. \quad (12)$$

The first expression permits us to determine, in accord with (5), the relation between the current density j and the intensity of the electric field E:

$$\mathbf{j}=2eh^{-3}\int \mathbf{v}f_1' d\tau_p.$$

This connection was found in Refs. 7 and 9. We are interested only in the function f' which makes possible the determination of the spin moment M:

$$\mathbf{M}=\chi\mathbf{B}+2\mu h^{-3}\int \mathbf{f}'d\tau_p. \quad (13)$$

For the solution of Eq. (12) we must write out the concrete form of the collision integral. The vector f' is changed in collisions both as a consequence of the redistribution of electrons in energy and momentum (with relaxation times t_0^ε and t_0^p), and as a consequence of the redistribution of their spins (with relaxation time T_{ff}). In this case, as has already been pointed out $T_{ff}\gg t_0$, so that the two types of collisions can be considered separately:

$$\left(\frac{\partial \mathbf{f}'}{\partial t}\right)_{col}=\left(\frac{\partial \mathbf{f}'}{\partial t}\right)_{t_0}+\left(\frac{\partial \mathbf{f}'}{\partial t}\right)_{T_{ff}}.$$

Without taking a specific form for these operators, let us write them out as is usually done, with the aid of the corresponding relaxation times. It is obvious that in a wholly equilibrium state, $f'=0$; therefore,

$$(\partial \mathbf{f}'/\partial t)_{T_{ff}}=\mathbf{f}'/T_{ff}.$$

Let us determine to what equilibrium value f'_{eq} the collisions without spin reversal. Since in such collisions the probability density of finding a given projection of the spin, independent of the values of the energy and momentum, does not change,

$$\int \mathbf{f}'d\tau_p=\int \mathbf{f}'_{eq}(\varepsilon)\,d\tau_p.$$

For simplicity, we shall consider that any change in energy in the collisions can be neglected. Then

$$\mathbf{f}_{eq}=\int \hat{\mathbf{f}}'\frac{ds}{v}\Big/\int\frac{ds}{v}\equiv\bar{\mathbf{f}}';\qquad \left(\frac{\partial \mathbf{f}'}{\partial t}\right)_{t_0}=\frac{\mathbf{f}'-\bar{\mathbf{f}}'}{t_0}.$$

(This is clearly valid either for sufficiently low temperatures, when $t_0^\varepsilon\gg t_0^p$, and the collisions can be regarded as elastic, or in sufficiently weak magnetic fields, in which $\mu H_0\ll kT$.) In the general case,

$$\left(\frac{\partial \mathbf{f}}{\partial t}\right)_{col}=\frac{1}{t_0^p}(\mathbf{f}-\bar{\mathbf{f}})+\frac{1}{t_0^\varepsilon}(\mathbf{f}-\tilde{\mathbf{f}}\chi^0/\tilde{\chi}^0),\ \tilde{\varphi}=\int\varphi\,d\tau_p,$$

$$\chi^0=\tfrac{1}{2}[f_0(\varepsilon-\Delta)-f_0(\varepsilon+\Delta)],\ |\tilde{\mathbf{f}}|=\tilde{\chi}^0.)$$

Thus the problem reduces to the solution of the Maxwell equations (2) with the current density j(E) determined in Refs. 7 and 9, and the magnetic moment

$$\mathbf{M}=\chi\mathbf{B}+2\mu h^{-3}\int \mathbf{f}'d\tau_p,$$

where f' satisfies the equation

$$\frac{\partial \mathbf{f}'}{\partial t}+\frac{\partial \mathbf{f}'}{\partial \zeta}v_\zeta+\frac{1}{T_0}\frac{\partial \mathbf{f}'}{\partial \tau}+[\mathbf{f}'\Omega]+\frac{\mathbf{f}'}{t_0^*}=\frac{\bar{\mathbf{f}}'}{t_0}-\frac{\partial \mathbf{f}^0}{\partial t},\quad \frac{1}{t_0^*}=\frac{1}{t_0}+\frac{1}{T_{eq}}$$

with boundary conditions

$$\mathbf{f}'(v_\zeta)\,|_{\zeta=0}=(1-q)\,\bar{\mathbf{f}}'\,|_{\zeta=0}+q\mathbf{f}'_1(-v_\zeta)\,|_{\zeta=0}.$$

In the case of a half space, evidently $\mathbf{f}'(-v_\zeta<0)=0$ for $\zeta=\infty$; the function f' must be periodic in τ with period $\theta=(\tfrac{1}{2}\pi m_0)\,\partial S/\partial\varepsilon$.

For simplicity, we shall consider that $\mu H/kT\ll 1$, so that $\partial \mathbf{f}^0/\partial t=-\mu f_0'(\varepsilon)\,\partial \mathbf{H}/\partial t$. Let us set $\mathbf{f}'=\mu f_0'(\varepsilon)\,\mathbf{w}'$. Then we get

$$\mathbf{M}=\chi(\mathbf{B}-\bar{\mathbf{w}}'), \quad (14)$$

$$\frac{\partial \mathbf{w}'}{\partial t}+\frac{\partial \mathbf{w}'}{\partial \zeta}v_\zeta+\frac{1}{T_0}\frac{\partial \mathbf{w}'}{\partial \tau}+[\mathbf{w}'\Omega]+\frac{\mathbf{w}'}{t_0^*}=\frac{\bar{\mathbf{w}}'}{t^0}+\frac{\partial \mathbf{B}}{\partial t},$$

$$\frac{1}{t_0^*}=\frac{1}{t_0}+\frac{1}{T_{ff}}. \quad (15)$$

We now introduce the cyclic variables w and w_z:

$$iwH_0=w'_x+iw'_y,\ w'_zB_0=w_z,$$
$$B_1=B_{1x}+iB_{1y},\ M_1=M_{1x}+iM_{1y}. \quad (16)$$

Then Eqs. (14) and (15) take the form

$$M_z = \chi B_0 (1 - \bar{w}_z), \quad M = -i\chi B_0 \bar{w},$$
$$\left(\frac{\partial}{\partial t} + \hat{D}\right) w_z = \bar{w}_z / t_0 + \mathrm{Re}\,(w\,\Omega_1^*),$$
$$\left(\frac{\partial}{\partial t} + \hat{D} - i\,\Omega_0\right) w = \frac{\bar{w}}{t_0} - i\,\frac{1}{B_0}\frac{\partial B_1}{\partial t} - \frac{2\mu}{\hbar} B_1 w_z, \tag{17}$$
$$\hat{D} = \frac{\partial}{\partial \zeta}\, v_\zeta + \frac{1}{T_0}\frac{\partial}{\partial \tau} + \frac{1}{t_0^*}, \quad \Omega = \frac{2\mu \mathbf{H}}{\hbar}.$$

We consider only that component Ω, which yields a resonance, *i.e.*, $\Omega_1 = \Omega_1 e^{i\omega t}$ (we shall denote the amplitude by the same letter as the function). Then the solution has the form: $w = we^{i\omega t}$; w_z does not depend on the time. The equations for the determination of $w(\zeta)$ and $w_z(\zeta)$ close to resonance, at $\omega = \Omega_0$, are written

$$\{\hat{D} + i\,(\omega - \Omega_0)\}\, w = \bar{w}/t_0 + \Omega_1 (1 - w_z),$$
$$\hat{D}\, w_z = \bar{w}_z / t_0 + \mathrm{Re}\,(\Omega_1^* w). \tag{18}$$

Thus the problem reduces to the solution of the system of Eq. (18) and the Maxwell equations. Evidently the system of these equations is non-linear in general, because of the nonlinearity of the coupling of the magnetic moment M with the field $B_1 = \hbar\,\Omega_1/2\mu$ [this coupling is also determined by the equations (18)].

Chief interest is presented by the case of sufficiently large fields B_1, in which the electron gas close to the metallic surface is almost completely depolarized: $w_z \approx 1$, but at sufficiently great depths, the depolarization is naturally small: $w_z \ll 1$. In this case the usual linearization is not possible. It would appear that an essential nonlinearity can take place only in the region close to resonance. Let us investigate this region in somewhat more detail. First of all, we note that the solution of the first of Eqs. (18):

$$\frac{\partial w}{\partial \zeta} v_\zeta + \frac{1}{T_0}\frac{\partial w}{\partial \tau} + \left\{\frac{1}{t_0} + \frac{1}{T_{\mathrm{ff}}} + i\,(\omega - \Omega_0)\right\} w = \frac{\bar{w}}{t_0} + \Omega_1 (1 - w_z) \tag{19}$$

has a sharply resonant character at $\omega T_{\mathrm{ff}} \gg 1$, ωt_0, *independently* of the relation between ω and $1/t_0$ (in the particular case when $\omega t_0 \ll 1$). This is connected with the fact that, at $\omega = \Omega_0$, $1/T_{\mathrm{ff}} = 0$ is an *eigenvalue* of Eq. (19), since in this case, the homogeneous equation

$$\frac{\partial w}{\partial \zeta} v_\zeta + \frac{1}{T_0}\frac{\partial w}{\partial \tau} + \frac{w}{t_0} - \frac{\bar{w}}{t_0} = 0$$

has the nontrivial solution $w = w(\varepsilon)$, which is independent of the coordinates and of τ.

In correspondence with this, the solutions of Eqs. (18) near resonance (for $|\omega - \Omega_0| \lesssim 1/T_{\mathrm{ff}} \ll 1/t_0$) will, in the first place, have a significantly larger $\Omega_1 t_0$ [since for $\omega = \Omega_0$ and $T_{\mathrm{ff}} \to \infty$, w generally diverges as $(t_0/T_{\mathrm{ff}})^{-1/2}$], meaning that it will differ only slightly from $\bar{w}$ and $\bar{w}_z$ (since $w - \bar{w} \sim \Omega_1 t_0$); in the second place, they are more slowly varying with distance than Ω_1 (the reason for this is discussed in Sec. 1), and in the third place they depend on the behavior of Ω_1 only at small distances [since Eq. (19) has a smoothly varying solution even for Ω_1 which is a δ-function in the coordinates]. Therefore,

$$\Omega_1 (1 - w_z(\zeta)) \approx \Omega_1 (1 - \bar{w}_z(\zeta)) \approx \Omega_1 (1 - \bar{w}_z(0));$$
$$\Omega_1^* w(\zeta) \approx \Omega_1^* \bar{w}(\zeta) \approx \Omega_1^* \bar{w}(0).$$

At large distances, Ω_1 changes as slowly as $\bar{w}$ and $\bar{w}_z$; however, as was pointed out, the value of the right side at such distances has no effect on the form of $\bar{w}$ and $\bar{w}_z$. Of course, all these assertions can be verified.

Thus, Eq. (18) near resonance can be written in the form

$$\{\hat{D} + i\,(\omega - \Omega_0)\}\, w = \bar{w}/t_0 + \Omega_1 [1 - \bar{w}_z(0)], \tag{20}$$

$$\hat{D} w_z = \bar{w}_z / t_0 + \mathrm{Re}\,[\Omega_1^* \bar{w}(0)]. \tag{21}$$

We set

$$w = [1 - \bar{w}_z(0)]\, u, \quad w_z = \mathrm{Re}\,[\bar{w}(0)\, u_z]. \tag{22}$$

Then Eqs. (20) take the form

$$\{\hat{D} + i\,(w - \Omega_0)\}\, u = \bar{u}/t_0 + \Omega_1,$$
$$u_z = u^*|_{\omega = \Omega_0} \tag{23}$$

$$u(0, v_\zeta) = (1 - q)\,\bar{u}(0) + q u(0, -v_\zeta), \quad v_\zeta > 0, \tag{24}$$

where

$$w_z(\zeta) = \frac{\mathrm{Re}\,[\bar{u}(0)\, u_z(\zeta)]}{1 + \mathrm{Re}\,[\bar{u}(0)\,\bar{u}_z(0)]},$$
$$w(\zeta) = \frac{u(\zeta)}{1 + \mathrm{Re}\,[\bar{u}(0)\,\bar{u}_z(0)]}. \tag{25}$$

The magnetization M_z and M and the polarization of the nuclei P are determined by Eqs. (17) and (1a), as before.

3. SOLUTION OF THE EQUATIONS FOR THE BULK METAL

a) *Special case*

Let us consider the simplest case (in mathematical behavior) of a quadratic dispersion $\varepsilon = p^2/2m^*$ (m^* = effective mass), a field H_0 perpendicular to the surface of the metal (here the z and ζ axes coincide) and specular reflection of the electrons from the surface, *i.e.*, $q = 1$. (We note that the quantity q does not depend on the qualitative results.) Then Eq. (23) takes the form (u independent of τ):

$$v_z \frac{\partial u}{\partial z} + \frac{u}{t} = \frac{\bar{u}}{t_0} + \Omega_1, \qquad \frac{1}{t} = \frac{1}{t_0} + \frac{1}{T_{\text{ff}}} + i(\omega - \Omega_0). \tag{26}$$

The boundary conditions are

$$u(0, v_z) = u(0, -v_z), \quad u(\infty, -v_z) = 0, \quad v_z > 0.$$

Finding the solution of Eq. (26), and averaging it over the Fermi surface, we get an integral equation for $\bar{u}$:

$$\bar{u}(z) = \int_{-\infty}^{\infty} R(|z-\zeta|) \left\{ \frac{t}{t_0} \bar{u}(\zeta) + t\,\Omega_1(\zeta) \right\} d\zeta,$$

$$R(|z-\zeta|) = \frac{1}{2l} \int_1^{\infty} \exp\left\{ -\frac{|z-\zeta|}{l} x \right\} \frac{dx}{x}, \tag{27}$$

$$l = v_0 t, \quad \Omega_1(-\zeta) = \Omega_1(\zeta).$$

[We note that for $\Omega_1 = 0$ and $t/t_0 = 1$, $\bar{u} = \text{const}$ is a solution of Eq. (27)]. From (27) we find

$$\bar{u}(z) = \frac{1}{\pi} \int_0^{\infty} \frac{R_k t_0 \Omega_{1k} \cos kz\, dk}{t_0/t - R_k}, \tag{28}$$

$$R_k = \tan^{-1} kl/kl, \quad \Omega_{1k} = 2\int_0^{\infty} \Omega_1(z) \cos kz\, dz.$$

by making use of a Fourier transformation. We note that close to resonance ($|\omega - \Omega_0| \sim 1/T_{\text{ff}}$) the only essential k are those for which $kl \lesssim (t_0/T_{\text{ff}})^{1/2}$. For such kl, $R_k \approx 1 - k^2 l^2/3$ and

$$\bar{u}(z) \approx \frac{1}{\pi} \int_0^{\infty} \frac{t_0 \Omega_{10} \cos kz\, dk}{t_0/T_{\text{ff}} + it_0(\omega - \Omega_0) + k^2 l^2/3}$$

$$= \frac{t_0 \Omega_{10}}{2l} \sqrt{\frac{3}{\varkappa}} \exp\left\{ -\frac{z}{l} \sqrt{3\varkappa} \right\},$$

$$\varkappa = t_0/T_{\text{ff}} + it_0(\omega - \Omega_0).$$

The Maxwell equations (2) for

$$H_1 = H_{1x} + iH_{1y} = H_1 e^{i\omega t};$$

$$E = E_x + iE_y = Ee^{i\omega t}; \quad j = j_x + ij_y = je^{i\omega t}$$

are written in the form

$$dE/dz = -\omega B_1/c; \quad dH_1/dz = -4\pi ij/c.$$

Therefore,

$$\Omega_{10} = 2\int_0^{\infty} \Omega_1(z)\, dz = \frac{4\mu c}{\hbar \omega} E(0),$$

where $E(0)$ is the field at the surface of the metal. Thus, close to resonance,

$$\bar{u}(z) = \frac{3cE(0)\,\delta_{\text{eff}}}{vB_0 l} e^{-z/\delta_{\text{eff}}};$$

$$\delta_{\text{eff}} = v \sqrt{\frac{t_0 T_{\text{ff}}}{3(1 + i(\omega - \Omega_0) T_{\text{ff}})}}. \tag{29}$$

It is seen from this equation that the width of the resonance line is determined only by the quantity T_{ff}: $|\omega - \Omega_0| \sim 1/T_{\text{ff}}$ which was first shown by Dyson[4].

For the magnetization, substituting the value of $\bar{u}(z)$ in Eq. (17), we get, at resonance,

$$M_z = \chi B_0 \left\{ 1 - \frac{|\alpha|^2}{1 + |\alpha|^2} e^{-z/\delta_{\text{eff}}} \right\},$$

$$M = M_x + iM_y = -i\chi B_0 \frac{\alpha}{1 + |\alpha|^2} e^{-z/\delta_{\text{eff}}},$$

where

$$\alpha = \frac{3c\{E_x(0) + iE_y(0)\}\,\delta_{\text{eff}}}{B_0 v_0 l}.$$

We note that for sufficiently weak field B_1, when saturation is absent, *i.e.*, $|\alpha| \ll 1$, the equations for M_x and M_y undergo (with accuracy up to an exponential factor) a transition to the Dyson formula[4], where we must set $\nu = \omega$.

Thus, we have shown that $\bar{u}(z)$ actually vanishes at the depth $\delta_{\text{eff}} \gg \delta$. Moreover, u and $\bar{u} \gg \Omega_1 t_0$, but $u - \bar{u} \sim \Omega_1 t_0$, *i.e.*, $u - \bar{u} \ll \bar{u}$. Thus the assumptions of the preceding section are valid.

We note that $H_1(z)$ can be represented qualitatively in the form of two parts: a large, rapidly attenuating part, and a small, slowly attenuating part:

$$H_1(z) \sim H_1(0)\, e^{-z/\delta - 4\pi i \chi H_0 \alpha e^{-z/\delta_{\text{eff}}}}.$$

b) *General case.*

Let us find the quantities of interest to use for arbitrary assumptions on the dispersion law $\varepsilon(\mathbf{p})$ and for arbitrary magnitude and direction of the constant field $\mathbf{H}_0$. For simplicity, we consider only the case of resonance. The reflection of the electrons from the surface we shall consider diffuse ($q = 0$) which is practically always the case.

As was shown, the problem reduced to finding a solution of the equation

$$v_\zeta \frac{\partial u}{\partial \zeta} + \frac{1}{T_0}\frac{\partial u}{\partial \tau} + \frac{u}{t_0^*} = \frac{\bar{u}}{t_0} + \Omega_1 \qquad (30)$$

which is periodic in τ with the boundary conditions:

$$u(0, \mathbf{vn}) = \bar{u}(0); \quad u(\infty, -\mathbf{vn}) = 0, \quad \mathbf{vn} > 0. \qquad (31)$$

We introduce

$$\xi = \zeta/r_0, \quad \gamma^* = T_0/t_0^*, \quad \gamma = T_0/t_0,$$

$$v_\zeta/v_0 = V_\zeta, \quad r_0 = v_0 T_0,$$

v_0 = characteristic velocity on the Fermi surface. Then Eq. (30) is written

$$\frac{\partial u}{\partial \xi} + \hat{L}u = \frac{\gamma}{V_\zeta}(\bar{u} + t_0\Omega_1) \equiv \frac{\gamma}{V_\zeta}\psi;$$

$$\hat{L} = \frac{1}{V_\zeta}\left(\frac{\partial}{\partial \tau} + \gamma^*\right). \qquad (32)$$

For solution of this equation, we apply the method developed in Ref. 9. We replace $\mathbf{p}$ in Eq. (32) by $-\mathbf{p}$; then we obtain for the function $u(-\mathbf{v})$ the equation

$$\partial u(-\mathbf{v})/\partial \xi - \hat{L}u(-\mathbf{v}) = -\gamma\psi/V_\zeta. \qquad (33)$$

Here use is made of the fact that
$\varepsilon(-\mathbf{p}) = \varepsilon(\mathbf{p})$, $\mathbf{v}(-\mathbf{p}) = -\mathbf{v}(\mathbf{p})$,

$$\frac{1}{T_0}\frac{\partial}{\partial \tau}\Big|_{\mathbf{p}} \equiv \left[\mathbf{v}\frac{\partial}{\partial \mathbf{p}}\right] = \frac{1}{T_0}\frac{\partial}{\partial \tau}\Big|_{-\mathbf{p}}.$$

Acting on Eq. (32) with the operator $\partial/\partial\xi - \hat{L}$, and on (33) with the operator $\partial/\partial\xi + \hat{L}$, and reducing them, we obtain an equation for the function $f = \frac{1}{2}[u(\mathbf{v}) + u(-\mathbf{v})]$:

$$(\partial^2/\partial\xi^2 - \hat{L}^2) f = -\gamma\psi\hat{L}/V_\zeta, \qquad (34)$$

where it is taken into account that $\bar{f}(\xi) = \bar{u}(\xi)$.

In this equation, we continue the functions $f(\xi)$ and $\Omega_1(\xi)$ as even functions into the region $\xi < 0$:

$$f(-\xi) = f(\xi), \quad \Omega_1(-\xi) = \Omega_1(\xi)$$

and go over to the Fourier transforms

$$\varphi(k) = \int_{-\infty}^{\infty} f(\xi) e^{ik\xi} d\xi, \quad \Omega_1(k) = \int_{-\infty}^{\infty} \Omega_1(\xi) e^{ik\xi} d\xi,$$

(obviously, $\bar{\varphi}(k) = \bar{u}(k)$):

$$(\hat{L}^2 + k^2)\varphi(k) = \gamma\psi(k)\hat{L}/V_\zeta - 2f'(0). \qquad (35)$$

For determination of $f'(0)$, we note that, from Eqs. (32) and (33),

$$f'(0) = -\tfrac{1}{2}\hat{L}\{u(\mathbf{v}) - u(-\mathbf{v})\}.$$

We now make use of the boundary condition (31). Since, for $V_\zeta > 0$ on the surface of the metal, independently of the other projections of the velocity $u = \bar{u} = \bar{f}$, then, as is easy to see,

$$u(\mathbf{v}) - u(-\mathbf{v}) = \operatorname{sign} V_\zeta \cdot (\bar{f}(0) - f(0)),$$
$$f'(0) = -\hat{L}\operatorname{sign} V_\zeta \cdot (\bar{f}(0) - f(0)).$$

Consequently, Eq. (35) takes the form

$$(\hat{L}^2 + k^2)\varphi(k)$$
$$= (2\hat{L}/V_\zeta)\{\tfrac{1}{2}\gamma\psi(k) + V_\zeta|[\bar{f}(0) - \bar{f}(0)]\},$$
$$\varphi(k) = \{(\hat{L} + ik)^{-1} + (\hat{L} - ik)^{-1}\}$$
$$\times\{\tfrac{1}{2}\gamma\psi(k) + |V_\zeta|[\bar{f}(0) - f(0)]\}\, 1/V_\zeta \equiv g_+ + g_-.$$

Computation of the right side of this expression reduces to finding the periodic solution of the linear equation

$$(\partial/\partial\tau + \gamma^* \pm ikV_\zeta)g_\pm$$
$$= \tfrac{1}{2}\gamma\psi(k) + |V_\zeta|[\bar{f}(0) - f(0)].$$

This solution has the form

$$g_\pm = [\exp(\gamma^*\theta \pm ik\tilde{V}_\zeta) - 1]^{-1}$$
$$\times \int_\tau^{\tau+\theta} \exp\{\gamma^*(\tau' - \tau) \pm ik\int_\tau^{\tau'} V_\zeta\, d\tau''\}\{\tfrac{1}{2}\gamma\psi(k)$$
$$+ |V_\zeta|[\bar{f}(0) - f(0)]\}\, d\tau';$$
$$\tilde{V}_\zeta = \int_0^\theta V_\zeta\, d\tau.$$

Therefore, remembering that $\psi(k) = \bar{u}(k) + t_0\Omega_1(k)$, we get

$$\varphi(k,\tau) = R(k,\tau)\,\bar{u}(k) + R(k,\tau)\,t_0\,\Omega_1(k) + \int_\tau^{\tau+\theta} N(k,\tau,\tau')\,[\bar{f}(0) - f(0)]\,d\tau', \tag{36}$$

where

$$R(k,\tau) = \mathrm{Re}\,\gamma\,[\exp(\gamma^*\theta + ik\tilde{V}_\zeta) - 1]^{-1} \int_\tau^{\tau+\theta} \exp\{\gamma^*(\tau'-\tau) + ik\int_\tau^{\tau'} V_\zeta\,d\tau''\}\,d\tau',$$

$$N(k,\tau,\tau') = 2\mathrm{Re}\,|V_\zeta|\,[\exp(\gamma^*\theta + ik\tilde{V}_\zeta) - 1]^{-1} \exp\{\gamma^*(\tau'-\tau) + ik\int_\tau^{\tau'} V_\zeta d\tau''\}.$$

(We note that although $\bar{f} = f \ll \bar{f}$, $\bar{f} - f \sim t_0\,\Omega_1$. Therefore we cannot neglect this difference.)

For convenience, we introduce

$$\Sigma(k,\tau) = \bar{\varphi}(k,\tau) - \varphi(k,\tau), \qquad \overline{\Sigma(k,\tau)} = 0,$$

$$S(\tau) = \overline{f(0,\tau)} - f(0,\tau) = \lim_{\xi\to 0} \frac{1}{\pi}\int_0^\infty \Sigma(k,\tau)\cdot\cos\xi k\cdot dk = \int_0^\infty \frac{1}{\pi}\Sigma(k,\tau)\,dk, \overline{S} = 0.$$

Then Eq. (36) can be written in the form

$$\Sigma(k,\tau) = [1 - R(k,\tau)]\,\bar{u}(k) - R(k,\tau)\,t_0\,\Omega_1(k) - \int_\tau^{\tau+\theta} N(k,\tau,\tau')\,S(\tau')\,d\tau'. \tag{37}$$

Averaging this equation over the Fermi surface, we find the function $\bar{u}(k)$:

$$\bar{u}(k) = \frac{\overline{R(k,\tau)}\,t_0\Omega_1(k)}{1 - \overline{R(k,\tau)}} + \frac{1}{1-\overline{R(k,\tau)}}\overline{\int_\tau^{\tau+\theta} N(k,\tau,\tau')\,S(\tau')\,d\tau'}. \tag{38}$$

For the determination of $S(\tau)$, we substitute $u(k)$ in Eq. (37) and integrate the latter over k from 0 to ∞. We then obtain the integral equation

$$S(\tau) = \frac{1}{\pi}\int_0^\infty \frac{\overline{R(k,\tau)} - R(k,\tau)}{1-\overline{R(k,\tau)}}\,t_0\Omega_1(k)\,dk$$

$$- \frac{1}{\pi}\int_0^\infty dk \int_\tau^{\tau+\theta} N(k,\tau,\tau')\,S(\tau')\,d\tau'$$

$$+ \frac{1}{\pi}\int_0^\infty \frac{1-R(k,\tau)}{1-\overline{R(k,\tau)}}\,dk \overline{\int_\tau^{\tau+\theta} N(k,\tau,\tau')\,S(\tau')\,d\tau'},$$

wherein we must set $\gamma^* = \gamma$. In a fashion similar to that of Ref. 9, we can solve the resultant equation by the method of successive approximations, and show that $S(\tau) \sim t_0\Omega_1(k)$ and that it has no singularities for any values of τ.

Returning to Eq. (38), we note that for sufficiently small k (such that $kl \ll 1$)

$$\overline{R(k,\tau)} = t_0^*/t_0 - l^2k^2,$$

where

$$l^2 = (\gamma/\vartheta\int dp_z)\int \frac{dp_z}{(e^{\gamma^*\theta}-1)^3}\int_0^\theta d\tau\int_0^\theta e^{\gamma^*\tau'}\varphi(\tau,\tau')\,d\tau',$$

$$\varphi(\tau,\tau') = e^{\gamma^*\theta}(e^{\gamma^*\theta}+1)\,\tilde{V}_\zeta^2$$

$$- 2\int_\tau^{\tau+\tau'} V_\zeta d\tau'' e^{\gamma^*\theta}(e^{\gamma^*\theta}-1)\,\tilde{V}_\zeta$$

$$+ \Big(\int_\tau^{\tau+\tau'} V_\zeta d\tau''\Big)^2 (e^{\gamma^*\theta}-1)^2.$$

It is easy to see that in weak fields, $H_0\,(\gamma \gg 1)\,l \sim 1/\gamma$. For strong fields $H_0\,(\gamma \ll 1)$ two cases are possible:

1. If the field H_0 forms an angle with the surface $\varphi \gtrsim \gamma$ (in this case $\tilde{V}_\zeta$ is not small), then $\varphi(\tau,\tau') \approx 2\tilde{V}_\zeta^2$ and, as before, $l \sim 1/\gamma$.

2. If the field H_0 forms and angle with the surface $\varphi \lesssim \gamma$ (in this case $\tilde{V}_\zeta \approx 0$), then $l \sim 1$.

As in case (a), we have

$$\bar{u}(\xi) = \frac{1}{\pi}\left\{t_0\Omega_1(0) + \int_{\tau}^{\tau+0} N(0,\tau,\tau')\,S(\tau')\,d\tau'\right\} \int_0^{\infty} \frac{\cos k\xi \cdot dk}{t_0/T_{\text{ff}} + l^2k^2}.$$

It follows from the Maxwell equations that $\Omega_1(0) = (4\mu c/\hbar\omega)E(0)$.

Taking it into account that $S(\tau) \sim t_0\Omega_1(0)$, we get

$$\bar{u}(\zeta) = A\frac{ct_0E(0)}{B_0r_0l}\sqrt{\frac{T_{\text{ff}}}{t_0}}\,e^{-\zeta/\delta_{\text{eff}}}, \quad \delta_{\text{eff}} = lr_0\sqrt{T_{\text{ff}}/t_0}, \quad A \sim 1, \quad E(0) = (cZ/4\pi)H_1(0), \tag{39}$$

Z is the surface impedance which was found in Ref. 7.

The exact value of l depends on the dispersion law and the direction of the field H_0. Thus, for quadratic dispersion and a constant field perpendicular to the surface of the metal, $l = 1/\gamma\sqrt{3}$, and we again obtain Eq. (29).

Making use of Eqs. (25) and (1a), we obtain the polarization of the nuclei in the bulk metal at resonance:

$$P = \frac{1}{I}\left\{\left(I+\frac{1}{2}\right)\coth\left(I+\frac{1}{2}\right)\frac{|\alpha|^2 e^{-\zeta/\delta_{\text{eff}}}}{1+|\alpha|^2}\,\frac{\mu H_0}{kT} - \frac{1}{2}\coth\frac{1}{2}\,\frac{|\alpha|^2 e^{-\zeta/\delta_{\text{eff}}}}{1+|\alpha|^2}\,\frac{\mu H_0}{kT}\right\},$$

$$\alpha = A\,(ct_0E(0)/H_0r_0l)\sqrt{T_{\text{ff}}/t_0}.$$

Thus, in the bulk metal, a substantial polarization of the nuclei takes place to a depth of $\delta_{\text{eff}} \sim v_0T_0(T_{\text{ff}}/t_0)^{1/2}$ in the case of a strong field H_0 parallel to the surface, and to a depth $\delta_{\text{eff}} \sim v_0\,t_0\,(T_{\text{ff}}/t_0)^{1/2}$ for all other cases.

4. SELECTIVE TRANSPARENCY OF A FILM

In order to find the transmission coefficient of an electromagnetic wave through a film of thickness d, it is necessary to solve Eq. (23) with the two boundary conditions (24).

For simplicity we consider the case of a square law of dispersion $\varepsilon = p^2/2m^*$, a field H_0 perpendicular to the surface, and mirror reflection of electrons from the surface: $q = 1$ (inasmuch as the character of the dispersion law and the boundary conditions affect the results only quantitatively, as we have already seen).

In this case, Eq. (23) takes the form (since u obviously does not depend on τ)

$$v_z\partial u/\partial z + u/t_0^* = \bar{u}/t_0 + \Omega_1. \tag{40}$$

The boundary conditions are written

$$u(0,\ v_z) = u(0,\ -v_z),\ u(d,\ -v_z) = u(d,\ v_z),\ v_z > 0.$$

Finding $u(z)$ and averaging it over the Fermi surface, we obtain the integral equation for $\bar{u}(z)$:

$$\bar{u}(z) = \frac{1}{2v_0}\int_{-k}^{k} R(|t-\zeta|)\,[\bar{u}(\zeta) + t_0\Omega_1(\zeta)]\,d\zeta, \tag{41}$$

$$k = \frac{d}{v_0t_0^*}, \qquad R(t) = \frac{t_0^*}{t_0}\int_1^{\infty}\frac{\cosh(k-t)x\,dx}{\sinh kx\quad x}.$$

The function $R(t)$ is even and periodic in the interval $(-2k,\ 2k)$ with period $2k$. Thanks to this, we can solve Eq. (41) by the expansion of all functions in Fourier series (cosines) with period π/k. The solution has the form

$$\bar{u}(z) = \frac{\bar{u}_0}{2} + \sum_{n=1}^{\infty}\bar{u}_n\cos\frac{\pi nz}{k},$$

$$\bar{u}_n = \frac{kt_0R_n\Omega_{1n}}{1-kR_n}, \qquad \Omega_{1n} = \frac{2}{k}\int_0^k \Omega_1(z)\cos\frac{\pi nz}{k}\,dz,$$

$$R_n = \int_0^{\infty} R(t)\cos\frac{\pi nt}{k}\,dt = \frac{t_0^*}{kt_0}\,\frac{\tan^{-1}(\pi n/k)}{\pi n/k}. \tag{42}$$

In resonance, the chief contributions in (42) are clearly made by the $\bar{u}_n$ with small n (so that $\pi n/k \ll 1$). In this case,

$$u_n \approx t_0\Omega_{1n}\Big/\left[\frac{t_0}{T_{\text{ff}}} + \frac{1}{3}\left(\frac{\pi n}{k}\right)^2\right].$$

But in $\Omega_1(z)$ the essential $z \lesssim \delta/v_0t_0$, where $\pi nz/k \lesssim \delta/\delta_{\text{eff}} \ll 1$; therefore,

$$\Omega_{1n} \approx \frac{2}{k}\int_0^k \Omega_1(z)\cos\frac{\pi nz}{k}\,dz \approx \frac{2}{k}\int_0^k \Omega_1(z)\,dz = \Omega_{10}.$$

Thus,

$$u_n \approx t_0\Omega_{10} \Big/ \left[\frac{t_0}{T_{ff}} + {}^1/_3\left(\frac{\pi n}{k}\right)^2\right]$$

$$\bar{u}(z) = \frac{u_0}{2} + \sum_{n=1}^{\infty} u_n \cos\frac{\pi n z}{k} = {}^1/_2\,\Omega_{10} T_{ff}\,\frac{d}{\delta_{eff}}\,\frac{|\cosh[(d-z)/\delta_{eff}]}{\sinh(d/\delta_{eff})}. \tag{43}$$

From Maxwell's equations we get

$$\Omega_{10} = (4\mu c/\hbar\omega)\,[E(0) - E(d)]/d.$$

(We note that for $d \to \infty$ Eq. (43) goes over into Eq. (29).

Of fundamental interest (see below) is the consideration of selective transparency of films for which $\delta \ll d \ll \delta_{eff}$. Here (at resonance),

$$\bar{u}(z) \approx cT_{ff}E(0)/H_0 d.$$

Hence

$$M = -i\chi B_0 \frac{\bar{u}}{1+|\bar{u}|^2} e^{i\omega t} \equiv M_0 e^{i\omega t}.$$

From Maxwell's equations,

$$E' = -\omega B_1/c, \quad H_1' = -4\pi i j/c;$$

since $H_1 = B_1 - 4\pi M$, then

$$E' = -\omega B_1/c, \quad B_1' = -4\pi i j/c,$$

i.e., B_1 in this approximation does not depend on the magnetization and falls off rapidly (at depths of order δ).

Consequently, at a depth $\delta_{eff} \gg z$, $d - z \gg \delta$, we have a homogeneous magnetic field $-4\pi M_0 e^{i\omega t}$ (obviously, this field always has circular polarization). Hence, taking into account the boundary conditions on the surface of the film, we easily obtain the transmission coefficient for electromagnetic waves through the film:

$$K = \left|\frac{H_{1trans}}{H_{1inc}}\right|^2 \approx \left|\frac{\chi T_{ff} c^3 Z^2}{2\pi d\,\{1 + |c^2 Z T_{ff} H_{1inc}/2\pi d H_0|^2\}}\right|^2,$$

where Z is the surface impedance without account of spin polarization.

The unusual form of the equation for K is connected with the specific change of the field in the film as a result of the diffusion of the spin [see Eq. (29a)].

The power of the previous wave W_{trans} will be maximum in that case in which

$$H_{inc}^{opt} = 2\pi d H_0/c^2 T_{ff}|Z|.$$

Here

$$W_{trans}^{max} = \frac{\pi}{16}\left(\frac{\chi\hbar c^2\,|\,Z\,|}{\mu\lambda}\right); \qquad H_{trans}^{max} = \frac{\pi\chi\hbar c^2\,|\,Z\,|}{2\mu\lambda},$$

i.e., both these quantities are independent of the thickness of the film (but $H_{inc}^{opt} \sim d$).

In the general case,

$$W_{trans} = 4W^{max}\{H_{1inc}/H_{1inc}^{opt}\}^2/\{1 + (H_{1inc}/H_{1inc}^{opt})^2\}^{-2};$$

$$H_{1trans} = 2H_{trans}^{max}\,|\,H_{1inc}/H_{1inc}^{opt}\,|\,/[1 + |\,H_{1inc}/H_{1inc}^{opt}\,|^2].$$

5. POLARIZATION OF NUCLEI IN FILMS

We write out the formula for the polarization of nuclei in films* (at resonance):

$$P = \frac{1}{I}\{(I + {}^1/_2)\coth(I + {}^1/_2)\,A - {}^1/_2\coth{}^1/_2\,A\};$$

$$A = \frac{|\alpha|^2}{1+|\alpha|^2}\,\frac{\mu H_0}{kT}\,\frac{\cosh[(d-z)/\delta_{eff}]}{\cosh(d/\delta_{eff})},$$

where

$$\alpha = \frac{cT_{ff}\,[E(0) - E(d)]}{H_0\delta_{eff}}\coth\frac{d}{\delta_{eff}}$$

for arbitrary d. In the case $d < \delta$,

$$\alpha = 4\mu T_{ff} H_1/\hbar,$$

i.e., we get the Overhauser formula. In the case $\delta \ll d \ll \delta_{eff}$:

$$\alpha = cT_{ff}E(0)/H_0 d = c^2 Z T_{ff} H_{inc}/2\pi d H_0.$$

Finally, for $d \gg \delta_{eff}$, we get the formula for the bulk metal:

$$\alpha = cT_{ff}E(0)/H_0\delta_{eff} = c^2 T_{ff} Z H_{inc}/2\pi d H_0.$$

*This formula is correct for $d - z \ll \delta$ since at such a distance from the second surface the polarization is significantly less.

[1] T. W. Griswold, A. F. Kip and C. Kittel, Phys. Rev. 88, 951 (1952); G. Feher and A. F. Kip, Phys. Rev. 95, 1343 (1954); G. Feher and A. F. Kip, Phys. Rev. 98, 337 (1955).

[2] A. W. Overhauser, Phys. Rev. 89, 689 (1953); A. W. Overhauser; Phys. Rev. 92, 411 (1953).

[3] T. R. Carver and C. P. Slichter, Phys. Rev. 92, 212 (1953).

[4] F. J. Dyson, Phys. Rev. 98, 349 (1955).

[5] V. P. Silin, J. Exptl. Theoret. Phys. (U.S.S.R.) 30, 421 (1956); Soviet Phys. JETP. 3, 305 (1956).

[6] K. Fuchs, Proc. Camb. Phil. Soc. 34, 100 (1938).

[7] W. E. H. Reuter, and E. H. Sondheimer, Proc. Roy. Soc. (London) 195A, 336 (1948); M. I. Kaganov and M. Ia. Azbel', Dokl. Akad. Nauk SSSR 102, 49 (1955); M. Ia. Azbel' and M. I. Kaganov, Dokl. Akad. Nauk SSSR 95, 43 (1953).

[8] Lifshitz, Azbel' and Kaganov, J. Exptl. Theoret. Phys. (U.S.S.R.) 30, 220 (1956). Soviet Phys. JETP. 3, 143 (1956).

[9] M. Ia. Azbel' and E. A. Kaner, J. Exptl. Theoret. Phys. (U.S.S.R.) 30, 811 (1956); Soviet Phys. JETP. 3, 772 (1956).

[10] Azbel', Gerasimenko and Lifshitz, J. Exptl. Theoret. Phys. (U.S.S.R.) 31, 357 (1956); Soviet Phys. JETP 4, 276 (1957).

Translated by R. T. Beyer
243

SOVIET PHYSICS JETP VOLUME 5, NUMBER 5 DECEMBER, 1957

Polarization Correlation in Nucleon-Nucleon Scattering

A. G. ZIMIN

(Submitted to JETP editor December 2, 1955)
J. Exptl. Theoret. Phys. (U.S.S.R.) 32, 1226-1232 (May, 1957)

Equations are obtained for the polarization correlation in proton-proton scattering, taking into account four phases: $^1S_0$, $^3P_0$, $^3P_1$, $^3P_2$ and Coulomb interaction. A computation using phases for the isotropic states as obtained from scattering data shows that the Coulomb interaction plays an essential role for energies of 10–30 Mev. Polarization correlation can thus be used to give a more precise determination of the isotropic phases (which do not give rise to polarization), and to estimate other phases in the energy region in which they begin to appear. We also consider the scheme of experiments for measuring the polarization correlation and obtain the combinations of components of the polarization tensor which are measured in the experiments.

1. INTRODUCTION

THE SCATTERING OF PARTICLES with spin is described by the average values of spin operators over the scattered wave. For two particles with spins $\sigma^{(1)}$ and $\sigma^{(2)}$, these operators are:

$$\hat{1},\ \sigma_i^{(1)},\ \sigma_i^{(2)},\ \hat{P}_{ik} = \hat{\sigma}_i^{(1)}\hat{\sigma}_k^{(2)}. \qquad (1)$$

The corresponding average values are: the scattering cross section, the polarization of the first (1) and second (2) particle, and the polarization correlation. This last quantity has a tensor character ($i, k = x, y, z$) and may be called the polarization tensor. If we represent the asymptotic form of the scattered wave as a sum of partial waves (with given j, l, s), these average quantities will be expressed in terms of the corresponding phases. The analysis of scattering of nucleons requires the inclusion of phases with $l > 0$. To determine them unambiguously we must measure all the characteristics of the scattering which relate the phases (cross section, polarization, and polarization correlation). As we shall show in detail later, measurement of the polarization correlation is especially important for determining the phases in the region of isotropic scattering of the protons. It is known that the scattering of protons is isotropic over a wide range of energy (up to 400–450 Mev), and is therefore described by the phases of the isotropic states $^1S_0$ and $^3P_0$. To separate them one might measure polarization in addition to the cross section. However, the isotropic phases give no nuclear polarization, while its Coulomb part is sizeable only at very small an-

gles of scattering [$\lesssim 5-10°$ in the center-of-mass system (c.m.s.) at medium energies], and is therefore difficult to measure. On the other hand, the polarization correlation has a measurable value even when only the singlet phase is included. Consequently its measurement (along with the cross section) makes it possible to determine these phases in the high energy region (> 100 Mev), where the Coulomb interference term, which enables us to separate these phases at low energies, becomes negligibly small.

In the present paper we derive equations for the polarization and polarization correlation in terms of the scattering phases for orbital angular momenta $l = 0$ and 1 ($J = 0, 1, 2$), with allowance for the Coulomb interaction which plays an important part in the scattering of charged particles (protons) for energies < 100 Mev.

2. DERIVATION OF EQUATIONS

The polarization correlation in the scattering of two particles is defined as the average of the operator $\hat{P}_{ik}$ over the scattered wave. It gives the probability that, after scattering, one of the particles (1) is in the spin state σ_i, while the other is in the state σ_k.

In order to express P_{ik} in terms of the scattering phases by means of the method of phase analysis, we consider the asymptotic expression for the wave function in the scattering of a plane wave with spin. We consider the scattering of initially unpolarized particles. In the c.m.s. the system of two particles with spins s_1 and s_2 is described by the plane wave $\chi_m^s \exp(i\mathbf{k}\cdot\mathbf{r})$, which is the product of the spin wave function χ_m^s with total spin $s_1 + s_2, \ldots |s_1 - s_2|$ and projection m on the axis of quantization (taken along the direction of relative motion of the particles), and the plane wave $\exp(i\mathbf{k}\cdot\mathbf{r})$ of the relative motion. Since the particles are not polarized prior to scattering, the scattering of waves with given s and $m = m_s$ proceeds independently, *i.e.*, $\chi_m^s \to \chi_{m'}^{s'}$ where the prime denotes quantities after the scattering. The asymptotic form of the scattered wave is:

$$\psi_{\text{sc}}(s'm') = \frac{e^{ikr}}{r} \sum_{sm} M_{s'm'}^{sm}(\theta, \varphi)\chi_m^s. \qquad (2)$$

After the scattering, the original spin s and its projection m are in general changed and take on some new values s', m'. The quantity which is conserved is the total angular momentum J, which we write schematically as a sum $\mathbf{J} = \mathbf{l} + \mathbf{s}$ of the spin and the orbital angular momentum of the relative motion.

The quantities $M_{s'm'}^{sm}$, whose angular dependence is given by generalized Legendre polynomials, are the amplitudes for transitions between spin states $(sm) \to (s'm')$. There quantities are the generalization of the single amplitude which appears in the scattering of spinless particles and which is given by the Legendre polynomial $P_l(\cos\theta)$. In the scattering of nucleons ($s_1 = s_2 = \frac{1}{2}$) the total spin takes on two values: $s = 0$ (singlet) and $s = 1$ (triplet), so that the scattering matrix M is made up from the 16 amplitudes $M_{s'm'}^{sm}$. It is easy to express all the quantities characterizing the scattering in terms of this matrix:

$$\text{cross section: } \sigma = \text{Sp}(M^+M), \qquad (3)$$

$$\text{polarization: } P_i = \text{Sp}(M^+\sigma_i M)/\text{Sp}(M^+M) \qquad (4)$$

polarization correlation:

$$P_{ik} = \text{Sp}(M^+\hat{\sigma}_i^{(1)}\hat{\sigma}_k^{(2)}M)/\text{Sp}(M^+M). \qquad (5)$$

As usual, Sp denotes the sum of the diagonal matrix elements and M^+ is the Hermitean conjugate.

A knowledge of the phases is necessary for a complete determination of the scattering matrix.

We first treat the scattering of two protons (n–n scattering is obtainable from the general formulas by setting the charge equal to zero). When the Coulomb interaction is included, the scattering matrix can be written as a sum of nuclear and Coulomb terms. The nuclear part is obtained from the asymptotic form of the scattered wave function, where the expansion of the plane wave must be carried out using radial Coulomb functions F and G in place of the free radial functions R_{kl}.

For the case of identical particles, the matrix must be symmetrized appropriately: the coordinate part must be symmetric for singlet states and antisymmetric for triplet states. Taking account of the symmetry, the Coulomb part of the matrix can be written in the form:

$$M_{\text{coul}} = K_{ss'}\delta_{ss'}\delta_{mm'}, \qquad (6)$$

where

$$K_s = -\tfrac{1}{4}\gamma_l\omega\,(s^{-2}e^{-i\alpha} + (-)^s c^{-2}e^{-i\beta})\exp(2i\sigma_0) \qquad (7)$$

is the Coulomb scattering amplitude. We have introduced the symbols

$$\eta_i = e^2/\hbar v, \quad c = \cos\vartheta/2, \quad s = \sin\vartheta/2,$$
$$\alpha = \eta_i \ln s^2, \quad \beta = \eta_i \ln c^2,$$

$\omega = \sqrt{(\gamma+1)/2\gamma^2}$; ω is a relativistic correction for small angles of scattering. In this part of the matrix, the spin variables appear in delta functions since the spin is conserved in a Coulomb field.

For identical particles there are no transitions with change of spin (singlet $\rightleftarrows$ triplet) in the nuclear part of the matrix.

The matrix elements of M are expressed in terms of generalized Legendre polynomials and the phase matrix

$$\overset{J}{S}{}^{sl}_{s'l'} = \exp(2i\overset{J}{\delta}{}^{sl}_{s'l'}),$$

which gives the connection between the incoming and outgoing spin amplitudes $(sl) \to (s'l')$.[1] The matrix S is defined for a given J and parity $P_+ = (--)^J$, $P_- = (-)^{J+1}$. In the case of no spin, the S matrix has one element $S_l = \exp(2i\delta_l)$ for each l. We shall calculate only that part of the matrix which is important for practical purposes, *i.e.*, the part with orbital angular momentum $l = 0$ and 1. Formulae for higher l's can be gotten without any fundamental difficulties (it is sufficient to include transitions between states with $l > 1$), but are very cumbersome.

Using the selection rules, we obtain from the asymptotic form of the scattered wave the following expressions for the nonzero elements of the scattering matrix (the Coulomb factor $\exp(2i\delta_l)$ is omitted):

$$M^{00}_{00} = \frac{1}{2}(1 - \overset{0}{S}{}^{00}_{00}), \quad M^{11}_{11} = M^{1-1}_{1-1} = \frac{3}{4}\cos\vartheta\,(2 - \overset{1}{S}{}^{11}_{11} - \overset{2}{S}{}^{11}_{11}),$$
$$M^{10}_{10} = \frac{1}{2}\cos\vartheta\left(3 - 2\overset{2}{S}{}^{11}_{11} - \overset{0}{S}{}^{11}_{11}\right), \quad M^{10}_{1-1} = -\frac{1}{2\sqrt{2}}e^{i\varphi}\sin\vartheta\left(\overset{0}{S}{}^{11}_{11} - \overset{2}{S}{}^{11}_{11}\right),$$
$$M^{11}_{10} = -\frac{3}{4\sqrt{2}}e^{i\varphi}\sin\vartheta\left(\overset{1}{S}{}^{11}_{11} - \overset{2}{S}{}^{11}_{11}\right), \quad M^{1-1}_{10} = \frac{3}{4\sqrt{2}}e^{-i\varphi}\sin\vartheta\left(\overset{1}{S}{}^{11}_{11} - \overset{2}{S}{}^{11}_{11}\right), \tag{8}$$
$$M^{10}_{11} = \frac{1}{2\sqrt{2}}e^{-i\varphi}\sin\vartheta\left(\overset{0}{S}{}^{11}_{11} - \overset{2}{S}{}^{11}_{11}\right).$$

The polarization tensor for identical particles is obviously symmetric in the particle and coordinate indices (since the particles are indistinguishable), *i.e.*, it must be written in the form:

$$\hat{P}_{ik} = \frac{1}{2}(\hat{\sigma}^{(1)}_i\hat{\sigma}^{(2)}_k + \hat{\sigma}^{(1)}_k\hat{\sigma}^{(2)}_i).$$

The action of the operator $\hat{P}_{ik}$ on the spin indices $(s'm')$ of the matrix $M^{sm}_{s'm'}$ is completely analogous to its action on the spin indices of the wave functions $\chi^s_{m'}$: for example

$$\hat{P}_{xx}\chi^0_0 = -\chi^0_0, \quad \hat{P}_{xx}\chi^1_0 = \chi^1_0, \tag{9}$$
$$\hat{P}_{yz}\chi^1_0 = -\frac{i}{\sqrt{2}}(\chi^1_{-1} + \chi^1_1)$$

etc.

To simplify the writing of the polarization tensor, we define the quantity

$$\sigma_{ik} = P_{ik}\,\mathrm{Sp}\,(M^+M). \tag{10}$$

Unlike the normalized P_{ik}, this quantity has the dimensions of a differential cross section (barns/sterad.). We choose our coordinate system as follows (*cf.* Fig. 1): the z axis is along the direction of the incident flux, the y axis is perpendicular to the plane of scattering.

Let us consider the scattering the c.m.s. in the (xz) plane, which corresponds to azimuthal angle $\varphi = 0$. From formula (5), by using (6) – (9), we get the following expressions for the components σ_{ik} in terms of the four phases: $\delta_0(^1S_0)$, $\delta^0_1(^3P_0)$, $\delta^1_1(^3P_1)$, $\delta^2_1(^3P_2)$, which for simplicity we write in terms of elements of the scattering matrix:

$$k^2\sigma_{xx} = 4\mathrm{Re}\,[(M^{11}_{11} + K_1)\,M^{11*}_{1-1}] + 2(|M^{10}_{11}|^2 - |M^{11}_{10}|^2) + |M^{10}_{10} + K_1|^2 - |M^{00}_{00} + K_0|^2,$$
$$k^2\sigma_{xz} = 2\sqrt{2}\,\mathrm{Re}\,[(M^{11}_{11} + K_1)\,M^{10*}_{11} + (M^{10}_{10} + K_1)\,M^{11*}_{10} - M^{11}_{1-1}M^{10*}_{11}],$$
$$k^2\sigma_{zz} = 2(|M^{11}_{11} + K_1|^2 + |M^{11}_{1-1}|^2 + |M^{11}_{10}|^2 - |M^{10}_{11}|^2) - |M^{10}_{10} + K_1|^2 - |M^{00}_{00} + K_0|^2; \tag{11}$$
$$k^2\sigma_{yy} = -4\mathrm{Re}\,[(M^{11}_{11} + K_1)\,M^{11*}_{11}] + 2(|M^{10}_{11}|^2 + |M^{11}_{10}|^2) + |M^{10}_{10} + K_1|^2 - |M^{00}_{00} + K_0|^2.$$

Thus only four components of the tensor are different from zero.

Similarly we get the expression for the polarization from formula (4):

$$\sigma_0 P_y = \frac{\sqrt{2}}{4} \operatorname{Re}\,[i\,(M_{10}^{11} - M_{11}^{10}) \times (M_{11}^{11} + M_{10}^{10} - M_{1-1}^{11} + 2K_1)^*]. \tag{12}$$

Only the y-component of the polarization is different from zero. The polarization is perpendicular to the plane of scattering because the polarization pseudovector is constructed from the two available vectors: $\mathbf{k}$ and $\mathbf{k}'$ (the wave vectors before and after scattering), so that $\mathbf{P} \sim \mathbf{k} \times \mathbf{k}'$.

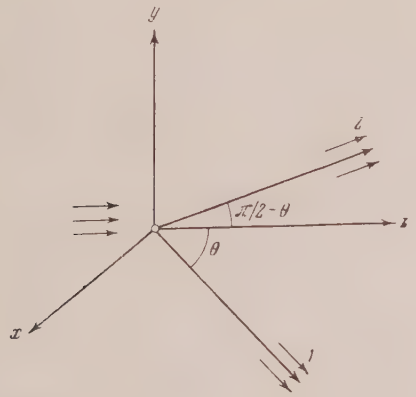

FIG. 1. Orientation of coordinate axes.

We first consider the formula for the polarization. It consists of two terms: a nuclear term and an interference term (proportional to $\eta = e^2/\hbar v$). Pure Coulomb terms naturally do not occur, since the Coulomb field does not change the polarization. In the nuclear part only the triplet phases occur, and they appear in linear combinations which vanish if they are equal or if one of them is equal to zero. It is clear that for isotropic phases only the Coulomb interference term is left, and this term is important only for very small angles of scattering ($\lesssim 5$–$10°$ in the c,m.s. at medium energies). The measurement of polarization at small, scattering angles presents well-known difficulties.

Next we treat the expressions for σ_{ik}. They consist of a nuclear, a Coulomb ($\sim \eta^2$), and an interference ($\sim \eta$) part. Unlike the polarization, the correlation contains pure Coulomb terms, so that it even occurs in the scattering in a pure Coulomb field. It is not hard to see that the Coulomb term is itself an interference between Coulomb scattering amplitudes and is consequently closely related to the identify of the particles. To make this clearer, we consider in particular the Coulomb term in the expression for P_{xx}.

The spin state is not changed during scattering in a Coulomb field, so that the scattering matrix is diagonal. The diagonal terms have the form $K_s = f(\theta) + (-)^s f(\pi - \theta) \equiv f_+ + (-)^s f_-$, while the scattered wave from a given spin state is $K_s \chi_m^s$.

We find the average value of $\hat{P}_{xx} = \hat{\sigma}_x^{(1)} \hat{\sigma}_x^{(2)}$ for the individual states, *i.e.*,

$$[(K_s \chi_m^s)^+, \quad \hat{\sigma}_x^{(1)} \hat{\sigma}_x^{(2)} (K_s \chi_m^s)] = K_s^* K_s (\chi_m^{s+} \hat{\sigma}_x^{(1)} \hat{\sigma}_x^{(2)} \chi_m^s).$$

For the singlet we get $-K_0^* K_0$; for the triplet with $m = 0$, $K_1^* K_1$; while for the triplets with $m = \pm 1$ we get zero, since, for example, $(\chi_1^1 \hat{P}_{xx} \chi_1^1) = (\chi_1^{1+} \chi_{-1}^1) = 0$. To determine P_{xx} we need only add the results obtained for singlet and triplet waves, multiplying them by the statistical weights which are equal to ¼, since there was no initial polarization. We get $\sigma_{xx}^c = K_1^* K_1 - K_0^* K_0 = -2(f_+^* f_- + f_+ f_-^*)$. In other words, this term occurs because singlet and triplet are scattered differently.

3. MEASURABLE CONBINATIONS OF CORRELATIONS

As was shown above, in the plane of scattering only four of the tensor components are different from zero: P_{yy}, P_{xx}, P_{xz}, P_{zz}. However, in an experiment we can only perform two independent measurements of the correlation: one in which the planes of the first and second scatterings are parallel, the other in which they are mutually perpendicular[2] (*cf.* Fig. 2). By the second scattering we mean the scattering by the nuclei of the analyzers (de-

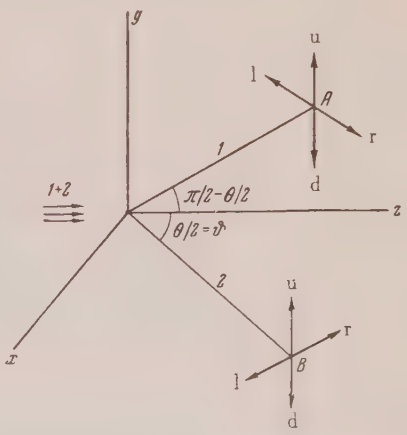

FIG. 2. Scheme of experiment for measurement of polarization correlation.

noted by A and B). The following two correlation measurements are independent:

1) By measuring the intensity when both particles are scattered upward (I_{uu}), both downward (I_{dd}), one scattered up, the other down (I_{ud}), and vice versa (I_{du}), we measure the correlation along the y axis:

$$P_{yy} = P_{\mathrm{I}} = \frac{\sigma_{\mathrm{I}}}{\sigma} = \frac{(I_{uu} - I_{du}) - (I_{ud} - I_{dd})}{I_{uu} + I_{du} + I_{ud} + I_{dd}}; \quad (13)$$

2) The second measurement is a measurement of the intensity when both particles are scattered to the left (I_{ll}), both scattered to the right (I_{rr}), the first to the right and the second to the left (I_{rl}) and vice versa (I_{lr}). By means of a formula analogous to (13) with the substitutions $u \to l$, $d \to r$, we determine a linear conbination of the remaining components: P_{xx}, P_{xz}, P_{zz}. These three components form a tensor in the xz plane. We bring it to axes $x'z'$ by a rotation through the angle ϑ ($\vartheta = \theta/2$ is the angle of scattering in the laboratory system). In this case we obviously are measuring the component of the rotated tensor with mixed indices, or more precisely the sum $\frac{1}{2}(P'_{x'z'} + P'_{z'x'})$ (in view of the identity of the particles). So the second combination is the following:

$$P_{\mathrm{II}} = \tfrac{1}{2}(P'_{x'z'} + P'_{z'x'}) = P_{xz}\cos 2\vartheta + \tfrac{1}{2}(P_{xx} - P_{zz})\sin 2\vartheta.$$

The formulas for P_{I} and P_{II} must be expressed in terms of the scattering angle in the lab system. Neglecting relativistic effects (for protons of a few hundred Mev), we must set $\theta = 2\vartheta$. The measurable combinations are

$$k^2\sigma_0 P_{\mathrm{I}} = k^2\sigma_{yy},$$

$$k^2\sigma_0 P_{\mathrm{II}} = \frac{1}{2\sin\theta}(|M_{11}^{10}|^2 - |M_{10}^{11}|^2).$$

4. PHASE ANALYSIS

Starting from the isotropy of the p–p scattering, an attempt was made to describe the scattering in terms of the two phases of the isotropic states δ_0 ($^1S_0$) and δ_1 ($^3P_0$).[3] Inclusion of the Coulomb interaction makes it possible, by analyzing experimental data on scattering cross sections, to determine magnitudes and signs of these phases in the energy region where the interference between Coulomb and nuclear scattering is not very small compared to the nuclear scattering. Protons with energies of 70–80 Mev in the laboratory system belong in this energy region.

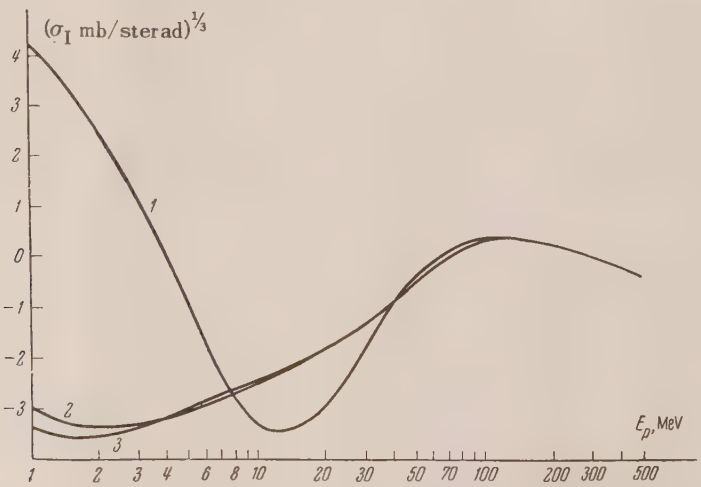

FIG. 3. Energy dependence of the polarization correlation, of measured with scattering planes perpendicular. *1.* Correlation for $\theta = 20°$; *2.* Correlation for $\theta = 90°$; *3.* Nuclear part for $\theta = 20°$.

For higher energies the interference term (which falls off essentially like $E^{-3/2}$) becomes so small that separation of the phases which are combined in the nuclear scattering cross section $\sigma_{\mathrm{nuc}} = f(\delta_0, \delta_1)$ is no longer possible. By using the energy dependence of the cross section, the

energy variation of the phases δ_0 and δ_1 over the whole region of isotropy (up to 400 – 450 Mev) was predicted[3].

We give a table of the values of the phases which we shall use in estimating the correlation:

E (Mev)	δ_0 (deg)	δ_1 (deg)	E (Mev)	δ_0 (deg)	δ_1 (deg)
0.5	18	~0	46	32	32
1	33	~0	100	10	52
1.5	42	~0	150	—7	61
2	46	~0	200	—23	70
10	56	2	300	—56	84
18	54	3	450	—90	90
30	48	11			

More accurate values for the phases can be obtained only from measurement of the polarization correlation (since, as already noted, measurement of the polarization gives nothing).

In order to estimate the importance of the polarization correlation, we give graphs of the energy dependence of σ_{ik} (for both σ_I and σ_{II}) for two typical angles: $\theta = 20°$ (where the Coulomb part is important), and $\theta = 90°$ (where the Coulomb part is neglibly small except at the very lowest energies). Figure 3 gives the quantity σ_I, which is measured when the planes of scattering are perpendicular, while Fig. 4 shows $\sigma_{II} = \sigma P_{II}$ while is measured with parallel planes of scattering. In order to make the drawings compact the energy is measured on a logarithmic scale, while the vertical axis gives the cube root of the correlation (in mb/sterad). Such a scale enables us to visualize the behavior of the curves over the whole energy range.

From the figures we see that the Coulomb terms play an important part not just for intermediate energies (*cf.* σ_I), which makes possible a more detailed phase analysis over the region of isotropy of the p–p scattering.

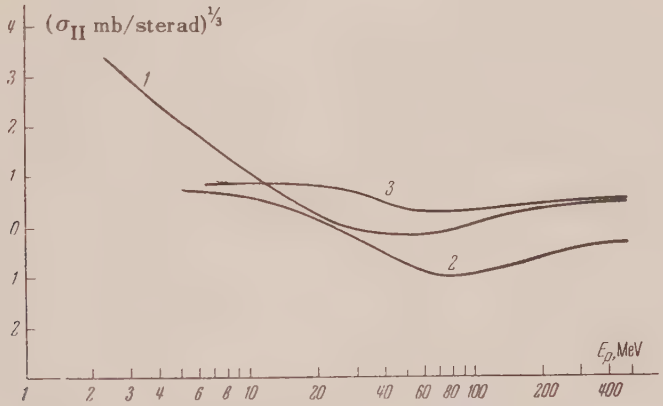

FIG. 4. Energy dependence of the polarization correlation, as measured with scattering planes parallel. *1.* Correlation for $\theta = 20°$; *2.* Total and nuclear correlation for $\theta = 90°$; *3.* Nuclear part for $\theta = 20°$.

We get the important result that the Coulomb terms cannot be neglected in an analysis which includes the polarization correlation. Measurement of the correlation at intermediate energies (20–100 Mev) will make it possible to get the isotropic phases more accurately and to determine the contribution of the anisotropic phases.

In conclusion, I express my thanks to Prof. Ia. A. Smorodinskii for suggesting this topic.

[1] J. M. Blatt and L. C. Biedenharn, Rev, Mod. Phys. **24**, 258 (1952).

[2] V. V. Vladimirskii and Ia. A. Smorodinskii, Dokl. Akad. Nauk SSSR **104**, 713 (1955).

[3] A. G. Zimin, Dokl. Akad. Nauk SSSR **105**, 73 (1955).

Translated by M. Hamermesh
244

The Problem of Saturation of the Hall "Constant" in Semiconductors in Strong Magnetic Fields

F. G. BASS AND M. I. KAGANOV
Physico-Technical Institute, Academy of Sciences, Ukrainian Soviet Socialist Republic

(Submitted to JETP editor April 13, 1956)
J. Exptl. Theoret. Phys. (U.S.S.R.) 32, 1233-1235 (May, 1957)

An expression is derived for the Hall "constant" in strong magnetic fields; it is valid for semiconductors that contain narrow bands.

1. A RECENTLY PUBLISHED work[1] explains the asymptotic behavior of the resistance and Hall "constant" of metals in strong magnetic fields. In particular, the following expression is obtained for the Hall "constant":

$$R = -1/ec(n_1 - n_2) \tag{1}$$

(n_1 and n_2 are the electron and hole densities). The expression is valid in those cases in which only closed equal-energy surfaces play a role. An analogous expression has also been obtained for semiconductors[2]. It reduces to the usual expressions in the special cases of a donor ($n_2 = 0$) and of an acceptor ($n_1 = 0$) semiconductor.

Formula (1) fails for an intrinsic semiconductor, since in this case $n_1 = n_2$. The subject of the present communication is the derivation of an expression for the Hall constant that is valid for intrinsic semiconductors and is especially effective for semiconductors with narrow bands.

For simplicity, a semiconductor is considered that possesses the energy spectrum represented in the figure. It is supposed that at $T = 0$, bands a and b are completely filled, band c empty. Upon increase of temperature, electrons from band b get into band c. The distance between the bottom of band b and the top of band a is so great that excitation of electrons from band a is known to be negligible. This is a representative model of an intrinsic semiconductor. By narrowing band b, we pass over to a donor semiconductor. Generalization to the case of several bands located close together, and likewise passage to an acceptor semiconductor in such a scheme, are trivial.

A considerable simplification results from the assumption that in band b there is *only one open surface*, and that in band c the open surfaces are located so high that excitation of electrons into these states may be neglected. A similar relation must clearly exist if band b is appreciably narrower than band c.

2. The treatment presented in Ref. 1 shows that in our case the conductivity matrix $\sigma_{ik}(H)$ has a form determined by expression (24) of that reference. This means that the Hall "constant" R in large fields is determined by

$$R = \sigma_{yx}/H = 1/\sigma_{xy}H. \tag{2}$$

It should be mentioned that in consequence of the smallness of the numbers of conduction electrons in semiconductors, use of formula (2) in this case is permissible at larger magnetic fields than in the case of metals.

In accordance with Eq. (25) of Ref. 1, the asymptotic expression for σ_{xy} may be written in our case in the following form:

$$\sigma_{xy} = -\frac{2ce}{H}\left\{\int_0^{\varepsilon_0} f_0'(\varepsilon)V(\varepsilon)\,d\varepsilon - \int_{\varepsilon_0}^{\varepsilon_1} f_0'(\varepsilon)V(\varepsilon)\,d\varepsilon + \int_{\varepsilon_2}^{\infty} f_0'(\varepsilon)V(\varepsilon)\,d\varepsilon\right\}. \tag{3}$$

Here ε_0 is the value of the energy on the open surface; the values ε_1 and ε_2 are evident from the figure (see below); $V(\varepsilon)$ is the volume *inside* the surface $\varepsilon(p) = \varepsilon$.* Upon integrating (3) by parts, we get

$$\sigma_{xy} = (2ce/Hh^3)\left\{-f_0(\varepsilon_0)[V(\varepsilon_0 - 0) + V(\varepsilon_0 + 0)] + \int_0^{\varepsilon_0} f_0(\varepsilon)V'(\varepsilon)\,d\varepsilon - \int_{\varepsilon_0}^{\varepsilon_1} f_0(\varepsilon)V'(\varepsilon)\,d\varepsilon + \int_{\varepsilon_2}^{\infty} f_0(\varepsilon)V'(\varepsilon)\,d\varepsilon\right\}.$$

*The exact definition of $V(\varepsilon)$ is evident from (22′) of Ref. 1.

Here

$$V(\varepsilon_0 - 0) = \lim_{\substack{\varepsilon \to \varepsilon_0 \\ (\varepsilon < \varepsilon_0)}} V(\varepsilon);\ V(\varepsilon_0 + 0) = \lim_{\substack{\varepsilon \to \varepsilon_0 \\ (\varepsilon > \varepsilon_0)}} V(\varepsilon),$$

and we have used the fact that $V(0) = V(\varepsilon_1) = V(\varepsilon_2) = 0$. Obviously $2h^{-3}[V_0(\varepsilon_0 - 0) + V(\varepsilon_0 - 0)] = N$ is the number of states in band b, and

$$2V'(\varepsilon)/h^3 = \begin{cases} n(\varepsilon) & 0 < \varepsilon < \varepsilon_0;\ \varepsilon_2 \leqslant \varepsilon; \\ -n(\varepsilon) & \varepsilon_0 < \varepsilon \leqslant \varepsilon_1, \end{cases}$$

where $n(\varepsilon)$ is the density of states per unit energy interval. We recall that $m > 0$ for $\varepsilon < \varepsilon_0$; but that for $\varepsilon_1 > \varepsilon > \varepsilon_0$, $m < 0$. From the normalization condition we have

$$\int_0^{\varepsilon_1} f_0(\varepsilon)\, n(\varepsilon)\, d\varepsilon + \int_{\varepsilon_2}^{\infty} f_0(\varepsilon)\, n(\varepsilon)\, d\varepsilon = N$$

Thus

$$R = 1/ecN\,(1 - f_0(\varepsilon_0));$$
$$f_0(\varepsilon_0) = [\exp\{(\varepsilon_0 - \mu(T))/kT\} + 1]^{-1}. \qquad (4)$$

If the band b is broad, the chemical potential $\mu(T)$ is located approximately in the middle of the forbidden band[3]. Then $e^{(\varepsilon_0 - \mu)/kT} \ll 1$, and expansion in the exponential gives

$$R = e^{(\mu - \varepsilon_0)/kT}/ecN. \qquad (5)$$

We are assuming that the distance on an energy scale from the open surface in band b to the chemical potential is less than the distance from μ to an open surface in band c. The appropriate generalization to take account of an open surface in band c is carried out in an obvious manner. The formula (5) obtained corresponds to an intrinsic semiconductor.

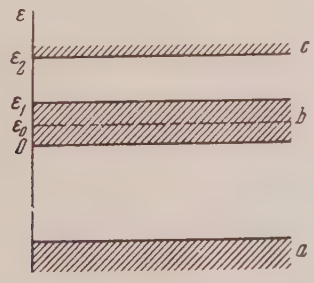

Qualitatively, the formula is evidently valid not only in the case of a single open surface, but also when a layer of open surfaces is narrow in comparison with the width of the band.

Passage to the limit of a donor level, $\varepsilon_1 = 0$, is accomplished as follows:

$$\int_0^{\varepsilon_1} f_0(\varepsilon)\, n(\varepsilon)\, d\varepsilon = N f_0(0);\ f_0(\varepsilon_0) = f_0(0).$$

Hence (*cf.* for example, Ref. 4)

$$R = \frac{1}{ecN(T)};\ N(T) = \int_{\varepsilon_2}^{\infty} f_0(\varepsilon)\, n(\varepsilon)\, d\varepsilon.$$

Here N is the number of electrons in the conduction band.

If the band b is very narrow ($\varepsilon_1 \ll kT$) but has a finite width, then the Hall "constant" can be written in the following form:

$$R = \frac{1}{ecN(T)}\left\{1 - \frac{\Delta N}{N(T)}\right\}.$$

Here $N(T)$ is the number of electrons in band c, and

$$\Delta N = f_0'(\varepsilon_0) \int_0^{\varepsilon_1} (\varepsilon - \varepsilon_0)\, n(\varepsilon)\, d\varepsilon.$$

It is necessary to set special limits to the applicability of the formulas obtained here. According to Swanson,[2] formula (1) is applicable when $H \gg H_0$, where H_0 is the magnetic field at which the period of revolution of an electron is equal to the relaxation time. However, since the electrons in a narrow band must have large effective masses, *i.e.*, small mobilities (as the width of the band approaches zero, the effective mass becomes infinite*), it may be concluded that H_0 is appreciably larger for semiconductors with narrow bands than for metals or for semiconductors of other types. Furthermore, one must keep in mind that the expression (3) that we have used for σ_{xy} is the first term of an expansion in powers of $1/H$. In the case of *low temperatures*, for an intrinsic semiconductor, the coefficient of $1/H$ will be so small [*cf.* Eq. (5)] that the next term of the expansion in powers of $1/H$ will be significant, and the formulas obtained here will be invalid. A similar situation always exists (practically at all temperatures) for metals with an equal number of electrons and "holes" (*cf.* Ref. 1).

The authors take this occasion to thank I. M. Lifshitz for useful discussions.

* For example, Samoilovich and Klinger[5] showed that $m_{eff} \sim 1/\varepsilon_1$. True, according to an estimate made in the the same work $m_{eff} \sim m_0$ (m_0 = mass of a free electron).

[1] Lifshitz, Azbel', and Kaganov, J. Exptl. Theoret. Phys. (U.S.S.R.) **30**, 220 (1956), Soviet Phys. JETP **3**, 143 (1956).

[2] J. A. Swanson, Phys. Rev. **99**, 1799 (1955).

[3] F. F. Vol'kenshtein, *Electrical Conductivity of Semiconductors* (Gostekhizdat, 1947).

[4] A. H. Wilson, *Theory of Metals* (Cambridge University Press, 1953), Chap. VIII.

[5] A. G. Samoilovich and M. I. Klinger, J. Tech. Phys. (U.S.S.R.) **25**, 2050 (1955).

Translated by W. F. Brown, Jr.
245

Letters to the Editor

The Nature of Field Fluctuations

M. M. MIRIANASHVILI, V. V. CHAVCHANIDZE AND IU. G. MAMALADZE
Institute of Physics, Academy of Sciences, Georgian SSR

(Submitted to JETP editor April 13, 1956)
J. Exptl. Theoret. Phys. (U.S.S.R.) 32, 1236-1237 (May, 1957)

AS IS WELL KNOWN, the neutral or charged nature of a given wave field, *i.e.*, the neutral or charged nature of the particles corresponding to that field, is closely connected with the character of the wave function. In the case of a neutral field, the wave function is real; in the case of a charged field, the wave function is complex. A neutral or charged nature means here, in fact, the absence or presence of interaction between the given wave field and the electromagnetic field. However, the wave fields do not interact with the electromagnetic field only. According to the contemporary meson theory, the meson fields interact with nucleons and with the electron-positron field.

However, whether a given wave field interacts with a given field of non-electromagnetic character cannot be ascertained from the form of the wave function, *i.e.*, from the algebraic construction of the wave function. This means that in the contemporary theory the existence of non-electromagnetic interactions between given wave fields does not impose conditions on the character of the corresponding field quantities, whereas in the case of interactions with the electromagnetic field such a condition exists (complex nature of the field function).

In fact, let us take, for example, a spinor field, characterized by a four-component spinor. If this field interacts with an electromagnetic field, then the wave function of the given spinor field should be complex. In the case of a real spinor (Majorana's theory for the neutrino) such an interaction cannot exist. There are no analogous conditions for the wave function relative to the interaction with the meson field. The interaction with the meson field is introduced in such a way that no conditions are imposed on the wave function of the spinor (or any other) field. This signifies that the electromagnetic field occupies a special position in the contemporary theory of wave fields.

This leads to one of two conclusions. Either it is to be acknowledged that the electromagnetic field occupies by its specific nature a special position distinguishing it from other wave fields, or it is necessary to admit that modern theory has not yet found an adequate apparatus for imposing supplementary conditions on the field quantities of interacting fields to reflect the particular characteristics of the existing wave fields.

The first conclusion is unacceptable for the reason that it does not lead out of the maze of contemporary meson theories. Even if it is valid, this does not give reason to deny the presence of particular characteristics of field quantities which describe interactions different from the electromagnetic one.

The second conclusion can serve as a basis for an attempt to generalize the concept of field functions. In other words, it is necessary to search for the conditions which must be imposed on the corresponding wave functions in order to carry through this or that interaction. As a hypothesis, it might be proposed that the field function of a wave field should be a hypercomplex number, in particular, a quaternion. Then the field function should have components in quaternion space with the base vectors $(1, i, j, k)$, where the base vectors satisfy the following conditions:

$$i^2 = j^2 = k^2 = -1, \quad ij = -ji = k,$$
$$jk = -kj = i, \quad ki = -ik = j.$$

In this space three independent rotations are possible; gauge transformations correspond to these rotations. Invariance under a gauge transformation (of the first type) will correspond to the conservation of certain three charges. We can thus expect that instead of the one known law of conservation of electromagnetic charge, two other laws of conservation of some charges g_n and g_μ (for example, nucleon and μ-meson charges) should exist.

Hypothetically, one can propose several ways of generalizing the concept of a field function. The simplest are the following assumptions: a) the field function is essentially a Hamiltonian quaternion[2,3] b) the field function is essentially a Dirac quaternion[4]. At present there is no need to employ more complex field functions.

It is known that the quaternion Q is equivalent to the complex number $Q = q_0 + iq_1$, if the components

at positions j and k are equal to zero[2]. It is also known that the wave functions of the field of electrically charged mesons φ and φ^* are made conjugate in the plane of the base vectors $(1, i)$. It is possible to assume, as a hypothesis, the existence of some special conjugation of the wave functions of the field, corresponding to the description of two nucleons with opposite $\pm g_n$-charges (g_n will be called the nucleon charge). Such a conjugation of the wave functions of the field can be carried out in the $(1, j)$ plane, where j does not coincide with the base vector i. If we do not go outside the $(1, j)$ plane, the algebraic properties of the wave functions of the field do not differ from the algebraic properties of complex functions. Therefore, the theory of particles with the g_n-charge (in other respects, neutral) can be developed analogously to the theory of electromagnetically charged particles. One of the authors of this note developed exactly such an approach to the theory of interaction of mesons with fermion fields[5].

However that may be, it is possible to consider that, together with electromagnetic conjugation, it is reasonable to introduce g_n-conjugation. The conjugation in the $(1, k)$ plane has not yet been employed. In the most general case, a particle having three charges, e, g_n, g_μ, should be described by a quaternion $\Psi = u_0 + iu_1 + ju_2 + ku_3$. A particle with charges $-e$, $-g_n$ and $-g_\mu$ will be described by the conjugate field function $\tilde{\Psi} = u_0 - iu_1 - ju_2 - ku_3$, where the sign $\sim$ means total conjugation in the case of Ψ and $\tilde{\Psi}$.

It can easily be shown that all possible combinations of the 3, 2, 1 and 0 charges, which the particles can have, can be described by 27 different quaternion field functions which have 3, 2, 1, 0 components.

The authors believe that the possibility described above of constructing a theory of particles which possess simultaneously three charges, is a new possibility in mesodynamics, opened up because of the broadening of the algebraic class of functions used as field functions.

In Ref. 5 a specific program of introducing field functions of a new algebraic class was outlined. However, other variants for using quaternions as field functions are equally conceivable.

[1] G. Wentzel, *Quantum Theory of Fields* (Russian translation) GTTI, 1947.

[2] M. Lagalli, *Vector Calculus*, ONTI, 1949.

[3] Iu. V. Linnick, Usp. Mat. Nauk (Progr. in Math. Sci.) 4, 49 (1949).

[4] Iu. B. Rumer, *Spinor Analysis*, ONTI, 1936.

[5] V. V. Chavchanidze, Dokl. Akad. Nauk SSSR **104**, 205 (1955).

Translated by G. E. Brown
246

Simplification of the Equations for the Distribution Function of Electrons in a Plasma

A. V. GUREVICH
P. N. Lebedev Physics Institute, Academy of Sciences, U.S.S.R.

(Submitted to JETP editor December 13, 1956; resubmitted March 14, 1957)
J. Exptl. Theoret. Phys. (U.S.S.R.) **32**, 1237-1238 (May, 1957)

DAVYDOV, starting from the Boltzmann kinetic equation, showed that for the electron distribution function

$$f(\mathbf{r}, \mathbf{v}, t) = f_0(\mathbf{r}, v, t) + \frac{\mathbf{v}}{v}\mathbf{f}_1(\mathbf{r}, v, t) + \chi(\mathbf{r}, \mathbf{v}, t)$$

in a plasma located in electric and magnetic fields the following system of equations is correct:

$$\frac{\partial f_0}{\partial t} + \frac{v}{3}\operatorname{div}\mathbf{f}_1 - \frac{e}{3mv^2}\frac{\partial}{\partial v}(v^2\mathbf{E}\mathbf{f}_1) - \frac{1}{v^2}\frac{\partial}{\partial v}\left\{\nu v^2\frac{kT}{M}\frac{\partial f_0}{\partial v} + \nu v^3\frac{m}{M}f_0\right\} = 0, \quad (1a)$$

$$\frac{\partial \mathbf{f}_1}{\partial t} + v\operatorname{grad} f_0 + \frac{e\mathbf{E}}{m}\frac{\partial f_0}{\partial v} + \frac{e}{mc}[\mathbf{H}\mathbf{f}_1] + \nu\mathbf{f}_1 = 0. \quad (1b)$$

Here e and m are the charge and mass of an electron, M is the mass of a molecule (ion), k is the Boltzmann constant, T is the temperature of the plasma, E and H are the intensities of the electric and magnetic fields, $\nu = \nu(v)$ is the frequency of collision of electrons with molecules or ions (see Ref. 2, §59). Terms of order χ (in comparison with f_0) have been neglected in the derivation of Eqs. (1). The evaluation carried out in Ref. 1 has shown that in a spatially uniform plasma $\chi \sim \delta f_0$, while in the presence of irregularities $\chi \sim \delta f_0 + l\partial f_1/\partial z$, that is, Eqs. (1) are true when the conditions

$$\delta \ll 1, \quad l\partial f_1/\partial z \ll f_0. \quad (2)$$

We shall now show that the system of equations (1) can be simplified. For this purpose we shall first consider the case of a spatially homogeneous plasma. In this case the symmetrical part of the electron distribution function (f_0) can be essentially changed only in a time of order $1/\delta\nu$, since $\partial f_0/\partial t \leq \delta\nu f_0$ (see Ref. 3). At the same time, as is clear from Eq. (1b), the current (directed) part of the distribution function ($\mathbf{f}_1$) changes essentially in a time of order $1/\nu$, since $\partial \mathbf{f}_1/\partial t \geq \nu \mathbf{f}_1$. Hence the function $\mathbf{f}_1$ changes more rapidly in time than f_0. For this reason the dependence of the function f_0 on t may be neglected in the integration of Eq. (1b). The solution obtained will then be correct to an accuracy which includes up to terms less than or of the order of δ, *i.e.*, to the same degree of accuracy to which Eqs. (1) themselves are correct.

Analogously, in the presence of spatial inhomogeneities the dependence of f_0 on t may be neglected in the integration of Eq. (1b) only on the condition that the function f_0 change much more slowly with time than $\mathbf{f}_1$, *i.e.*, that $\partial f_0/\partial t \ll \nu f_0$. On the other hand, it follows from Eq. (1a) that $\partial f_0/\partial t \lesssim \delta\nu f_0 + v\partial f_1/\partial z$, where z is the direction in which the function $|\mathbf{f}_1|$ changes most sharply. Hence the dependence of the function f_0 on t may be neglected in the integration of Eq. (1b) only if $\nu f_0 \gg \delta\nu f_0 + v\partial f_1/\partial z$, *i.e.*, if $\delta \ll 1$ and $l\partial f_1/\partial z \ll 1$, which coincides exactly with conditions (2).

Taking account of this circumstance (and knowing precisely how the fields E and H change with time), we can integrate Eq. (1b) without difficulty. The result obtained is a simple approximate expression for the function $\mathbf{f}_1$, which, as remarked above, is correct (*i.e.*, to the same degree of accuracy with which Eqs. (1) themselves are correct) when conditions (2) are fulfilled. Thus the problem of finding the electron distribution function reduces to the integration of the single equation (1a)*. For example, in the case of a spatially homogeneous plasma we have

$$\mathbf{f}_1 = -\mathbf{u}\frac{\partial f_0}{\partial v},$$

$$\frac{\partial f_0}{\partial t} - \frac{1}{v^2}\frac{\partial}{\partial v}\left\{v^2\left[\frac{e\mathbf{E}\mathbf{u}}{3m} + \nu\frac{kT}{M}\right]\frac{\partial f_0}{\partial v} + \nu v\frac{m}{M}f_0\right\} = 0.$$

Here $\mathbf{u}$ is the velocity of the directed motion of the electron produced by external fields. The velocity $\mathbf{u}$ is determined by the Lorentz equation of motion of the electron

$$\frac{\partial \mathbf{u}}{\partial t} + \nu\mathbf{u} = \frac{e}{m}\left(\mathbf{E} + \frac{1}{c}\mathbf{u}\times\mathbf{H}\right), \tag{3}$$

which is ordinarily easily solved.

If spatial inhomogeneities are present in the plasma, the expression for the current function (in a constant magnetic field) takes the form

$$\mathbf{f}_1 = -\mathbf{u}\frac{\partial f_0}{\partial v} - \frac{l}{1+\gamma^2}\{\operatorname{grad} f_0 \cdot$$

$$+ \gamma^2 H^{-2}\mathbf{H}(\mathbf{H}\operatorname{grad} f_0) + \gamma[\mathbf{H}\operatorname{grad} f_0]/H\},$$

where $\gamma = eH/mc\nu$ and the velocity $\mathbf{u}$ is determined, as before, by Eq. (3).

In the case of a Maxwellian distribution of the electron velocities, the equations for the distribution function lead, as is well-known, to a system of equations for the temperature T_e and the density n of the electrons (the needed expressions for the current and for the energy flux carried by the electrons are calculated with the aid of the expression obtained above for the current function). These equations were obtained in Ref. 1 for a varying magnetic field ($\mathbf{E} = \mathbf{E}_0(\mathbf{r})\cos\omega t$) of low frequency ($\omega^2 \ll \nu^2$). For high frequency $\omega^2 \gg \nu^2$ the electron distribution is stationary. The equations for the temperature and density of the electrons become essentially simpler in this case. For example, if we assume that $l \neq l(v)$ (collision with neutral particles), then for $H = 0$

$$\theta - \frac{l^2}{3\delta}\operatorname{div}\operatorname{grad}\theta = 1 + \frac{e^2E_0^2(\mathbf{r})}{3kTm\delta\omega^2},$$

$$n = (n_0/\theta^{1/2})(V/\int_V \theta^{-1/2}dV),$$

where $\theta = T_e/T$ and n_0 is the electron density in a plasma undisturbed by an electric field.

* It should be noted that in the case of a constant magnetic field the system of equations (1) can also, generally speaking, be reduced to a single equation by means of an exact integration of Eq. (1b). However, such an integration does not lead to any simplification of the problem, since at the same time Eq. (1a) has its order increased and becomes integro-differential.

[1] B. I. Davydov, J. Exptl. Theoret. Phys. (U.S.S.R.) **7**, 1069 (1937).

[2] Al'pert, Ginzburg and Feinberg, *The Propagation of Radio Waves*, GTTI, 1953.

[3] A. V. Gurevich, J. Exptl. Theoret. Phys. (U.S.S.R.) **30**, 1112 (1956); Soviet Phys. JETP **3**, 895 (1957); Dokl. Akad. Nauk SSSR **104**, 201 (1955).

Translated by M. G. Gibbons
247

Application of Correlation Polarization in the Phase Analysis of $p-p$ Scattering

A. G. ZIMIN

(Submitted to JETP editor December 14, 1956)
J. Exptl. Theoret. Phys. (U.S.S.R.) 32, 1239-1240
(May, 1957)

EXPERIMENTS ON THE three-fold scattering of 310 Mev protons by protons have been conducted recently in Berkeley [1]. In these experiments there were measured two quantities which characterize the change of polarization of one of the interacting particles in the ensuing scattering, namely, the depolarization D and the rotation of the polarization R. Together with the scattering cross section and the value of the polarization, this gives the four essential quantities which characterize the scattering matrix. Phase analysis, carried out with the aid of the designated quantities [2], yields five groups of permissible phases with momenta $l \leqslant 4$.

State	Number of group 1	2	2*	3	4
$^1S_0$	$-10.9\pm4.9°$	$-19.5°$	$-27\pm3.9°$	$-10.1\pm4.9°$	$-0.3\pm4.6°$
$^1D_2$	$13.3\pm1.5°$	$4.3°$	$4.8\pm1.2°$	$12.8\pm1.4°$	$12.9\pm1.2°$
$^1G_4$	$1.1°$	$1.3°$	$1.0°$	$1.0°$	-1.0
$^3P_0$	-4.1 ± 2.7	-36	$-25.4+3.8$	-14.3 ± 4.3	-64.7 ± 3.8
$^3P_1$	-19.8 ± 1.6	-11.7 ± 2	-7.3 ± 2	-26.7 ± 1.9	8.1 ± 1
$^3P_2$	22.6 ± 1.3	18.8	23.1 ± 1.5	-12.6 ± 1.9	8.1 ± 1
ε_2	-1.8 ± 2	9.3	7.5	-0.8 ± 4	0.2 ± 6.2
$^3F_2$	2.0 ± 1.1	-0.5	-1.4 ± 1.8;	-1.3 ± 2	-2.1 ± 1.3
$^3F_4$	-0.5 ± 0.9	2.5	2.6 ± 1.5;	3.2 ± 1	3.3 ± 0.5
ε_4	-0.9	1.5	0.9	1.1	-1.3
$^3H_4$	-1.1	2.1	-0.7	1.4	2.2
$^3H_5$	0.9	-1.4	0.9	0.1	-2.0
$^3H_6$	-0.6	1.6	-0.8	1.3	0.3
$^3F_3$	$-2.6\pm1.1°$	0.2	1.5 ± 0.7	2.1 ± 1.5	$3.0\pm2.2°$

Such lack of single-valuedness arises because the four designated quantities do not constitute a complete set of experimental data. For a single-valued phase analysis, it is necessary to carry out supplementary experiments, *viz:* there-fold scattering with the application of a field or else with correlation polarization. As Chamberlain reports [6], the application of magnetic fields in three-fold scattering does not produce complete single-valuedness of the phase analysis. As shown by the calculations which follow, the values of correlation polarization corresponding to different phase groups differ markedly from one another. This fact makes possible the complete separation of the designated groups by measuring only a single correlation polarization.

As is known [3,4], the measurement of the correlation polarization, *i.e.*, $\langle \sigma_i^{(1)}\ \sigma_k^{(2)} \rangle (i, k = x, y, z)$, can be carried out through two-fold proton-proton scattering. Here two quantities are measured directly:

$$\sigma_{\mathrm{I}} = \sigma_{yy} = \sigma_{y'y'} \text{ and } \sigma_{\mathrm{II}}$$

$$= \sigma_{xz}\cos 2\vartheta + {}^1/_2(\sigma_{xx} - \sigma_{zz})\sin 2\vartheta = \sigma_{x'z'},$$

where ϑ is the scattering angle in the laboratory coordinate system, and the primed quantities refer to the coordinate system with axes x' and z' which are oriented in the directions taken by the two scattered particles. Measuring the component combinations of the tensor $\sigma_{ik} = \sigma_i^{(1)}\sigma_k^{(2)}$, the expression for the matrix parameters of the scattering

$$M = aS + c(\sigma_n^1 + \sigma_n^2) + {}^1/_2 g(\sigma_k^1\sigma_k^2 + \sigma_p^1\sigma_p^2)T$$
$$+ {}^1/_2 h(\sigma_k^1\sigma_k^2 - \sigma_p^1\sigma_p^2)T + m\sigma_n^1\sigma_n^2 T,$$

takes the following form:

$$\sigma\sigma_{y'y'} = 2\mathrm{Re}(am^*) + 2(cc^* + hh^* - gg^*),$$
$$\sigma\sigma_{x'z'} = 4\mathrm{Re}(ich^*).$$

The results of the calculation of σ_{I} upon adduction of the phase grouping are shown graphically. The value of σ_{I} proves to be quite dependent upon the group number, especially for angles less than 50 degrees. Therefore measurement of σ_{I} for angles less than 50° permits isolation of the correct phase grouping. σ_{II} is less dependent on the group number, so that calculation of σ_{II} is not of interest (taking

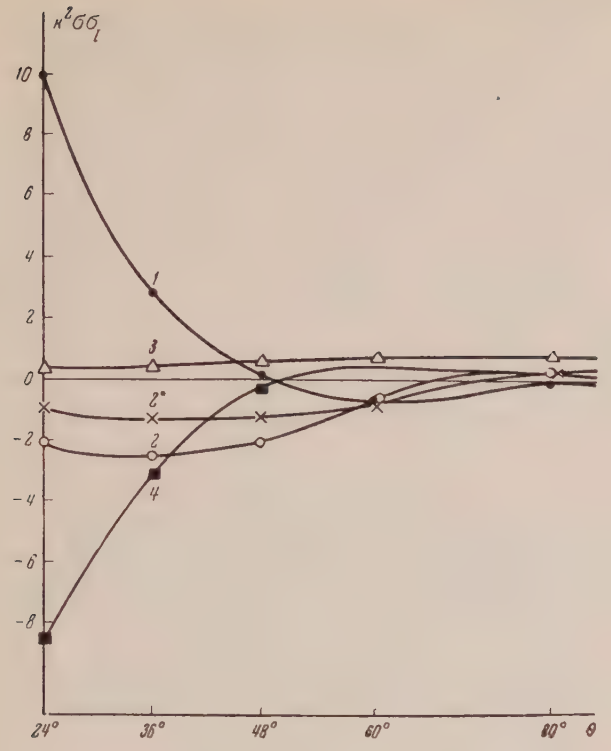

into account the large deviations from the phase values in a given group).

As is shown by phase analysis which takes into account only phases of isotropic states[5] (first approximation), the S-phase, for the energy under consideration should have a large negative value. Groups 2 and 2* show agreement with this statement, besides yielding only minor mean square deviations. Groups 1 and 4, whose phases differ greatly from those of 2 and 2*, show a sharply different behavior of σ_I for small angles. This circumstance permits sorting them out by measuring σ_I.

This work has been carried out on the suggestion of Professor Ia. A. Smorodinskii, to whom I wish to express my appreciation. I also wish to thank Professor O. Chamberlain (USA) for furnishing data on phase analysis.

[1] T. J. Ypsilantis, Experiments on Polarization in Nucleon-Nucleon Scattering at 310 Mev, University of California Rad. Lab., Berkeley (1956).

[2] H. P. Stapp, On the Analysis of p–p Polarization Experiments, University of California Rad. Lab., Berkeley (1956).

[3] Ia. A. Smorodinskii and V. V. Vladimirskii, Dokl. Akad. Nauk SSSR **103**, No 6 (1955).

[4] A. G. Zimin, J. Exptl. Theoret. Phys. (U.S.S.R.) **32**, 1226 (1957), Soviet Phys. JETP, **5**, 996 (1957).

[5] A. G. Zimin, Dokl. Akad. Nauk SSSR **105**, 73 (1955).

[6] O. Chamberlain, *Transactions of Conference on High Energies*, M. (1956).

Translated by D. A. Kellog
248

Polarization of Deuterons in Elastic Scattering

O. D. CHEISHVILI
Tbilisi State University

(Submitted to JETP editor December 25, 1956; resubmitted after revision February 28, 1957)
J. Exptl. Theoret. Phys. (U.S.S.R.) **32**, 1240-1242 (May, 1957)

WE CONSIDER IN THIS WORK several questions concerning the polarization of deuterons during their elastic scattering by nuclei. Lakin[1] and the author[2] made calculations on the polarization of deuterons, but these were based only on general considerations of invariance and did not yield concrete results with regard to polarization. For the interaction potential of the deuteron and the nucleus we shall take (in analogy to the interaction potential of a nucleon with a nucleus[3])

$$V_{dA}(\mathbf{r}) = \int \psi_d^*(|\mathbf{r}_n - \mathbf{r}_p|)\,[V_{nA}(\mathbf{r}_n) + V_{pA}(\mathbf{r}_p)]\,\psi_d(|\mathbf{r}_n - \mathbf{r}_p|)\,d(\mathbf{r}_n - \mathbf{r}_p). \quad (1)$$

The interaction potentials for neutrons and protons with nuclei are taken as

$$V_{nA}(\mathbf{r}) = V_0\rho(r) + V_1\frac{1}{r}\frac{\partial\rho(r)}{\partial r}(\sigma_n \mathbf{L}), \quad (2)$$

$$V_{pA}(\mathbf{r}) = V_0\rho(r) + V_1\frac{1}{r}\frac{\partial\rho(r)}{\partial r}(\sigma_p \mathbf{L}) + V_c(r). \quad (3)$$

The Coulomb interaction potential of the proton with a nucleus is taken as

$$V_c(r) = \begin{cases} (3R^2 - r^2)\,Ze^2/2R^3, & \text{for } r < R \\ Ze^2/r, & \text{for } r > R \end{cases} \quad (4)$$

where R is the nuclear radius and Z is the nuclear charge. The spin-orbital Coulomb interaction is not taken into consideration, since it is small compared with the spin-orbital nuclear interaction.

The calculation is carried out by the Born approximation; it is assumed that the deuteron is in the

s-state. The differential scattering cross section of the polarized deuteron beam in this case takes the form

$$I(\vartheta, \varphi) = \left(\frac{2M}{\hbar^2}\right)^2 \left(\frac{4\alpha}{q}\right)^2 \left(\tan^{-1}\frac{q}{4\alpha}\right)^2 \left\{|A|^2 + \frac{2}{3}|B|^2 + \right.$$
$$\left. + 2\sqrt{\frac{2}{3}}\sqrt{\frac{4\pi}{3}}\,\mathrm{Im}(AB^+)\sum_M \langle T_{1M}\rangle Y^*_{1M}(\mathrm{n}) + \frac{\sqrt{2}}{3}\sqrt{\frac{4\pi}{5}}|B|^2 \sum_M \langle T_{2M}\rangle Y^*_{2M}(\mathrm{n})\right\},$$
$$A(\vartheta) = \frac{2V_0}{q}\int_0^\infty j_1(qr)\,\frac{\partial\rho(r)}{\partial r}\,r^2 dr + \frac{Ze^2}{R}\left\{\frac{3}{2}\,\frac{1}{q^3}\sin qR - \right. \qquad (5)$$
$$\left. - \frac{3}{2}\,\frac{R}{q^2}\cos qR + \frac{3R^2}{2q}\left(1 + \frac{2}{(qR)^2}\right) j_1(qR)\right\},$$
$$B(\vartheta) = \frac{2V_1}{q}\,k^2 \sin\vartheta \int_0^\infty j_1(qr)\,\frac{\partial\rho(r)}{\partial r}\,r^2\,dr, \quad q = 2k\sin\frac{\vartheta}{2}, \qquad \mathrm{n} = \frac{[\mathbf{k}, \mathbf{k}_0]}{k^2\sin\vartheta},$$

where M is the mass of the deuteron, $\mathbf{k}_0$ and $\mathbf{k}$ the wave vectors of the deuteron before and after scattering, $j_1(qr)$ the first-order spherical Bessel function, Y_{jM} the associated Legendre polynomials, and T_{jM} the tensor operator of the deuteron spin [1]. Equation (5) can be considered as the formula for double elastic scattering of unpolarized deuterons by nuclei, provided $\langle T_{1M}\rangle$ and $\langle T_{2M}\rangle$ are replaced by the value of the deuteron polarization after the first scattering.

If after the first scattering the deuteron travels in the direction of the z axis, while the y axis is perpendicular to the plane of the first scattering, then

$$I(\vartheta, \varphi) = I_0(\vartheta)\{1 + P_{20}(\vartheta)P_{20}(\vartheta_1) + 2P_{11}(\vartheta)P_{11}(\vartheta_1)\cos\varphi + 2P_{22}(\vartheta)P_{22}(\vartheta_1)\cos 2\varphi\}, \quad (6)$$

where

$$P_{20}(\vartheta) = -\frac{1}{3\sqrt{2}}\,\frac{|B|^2}{|A|^2 + {}^2/_3|B|^2} = \langle T_{20}\rangle,$$
$$iP_{11}(\vartheta) = -\frac{2i}{\sqrt{3}}\,\frac{\mathrm{Im}(AB^+)}{|A|^2 + {}^2/_3|B|^2} = \langle T_{11}\rangle,$$
$$P_{22}(\vartheta) = -\frac{1}{2\sqrt{3}}\,\frac{|B|^2}{|A|^2 + {}^2/_3|B|^2} = \langle T_{22}\rangle.$$

The differential cross section for the unpolarized deuterons is

$$I_0(\vartheta) = \left(\frac{2M}{\hbar^2}\right)^2 \left(\frac{4\alpha}{q}\right)^2 \left(\tan^{-1}\frac{q}{4\alpha}\right)^2 \left\{|A|^2 + \frac{2}{3}|B|^2\right\}, \quad (7)$$

where ϑ_1 and ϑ are the angles of the first scattering and of the corresponding second scattering. Equation (6) contains those quantities which characterize the interactions of nucleons with nuclei.

Assuming that each nucleon of the moving deuteron has half the energy of the deuteron (the experiment was carried out [5] with deuterons of high energy – 167 Mev), and calculating the interaction potential by using the optical model of the nucleus [6], we obtain for the central part of the potential

$$V_0\rho(r) = \begin{cases} -(28 + i16)\ \mathrm{Mev}, & \text{for } r < R \\ 0, & \text{for } r > R \end{cases}$$

If we take the spin-orbital part of the potential to be 15 times larger than the Thomas expression for the real part of the central potential [7], then

$$V_1 = 9 \times 10^{-26}\ \mathrm{Mev\ cm^2}.$$

If both scatterings occur in carbon, and the scattering angles ϑ_1 and ϑ are both 20°, Eq. (6) takes the form

$$I(20°, \varphi) = (p + q\cos\varphi + r\cos 2\varphi) \times 10^{-27}\ \mathrm{cm^2/steradian}$$

where $p = 18.1$, $q = 5.5$, $r = 2.4$. The following results were obtained experimentally: $p = 50.3 \pm 2.2$, $q = 15.3 \pm 1.9$, $r = -1.8 \pm 3.6$. The experimental statistical errors are correct only as concerns the relative values of p, q, and r, and not as regards absolute values.

The $p : q$ ratio obtained above agrees with experiment, but the $p : r$ ratio is somewhat low.

Reference 8 gives the results of double scattering of deuterons into various scattering angles by various scattering materials. We have made a comparison for the case where both scattering targets are carbon and the deuteron energy is 156 Mev.

For this experiment the first scattering angle was 16°. The second scattering angle was varied in the interval 11° to 28°. For a second scattering angle

greater than 16°, there is satisfactory agreement with the experimental results in the $p : q$ ratio. For smaller angles the agreement breaks down, and our calculation of the coefficient r of the term $r \cos 2\varphi$ comes out to be several times larger than the experimental value.

As is proposed in Ref. 1, it is necessary to consider that the state of the deuteron makes a major contribution, and leads to the diminuation of the coefficient r in front of $\cos 2\varphi$.

I wish to express my thanks to Professor G. P. Khutsishvili for his never-failing interest in the work and for his valuable discussions.

[1] W. Lakin, Phys. Rev. **98**, 139 (1955).
[2] O. Cheishvili, J. Exptl. Theoret. Phys. (U.S.S.R.) **30**, 1147 (1956), Soviet Phys. JETP **3**, 974 (1957).
[3] Lane, Thomas, and Wigner, Phys. Rev. **98**, 693 (1955).
[4] K. Gatha and R. Riddell, Phys. Rev. **86**, 1035 (1952).
[5] Chamberlain, Segre, Tripp, Wiegand and Ypsilantis, Phys. Rev. **95**, 1104 (1954).
[6] Fernbach, Serber, and Taylor, Phys. Rev. **75**, 1352 (1949).
[7] E. Fermi, Nuovo cimento **11**, 407 (1954).
[8] Baldwin, Chamberlain, Segre, Tripp, Wiegand, and T. Ypsilantis, Phys. Rev. **102**, 1502 (1956).

Translated by D. A. Kellog
249

Some New Possibilities of Ionic Phenomena in Metastable Liquids

G. A. ASKAR'IAN
P. N. Lebedev Physics Institute, Academy of Sciences, U.S.S.R.

(Submitted to JETP editor January 8, 1957; resubmitted February 23, 1957)
J. Exptl. Theoret. Phys. (U.S.S.R.) **32**, 1242-1244 (May, 1957)

IONIZING PARTICLE TRACKS are produced in the usual bubble chambers[1] through the budding of nucleation voids directly accompanying the passage of ionizing particles, and are generated as the result of ponderomotive micro-entrainment among the accumulated mutually repelling ions or else as the result of micro-explosions due to local heating. The short lifetime of these phase nuclei does not permit their use for delayed track production, which to a certain extent limits the usefulness of the usual bubble chambers, assuming only semiautomatic registration of particles in preliminary saturation. (This condition increases interest in the investigation of the density, lifetime and dynamic growth of these *primary* phase centers, and in attempts at very high speed photographic registration of the tracks, such as could be done by using pulses from highly sensitive electro-optical tubes[2] or by other optical recorders, activated by the scattering or the emission of light by these optical inhomogeneities. Such inhomogeneities arise virtually along the entire particle track, not only under metastable conditions, but even without pressure drops, in stable heated or aerated liquids, for example, near the boiling point, and especially strongly near the critical point).

A series of suggested methods for the proposed accomplishment of the automatic operation of bubble chambers employs the possibility of formation of *secondary* centers for the initiation of the action on the remaining ions. Among such methods are, for example, the proposal[3] to use the local energy liberated upon the recombination of ions, the formation of phase nuclei through dissipative drifting of ions in an external electric field or else in the field of an approaching ion of opposite charge, attempts at influencing the ions by high frequency electromagnetic waves[4], *etc.*, using various ways of changing the dynamics of recombination of the ions by the application of an external electric field.

Without stopping to evaluate the effectiveness of these methods for various working liquids in bubble chambers, let us examine possible new methods of revealing the presence of single ions, based on the stratification of a working liquid composed of heterogeneous components in ion fields.

Let us assume that the molecules of a profusely dissolved substance (for example, a gas, vapor or liquid) possess a dipole moment markedly exceeding the dipole moment of the solvent liquid. Then the strong inhomogeneous electric field due to ion formation leads to a sharp change in the concentration of the solution in the vicinity of the ions (local enrichment or quasi-liquid complex formation). If the lifetime of the ion exceeds the time needed to establish localized statistical diffusion equilibrium (and it is indeed these relatively long-lived ions, for which this condition is known to be fulfilled, that we are interested in), then in accord with the Boltzmann formula the local concentration of the solution at a distance r from the center of

the ionic field is equal to:

$$K(r) = \frac{n_s}{n_l} = K(\infty) \exp\left\{\frac{1}{kT} \int_0^{E'(r)} (p_s - p_l)\, dE'\right\},$$

where p_s and p_l are the effective averaged (over the direction of the field) molecular dipole moments of the dissolved substance and solvent liquid respectively. These quantities depend, generally speaking, on the field intensity and on the temperature. E' is the effective electric field acting on the molecules ($E' \approx a(r)e/r^2$, where e is the ionic charge, and $a(r) \approx \frac{2}{3\varepsilon(r)} + \frac{1}{3}$) takes the local polarization of the mixture into account, can vary only in a narrow range: $0.3 < a(r) > 1$.

For the sake of illustration we shall evaluate the order of magnitude of the dimensions of the zone of adequate enrichment. Assuming for the sake of simplicity on the zone boundary $(p_s - p_l) \sim 10^{-18}$ C.G.S. electrostatic units, approximately equal in order of magnitude to the intrinsic dipole moment of a polar molecule, let us examine a solution of polar gas molecules in a less polar or nonpolar liquid. Then, the condition of adequate enrichment, say for $\ln \frac{K(r_1)}{K(\infty)} \sim 2$, yields $r_1 > 10^{-7}$ cm for $T < 300°$ K.

For a very weak or vanishingly small electric field in the zone of enrichment (with approach toward or recombination with a center of opposite charge, or with neutralization of the ion at the electrode, occurring in surface development of the track projection on the electrode, *etc.*) the attraction power acting on the molecule in the zone of enrichment is sharply decreased. The excess quasi-gaseous pressure (if the dissolved substance has sufficient volatility) exerts an effect on the adjacent layer of the liquid and is able to promote a microexplosion of the liquid and the production of nucleation voids, resulting in a bubble with assured instability of the state (superheat or supersaturation of the working liquid).

This process of ion development, which is basically different from the development mechanism used in the usual bubble chambers, produces development centers as long as the recombination of ions continues. This process can be used not only during preliminary saturation, but also during delayed instability.

Obviously, the greater the relative difference of the dipole moments or polarizability of the solvent and solute molecules, the more valid is this description of the possible mechanism of development; the faster it occurs, and the greater is the instability of the system.

Among the shortcomings of methods for delayed track development which use the effects arising on the recombination of ions is the need for providing enough recombining ions, during a given time interval, to produce supersaturation also in the time interval during which a strongly unstable state exists. In view of the sharp decrease in the number of ions recombining per unit time, it is apparently necessary to use special electric fields, such as an alternating field to attract and repel the ions at certain instants of time.

In this regard the proposed methods of development which utilize the effect of electric fields from the side on the ions, excel markedly, since in this case the effectiveness of development is determined by the number of ions caught up rapidly by the effected influence, and not by the change in the number of ions, as was the case previously. The application of the field can be accomplished with negligibly small delay (with an associated small instability of the state), or else fortuitously combined with the field that weakens of the recombination of the ions (upon triggering of the system by the passing particle).

The effect of the formation of phase nuclei in heated or aerated liquids in the presence of ions moving under the influence of an electric field, or in the presence of changes in the local ionic fields, holds great interest not only in regard to the possibility of automatic particle track registration, but also because it is a unique means of initiating phase transitions under the influence of electric fields.

Among other manifestations of the effect of electric fields in the specific conditions considered above, it is worth noting that the establishment of easier conditions for the production of nucleation bubbles and a high ion density along the particle track in the liquid can facilitate the localization of discharge along the track and the production of a gas-vapor canal for visualization of the track (for example, limited discharge along the track, intersecting a series of flat thin electrodes submerged in the liquid with alternating potentials, *etc.*).

It is also of interest to investigate the dynamics of current-induced compression of discharge in liquid systems of special physical interest metastable or near-boiling liquids, which consequently exhibit a low breakdown resistance to the discharge voltage actually produced in the gas-vapor phase

(special dissolved gas or liquid vapor).

[1] D. Glaser, Suppl. del Nuovo cimento 11, Ser. IX, 2, 361 (1954).

[2] G. A. Askar'ian, J. Exptl. Theoret. Phys. (U.S.S.R.) 28, 636 (1955), Soviet Phys. JETP 1, 571 (1955).

[3] G. A. Askar'ian, J. Exptl. Theoret. Phys. (U.S.S.R.) 31, 897 (1956), Soviet Phys. JETP 4, 761 (1957).

[4] Bertranza, Franzini, Martelli and Tallini, Paper presented at CERN Symposium, Geneva, June 1956.

Translated by D. A. Kellog
250

Phenomenological Study of the Effect of Nonconducting Medium in Quantum Electrodynamics

M. I. RIAZANOV
Moscow Engeneering-Physics Institute

(Submitted to JETP editor February 13, 1957)
J. Exptl. Theoret. Phys. (U.S.S.R.) 32, 1244-1246
(May, 1957)

AS IS KNOWN (see, for instance, the review by Feinberg [1]), the influence of the surrounding medium on the collision of particles with a small longitudinal momentum transfer can become considerable even for high energies. Furthermore, the influence of the surrounding medium must necessarily be important in the higher order perturbation calculations because, in the integration over the 4-momentum of virtual photons, one necessarily has to include the wavelength region for which the presence of the neighboring atoms cannot be ignored. This was pointed out for the first time by Landau and Pomeranchuk [2] who noted that the magnitude of the radiative corrections is strongly influenced by the multiple scattering of the electron in the medium. Ter-Mikaelian [3] noted that the radiative corrections should be especially strongly influenced by the deviation, for soft quanta, of the dielectric susceptibility $\varepsilon(\omega)$ from unity.

In view of this, it would be of some interest to construct a covariant Feynman-Dyson perturbation theory for a phenomenological quantum electrodynamics in a medium.

A non-covariant formulation of quantum electrodynamics was given by Ginzburg [4] and Sokolov [5] and was later expanded by Watson and Jauch [6]. For the construction of a covariant perturbation theory in a medium, it is convenient to use the formulation of phenomenological quantum electrodynamics proposed by Tamm, in which the properties of the medium are described by the dielectric and magnetic susceptibility tensor $\varepsilon_{\nu\lambda\rho\sigma}$ which relates the field tensor $F_{\nu\lambda}$ to the induction tensor $H_{\nu\lambda}$:

$$H_{\nu\lambda} = \varepsilon_{\nu\lambda\rho\sigma} F_{\rho\sigma}. \tag{1}$$

In homogeneous isotropic matter, $\varepsilon_{\nu\lambda\rho\sigma}$ has the form

$$\varepsilon_{\nu\lambda\rho\sigma} = \mu^{-1} (\delta_{\nu\rho} + \varkappa u_\nu u_\rho)(\delta_{\lambda\sigma} + \varkappa u_\lambda u_\sigma). \tag{2}$$

Here u_ρ is the 4-velocity of the medium, μ is the magnetic susceptibility, $\varkappa = \varepsilon\mu - 1$, $\varkappa$ and μ are invariants; the Feynman notation is used. If the potential of the electromagnetic field is introduced in the usual way

$$F_{\rho\sigma} = \partial_\rho A_\sigma - \partial_\sigma A_\rho \tag{3}$$

and the components are constrained to the auxiliary condition

$$\partial_\rho (A_\rho + \varkappa u_\rho u_\sigma A_\sigma) = 0, \tag{4}$$

then, from the field equation

$$\partial_\nu H_{\nu\lambda} = -j_\lambda \tag{5}$$

and from (2) – (4) one obtains the following equation for the potential

$$\mu^{-1} (\partial_\rho^2 + \varkappa (u_\rho \partial_\rho)^2)(\delta_{\lambda\sigma} + \varkappa u_\lambda u_\sigma) A_\sigma = -j_\lambda. \tag{6}$$

In the Heisenberg representation of quantum theory, the field operators satisfy the same equation (5); the commutation relations for the free field operators have been found in Ref. 6. The rules for the computation of the scattering matrix elements can be easily obtained, for instance by the method of Galanin [8]. But, instead of the usual Green function for photon, the formulae will involve the Green function for the free equation (6), determined by

$$\mu^{-1} (\partial_\rho^2 + \varkappa (u_\rho \partial_\rho)^2)(\delta_{\lambda\sigma} + \varkappa u_\lambda u_\sigma) G_{\lambda\nu}(x, x') = -\delta_{\sigma\nu}\delta(x - x'), \tag{7}$$

Changing to the momentum representation, it is easy to obtain the following expression for the Green function:

$$G_{\lambda\nu}(x, x') = (2\pi)^{-2} \int d^4k\mu \left(\delta_{\lambda\nu} - \frac{\varkappa}{1+\varkappa} u_\nu u_\lambda\right) \times \{k_\rho^2 + \varkappa (u_\rho k_\rho)^2\}^{-1} \exp ik(x - x'). \tag{8}$$

The choice of the integration path with respect to the poles is determined in the following way: for positive frequencies, it is required that an infinitesimal absorption occur. For negative frequencies, the contour is chosen in such a way as to make the theory symmetric with respect to past and future.

It is also necessary to note that the denominator of the integrand in (8) vanishes if both $u_\rho k_\rho$ and k_ρ^2 tend to zero. This is due to the fact that perturbation theory is not applicable to soft quanta and leads to singularities in the expressions for the radiative corrections ("infrared catastrophe"). In order to obtain converging expressions, it is necessary to limit, in a covariant way, the integration region from the soft-quanta end. In analogy with perturbation theory in vacuum, let us introduce an additional term in the denominator of the Green function (8) – a constant λ^2 which cuts off the infrared region. The magnitude of λ depends only on the conditions of applicability of the perturbation theory and can be left unspecified if one is interested only in final results independent of λ. Taking this into account, the final expression for the Green function can be obtained in the following form

$$G_{\lambda\nu}(x, x') = (2\pi)^{-2}\int d^4k g_{i\lambda}\{k_\rho^2 + \varkappa(u_\rho k_\rho)^2 - \lambda^2\}^{-1} g_{i\nu}\exp ik(x-x'),$$
$$g_{i\lambda} = e_{i\sigma}(\delta_{\lambda\sigma} - u_\lambda u_\sigma[1-(1+\varkappa)^{-1/2}]);\ e_{i\lambda}e_{i\nu} = \delta_{\lambda\nu};\ e_{i\lambda}e_{k\lambda} = \delta_{ik}. \tag{8'}$$

This way, the matrix elements can be computed using the standard diagram technique, where an internal photon line corresponds in the momentum representation, to the factor

$$\{k_\rho^2 + \varkappa(u_\rho k_\rho)^2 - \lambda^2\}^{-1}, \tag{9}$$

and the vertices at its ends correspond to the operators

$$g_{i\nu}\gamma_\nu \tag{10}$$

To obtain the factor corresponding to a vertex with an exterior photon line, it is convenient to make use of a method mentioned by Feynman in a footnote in the second section of his paper[9]. After integrating (8) over k_4 it is easy to see that the factor corresponding to an internal line can be interpreted as the result of exchange by real photons of all possible momenta and polarizations. Since an external line corresponds to emission (absorption) of a real photon with definite momentum and polarization, it is easy to determine the relationship between the factors. The result can be formulated in the following way: in the momentum representation, a vertex with an external photon line corresponds to the operator

$$g_{i\nu}\gamma_\nu[2k_4 + u_4 2(u_\rho k_\rho)\varkappa + u_4(u_\rho k_\rho)^2\partial\varkappa/\partial(u_\rho k_\rho)]^{-1/2}. \tag{11}$$

Here, in contrast with (9) and (10), the components k_ρ are related by

$$k_\rho^2 + \varkappa(u_\rho k_\rho)^2 = \lambda^2, \tag{12}$$

which has to be considered as a definition of the dependence $\mathbf{k}(k_4)$. The other factors of the matrix element have the same form as in the case of vacuum. Let us illustrate the application of the theoretical apparatus with an example of Cerenkov radiation. The matrix element of the process is

$$S^{(1)} = -e(2\pi)^4(\bar{u}_2,\ g_{i\nu}\gamma_\nu u_1)$$
$$\times\left\{2\omega\left(1+\varkappa+\frac{1}{2}\omega\frac{\partial\varkappa}{\partial\omega}\right)\right\}^{-1/2}\delta(p_1+k_1-p_2). \tag{13}$$

The emission probability of a non-polarized photon by a non-polarized electron can be obtained in the form (medium at rest):

$$dW = \mu\frac{e^2}{4\pi}d\omega\beta\left\{1-\beta^{-2}(1+\varkappa)^{-1} + \frac{\omega}{p\beta}\frac{\varkappa}{1+\varkappa} - \frac{\omega^2}{4p^2}\left[\varkappa+\frac{\varkappa}{1+\varkappa}\right]\right\}. \tag{14}$$

The energy radiated by the electron per unit time is equal to

$$W = \frac{e^2}{4\pi}\mu\beta\int_{\omega_{\min}}^{\omega_{\max}}\omega d\omega\left\{1-\beta^{-2}(1+\varkappa)^{-1} + \frac{\omega}{p\beta}\frac{\varkappa}{1+\varkappa} - \frac{\omega^2}{4p^2}\left[\varkappa+\frac{\varkappa}{1+\varkappa}\right]\right\}. \tag{15}$$

The conservation laws determine the direction of the radiation and the limits of integration

$$\cos\vartheta = (1/\beta\sqrt{1+\varkappa}) - (\omega/2m\beta)\sqrt{1-\beta^2\varkappa}/\sqrt{1+\varkappa}. \tag{16}$$

The results coincide completely with those of Refs. 4 and 5 for $\mu = 1$ and go into the classical formula as the electron's recoils are neglected.

As a conclusion, I wish to express my gratitude

to E. L. Feinberg and M. L. Ter-Mikaelian for constant interest in this work and for valuable discussions.

[1] E. L. Feinberg, Usp. Fiz. Nauk **58**, 193 (1956).
[2] L. D. Landau and I. Ia. Pomeranchuk, Dokl. Akad. Nauk SSSR **92**, 735 (1953).
[3] M. L. Ter-Mikaelian, Izv. Akad. Nauk SSSR, Ser. Fiz. **19**, 657 (1955).
[4] V. L. Ginzburg, J. Exptl. Theoret. Phys. (U.S.S.R.) **10**, 589 (1940).
[5] A. A. Sokolov, Dokl. Akad. Nauk SSSR **28**, 415 (1940).
[6] K. M. Watson and J. M. Jauch, Phys. Rev. **74**, 950, 1485 (1948), **75**, 1247 (1949).
[7] I. E. Tamm, Zhurn. Russ. Fiz. Khim. Obshch. (J. of Russ. Chem. & Phys. Soc.) **56**, 248 (1924).
[8] A. D. Galinin, J. Exptl. Theoret. Phys. (U.S.S.R.) **22**, 448, 462 (1952).
[9] R. P. Feynman, Phys. Rev. **76**, 769 (1949).

Translated by S. Troubetzkoy
251

Two Possible Schemes of Non-Conservation Of Parity in Weak Interactions

B. L. IOFFE

(Submitted to JETP editor January 19, 1957)
J. Exptl. Theoret. Phys. (U.S.S.R.) **32**, 1246-1248
(May, 1957)

ONE OF THE possible explanations of the decay of K^+-mesons into two and three π-mesons consists in the supposition that spatial parity is not conserved in weak interactions[1]. If one accepts this hypothesis then the question arises: should charge parity and parity relative to reflection in time be conserved in weak interactions. As is well known[2], the connection between spin and statistics requires that all interactions be invariant under the product of the three transformations: reflection of the three spatial coordinates I, reflection in time T and charge conjugation C, *i.e.*, symbolically $ITC = 1$. Therefore[3] with violation of spatial parity in weak interactions ($I \neq 1$) there are three possibilities: I) weak interactions are invariant under reflection in time ($T = 1$), but are not invariant under charge conjugation, so that $IC = 1$; II) weak interactions are invariant under charge conjugation ($C = 1$) but are not invariant under reflection in time and $IT = 1$; III) weak interactions are not invariant under either charge conjugation or reflection in time, but $ITC = 1$. If one accepts the last possibility, then the fact that a K^0-meson with a long lifetime exists[4] would appear to be a pure coincidence in so far as the argument of Gell-Mann and Pais[5], on the basis of which it was predicted, and would be valid only under conservation of either charge parity or parity relative to reflection in time. This forces us to discard the third possibility and consider only the first two.

In this article we consider what physical phenomena could occur with either of these alternative possibilities.

The first of these possibilities, as remarked by Landau[6], corresponds physically to the assumption that all interactions are invariant under simultaneous interchange of right and left and change from particle to antiparticle. The physical significance of the second assumption is that all interactions remain unchanged only if the motion proceeds backwards in time together with the transition from right to left.

We consider first scheme I, *i.e.*, when, together with violation of spatial parity, invariance relative to reflection in time is conserved. At $t \to -\infty$ let there be a system of particles in state a, with particle momenta $\mathbf{p}_a$ and a mean value of spins $\mathbf{s}_a$. Let, further, as a result of interaction, this system go into a different system of particles (at $t \to \infty$) with momenta $\mathbf{p}_b$ and mean values of the spins $\mathbf{s}_b$. From the invariance under reflection in time it follows[7] that the transition matrix element $S^I_{ab}(\mathbf{p}_a, \mathbf{s}_a; \mathbf{p}_b, \mathbf{s}_b)$ is connected in the following way with the matrix element of the inverse process $S^I_{ba}(\mathbf{p}_b, \mathbf{s}_b; \mathbf{p}_a, \mathbf{s}_a)$

$$S^I_{ab}(\mathbf{p}_a, \mathbf{s}_a; \mathbf{p}_b, \mathbf{s}_b) = S^I_{ba}(-\mathbf{p}_b - \mathbf{s}_b; -\mathbf{p}_a, -\mathbf{s}_a). \quad (1)$$

The matrix element S_{ba}, viewed as a function of its arguments $\mathbf{p}_a$, $\mathbf{p}_b$, *etc.*, does not have, in general, the same functional form as the function S_{ab}. Thus, we cannot extract any help directly from Eq. (1). However, if the transition $a \to b$ is considered to go as a result of a weak interaction, then in the first non-vanishing approximation of this interaction, the relation of detailed reversibility holds:

$$S_{ab}(\mathbf{p}_a, \mathbf{s}_a; \mathbf{p}_b, \mathbf{s}_b) = -S^*_{ba}(\mathbf{p}_b, \mathbf{s}_b; \mathbf{p}_a, \mathbf{s}_a). \quad (2)$$

[For the validity of (2) it is important that the transition proceed as a result of a weak interaction, but it is not necessary that the particle motion as a whole in the initial or final states be describable

by free wave functions.] Eliminating S_{ba} from Eqs. (1) and (2), we find that in the case of invariance of the interaction under reflection in time, the transition matrix element should satisfy the equation

$$S^{I}_{ab}(\mathbf{p}_a, \mathbf{s}_a; \mathbf{p}_b, \mathbf{s}_b) = -S^{I*}_{ab}(-\mathbf{p}_a, -\mathbf{s}_a; -\mathbf{p}_b, -\mathbf{s}_b) \tag{3}$$

and, consequently, the transition probability

$$W^{I}_{ab}(\mathbf{p}_a, \mathbf{s}_a; \mathbf{p}_b, \mathbf{s}_b) = W^{I}_{ab}(-\mathbf{p}_a, -\mathbf{s}_a; -\mathbf{p}_b, -\mathbf{s}_b). \tag{A}$$

In the case of the second possible scheme, where all interactions are invariant under charge conjugation, one can carry out analogous arguments. Only here, instead of reflection in time, it is necessary to consider the transformation of reflection of all four coordinates. The matrix elements of the direct and inverse transitions turn out to be connected by the following relation:

$$S^{II}_{ab}(\mathbf{p}_a, \mathbf{s}_a; \mathbf{p}_b, \mathbf{s}_b) = S^{II}_{ba}(\mathbf{p}_b, -\mathbf{s}_b; \mathbf{p}_a, -\mathbf{s}_a). \tag{4}$$

For the validity of Eq. (2), it is only necessary that the interaction Hamiltonian be hermitean, which, obviously, occurs also in this case. Substitution from Eq. (2) into Eq. (4) gives

$$S^{II}_{ab}(\mathbf{p}_a, \mathbf{s}_a; \mathbf{p}_b, \mathbf{s}_b) = -S^{II*}_{ab}(\mathbf{p}_a, -\mathbf{s}_a; \mathbf{p}_b, -\mathbf{s}_b). \tag{5}$$

Thus, in the case of scheme II, the transition probability should satisfy the equation

$$W^{II}_{ab}(\mathbf{p}_a, \mathbf{s}_a; \mathbf{p}_b, \mathbf{s}_b) = W^{II}_{ab}(\mathbf{p}_a, -\mathbf{s}_a; \mathbf{p}_b, -\mathbf{s}_b). \tag{B}$$

Using (A) and (B) it is easy to establish the general form of the transition amplitudes for both possible schemes of non-conservation of parity.

We consider, for example, the decay of a stationary polarized λ-particle, $\lambda^0 \to p + \pi^-$. In this case, the λ-particle decay is characterized by three vectors: the spin vector of the λ-particle $\mathbf{s}_\lambda$, the proton momentum $\mathbf{p}_p$ and the proton spin $\mathbf{s}_p$. We will be interested only in pseudoscalar quantities, arising because of non-conservation of parity. From these three vectors it is possible to construct three such quantities: $\mathbf{s}_p\mathbf{p}_p$, $\mathbf{s}_\lambda\mathbf{p}_p$ and $[\mathbf{s}_\lambda\mathbf{s}_p]\mathbf{p}_p$. From Eqs. (A) and (B) it then follows that in the case of scheme I the probability can contain terms proportional to $\mathbf{s}_p\mathbf{p}_p$ and $\mathbf{s}_\lambda\mathbf{p}_p$ whereas in the case of scheme II only terms proportional to $[\mathbf{s}_\lambda\mathbf{s}_p]\mathbf{p}_p$ can enter into the probability. Thus in scheme I, upon decay of the λ^0-particle one can expect polarization of the decay protons parallel (or anti-parallel) to the direction of their momenta, and, if the λ-particle is polarized, most of the decay protons will have momenta parallel (or anti-parallel) to the spin of the λ-particle. (This effect was considered by Lee and Yang[1].) In scheme II the effect of non-conservation of parity can be detected only by observing the polarization of the protons in decay of polarized λ-particles, or, equivalently, by measuring the directions of the momentum and spin of the proton relative to the normal of the plane in which the λ-particle was produced.

Type of decay	Scheme I T = inv.	Scheme II C = inv.
Λ	$\mathbf{s}_p\mathbf{p}_p$; $\mathbf{s}_\Lambda\mathbf{p}_p$	$[\mathbf{s}_\Lambda\mathbf{s}_p]\,\mathbf{p}_p$
β	$\mathbf{s}_e\mathbf{p}_e$; $\mathbf{s}_e\mathbf{p}_N$ $\mathbf{I}_N\mathbf{p}_e$; $\mathbf{I}_N\mathbf{p}_N$	$[\mathbf{s}_e\mathbf{I}_N]\,\mathbf{p}_e$ $[\mathbf{s}e\mathbf{I}_N]\,\mathbf{p}_N$
π	$\mathbf{s}_\mu\mathbf{p}_\mu$	—
μ	$\mathbf{s}_\mu\mathbf{p}_e$; $\mathbf{s}_e\mathbf{p}_e$	$[\mathbf{s}_\mu\mathbf{s}_e]\,\mathbf{p}_e$

Analogously, one can determine the pseudoscalar quantities acceptable in each scheme for other weak decays. The results given in the table (the indices λ, p, e, μ denote the spin and momenta of the respective λ^0, proton, electron, μ-meson; in the case of β-decay: I_N is the spin of the initial nucleus, $\mathbf{p}_N$ is the nuclear recoil momentum, the remaining momenta are averaged over).

It is interesting to note that dipole moments of the nucleus are absent[6] in scheme I, but can occur in scheme II. In fact, the energy of interaction of a dipole moment with an electric field is proportional to $\mathbf{sE}$. Under time reflection, $\mathbf{s} \to -\mathbf{s}$ and $\mathbf{E} \to -\mathbf{E}$, and under reflection of all four coordinates $\mathbf{s} \to -\mathbf{s}$ and $\mathbf{E} \to -\mathbf{E}$ so that $\mathbf{sE} \to -\mathbf{sE}$ in scheme I and $\mathbf{sE} \to \mathbf{sE}$ in scheme II.

The author is grateful to Academician L. D. Landau, whose work in the field of non-conservation of parity stimulated the present work, and also to L. B. Okun' and A. P. Rudik for discussions which greatly furthered the consideration of the problems touched upon here.

[1] T. D. Lee and C. N. Yang, Phys. Rev. **104**, 254 (1956).

[2] W. Pauli, *Niels Bohr and the Development of Physics*, 1955.

[3] Ioffe, Okun', and Rudik, J. Exptl. Theoret. Phys. (U.S.S.R.) **32**, 396 (1957), Soviet Phys. JETP **5**, 328 (1957).

[4] Lande, Booth, Impeduglia, Lederman and Chinowsky, Phys. Rev. 103, 1901 (1956). Fry, Schneps, and Swami, Phys. Rev. 103, 1904 (1956).

[5] M. Gell-Mann and A. Pais, Phys. Rev. 97, 1387 (1955).

[6] L. D. Landau, J. Exptl. Theoret. Phys. (U.S.S.R.) 32, 405 (1957), Soviet Phys. JETP 5, 336 (1957).

[7] J. Blatt and V. F. Weisskopf, *Theoretical Nuclear Physics*, IIL, 1954 (Russian translation).

Translated by G. E. Brown
252

Non-Conservation of Parity and Hyperon Decay

S. G. MATINIAN
Institute of Physics, Academy of Sciences, Georgian SSR

(Submitted to JETP editor January 24, 1957)
J. Exptl. Theoret. Phys. (U.S.S.R.) 32, 1248-1249 (May, 1957)

THE NON-CONSERVATION of parity in weak decay interactions[1,2] leads to a series of effects, the study of which allows one to establish whether, in reality, weak interactions are non-invariant relative to reflection of spatial coordinates, and also to clarify a number of other questions connected with this. In this note, the decay of hyperons by interactions which do not conserve spatial parity is considered. For simplicity we restrict ourselves to non-derivative couplings and to hyperon spins equal to ½.

The interaction Hamiltonian leading to the decay has the form

$$H = g\bar{\psi}_N(1+\lambda\gamma_5)\psi_Y\varphi_\pi^* \qquad (1)$$

where ψ are spinor wave functions and φ_π is the wave function of the π-meson; λ is a quantity, which is complex in general, characterizing the degree of non-conservation of parity. The existence of K^0-particles with long lifetimes[3] can be made compatible with non-conservation of parity if we assume that either temporal or charge parity is conserved (see Ref. 4 with regard to this). In the first case λ is a real constant, in the second purely imaginary.

We now consider a hyperon at rest, the spin of which is directed along the unit vector $\boldsymbol{\eta}$. Calculation of the square of the matrix element M of the interaction (1), leading to emission of a nucleon with a given direction of momentum $\mathbf{n}$ and spin along the unit vector $\boldsymbol{\zeta}$, gives

$$|M|^2 = \frac{1}{4}\left\{\left(1+\frac{m}{E_N}\right)(1+\eta\zeta) + |\lambda|^2\left(1-\frac{m}{E_N}\right)(1-\eta\zeta)\right.$$
$$+2|\lambda|^2 p^2[(n\eta)(n\zeta)/E_N(E_N+m)] \qquad (2)$$
$$\left.+(\lambda+\lambda^+)\frac{p}{E_N}(n\eta+n\zeta)+i(\lambda-\lambda^+)\frac{p}{E_N}(n[\eta\zeta])\right\}.$$

Here m is the mass of the nucleon, $E_N = \sqrt{p^2+m^2}$, $p = \sqrt{2\mu^* Q}$, where μ^* is the reduced mass of the π-meson and nucleon; Q is the energy of decay of the hyperon; $\hbar = c = 1$. The first three terms in the braces correspond to the usual treatment with conservation of charge for even (terms with $|\lambda|^2$) and odd (terms without $|\lambda|^2$ hyperons. Non-conservation of parity leads to the appearance of the pseudoscalar (relative to spatial reflection) quantities: $\mathbf{n}\eta$, $\mathbf{n}\zeta$, $\mathbf{n}[\eta\times\zeta]$.

If the Hamiltonian H is invariant relative to time-reflection, then the term $\mathbf{n}[\eta\times\zeta]$ drops out. In this case, contrary to the usual situations, even in the decay of unpolarized hyperons (absence of the term with η) there will be a term of the order of the nucleon velocity (v/c) giving nucleons polarized along $\mathbf{n}$. This term would be particularly noticeable for Σ-hyperons.

In case of invariance of H relative to charge conjugation the terms with $\mathbf{n}\eta$ and $\mathbf{n}\zeta$ drop out and the term proportional to $\mathbf{n}[\eta\times\zeta]$ remains, giving an additional correlation of the spins of the polarized hyperons and nucleons, different from that which would occur for variants with conservation of parity (this term leads to a mutually-perpendicular orientation of the spins). A similar situation arises in the case of gradient coupling.

Ioffe[5] arrived at analogous conclusions, starting from general considerations (within the framework of perturbation theory), about invariance of the decay probabilities relative to time-reflection and charge conservation, respectively.

In conclusion, we note that if there is invariance under reflection in time, then non-conservation of parity leads to correlation between the direction of emission of the Λ^0-particle in the decay of the Ξ^--hyperon and the direction of emission of the nuclei in the rest system of the Λ^0-particle in its subsequent decay, even for a Λ^0-spin equal to ½. A simple consideration leads to a correlation function of the form $a + b\cos\vartheta$, where ϑ is the angle between the directions indicated above.

In the case of invariance under charge conjugation, this effect does not arise.

I would like to express my gratitude to B. L. Ioffe for a useful discussion.

[1] T. D. Lee and C. N. Yang, Phys. Rev. **104**, 254 (1956).

[2] L. D. Landau, J. Exptl. Theoret. Phys. (U.S.S.R.) **32**, 405 (1957). Soviet Phys. JETP **5**, 336 (1957).

[3] Lande, Booth, Impeduglia, Lederman and Chinowsky, Phys. Rev. **103**, 1901 (1956). Fry, Schneps and Swami, Phys. Rev. **103**, 1904 (1956).

[4] Ioffe, Okun', and Rudik, J. Exptl. Theoret. Phys. (U.S.S.R.) **32**, 396 (1957), Soviet Phys. JETP **5**, 328 (1957).

[5] B. L. Ioffe, J. Exptl. Theoret. Phys. (U.S.S.R.) **32**, 1246 (1957). Soviet Phys. JETP **5**, 1015, this issue (1957).

Translated by G. E. Brown
253

Nuclear Photoeffect in Be^9 at High Energies

T. I. KOPALEISHVILI
Tbilisi State University

(Submitted to JETP editor January 30, 1957)
J. Exptl. Theoret Phys. (U.S.S.R.) **32**, 1249-1250
(May, 1957)

ÜBERALL [1] HAS INVESTIGATED the $Be^9(\gamma_1 n)Be^8$ reaction on the basis of the one particle model in the γ-energy interval 20–200 Mev. The interaction energy curve of the (Be^8, n) system is taken in the form of a potential well having spherical symmetry. He studies both the electric and magnetic transitions of the system taking account of retardation.

The Born approximation gives a photoneutron angular distribution proportional to $\sin^2\theta$ as well as the energy dependence of the total effective cross section. The cross section curve, generally falling with increasing energy, has zeros at several energy values (curve *1* of the figure), which do not correspond with the experimental data.

Überall shows that such an oscillation of the total cross section curve is possibly due to the special choice of the potential in the form of a square well. One can expect that with a different choice of the interaction potential the total cross section may not oscillate. To test this idea we investigated the same reaction taking as the interaction potential of the (Be^8, n) system the potential of an oscillator, terminated at some point $r = r_0$.

Our work [2] showed that with this choice of potential the wave function of the (Be^8, n) system can be represented with satisfactory approximation in the form

$$R(r) = \sqrt{2/3}\,(2\pi)^{-1/4}(r_0')^{-3/2}\exp\{-1/4\,(r/r_0')^2\}\,r/r_0', \tag{1}$$

where r_0' is a parameter proportional, on one hand, to the most probable distance between the nuclear core of B^8 and the neutron, and on the other hand, to the nuclear radius. The parameter r_0' may be regarded as the quantity which characterizes the behavior of the wave function inside the nucleus and hence in some measure takes into account the structure of the nucleus.

The differential cross section, found from Eq. (1), is likewise proportional to $\sin^2\theta$. The total effective cross section, as found by us, takes the form:

$$\sigma = 4.82\cdot 10^{-29}\delta^5\,[\hbar\omega]^{3/2}\exp[-0.094\delta^2\hbar\omega], \tag{2}$$

where $\delta = r_0' \times 10^{13}$ cm^{-1}, and $\hbar\omega$ is in Mev. Equation (2) shows the total effective cross section falling off exponentially with increasing γ-energy, while the damping coefficient depends upon r_0'.

It is easily seen that to get quantitative agreement between theory and experiment it is sufficient to set

$$\delta = 1.6\,(20/\hbar\omega)^{2/5}. \tag{3}$$

In this case we will have for the total effective cross section

$$\sigma = 2.36\cdot 10^{-25}\exp[-5.15\,(\hbar\omega/20)^{1/5}]\,(\hbar\omega)^{-1/2}. \tag{4}$$

The energy dependence of the effective cross section obtained from Eq. (4) is shown by Curve *2* of the figure. The experimental points, shown by crosses, fit the theoretical curve well.

The energy dependence of the parameter r_0', expressed by Eq. (3), can be determined approximately from the wave function (1). The point is that at high γ-energies the excitation of the nucleus is so large that it is not legitimate to assume that the liberated neutron leaves the nucleus in the definite stationary state given by the wave function (1). The energy dependence of r_0', apparently, in some measure takes account of the change in state of the (Be^8, n) system under the influence of radiation. As Eq. (3) shows, an increase in the γ-energy reduces r_0', which is natural, since with increasing excitation of the nucleus the role of the smaller dis-

tances should become more and more important in releasing the neutron.

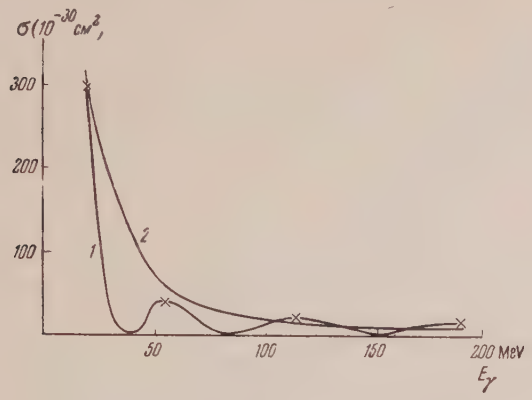

At $\hbar\omega = 5$–8 Mev Eq. (3) gives $r_0' \approx 2.6 \times 10^{-13}$ cm. This particular value agrees with the experiment on the collision of the deuteron with the beryllium nucleus, treated in Ref. (2).

If we consider that in the energy range 20–200 Mev, where there is a satisfactory agreement between theory and experiment, r_0' changes only by a factor 2.5, we can conclude that the assumption of a slow energy dependence of r_0' will explain the experimental data over a wide range of γ-energies.

In conclusion I wish to thank Prof. V. I. Mamasakhlisov for helpful discussions.

[1] H. Überall, Z. Naturforsch., 8a, 142 (1953).

[2] T. I. Kopaleishvili. Trudy (Transactions), Tbilisi State University, 62, 1957 (in press).

Translated by C. V. Larrick
254

Distribution of the Electron-Photon Component on the Periphery of Extensive Air Showers of Cosmic Rays

S. I. NIKOL'SKII AND V. M. SELEZNEV
P. N. Lebedev Physics Institute, Academy of Sciences, U.S.S.R.

(Submitted to JETP editor February 4, 1957)
J. Exptl. Theoret. Phys. (U.S.S.R.) 32, 1250-1252 (May, 1957)

INVESTIGATIONS of the lateral distribution function of the electron-photon component of extensive air showers at 3860 m were carried out by means of an experimental set-up [1] consisting of a large number of hodoscoped counters placed at various distances from each other. Counters intended for the measurement of the flux density of all charged particles in the shower were placed under thin covers made of aluminum and wood ($\sim 2 g/cm^2$). The particle flux density at a given distance from the axis of the shower was determined according to the formula

$$\rho(r) = \frac{1}{\sigma} \ln \frac{n}{n-m}$$

This formula makes it possible to determine the most probable value of the flux density of charged particles that discharge m out of the total number of n counters, each of area σ, situated in the given place of observation.

In the case when $\rho\sigma n \lesssim 1$ the determination of the particle flux density in an individual case of shower detection is impossible. In such cases the particle flux density was determined for a group of showers identical with respect to the total number of particles and the position of the shower axes. It was assumed that n equals the product of the total number of counters by the number of showers of a given group and m is the total number of counter discharges during the passage of all showers of the group. Test computation showed that the probable value of the particle flux density in a given group of showers is, within the limits of statistical accuracy, the same as the mean weighted value of the probable values of the particle flux density determined for each separate shower of the group.

We considered three groups of extensive air showers with definite axis positions. The first group comprised showers with a total number of particles between 5×10^4 and 1×10^5. The energy of primary particles producing these showers can be estimated [2] as $\bar{E}_0 = 1.6 \times 10^{14}$ ev. The limits of the total number of shower particles and the corresponding mean energy of primaries for the second and third group were $1.5 \times 10^5 - 2.6 \times 10^5$ ($\bar{E}_0 = 5 \times 10^{14}$ ev) and $5 \times 10^5 - 13 \times 10^5$ ($\bar{E}_0 = 16 \times 10^{14}$ ev). The lateral distribution functions of all charged particles obtained for the three groups of showers are shown in Fig. 1. The plotted lateral distributions for distances from the axis smaller than 40 m are based on previously published results [3].

The experimental data given in Fig. 1 characterize the lateral distribution of the electron-photon component of the shower only at distances from the axis smaller than ~ 100 m, where the relative contribution of penetrating particles is not appreciable.

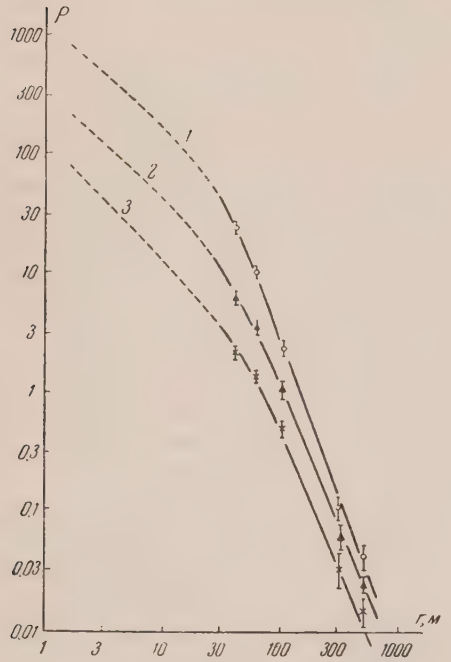

FIG. 1

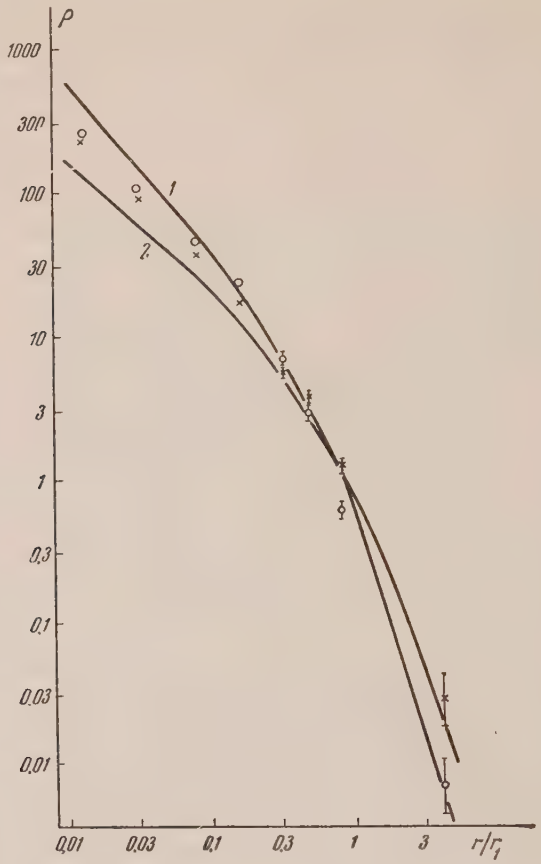

FIG. 2

FIG. 1. Lateral distribution of charged particles in extensive atmospheric showers, caused by particles with different energies. $1-\bar{E}_0 \approx 1.6\times 10^{15}$; $2-\bar{E}_0 \approx 5\times 10^{14}$; $3-\bar{E}_0 \approx 1.6\times 10^{14}$ ev.

FIG. 2. Lateral distribution of electron-photon component of extensive atmospheric showers. Number of electrons in showers: $\circ - 7.4\times 10^5$; $\times - 7.7\times 10^4$; value of s is: for $1-1$, for $2-1.4$; $r_1 = 125$ m.

To determine of the lateral distribution of the electron-photon component on the shower periphery it is necessary to account for the share of μ-mesons in the total flux of charged particles. The lateral distribution and the energy spectrum at various distances from the axis were obtained in the same series of measurements [1,4]. In consistence with these, the number of μ-mesons with energy $\geqslant 250$ Mev, multiplied by 1.3, was substracted from the total flux of charged particles at 100 and 500 meters from the axis, to account for the electron-photon component in equilibrium with the μ-mesons. The results for showers with 7.4×10^5 and 7.7×10^6 electrons not in equilibrium with μ-mesons are shown in Fig. 2. The functions of the lateral distribution of electrons calculated according to the electromagnetic cascade theory [5] for two values of the parameter s are shown in the same figure. The experimental values of the electron flux density at various distances from the axis and the theoretically calculated functions of lateral distribution are normalized to the same number of electrons at distances between 0 and 1000 m (2×10^5).

It can be seen from Fig. 2 that the lateral distribution of electrons on the periphery of extensive air showers varies with the energy of the shower-producing primary. Comparison of the experimental data with the calculations of Nishimura and Kamata [5] indicates that the lateral distribution of electrons in extensive air showers produced by primaries with the energy of $\sim 2\times 10^{14}$ ev coincides with the calculated distribution of the electron-photon cascade for the parameter $s = 1.2$. Such a value of the parameter can be expected from the altitude develop-

ment of extensive air showers[6,7].

The lateral distribution of electrons in extensive air showers produced by primaries with the energy of $(1-2) \times 10^{15}$ ev does not conform with the functions calculated by Nishimura and Kamata for the distribution of electrons in the electron-photon cascade for any value of the parameter s, including $s = 1.2$.

[1] Vavilov, Evstigneev, and Nikol'skii, J. Exptl. Theoret. Phys. (U.S.S.R.) 32, 1319 (1957), Soviet Phys. JETP 5, in press (1957).

[2] K. Greisen, Progress in Cosmic Ray Physics, v. III, Amsterdam 1956.

[3] Dobrovol'skii, Nikol'skii, Tukish, and Iakovlev, J. Exptl. Theoret. Phys. (U.S.S.R.) 31, 939 (1956), Soviet. Phys. JETP 4, 799 (1957).

[4] Dovzhenko, Nelepo, and Nikol'skii, J. Exptl. Theoret. Phys. (U.S.S.R.) 32, 463 (1957), Soviet Phys. JETP 5, 391 (1957).

[5] I. Nishimura and K. Kamata, Progr. Theor. Phys. 6, 628 (1951).

[6] I. L. Rozental', J. Exptl. Theoret. Phys. (U.S.S.R.) 22, 92 (1952).

[7] G. B. Khristiansen, The Oxford Conference on Extensive Air Showers, s. 11, Harwell, 1956.

Translated by H. Kasha
255

On Quasiclassical Single-Electron Wave Functions

N. I. ZHIRNOV
Moscow State Pedagogical Institute

(Submitted to JETP editor February 13, 1957)
J. Exptl. Theoret. Phys. (U.S.S.R.) 32, 1252-1254
(May, 1957)

FOR THE PURPOSE OF evaluating the matrix elements for various interactions between matter and a radiation field it is necessary to have good nonrelativistic wave functions of the radiating electron. Hydrogen-like functions or Slater functions are ordinarily used in calculations. However, the results obtained by using these functions are not accurate because they do not take into account the influence of all other electrons of an atom on the radiating electron, or do so insufficiently.

We have constructed approximate wave functions for an electron in bound states which allow for the electrostatic screening effect of the atomic electrons on the radiating electron. The calculations were based on a combination of the Fermi-Thomas statistical method of obtaining the effective electrostatic field which acts on an individual electron in an atom with a generalized quasiclassical method of calculating wave functions in a given potential field.

The effective electrostatic field acting on a radiating electron in a heavy atom can be described by the Thomas-Fermi potential corrected at small and large distances from the nucleus, as follows:

$$U(r) = \begin{cases} -Z(1-\alpha r)/r, & r \leqslant 1/Z; \\ -\dfrac{1}{r} - \dfrac{(Z-1)}{r}\varphi_0\left(\dfrac{r}{\mu}\right); & 1/Z \leqslant r \leqslant r_0, \\ -1/r; & r \geqslant r_0, \end{cases} \quad (1)$$

where r_0 is the boundary radius of a $(Z-1)$-fold ionized atom in the Thomas-Fermi statistical model and the constant α is determined from the continuity of the potential at $r = 1/Z$ [all quantities in Eq. (1) are measured in atomic units].

Since $U(r)$ is a centrally symmetrical field the angular dependence of the eigenfunctions ψ is exactly the same as in the case of the hydrogen atom. The problem is therefore reduced to the calculation of the radial functions $R_{nl}(r)$ from the equation

$$d^2\varkappa_{nl}(r)/dr^2 + \{2[\varepsilon_{nl} - U(r)] - l(l+1)/r^2\}\varkappa_{nl}(r) = 0,$$
$$\varkappa_{nl}(r) = rR_{nl}(r), \quad (2)$$

where $U(r)$ is taken from (1).

The solutions of (2) are obtained quasiclassically in the generalized form first indicated by Fock and by Petrashen'[1] and later by other authors[2]. Using the Fock-Petrashen' method the desired solutions of (2) can be represented approximately as

$$\varkappa_{nl}(r) = A(S')^{-1/2}\varphi[S(r)], \quad (3)$$

where $\varphi(S)$ is the solution of the radial Schroedinger equation with a Coulomb potential:

$$\varphi(S) = SR_{nl}^{\text{hydr}}(S),$$

and $S = S(r)$, which we shall call the screening function, is determined from the equation

$$\int_{r_1}^{r} \sqrt{2[\varepsilon_{nl} - U(r)] - \frac{l(l+1)}{r^2}}\, dr = \int_{S_1}^{S} \sqrt{-\frac{Z^2}{n^2} + \frac{2Z}{S} - \frac{l(l+1)}{S^2}}\, dS. \quad (4)$$

The approximate energy eigenvalues ε_{nl} are obtained from

$$\int_{r_1}^{r_2} \sqrt{2[\varepsilon_{nl} - U(r)] - \frac{l(l+1)}{r^2}}\, dr = \pi [n - \sqrt{l(l+1)}].$$

(for states with $l \neq 0$) and

$$\int_0^{r_1} \sqrt{2[\varepsilon_{no} - U(r)]}\, dr = n\pi$$

(for s states), where r_1, r_2 and S_1, S_2 are the roots of the integrands.

Energy values have been calculated for Ag and In atoms in 1s, 2s, 2p, 3s, 3p, 3d and 4p states and Gd in 3p, 3d, 4p and 4d states. These energies (in Rydbergs) are given in Table 1.

TABLE 1.

Atom	1s	2s	2p	3s	3p	3d	4p	4d
Ag	1791.2	260.5	241.7	50.0	42.6	29.4	5.9	—
In	1956.4	289.9	268.4	57.2	48.7	34.6	7.2	—
Gd	—	—	—	—	108.6	87.1	20.4	12.2

Our calculated energy levels are in quite satisfactory agreement with experiment[3]; the discrepancies do not exceed 6 to 7% except for the outermost electronic shells. For such shells the statistical method of describing the electrostatic field is no longer valid.

The single-electron wave functions obtained by the Fock-Petrashen' method are continuous over the entire field under consideration, so that they can be used for calculation of the matrix elements. But the screening function $S(r)$, as seen from Eq. (4), cannot be represented in exact analytic form; therefore the matrix elements based on the approximate single-electron functions (3) can only be calculated numerically. In order to avoid numerical integration and represent the approximate radial functions (3) in analytic form the screening function must be suitably approximated. Numerical calculations of the screening functions for several of the above states showed that they can be approximately represented by logarithmic functions of the form $a \ln(1 + br)$, where a and b are such that

$$a \ln(1 + br_2) = S_2,\ (dS/dr)_{r=r_2} = ab/(1 + br_2)$$

The screening function is very well approximated by $S(r) = a \ln(1 + br)$ in the spatial region which is most important for calculation of the matrix elements. This approximation of the screening functions also permits a relatively easy calculation of the normalization constants A in the approximate wave functions (3).

The approximate radial functions (3) are finally of the form (the 3p state of indium being used as an example):

$$R_{31} = \frac{1{,}887 \cdot 10^3}{a_0^{1/2}} \left\{ \left[\ln\left(\frac{0{,}789}{a_0} r + 1\right) \right]^2 \right.$$

$$\left. r \left(\frac{0{,}789}{a_0} r + 1\right)^{17{,}76} \right\} \left[1 - 9{,}13 \ln\left(\frac{0{,}789}{a_0} r + 1\right) \right].$$

Our approximate radial functions (3) have been used to calculate the relative intensities of the K-series lines of silver and indium X-ray spectra. The intensities are listed in Table 2 (with the intensity of K_{α_1} taken as 100) and compared with the available experimental values[4,5].

TABLE 2.

Transition	Line	Ag			In		
		Calculated intensity	Experimental values		Calculated intensity	Experimental values	
			Meyer[4]	Williams[5]		Meyer[4]	Williams[5]
$K \to L_{II}$	K_{α_2}	50	51.7	49.9	50	51.8	49.9
$K \to L_{III}$	K_{α_1}	100	100	100	100	100	100
$K \to M_{II+III}$	$K_{\beta_1+\beta_3}$	27.2	24	29	24.7	21.7	29.6
$K \to N_{II+III}$	K_{β_2}	5.14	4.22	6.17	4.48	3.65	6.47

A comparison of our results with the theoretical calculations of others who used hydrogen-like wave functions shows that our quasiclassical radial functions give much better agreement with experiment. lines as calculated by the use of hydrogen-like functions are 50: 100: 34: 12 for all atoms, which does not agree with experiment.

In conclusion I must express my gratitude to B. T. Geilikman, who directed this work.

[1] V. A. Fock, Dokl. Akad. Nauk SSSR 3, 147 (1934). M. I. Petrashen', Uch. Zap. LGU, Ser. Fiz., 7, 59 (1949); Dokl. Akad. Nauk SSSR 50, 147 (1945).

[2] S. C. Miller and R. H. Good, Phys. Rev. 91, 174 (1953); S. C. Miller, Phys. Rev. 94, 1345 (1954).

[3] E. Vainshtein and M. Kakhana, *Tables for X-Ray Spectroscopy*, Acad. Sci. U.S.S.R., 1953.

[4] H. T. Meyer, Wissenschaftliche Veroeffentlichungen aus dem Siemens-Konzern 7, 108 (1929).

[5] J. H. Williams, Phys. Rev. 7, 661 (1930) [sic!].

Translated by I. Emin
256

Magnetic Properties of Oxides of Manganese at Temperatures from 20 to 300° K

A. S. BOROVIK-ROMANOV AND M. P. ORLOVA
All-Union Scientific Research Institute of Physico-Technical and Radiotechnical Measurements

(Submitted to JETP editor Feb. 7, 1957)
J. Exptl. Theoret. Phys. (U.S.S.R.) 32, 1255-1256 (May, 1957)

IN CONNECTION with the anomaly in the magnetic properties of manganese carbonate below 31° K, discovered by the authors[1], it was deemed of interest to study the magnetic properties of oxides of manganese at low temperatures. These were the most probable impurities in the preparations studied. The magnetic properties of manganese monoxide (MnO) and of manganese dioxide (MnO_2) have been studied in detail by a number of authors[2]. Both compounds become antiferromagnetic at temperatures 122° K (MnO) and 84°K (MnO_2).

Measurements of the magnetic susceptibility of Mn_2O_3 and Mn_3O_4 were carried out on natural samples of these compounds in the temperature range 20 to 300° K. The measurements were made on the same samples of hausmannite (Mn_3O_4) and of braunite (Mn_2O_3) for which a physico-chemical analysis had earlier been made by Rode[3]. In Rode's judgment, the composition of these samples was quite close to stoichiometric.

The results of the measurements of the magnetic susceptibility of hausmannite (Mn_3O_4), in the temperature range 43 to 300° K, are presented in Fig. 1 as a plot of $1/\chi$ *vs.* T (curve 1). Below 42.5° K, hausmannite exhibits characteristic ferromagnetic properties. In Fig. 2 is drawn a curve showing the dependence of the magnetic moment M on the field H for 20.4° K. Hausmannite has the structure of a spinel elongated in the [001] direction[4]. Therefore it is natural to suppose that hausmannite, like the ferrites, is antiferromagnetic with an uncompensated moment. The ordering temperature is $T_C = 42.5°$ K.

The temperature dependence of the inverse magnetic susceptibility in the paramagnetic range agrees qualitatively with the formula proposed by Néel[5] for such substances,

$$1/\chi = \frac{T}{C_{\text{mol}}} + \frac{1}{\chi_0} - \frac{s}{(T-\Theta)}. \qquad (1)$$

Curve 2 of Fig. 1 corresponds to formula (1) with the following values of the constants:

$$C_{\text{mol}} = C\,(Mn^{++}) + 2C\,(Mn^{+++}) = 10{,}4;$$

$$1/\chi_0 = 91{,}3;\ s = 3480,\ \Theta = 31{,}1.$$

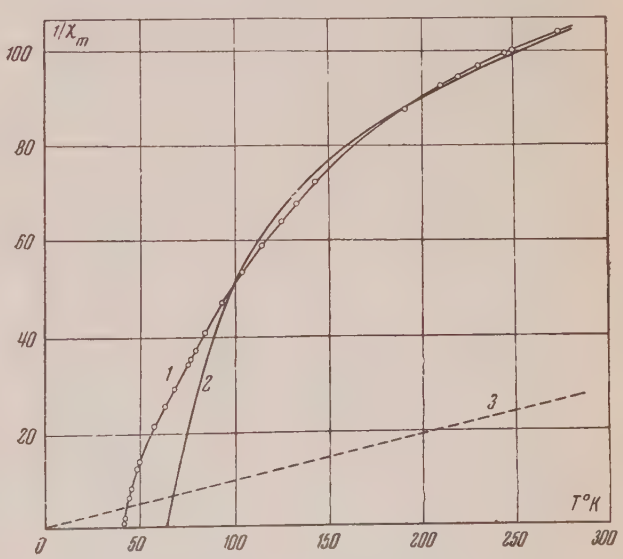

FIG. 1. Temperature dependence of the inverse magnetic susceptibility (molar) of hausmannite (Mn_3O_4). 1—experimental curve; 2—Néel's formula; 3—Curie's law.

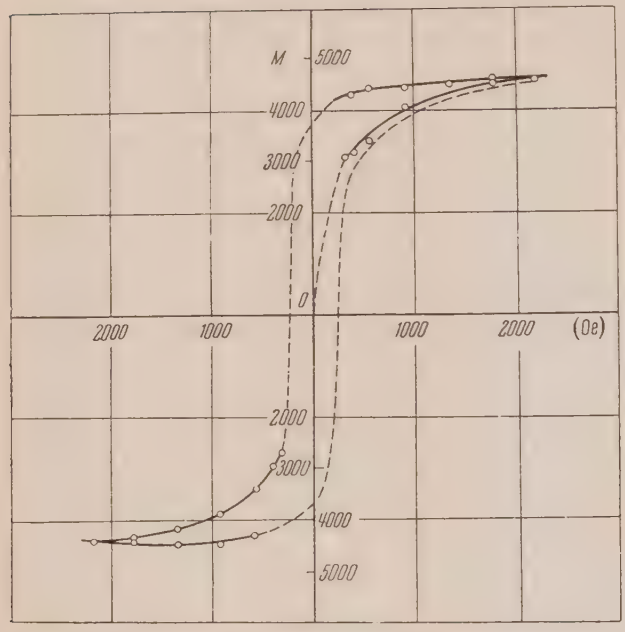

FIG. 2. Dependence of the magnetic moment (molar) of hausmannite on the field ($T = 20.4°$ K).

For comparison, Curve 3 has been drawn in Fig. 1; it corresponds to Curie's law with the constant C_{mol} given above.

Figure 3 shows the curve obtained by us for the temperature dependence of the inverse magnetic susceptibility of braunite (Mn_2O_3). Braunite remains paramagnetic over the whole range of temperatures studied. Below 120° K we observe an anomalous behavior of the susceptibility. The reason for this anomaly is not clear. It may be due to insufficient purity of the sample.

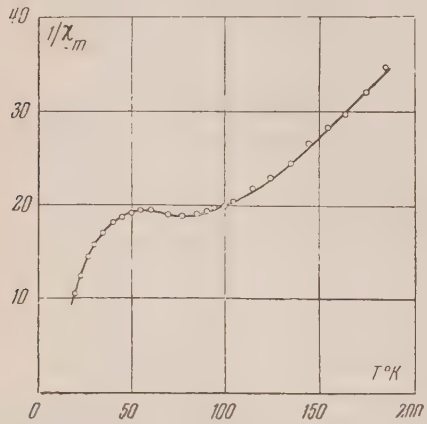

FIG. 3. Temperature dependence of the inverse magnetic susceptibility of braunite (Mn_2O_3).

[1] A. S. Borovik-Romanov and M. P. Orlova, J. Exptl. Theoret. Phys. (U.S.S.R.) 31, 579 (1956), Soviet Phys. JETP 4, 531 (1957).

[2] Bizette, Squire, and Tsai, Compt. rend. 207, 449 (1938); H. Bizette, J. phys. et radium 12, 161 (1951).

[3] V. V. Rode, Izv. sektora fiz.-khim. analiza Akad. Nauk SSSR 19, 5 (1949).

[4] R. Wyckoff, Crystal Structures, vol. 2 (Interscience Publishers, Inc., New York, 1951).

[5] L. Néel, Ann. phys. 3, 137 (1948).

Translated by W. F. Brown, Jr.
257

Visual Observation of the Stratification of Solutions of He^3-He^4

V. P. PESHKOV AND K. N. ZINOV'EVA
Institute for Physical Problems,
Academy of Sciences, U.S.S.R.

(Submitted to JETP editor February 14, 1957)
J. Exptl. Theoret. Phys. (U.S.S.R.) 32, 1256-1257
(May, 1957)

AS WALTERS AND FAIRBANK[1] have recently pointed out, solutions of He^3-He^4 at temperatures below 0.8° K separate into two phases with different concentrations of He^3. Making use of the nuclear resonance technique, these authors carried out measurements of the phase diagram of solutions of He^3-He^4 in the temperature range 0.25–0.85° K.

We have set up experiments on the visual observation of the stratification of solutions of He^3-He To obtain the low temperatures, we pumped vapors of He^3 which were condensed in a small transparent Dewar of volume of about 3 cm^3 (Fig. 1).

A glass ampoule *b* with a volume of about 200 mm^3 (diameter of the ampoule 3.5 mm, height 20 mm) was placed inside the Dewar *a*. The ampoule was joined by the copper link *c* to a thin steel capillary *d*, of internal diameter 0.5 mm, which led out of the Dewar.

The gaseous mixture He^3-He^4 along the capillary was condensed in the ampoule so that the meniscus between the liquid and the vapor remained below the copper connection. A mixture of 51.1% He^3-He^4 concentration was used in the experiment. Condensation took place at 1.1° K. At this temperature, the solution was a homogeneous transparent liquid.

Under a slow decrease of temperature, the solu-

tion remained homogeneous down to 0.81° K. The temperature of the solution was determined by the vapor pressure of He^3, measured with a McLeod gauge. Upon reaching a temperature 0.81 ± 0.01° (vapor pressure of He^3 = p = 3.0 ± 0.1 mm Hg), a thin transparent layer appeared on the surface of the liquid. This layer sharply defined the horizontal boundary below.

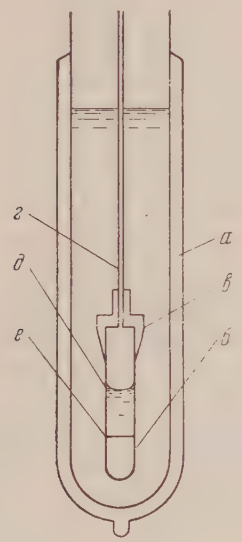

FIG. 1. *a* – Dewar with He^3, *b* – glass ampoule, *c* – copper link, *d* – steel capillary, *e* – liquid-vapor meniscus, *f* – stratification boundary.

As the temperature falls, the boundary dividing the two phases of the solution moves downward; at 0.5° K it occupies a position corresponding to that shown in Fig. 2. Upon increase in the temperature, the dividing boundary slowly rises, and at 0.81° K it combines with the meniscus of the liquid-vapor. In contrast with the concave meniscus of the upper phase, the boundary dividing the two phases has the form of a horizontal line for all temperatures. Shaking and jarring the apparatus has no effect on the position of the boundary.

The temperature of the stratification of the solution with concentration 51.1% was determined by a series of repeated observations of the appearance and disappearance of the boundary on cooling and heating. The value of 0.81° K which we found here agrees well with the measurements of Walters and Fairbank.

It was of interest to establish whether the liquid in the upper phase was normal or superfluid. Measurements of the λ-transitions in solutions of high concentration, carried out by Daunt and Heer[2], suggest the normal state for this phase; however, their measurements are not sufficiently dependable. In accord with the latest data of Esel'son, Berezniak and Kaganov[3], the curve of the λ-point for solutions with concentrations to 38% is significantly higher than the previous curve[4]. Extrapolation of the data of Esel'son *et al.* in the direction of higher concentrations does not contradict superfluidity of both phases.

FIG. 2. Photograph of stratification of a solution with 51.1% concentration at 0.5° K.

We set up an experiment in which a glass test tube, open from above, with inside diameter 1 mm and length 8 mm, was suspended on a wire inside the ampoule. According to the character of the overflow of the stratified liquid, we could say that in all probability, the upper, as well as the lower, phase was superfluid. However, a final conclusion can be made only as a result of a fuller investigation. This investigation of the properties of the solution is continuing at the present time.

The authors express their deep gratitude to Academician P. L. Kapitza for his constant interest and attention to the research.

[1] G. K. Walters and W. M. Fairbank, Phys. Rev. 103, 262 (1956).
[2] J. G. Daunt and C. V. Heer, Phys. Rev. 79, 46 (1950).
[3] B. N. Esel'son, Berezniak and Kaganov, Dokl. Akad. Nauk SSSR 111, 568 (1956).
[4] Abraham, Weinstock and Osborne, Phys. Rev. 76, 864 (1949).

Translated by R. T. Beyer
258

Fine Structure of the α-Spectra of U^{234} and U^{238}

B. A. BOCHAGOV, A. P. KOMAR AND G. E. KOCHAROV
Leningrad Physico-Technical Institute
Academy of Sciences, U.S.S.R.

(Submitted to JETP editor February 16, 1957)
J. Exptl. Theoret. Phys. (U.S.S.R.) 32, 1257-1259
(May, 1957)

FOR THE STUDY OF the fine structure of the α-spectra of long-lived isotopes such as U^{238} and Th^{232}, magnetic spectrometers are practically useless because of their low sensitivity. To solve such problems it is therefore advisable to use pulsed ionization chambers, which exceed the sensitivity of magnetic spectrometers by several orders of magnitude. (The product of source area and solid angle is greater.)

Although they are more sensitive, ionization chambers are somewhat inferior to magnetic spectrometers in resolution. As a rule, the half-width of the lines of the α-spectra of a pulse ionization chamber, which determines its energy resolution, is 50–70 kev. This high value of this quantity is ascribable to circuit noise, in addition to other causes. We were able[1] to reduce the mean square value of the circuit noise to 6.8 kev, which is 3.2 kev less than the best work abroad[2]. In addition, the method of electrical collimation worked out in our laboratory permitted complete utilization of the sensitivity of the apparatus. The resultant apparatus had a line half-width of 30 kev and good sensitivity.

We used this apparatus to study the energy spectra of the α-particles of U^{234} and U^{238}. A natural mixture of uranium isotopes was used as a source of α-particles. The results obtained are shown in Figs. 1 and 2. Figure 1 shows the energy spectrum of the α-particles from U^{234}. Along with the basic group of 4.77 Mev α-particles there is a clearly

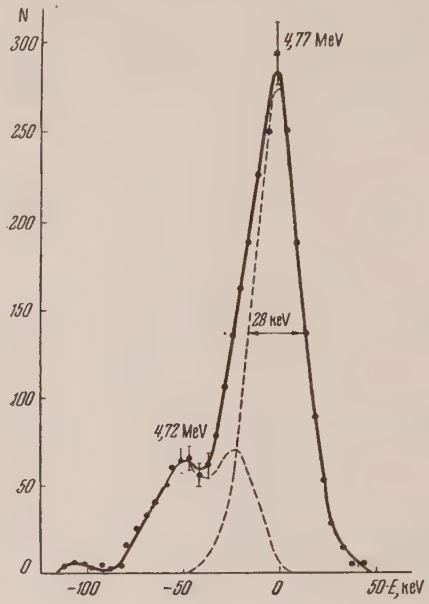

FIG. 1

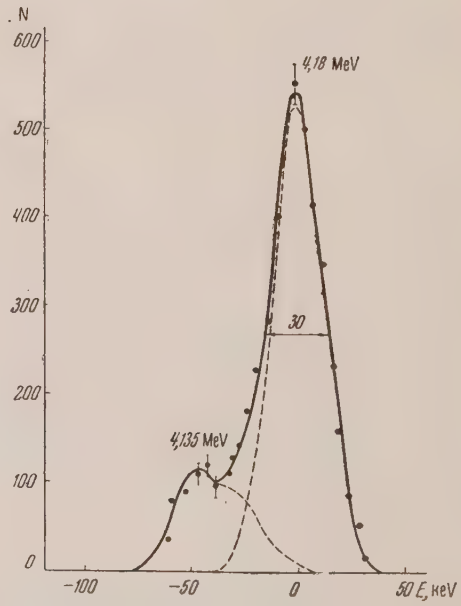

FIG. 2

defined 4.72 Mev group corresponding with the transition to the first rotational level of Th^{230}. The intensities of these two lines are 72 and 28% respectively. These data are in good agreement with the data found by Goldin, Tretyakov and Novikov[3].

Figure 2 shows the energy spectrum of the α-particles of U^{238}. In this case, too, a fine structure was revealed. The fine structure line is separated from the fundamental by 45 kev. The ratio of intensity of the fundamental to the fine structure line is 4. The half-width of the lines is about 30 kev.

An analysis of the curves has shown that they cannot be represented by the sum of two gaussians, corresponding to a fundamental group and a fine structure group. The existence of a third group of α-particles had to be assumed with an energy lying between the fundamental and the fine structure group. This is reasonable since immediately after emitting a low-energy α-particle the nucleus emits a conversion electron. Half of the total number of emitted conversion electrons, falling in the working volume of the chamber, produce additional ionization. Consequently, half of the pulses v_α from the α-particles of the fine structure line are registered simultaneously with the pulses v_e from the conversion electrons, and what we get is the sum of the pulses, equal to $v_\alpha + v_e$, corresponding so to speak to a group of α-particles of intermediate energy $E = E_\alpha + E_e$. The other half of the pulses is registered as α-particle pulses of energy E_α. Our analysis of the curves shows the existence of such lines. The separation between the lines is about 30 kev, which corresponds to the kinetic energy of the electrons emitted from the L-shell of the atom.*

The intensities of the groups are identical which shows that the conversion is practically 100%.

It should be noted that number of authors[4-6] have studied the fine structure of the α-spectrum of U^{238} by an indirect method, viz., by studying the conversion electrons accompanying α-decay, using electron sensitive emulsions impregnated with a uranium salt. From the data of the above authors, the intensity of the transition to the first excited level amounts fo 23 ± 3%. After finishing our measurements it became known (private communication from J. Teillac) that the fine structure of the α-decay had been studied by Valladas using an ionization chamber with ion collection. He plotted the energy spectrum of the α-particles of U^{238} by means of the coincidences of the α-particles and the γ-radiation accompanying conversion, thereby avoiding registering the fundamental group of α-particles. His results agree with ours.

The authors wish to thank G. F. Kirshin, a student at the M. I. Kalinin Polytechnic Institute in Leningrad, for his active aid in the work, as well as S. N. Nikolaev and his group for building and setting up the apparatus.

*The mean energy going into the formation of one ion pair by electrons is the same as for α-particles.

[1] Bochagov, Kocharov, and Krishin, "Signal to Noise Ratio in Pulse Ionization Chambers," Pribori i Tekhnika Eksperimenta (in press).

[2] D. W. Engelkemeir, L. B. Magnusson, Rev. Sci. Instr. 26, 295 (1955).

[3] L. L. Goldin, E. F. Tretyakov, G. I. Novikov, Report of the Session of the Academy of Sciences of the U.S.S.R. on the Peaceful Uses of Atomic Energy, July 1–5, 1955.

[4] B. B. Zajac, Phil. Mag. 43, 264 (1952).

[5] D. C. Dunlavey and G. T. Seaborg, Phys. Rev. 87, 165 (1952).

[6] G. Albouy and J. Teillac, Compt. rend. 234, 829 (1952).

Translated by C. V. Larrick
259

On the Theory of Skin Effect in Metals

M. IA. AZBEL'
Physico-Technical Institute, Academy of Sciences, Ukrainian SSR

(Submitted to JETP editor February 18, 1957)
J. Exptl. Theoret. Phys. (U.S.S.R.) 32, 1259 (May, 1957)

IN ANY THEORY of skin effect in metals one usually assumes $B = H$ since the magnetic susceptibility of metals is very slight ($\chi \sim 10^{-6}$). However, it is easy to see that neglect of the spin paramagnetism of the free electrons would lead to a substantial error in determining the coefficient of electromagnetic wave transmission through a sufficiently thick film. As was shown in Ref. 1, this is due to the damping of the magnetic moment due to spin paramagnetism at a depth

$$\delta_{\text{eff}} \sim v\,[t_0 T_{\text{sp}} / 3\,(1 + \omega T_{\text{sp}})]^{1/2}$$

(v is the limiting Fermi electron velocity, ω is the electromagnetic field frequency, T_0 and T_{sp} are the electron free path times without and with spin transfer). Since the usual skin layer depth is

$$\delta \sim \sqrt{c^2 / 2\pi\omega\sigma}, \quad \text{then}$$

$$\delta / \delta_{\text{eff}} \lesssim (c / vt_0) \sqrt{m / 2\pi ne^2} \sim 10^{-14}\,\text{sec} / t_0 \ll 1$$

(n, m, and e are the density, effective mass, and

charge of the electron, while σ is the conductivity of the metal). Therefore, taking the spin magnetic moment into account leads to an albeit small but slowly-damped addition. In this paper, the coefficient of wave transmission through a sufficiently thick film $[d \gtrsim 2\delta \ln (\delta_{\text{eff}}/4\chi\delta)]$ is calculated taking this addition into account.

In this case, the complete system of equations is [see Eq. (14) of Ref. 1]

$$\operatorname{curl} \mathbf{E} = -i\omega \mathbf{B}/c; \quad \operatorname{curl} \mathbf{H} = 4\pi \mathbf{j}/c;$$

$$\mathbf{H} = \mathbf{B} - 4\pi \mathbf{M}; \quad \mathbf{M} = \chi (\mathbf{B} - \mathbf{w});$$

$$\frac{\partial \mathbf{w}}{\partial z} v \cos\theta + \frac{\mathbf{w}}{t_0^*} = \frac{\overline{\mathbf{w}}}{t_0} + i\omega \mathbf{B};$$

$$\frac{1}{t_0^*} = \frac{1}{t_0} + \frac{1}{T_{\text{sp}}} + i\omega; \quad \overline{f} = \frac{1}{2} \int_0^{\pi} f \sin\theta \, d\theta.$$

The solution of this system is completely analogous to the solution of the system (26) of Ref. 1 and leads to the following formula for the transmission coefficient:

$$K \sim \left| \frac{\chi c^3 Z^2}{2\pi d (\omega + 1/T_{\text{sp}})} \right|^2, \quad 2\delta \ln \frac{\delta_{\text{eff}}}{4\pi\chi\delta} \ll d \ll \delta_{\text{eff}}.$$

In particular, for normal skin effect and $\omega \gg 1/T_c$

$$K \sim \left(\frac{2\chi c}{\sigma d}\right)^2 \gtrsim \frac{2\pi\chi^2\omega}{\sigma} \ln^{-2} \frac{c}{v\sqrt{2\pi\sigma t_0}} \sim 10^{-17}.$$

In conclusion, I would like to express my gratitude to I. M. Lifshitz and M. I. Kaganov for valuable discussions.

---

[1] Azbel', Gerasimenko, and Lifshitz, J. Exptl. Theoret. Phys. (U.S.S.R.) **32**, 1212 (1957), Soviet Phys. JETP **5**, 986, this issue (1957).
Translated by M. D. Friedman
260

Radiation From a Point Charge, Moving Uniformly Along the Surface of an Isotropic Medium

A. I. MOROZOV
Moscow State University
(Submitted to JETP editor February 18, 1957)
J. Exptl. Theoret. Phys. (U.S.S.R.) **32**, 1260-1261 (May, 1957)

THE MOTION OF CHARGED particles close to the surface of a dielectric material has been treated in a number of papers [1,2]. The case of a straight charge line moving close to a medium with arbitrary ε' and μ' was already treated by the author [3].

We shall now give some results of the corresponding case of a point charge. It is known [4] that in a uniform motion of a particle at a distance l from the surface the radiation into the surface is limited to wavelengths $\lambda \gtrsim l\sqrt{\mu'\varepsilon'}$ (more accurately $\lambda \gtrsim l\beta$). This allows to obtain a qualitative picture assuming a nondispersive medium. Then the energy emitted per unit time by Cerenkov radiation by a particle moving at a distance l from the medium with a a velocity $v = \beta c$ is given by

$$P = -\frac{e^2}{2\theta l^2} \frac{c}{\sqrt{\mu'\varepsilon' - 1}} \left\{ \theta^2 \mu' \left(1 - \frac{\mu'}{\sqrt{\mu'^2 + \Gamma^2}}\right) + \frac{\mu'\varepsilon - 1}{\varepsilon' - \mu'} \left(\frac{\mu'}{\sqrt{\mu'^2 + \Gamma^2}} - \frac{\varepsilon'}{\sqrt{\varepsilon'^2 + \Gamma^2}} \right) \right\}, \qquad (1)$$

$$\theta^2 = 1 - \beta^2, \quad \Gamma = \gamma\theta, \quad \gamma^2 = \mu'\varepsilon'\beta^2 - 1.$$

We note for comparison that the radiation per unit length from a charge filament of linear charge density ρ is [3]

$$P_l = (2v\rho^2/l)\, \varepsilon'\Gamma/(\varepsilon'^2 + \Gamma^2). \qquad (2)$$

From these formulae we deduce that:

a) In the relativistic case $\theta \to 0$, independently of the characteristics of the medium, the radiated power approaches the limits

$$P \to e^2 c/2l^2; \quad P_l \to 0. \qquad (3)$$

b) In the nonrelativistic case but if $\beta\sqrt{\varepsilon'} \gg 1$

$$P \approx \frac{e^2}{2l^2} \frac{c}{\sqrt{\varepsilon'}} \beta^2; \quad P_l \approx 2 \frac{\rho^2}{l} \frac{c}{\sqrt{\varepsilon'}} \beta^2. \qquad (4)$$

This means physically that at low velocity the field enters the medium practically perpendicularly to the surface if $\varepsilon' \gg 1$.

c) For a magnetic material ($\varepsilon' = 1$) at $\beta^2\mu' \gg 1$ and nonrelativistic velocity the radiated power is given by

$$P \approx e^2 c/2l^2 \sqrt{\mu'}, \quad P_l \approx 2\rho^2 c/l\sqrt{\mu'}. \qquad (5)$$

The form of these expressions is due to the fact that at particle velocities above the inversion velocity (see below) the field is being expelled from the magnetic medium.

d) Finally, for a medium of the type of a ferrite ($\mu' \gg \varepsilon' \gg 1$) we have for $\mu'\beta^2 \gg \varepsilon'$ and $\theta \approx 1$

$$P \approx (e^2 c/2l^2)\sqrt{\varepsilon'/\mu'}, \quad P_l \approx (2\rho^2 c/l)\sqrt{\varepsilon'/\mu'}. \tag{6}$$

These expressions can be interpreted in an analogous fashion as the previous ones.

The force acting on the particle in a direction normal to the surface of the medium is given by

$$F = -\frac{e^2}{\pi\theta l^2}\left\{\frac{\mu'\varepsilon'-1}{\mu'-\varepsilon'} L(\varepsilon') - \left(\frac{\mu'\varepsilon'-1}{\mu'-\varepsilon'} + \mu'\theta^2\right) L(\mu') + \frac{\pi}{4}\theta^2\right\}, \tag{7}$$

$$L(\lambda) = \frac{\lambda}{\sqrt{(\lambda^2-1)(\lambda^2+\Gamma^2)}} \tan^{-1}\left(\sqrt{\frac{\lambda^2-1}{\lambda^2+\Gamma^2}}\,\Gamma\right) + \int_0^{\tan^{-1}\Gamma} \frac{d\alpha}{\lambda + \sqrt{1-(\Gamma^2+1)\sin^2\alpha}}. \tag{8}$$

The equivalent force per unit length acting on a charged line is

$$F_l = (\rho^2/l)(\varepsilon'^2-\Gamma^2)/(\varepsilon'^2+\Gamma^2). \tag{9}$$

One sees from (8) that in the case of a magnetic medium ($\mu' \gg 1$, $\varepsilon' = 1$) the force is attractive up to $\Gamma \sim 1$ and becomes attractive again at $\Gamma \approx \mu'$. For $\mu' \gg \Gamma \gg 1$ the repulsive force equals $e^2/(4l^2)$. On the other hand, in the case of a dieletric, the force is always attractive and has a value close to $-e^2/(4l^2)$.

For comparison we note that for a charged line the force is repulsive beginning at the inversion velocity (*i.e.*, at the velocity where $\Gamma = \varepsilon'$) and remains repulsive from there on for all velocities.

In conclusion, the author wishes to express his gratitude to Prof. A. A. Sokolov for his interest in this work, to I. Kvasnitsa for the discussion of the calculations, and to V. Pafomov for acquainting the author with his work[2].

[1] M. Danos, J. Appl. Phys. **26**, 2 (1955).

[2] V. E. Pafomov, J. Exptl. Theoret. Phys. (U.S.S.R.) **32**, 610 (1957), Soviet Phys. JETP **5**, 504 (1957).

[3] A. I. Morozov, Vestn. MGU. **1**, (1957).

[4] V. L. Ginzburg and I. M. Frank, Dokl. Akad. Nauk SSSR **56**, 699 (1947).

Translated by M. Danos
261

Photon Green Function Accurate to e^4

S. N. SOKOLOV
Joint Institute of Nuclear Study

(Submitted to JETP editor March 1, 1957)
J. Exptl. Theoret. Phys. (U.S.S.R.) **32**, 1261-1262
(May, 1957)

THE SUM OF DIAGRAMS for the self energy of the photon, inclusive of fourth-order diagrams, was calculated. After carrying out renormalization in the usual way and evaluating the integrals over the momenta, the following expression was obtained

$$iG_{\mu\nu} = \frac{k^2\delta_{\mu\nu} - k_\mu k_\nu}{k^4}\left\{1 + \frac{e^2}{2\pi^2}\int_0^1 dx\, X \ln\left(1+\frac{k^2}{m^2}X\right) + \left[\frac{e^2}{2\pi^2}\int_0^1 dx\, X \ln\left(1+\frac{k^2}{m^2}X\right)\right]^2 \right.$$
$$+ \frac{e^4}{16\pi^4}\left[\left[\frac{1}{2}\int_0^1 dx \ln\left(1+\frac{k^2}{m^2}X\right)\right]^2 + \int_0^1 dx\,(2-3x+2x^2)\ln\left(1+\frac{k^2}{m^2}X\right)\right.$$
$$+ \int_0^1 dx\int_0^1 dy\left(y-2y^2-\frac{y}{x}\right)\ln\left(1+\frac{k^2 Yx}{m^2(1-y+yx)}\right) + \int_0^1 dx\int_0^1 dy\int_0^1 dz\int_0^1 dt \tag{1}$$
$$\times \frac{k^2[1-x(1-t)-zt][x(1-t)+zt]+m^2\{1+2[x(1-t)+zt][yx(1-t)+yzt+x(1-y)]\}}{(1-t)(k^2X+m^2)+y[t(k^2Z+m^2)+k^2T(z-x)^2]}$$
$$\left.\left. - \int_0^1 dx\int_0^1 dy\int_0^1 dz\,\frac{2m^2(3-x)yz^2(1-yz)}{k^2x(Yz+Zy^2)+m^2(1-z+zx)} + \frac{49}{54} + \frac{5}{12} - \frac{11}{6}\zeta(2)\right] + \cdots\right\},$$

where

$$X = x(1-x), \quad Y = y(1-y),$$
$$Z = z(1-z), \quad T = t(1-t).$$

We will consider that the sum

$$A = \alpha + \beta \ln \frac{k^2}{m^2} + \gamma \left(\ln \frac{k^2}{m^2} \right)^2 \tag{2}$$

is the asymptotic form of the function f if

$$\lim [f(k^2/m^2) - A(k^2/m^2)] = 0 \text{ as } k^2/m^2 \to \infty. \tag{3}$$

Then the asymptotic form of the Green function of the photon is, in the approximation considered

$$iG_{\mu\nu} \sim \frac{k^2\delta_{\mu\nu} - k_\mu k_\nu}{k^4} \left\{ 1 + \frac{e^2}{12\pi^2} \left(\ln \frac{k^2}{m^2} - \frac{5}{3} \right) + \left[\frac{e^2}{12\pi^2} \left(\ln \frac{k^2}{m^2} - \frac{5}{3} \right) \right]^2 + \frac{e^4}{64\pi^4} \left(\ln \frac{k^2}{m^2} + \frac{139}{54} - \frac{22}{3}\zeta(2) + 4\zeta(3) \right) \right\}, \tag{4}$$

where $\zeta(2)$ and $\zeta(3)$ are the Riemann Zeta functions [see Eq. (5.10) of Ref. 1].

The coefficient $e^4/64\pi^4$ coincides with the coefficient obtained earlier by Jost and Luttinger[2] by a different procedure.

We give the numerical value of the constant contained in the asymptotic form:

$$C = \frac{139}{54} - \frac{22}{3}\zeta(2) + 4\zeta(3) = -4.680\,548\ldots \tag{5}$$

Taking the constant C into account does not change the structure of Eq. (30) of Ref. 3 for the asymptotic form of the Green function of the photon, but the charge e which comes into this formula is given now by the expression

$$e^2 = e_0^2 \Big/ \left[1 + \frac{5}{3}\frac{e_0^2}{3\pi} + \frac{e_0^4}{4\pi^2} 4{,}68 \right]. \tag{6}$$

The author is very grateful to N. P. Klepikov for help in this work, and also to V. G. Solov'ev for valuable advice.

[1] M. Gell-Mann and F. Low, Phys. Rev. **95**, 1300 (1954).

[2] R. Jost and J. M. Luttinger, Helv. Phys. Acta **23**, 201 (1950).

[3] N. N. Bogoliubov and D. V. Shirkov, J. Exptl. Theoret. Phys. (U.S.S.R.) **30**, 77 (1956), Soviet Phys. JETP **3**, 57 (1956).

Translated by G. E. Brown
262

Reduction of the Two-Nucleon Problem to a Single-Nucleon Problem in the Nonrelativistic Range

IU. V. NOVOZHILOV
Leningrad State University

(Submitted to JETP editor February 25, 1957)
J. Exptl. Theoret. Phys. (U.S.S.R.) **32**, 1262-1264 (May, 1957)

WE SHALL CONSIDER the interaction between two nucleons at the fixed points $\mathbf{r}_1$ and $\mathbf{r}_2$ and shall attempt to express the renormalized two-nucleon matrix elements in terms of renormalized single-nucleon matrix elements. We shall use as a basis the papers of Chew and Low[1] and Wick[2], in which single-nucleon problems are treated.

The energy operator is

$$H = H_0 + U_1 + U_2, \tag{1}$$

$$U_A = \sum_{\mathbf{k}} V_{\mathbf{k}}^0(A)\, e^{i\mathbf{k}\mathbf{r}_A} a_{\mathbf{k}} + V_{\mathbf{k}}^0(A)\, e^{-i\mathbf{k}\mathbf{r}_A} a_{\mathbf{k}}^+; \quad A = 1, 2. \tag{2}$$

Here $V_{\mathbf{k}}^0(A)$ contains the operators σ_A and τ^A, which apply to nucleon A; the rest of the notation is taken from Ref. 1.

The state Ψ_σ with two interacting physical nucleons is an eigenfunction of the Hamiltonian (1):

$$H\Psi_\sigma(1, 2, \bar{a}) = [2E_0 + E_\sigma(\rho)]\,\Psi_\sigma(1, 2, \bar{a}), \quad (\rho = \mathbf{r}_1 - \mathbf{r}_2), \tag{3}$$

where E_0 is the nucleon self-energy and $E_\sigma(\rho)$ is the static interaction energy of the nucleons. The symbol $\sigma \equiv (I', S', I_3', S_3')$ denotes the eigenvalues of the total spin, the total isotopic spin, and their three projections. In the representation where the creation operator $a_{\mathbf{k}}^+$ is equivalent to multiplication by $\bar{a}_{\mathbf{k}}$ *i.e.*, $a_{\mathbf{k}}^+\Psi = \bar{a}_{\mathbf{k}}\Psi$, the state vector Ψ_σ will be a function of $\bar{a}_{\mathbf{k}}$.

As the basic set of functions we shall use the products of single-nucleon state vectors $F_{\alpha\beta}(1, 2, \bar{a}) = F_\alpha(1, \bar{a})\, F_\beta(2, \bar{a})$, where α and β are spin and isotopic spin indices. $F_\alpha(1, \bar{a})$, which describes a nucleon in a meson cloud, is the solution of the Schroedinger equation

$$(H_0 + U_1) F(1, \bar{a}) = E_0 F(1, \bar{a}). \quad (4)$$

It can be shown[3] that for $\rho \to \infty$ the products $F_{\alpha\beta}(1, 2, \bar{a}) = F_\alpha(1, \bar{a}) F_\beta(2, \bar{a})$ are solutions of (3) and are subject to the orthogonality condition

$$(F_{\alpha\beta}(1, 2, \bar{a}), \quad F_{\alpha'\beta'}(1, 2, \bar{a})) = \delta_{\alpha\alpha'}\delta_{\beta\beta'}.$$

However for finite ρ these products are nonorthogonal functions of ρ.

We shall obtain Ψ_σ in the form

$$\Psi_\sigma = \Phi_\sigma + \chi_\sigma,$$

where $\Phi_\sigma = \sum c^\sigma_{\alpha\beta} F_{\alpha\beta}$ coincides with Ψ_σ for $\rho \to \infty$. When χ_σ is expanded in eigenfunctions of the total Hamiltonian H we shall restrict ourselves to the states Ψ_μ (without real mesons) and Ψ^q_μ (with one real meson) so that

$$\Psi_\sigma = \frac{1}{(\Psi_\sigma, \Phi_\sigma)} \Bigg[\Phi_\sigma - \sum_{\mu \neq \sigma} (\Psi_\mu, \Phi_\sigma) \Psi_\mu - \sum_{\mu, q} \frac{1}{q_0} (\Psi^q_\mu, [H - 2E_0 - E_\sigma] \Phi_\sigma) \Psi^q_\mu \Bigg]. \quad (5)$$

In the nonrelativistic approximation where small distances are unimportant Ψ_σ in the right-hand side can be replaced by Φ_σ. The principal difficulty here lies in the calculation of the matrix elements

$$(\alpha\beta \mid L \mid \alpha'\beta') = (F_\alpha(1, \bar{a}) F_\beta(2, \bar{a}), L(a, a^+) F_{\alpha'}(1, \bar{a}) F_{\beta'}(2, \bar{a})) \quad (6)$$

without being able to use the explicit single-nucleon states $F(1, \bar{a})$ and $F(2, \bar{a})$.

We introduce a different notation for the meson field variables in $F_{\alpha'}(1, \bar{a})$ and $F_{\beta'}(2, \bar{a})$, as follows:

$$F_{\alpha'}(1, \bar{a}) = F_{\alpha'}(1, \bar{a}_1), \quad F_{\beta'}(2, \bar{a}) = F_{\beta'}(2, \bar{a}_2)$$

(without any special assumptions). Then, for example, the matrix element (6) with $L = 1$ will be written as

$$F^*_\alpha\left(1, \frac{\partial}{\partial \bar{a}_1} + \frac{\partial}{\partial \bar{a}_2}\right) F^*_\beta\left(2, \frac{\partial}{\partial \bar{a}_1} + \frac{\partial}{\partial \bar{a}_2}\right) \times F_{\alpha'}(1, \bar{a}_1) F_{\beta'}(2, \bar{a}_2)\big|_{\bar{a}_1 = \bar{a}_2 = 0}. \quad (7)$$

Assume now that a meson cloud interacts much more strongly with its "own" nucleon than with another nucleon. Then in $F^*_\alpha(1, \partial/\partial\bar{a}_1 + \partial/\partial\bar{a}_2)$ the operator $\partial/\partial\bar{a}_2$ will be small compared with $\partial/\partial\bar{a}_1$ and in $F^*_\beta(2, \partial/\partial\bar{a}_1 + \partial/\partial\bar{a}_2)$ the operator $\partial/\partial\bar{a}_1$ will be small compared with $\partial/\partial\bar{a}_2$. Since for small $\bar{a}_2$

$$F(1, \bar{a}_1 + \bar{a}_2) \approx F(1, \bar{a}_1) + \sum_{\mathbf{k}} a^+_{2\mathbf{k}} a_{1\mathbf{k}} F(1, \bar{a}_1) + \ldots, \quad (8)$$

we obtain when we limit ourselves to the linear term in (8)

$$(\alpha\beta \mid \alpha'\beta') = (F_\alpha(1, \bar{a}_1) F_\beta(2, \bar{a}_2), (1 + \hat{N}) F_{\alpha'}(1, \bar{a}_1) F_{\beta'}(2, \bar{a}_2)), \quad (9)$$

$$N = \sum_{\mathbf{q}} [a^+_{1\mathbf{q}} a_{2\mathbf{q}} + a^+_{2\mathbf{q}} a_{1\mathbf{q}}], \quad (10)$$

with $[a_{1\mathbf{q}}, a^+_{2\mathbf{q}}] = 0$, $[a_{1\mathbf{q}}, a^+_{1\mathbf{q}'}] = \delta_{\mathbf{q}\mathbf{q}'}$ etc.

In general, for the calculation of (6) all $a_{\mathbf{k}}$ and $a^+_{\mathbf{k}}$ must first operate on the functions $F(1, \bar{a})$ and $F(2, \bar{a})$, following which (7) and (8) will be used. For example,

$$(\alpha\beta \mid H - 2E_0 \mid \alpha'\beta') = (F_\alpha(1, \bar{a}_1) F_\beta(2, \bar{a}_2), (1 + \hat{N}) [U^+_1(a_2) + U^+_2(a_1)] F_{\alpha'}(1, \bar{a}_1) F_{\beta'}(2, \bar{a}_2)), \quad (11)$$

where $U^+_1(a_2)$ is the annihilation component of the operator U_1 with annihilation operators $a_{2\mathbf{k}}$. The right-hand sides of (9) and (11) can be expressed in terms of the single-nucleon matrix elements $(F_\alpha, V^0_{\mathbf{k}} F_{\alpha'})$ and $(F^q_\alpha, V^0_{\mathbf{k}} F_{\alpha'})$, where F^q_α is the state with a nucleon and one (real) meson q. The first of these matrix elements is known to be $(u_\alpha, V_{\mathbf{k}} u_{\alpha'})$, where u is the spin-isotopic spin function of the bare nucleon and $V_{\mathbf{k}}$ contains the renormalized charge f. The second matrix element is associated with the meson-nucleon elastic scattering amplitude. The rule for calculating expressions such as (6) can be expressed as follows. In the coordinate representation the annihilation component $\varphi^{(+)}(\mathbf{r}_1)$ of the meson operator $\varphi(\mathbf{r}_1)$ is

$$\varphi^{(+)}(\mathbf{r}_1) = \int \Delta^{(+)}(\mathbf{r}_1 - \mathbf{r}) \frac{\delta}{\delta\varphi^{(-)}_{(\mathbf{r})}} d^3\mathbf{r}, \quad (12)$$

where $\Delta^{(+)}(\mathbf{r}_1 - \mathbf{r}) = [\varphi^{(+)}(\mathbf{r}_1), \varphi^{(-)}(\mathbf{r})]$,

where $\varphi^{(-)}(\mathbf{r})$ is the creation component of $\varphi(\mathbf{r})$. If τ_1 and τ_2 are the regions occupied by the meson clouds of nucleons 1 and 2, $F(1, \bar{a})$ will depend on $\varphi^{(-)}(\mathbf{r})$, where $\mathbf{r}$ lies in the region τ_1, and $F(2, \bar{a})$

will depend on $\varphi^{(-)}(\mathbf{r})$ in the volume τ_2. Then division of the operator $\partial/\partial\overline{a}_1 + \partial/\partial\overline{a}_2$ in $F_\alpha^*(1)$ [Eq. (7)] into a larger part $\partial/\partial\overline{a}_1$ and a smaller part $\partial/\partial\overline{a}_2$ corresponds to division of $\varphi^{(+)}(\mathbf{r}_1)$ into two terms – an integral over τ_1 (the larger part) and an integral over τ_2 (the smaller part).

Equation (8) is not an expansion with respect to renormalized charge because the single-nucleon matrix element $(F_\alpha^q, V_{\mathbf{k}}^0 F_{\alpha'})$ cannot be calculated by ordinary perturbation theory. Its value must either be calculated exactly or obtained from pion-nucleon scattering experiments.

[1] G. F. Chew and F. E. Low, Phys. Rev. 101, 1570 (1956).

[2] G. C. Wick, Revs. Modern Phys. 27, 339 (1955).

[3] H. Ekstein, Nuovo cimento 4, 1017 (1956).

Translated by I. Emin
263

CONTENTS – *continued*

CONTENTS

(*Contents continued on inside back cover*)